



Environmental Effects Monitoring Program

Quarterly Report: July – September 2019

September 30, 2019

Fundy Ocean Research Center for Energy
1156 West Bay Road | Parrsboro, Nova Scotia
PO Box 2573, Halifax, Nova Scotia
902-406-1166
fundyforce.ca

Executive Summary

Generating electricity from tidal stream technology devices using the ebb and flow of the tides is an emerging marine renewable energy sector that is being explored by countries around the world.

FORCE was established in 2009 after undergoing a joint federal-provincial environmental assessment with the mandate to enable the testing and demonstration of tidal stream energy devices. Since that time, more than 100 related research studies have been completed or are underway with funding from FORCE, the Offshore Energy Research Association of Nova Scotia (OERA), and others. These studies have considered socioeconomics, biological, and other research areas.

The latest monitoring programs at the FORCE site were initiated in 2016 in anticipation of turbine deployments by one of FORCE's berth holders, Cape Sharp Tidal Venture (CSTV) in 2016. These efforts are divided into two components: mid-field monitoring activities led by FORCE >100 metres from a turbine, and near-field or 'turbine-specific' monitoring led by individual tidal energy developers at the FORCE site ≤100 metres from a turbine. All plans are reviewed by FORCE's independent Environmental Monitoring Advisory Committee (EMAC) and federal and provincial regulators prior to implementation.

Mid-field monitoring at the FORCE site presently consists of monitoring for fish, marine mammals, seabirds, lobster, and marine sound. Since the start of this latest monitoring effort in 2016, FORCE has completed:

- ~408 hours of hydroacoustic fish surveys;
- more than 3,780 'C-POD' marine mammal monitoring days;
- bi-weekly shoreline observations;
- 49 observational seabird surveys;
- four drifting marine sound surveys and additional sound monitoring; and
- 11 days of lobster surveys

Analysis of fifteen hydroacoustic fish surveys conducted in the Minas Passage between 2011-2017 as part of FORCE's Environmental Effects Monitoring Program (EEMP) has been recently completed by the University of Maine and is included in this report and in Appendix IV. The report by the University of Maine provides an overall approach for understanding the information contained within the hydroacoustic data sets, including data visualization and statistical analyses. Moreover, the University of Maine has provided FORCE with the data scripts/coding required for analysis and data visualization so that deeper explorations of the data may be undertaken to investigate questions that are specific to the needs of FORCE.

FORCE recently completed the field component for the comparative passive acoustic monitoring (PAM) study outlined in its regulator approved 2019 EEMP plan. This study aims to understand the relative performance of multiple PAM devices (C-POD, F-POD, SoundTrap, icListenHF, and AMAR) across the range of tidal flows experienced at the FORCE site. The first phase of the study involved Aquatron testing and confirmed that each device could detect synthetic click trains emitted by an icTalk used to mimic harbour porpoise vocalizations. FORCE recently completed the field trial component of this study and has sent the data to SMRU Consulting for analyses. Further information is included in this report.

In another PAM-related study, FORCE recently commissioned JASCO Applied Sciences (Canada) Ltd. to conduct a comparative integrated analysis of acoustic data sets collected by various hydrophones mounted on and deployed around the CSTV turbine at the FORCE site. Study details are contained herein, and the report is included as Appendix IX. Results demonstrated that flow noise increased with the height of the hydrophone off the seabed and impacted the hydrophone mounted on the top of the CSTV turbine the most. The least affected hydrophones were those mounted at the 'aft' position on the CSTV turbine and the autonomously deployed AMAR. In fact, flow noise at these locations was low enough to successfully measure the sound from the turbine during the brief period prior to the malfunction of the turbine's rotor in August 2018 (see below).

FORCE is working collaboratively with the OERA to advance 'The Pathway Program' to identify effective and regulator approved monitoring solutions for the tidal energy industry in Nova Scotia. The first phase of this program was a Global Capability Assessment that was recently completed. It involved comprehensive literature reviews about the use of different classes of environmental monitoring technologies such as PAM, imaging sonars, and echosounders for monitoring tidal energy devices around the world. Subject matter experts were commissioned to provide reports on these instrument classes, and FORCE has received final reports for these technology classes. Further information is included in this report and Appendix V (PAM), Appendix VI (imaging sonars), and Appendix VII (echosounders). Phase II, Advancing Data Processing and Analysis, has commenced and work is underway with DeepSense (Dalhousie University) to automate the post-processing of hydroacoustic fish survey data. Automation of other types of monitoring data such as PAM will commence in the near future. Phase III, Technology Validation, has also begun and FORCE is working collaboratively with Sustainable Marine Energy Canada (SME) to assess the capabilities of different classes of environmental monitoring technologies in high flow environments.

In July 2018, CSTV installed a two-megawatt OpenHydro turbine at 'Berth D' in the FORCE Crown Lease Area. Due to the insolvency of OpenHydro which was announced four days after turbine installation, the approved near-field monitoring program and contingency monitoring program for this turbine could not be immediately initiated. Efforts were taken to monitor the turbine in the interim, with a focus on fish and marine mammals, until the turbine was re-energized on September 4, 2018. At that time, it was confirmed that the turbine's rotor was not turning, and the turbine-mounted monitoring sensors were re-energized.

As a result of the status of the turbine's rotor, the monitoring requirements and reporting timelines approved as part of CSTV's authorization from Fisheries and Oceans Canada were modified to monthly confirmation of the turbine rotor's status. This is done using data collected from turbine-mounted Acoustic Doppler Current Profilers (ADCP) during peak tidal flow. CSTV provided these monthly reports to regulators from October 2018 through February 2019, but notified Nova Scotia Environment and FORCE on March 15, 2019, that it intended to cease this monthly reporting requirement due to issues surrounding its insolvency. Consequently, FORCE took on this responsibility and has provided regulators with monthly turbine status reports from March 2019 through September 2019 that confirm the continued non-operational status of the CSTV turbine. FORCE intends to provide these monthly reports until the CSTV turbine is retrieved. Beyond the ADCPs, data from other operating turbine-mounted sensors are being used by FORCE and its partners to inform research objectives. Further information regarding the turbine's status, CSTV project updates, and contingency monitoring efforts, is included in this report and Appendix I.

This report provides a summary of monitoring activities and data analysis completed at the FORCE site up to the end of the third quarter of 2019. In addition, it also highlights findings from international research efforts, previous data collection periods at the FORCE site, and additional research work that is being conducted by FORCE and its partners. This includes supporting fish tagging efforts with Acadia University and the Ocean Tracking Network, radar research projects, and subsea instrumentation platform deployments through the Fundy Advanced Sensor Technology (FAST) Program. Finally, the report presents details regarding future research and monitoring efforts at the FORCE test site.

All reports, including quarterly monitoring summaries, are available online at www.fundyforce.ca/document-collection.

Contents

Acronyms.....	5
Introduction	7
International Experience & Cooperation	10
Mid-Field Monitoring Activities.....	12
Lobster	14
Fish	15
Marine Mammals.....	17
Marine Sound (Acoustics).....	20
Seabirds	21
Near-field Monitoring Activities.....	22
Other FORCE Research Activities	23
Discussion	27
References	27

Appendices

Appendix I	Cape Sharp Tidal Venture Update
Appendix II	Passive Acoustic Monitoring Workshop Report
Appendix III	Using radar data to evaluate seabird abundance and habitat use at the Fundy Ocean Research Centre for Energy site near Parrsboro, NS
Appendix IV	Marine fish monitoring at FORCE: Updated report on processing and analysis
Appendix V	Passive acoustic monitoring in tidal channels and high flow environments
Appendix VI	Imaging sonar review for marine environmental monitoring around tidal turbines
Appendix VII	Final report: Scientific echosounder review for instream tidal turbines
Appendix VIII	Active sonar environmental monitoring for Fundy tidal energy project: A panel discussion by subject matter experts
Appendix IX	Passive acoustic monitoring in a tidal energy environment: Comparing acoustic data from three measurement positions in the Minas Passage

Acronyms

AAM	Active Acoustic Monitoring
ADCP	Acoustic Doppler Current Profiler
AMAR	Autonomous Multichannel Acoustic Recorder
BACI	Before/After, Control/Impact
BC	British Columbia
BoFEP	Bay of Fundy Ecosystem Partnership
CFI	Canadian Foundation for Innovation
CLA	Crown Lease Area
cm	Centimetre(s)
CPUE	Catch Per Unit Effort
CSTV	Cape Sharp Tidal Venture
DFO	Department of Fisheries and Oceans (Canada)
DEM	Department of Energy and Mines (Nova Scotia)
EA	Environmental Assessment
EEMP	Environmental Effects Monitoring Program
EMAC	Environmental Monitoring Advisory Committee
EMP	Environmental Management Plan
FAD	Fish Aggregation Device
FAST	Fundy Advanced Sensor Technology
FAST-EMS	Fundy Advanced Sensor Technology – Environmental Monitoring System
FERN	Fundy Energy Research Network
FORCE	Fundy Ocean Research Center for Energy
GPS	Global Positioning System
hr	Hour(s)
IEA	International Energy Agency
kg	Kilogram(s)
km	Kilometer(s)
kW	Kilowatt(s)
m	Meter(s)
MET	Meteorological
MRE	Marine Renewable Energy
MREA	Marine Renewable-electricity Area
NL	Newfoundland and Labrador
NRCan	Natural Resources Canada
NS	Nova Scotia
NSDEM	Nova Scotia Department of Energy and Mines
NSE	Nova Scotia Department of Environment
NSERC	Natural Sciences and Engineering Research Council
NSPI	Nova Scotia Power Inc.
OERA	Offshore Energy Research Association of Nova Scotia
OES	Ocean Energy Systems
ONC	Ocean Networks Canada
ORJIP	Offshore Renewables Joint Industry Programme
OSC	Ocean Supercluster
OTN	Ocean Tracking Network
PAM	Passive Acoustic Monitoring
Q1/2/3	Quarter (1, 2, 3), based on a quarterly reporting schedule
R&D	Research and Development
TC114	Technical Committee 114

TISEC	Tidal In-Stream Energy Converter
SUBS	Streamlined Underwater Buoyancy System
SME	Sustainable Marine Energy (Canada)
UAV	Unmanned Aerial Vehicle
UK	United Kingdom
VEC(s)	Valuable Ecosystem Component(s)

Introduction

This report outlines monitoring activities occurring at the Fundy Ocean Research Center for Energy test site in the Minas Passage, Bay of Fundy throughout the third quarter of 2019, from July 1 to September 30. Specifically, this report highlights results of environmental monitoring activities conducted in the mid-field and near-field zones and other research and development activities conducted at the FORCE site. This report also provides a summary of international research activities around tidal stream energy devices.

About FORCE

FORCE was created in 2009 to lead research, demonstration, and testing for high flow, industrial-scale tidal stream energy devices. FORCE is a not-for-profit entity that has received funding support from the Government of Canada, the Province of Nova Scotia, Encana Corporation, and participating developers.

FORCE has two central roles in relation to the demonstration of tidal stream energy converters in the Minas Passage:

1. Host: providing the technical infrastructure to allow demonstration devices to connect to the transmission grid; and
2. Steward: research and monitoring to better understand the interaction between devices and the environment.

The FORCE project currently consists of five undersea berths for subsea turbine generators, four subsea power cables to connect the turbines to land-based infrastructure, an onshore substation and power lines connected to the Nova Scotia Power transmission system, and a Visitor Centre that is free and open to the public from May to November annually. These onshore facilities are located approximately 10 km west of Parrsboro, Nova Scotia.

The marine portion of the project is located in a 1.6 km x 1.0 km Crown Lease Area in the Minas Passage. It is also identified as a Marine Renewable-electricity Area under the Province's Marine Renewable-energy Act. This area consists of five subsea berths that are leased to tidal energy companies¹ selected by the Nova Scotia Department of Energy and Mines. Current berth holders at FORCE are:

Berth A: Minas Tidal Limited Partnership
Berth B: Sustainable Marine Energy (Canada)²
Berth C: Rio Fundo Operations Canada Limited³
Berth D: Unassigned (formerly Cape Sharp Tidal Venture)⁴
Berth E: Halagonia Tidal Energy Limited⁵

¹ Further information about each company may be found at: www.fundyforce.ca/technology

² On May 15, 2019 the Department of Energy and Mines issued an approval for Black Rock Tidal Power to change its name to Sustainable Marine Energy (Canada) Ltd. with the transfer of assets from SCHOTTEL to Sustainable Marine Energy. Learn more: sustainablemarine.com/news/schottel

³ On April 30, 2019 the Department of Energy and Mines approved the transfer of the Project Agreement and FIT approvals from Atlantis Operations (Canada) Ltd. to Rio Fundo Operations Canada Ltd.

⁴ On April 1, 2019 the Department of Energy and Mines revoked Cape Sharp Tidal's Marine Renewable Electricity License thereby triggering a default of the company's berth holder status at FORCE.

⁵ Berth E does not have a subsea electrical cable provided to it.

Research, monitoring, and associated reporting is central to FORCE's steward role, to assess whether tidal stream energy devices can operate in the Minas Passage without causing significant adverse effects on the environment, electricity rates, and other users of the Bay.

As part of this mandate FORCE has a role to play in supporting informed, evidence-based decisions by regulators, industry, the scientific community, and the public. As deployments of different technologies are expected to be phased in over the next several years, FORCE and regulators will have the opportunity to learn and adapt environmental monitoring approaches as lessons are learned.

Background

The FORCE demonstration project received its environmental assessment (EA) approval on September 15, 2009 from the Nova Scotia Minister of Environment. The conditions of its EA approval⁶ provide for comprehensive, ongoing, and adaptive environmental management. The EA approval has been amended since it was issued to accommodate changes in technologies and inclusion of more berths to facilitate provincial demonstration goals.

In accordance with this EA approval, FORCE has been conducting an Environmental Effects Monitoring Program to better understand the natural environment of the Minas Passage and the potential effects of turbines as related to fish, seabirds, marine mammals, lobster, marine sound, benthic habitat, and other environmental variables. All reports on site monitoring are available online at: www.fundyforce.ca/document-collection.

Since 2009, more than 100 related research studies have been completed or are underway with funding from FORCE, the Offshore Energy Research Association and others. These studies have considered socioeconomics, biological, and other research areas.⁷

Monitoring at the FORCE site is currently focused on lobster, fish, marine mammals, seabirds, and marine sound and is divided into 'near-field' (≤ 100 m from a turbine) and 'mid-field' or 'site-level' (> 100 m from a turbine) monitoring. As approved by regulators, individual berth holders are responsible for leading near-field monitoring in direct vicinity of their turbine(s), in recognition of the unique design and operational requirements of different turbine technologies. FORCE completes 'mid-field' monitoring activities as well as supporting integration of data analysis between these monitoring zones, where applicable.

All near-field and mid-field monitoring programs are reviewed by FORCE's Environmental Monitoring Advisory Committee, which includes representatives from scientific, First Nations, and local fishing communities.⁸ These programs are also reviewed by federal and provincial regulators prior to turbine installation. In addition, FORCE and berth holders also submit an Environmental Management Plan (EMP) to regulators for review prior to turbine installation. EMP's include: environmental management roles and responsibilities and commitments, environmental protection plans, maintenance and inspection requirements, training and education requirements, reporting protocols, and more.

⁶ FORCE's Environmental Assessment Registration Document and conditions of approval are found online at: www.fundyforce.ca/environment/enviromental-assesment.

⁷ OERA's Tidal Energy Research Portal (<http://tidalportal.oera.ca/>) includes studies pertaining to infrastructure, marine life, seabed characteristics, socio-economics and traditional use, technology, and site characterization.

⁸ Information about EMAC may be found online at: www.fundyforce.ca/about/advisory-committees

Turbine Deployments

Since FORCE's establishment in 2009, turbines have been installed at the FORCE site three times: once in 2009/2010, November 2016 – June 2017, and July 2018 – present. Given the limited timescales in which a tidal turbine has been present and operating at the FORCE site, environmental studies to-date have largely focused on the collection of baseline data and developing an understanding of the capabilities of monitoring devices in high flow tidal environments.

On July 22, 2018, CSTV installed a two-megawatt OpenHydro turbine at Berth D of the FORCE site and successfully connected the subsea cable to the turbine. CSTV confirmed establishment of communication with the turbine systems two days later on July 24. On July 26, 2018, Naval Energies unexpectedly filed a petition with the High Court of Ireland for the liquidation of OpenHydro Group Limited and OpenHydro Technologies Limited.⁹ For safety purposes, the turbine was isolated from the power grid on July 26. On September 4, 2018, work began to re-energize the turbine. In the days following, it was confirmed that the turbine's rotor was not turning. It is believed that an internal component failure in the generator caused sufficient damage to the rotor to prevent its operation. Environmental sensors located on the turbine and subsea base continued to function at that time with the exception of one hydrophone.

As a result of the status of the turbine, the monitoring requirements and reporting timelines set out in CSTV's environmental effects monitoring program were subsequently modified under CSTV's Authorization from Fisheries and Oceans Canada. The modification requires that CSTV provide written confirmation to regulators on a monthly basis that the turbine is not spinning by monitoring its status during the peak tidal flow of each month. This began October 1, 2018 and was expected to continue until the removal of the turbine; however, as a result of the insolvency of OpenHydro Technology Ltd., all near-field reporting activities by CSTV ceased as of March 1, 2019. Since that time, FORCE has provided monthly reports to regulators confirming the continued non-operational status of the CSTV turbine. An update prepared by CSTV is included in Appendix I of this report.

Additional turbines are expected to be deployed at the FORCE site in the coming years. In 2018, Sustainable Marine Energy (formerly Black Rock Tidal Power) installed a PLAT-I system in Grand Passage, Nova Scotia under a Demonstration Permit.¹⁰ This permit allows for a demonstration of the 280 kW system to help SME and its partners learn about how the device operates in the marine environment of the Bay of Fundy. Also in 2018, Natural Resources Canada announced a \$29.8 million contribution to Halagonia Tidal Energy's project at the FORCE site through its Emerging Renewable Power Program.¹¹ The project consists of submerged turbines for a total of nine megawatts—enough capacity to provide electricity to an estimated 2,500 homes.

Each berth holder project will be required to develop a turbine-specific monitoring program, which will be reviewed by FORCE's EMAC and federal and provincial regulators including Fisheries and Oceans Canada, the Nova Scotia Department of Environment, and the Nova Scotia Department of Energy and Mines prior to turbine installation.

⁹ See original news report: <https://www.irishexaminer.com/breakingnews/business/renewable-energy-firms-with-more-than-100-employees-to-be-wound-up-857995.html>.

¹⁰ To learn more about this project, see: <https://novascotia.ca/news/release/?id=20180919002>.

¹¹ To learn more about this announcement, see: <https://www.canada.ca/en/natural-resources-canada/news/2018/09/minister-sohi-announces-major-investment-in-renewable-tidal-energy-that-will-power-2500-homes-in-nova-scotia.html>.

International Experience & Cooperation

The research and monitoring being conducted at the FORCE test site is part of an international effort to evaluate the risks tidal energy poses to marine life (Copping et al., 2016). Presently, countries such as China, France, Italy, the Netherlands, South Korea, the United Kingdom, and the United States (Marine Renewables Canada, 2018) are exploring tidal energy, supporting environmental monitoring and innovative R&D projects. Tidal energy and other marine renewable energy technologies such as tidal range, tidal current, wave, and ocean thermal energy offer significant opportunities to replace carbon fuel sources in a meaningful and permanent manner. Some estimates place MRE's potential as exceeding current human energy needs (Gattuso et al., 2018; Lewis et al., 2011). Recent research includes assessments of operational sounds on marine fauna (Lossent et al., 2017; Schramm et al. 2017; Polagye et al. 2018; Pine et al. 2019), the utility of PAM sensors for monitoring marine mammal interactions with turbines (Malinka et al., 2018) and collision risk (Joy et al. 2018), and the influence of tidal turbines on fish behavior (Fraser et al. 2018).

Through connections to groups supporting tidal energy demonstration and R&D, FORCE is working to inform the global body of knowledge pertaining to environmental effects associated with tidal power projects. This includes participation in the Fundy Energy Research Network,¹² the Bay of Fundy Ecosystem Partnership,¹³ TC114,¹⁴ and the Atlantic Canadian-based Ocean Supercluster.¹⁵

Another key group is OES Environmental (formerly Annex IV); a forum to explore the present state of environmental effects monitoring around MRE devices.¹⁶ Last year FORCE worked with OES Environmental members¹⁷ to discuss best management practices regarding data transferability, “using data from an already permitted/consented MRE project or analogous industry to be ‘transferred’ to inform potential environmental effects and consenting for a future MRE project” (Copping et al., 2018, p. 4), and collection consistency—that is, transferring practices and learnings across jurisdictions and project sites. FORCE will continue to work closely with OES Environmental and its members to document and improve the state of knowledge pertaining to MRE devices’ interactions with the marine environment.

As part of this effort, Dr. Daniel Hasselman, FORCE’s science director, attended a one-day workshop in Edinburgh, Scotland led by OES Environmental and the Offshore Renewables Joint Industry Programme (ORJIP)¹⁸ to discuss collision risks associated with MRE devices. The purpose of the workshop was to overview pre-existing data in an effort to understand the risk profile of fish and marine mammal collision – that is, to determine the relative probability of a

¹² FERN is a research network designed to “coordinate and foster research collaborations, capacity building and information exchange” (Source: fern.acadiau.ca/about.html). FORCE participates in the Natural Sciences, Engineering, and Socio-Economic Subcommittees of FERN.

¹³ BoFEP is a ‘virtual institute’ interested in the well-being of the Bay of Fundy. To learn more, see www.bofep.org.

¹⁴ TC114 is the Canadian Subcommittee created by the International Electrotechnical Commission (IEC) to prepare international standards for marine energy conversion systems. Learn more: tc114.oreg.ca.

¹⁵ The OSC was established with a mandate to “better leverage science and technology in Canada’s ocean sectors and to build a digitally-powered, knowledge-based ocean economy.” Learn more: www.oceansupercluster.ca.

¹⁶ Annex IV was established by the International Energy Agency (IEA) Ocean Energy Systems (OES) in January 2010 to examine environmental effects of marine renewable energy development. Further information is available at <https://tethys.pnnl.gov>.

¹⁷ Member nations of OES Environmental are: Australia, China, Canada, Denmark, France, India, Ireland, Japan, Norway, Portugal, South Africa, Spain, Sweden, United Kingdom, and United States.

¹⁸ ORJIP has a mandate to bring together industry, regulators, academia, and others to work on key environmental and consenting issues in the offshore wind and ocean energy sectors. To learn more, visit: www.orjip.org.uk.

collision with a turbine and the relative consequence of the collision, should it occur. The workshop included a series of presentations from key groups working to understand turbine-animal interactions and included an overview of various integrated sensor platforms used in monitoring. Break-out groups convened for the afternoon in an effort to develop detailed project plans for strategic research projects relevant to collision risk.

Overall, the risks associated with single device or small array projects are anticipated to be low given the relative size/scale of devices (Copping, 2018). For example, at the FORCE site a single two-megawatt OpenHydro turbine occupies $\sim 1/1,000^{\text{th}}$ of the cross-sectional area in the Minas Passage (Figure 1). A full evaluation of the risks of tidal stream energy devices, however, will not be possible until more are tested over a longer-term period with monitoring that documents local impacts, considers far-field and cumulative effects, and adds to the growing global knowledge base.

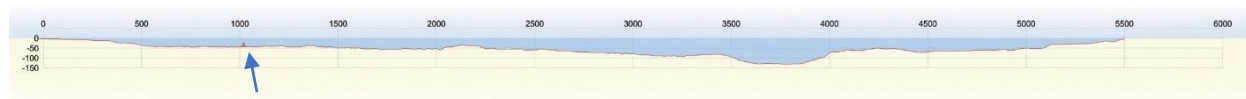


Figure 1: The scale of a single turbine (based on the dimensions of the OpenHydro turbine deployed by CSTV, indicated by the red dot and above the blue arrow) in relation to the cross-sectional area of the Minas Passage. The Passage reaches a width of ~ 5.4 km and a depth of 130 m.

The global understanding of the potential impacts of MRE devices is presently based on a few deployments—often of single devices and increasing numbers of small arrays, notably the MeyGen project in Pentland Firth, Scotland¹⁹ and a project led by Nova Innovation in Bluemull Sound, Scotland.²⁰ To gain understanding of the environmental monitoring conducted for projects in the United Kingdom and insight into operational limitation of sensors used, staff from FORCE (Dr. Hasselman and two ocean technologists, Tyler Boucher and Ray Pieroway) visited Scotland in early February. FORCE met with staff and graduate students at Marine Scotland Science (MSS), the University of Aberdeen (UoA), and the University of Highlands and Islands-Environmental Research Unit (UHI-ERI). Each group provided overview presentations of monitoring activities and there was discussion about the common challenge of monitoring in high flow environments. While the regulatory environment may differ in the UK versus Canada, it's important to acknowledge that researchers in the UK are still working towards developing monitoring techniques that are suitable for turbine-animal interactions. A major take away from this trip was the difference in access to infrastructure and human resources and how that has influenced monitoring capabilities and the advancement of our understanding of how to monitor environmental effects. Marine Scotland Science has access to two research vessels, the 'Alba na Mara' and the 'Scotia', that can house multiple scientists and stay at sea for extended periods of time for monitoring. Similarly, UoA and UHI-ERI have access to a cadre of graduate students who have each dedicated 4-6 years of effort towards addressing monitoring challenges for the MRE sector. Overcoming the monitoring challenges at FORCE requires a similar level of dedication and access to resources.

Dr. Hasselman attended a workshop entitled 'Retiring Risks of Effects on Marine Animals from Electromagnetic Field (EMF) and Underwater Noise from Marine Energy Devices' hosted by OES Environmental and ORJIP at the recent European Wave and Tidal Energy Conference

¹⁹ To learn more about this project, visit <https://simecatlantis.com/projects/meygen>.

²⁰ To learn more about this project, visit <https://www.novainnovation.com/bluemull-sound>.

(EWTEC) in Naples, Italy. The purpose of the workshop was to review the current state of knowledge about EMF and acoustics near MRE devices to determine whether enough information had been accumulated through research projects to retire the risk posed by EMF and MRE generated noise (from a single MRE device) to marine animals. The workshop was well attended by a host of international participants representing academia, industry, government, and NGOs, and included world experts in EMF (Dr. Andrew Gill) and marine acoustics (Dr. Brian Polagye). Break-out sessions were held and included an exercise where participants considered the information available for EMF and acoustics from a regulatory perspective and addressed whether enough data existed to retire the risks for consenting on single MRE devices. Although consenting on individual projects is context-specific, the break-out sessions largely revealed that enough data had been accumulated from EMF and acoustics research around MRE devices to justify retiring these risks for consenting on future single MRE devices.

On May 23, 2019, Dr. Hasselman co-chaired a round-table discussion by a panel of international subject matter experts on the use of active acoustics for monitoring in high flow environments. This panel was hosted at the Center for Ocean Ventures and Entrepreneurship (COVE) and the report is provided herein as Appendix VIII. The panel discussed the challenges presented by turbulence and entrained air that are common in high flow environments to monitoring using active acoustic devices. Specifically, entrained air and sediment in the water column generate a substantial amount of backscatter ‘noise’ for active acoustic devices, and the primary challenge lies in separating the signal generated by biological targets from the noise in these conditions. The group sought to address whether the challenge is a limitation of current active acoustic technologies that have not been optimized for high flow environments, or if these limits are imposed by the physics of the environment itself. The discussion generated multiple suggestions including increasing the frequency of the active acoustic devices to decrease the volume of backscatter noise or decreasing the frequency to reduce the amount of backscatter from entrained air. Ultimately, the panel reached consensus that while we are not at the limit of technology, commercially available technology might not be particularly well suited for monitoring in high flow environments.

To increase FORCE’s international cooperation efforts even further, Dr. Dan Hasselman is also leading a team of international researchers to draft the chapter on ‘Environmental Monitoring Approaches and Technologies’ for the OES Environmental 2020 State of the Science Report. The objectives of the chapter are to describe i) the state of development of environmental monitoring for tidal stream energy devices and wave energy converters, ii) the outcomes that have been shown, and iii) a process for applying consistent monitoring practices. To that end, the chapter overviews the importance of environmental monitoring to support permitting, key monitoring questions, the state of the science in environmental monitoring/methodologies, lessons learned from monitoring activities, and provides recommendations for quality data collection, management and analysis.

Mid-Field Monitoring Activities

FORCE has been leading ‘mid-field area’ or ‘site-level’ monitoring for a number of years, focusing on a variety of environmental variables. FORCE’s present environmental effects monitoring program, introduced in May 2016, was developed in consultation with SLR Consulting (Canada);²¹ strengthened by review and contributions by national and international experts and scientists, DFO, NSE, and FORCE’s EMAC; and has been adjusted based on experience and lessons learned, in keeping with the adaptive management approach—the

²¹ This document is available online at: www.fundyforce.ca/environment/monitoring.

process of monitoring, evaluating and learning, and adapting (AECOM, 2009) that has been used at the FORCE site since its establishment in 2009.²²

FORCE's EEMP currently focuses on the impacts of operational turbines on lobster, fish, marine mammals, and seabirds as well as the impact of turbine-produced sound. Overall, these research and monitoring efforts, detailed below, were designed to test the predictions made in the FORCE EA. Since the latest EEMP was initiated in 2016, FORCE has completed approximately:

- 408 hours of hydroacoustic fish surveys;
- more than 3,780 'C-POD' (marine mammal monitoring) days;
- bi-weekly shoreline observations;
- 49 observational seabird surveys;
- four drifting marine sound surveys and additional bottom-mounted instrument sound data collection; and
- 11 days of lobster surveys.

The following pages provide a summary of the mid-field monitoring activities conducted at the FORCE site so far in 2019 (January 1 – September 30), including data collection, data analyses performed, initial results, and lessons learned building activities and analyses from previous years. Where applicable this report also presents analyses that have integrated data collected through the near-field and mid-field monitoring programs in an effort to provide a more complete understanding of turbine-marine life interactions.

This year represents a pivotal period in the continued adaptation of FORCE's EEMP. If the CSTV turbine is non-operational and its rotor is not spinning, its full range of environmental effects cannot be fully assessed. Further, some monitoring during this time may not contribute to enhancing baseline data as a non-functional turbine could serve as an artificial reef to which some marine animals might be attracted to seek shelter in and around (Langhamer et al., 2009; Wilson and Elliott, 2009; Andersson and Öhman, 2010; Langhammer, 2012) thereby influencing the data collected. In consequence FORCE will use this period of time to continue to evaluate the utility of environmental sensors and protocols for environmental monitoring in high-flow sites. Building on advice from regulators and FORCE's EMAC, FORCE will focus its efforts in 2019 on evaluating monitoring instrumentation capabilities, data synthesis and integration activities, and mid-field monitoring (elaborated below), where appropriate.

Monitoring Objectives

The overarching purpose of environmental monitoring is to test the accuracy of the environmental effect predictions made in the original EA. These predictions were generated through an evaluation of existing physical, biological, and socioeconomic conditions of the study area, and an assessment of the risks the tidal energy demonstration project poses to components of the ecosystem.

A comprehensive understanding of turbine-marine life interactions will not be possible until turbine-specific and site-level monitoring efforts are integrated and additional data is collected in relation to operating turbines. Further, multi-year data collection will be required to consider

²² The adaptive management approach is necessary due to the unknowns and difficulties inherent with gathering data in tidal environments such as the Minas Passage and allows for adjustments and constant improvements to be made as knowledge about the system and environmental interactions become known. This approach has been accepted by scientists and regulators.

seasonal variability at the FORCE test site and appropriate statistical analyses of this data will help to obtain a more complete understanding of marine life-turbine interactions.

Table 1 outlines the objectives of the respective mid-field monitoring activities conducted at the FORCE demonstration site. Further information about near-field monitoring is included in this report and detailed information is provided by CSTV in Appendix I. Appendices and Near-field Monitoring Summary sections will be updated as additional turbines are scheduled for demonstration at the FORCE demonstration site.

At this time, and considering the scale of turbine deployments in the near-term at FORCE, it is unlikely that significant effects in the far-field will be measurable (SLR, 2015). Far-field studies such as sediment dynamics will be deferred until such time they are required. As more devices are scheduled for deployment at the FORCE site and as monitoring techniques are improved, monitoring protocols will be revised in keeping with the adaptive management approach. These studies will be developed in consultation with FORCE's EMAC, regulators, and key stakeholders.

Table 1: The objectives of each of the 'mid-field' environmental effects monitoring activity, which consider various Valued Ecosystem Components (VECs), led by FORCE.

<i>Mid-Field Environmental Effects Monitoring VEC</i>	<i>Objectives</i>
Lobster	<ul style="list-style-type: none"> to determine if the presence of a tidal stream energy turbine affects commercial lobster catches
Fish	<ul style="list-style-type: none"> to test for indirect effects of tidal stream energy turbines on water column fish density and fish vertical distribution to estimate probability of fish encountering a device based on fish density proportions in the water column relative to turbine depth in the water column
Marine Mammals	<ul style="list-style-type: none"> to determine if there is permanent avoidance of the mid-field study area during turbine operations to determine if there is a change in the distribution of a portion of the population across the mid-field study area
Marine Sound (Acoustics)	<ul style="list-style-type: none"> to conduct ambient sound measurements to characterize the soundscape prior to and following deployment of the in-stream turbines
Seabirds	<ul style="list-style-type: none"> to understand the occurrence and movement of bird species in the vicinity of tidal stream energy turbines to confirm FORCE's Environmental Assessment predictions relating to the avoidance and/or attraction of birds to tidal stream energy turbines

Lobster

In fall 2017, FORCE conducted a baseline lobster catchability survey (NEXUS Coastal Resource Management Ltd., 2017). The survey design consists of the deployment of commercial lobster traps at varying distances from an operating turbine or, as the case was in 2017, the location for a turbine. The catch-and-release survey was completed by NEXUS Coastal Resource Management Ltd (Halifax, NS) over 11 days in fall 2017. Lobsters were retrieved from traps and measured (carapace length), sex and reproductive stage were determined (male, female, and berried female), and shell condition evaluated.

Overall, the 2016 survey noted high catchability rates ($> 2.7 \text{ kg/trap}$)²³ and measured 351 lobsters. Preliminary qualitative analysis by NEXUS indicates that catch rates declined during the survey period, likely due to increasing tidal velocities during the progression of the study – there was a statistically significant negative relationship between catch rates and maximum tidal range, indicating lower catch rates during higher flows. Catch rates, further, did not increase significantly with depth, and qualitative analyses suggested no significant difference in catch rates across different locations from the turbine location. These initial results may indicate the impact of turbines may be higher on lobster catchability than anticipated in the EA (AECOM, 2009); however, data collection in the presence of an operational turbine is needed to compare to the 2017 survey dataset and to verify the EA predictions.

FORCE and NEXUS had planned to conduct a second lobster catchability survey in fall 2018 to complete a comparative analysis with the baseline data from 2017. The intent of the comparative study is to determine if the presence of a tidal stream energy turbine affects commercial lobster catches within the Minas Passage. Specifically, this study – with pre-installation and operating turbine data collection periods – is designed to test the EA prediction that tidal stream turbines will have minimal impacts on lobster populations within the FORCE test site (AECOM, 2009).

This plan, however, was contingent on the presence of an operational turbine in order to assess the impacts a turbine might have on lobster in the Minas Passage. Given the non-operational status of the CSTV turbine, the objectives of the 2018 survey effort could not be achieved, and the survey has been postponed until such time as an operational turbine is present at the site. In the interim FORCE is continuing to examine alternative lobster monitoring methods, including non-catchability studies, in the Minas Passage.

Fish

FORCE and its partner the University of Maine (Orono, Maine) have been conducting mobile fish surveys since May 2016 to:

- test for indirect effects of tidal stream energy turbines on water column fish density and fish vertical distribution; and
- estimate the probability of fish encountering a device based on any ‘co-occurrence’ relative to turbine depth in the water column.

These goals were laid out to test the EA prediction that tidal stream turbines are unlikely to cause substantial impacts to fishes at the test site (AECOM, 2009). These surveys are designed to permit a comparison of data collected before a turbine is installed with data collected while a turbine is operational at the FORCE site as well as in relation to a reference site along the south side of the Minas Passage – the nature of this design is referred to as ‘BACI’: Before/After, Control/Impact.

The surveys occur over a 24-hour period to include two tidal cycles and day/night periods using a scientific grade echosounder, a Simrad EK80, mounted onto a vessel, the Nova Endeavor (Huntley's Sub-Aqua Construction, Wolfville, NS). This instrument is an active acoustic monitoring device as it uses sonar technology to detect fish by recording reflections of a fish's swim bladder. In January 2019, FORCE staff underwent additional training on the EK80 from Kongsberg Maritime Canada Ltd. (Dartmouth, NS) to learn about the software through an

²³ This is classified as ‘high’ according to DFO's Catch Per Unit Effort (CPUE) index (Serdynska and Coffen-Smout, 2017).

operational review detailing the features and new updates for the EK60, EK80 and WBAT instruments. The training highlighted ways to optimize data collection and options available for real-time trouble shooting. Throughout the course attendees presented their user experience to Kongsberg staff as well. These lessons will be an asset for future fish surveys to know the limits of the equipment and to ensure quality data is collected.

Analyses of hydroacoustic fish surveys completed during baseline studies in 2011 and 2012 (Melvin and Cochrane, 2014) and surveys May 2016 – August 2017 (Daroux and Zydlewski, 2017) have observed similar fish densities at the FORCE test site and the reference site, including similar patterns of seasonal change. These analyses also evaluated changes in fish densities in association with diel stage (day/night), tidal stage (ebb/flood), and turbine presence or absence. During the evaluated periods an OpenHydro turbine was present November 2016 – June 2017. Results to-date support the EA prediction that tidal stream devices have minimal impact on marine fishes, however further data in relation to an operating turbine is required to fully test this prediction. FORCE is continuing to process and will analyze datasets from surveys conducted in late 2017 and throughout 2018 which will help to contribute to the growing body of knowledge of fish species at the FORCE site.

The University of Maine has recently completed a thorough analysis and report for 15 hydroacoustic fish surveys conducted at FORCE from 2011-2017 (Appendix IV). The hydroacoustic data set included six ‘historical’ surveys conducted between August 2011-May 2012, and nine ‘contemporary’ surveys conducted between May 2016 and August 2017. The report provides an overall approach for understanding the information contained within the hydroacoustic data sets, including data visualization and statistical analyses. Moreover, the University of Maine has provided FORCE with the data scripts/coding and hands-on training required for analysis and data visualization so that deeper explorations of the data may be undertaken to investigate questions that are specific to the needs of FORCE. The analyses included comparisons of fish presence/absence and relative fish density with respect to a series of temporal (historical vs. contemporary, or by survey), spatial (CLA vs. reference study area, or by transect) and environmental (tide phase, diel state, or with and against predicted tidal flow) explanatory variables. The report identified a statistically significant difference in fish presence/absence and relative fish density between the historical and contemporary data sets that may be attributable to differences in the survey design/execution between the time periods or could reflect changes in fish usage of the site. Considering this result, remaining analyses were restricted to the contemporary data sets alone. The authors identified a statistically significant difference in fish presence/absence and relative density between the CLA and the reference site suggesting that the reference site may not be sufficiently representative to serve as a reference for the CLA. Other key findings include: i) data collection during the ebb tide and during the night are both important factors for understanding fish presence in the CLA, ii) a variety of explanatory variables and their additive effects should be explored further, iii) increasing the frequency of surveys within each month (perhaps on consecutive days), particularly during May, may be required to understand patterns and variability of fish presence and density in Minas Passage, and iv) results suggest modifying the survey design to exclude adjacent pairings of transects.

It is important to note, however, that like the lobster survey program, the fish monitoring program requires the presence of an operational turbine at the FORCE site in 2018 for testing its effects. Further, a non-operational turbine may bias baseline data collection as the turbine may serve as a Fish Aggregation Device (i.e., a ‘FAD’) (Wilhelmsson et al. 2006). FORCE was planning to conduct fish surveys during known periods of peak migration in 2019 – notably, in spring to capture migration periods of alewife, Atlantic herring, striped bass, Atlantic sturgeon,

American shad, Atlantic mackerel, and rainbow smelt (Baker et al., 2014; Stokesbury et al., 2016) and also in late fall in consideration of outward migration of Atlantic herring, blueback herring, and alewife (Townsend et al., 1989). These data collection efforts were contingent on operational status of the turbine and suitable weather conditions. Given that the CSTV turbine currently remains at the FORCE site, spring surveys were not conducted.

In the interim, FORCE in cooperation with Echoview Software (Tasmania, Australia) and the University of Maine, has been focusing efforts on data processing and analysis of fish survey data as well as in support of a comparative analysis with data collected from a bottom-mounted system (see 'Platform Projects' below). FORCE staff (Research Scientist Jeremy Locke and Ocean Technologists Jessica Douglas and Tyler Boucher) completed the Echoview software training course in Q2 2019 to build the skillset of processing hydroacoustic data within Nova Scotia. This training enables the FORCE team to better complete data collection activities moving forward. Presently, FORCE staff are undertaking data processing to enable Echoview staff to complete data analysis and reporting and to improve the efficiency data processing.

Marine Mammals

In 2019, FORCE continues to conduct two main activities aimed at testing the EA prediction that project activities are not likely to cause significant adverse residual effects on marine mammals within the FORCE test site (AECOM, 2009). These activities have been ongoing on a regular basis since 2016. Specifically, FORCE is continuing to:

- conduct passive acoustic monitoring (PAM) using 'click recorders' known as C-PODs; and
- implement an observation program that includes shoreline, stationary, and vessel-based observations.

Passive Acoustic Monitoring

The first component of FORCE's marine mammal monitoring program involves the use of PAM mammal detectors known as C-PODs, which record the vocalizations of toothed whales, porpoises, and dolphins.²⁴ The program focuses mainly on harbour porpoise – the key marine mammal species in the Minas Passage that is known to have a small population that inhabits the inner Bay of Fundy (Gaskin, 1992). The goal of this program is to understand if there is a change in marine mammal presence in proximity to a deployed tidal stream energy device and builds upon baseline C-POD data collection within the Minas Passage since 2011.

From 2011 to early 2018, more than 4,695 'C-POD days'²⁵ of data were collected in the Minas Passage. Over the study period, it was found that harbour porpoise use and movement varies over long (i.e., seasonal peaks and lunar cycles) and short (i.e., nocturnal preference and tide stage) timescales. This analysis, completed by Sea Mammal Research Unit (Canada) (Vancouver, BC), showed some evidence to suggest marine mammal exclusion within the near-field of CSTV turbine when it was operational (November 2016 – June 2017) (Joy et al., 2018). This analysis showed that the C-PODs in closest proximity to the turbine (230 m and 210 m distance) had shown decreases in detections whereas there is no evidence of mid-field avoidance with a turbine present and operating. The latest findings also showed a decrease in detections during turbine installation activities which is consistent with previous findings (Joy et

²⁴ The C-PODs, purchased from Chelonia Limited, are designed to passively detect marine mammal 'clicks' from toothed whales, dolphins, and porpoises.

²⁵ A 'C-POD day' refers to the number of total days each C-POD was deployed times the number of C-PODs deployed.

al., 2017), but will require additional data collected in relation to an operating turbine to allow for a full assessment of the EA predictions.

The C-PODs were deployed on December 6, 2018 and recovered on March 29, 2019. Following inspection and data-recovery, maintenance activities included replacement of CPOD batteries, replacement of acoustic release batteries, refurbishment of one SUBS package, and the fabrication and installment of mounts for the MetOcean Telematics (Dartmouth, NS) beacons. The C-PODs were subsequently re-deployed on May 3, 2019. The delay for the re-deployment was caused by the amount of maintenance required during that period as well as the vessel availability for the operation. The vessels normally used for this operation were both away on location for other jobs. It took a special weather window for a vessel to return to the area, and also have time for the deployment. This summer, the C-PODs were recovered on August 14th to download data, were re-deployed during the same day, and are currently collecting data.

In 2019 FORCE received an F-POD from Chelonia Limited (makers of the C-PODs; Cornwall, UK), which it deployed at the FORCE site. This instrument was included in FORCE's comparative PAM study outlined in its 2019 EEMP plan. This study aims to understand the relative performance of multiple PAM devices (i.e., C-POD, F-POD, SoundTrap, icListenHF, and AMAR) across the range of tidal flows experienced at the FORCE site. The first phase (i.e., Aquatron testing; Figure 2) was completed and confirmed that each device could detect synthetic click trains emitted by an icTalk used to mimic harbour porpoise vocalizations. FORCE subsequently deployed the devices on a FAST platform at the FORCE site to complete the field trial component of this study (Figure 3, 4). The field trials included playing the synthetic click trains with the icTalk while passively drifting over the FAST platform over the course of a full tidal cycle, followed by a week of data collection for harbour porpoise transiting the FORCE site. The platform was recovered on September 13th, and the data was downloaded from the instruments and sent to Sea Mammal Research Unit (Canada) for analyses. FORCE expects to receive a report on the relative performance of each PAM device by the end of 2019.

Harbor porpoise (Phocoena phocoena) monitoring at the FORCE Test Site, Canada featured on Tethys (by FORCE and SMRU): <https://tethys.pnnl.gov/tethys-stories/harbor-porpoise-phocoena-phocoena-monitoring-force-test-site-canada>

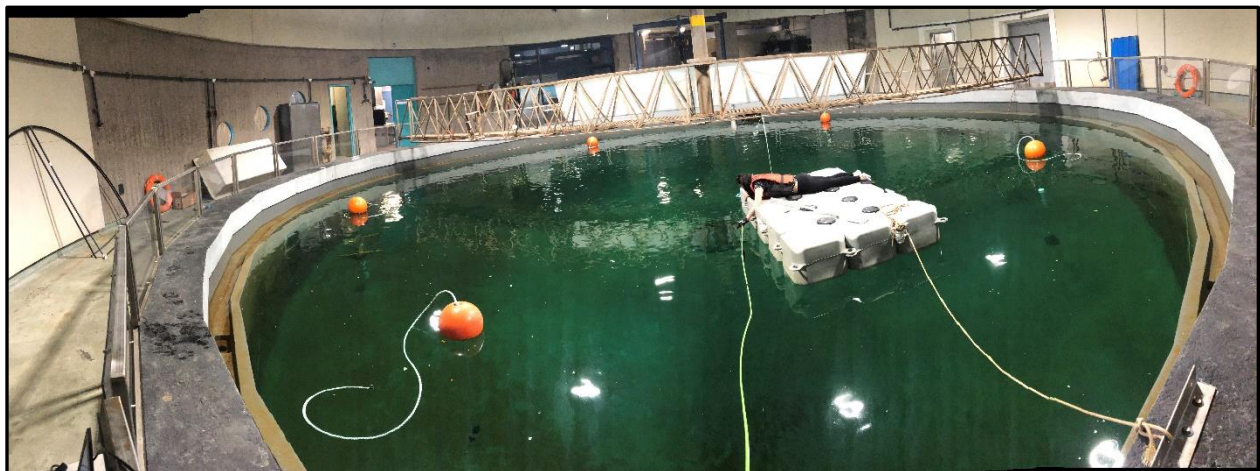


Figure 1: One of FORCE's Ocean Technicians assists with testing PAM devices in the Aquatron pool-tank facility at Dalhousie University.

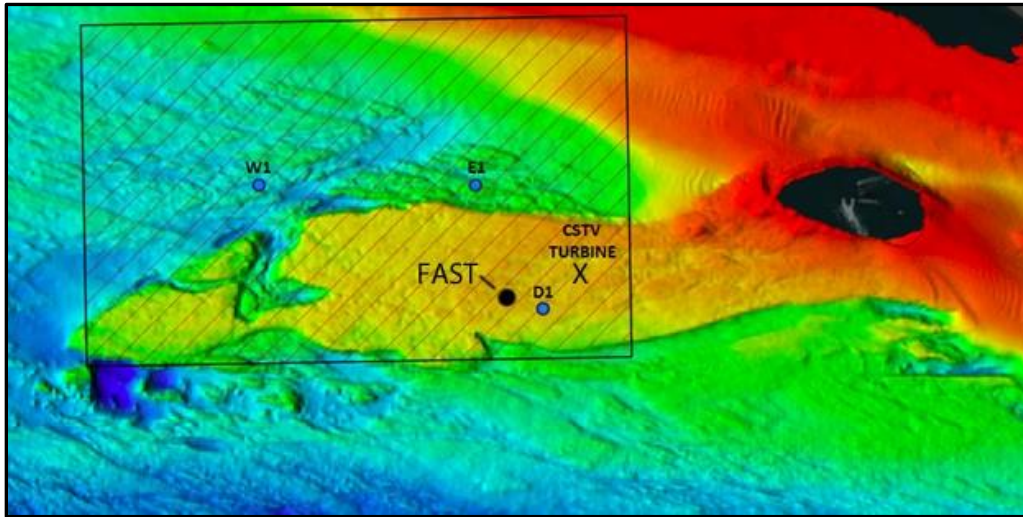


Figure 2: Map of FORCE test site showing approximate locations for C-PODs deployed on SUBS packages (W1, E1, D1), and the planned location for deployment of the FAST platform mounted with PAM devices (•). The location of the Cape Sharp Tidal Venture Tur

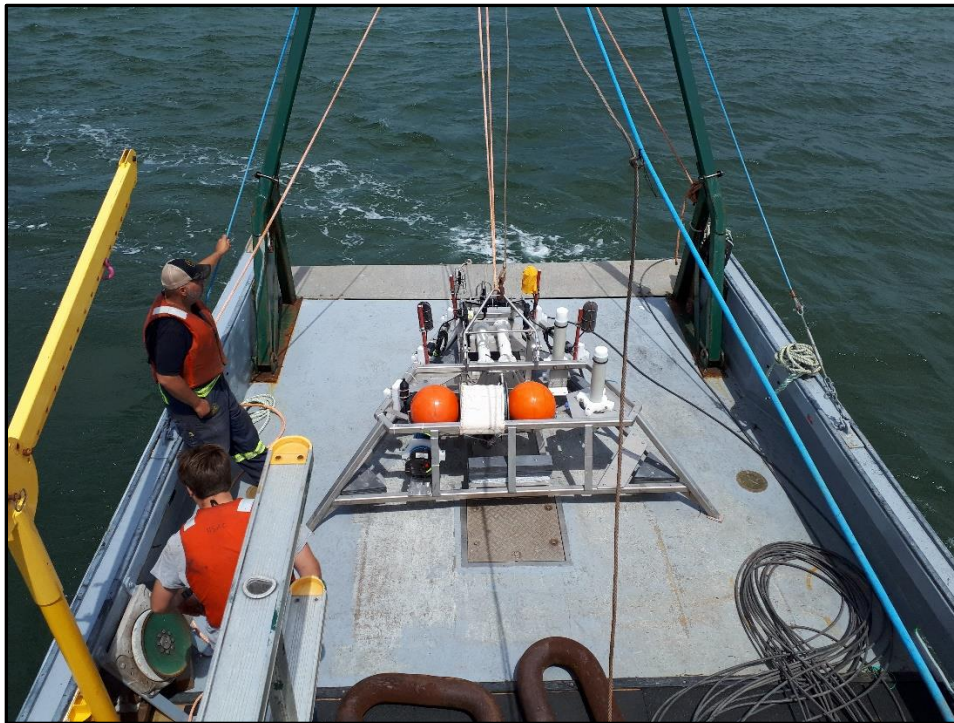


Figure 3: Five PAM devices were mounted on the FAST platform for the comparative PAM study. Photograph depicts the platform on the deck of the Nova Endeavour prior to deployment at the FORCE site.

Observation Program

FORCE's marine mammal observation program in 2019 includes observations made during bi-weekly shoreline surveys, stationary observations at the FORCE Visitor Centre, and marine-based observations during marine operations. All observations and sightings are recorded, along with weather data, tide state, and other environmental data. Any marine mammal observations are shared with SMRU Consulting to support validation efforts of PAM activities.

FORCE will also continue to explore the utility of using an Unmanned Aerial Vehicle (UAV) for collecting observational data along the shoreline and over the FORCE site using transects by programming GPS waypoints in the UAV to standardize the flight paths. In recent months a number of FORCE staff including Science Director Dan Hasselman, Facility Manager Sandra Currie, and Ocean Technologists Ray Pieroway, Tyler Boucher, Jessica Douglas, and Megan Elliott received training to operate a UAV. Recent changes to Transport Canada's regulations for Remotely Piloted Aircraft Systems (RPAS) necessitated FORCE staff acquiring UAV pilot certification by successfully passing the 2019 Canadian Drone Pilot Basic Operations Examination. Several trained staff have now acquired this certification and are licensed to safely operate a drone at the FORCE site. To assess the relative utility of a UAV-based versus walking-based observational survey, FORCE recently developed and conducted a study using a series of objects randomly distributed along the FORCE beach. This assessment revealed that the UAV performed as well as a walking-based observational survey, but requires less time and human resource to achieve. FORCE also hosts a public reporting tool that allows members of the public to report observations of marine life: mmo.fundyforce.ca

Marine Sound (Acoustics)

Marine sound – often referred to as 'acoustics' or 'noise' – monitoring efforts are designed to characterize the soundscape of the FORCE test site. Data collected from these monitoring efforts will be used to test the EA predictions that operational sounds produced from operating tidal stream turbines are unlikely to cause mortality, physical injury or hearing impairment to marine animals (AECOM, 2009).

FORCE convened a working group of experts in passive acoustic monitoring (PAM) data collection and analyses from local academic institutions, industry partners, and other stakeholders in late 2018. The purpose of the workshop was to discuss the challenges and operational limitations inherent with using PAM technologies for marine mammal and sound monitoring in high-flow environments like the FORCE test site and to identify potential solutions to improve environmental effects monitoring capabilities for operational tidal stream energy turbines in the future. The workshop sought to address questions from regulators regarding the integration or corroboration of results from multiple PAM technologies deployed in and around the FORCE test site. The workshop also explored potential future projects to support further environmental monitoring using PAM technologies with the end goal of lending confidence to environmental effects monitoring technologies and approaches used in support of tidal energy devices. A copy of the workshop report, including outcomes and identified next steps may be found in Appendix II.

Building on this workshop, FORCE recently commissioned JASCO Applied Sciences (Canada) Ltd. to conduct a comparative integrated analysis of acoustic data sets collected by various hydrophones (i.e., underwater sound recorders) mounted on and deployed autonomously around the CSTV turbine at the FORCE site (see Appendix IX). This integrated comparative analysis examined near-field sound data collected by hydrophones located:

- on the CSTV turbine, collecting data since September 4, 2018 (three icListen hydrophones);
- two icListen hydrophones mounted on a Fundy Advanced Sensor Technology (FAST) platform deployed approximately 35 m from the turbine from September 5 – 21, 2018;
- an AMAR (Autonomous Multichannel Acoustic Recorder) deployed approximately 100 m from the turbine from June 29 – November 19, 2018.

In addition, an acoustic Doppler current profiler mounted on the CSTV turbine has collected current data since September 4, 2018. Analyses of the acoustic data revealed that flow noise increased with the height of the hydrophone off the seabed and impacted the hydrophone mounted on the top of the CSTV turbine the most. The least affected hydrophones were those mounted at the 'aft' position on the CSTV turbine and the autonomously deployed AMAR. In fact, flow noise at these locations was low enough to successfully measure the sound from the turbine during the brief period prior to the malfunction of the turbine's rotor in August 2018. Indeed, when the turbine was present (and presumably free spinning prior to this malfunction), the sound levels increased in the 30-1000 Hz band. Details are contained in the report provided as Appendix IX. This comparative analysis provides valuable information about future marine sound monitoring technologies and protocols while building on previous acoustics analysis at the FORCE site.

Results from previous acoustic analyses completed at the FORCE site indicate that the turbine is audible to marine life at varying distances from the turbine, but only exceeded the threshold for behavioural disturbance at very short ranges and during particular tide conditions (Martin et al., 2018). This is consistent with findings at the Paimpol-Bréhat site in France where an OpenHydro turbine was also deployed – data suggests that physiological trauma associated with a tidal turbine is improbable, but that behavioural disturbance may occur within 400 m of a turbine for marine mammals and at closer distances for some fish species (Lossent et al., 2017).

Seabirds

FORCE's seabird monitoring program is designed to test the EA prediction that project activities are not likely to cause adverse residual effects on marine birds within the FORCE test area (AECOM, 2009). Over the last several years, FORCE and Envirosphere Consultants Ltd. (Windsor, NS) have collected observational data from the deck of the FORCE Visitor Centre, documenting bird species presence, behaviour, and seasonality throughout the FORCE site (Envirosphere Consultants, 2009, 2017; Stewart and Lavender, 2010; Stewart et al., 2011, 2012, 2013; Stewart et al., 2018). Overall, these surveys have documented the distribution, abundance, and seasonality of water-associated birds in the Minas Passage, but there has been limited opportunity to determine potential effects and test the EA predictions given the short time period with an operational turbine present at the FORCE site.

The non-operational turbine currently present at the FORCE site has the potential to serve as a FAD (Wilhelmsson et al., 2006). This could have potential cascading ecological effects for predatory diving seabirds (Wilson and Elliott, 2009; Boehlert and Gill, 2010), and therefore, have indirect consequences for seabird monitoring. Diving seabirds may be drawn to the FORCE site if the abundance of prey species increases as a consequence of the non-operational CSTV turbine (Wilhelmsson et al. 2006; Andersson and Öhman 2010; Boehlert and Gill 2010). Observational surveys under these circumstances contribute neither to effects testing nor to enhancing the seabird baseline. In consequence FORCE will not conduct observational seabird surveys in 2019 and will instead pursue a synthesis of existing baseline data and integration with radar to improve monitoring protocols for the future (see below).

FORCE has begun a collaboration with EnviroSphere and Dr. Phil Taylor at Acadia University (Wolfville, NS) to synthesize previous observation-based seabird baseline datasets (2017-2018) and to integrate this information with data from radar-based monitoring (Walker and Taylor, 2018). Radar based monitoring, based on an X-band radar located at the FORCE Visitor Centre has typically been used for flow characterization, but can be used to monitor bird movements throughout and around the FORCE test site. Similar to the observational studies, radar analysis shows a clear seasonal pattern of activity with very few birds present in the winter and peaks during spring and fall migrations (Walker and Taylor, 2018; Appendix III).

This integrated work will help to quantify the risk for seabirds in relation to operating tidal energy turbines at the FORCE site. This work will examine the potential of statistical models to improve the precision and certainty in detecting impacts to seabirds. This work will advance the ability to describe seabird abundance, species composition, spatial and temporal distribution, and seasonality.

Near-field Monitoring Activities

While FORCE completes site-level or ‘mid-field’ monitoring activities at the FORCE site, near-field monitoring is led by individual berth holders. Like the mid-field monitoring programs, the near-field monitoring plans and reports undergo review by FORCE’s EMAC and regulators.

In September 2018, it was confirmed that that CSTV turbine rotor was not spinning. Since that time, CSTV had been providing written confirmation to regulators on a monthly basis that the turbine is not spinning by monitoring its status during the peak tidal flow of each month. However, as a result of the insolvency of OpenHydro Technology Ltd., all reporting activities by CSTV ceased as of March 1, 2019. Data collection from the turbine-mounted ADCPs to confirm the turbine is no longer spinning is being managed and reported by FORCE to regulators on a monthly basis. Data is also still being collected from two of the four hydrophones on the CSTV turbine. An update prepared by CSTV is included in Appendix I of this report.

Throughout 2018 and into Q3 2019, FORCE has been taking steps to enhance its near-field monitoring capabilities. In 2018, FORCE deployed multiple Fundy Advanced Sensor Technology (FAST) platforms in proximity to the Cape Sharp Tidal turbine (within 15m – 35m from the turbine) containing hydrophones and ADCPs to measure turbine-produced sound and flow impacts of the turbine respectively. These measurements are being used to inform marine acoustics and also to better understand flow dynamics at the FORCE test site.

FORCE staff (Science Director Dan Hasselman and Ocean Technologists Ray Pieroway and Tyler Boucher) also underwent training in Q1 2019 to understand a near-field monitoring instrument, a Gemini imaging sonar. This training was led by the maker of the Gemini, Tritech International Ltd. (Aberdeen, Scotland) and included an overview of the instrument’s capabilities and limitations, best practices for use, and setting optimization for in-situ data recording. The training also incorporated the specialized software used to track marine life targets in the water column. This training will serve to be beneficial for use and testing of the Gemini at the FORCE test site.

As additional near-field, device-specific environmental effects monitoring programs are required and implemented for deployed tidal stream devices, berth holder updates will be included as appendices to this report.

Other FORCE Research Activities

The Pathway Program

The Pathway Program is a collaborative effort between FORCE and OERA to identify an effective and regulator approved monitoring solution for the tidal energy industry in Nova Scotia. The Pathway Program involves several phases, including i) Global capability Assessment, ii) Advancing Data Processing and Analytics, and iii) Technology Validation. The first phase of this program, a Global Capability Assessment, involves a comprehensive literature review about the use of different classes of environmental monitoring technologies (i.e., PAM, imaging sonars, echosounders) for monitoring tidal energy devices around the world. Subject matter experts were commissioned to provide reports on these instrument classes, and FORCE has now received final reports for each of these.

Dr. David Barclay (Oceanography Department, Dalhousie University) authored a report that provides an overview of PAM technologies, methodologies, and data processing techniques used to make passive acoustic measurements in tidal channels, with a focus on the tools and techniques used for marine mammal monitoring around tidal energy devices (Appendix V). Despite a growing body of underwater acoustics research related to assessing the environmental effects of tidal power development, there are no commercially available, purpose-built acoustic monitoring systems that have been designed specifically for operation in turbulent tidal channels. Nonetheless, experimental deployments of various PAM technologies have been attempted in high-flow conditions for marine mammal monitoring, with varying success. Dr. Barclay's review suggests that the ideal PAM system for marine mammal monitoring in high flow environments has the highest sensitivity, best mitigation of flow noise, and records the entire pressure time series. This would include technologies like the SoundTrap, icListenHF, and AMAR-G4 series of hydrophones.

Dr. James Joslin (Applied Physics Laboratory, University of Washington) authored a report on the use of imaging (multibeam) sonars for monitoring fish and marine mammals around tidal energy devices (Appendix VI). While there are currently more than a dozen commercially available imaging sonars that have been developed for use in high energy marine environments (each differing in functional range, resolution, field of view, and mechanical configuration), the typical application is for underwater vehicle navigation and situational awareness. Further, not all imaging sonars have been designed for long term deployments without regular maintenance, and most use cases do not require the sonar control software to be integrated on a multi-instrument platform with other active acoustics. Thus, many of the commercially available imaging sonars are not well suited for monitoring tidal energy devices and the best options are those that have been demonstrated on previous projects. This report demonstrates how imaging sonars have been used successfully on both bottom and surface mounted platforms to monitor fish, marine mammals and seabirds. Further, target classification from imaging sonars is best achieved by pairing the instrument with optical cameras or echosounders. Dr. Joslin's report recommends that the best imaging sonars for fish and marine mammal monitoring at the FORCE site are the Triton Gemini 720is and the Teledyne Blueview M900/2250.

Dr. John Horne (School of Aquatic and Fishery Sciences, University of Washington) provided a report on the features and performance of scientific echosounders for monitoring fish around tidal energy devices (Appendix VII). The report highlights the challenges of using active acoustic devices in high flow environments due to the presence of turbulence and entrained air, and identifies the need to maximize the signal to noise ratio for using echosounders effectively. The report provides the required background, necessary context and relevant information to understand acoustic theory and how it relates to the challenge of monitoring fish in high flow

environments using acoustic technology, and contains a suite of manufacturer instrument specification sheets that some readers may find valuable. The report also makes recommendations about which scientific echosounders are most suitable for monitoring in high flow environments based on whether they i) can be calibrated, ii) have been vetted by the scientific community, and iii) provide digital output. Based on these criteria, the report recommends using the Kongsberg-Simrad EK80 line of scientific echosounders. This includes instruments like the EK80, WBAT, WBT Mini, and WBT Tube; instruments that FORCE has been using for years in its fish monitoring efforts.

Fundy Advanced Sensor Technology (FAST) Activities

FORCE's Fundy Advanced Sensor Technology Program is designed to advance capabilities to monitor and characterize the FORCE site. Specifically, the FAST Program was designed to achieve the following objectives:

- 1) To advance capabilities of site characterization;
- 2) To develop and refine environmental monitoring standards and technologies; and
- 3) To enhance marine operating methodologies.

FAST combines both onshore and offshore monitoring assets. Onshore assets include a meteorological station, video cameras, an X-band radar system, and tide gauge. Offshore assets include modular subsea platforms for both autonomous and cabled data collection and a suite of instrumentation for a variety of research purposes. Real-time data collected through FAST assets is broadcasted live on the Ocean Networks Canada's (ONC; Victoria, BC) website.²⁶

The FORCE tide gauge began experiencing issues with data collection on April 9, 2019. The instrument was recovered for inspection, and it was determined that there was a leak in the data/power cable. The cable was replaced, re-terminated, and tested before re-deployment on June 6, 2019 (Figure 5).



Figure 4: One of FORCE's Ocean Technicians prepares the tide gauge for deployment.

Platform Projects

The first and largest of the FAST platforms houses an instrument called the Vectron. Developed in partnership with Nortek Scientific (Halifax, NS), Memorial University (St. John's, NL), and Dalhousie University (Halifax, NS), the Vectron is the world's first stand-alone instrument to remotely measure, in high resolution, turbulence in the mid-water column. Measurements and analysis from the Vectron will help tidal energy companies to better design devices, plan marine operations, and characterize the tidal energy resource.

A smaller platform called FAST-3 has been used for the last two years to monitor fish densities in the mid-field of the turbine. Data collection activities for this project was completed in 2018 and FORCE and its partners, including Echowiew Software, will conduct data processing and analysis in 2019. This project will integrate the data collected from the FAST-3 platform with

²⁶ This is available online at: www.oceannetworks.ca/observatories/atlantic/bay-fundy

data collected from a vessel-mounted hydroacoustic echosounder used as part of the mid-field fish monitoring activities previously referenced, to evaluate the temporal and spatial representativeness of each method and determine the degree to which results are corroborative (depicted in Figure 6). This project is funded by Natural Resources Canada (NRCan), the NSDEM, and the OERA.

Marine Operations

FORCE has partnered with Operational Excellence Consulting Inc. (Halifax, NS) to document lessons learned from various marine operations over the last few years. The report, *Lessons Learned: Marine Operations in the Minas Passage* (2019), documents operational constraints, information to address commonly-encountered situations, and learnings to-date in an effort to help support and de-risk future projects at the FORCE test site. This work was funded by the OERA.

FORCE and Operational Excellence webinar presentation: 'FORCE Site Marine Operations Lessoned Learned' (March 21st, 2019):
<http://www.oera.ca/oera-webinar-series-andrew-lowery-fundy-ocean-research-center-for-energy-force-jason-clarkson-operational-excellence-consulting/>

Fish Tracking

To enhance fish monitoring and to expand its data collection capacity, FORCE partnered with the Ocean Tracking Network (OTN)²⁷ and attached one VEMCO²⁸ fish tag receiver (a VR2 receiver) to each C-POD mooring/SUBS (Streamlined Underwater Buoyancy System) package (see above). These receivers are used to supplement OTN's ongoing data collection program within the Minas Passage and are referred to as 'Buoys of Opportunity.' Upon retrieval of the C-PODs and receivers, instruments are shared with OTN where data is offloaded prior to redeployment. This effort will support increased knowledge of fish movement within the Minas Passage, which has applicability beyond tidal energy demonstration, as well as complement FORCE's hydroacoustic data collection efforts that do not allow for species identification.

OTN data managers are in the process of acquiring information, including species identification, and sharing this with FORCE. Initial results show that the OTN receivers deployed by FORCE have detected tags from the following projects:

- Maritimes Region Atlantic salmon marine survival and migration (Hardie, D.C., 2017);
- Quebec MDDEFP Atlantic Sturgeon Tagging (Verreault, G., Dussureault, J., 2013);
- Gulf of Maine Sturgeon (Zydlewski, G., Wippelhauser, G. Sulikowski, J., Kieffer, M., Kinnison, M., 2006);
- OTN Canada Atlantic Sturgeon Tracking (Dadswell, M., Litvak, M., Stokesbury, M., Bradford, R., Karsten, R., Redden, A., Sheng, J., Smith, P.C., 2010);
- Darren Porter Bay of Fundy Weir Fishing (Porter, D., Whoriskey, F., 2017);

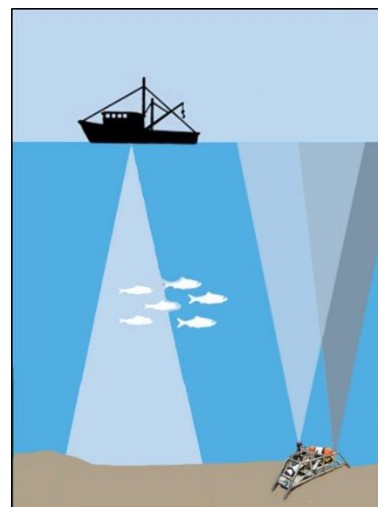


Figure 5: A representation of the data collection methods of the FORCE mid-field fish EEMP and the FAST-3 platform.

²⁷ Ocean Tracking Network's website: www.oceantrackingnetwork.org.

²⁸ VEMCO is "the world leader in the design and manufacture of acoustic telemetry equipment used by researchers worldwide to study behaviour and migration patterns of a wide variety of aquatic animals." Learn more: www.vemco.com.

- Movement patterns of American lobsters in the Minas Basin, Minas Passage, and Bay of Fundy Canada (2017);
- Shubenacadie River Monitoring Project: Tomcod (Marshall, J., Fleming, C., Hunt, A., and Beland, J., 2017);
- MA Marine Fisheries Shark Research Program (Skomal, G.B., Chisholm, J., 2009);
- UNB Atlantic Sturgeon and Striped Bass tracking (Curry, A., Linnansaari, T., Gautreau, M., 2010); and
- Inner Bay of Fundy Atlantic Salmon (Bradford, R., LeBlanc, P., 2012).

Further information about these Buoys of Opportunity, and the projects listed above, can be found on OTN's website: <https://members.oceantrack.org/project?ccode=BOOFORCE>

Starting in 2018, FORCE has worked in collaboration with Dr. Mike Stokesbury at Acadia University to install additional VEMCO receivers of a new design on FORCE's C-POD moorings/SUBS packages. These new receivers are expected to be even more effective in picking up acoustic detections in high flow environments, where tag signals can be obscured by noise. This partnership will contribute additional information regarding movement patterns of Atlantic salmon, sturgeon, striped bass, and alewife in Minas Passage and Basin. This work is sponsored by the OERA, NRCan, NSDEM, the Natural Sciences and Engineering Research Council of Canada (NSERC), and the Canadian Foundation for Innovation (CFI).²⁹

Wetlands Monitoring

In addition to marine monitoring, FORCE will also be completing onshore terrestrial monitoring in 2019. This work will be done to verify impact predictions made in relation to its work in the marsh wetlands along Black Rock Beach to install four electrical cables and a data cable.

This monitoring work has been ongoing since the installation of the cables in 2014. Completed by Envirosphere Consultants, this includes periodic walkovers by a biologist and a botany survey in the disturbed area, repeating baseline work done in 2014 and monitoring work completed in 2015, 2016 and in August 2019. To-date, this monitoring work has shown the wetland is well-vegetated and has largely recovered from the trenching operations associated with the cable installation. A report on the status of the recovery of the wetland is anticipated in fall 2019 and will be included in FORCE's 2019 annual report.

²⁹ Information about this project, and others funded through this program, is available online at: www.oera.ca/press-release-research-investments-in-nova-scotia-in-stream-tidal-technology-research/

Discussion

This year represents a strategic opportunity for FORCE and its partners to learn from previous experiences and to re-evaluate approaches to research and monitoring in the high flows of the Minas Passage.

Given the present status of the CSTV turbine, monitoring efforts have been curtailed to avoid biasing datasets. This is because a non-operational turbine has implications for monitoring – a turbine that is not spinning does not allow us to test its true environmental effects while also potentially acting as an artificial reef, and thereby biasing any attempts at capturing baseline data. At this time, FORCE is not aware of any timelines for turbine removal but will continue to monitor its non-operational status and use, where applicable, its sensors in a way to advance monitoring capabilities.

In 2019 FORCE and its partners plan to deliver a number of efforts that will improve monitoring capabilities – this will occur through continued learning from the experiences of local and international partners, local capacity and skills development, testing new sensor capabilities such as radar for seabird monitoring or testing new PAM devices like the F-POD, and integrating results from various instruments. Reports and updates will undergo review by FORCE's EMAC and regulators, along with continued results from FORCE's ongoing monitoring efforts. These efforts will provide an opportunity for adaptive management and further develop and refine the scientific approaches, tools, and techniques necessary in the near- and mid-field study areas to effectively monitor tidal stream energy devices in high-flow environments.

Ongoing monitoring efforts will continue to build on the present body of knowledge of marine life-turbine interactions. While it is still early to draw conclusions, initial findings internationally and at the FORCE test site have documented some disturbance of marine mammals primarily during marine operations associated with turbine installation/removal activities, but otherwise have not observed significant effects.

FORCE will continue to conduct environmental research and monitoring to increase our understanding of the natural conditions within the Minas Passage and, when the next turbine(s) are deployed and operating, test the EA prediction that tidal energy is unlikely to cause significant harm to marine life. In the longer-term, monitoring will need to be conducted over the full seasonal cycle and in association with multiple different turbine technologies in order to understand if tidal energy can be a safe and responsibly produced energy source. FORCE will continue to report on progress and release results and lessons learned in keeping with its mandate to inform decisions regarding future tidal energy projects.

References

- AECOM. (2009). *Environmental Assessment Registration Document – Fundy Tidal Energy Demonstration Project Volume I: Environmental Assessment*. Available at www.fundyforce.ca.
- Andersson, M.H., and Öhman, M.C. (2010). *Fish and sessile assemblages associated with wind-turbine constructions in the Baltic Sea*. Mar. Freshw. Res. 61(6): 642 – 650.
- Baker, M., Reed, M., and Redden, A. (2014). *Temporal Patterns in Minas Basin Intertidal Weir Fish Catches and Presence of Harbour Porpoise during April – August 2013*. Acadia Center for Estuarine Research, Wolfville, NS. Tech. Rep. 120.
- Boehlert, G., and Gill, A. 2010. *Environmental and Ecological Effects of Ocean Renewable Energy Development – A Current Synthesis*. Oceanography 23(2): 68–81.
- Copping, A., Sather, N., Hanna, L., Whiting, J., Zydlewski, G., Staines, G., Gill, A., Hutchison, I., O'Hagan, A., Simas, T., Bald, J., Sparling, C., Wood, J., and Masden, E. (2016). *Annex IV 2016 State of the Science Report: Environmental Effects of Marine Renewable Energy Development Around the World*. Available at tethys.pnnl.gov.
- Copping, A. (2018). *The State of Knowledge for Environmental Effects: Driving Consenting/Permitting for the Marine Renewable Energy Industry*. Available at: tethys.pnnl.gov.
- Copping, A., Freeman, M., and Gorton, A. (2018). *Optimizing Permitting for MRE through Data Transferability*. Webinar for the MRE Community. Available at: tethys.pnnl.gov.
- Daroux, A. and Zydlewski, G. (2017). *Marine Fish Monitoring Program Tidal Energy Demonstration Site – Minas Passage*. Prepared for Fundy Ocean Research Center for Energy.
- Envirosphere Consultants Limited. (2017). *Marine Seabirds Monitoring Program – Tidal Energy Demonstration Site – Minas Passage, 2016 – 2017*. Prepared for Fundy Ocean Research Center for Energy.
- Envirosphere Consultants Limited. (2009). *Marine Bird and Mammal Observations—Minas Passage Study Site*. Prepared for Minas Basin Pulp and Power Co. Ltd.
- Fraser, S.; Williamson, B.; Nikora, V.; Scott, B. (2018). *Fish Distributions in a Tidal Channel Indicate the Behavioural Impact of a Marine Renewable Energy Installation*. Energy Reports, 4, 65-69.
- Gaskin, D.E. (1992). *Status of the harbour porpoise, Phocoena phocoena, in Canada*. Canadian Field-Naturalist 196: 36 – 54.
- Gattuso J.-P., Magnan A.K., Bopp L., Cheung W.W.L., Duarte C.M., Hinkel J., Mcleod E., Micheli F., Oschlies A., Williamson P., Billé R., Chalastani V.I., Gates R.D., Irisson J.-O., Middelburg J.J., Pörtner H.-O. and Rau G.H. (2018). *Ocean Solutions to Address Climate Change and Its Effects on Marine Ecosystems*. Frontiers in Marine Science. 5:337.
- Joy, R., Wood, J., Robertson, F., and Tollit, D. (2017). *FORCE Marine Mammal Environmental Effects Monitoring Program – 1st Year (2017) Monitoring Report*. Prepared by SMRU Consulting (Canada) on behalf of FORCE.
- Joy, R., Wood, J., and Tollit D. (2018). *FORCE Echolocating Marine Mammal Environmental Effects Monitoring Program – 2nd Year (2018) Monitoring Report*. Prepared by SMRU Consulting (Canada) on behalf of FORCE, December 8, 2018.

- Joy, R.; Wood, J.; Sparling, C.; Tollit, D.; Copping, A.; McConnell, B. (2018). *Empirical measures of harbor seal behavior and avoidance of an operational tidal turbine*. Marine Pollution Bulletin, 136, 92-106.
- Langhamer, O. (2012). *Artificial reef effect in relation to offshore renewable energy conversion*. State of the art. Sci. World. J.
- Langhamer, O., Wilhelmsson, D., and Engström, J. (2009). *Artificial reef effect and fouling impacts on offshore wave power foundations and buoys – a pilot study*. Estuar. Coast. Shelf Sci. 82(3): 426 – 432.
- Lewis, A., Estefen, S., Huckerby, J., Musial, W., Pontes, T., Torres-Martinez, J., et al. (2011). “Ocean energy,” in *Renewable Energy Sources and Climate Change Mitigation. Special Report of the Intergovernmental Panel on Climate Change*, eds O. Edenhofer, R. Pichs-Madruga, Y. Sokona, K. Seyboth, P. Matschoss, S. Kadner, et al. (Cambridge: Cambridge University Press), 497–534.
- Lossent, J.; Gervaise, C.; Iorio, L.; Folegot, T.; Clorennec, D.; Lejart, M. (2017). *Underwater operational noise level emitted by a tidal current turbine and its potential impact on marine fauna*. The Journal of the Acoustical Society of America, 141(5).
- Malinka, C.; Gillespie, D.; Macaulay, J.; Joy, R.; Sparling, C. (2018). *First in situ Passive Acoustic Monitoring for Marine Mammals during Operation of a Tidal Turbine in Ramsey Sound, Wales*. Marine Ecology Progress Series, 590, 247-266.
- Marine Renewables Canada. (2018). *State of the Sector Report: Marine Renewable Energy in Canada*.
- Martin, B., Whitt, C., and Horwich, L. (2018). *Acoustic Data Analysis of the OpenHydro Open-Centre Turbine at FORCE: Final Report*. Document 01588, Version 3.0b. Technical report by JASCO Applied Sciences for Cape Sharp Tidal and FORCE.
- Melvin, G.D., and Cochrane, N.A. (2014). *Investigation of the vertical distribution, movement, and abundance of fish in the vicinity of proposed tidal power energy conversion devices*. Final Report for Offshore Energy Research Association. Research Project 300-170-09-12.
- NEXUS Coastal Resource Management Ltd. (2017). *Lobster Catchability Study Report*.
- Operational Excellence Consulting. (2019). *Lessons Learned: Marine Operations in the Minas Passage*.
- Pine, M.; Schmitt, P.; Culloch, R.; Lieber, L.; Kregting, L. (2019). Providing ecological context to anthropogenic subsea noise: Assessing listening space reductions of marine mammals from tidal energy devices. Renewable and Sustainable Energy Reviews, 103, 49-57.
- Polagye, B.; Wood, J.; Robertson, F.; Joslin, J.; Joy, R. (2018). *Marine Mammal Behavioral Response to Tidal Turbine Sound*. Report by Sea Mammal Research Unit (SMRU) and University of Washington. pp 65.
- Schramm, M.; Bevelhimer, M.; Scherelis, C. (2017). Effects of hydrokinetic turbine sound on the behavior of four species of fish within an experimental mesocosm. *Fisheries Research*, 190, 1-14.

- Serdynska and Coffen-Smout. (2017). *Mapping inshore lobster landings and fishing effort on a Maritimes Regional statistical grid (2012-2014)*. Dartmouth, Nova Scotia: Fisheries and Oceans Canada.
- SLR Consulting. (2015). *Proposed Environmental Effects Monitoring Programs 2015-2020 for Fundy Ocean Research Center for Energy (FORCE)*.
- Stewart, P.L., Kendall, V.J., and Lavender, F.L. (2018). *Marine Seabirds Monitoring Program Tidal Energy Demonstration Site – Minas Passage, Year-2: 2017 – 2018*. Prepared for Fundy Ocean Research Center for Energy.
- Stewart, P.L., and Lavender, F.L. (2010). *Marine Mammal and Seabird Surveys Tidal Energy Demonstration Site — Minas Passage, 2009*. Prepared for Fundy Ocean Research Center for Energy.
- Stewart, P.L., Lavender, F.L., and Levy, H. A. (2013). *Marine Mammal and Seabird Surveys Tidal Energy Demonstration Site — Minas Passage, 2012*. Prepared for Fundy Ocean Research Center for Energy.
- Stewart, P.L., Lavender, F.L., and Levy, H. A. (2012). *Marine Mammal and Seabird Surveys Tidal Energy Demonstration Site — Minas Passage, 2011*. Prepared for Fundy Ocean Research Center for Energy.
- Stewart, P.L., Lavender, F.L., and Levy, H. A. (2011). *Marine Mammal and Seabird Surveys Tidal Energy Demonstration Site — Minas Passage, 2010*. Prepared for Fundy Ocean Research Center for Energy.
- Stokesbury, M., Logan-Chesney, L., McLean, M., Buhariwalla, C., Redden, A., Beardsall, J., and Dadswell, M. (2016). *Atlantic sturgeon spatial and temporal distribution in Minas Passage, Nova Scotia, Canada, a region of future tidal energy extraction*. PLoS One, 11(7), e0158387.
- Townsend, D., Radtke, R., Morrison, M., and Folsom, S. (1989). *Recruitment implications of larval herring overwintering distributions in the Gulf of Maine, inferred using a new otolith technique*. Marine Ecological Progress Series. 55, 1 – 13.
- Walker, J. and Taylor, P. (2018). *Using radar data to evaluate seabird abundance and habitat use at the Fundy Ocean Research Center for Energy site near Parrsboro, NS*.
- Wilhelmsson, D., Malm, T., and Öhman, M.C. (2006). *The influence of offshore windpower on demersal fish*. ICES J. Mar. Sci. 63(5): 775–784.
- Wilson, J.C., and Elliott, M. (2009). *The habitat-creation potential of offshore wind farms*. Wind Energy 12(2): 203 -212.

Appendix 1

Cape Sharp Tidal Venture Update

ABOUT CAPE SHARP TIDAL VENTURE

Cape Sharp Tidal Venture (CSTV) is a joint venture between tidal energy technology developer, OpenHydro Technology, a Naval Energies company, and Halifax-based energy company Emera Inc. The CSTV project used OpenHydro's Open-Centre Turbine (Figure A.1). This turbine technology has four key components:

- a horizontal axis rotor;
- a magnet generator;
- a hydrodynamic duct; and
- a subsea gravity base foundation.

The turbine design has 10 fins, each approximately 2.4 m wide x 4.8 m long, manufactured from glass-reinforced plastic. The thickness of each fin ranges from 21 cm at the root (outer diameter) to 1.5 cm at the tip (inner diameter). The turbine is supported by a triangular-shaped gravity foundation subsea base structure. The entire unit sits on the sea floor without requiring drilling or any preparation to the substrate.

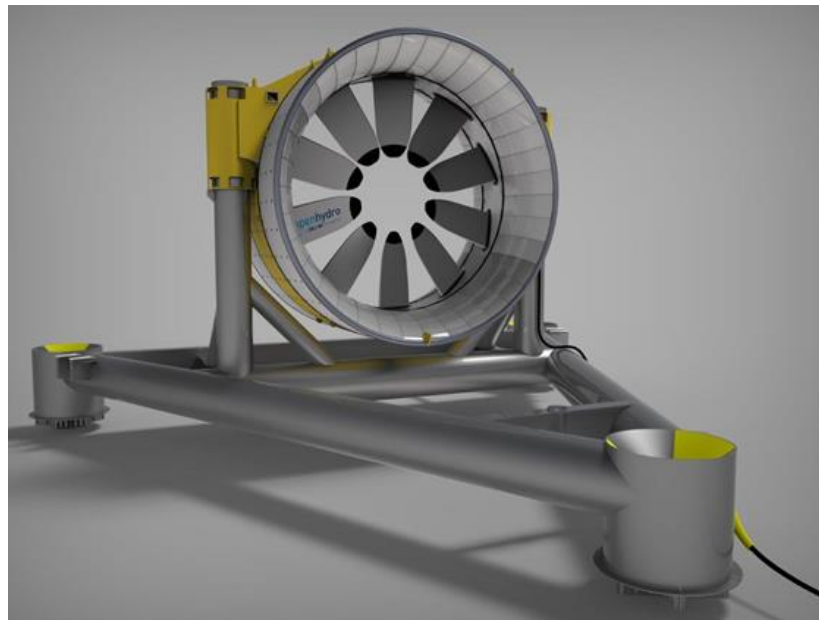


Figure A.1: An image of the OpenHydro Open-Centre Turbine design.

Previously, CSTV deployed a 2-megawatt (MW) in-stream tidal energy turbine at the FORCE site on November 7, 2016. This turbine was retrieved on June 15, 2017. Following retrieval, the turbine and subsea base were towed to port facilities in Saint John, New Brunswick. Details of the marine operations around the retrieval were provided in the 2017 Environmental Effects Monitoring (EEMP) Reports (www.capesharptidal.com/eemp/).

A second turbine was deployed on July 22, 2018 and on July 24, 2018 OpenHydro successfully connected the subsea cable to the turbine and confirmed establishment of communication with the turbine systems. Two days later, on July 26, 2018 Naval Energies filed a petition with the High Court of Ireland for the liquidation of OpenHydro Group Limited and OpenHydro Technologies

Limited. In order to ensure safety, the OpenHydro commissioning team isolated the turbine from the Nova Scotia Power Inc. grid, which consequently disabled the monitoring devices. On September 4, 2018 the turbine was re-energized and power was restored to the environmental sensors. At that time it was confirmed that the turbine was not spinning and that one hydrophone was not communicating.

As a result of the OpenHydro insolvency, on August 13, 2018, Emera formally notified OpenHydro and OpenHydro's provisional liquidator that the company was withdrawing from its involvement in Cape Sharp Tidal. These processes are ongoing in Q1 2019.

At this time, the turbine remains at the FORCE berth where it was deployed in July. The turbine rotor is stationary and some of the environmental sensors are operating and continuously transmitting data to shore. An internal component failure in the generator has caused sufficient damage to prevent the rotor from turning.

Q1 2019 OPERATIONAL UPDATE

The focus of operations during this reporting period (January 1 – March 31, 2019) was regular reports to regulators to confirm that the turbine rotor remains stationary (i.e., not turning).

On September 19, 2018, the Department of Fisheries and Oceans (DFO) confirmed a modification of monitoring requirements under the CSTV *Fisheries Act* Authorization to be comprised of a monthly status updates on the turbine to confirm that the rotor is not spinning by monitoring turbine status during the peak tidal flow of each month. This program began October 1, 2018. CSTV suspended reporting on March 1, 2019 due to lack of funds from OpenHydro Technology LTD (as it is presently in liquidation).

Acoustic Doppler current profiler (ADCP) data indicate that during the months of January and February the turbine rotor remained stationary.

NEAR-FIELD ENVIRONMENTAL EFFECTS MONITORING – Q1 2019 UPDATE

As indicated above, while FORCE completes site-level or 'mid-field' monitoring activities at the FORCE site, near-field monitoring (i.e., device-specific monitoring within 100 m of a turbine) is completed by individual berth holders. Like the mid-field monitoring programs, the near-field monitoring plans and reports undergo review by FORCE's EMAC and regulators.

Moving forward, each berth holder's monitoring activities will be included as appendices below. Updates from future berth holders will be provided as others develop and implement near-field, device-specific environmental effects monitoring programs.

As noted above, CSTV is currently not completing near-field monitoring at 'Berth D' since it has been confirmed that the turbine rotor is not spinning.

Data is still being collected by two hydrophones (a third was confirmed to be non-operating in March 2019) mounted in separate locations on the turbine rotor and the subsea base. The three ADCP devices mounted on the turbine are also collecting data on water flow.

Appendix II

Passive Acoustic Monitoring Workshop Report



FORCE

Fundy Ocean Research Center for Energy

Passive Acoustic Monitoring in association with Tidal Energy Turbines in the Minas Passage: Workshop Report

Original: 26 November 2018

Revised: 11 March 2019

Fundy Ocean Research Center for Energy
1156 West Bay Road | Parrsboro, NS
1690 Hollis Street, 10th Floor | Halifax, NS
www.fundyforce.ca

Executive Summary

In November 2018, the Fundy Ocean Research Center for Energy (FORCE) convened a workshop of regional experts (i.e., industry partners, academics, stakeholders) in Passive Acoustic Monitoring (PAM) data collection and analyses. FORCE's Environmental Effects Monitoring Program (EEMP) utilizes PAM equipment as its primary means of monitoring marine mammals and for understanding the effects of sound generated by turbines deployed at the FORCE test site, located in the Minas Passage, Bay of Fundy. The FORCE test site is exposed to tidal flows that may restrict the utility of particular types of PAM equipment that are suitable for environmental monitoring elsewhere. Further, regulators have requested clarification regarding the ability of different PAM technologies to detect harbour porpoise (*Phocoena phocoena*) echolocations at the FORCE site, including rates of false-positive detections. Therefore, the purpose of the PAM workshop was to discuss the inherent challenges and operational limitations associated with PAM technologies and methodologies in high-flow environments, and to identify future projects that could facilitate the deployment of PAM technologies best suited for marine mammal and sound monitoring in the Minas Passage. Participants discussed previous and ongoing PAM projects in the Bay of Fundy including challenges, methodologies for overcoming the difficult conditions presented by high-flow environments and initial findings. Importantly, the group discussed opportunities for improvements to PAM technologies, and potential projects and collaborations for the near-future. It is anticipated that members of this group will continue to meet on a semi-regular basis to pursue collaborations and opportunities to improve the utility of PAM technologies in the challenging conditions of the Bay of Fundy.

Table of Content

Acronyms	3
Introduction	4
Background	4
Attendees.....	6
Proceedings.....	7
Present Situation at FORCE.....	7
Instrumentation Evaluation	9
PAM Analysis from November 2016 – June 2017.....	9
C-POD Utility	11
Calibration and Instrumentation Life.....	12
Laboratory and In Situ Tests	12
Additional Studies & Resources	12
Recommendations & Next Steps	12
References & Further Reading.....	14

List of Figures

Figure 1: The locations of the four hydrophones placed on the OpenHydro turbine. Hydrophone 2 (fore port) is presently not communicating.	8
Figure 2: Median pressure spectral densities for three different long-term recording positions, the reference recording from the outer Bay of Fundy as well as the drifter measurements from 27 Mar 2017. Frequency-5/3 is the expected slope for turbulent flow noise (Martin et al., 2018).	10
Figure 3: Power spectral density versus tidal increment time, turbine state, and recorder. The horizontal axis is time in hours since high tide. Times with less than 30 samples of data are blocked out in red (JASCO, 2018).	11

Acronyms

AAM	Active Acoustic Monitoring
ADCP	Acoustic Doppler Current Profiler
AMAR	Autonomous Multichannel Acoustic Recorder
CSTV	Cape Sharp Tidal Venture
dB	Decibel
DRDC	Defense Research and Development Canada
FAST	Fundy Advanced Sensor Technology
FORCE	Fundy Ocean Research Center for Energy
HR	High Residence
Hz	Hertz
ISEM	Integrated active and passive acoustic System for Environmental Monitoring of fish and marine mammals in tidal energy sites
kHz	Kilohertz
NS	Nova Scotia
NSERC	Natural Sciences and Engineering Research Council of Canada
OERA	Offshore Energy Research Association of Nova Scotia
PAM	Passive Acoustic Monitoring
PPM	Pulse Position Modulation
SMRU	Sea Mammal Research Unit
STREEM	Sensor Testing Research for Environmental Effects Monitoring
SUBS	Streamlined Underwater Buoyancy System
TL	Transmission Loss

Introduction

On 23 November 2018, the Fundy Ocean Research Center for Energy (FORCE) convened a workshop of regional experts (e.g., industry partners, academia, stakeholders) in passive acoustic monitoring (PAM) data collection and analyses. The purpose of the workshop was to discuss the challenges and operational limitations inherent with using PAM technologies for marine mammal and sound monitoring in high-flow environments like the FORCE test site in Minas Passage, Bay of Fundy, and to identify potential solutions to improve environmental effects monitoring capabilities for operational in-stream tidal energy turbines in the future. The workshop sought to address questions from provincial (Nova Scotia Department of Environment) and federal (Canada Department of Fisheries and Oceans) regulators with respect to the integration or corroboration of results from multiple PAM technologies to inform predictions made in the FORCE Environmental Assessment (AECOM, 2009). The workshop also explored potential future projects to support further environmental monitoring using PAM technologies with the end goal of lending confidence to environmental effects monitoring technologies and approaches used in support of tidal energy devices.

Background

Passive acoustic monitoring has been ongoing at the FORCE test site for many years. Recent environmental effects monitoring efforts increased in 2016 in anticipation of the installation of a single two-megawatt OpenHydro turbine by Cape Sharp Tidal Venture (CSTV) at the FORCE site.

Mid-field or 'site-level' monitoring using PAM technologies and in relation to the FORCE Environmental Assessment (AECOM 2009) is completed by FORCE and its contractors. Presently, this monitoring has focused on two main initiatives: C-PODs and drifting hydrophones. Mid-field monitoring for marine mammals at FORCE consists of near-continuous autonomous deployment of five C-PODs (designed to record marine mammal echolocations) ranging from 210m – 1,700m from the turbine, building on previous years of C-POD deployments throughout the Minas Passage. FORCE deploys and recovers the instrumentation and analysis has been completed by Sea Mammal Research Unit (SMRU) Canada Ltd.

During the 2016 - 2017 deployment of the CSTV OpenHydro turbine, FORCE conducted a drifting hydrophone survey to coincide with the deployment of autonomous and turbine-mounted hydrophones to monitor turbine-generated sounds at the FORCE test site. An integrated analysis was completed by JASCO Applied Sciences (JASCO) (Martin et al., 2018).

Parallel to the FORCE's efforts, a research project was initiated by CSTV to study the potential for integrating active acoustic monitoring (AAM) and PAM technologies on an operating in-stream tidal energy turbine. This research project, 'Integrated Active and Passive Acoustic System for Environmental Monitoring of Fish and Marine Mammals in Tidal Energy Sites (ISEM)', was developed to explore technologies that could operate as an integrated environmental monitoring system using data analysis software and encompassing active and passive acoustic sensors in order to provide real time detection, classification, localization, and tracking of fish and marine mammals at high energy sites.

Although the success of the ISEM project tasks and objectives have been directly affected by the disruption of the CSTV turbine operation, some successes were realized and will be reported on in the final project report planned for spring 2019. The report will also address lessons learned and recommendations for moving these types of monitoring programs forward to increase understanding of monitoring in tidal energy sites.

Additional PAM activities happening in the Bay of Fundy include:

Integrated Lander Platform

Acadia University and collaborators at SMRU Canada Ltd. have been measuring harbour porpoise (*Phocoena phocoena*) detections in Minas Passage since 2010 (Tollit et al., 2011; Wood et al., 2013; Porskamp, 2013). Acadia University and SMRU Canada Ltd. established PAM (i.e., C-POD) monitoring sites in and around the FORCE test site during December 2013 – June 2014. In order to better assess PAM monitoring methods, Acadia and OceanSonics Ltd. deployed a lander (sub-sea) platform at the FORCE test site in June 2014. Among other instrumentation, the platform carried icListenHF hydrophones, C-PODs, and VR2W receivers that detect acoustic tags. Analysis of the data collected using this sensor suite provided a comparison of C-PODs and broadband hydrophones for monitoring harbour porpoise (Porskamp, 2015; Porskamp et al., 2015). Acadia has also undertaken a great deal of monitoring for acoustically tagged fish (Broome, 2014; Broome et al., 2015; Keyser et al., 2016).

Drifting Platform

Results from the integrated lander platform work generated questions that prompted a long series of experiments using a passive acoustic drifting platform (i.e., ‘drifter’) to make targeted PAM measurements. Drifter work in 2016 focused on detection range for acoustic tags (Sanderson et al., 2017) and PAM to measure ambient sound and harbour porpoise presence. Drifter work in June 2017 focused on comparison of C-POD data, icListen-coda, and visual harbour porpoise sightings (Adams, 2018; Adams et al., 2018). This work included some preliminary assessments of harbour porpoise localization (Sanderson et al., 2018b), and detections of tagged fish and comparisons of harbour porpoise detections with moored instruments (Sanderson, personal research notes). Drifter work in June 2018 used an array of four synchronized hydrophones and is presently being analysed for porpoise localization. Drifters were also used to demonstrate ‘quasi-stable’ platform trajectories in the currents of Minas Passage which may prove useful for future monitoring and research (Sanderson et al., 2018b). The 2018 work also undertook further range testing of acoustic tags, particularly to determine the efficacy of Pulse Position Modulation (PPM) transmissions relative to High Residence (HR) transmissions.

Passive and Active Acoustic Measurements

The ‘Sensor Testing Research for Environmental Effects Monitoring’ (STREEM) project in Grand Passage, Nova Scotia involves assessment of both passive and active acoustic instruments. Preliminary work (October 2018) involved passively drifting a variety of targets to quantify detection capabilities of an imaging sonar (i.e., Tritech Gemini 720is). Sometimes the targets were acoustically active, in which case their effects on the imaging sonar were identified. Other times, hydrophones were used as targets in order to measure how the imaging sonar interacted with PAM instruments. Interactions between echosounders, acoustic tags, the imaging sonar, broad-band hydrophones, and HR2 receivers were also measured. A drifting hydrophone array is also being used to measure sounds from the turbine platform (a PLAT-I from Sustainable Marine Energy Canada) installation. The major thrust for STREEM will be the application of imaging sonars, optical cameras, and hydrophones to study fish-turbine interactions. This work is ongoing, with the major experiment planned for spring/summer 2019.

Long-term Acoustic Monitoring

JASCO Applied Sciences Canada Ltd. and Dalhousie University (Dr. David Barclay; Oceanography Department) are undertaking a long-term acoustic monitoring AMAR (Autonomous Multichannel Acoustic Recorder) study in Grand Passage. The purpose of this work is to understand the effects of this turbulent environment on the ability to detect marine life and the ability of marine life to detect tidal turbines. Data analyses for this project has commenced.

Workshop Objective

In early 2018, regulators (Nova Scotia Department of Environment, 2018) provided feedback to FORCE and CSTV regarding passive acoustic data collection during the 2016-2017 deployment of an OpenHydro turbine at the FORCE site. Specifically, regulators requested clarity regarding harbour porpoise detections between turbine-mounted icListen hydrophones and C-PODs.

“[Fisheries and Oceans Canada] requests that a direct comparison of data collected by the icListen hydrophone used for near-field monitoring at Berth D to data collected by the C-PODs deployed at East1 and D1 [C-POD locations] during the 2016/2017 deployment period be provided [...] Specifically, provide a clear discussion of the results of the Days with Detected Porpoise Clicks with the Lucy Click Detector relative the Number of Calendar Days reported for deployment period” (Nova Scotia Department of Environment, 2018).

In response, FORCE consulted with the workshop attendees to develop a response for its second quarterly report in 2018 (FORCE, 2018) and began planning this workshop for fall 2018.

Problem Statement

Recognizing that C-POD data files are not comparable with icListen data files (Porskamp et al., 2015) and that there were observed discrepancies in ‘Days with Detected Porpoise Clicks’ between the turbine-mounted icListen hydrophones and the Chelonia C-PODs deployed in proximity to the CSTV turbine, a further examination of PAM devices is warranted at the FORCE site.

The differences in detection rates between these instruments can partly be attributable to their functioning. The icListen hydrophone is considered more sensitive but may be masked by the noise of the turbine during periods of high flow. Research has also demonstrated that C-POD units can sometimes record false positive detections (although this is at fairly low rates), whereas the icListen hydrophones and associated software programs have been developed to separate out the different high frequency sounds to make a positive identification of porpoise clicks. The icListen hydrophones appear to have a greater accuracy in detection rates of high frequency sounds in noisy environments; however, the continued use of C-PODs at the FORCE site is important as it provides a direct comparison to baseline data that was collected at the FORCE site prior to any turbine deployments within the mid-field study area.

A statistical model that accounted for relevant environmental variables and ‘Percent Time Lost’ was applied to the C-POD data, and was used to test for changes in the distribution and activity of harbour porpoise in relation to the installation and operation of the turbine. The overall effect of turbine operations on porpoise detection rates were found to be significant ($P < 0.01$). East1, a site 210 m north of the turbine at 41 m depth, and D1, a site 230 m south of the turbine at 33 m depth both showed significantly fewer porpoise detections post-installation of the turbine. Both of these sites had overall lower activity levels both with and without the turbine, whereas the sites > 1 km west and south of the turbine had overall higher activity levels and showed no decrease in porpoise detections with the turbine. Given that detection ranges of harbour porpoise are small ($< 2\text{--}300$ m), it is possible that the lower detection rates recorded by the icListen hydrophone mounted on the turbine reflect near-field avoidance by harbour porpoise.

For both types of monitoring devices, additional data collection will be required to cover seasonal and inter-annual variation to understand behaviours of marine mammals in relation to an operational turbine in the mid-field and near-field. The issues experienced during the 2016-2017 turbine deployment have

been mitigated through a series of pre-deployment commissioning tests of the icListen hydrophones, new protocol for transfer and management of data, hydrophone synchronization and recognition of the importance of protective measures and specific cabling for all icListen hydrophones.

Attendees

Attendees included representatives from:

- Acadia University (Wolfville, NS): Mike Adams, Anna Redden, Brian Sanderson
- Dalhousie University (Halifax, NS): David Barclay
- Emera/Cape Sharp Tidal Venture (Halifax, NS): Carys Burgess
- FORCE: Tyler Boucher, Jessica Douglas, Dan Hasselman, Melissa Oldreive
- GeoSpectrum Technologies Inc. (Dartmouth, NS): Matt Coffin
- JASCO Applied Sciences (Dartmouth, NS): Bruce Martin
- Ocean Sonics (Great Village, NS): Mark Wood
- Offshore Energy Research Association of Nova Scotia (Halifax, NS): Jennifer Pinks

SMRU Canada Ltd. (Vancouver, British Columbia) was unable to attend due to travel restrictions and provided advice beforehand. In addition, Dr. Dom Tollit presented at the Marine Renewables Canada Research Forum on 20 November 2018, highlighting the experience of SMRU Canada Ltd. with marine mammal monitoring at the FORCE test site.

All parties have had experience in data collection methodologies and/or analysis experience with PAM data collected within the Minas Passage, Bay of Fundy.

Proceedings

After a general roundtable introduction amongst participants, the workshop's objectives and the intent to form broad-scale collaborations for dissemination of research and technical challenges and developing joint research project area were discussed. This is especially important as some valuable lessons learned are not always outlined in publications.

Present Situation at FORCE

Dan Hasselman provided an update regarding the present situation at the FORCE test site in consideration of the OpenHydro turbine (i.e., turbine itself is non-operational, but three of four turbine-mounted icListen hydrophones are operating). It was agreed that it is critical to focus on the near-field at this time: this is key to enable future device developments.

For instance, FORCE has commissioned GeoSpectrum Technologies Inc. and Dalhousie University to examine data from the three turbine-mounted icListen hydrophones (depicted in Figure 1: The locations of the four hydrophones placed on the OpenHydro turbine. Hydrophone 2 (fore port) is presently not communicating.), an autonomous Fundy Advanced Sensor Technology (FAST) platform with two icListen hydrophones, and an AMAR system deployed by JASCO Applied Sciences Canada Ltd. The purpose of this work is to examine the data collected in summer/fall 2018 in the near-field region of the OpenHydro turbine to i) characterize ambient noise levels with a stationary turbine, and ii) evaluate the performance of each hydrophone configuration to provide information about how best to monitor sound at the FORCE test site in the future. Utilization of this near-field data will advance our understanding of the soundscape of the site and will provide valuable information about future mid-field and near-field monitoring at the FORCE site.

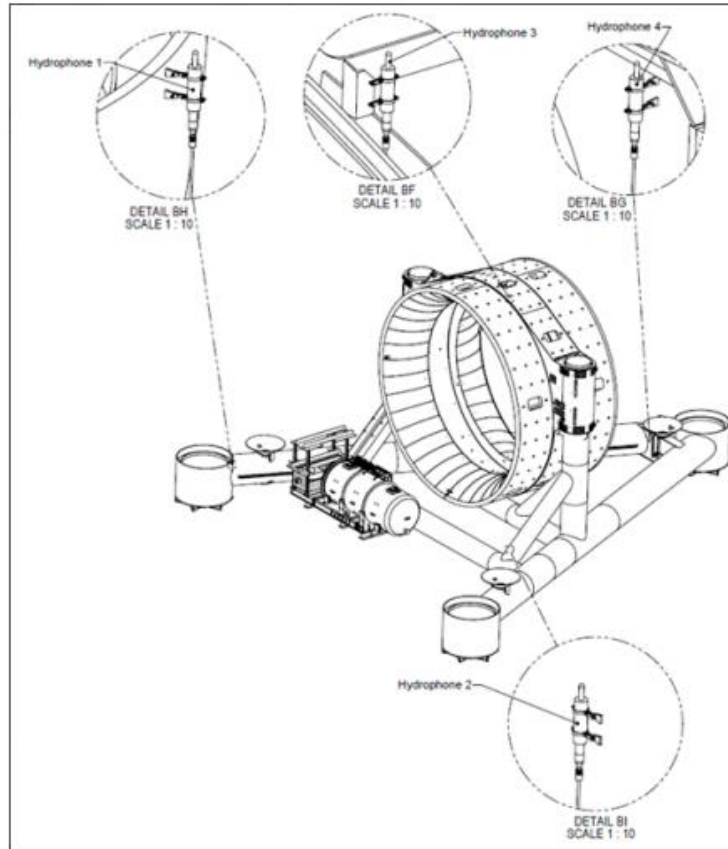


Figure 1: The locations of the four hydrophones placed on the OpenHydro turbine. Hydrophone 2 (fore port) is presently not communicating.

Matt Coffin (GeoSpectrum Technologies Inc.) elaborated on the data collected from the icListen hydrophones mounted on the FAST platform. Specifically, taking five-minute averages at two-hour intervals, flow noise can be seen in the spectra and is comparable to the flow noise observed in the data from the turbine-mounted icListen hydrophones. Matt pointed out that the sample rate of the raw icListen hydrophone data is 8 kHz, resulting in a 4 kHz cut-off frequency in the spectra. Mark Wood (Ocean Sonics) pointed out that high-frequency spectra are saved in addition to the raw time-series data. After the workshop, Matt located the high-frequency spectra and updated the spectral plots to include these data. Again, the spectra agree well with the turbine-mounted icListen hydrophone data.

Although Bruce Martin (JASCO Applied Sciences Canada Ltd.) has analyzed previous icListen hydrophone data, none of that data was collected when the turbine was non-operational. Therefore, the current data could be used to estimate ambient noise in the Minas Passage with the CSTV turbine present but stationary. This would be valuable information.

While there is accompanying ADCP (Acoustic Doppler Current Profiler) data for the data collection period, GeoSpectrum Technologies Inc. has not analyzed these data. For simplicity, Matt used tidal prediction times to estimate flow speed at the times corresponding to the spectral measurements instead.

Following the meeting, GeoSpectrum Technologies Inc., David Barclay, and Bruce Martin met to discuss the results of the preliminary analysis and developed a statement of work defining more in-depth analysis to follow.

Brian Sanderson (Acadia University) discussed how beam patterns from the various instruments can help with directionality and localization, allowing monitoring to move from presence/absence data to quantitative measurements (i.e., abundance estimates).

The three turbine-mounted icListen hydrophones provide an opportunity to continue PAM research objectives in the Minas Passage regardless of whether the turbine is operational or not. Mark Wood has been surprised by the level of animal activity recorded so far by the icListen hydrophones. Further examination during the winter months will provide additional information about harbour porpoise presence and activity. Mark also noted that this could provide an opportunity to better understand if AAM instruments are interfering with PAM devices. Data from the ADCPs mounted on the turbine are under review; an evaluation of PAM and AAM devices could be worthwhile right now.

Work with fish acoustic telemetry (i.e., fish tagging) (Mike Stokesbury; Acadia University) was discussed. A project that considers the new high-frequency hydroacoustic tags (180 and 170 signal) could provide further clarity about animal movements across instrumentation recorder locations. While tagging efforts are recognized as expensive and extensive, it was agreed that FORCE could coordinate multiple groups to develop a project that uses hydrophones to supplement tag receivers.

Instrumentation Evaluation

Brian Sanderson discussed how AAM devices such as ADCPs interfere with PAM devices. Dr. Haley Viehman (Echoview Software Pty Ltd.; previously Acadia University) has done work on the interference of active acoustic instrumentation on other AAM devices (e.g. Tritech Gemini sonar and ADCPs); additional work focused on AAM-AAM and AAM-PAM instrumentation interference is worthwhile and would facilitate discussions with regulators about the utility of setting duty cycles (i.e., sequentially turning acoustic monitoring devices on/off) to avoid interference and thereby improving the quality of data collected by all acoustic monitoring devices.

It was noted that SMRU Canada Ltd. had engaged the University of St Andrews (Scotland) to look at the interference between the Tritech Gemini imaging sonar with hydrophone data. The ISEM project (in collaboration with SMRU Canada Ltd., Acadia University, and Ocean Sonics) is presently examining the quality of Tritech Gemini data collected during the 2018 CSTV turbine deployment.

PAM Analysis from November 2016 – June 2017

Bruce Martin highlighted sections in the JASCO Applied Sciences Canada Ltd. report (Martin et al., 2018) that compared various turbine-mounted hydrophones to passively drifting icListen hydrophones deployed by FORCE and the AMAR (Figure 2: Median pressure spectral densities for three different long-term recording positions, the reference recording from the outer Bay of Fundy as well as the drifter measurements from 27 Mar 2017. Frequency-5/3 is the expected slope for turbulent flow noise (Martin et al., 2018).) during the 2016-2017 CSTV turbine operation. At 69 Hz, the data from the AMAR and the turbine-mounted hydrophones correlate well. Further, consistency was observed across instruments and tidal stage – the directional sound source could be due to sediment movement in the water column.

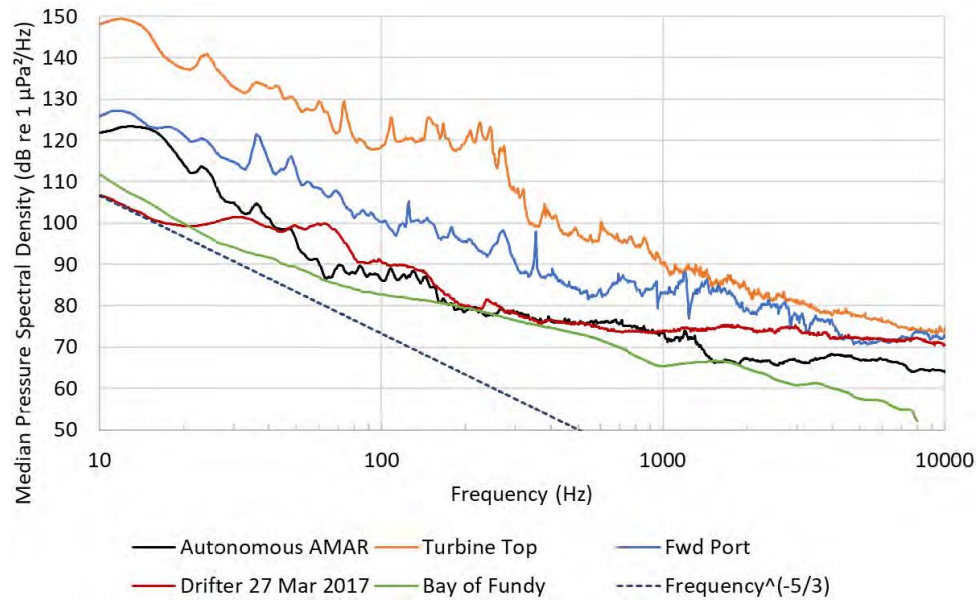


Figure 2: Median pressure spectral densities for three different long-term recording positions, the reference recording from the outer Bay of Fundy as well as the drifter measurements from 27 Mar 2017. Frequency-5/3 is the expected slope for turbulent flow noise (Martin et al., 2018).

It was also observed that the measurements from the AMAR had more vibrational energy, due to its proximity to the sound-source (i.e., CSTV turbine). It was observed that the shape of the lines for the AMAR data when the CSTV turbine was generating power were ‘arrowed’, indicating a stationary Lloyd’s Mirror Effect. At higher frequencies, dramatically different ebb and flood characteristics were detected among the various hydrophone locations on the turbine.

There was discussion regarding the turbine-generated sound (in its various states) relative to vessel traffic elsewhere in the Bay of Fundy, as well as the pre-existing soundscape in the Bay of Fundy.

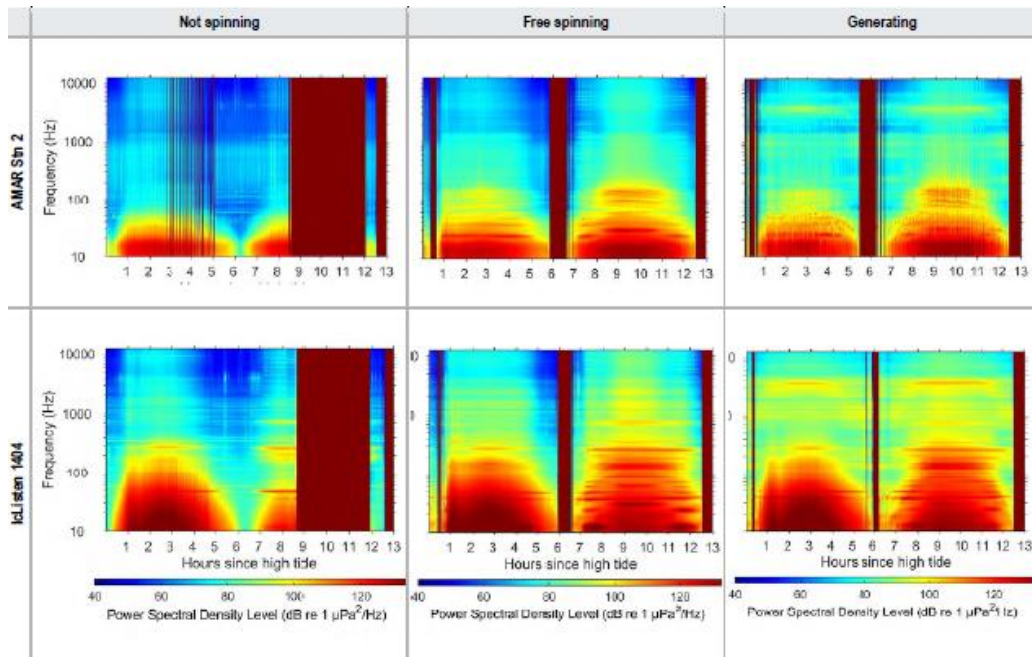


Figure 3: Power spectral density versus tidal increment time, turbine state, and recorder. The horizontal axis is time in hours since high tide. Times with less than 30 samples of data are blocked out in red (JASCO, 2018).

C-POD Utility

Brian Sanderson and Anna Redden (Acadia University) presented the issue of C-POD false detections, and issues with interfering noise and related data loss. C-POD performance is compromised above certain flow thresholds and does not assist with localization or abundance measurements. Some targeted experiments on the moorings used for C-PODs in the Minas Passage (known as SUBS – Streamlined Underwater Buoyancy System) are required.

SMRU Canada Ltd. undertook additional analyses to assess loss of data by C-PODs under high flow conditions. Data loss occurs when the 1-minute long internal memory buffer of the C-POD is filled with clicks before the end of that minute of monitoring (termed ‘Percent Time Lost’). Percent Time Lost had little effect on data quality between ebb current speeds < 2.4 m/s (95.0% of 10-minute periods) and flood current speeds < 2 m/s (71% of 10-minute periods). At ebb current speeds up to 2.9 m/s (99.0% of 10-minute periods) and flood current speeds up to 3.5 m/s (95.5% of 10-minute periods), Percent Time Lost does not exceed 65.0%. Despite the use of statistical methods to take Percent Time Lost into account, C-POD monitoring performance above these current speeds appears less reliable, noting that these speeds only occur over a small fraction of the tidal cycle.

Bruce Martin mentioned how geometry and directionality (including beam patterns and signals) are critical elements for proposed experimental trial work and must be considered in instrument mounting configuration (either on platforms, moorings, or turbines).

Dan Hasselman highlighted communications from Dom Tollit regarding a new PAM instrument called ‘Sound Trap 300 HF’, which can achieve continuous audio recordings at a low sample rate, while simultaneously capturing short audio snippets of each click detection at full 576 kHz sample rate. This is a compact acoustic recorder developed by Ocean Instruments New Zealand in collaboration with SMRU Ltd.

and uses the PAMGuard software to detect porpoise clicks.¹ Bruce highlighted a new instrument, an F-POD, which is under development by Chelonia (provider of the C-PODs) and is available for testing.

Calibration and Instrumentation Life

It was noted that C-PODs operate best in the first year of life. There will be a need for FORCE to recalibrate/refurbish these instruments soon.

Laboratory and In Situ Tests

Mark Wood described a test completed at the Aquatron facility (Dalhousie University), which resulted in less useful data as the walls of the facility ‘clip’ the hydrophone.

Anna Redden and Brian Sanderson discussed open water testing, which suffered from interference with boats and echosounders (which can be quite large – 200 dBs at times).

While it was recognized that laboratory facilities are useful in certain contexts (e.g., isolate signals, turbidity changes, multiple instruments, etc.), it was determined that open water test sites are preferable for PAM. Some tests were done in Saint Mary’s Bay, but the data is not yet analyzed. More data will be collected, but that work has been delayed until 2019 (spring/summer) due to weather.

Additional Studies & Resources

Care will be required in designing and interpreting any detection experiments. Ideally, all sensors being compared should be co-located. Where they are not co-located, the experiment should be designed to help reduce the impact of spatial and temporal variations in transmission loss (TL). GeoSpectrum Technologies Inc. has conducted a number of TL studies and similar experiments where many pulses have been transmitted over a period of time to various sensors. Even small changes in location and time (e.g., on the order of a wavelength and seconds to minutes) have resulted in TL variations on the order of 10 dB. Thus, any detection experiments should do their best to overlap sampling in space and time and ensure sufficiently long duration and variation in source location to try to ensure that all sensor locations are presented with similar test data.

Recommendations & Next Steps

All attendees agreed that it was useful for this group to reconvene again to discuss research projects (present and future) and lessons learned in greater detail. The strength in a group that shares best practices that are not necessarily found in publications is valuable and was recognized by all. It was also recognized that there is a good understanding of existing PAM technologies available, which provides a suitable background for beginning newer, innovative research projects.

The following were identified as potential research projects (in no particular order):

- Take advantage of the opportunity to continue acoustic research with the OpenHydro turbine before it is removed (options highlighted below).
- Assessment of beam patterns of commercially available tools and the potential for their interactions in a specific experimental design.

¹ More information: <http://www.oceaninstruments.co.nz/soundtrap-click-detector/>

- Exploration of mooring systems to optimize C-POD deployments and data collection. A comparison of existing C-POD mooring systems (utilizing SUBS packages), a (cabled) FAST platform, a lift-tilt system, and a deep-water drifter could provide a proper assessment of false positive detections, and most importantly differences in detection rate probabilities in the high-flows of the Minas Passage. This would allow for a comparison between previous baseline detection rates and detection rates using alternative devices and platforms. This approach could increase our understanding of C-POD limitations, possibly quantifying these limits.
- Synthesis of pre-existing data and baseline information collected by PAM receivers within the Minas Passage. This would include:
 - Revisiting C-POD data in consideration of poorer quality data points in order to evaluate the efficiency of these instruments;
 - Analysis of ambient conditions, including an AMAR deployment (June – November 2018); and
 - Quantify noise and transmission loss.
- Co-location of instrumentation near an operating tidal energy turbine. Potential options include:
 - Co-locating a C-POD with a newer Chelonia instrument known as an ‘F-POD’ (to be acquired from Chelonia);
 - Co-location of a C-POD with an icListen hydrophone on a FAST platform (cabled is preferred given the quantity of data from hydrophone); and
 - Placing a C-POD near the CSTV turbine, which has three operating hydrophones on it, on a FAST platform or with a SUBS package.
- An evaluation of harbour seal (*Phoca vitulina concolor*) and grey seal (*Halichoerus grypus*) within the Minas Passage. This could include an evaluation of habitat use, estimated abundance, and include the use of visual observations.
- Using synthetic clicks to assess instrumentation performance. Using a fixed-point source from Ocean Sonics, the ability of instruments to detect vocalizations across different tidal states, configurations, and in different sections of the water column would be assessed.
- Troubleshooting the fourth non-communicating icListen hydrophone on the OpenHydro turbine. Access to FORCE substation is required to communicate with the devices.
- Cumulative sound profiling at the FORCE site. This model could consider multiple turbines and their relative sound profile within the Minas Passage over different tidal stages but start with a single operating turbine when it is deployed.
- An evaluation of AAM interference with PAM devices in the Minas Passage.
- An examination of fish tag detections using pre-deployed hydrophones in the FORCE test site in cooperation with tag manufacturers.
- Continued PAM research options in Grand Passage as step-wise approach to Minas Passage deployments.

The possibility of working towards a submission to the OERA’s Open Call Program was discussed.² A discussion was also had regarding the required resources to complete this work.

The group agreed to its continued value and will attempt to reconvene in 2019.

² More information: <http://www.oera.ca/news/requests-for-proposals-funding/open-call-program/>

References & Further Reading

- Adams, M.J. (2018). *Application of a Multi-Hydrophone Drifter And Porpoise Detection Software for Monitoring Atlantic Harbour Porpoise(Phocoena Phocoena) Activity in and Near Minas Passage*. B.Sc. Honours, Biology, Acadia University, April 2018.
- Adams, M., Sanderson, B., Redden, A. (2018). *Comparison of Codeployed Passive Accoustic Monitoring Tools: icListenHF CODA and CPODs*. Proceedings of the 2018 Marine Renewables Canada Research Forum, Halifax, Canada, November 20, 2018.
- AECOM. (2009). *Environmental Assessment Registration Document – Fundy Tidal Energy Demonstration Project Volume I: Environmental Assessment*. Available at www.fundyforce.ca/environment.
- Broome, J.E., Redden, A.M., Keyser, F.M. (2015). *Passive acoustic telemetry detection of Striped Bass at the FORCE TISEC test site in Minas Passage, Nova Scotia, Canada*. Proceedings of the 3rd Marine Energy Technology Symposium, Washington, D.C., April 27-29, 2015
- Broome, J.E. (2014). *Population characteristics of striped bass (Moronesaxatilis, Walbaum 1792) in Minas Basin and patterns of acoustically detected movements within Minas Passage*. Master's thesis, Acadia University, Biology, 2014.
- Fundy Ocean Research Center for Energy. (Q2 2018). Environmental Effects Monitoring Program Quarterly Report: April - June 2018. Available online: www.fundyforce.ca/monitoring.
- Joy, R., Wood, J., Robertson, F. and Tollit D. (2017). Force Marine Mammal Environmental Effects Monitoring Program – 1st Year (2017) Monitoring Report. Prepared by SMRU Consulting (Canada) on behalf of FORCE, May 2, 2017.
- Joy, R., Wood, J., and Tollit D. (2018). Force Marine Mammal Environmental Effects Monitoring Program – 2nd Year (2018) Monitoring Report. Prepared by SMRU Consulting (Canada) on behalf of FORCE, Oct 11, 2018.
- Keyser, F.M., Broome, J.E., Bradford, R.G., Sanderson, B.G. and Redden, A.M. (2016). *Winter presence and temperature-related diel vertical migration of striped bass (Morone saxatilis) in an extreme high-flow passage in the inner Bay of Fundy*. Canadian Journal of Fisheries and Aquatic Sciences. Published on the web 02 June 2016, 10.1139/cjfas-2016-0002
- Martin, B., C. Whitt, and L. Horwich. (2018). *Acoustic Data Analysis of the OpenHydro Open-Centre Turbine at FORCE: Final Report*. Document 01588, Version 3.0b. Technical report by JASCO Applied Sciences for Cape Sharp Tidal and FORCE.
- Nova Scotia Department of Environment. (1 March 2018). *Fundy Ocean Research Center for Energy (FORCE) Demonstration Project Environmental Effects Monitoring Program (EEMP)*. Regulator Feedback. Available online: www.fundyforce.ca/monitoring
- Porskamp, P.H.J. (2015). *Detecting and Assessing Trends In Harbour Porpoise (Phocoena Phocoena) Presence In And Near The Force Test Site*. M.Sc. Thesis (Biology), Acadia University, Fall Graduation 2015.
- Porskamp, P. (2013). *Passive acoustic detection of harbour porpoises (Phocoena phocoena) in the Minas Passage, Nova Scotia, Canada*. B.Sc. (Hon) thesis. Acadia University, Canada.

Porskamp, P.H.J., Broome, J.E., Sanderson, B., and Redden, A.M. (2015). *Assessing the performance of passive acoustic monitoring technologies for porpoise detection in a high flow tidal energy test site*. Acoustics Week in Canada 2015.

Sanderson, B., Adams, M., and Redden, A. (2018). *Quasi-stable drifter trajectories in the minas channel-passage-basin enable efficient monitoring in the coordinate system of marine animals*. Proceedings of the 2018 Marine Renewables Canada Research Forum, Halifax, Canada, November 20, 2018.

Sanderson, B., Adams, M., and Redden, A. (2018). *Using reflected clicks to Monitor range and depth of porpoise*. Proceedings of the 2018 Marine Renewables Canada Research Forum, Halifax, Canada, November 20, 2018.

Sanderson, B., Buhariwalla, C., Adams, M., Broome, J., Stokesbury, M., and Redden, A. (2017). *Quantifying Detection Range of Acoustic Tags for Probability of Fish Encountering MHK Devices*. Proc. 12th EWTEC Conference 2017.

Tollit, D., Wood, J., Broome, J., and Redden, A. (2011). *Detection of marine mammals and effects monitoring at the NSPI (OpenHydro) turbine site in the Minas Passage during 2010*. Final Report for FORCE and OERA.

Wood, J., Tollit, D., Redden, A., Porskamp, P., Broome, J., Fogarty, L., Booth, C., Karsten, R., (2013). *Passive acoustic monitoring of cetacean activity patterns and movements in Minas Passage: Pre- turbine baseline conditions (2011/2012)*. Final Report for FORCE and OERA.

Appendix III

Using radar data to evaluate seabird abundance and habitat use at the Fundy Ocean Research Centre for Energy site near Parrsboro, NS

Using radar data to evaluate seabird abundance and habitat use
at the Fundy Ocean Research Centre for Energy site near
Parrsboro, NS

Project #: 300-223

Final Report for April 1 to September 30, 2018

Recipient: Acadia University

Author: Jacob Walker

Project Lead: Dr. Philip Taylor

Submitted: September 28, 2018

CONTENTS

Executive Summary	3
Introduction.....	3
Objectives.....	4
Methodology	4
Data Processing.....	4
Data Analysis	5
Results.....	6
Number of tracks.....	6
Effects of date, time, tide, and wind	6
Figure 1. The number of tracks (log ₁₀ scale) detected on each five-minute clip, by Julian date, including a separate smooth for each year	8
Figure 2. Map of tracks classified as floating objects, separated by tidal direction.	9
Figure 3. Histogram of the number of tracks detected by range.....	9
Figure 4. Map showing density of beginning and end points of bird tracks detected by the radar	10
Figure 5. Predicted values from the general additive model for number of tracks by Julian date.....	11
Figure 6. Violin plot showing histograms of track velocities by month.....	11
Figure 7. Interaction plot showing the number of tracks by Julian date for each combination of tidal stage and time of day.....	12
Figure 8. Interaction plot showing the how the effect of wind speed varies with wind direction	12
Table 1. Anova table from the general additive model.....	13
Table 2. Parameter coefficients from the general additive model	13
Conclusions	14
Recommendations	15
Literature cited	16
Budget	17
Employment Summary	17
Appendix 1. Table of radR settings used for processing data.....	18

EXECUTIVE SUMMARY

Radar scans from an open-array Furuno marine radar at the Fundy Ocean Research Centre for Energy (FORCE) site were assessed to determine if the data could be used to monitor seabird activity at the site. The radar unit was installed to monitor the surface of the water in the Minas Passage, to determine flow rates and turbulence at the site. Radar scans from the site have been archived since 2015 in SQLite and .jpg formats, and have somewhat less resolution than the raw radar data. The archived radar scans in .jpg format were subsampled and converted into five-minute long clips, and analysed using the radR program in the R statistical programming language. After filtering out areas with persistent interference due to waves on the surface of the water, bird targets were successfully tracked using tracking algorithms in the radR program. Clips from a wide range of dates, tidal stages, and times of day were analysed to characterize seabird use at the site over four years. A general additive model was used to simultaneously account for the effects of wave clutter, date, tidal stage, time of day, and wind speed and direction on the number of bird tracks detected. The results showed a clear seasonal pattern, with few bird tracks detected in winter, peaks during spring and fall migration, and a period of high activity during the summer. Effects of time of day and tidal stage were complex, and intertwined, as the effect of tidal stage on the number of bird tracks detected was dependent on the time of day and vice versa. The effect of wind speed and direction indicated that strong southwest or southeast winds produce higher numbers of bird tracks at the site, but strong winds from other directions produce fewer bird tracks. Recommendations were made for future use of radar monitoring at the site, and for how the data from this study could be used to modify the sampling regime of observer-based seabird surveys.

INTRODUCTION

The Fundy Ocean Research Centre for Energy (hereafter FORCE) is a demonstration site for in-stream tidal turbines in the Minas Passage, located west of Parrsboro, NS. To date, three turbines have been installed at the FORCE site, though no more than one have been deployed at any time (FORCE 2018). The Environmental Effects Monitoring Program (hereafter EEMP) was initiated in 2009 to monitor any effects of the turbines on the local ecosystem (FORCE 2018). Seabirds are one guild that have been selected for monitoring by the EEMP. Monthly observer-based seabird surveys have been conducted at the site from 2016 to present to determine species composition, habitat use, and effects of turbine placement at the site (FORCE 2018). To complement the observer-based seabird surveys, radar data from the FORCE site were analysed in this study to determine patterns of seabird use in relation to season, tidal cycle, time of day, and weather.

An open-array Furuno marine radar unit has been operating nearly continuously at the FORCE site since 2015. The radar was deployed to monitor the flow of water and turbulence at the FORCE site, however bird targets were also evident on the scans. The radar scans have been archived in two formats, initially in SQLite databases, and more recently in .jpg format. The raw radar scans were converted to .jpgs to save storage space, but in doing so some resolution was likely lost in the compression process. The primary objective of this study was to determine to what extent the existing radar data could be used to monitor seabirds at the FORCE site.

OBJECTIVES

To determine appropriate methodology for extracting bird targets from the radar scans archived in .jpg format from the radar unit at the FORCE site.

To provide a comprehensive analysis of bird use at the FORCE site, summarized by time of day, tidal cycle, and season.

METHODOLOGY

Data Processing

An open array Furuno marine radar unit was installed at the FORCE site in January 2015 to monitor tidal flow in the Minas Passage at the following coordinates (Latitude 45.3714°, Longitude -64.4029°). Scans from this radar unit were archived in SQLite databases until November 2015, and subsequent scans were and continue to be archived in .jpg format. Archived scans were acquired from John Brzustowski on several external hard drives. Analysis of scans was performed using radR program in the R statistical computing language (Taylor et al. 2010, R Core Team 2016). The radR program does not read in scans in either SQLite or .jpg formats, so scans were converted into .mp4 clips of 5-minute duration using the program FFmpeg, which could then be read into radR (FFmpeg Developers 2016). The scope of the project allowed for scans archived in .jpg format to be analysed in this study, but not those archived in SQLite databases. When splicing the .jpg scans into .mp4 clips, FFmpeg settings included a frame rate of 0.46 frames per second, the libx264 codec, and a pad of 1 black pixel (pad=1876:1866:0:0:black) on the side to make the dimensions in an even number of pixels.

Radar data in .jpg format were available between Nov 17, 2015 and July 2, 2016, and between May 22, 2017 and April 11, 2018. The hard drive containing scans between July 2016 and May 2017 was not obtained. Though radar data presently continue to be archived at the FORCE site, .jpgs were converted to .mp4s on Apr 11, 2018, hence the end date. The available radar data were subsampled to obtain 5-minute clips from four times of day (sunrise, three hours after sunrise [morning], three hours before sunset [afternoon], and sunset) thought to represent diurnal sea bird activity at the site. Clips from these four times of day were taken from one day per week throughout the year, and were selected from the day of that week that had the lowest average wind speed during diurnal hours. While the effects of wind and wind direction were of interest on sea bird use, it was clear after initially processing numerous clips from randomly selected days that the birds were not readily detectable over the waves when it was windy. Historic weather data were obtained for the Parrsboro, NS weather station from the Environment and Climate Change Canada website (http://climate.weather.gc.ca/climate_data/) to determine days with little wind and precipitation, and for use in the data analysis. Dates with >5mm of precipitation were not considered due to the difficulty in filtering rain or snow from the radar data. By selecting clips from these four times of day and the range of dates, it also ensured that each stage of the tidal cycle would have adequate representation. Tide predictions were calculated for Cape Sharp using the following website: tides.mobilegeographics.com. Based on the above criteria, 305 clips were created and processed (some of the time periods were missing

data on some days), though only 294 clips contained usable data due to radar malfunctions, fog, or other unknown reasons.

Each clip was read into radR using the video plugin, and processed using the radR settings shown in Appendix 1. The settings were selected after much trial and error specifically to reduce the effects of interference from waves on the surface of the water. Radar scans from the FORCE site are collected with an open-array antenna which records data in two dimensions, range and bearing, so objects detected at all altitudes are combined in a single plane. Additionally, the radar unit at the FORCE site was set up to intentionally detect the surface of the water, so there is significant amount of wave interference on most clips. The declutter plugin in radR was used to eliminate areas with persistent wave interference, which varied in each clip depending on wind speed, wind direction, and tidal stage. A separate clutter map was created for each clip, and was used to filter out waves on that clip and saved for use in the analysis. Additionally, the radar data were filtered to include only blips from within four kilometres of the radar, as there was an increasing amount of noise beyond that range.

Once the most problematic areas with persistent waves were removed from each clip, it was possible to use the tracker plug-in in radR to track flights of individual birds. The multi-frame correspondence algorithm was used, with the settings shown in Appendix 1, and the resulting tracks were saved in a .csv file. Finding appropriate settings that tracked birds effectively without producing unwanted tracks using blips from waves and other clutter was a difficult task, and the optimum settings found were a balance between the false positive and false negative tracks. The optimum settings were identified, however the process could not be fully automated due to excessive noise from the surface of the water, and manual corrections for false positive and false negative tracks were necessary. Specifically, each clip was watched as it was processed using the declutter, tracker, and blip trails (displays blips from previous scans in a different colour to help visualize tracks) plugins. The tracker plugin displays tracks it identifies by drawing a line through them on the plot of the radar scans. Tracks arising from clutter (false positives) were identified and deleted, and the beginning and endpoints of visible tracks not picked up by the tracking algorithm were recorded. An example of a clip being processed in radR is included in a separate .gif file as Appendix 2. Tracks are displayed in orange and blip-trails in green.

Data Analysis

Average velocities and bearings were calculated for tracks recorded by the tracking algorithm in radR. Tracks with average velocities below 20 kilometers per hour (kph) and bearings between 100 and 125 degrees or between 280 and 295 degrees were considered to be objects floating with the tides, and were removed from the other track data prior to further analysis. To determine the effects of date, time of day, and tidal stage on bird activity in the area, a general additive model was created using the package mgcv in R (Wood 2011). The number of tracks on a clip was the response variable, and predictor variables included a circular smoothed term for Julian day, the size of the wave clutter file (in Kilobytes), an interaction between tidal stage (factor with six levels) and time of day (factor with four levels), and an interaction between wind speed (hourly average kph from time of clip) and wind direction (factor with nine levels). The size of the

clutter file from the declutter plugin is representative of the amount of wave clutter on each clip, so this term was used to account for the amount of interference from waves. The tidal stages used are as follows: High (one hour before to one hour after high tide), High Falling (one hour after high tide to mid tide), Low Falling (mid tide to one hour before low tide), Low (one hour before to one hour after low tide), Low Rising (one hour after low tide to mid tide), and High Rising (mid tide to one hour before high tide). The factor for wind direction included the directions: N, NE, E, SE, S, SW, W, NW, and a level for calm for which no wind direction was specified. A negative binomial distribution was used for the model as the counts of tracks were overdispersed, and the model fit much better than it did with a Poisson or quasi-Poisson distribution. Predicted values were calculated using the model to aid in interpretation of plots, and used the average amount of clutter, wind speeds of 0, 5, 10, 15, and 20 kph, and the full range of values for other variables. Data from multiple years were included in the model, however there was insufficient overlap in dates between years to model separate year effects.

RESULTS

Number of tracks

Bird flights were detected on 233 of the 294 (79%) clips processed. Most of the clips lacking birds had high levels of wave interference, however there were several clips from calm days that also lacked birds. A total of 12,753 tracks from birds were recorded, with an average of 54.84 tracks per clip on clips where at least one track was detected. Of the 12,753 tracks detected, 10,928 were identified by the tracking algorithm in radR and an additional 1,825 (14%) were detected manually. The maximum number of tracks detected on a clip was 628. The raw number of tracks detected by date is depicted in Figure 1, however these numbers are not corrected for the amount of clutter, wind, tide, or any other variables considered. An additional 1005 tracks were detected that were considered to be floating objects (Figure 2). While some of these tracks could have been birds sitting on the surface of the water, we have no way to distinguish them from other floating objects. Birds were detected up to the range cut-off of four kilometers, however there appeared to be a decrease in detection probability at ranges over one kilometer (Figure 3). Beginning and end points of tracks were plotted to determine core areas of bird activity, but the only clear pattern indicated that the area of water between Black Rock and the small inlet west of the FORCE site was heavily used (Figure 4). Similar plots were also examined with tracks separated by time of day and tide, but none of these plots indicated a pattern different from the overall pattern, and are not depicted.

Effects of date, time, tide, and wind

The general additive model considered the effects of multiple explanatory variables simultaneously, including the effects of wave interference, to enable interpretation of the effects of each variable separately after the effects of the other variables had been accounted for. The model converged with an adjusted R^2 of 0.347 and 65% of the deviance explained, and all terms including the interactions were statistically significant at $\alpha = 0.05$ (Table 1). Estimates of parametric coefficients are shown in Table 2. The term for clutter is the most explanatory, which was expected due to the strong influence of wave interference on the ability to isolate tracks from birds. The smoothed term for date was highly explanatory ($\chi^2_8 = 234$, $P < 0.0001$), and

predicted values for the effect of date are shown in Figure 5. It was clear from the model, and the raw data, that there are very few bird tracks in the winter, and that the number of tracks increases markedly in March (Figures 1 and 5). An influx of spring migrants begins in March and peaks in late May, followed by a period of high activity in summer. There is another peak in late summer and early fall depicting fall migrants, which gradually tails off as winter approaches. A violin plot of track velocities by month helps document the presence of migrants, which should have higher track velocities than resident or breeding birds (Figure 6). Velocities are highest in March and April when many sea birds are migrating, and nearly bimodal in May when both migrant and breeding birds are present. Velocities in the summer are generally low, but increase again in the fall.

The effects of time of day, tide, and wind were not as easily interpretable due to the complex nature of the system involving multiple species of birds and their behaviours related to tidal cycles, times of day, and weather patterns. Two 2nd order interactions were modeled, both of which proved to be statistically significant, however these still likely downplay the complexity of the system. The interactions are most easily interpreted by plots of predicted values. Figure 7 depicts the interaction between time of day and tidal stage, and Figure 8 illustrates the interaction between wind speed and wind direction. The interaction between time of day and tidal stage indicates that bird species behave differently each day depending on the timing of the tides. A high tide in the afternoon, falling tide in the morning, or a low tide at sunset seem to produce the highest number of tracks (Figure 7). Strong winds from the SW or SE produce large numbers of bird tracks, but winds from due S or other directions do not have the same effect (Figure 8).

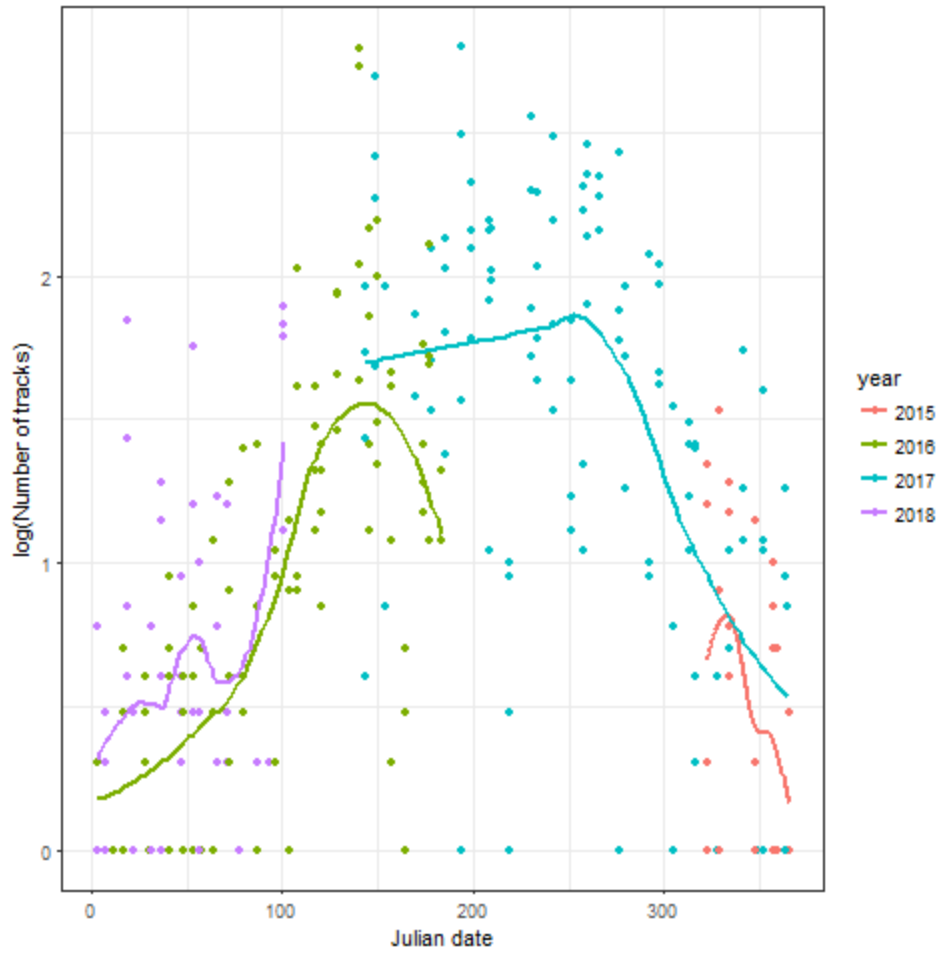


Figure 1. The number of tracks (\log_{10} scale) detected on each five-minute clip, by Julian date, including a separate smooth for each year.

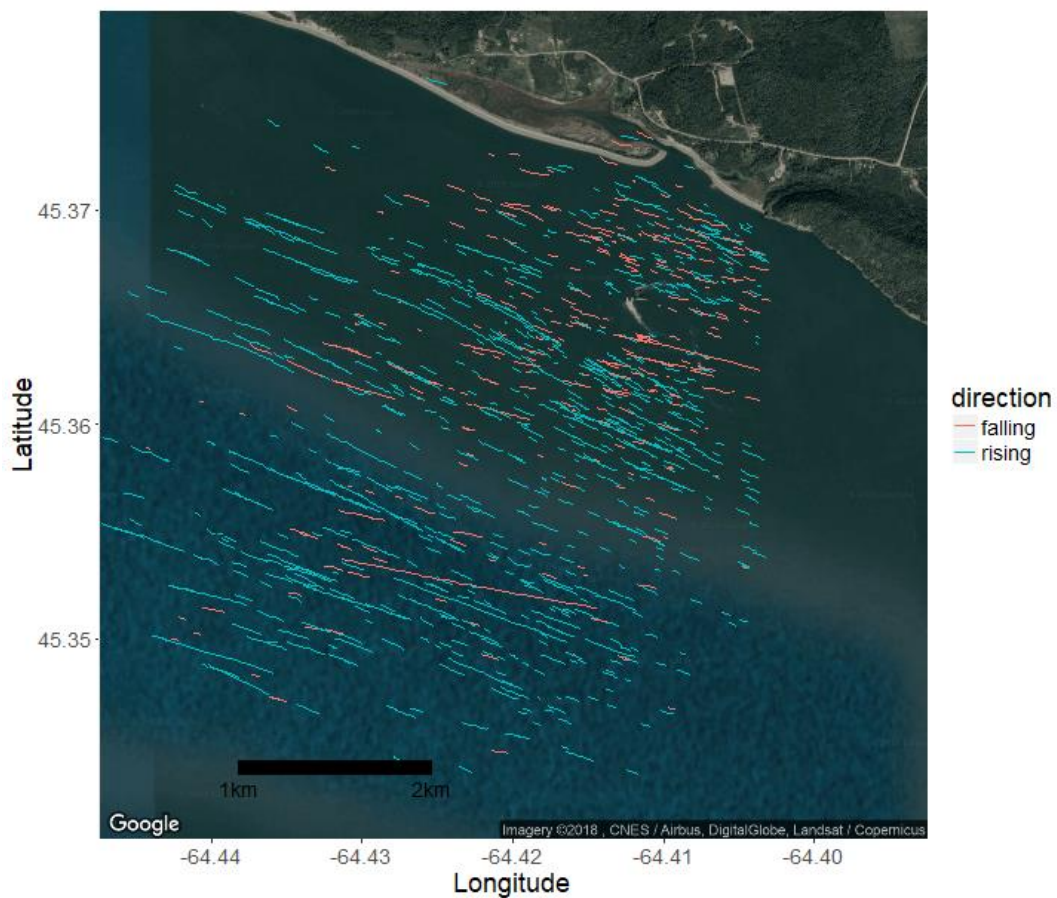


Figure 2. Map of tracks classified as floating objects, separated by tidal direction.

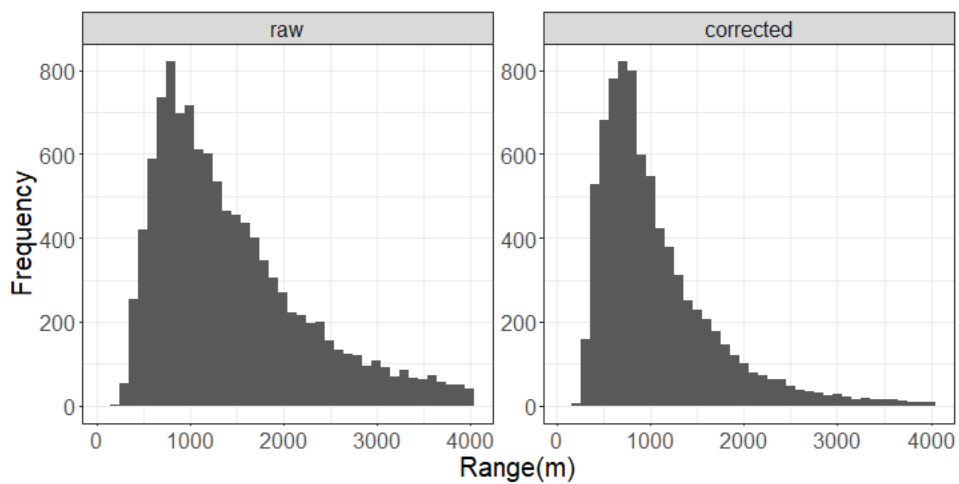


Figure 3. Histogram of the number of tracks detected by range. The left panel is the raw number of tracks and the right panel is corrected for the area sampled, which increases with range.

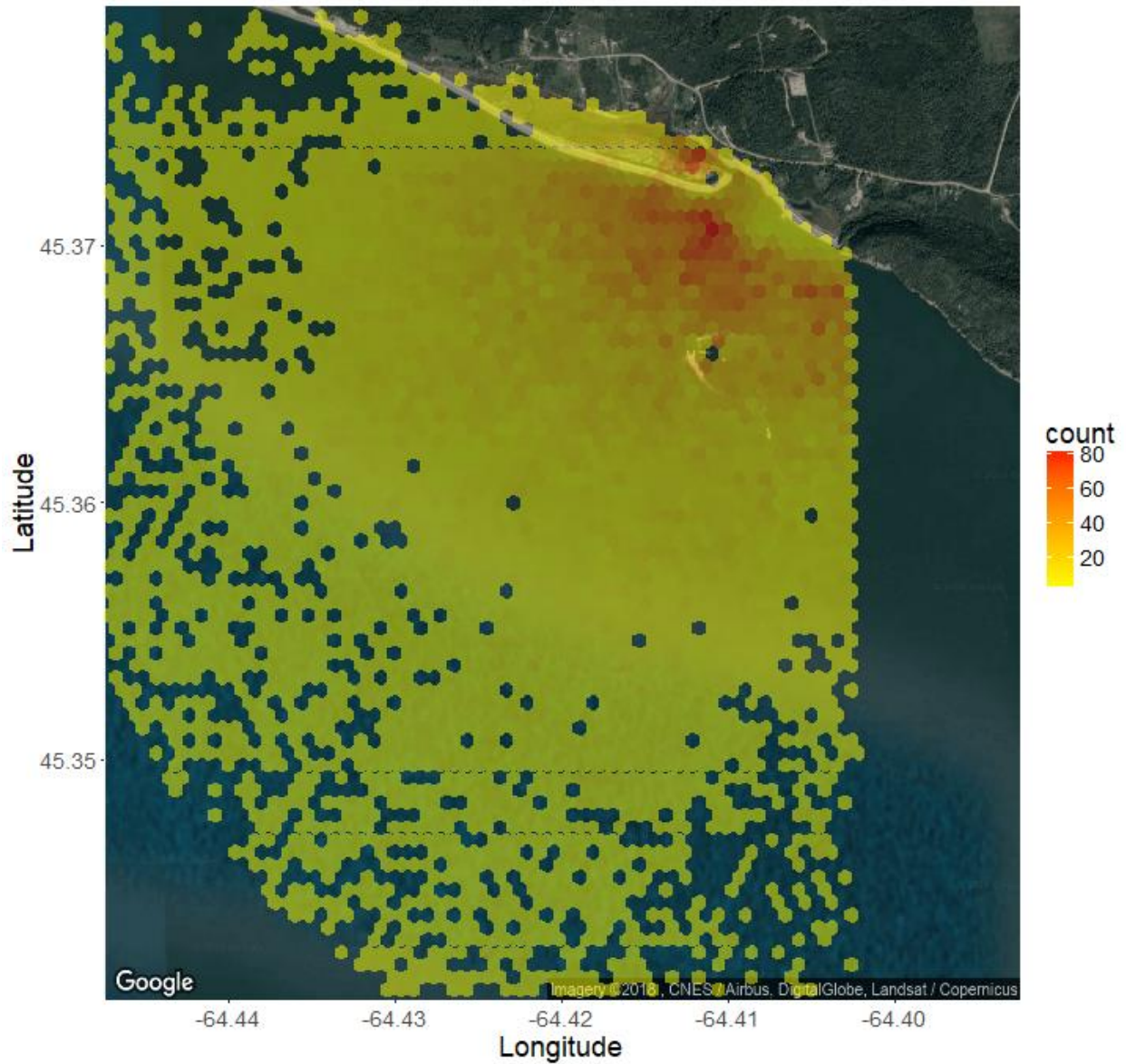


Figure 4. Map showing density of beginning and end points of bird tracks detected by the radar. The colors represent the number of tracks in each hexagonal bin.

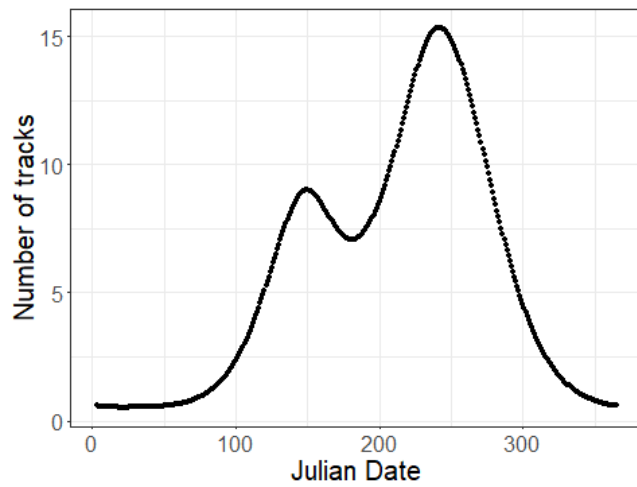


Figure 5. Predicted values from the general additive model for number of tracks by Julian date. The y-axis ticks are arbitrary, and based on the levels of the other variables in the model, but the relative effect of date remains constant. In this case, the levels of the other variables were: an average amount wave interference, at sunrise, at high tide, and with a north wind of 10kph.

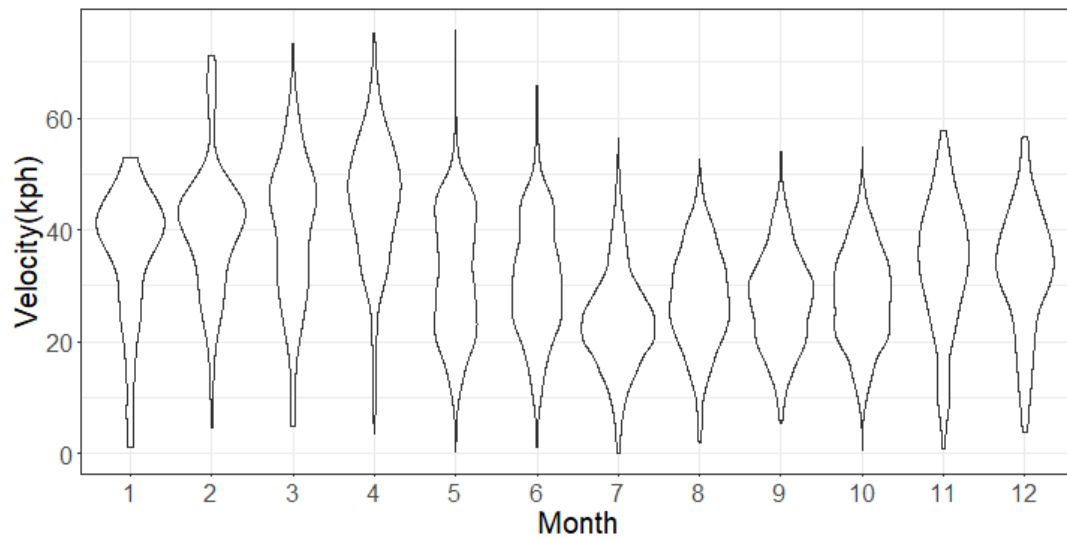


Figure 6. Violin plot showing histograms of track velocities by month.

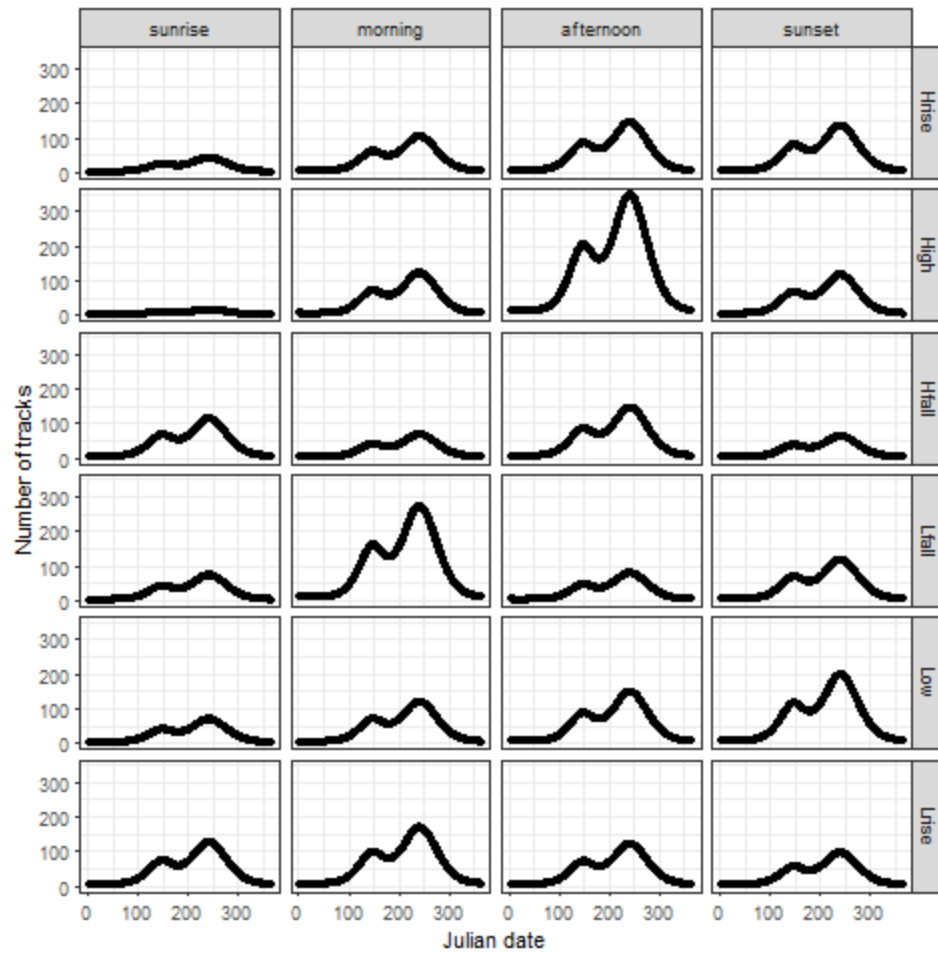


Figure 7. Interaction plot showing the number of tracks by Julian date for each combination of tidal stage and time of day.

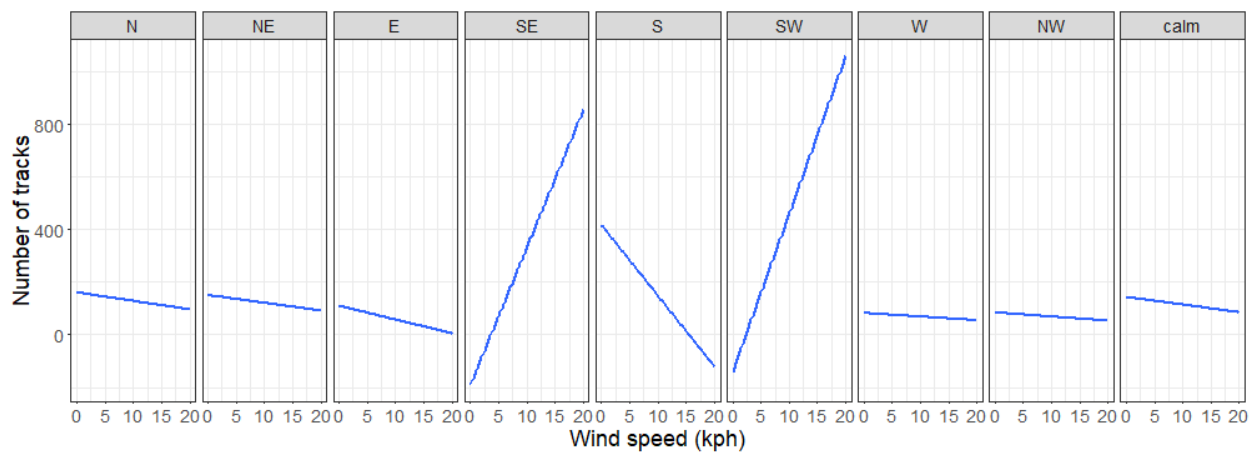


Figure 8. Interaction plot showing the how the effect of wind speed varies with wind direction.

Table 1. Anova table from the general additive model showing the degrees of freedom, χ^2 value, and P value for each term in the model.

Term	df	χ^2	P
time	3	18.0542	0.0004
tide	5	12.4602	0.0290
clutter	1	88.1319	<0.0001
wind direction	8	18.6458	0.0169
wind speed	1	0.4858	0.4858
time:tide	15	30.3152	0.0108
wind speed:wind direction	7	14.8963	0.0374

Table 2. Parameter coefficients from the general additive model, with their standard errors (se), t values, and P values. Statistically significant parameters at $\alpha=0.05$ are shown in bold font.

Parameter	Coefficient	se	t	P
intercept	2.9352	0.6941	4.2289	<0.0001
timemorning	2.0641	0.7109	2.9034	0.0037
timeafternoon	3.1177	0.7407	4.2089	<0.0001
timesunset	2.0184	0.7107	2.8401	0.0045
tideHfall	1.9951	0.6996	2.8519	0.0043
tideHrise	1.0004	0.7312	1.3681	0.1713
tideLfall	1.5555	0.7029	2.2130	0.0269
tideLow	1.5029	0.7798	1.9272	0.0540
tideLrise	2.1051	0.7137	2.9495	0.0032
clutter	-0.0058	0.0006	-9.3879	<0.0001
wdirNE	-0.0651	0.6154	-0.1058	0.9157
wdirE	-0.2742	0.6033	-0.4545	0.6495
wdirSE	-2.7550	0.8200	-3.3599	0.0008
wdirS	1.3517	0.9275	1.4574	0.1450
wdirSW	-1.2065	0.7299	-1.653	0.0983
wdirW	-0.6717	0.4410	-1.523	0.1278
wdirNW	-0.6456	0.5930	-1.0887	0.2763
wdircalm	-0.1167	0.3634	-0.3212	0.7480
windkph	-0.0255	0.0366	-0.697	0.4858
time morning:tideHfall	-2.5862	0.8680	-2.9796	0.0029
time afternoon:tideHfall	-2.8656	0.8404	-3.4097	0.0007
time sunset:tideHfall	-2.6125	0.8834	-2.9574	0.0031
timemorning:tideHrise	-1.1587	0.8762	-1.3225	0.1860
time afternoon:tideHrise	-1.8739	0.8939	-2.0962	0.0361
timesunset:tideHrise	-0.8499	0.8867	-0.9585	0.3378
timemorning:tideLfall	-0.7446	0.8614	-0.8644	0.3874
time afternoon:tideLfall	-3.0377	0.8833	-3.4391	0.0006

Parameter	Coefficient	se	<i>t</i>	<i>P</i>
timesunset:tideLfall	-1.5359	0.8341	-1.8415	0.0656
timemorning:tideLow	-1.5117	0.9050	-1.6703	0.0949
timeafternoon:tideLow	-2.3483	0.9385	-2.5021	0.0123
timesunset:tideLow	-0.9676	0.9364	-1.0332	0.3015
timemorning:tideLrise	-1.7710	0.8549	-2.0716	0.0383
timeafternoon:tideLrise	-3.1605	0.8746	-3.6137	0.0003
timesunset:tideLrise	-2.3006	0.8645	-2.6611	0.0078
wdirNE:windkph	0.0008	0.0899	0.0091	0.9928
wdirE:windkph	-0.0763	0.0931	-0.8198	0.4123
wdirSE:windkph	0.2615	0.0993	2.6334	0.0085
wdirS:windkph	-0.3510	0.1992	-1.7615	0.0781
wdirSW:windkph	0.1905	0.1037	1.8378	0.0661
wdirW:windkph	0.0052	0.0530	0.0989	0.9212
wdirNW:windkph	0.0025	0.0751	0.0339	0.9730
wdircalm:windkph	0	0	NA	NA

CONCLUSIONS

Data from the radar unit installed at the FORCE site to monitor currents, waves, and turbulence can be used to effectively monitor bird movements at the site, with some limitations. Bird targets were detected at ranges of at least up to four kilometers from the site. There was some evidence that fewer birds were detected as range increased, however if birds were selectively using areas closer to shore as indicated by the observer-based seabird surveys, it would confound this result. Interference from waves on the surface of the water are a major impediment to the identification of bird tracks, but methods were developed to eliminate areas with persistent wave clutter to enable tracking of birds in other parts of the study area. As a consequence, however, any birds using areas with persistent waves could not be isolated and tracked by the radar. It may be possible to develop algorithms to filter out wave interference while retaining blips from birds flying over the water, but this was beyond the scope of this project. Models using the radar data were corrected for the area obscured by wave interference, but the highly variable level of interference precluded an in-depth analysis of habitat use at the site.

The tracking algorithm in radR successfully tracked many of the birds present, though missed approximately 14% of the total based on manual estimates. Relaxing the settings of the tracking algorithm, such as allowing faster average velocities, allowing larger changes in bearing, or allowing more scans to be missing blips from the tracked target effectively reduced the number of bird tracks missed by the algorithm, but resulted in many spurious tracks consisting of wave clutter. Additionally, the tracking algorithm sometimes assigned multiple tracks to the same bird, which happened if the bird changed velocities, turned abruptly, or disappeared from the radar by passing behind a wave or by passing through an area filtered out by the declutter plugin. Also, any birds that landed and then later took off would be assigned a new track. As a

consequence, the number of tracks presented in the results should not be interpreted as the number of birds detected during a five minute clip, but as a record of activity that should be reflective of and proportional to the number of birds present.

The results clearly show a seasonal pattern of activity at the site across years. There are very few birds present at the site during the winter, and peaks of activity during spring and fall migration are obvious. Bird activity at the site during the summer months is much higher than during the winter. There was no clear pattern of how birds use the site at different tidal cycles or times of day, though it was clear that both tidal stage and time of day do have effects on the number of bird flights at the site. This is likely due to the multitude of species that use the site which varies by season. Adding a seasonal component to the interaction between time of day and tidal stage might tease out some of these differences, but the added complexity would require an enormous quantity of data and would be difficult to interpret. The interaction between wind speed and direction matched our expectations, showing that strong SW winds blow seabirds into the inner Bay of Fundy, and strong SE winds aligned with the shorelines of the Minas Passage increased the number of birds present. There is likely a seasonal component to this interaction as well, but adding another variable to this interaction would increase the complexity of the model markedly. Many of the clips with numerous tracks come from the summer months, so the effects of the interactions between time of day and tide and between wind speed and direction may be driven by the dominant species present then, namely gulls and cormorants (FORCE 2018).

One major limitation of the radar data is that it is difficult or impossible to determine the species of birds tracked by the radar. It may be possible to differentiate some species based on the size of the blips and speed of the tracks, but there will always be a need for observer-based surveys to accurately determine species composition, and how different species utilize the site. The radar data largely agreed with the observer-based seabird surveys in terms of seasonal peaks in activity, however the radar data indicate higher levels of activity in the summer than the observer based surveys (FORCE 2018, Figures 1 and 3). Additionally, radar data from multiple years indicated that there were large quantities of birds present at the site in late May. To date, none of the observer-based surveys have been conducted in late May, so these large flights of birds have not been recorded by the monitoring program. Future observer-based monitoring should continue, and should use the results of this radar study as a guideline for scheduling survey dates so they coincide with periods of peak activity. Weather should be considered when scheduling these surveys, since SE and SW winds can have marked effects on the number of tracks detected.

RECOMMENDATIONS

Effective monitoring of sea birds using radar is inextricably dependent on filtering wave-clutter from the data. Many sea birds fly at low altitudes, often in the troughs of waves, so there is no effective way to detect sea birds without also detecting the surface of the water. To specifically monitor birds, data from a dish antenna may be easier to analyze and interpret than those from an open array antenna since the scans and data are recorded in three dimensions, including altitude. This would likely facilitate the separation of bird targets from waves, but would require running a separate radar unit specifically to monitor birds. Classifying tracks to species would

still be nearly as difficult as with an open array antenna, but there would be additional information from the scans that could be used.

If bird monitoring via radar is to continue but using data from an open array antenna, the next advancement would be to develop an algorithm for detecting birds in sectors of the radar sweep with wave clutter. For the tracking algorithms to work effectively, the blips from waves will need to be removed while retaining those of the birds above the waves. This will be a complex and difficult task, especially considering that it is not possible to visually discern the blips from birds from the background noise with the human eye on the radR display. If wave clutter can be effectively filtered out, it would be possible to automate the processing of the radar data. This would provide a nearly complete record of bird activity at the site since 2015, allowing full analyses of inter-annual variability more detailed analyses of variation by weather, tide, and time of day. Additionally, modifications to the radR code should be made to allow .jpg files to be read into the program directly, so that .jpgs do not need to be spliced into videos prior to analysis. This modification would not only save time and computing power, but would preserve time stamp information included in the .jpg files.

Determining effects of a bottom-mounted turbine on sea birds at the FORCE site is very complex, especially due to the variation in sea bird abundance and behaviour by season, tidal stage, time of day, and weather. Each species of sea bird may need to be considered separately, since they use the site in different ways and are present at different times of year and under different weather conditions. Risk to birds would likely be restricted to diving species, though some species may be deterred from using the site by increased waves, noise, or turbulence. Some species could change their feeding patterns if there is an effect on fish or invertebrate species caused by the turbine. Detecting such varied effects in an already highly variable system will require careful thought as to which species are of interest and what the potential effects of a turbine might be.

LITERATURE CITED

FFmpeg Developers. 2016. ffmpeg tool (Version be1d324) [Software]. URL: <http://ffmpeg.org/>

Fundy Ocean Research Center for Energy (FORCE). 2018. Environmental Effects Monitoring Program. Annual Report 2017. URL: fundyforce.ca/wp-content/uploads/2012/05/Q4-2017-FORCE-EEMP.pdf

R Core Team. 2016. R: A language and environment for statistical computing. R Foundation for Statistical Computing, Vienna, Austria. URL: <https://www.R-project.org/>

Taylor, P.D., J.M. Brzustowski, C. Matkovich, M. L. Peckford, D. Wilson. 2010. radR: an open-source platform for acquiring and analysing data on biological targets observed by surveillance radar. *BMC Ecology* 2010, 10:22; doi:10.1186/1472-6785-10-22.

Wood, S. N. 2011. Fast stable restricted maximum likelihood and marginal likelihood estimation of semiparametric generalized linear models. *Journal of the Royal Statistical Society (B)* 73(1):3-36.

APPENDIX 1. TABLE OF radR SETTINGS USED FOR PROCESSING DATA

Plugin	Setting	Value
Video	frame rate	0.46 frames/sec
	image width	1876 pixels
	image height	1866 pixels
	x offset	-936 pixels
	y offset	-273 pixels
	scale	4.8 m/pixel
Antenna	angle of beam above rotaion	0 degrees
	horizontal aperture of beam	1 degree
	vertical aperture of beam	1 degree
	bearing offset	0 degrees
	elevation	10 metres
	true range of first sample	0 metres
	latitude	45.4 degrees
	longitude	-64.4 degrees
	rotation axis	90 degrees
Blip processing	tilt	0 degrees
	noise cutoff	0
	find blips	on
	learning scans	15
	update stats every scan	on
	exclude stats from blip update	on
	old stats weighting	0.95
	hot score threshold high	2.5
	hot score threshold low	-128
	samples per cell	4
	pulses per cell	4
	blips extend diagonally	off
	blip centroids by area not intensity	off
	filter blips	on
	min blip samples	8
	max blip samples	5000
	min blip area	150
	max blip area	20000
	min angular span	1
	max angular span	-1
	min radial span	1
	max radial span	-1

Plugin	Setting	Value
Blip processing	filter by logical expression	on
	logical expression	$\text{int} > 0.08 \ \& \ \text{sqrt}(x^2 + y^2) < 4000 \ \& \ 2 * \text{aspan} > \text{rspan}$
Declutter	blip cutoff for mean occupancy rate	0.03
Tracker controls	minimum number of blips required for a track	4
	maximum speed of tracked objects	80 kph
	minimum number of blips before track is plotted	4
	how long to retain plots of complete tracks	300
Multiframe correspondence controls	number of scans to backtrack over in building tracks	4
	weight of directional coherence vs proximity to prediction	0.64
	maximum gain for a blip to join a track (log units)	19
	small penalty for blips missing from tracks (gain units)	0

Appendix IV

Marine fish monitoring at FORCE: Updated report on processing and analysis

Marine Fish Monitoring at FORCE:

Updated Report on Processing and Analysis

Historical Dataset: August 2011 thru May 2012

and

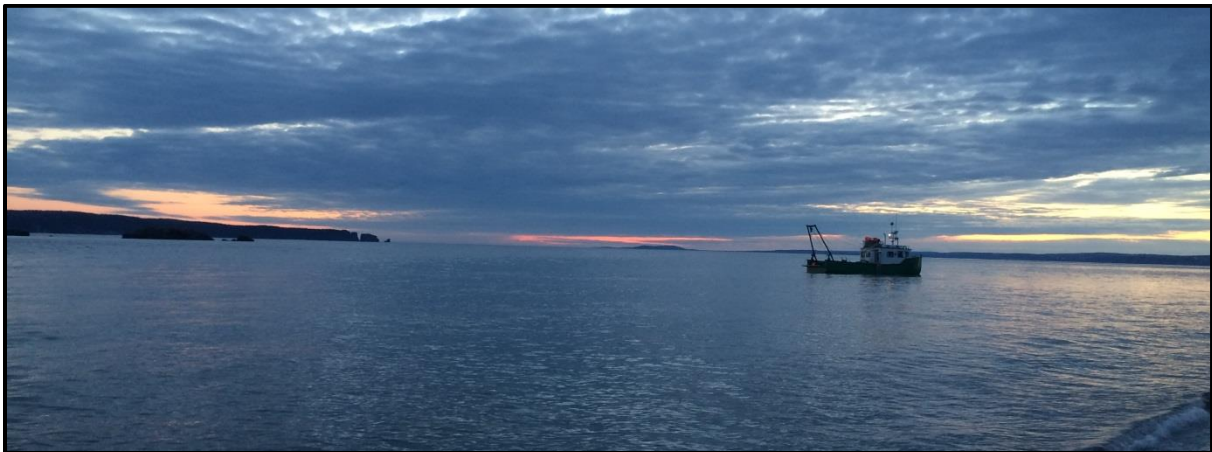
Contemporary Dataset: May 2016 thru August 2017

Prepared by: Louise P. McGarry, Ph.D. and Gayle B. Zydlewski, Ph.D.

University of Maine, School of Marine Sciences

May 2, 2019

Update: June 12, 2019 (Appendix C only)



Executive Summary

This is a report of the Environmental Effects Monitoring Plan (EEMP) for sixteen hydroacoustic fish surveys conducted in Minas Passage between August 2011 through August 2017. Six surveys were led by Dr. Gary Melvin between August 2011 and May 2012 (herein “historical”). The nine FORCE-funded surveys were conducted between May 2016 and August 2017 (herein “contemporary”).

The four main objectives of this report are to:

1. provide FORCE personnel information relevant to understanding the historical and contemporary datasets, including technical guidance.
2. convey to FORCE a set of scripts that can be used to automate preparation of hydroacoustic data for analyses.
3. provide examples of data visualizations, including a case study example of drilling down into the data to gain insight into the summarized data.
4. provide a statistically rigorous analytical *approach* to quantifying the relationship between observed volume backscattering strength (S_v : proxy for fish density) and predictor variables (e.g., site, season, tide phase). *This approach was designed and approved by a University of Maine statistician.*

An overall *approach* to understand the information contained within the hydroacoustic datasets, including data visualization and statistical analyses are detailed in the report. In addition, the scripts with coding for the analytical approach and data visualizations are provided such that deeper explorations of the data may be taken to investigate questions specific to the needs of FORCE. Selected results are presented below.

Because of the large percentage of “zero” observations (59%) contained in the dataset, the analytical steps were separated into two steps: (1) implement a statistical modeling approach (GLM) to examine fish presence:absence in relation to the predictor variables, and (2) implement a statistical test (ANOVA) to examine relative fish density (backscattering strength, S_v , as proxy) in relation to the predictor variables. The predictor (or explanatory) variables available in the dataset were: temporal (historical vs. contemporary, or by survey), spatial (CLA vs. reference study area, or by transect), and environmental (tide phase, diel state, or with and against predicted tidal flow). Metrics of interest, such as minimum, maximum, mean, and median S_v as well as the estimated marginal means used in the relative fish density analyses are included within the report.

Highlights from the analytical approaches for understanding how fish presence:absence and relative density compare for the following data aggregation levels:

1. Research Program, the data collected included historical (2011-2012) and contemporary (2016-2017) data, when compared:
 - highest maximum relative fish density was observed during the contemporary program
 - the probability of observing fish was higher during the contemporary program (42.8%) and statistically differed from the probability of observing fish during the historical program (31.5%)
 - relative fish density during the contemporary program was statistically different from the relative fish density during the historical program

Implications: Based on both metrics (presence:absence and S_v), the historical and contemporary datasets were statistically different. The differences may be artifact due to differences in survey design and execution, and therefore the datasets are simply not comparable, or the differences may signal that fish use of the site has changed. Additional analyses would need to be conducted to examine whether or not future comparisons with the historical dataset would be constructive. Given the statistical differences between the historical and contemporary research programs, the remaining analyses were conducted using the **contemporary dataset only**.

2. Study Area, data were collected in two distinct locations, CLA and reference, when compared:
 - highest maximum relative fish density was observed in the CLA study area
 - the probability of observing fish was higher in the CLA study area (44.9%) and statistically differed from the probability of observing fish in the reference study area (38.4%)
 - relative fish density within the CLA study area statistically differed from within the reference study area

Implication: The statistically significant differences between the CLA and reference site may indicate that the reference site is not sufficiently representative to serve as reference for the CLA.

3. Tide Phase, data were collected during the following stages: high-slack, ebb, low-slack, flood, when compared:
 - highest maximum relative fish density was observed during low-slack
 - the probability of observing fish was highest during the ebbing tide flow (49.3%) and statistically differed from the probability of observing fish during any of the remaining three tide phases
 - relative fish density observed during the ebbing tide flow statistically differed from all other tide phases

Implication: The ebb tide is an important tidal phase to focus on for an understanding of fish in this site.

4. Diel State, data were collected during the following time periods: dawn, day, dusk, night, when compared:
 - highest maximum relative fish density was observed during the day
 - the probability of observing fish was highest during the night (52.5%) and statistically differed from the probability of observing fish during any of the remaining three diel states
 - relative fish density observed during night statistically differed from observations during all other diel states

Implication: Data collection at night is important for understanding fish presence in this location.

5. Tide Phase and Diel State

Tide Phase and Diel State were used as an example scenario of combining explanatory variables where the effects of the tide phase and diel state add to one another (additive) and where the effects of the tide phase interact with the diel state (interactive):

- variance in the probability of observing fish was better explained (statistically significant) using the complexity of the interaction of the two explanatory variables

Implications: The influence of the variety of predictor variables and their additive versus interactive impact should be further explored.

6. Survey, data were collected during nine contemporary surveys, May 2016 through August 2017, when compared:

- the probability of observing fish and observations of relative fish density varied among surveys
- no seasonal trends were noted

Implications: Given the absence of a seasonal pattern and the preponderance of statistical differences between surveys, it may be advisable to increase sampling frequency within each month, sampling on consecutive days in order to get a finer scale understanding of the patterns and variability of fish presence and density in Minas Passage. May, with its particularly high and wide-range of observed backscattering values and apparently distinctive spatial pattern, appears to be an important month for surveying to continue to gather time-series data to help with interpretation.

7. Transect, data were collected along nine transects, six in the CLA study area (N0, N1, N2, N3, N4, N5) and three in the reference study area (S1, S2, S3), when compared:

- highest maximum relative fish density was observed on transects N0, N1, N2
- probability of observing fish on transect N0 statistically differed from all other transects
- relative fish density observed on transect N0 statistically differed from all other transects
- among the remaining transects there were several pairs of adjacent transects for which the probability of observing fish was not statistically significant
- the spatial pattern of the statistical significance of the observed relative fish density was more complex than the pairs noted in the probability of observing fish

Implications: The adjacent pairing of transects for which the probability of observing fish were not statistically different could provide guidance if a decision was at hand to adjust the survey design to include one of each pair rather than both. The transect groupings as produced by the relative fish density findings must also be considered. Given that these findings were based on highly summarized data (the full contemporary dataset summarized by transect), exploration of the statistical results at finer scales, such as transect data summarized by survey, may provide more robust guidance.

General observations

Within the contemporary dataset, where the number of categories within a predictor variable exceeded two, the statistical results of the presence:absence analysis generally differed from that of the relative fish density analysis in terms of which of the categories statistically differed or not. These findings suggest that the presence:absence ratio of observations was not an indicator of the relative density of fish passing under the transducer.

To gain insight into these findings, further analyses should be conducted on data summarized at finer scales. For example, is night the period of highest probability of observing fish when examined at the level of each monthly survey? Using the scripts provided (to prepare and analyze the data), FORCE personnel can apply the same approach to answer questions pertinent to the needs of FORCE.

It should be noted that echosounder gain settings used in the contemporary dataset were standardized rather than calibrated with each survey. This approach was used because data collection procedures for calibration data were insufficient to provide reliable calibration settings. Calibration procedures were subsequently updated starting with survey 15. For more information see the Calibration Quality Control Report (McGarry and Zydlewski, 2018) and the Notes for EK80 CW Calibration Settings (McGarry and Zydlewski, 2019).

Contents

Executive Summary	2
Introduction	8
Methods	9
Study Area	9
Historical Data: 2011-2012	9
Contemporary Data: 2016-2017	10
Data Processing	12
Full Water Column x 20-m Along-Shiptrack data	12
Analytical Approach	14
Exploratory Data Visualizations	15
Analyses – Fish Presence:Absence	15
Analyses – Fish Density (using S_v as proxy)	17
Results	20
Data Visualizations	20
Analytical Approach: Fish Presence:Absence	31
GLM Output	32
Research Program	36
Study Area	38
Tide Phase	40
Diel State	41
Survey	43
Transect	45
Example: Modeling with Additive and Interactive Explanatory Variables	47
Analytical Approach: Relative Fish Density (as inferred from S_v)	49
Research Program	50
Study Area	52
Tide Phase	55
Diel State	58
Survey	61
Transect	64
DISCUSSION	70
Literature Cited	74

APPENDIX A: Technical Notes	75
Historical Survey Detail	75
Contemporary Survey Detail	79
Survey Characteristics – Historical and Contemporary Surveys	84
Survey Design Notes – Contemporary Surveys.....	86
EV Exported Data Notes – Historical and Contemporary	87
APPENDIX B: Notes Going Forward	88
Cautions – Analytical.....	88
Cautions – Data Processing Procedures.....	88
Cautions – Datasets	90
Cautions – Data Collection (Simrad) and Data Processing (Echoview) Software	90
APPENDIX C: Data Export and Processing Scripts	91
Export Scripts	91
Processing Scripts.....	92
APPENDIX D: Additional Files Transferred with this Report.....	94
APPENDIX E: Glossary and Abbreviations	95

Introduction

In preparation for tidal power development, FORCE-funded 24-hour mobile hydroacoustic surveys have been conducted since May 2016 to establish a baseline understanding of fish presence in the region of the Crown Lease Area (CLA) in Minas Passage. The ultimate goal of the hydroacoustic surveys was to collect sufficient data to document changes in fish presence that may be attributed to the presence of devices engineered to convert tidal energy to electricity (e.g. TISEC: Tidal In Stream Energy Conversion devices). Nine surveys were conducted between May 2016 and August 2017. Each survey traversed an established grid of transects, including six transects within the CLA and three reference transects located near the south shore of the channel, outside the region influenced by the presence of turbines in the CLA. Data collected in the reference region were to be used to help interpret changes in fish presence in the CLA. Herein, this dataset will be referred to as the “contemporary” dataset.

In addition to the contemporary dataset, an “historical” dataset of seven surveys was available for inclusion in analyses. The historical surveys, led by Dr. Gary Melvin (Melvin and Cochrane, 2014), were conducted between August 2011 and May 2012. Similar to the FORCE surveys, the historical surveys traversed an established grid: nine transects within the CLA and one reference transect located near the south shore of the channel.

There are four main objectives for this report:

1. provide FORCE personnel information relevant to understanding the historical and contemporary datasets, including technical guidance. That information is contained mainly in the Methods, Results, Appendix A, and Appendix B sections of this document. A glossary and list of abbreviations is available in Appendix E.
2. convey to FORCE a set of scripts that can be used to automate processing of hydroacoustic data (Appendix C), including export from Echoview in a variety of echo integration configurations and the preparation of the exported data for analyses. The processing steps are described in the Methods section of this report and are described more fully in comments internal to the processing scripts. In addition, scripts by which to generate visualizations of the data, and execute analyses are included (Appendix C).
3. provide examples of the data visualizations, including a case study example of drilling down into the data to gain insight into the summarized data. The TISEC presence:absence data were used in this example (see: Results – Data Visualizations).
4. provide an analytical approach to quantifying the relationship between the observed volume backscattering strength (S_v) and the variety of “predictor” variables in the dataset. Because of the large percentage of “zero” observations (59%) contained in the dataset, the analytical steps were separated into two steps: (1) implement a generalized linear model (GLM) to examine fish presence:absence in relation to the predictor variables, and (2) implement an analysis of

variance to examine fish density in relation to the predictor variables (see: Methods – Analytical Approach and Results – Analytical Approach). *This approach was designed and approved by a University of Maine statistician.*

Presented here is an overall approach to understanding the information contained within the hydroacoustic datasets. The scripts are provided such that deeper explorations of the data may be taken to investigate questions specific to the needs of FORCE.

Methods

Study Area

Minas Passage is located at the entrance to Minas Basin. The hydroacoustic survey design encompassed a rectangle approximately 5-km long by 2-km wide, reaching nearly shore-to-shore. A set of transects were executed in the Crown Lease Area (CLA) along with a set of reference transects near the southern shore (Figure 1).

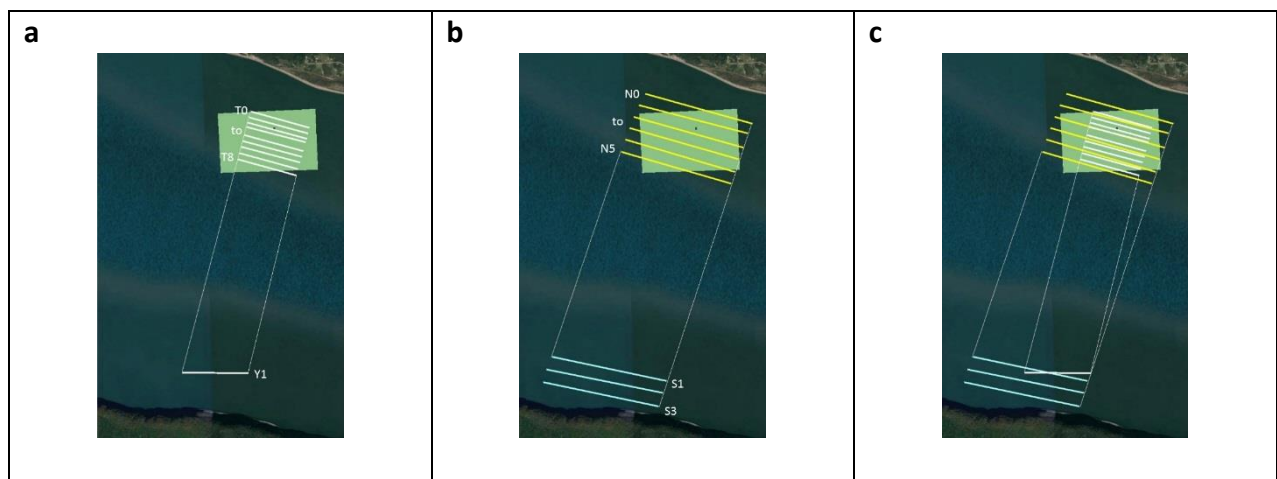


Figure 1. Grid Survey Plan for each Research Program. CLA region is shown as green box for reference. (a) historical survey grid, (b) contemporary survey grid, and (c) historical survey grid superimposed on the contemporary grid to show match/mismatch in survey area.








Historical Data: 2011-2012

In 2011 and 2012, seven mobile hydroacoustic surveys (Table 1) were conducted using a split-beam echosounder (Simrad EK60) operating at 120 kHz using the charter vessel FUNDY SPRAY (Melvin and Cochrane, 2014). The mobile surveys traversed an established grid (Figure 1a) with nine, generally east-west trending, transects (T0 – T8) executed in the CLA study area and one reference transect (Y1) positioned along the 30 m contour across the channel near the southern

shore. Transects were nominally one kilometer in length. During each grid pass, the transects were traversed once, alternating survey direction on each successive line. That is, each transect was traversed in a direction either with the direction of tidal flow or against the direction of tidal flow. Data were collected during the cross-channel transits (X1 and X2) between the CLA and reference study areas. Data from the cross-channel transits are excluded from analysis. No TISEC devices were present during the seven surveys. Herein this dataset will be referred to as the “historical” dataset. Calibration settings provided as Cal2012_120.ecs by Gary Melvin were used as the calibration settings for the historical datasets.

See additional notes regarding the historical dataset in Appendix A: Historical Survey Detail.

Table 1. Historical Surveys. Each survey consists of three to twelve repeats of the grid defined by the following transect lines: T0, T1, T2, T3, T4, T5, T6, T7, T8, X1, Y1, X2. Numbers in parentheses in the Month column indicate grid coverage (partial grids:completed grids). Historical survey data were time-stamped with Greenwich Mean Time (GMT). Time posted to the Start Time and End Time columns are shown in GMT with local time shown in parentheses. Only data collected from “T” and “Y” transects were included for analyses. **Please see extensive notations to this table in Appendix A (Table A1).**

Survey	Month	Start date	Start time	End date	End time	Day/ Night	Temperature (°C)	Turbine presence	Moon Phase Tide Range
1	Aug 2011 (4:3)	2011-08-22	11:45 (08:45)	2011-08-22	21:28 (18:28)	D	15.4	No	 7 m
2	Sep 2011 (4:3)	2011-09-19	10:55 (07:55)	2011-09-19	20:23 (17:23)	D	15.7	No	 8 m
3	Oct 2011 (4:3)	2011-10-03	09:53 (06:53)	2011-10-03	20:18 (17:18)	D	15.0	No	 10 m
4	Nov 2011 (3:3)	2011-11-22	14:22 (10:22)	2011-11-22	22:32 (18:32)	D	10.3	No	 11 m
5	Jan 2012 (10:9)	2012-01-25	18:32 (14:32)	2012-01-26	16:15 (12:15)	D/N	3.6	No	 11 m
6	Mar 2012 (12:11)	2012-03-19	14:23 (11:23)	2012-03-20	13:33 (10:33)	D/N	2.5	No	 9 m
7	May 2012 (5:4)	2012-05-31	12:09 (09:09)	2012-05-31	23:12 (20:12)	D	9.5	No	 10 m










Contemporary Data: 2016-2017

In 2016 and 2017, nine mobile hydroacoustic surveys (Table 2) were conducted by FORCE personnel using a split-beam echosounder (Simrad EK80) operating at 120 kHz using the charter vessel NOVA ENDEAVOR. Each survey traversed an established grid (Figure 1b) of transects similar to the historical survey-grid but differing in some fundamental ways. Transects were

nominally two kilometers in length, generally trending east-west. Unlike the historical dataset, during each grid pass each transect was traversed twice before moving to the next transect line. That is, each transect was traversed once in the direction of tidal flow, “with”, and once in the direction counter to tidal flow, “against”. Six transects were located within the CLA study area and three reference transects were located near the south shore of the channel, outside the region influenced by the presence of turbines in the CLA. Data collected in the reference study area was intended to be used to help interpret changes in fish presence in the CLA. A TISEC device was present during four of the surveys: Nov 2016, Jan 2017, Mar 2017, and Jul 2017 (Table 2). Herein, this dataset collected by FORCE personnel will be referred to as the “contemporary” dataset. See Appendix A for a table summarizing the survey design characteristics for the historical and contemporary datasets (Table A3). Table A4 provides a visual display of the survey timing within each year. See additional notes regarding the contemporary dataset in Appendix A: Contemporary Survey Detail.

Calibration gain parameters for contemporary surveys 1 through 9 were “standardized” such that TransducerGain and SaCorrection were set to Simrad default settings of 27.00 dB and 0.0 dB. The remaining calibration parameters were in keeping with standard practice: Beam pattern settings were as per the Simrad factory transducer measurements upon delivery of the instrument. Survey environmental settings for salinity and temperature were as provided by FORCE personnel. Soundspeed and absorption coefficient were calculated from the measured salinity and temperature using the Echoview Sonar Calculator (Echoview Software Pty Ltd). This approach was used because data collection procedures for calibration data were insufficient to provide reliable calibration gain settings. While this approach is not in keeping with standard practices, and should not be relied upon for future surveys, it was a resolution settled upon after consultation with experts in the hydroacoustic community. Calibration data collection procedures were updated subsequently starting with survey 15. For more information see the Calibration Quality Control Report (McGarry and Zydlewski, 2018) and the Notes for EK80 CW Calibration Settings (McGarry and Zydlewski, 2019).

Table 2: Contemporary Surveys. Each survey consists of 4 repeats of the grid defined by the following transect lines: N0, N1, N2, N3, N4, N5, South_CW, S1, S2, S3, North_FM with calibration files. Contemporary survey data were time-stamped with local time. Time posted to the Start Time and End Time columns are shown in local time. Only data collected from “N” and “S” transects were included for analysis. Please see extensive notations to the table below in Appendix A (Table A2).

Survey	Month	Start date	Start time	End date	End time	Day/ Night	Temperature (°C)	Turbine presence	Moon Phase Tide Range
1	May 2016	2016-05-28	06:01	2016-05-29	05:35	D/N	7	No	 10 m
2	Aug 2016	2016-08-13	09:09	2016-08-14	07:40	D/N	15	No	 7 m
3	Oct 2016	2016-10-07	05:45	2016-10-08	04:21	D/N	15	No	 8 m
4	Nov 2016	2016-11-24	08:38	2016-11-25	09:07	D/N	8.0	Yes	 8 m
5	Jan 2017	2017-01-21	06:55	2017-01-22	05:55	D/N	1.5	Yes	 7 m
6	Mar 2017	2017-03-21	08:24	2017-03-22	06:04	D/N	4	Yes	 7 m
7	May 2017	2017-05-04	19:57	2017-05-05	18:21	D/N	5	Yes (free spinning)	 9 m
8	Jul 2017	2017-07-03	21:34	2017-07-04	19:09	D/N	12	No	 8 m
9	Aug 2017	2017-08-30	18:53	2017-08-31	17:37	D/N	15.7	No	 7 m

Data Processing

Echosounder data files were processed using Echoview (“EV”; Echoview Software Pty Ltd): Version 7 for the historical EK60 dataset and Version 8 for the contemporary EK80 dataset. Data were processed to remove backscatter from the region of the transducer nearfield and from non-biological sources (e.g. bathymetry and entrained air). Minimum thresholds were set for volume backscattering strength (S_v : -66 dB re 1 m^{-1}) and target strength (TS: -60 dB re 1 m^2) as described in Daroux and Zydlewski (2017). More information about processing details is available in the Historical Survey Detail section of Appendix A. Using Echoview, the processed data were then integrated and exported in a variety of echo integration configurations for use in analyses. Additional processing to prepare the exported data for analysis was conducted using R Software (R Core Team 2018), an integrated suite of software facilities for data manipulation, calculation, and graphical display.

Full Water Column x 20-m Along-Shiptrack data

To examine the distribution of relative fish densities throughout the study area, echo integration data were exported from Echoview binned in 20-m along-shiptrack distances, integrated over the full water column (Figure 2), herein referred to as the “20-m dataset”. The 20-m along-shiptrack distance was selected to minimize autocorrelation (Daroux and Zydlewski,

2017). To place the echo integration data within a meaningful environmental context, using date and time as the common variable, the exported echo integration data were merged with a file holding the necessary metadata such as: diel state (i.e. dawn, day, dusk, night: a proxy for light level), tide phase (i.e. ebb, low-slack, flood, high-slack), study area (i.e. CLA, reference site), grid pass (i.e. “1”, “2”, “3”, etc.), transect number (i.e. “T0”, “T1”, ... “Y1”, “N0”, “N1”, ... “S1”, “S2”, “S3”, etc.), data collection direction (i.e. “with” the direction of tidal flow or “against” direction of tidal flow or “along” designating the cross-channel transits), and turbine presence (true, false), among others. Additional steps were required for the historical dataset before the metadata merge could be executed.

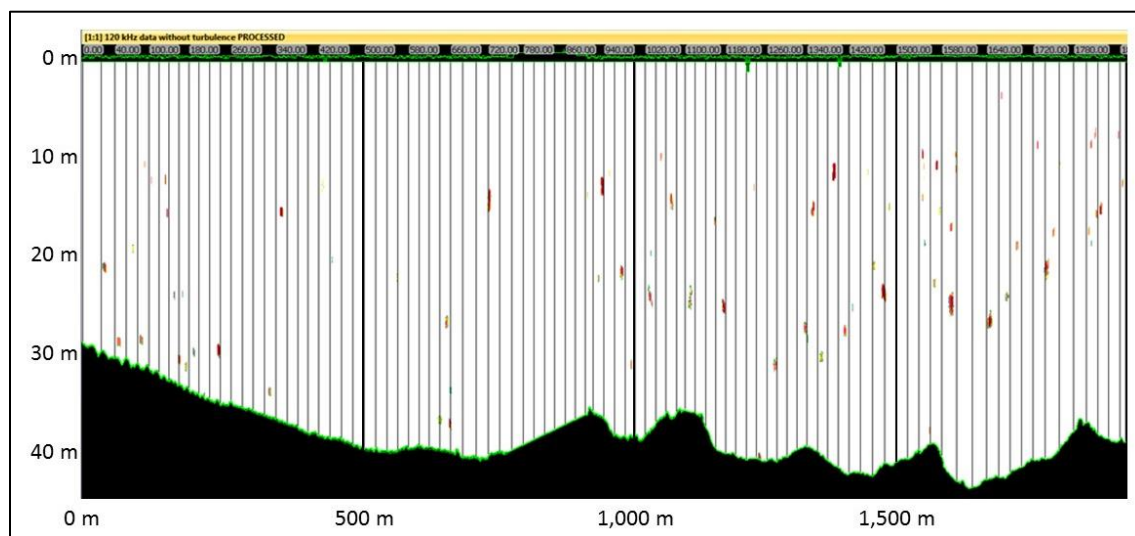


Figure 2. Configuration of the “20-m dataset”. Echogram shows data collected along one example transect. Colored marks indicate recorded backscatter from target in the water column. These are interpreted to be fish or fish aggregations. Vertical lines demarcate the “20-m along-shiptrack distances, over the full water column” integration cells used for analysis. x-axis is distance along transect. y-axis is range from transducer.

Because the historical echosounder dataset and the associated historical datasheets were recorded with “time” set to Greenwich Mean Time (GMT), and because the contemporary data were recorded and will continue to be recorded with “time” set to local time, historical time in GMT was converted to local time for both the exported echo integrated data and the datasheet, paying special attention to periods crossing midnight such that the date was updated as needed, and paying attention to time of year as the conversion from GMT to local time is 3 or 4 hours depending on time of year. With the datasheet populated with local time, the appropriate diel, tide, and with/against phases were posted and the merge then generated a historical dataset with appropriately associated metadata. See notation “2” to Table A1 in Appendix A for more information regarding the conversion of the historical dataset time from GMT to local time.

In preparing the full dataset (historical plus contemporary) for analysis, in addition to appending columns associating the metadata to the echo integration data, columns were calculated from the data exported from Echoview to facilitate calculations (e.g. converting the backscattering strength (S_v) exported by Echoview to its linear form (s_v) using the relationship in Equation 1 (MacLennan *et al.*, 2002). Additionally, commands were executed to exclude data meeting certain criteria such as the “along” data collection direction in order to exclude the cross-channel transit data, and to exclude any “Interval” assigned a value of 0. (See the EV Exported Data Notes section of Appendix A for more information about “Interval”.)

$$S_v = 10 * \log_{10}(s_v) \quad \text{Equation 1}$$

To standardize the number of grid passes per historical survey, which varied from three to twelve passes and not all of which were complete grid passes, three grid passes from each survey were selected for inclusion in analyses, excluding data from all other historical grid passes. See notation “3” to Table A1 in Appendix A for the list of grids included for each survey and notes regarding selection criteria. The derived “20-m dataset” of historical and contemporary data resulted in a dataset of 71,016 observations (11,347 and 59,669, respectively). The analytical variable of interest here is the mean volume backscattering strength (S_v).

Due to logistical difficulties and safety considerations, physical sampling was not available by which to confirm the identity and sizes of the fish generating the observed backscatter. Therefore, in this report we are using the observed mean volume backscattering strength (S_v) as a proxy for relative fish density. “ S_v ” and “relative fish density” are used interchangeably.

Analytical Approach

Data visualizations and analyses were produced using R Software (R Core Team 2018).

The 71,016 datapoints that constituted the “20-m dataset” included 29,105 non-zero S_v values (41%) and 41,911 zero values (59%). A zero-value indicated that no observations above the thresholds were observed in a cell size of 20-m along-shiptrack distance integrated over the whole water column (thresholds: $S_v = -66$ dB and $TS = -60$ dB; Daroux and Zydlewski, 2017). In order to implement analyses for a dataset of which zero values constituted 59% of the observations, a three-pronged approach to the analyses was undertaken. First, a set of data visualizations were constructed to explore the observations contained in the dataset. Second, to investigate the relationship between fish presence and the spatial and temporal variables, integrated S_v values were converted to fish “presence” and “absence” which was then used in the analyses. Third, because the relationships of the magnitude of relative fish density is also of interest, the non-zero S_v values were analyzed in relation to the spatial and temporal variables.

Exploratory Data Visualizations

To gain an understanding of the underlying historical and contemporary data available for spatial and temporal analyses, a series of data visualizations were produced in the form of histograms, boxplots, and frequency plots. The preponderance of zero observations created special challenges for data visualizations due to the data range when including zeros, and the overriding influence of the preponderance of zero-values. Therefore, the produced plots exclude zero values. In addition, the 29,105 non-zero backscattering values available to plot were distributed over a range of nearly 8 orders of magnitude, $3.6\text{e-}12 \text{ m}^{-1}$ to $8.4\text{e-}5 \text{ m}^{-1}$. Calculations were done with the data in linear form (s_v : mean volume backscattering coefficient) and converted to the log form (S_v : mean volume backscattering strength) in order to display the full dynamic range of the data (S_v : -114.4 dB to -40.8 dB). In its log form, a change in S_v of 3 dB represents a doubling (+3 dB) or a halving (-3 dB) in linear terms. A change in S_v of 10 dB indicates a change of one order of magnitude, whereas 20 dB indicates a change of two orders of magnitude. R coding to produce these and other plots are included with this document (Appendix C), including coding to produce the plots with or without zeros and/or using the linear volume backscattering coefficient (s_v).

Boxplot Conventions

The central rectangle in the box plots include the 25th through 75th data percentiles. Thick line indicates median. The mean, calculated in its linear form (s_v), is indicated by an open square. Whiskers are placed at the minimum and maximum extremes of the data unless the range to the extremes are greater than 1.5 times the size range of the box. Where the range to the extreme is greater than 1.5 times the size range of the box, the whisker is placed at the 1.5 distance range from the edge of the box and any datapoints beyond the 1.5x are plotted individually as open circles. All calculations were made with the data in its linear form (s_v) and then converted to its log form (S_v) for display. The physical length of the whiskers, although symmetrical on a linear scale relative to the central rectangle, become asymmetrical when plotted on a log scale.

Analyses – Fish Presence:Absence

To investigate the relationship between the spatial and temporal distribution of the presence of fish and the predictor variables available in the “20-m dataset”, a binary logistic regression was implemented in R using the Generalized Linear Model (GLM) function. The binary logistic regression was chosen because the dataset contained a high percentage of zeros (59%). To prepare the dataset for analyses, a variable called “FishPresence” was created. The variable was populated with “zero” wherever the observed integrated mean volume backscattering strength (S_v) was zero. Wherever S_v was any value other than zero, the variable was populated with “one”. This created a binary “response” variable denoting presence (“1”) or absence (“0”) that could then be evaluated in relation to the “predictor” variables in the dataset. The predictor variables in the dataset were categorical: temporal (historical vs. contemporary, or by survey),

spatial (CLA vs. reference study area, or by transect), and environmental (tide phase, diel state, or with and against the tidal flow). While a 50:50 ratio of fish presence:absence is not intrinsically of biological interest, the 50:50 ratio provides a baseline against which the significance of the differences in fish presence relationships to the explanatory variables can be measured.

The R output from the GLM model includes a table of the coefficients for each of the variables. The first variable listed is designated as the “reference” variable. The results reported in the reference row are in direct reference to the null hypothesis: “Is the ratio of fish-presence:fish-absence equal to 50:50?”. The table includes estimates of the y-intercept of the resulting model, the standard error, and associated p-value for each categorical variable. The closer the presence:absence ratio to 50:50 for the reference variable (the first variable in the list), the closer to zero is the estimated intercept. For a reference variable intercept that is not equal to zero, the p-value for that row will indicate whether the divergence from 50:50 is significant ($p < 0.05$). For all variables other than the reference variable, the values reported in the table are relative to the reference variable. Therefore, the p-values listed on each subsequent row of the table are a measure of the significance in the difference of the fish presence:absence ratio from that of the reference variable.

Given that each subsequent row is reported relative to the reference variable, the sign and magnitude of the values in the y-intercept column give an indication as to whether presence:absence ratio is very different from that of the reference variable and in which direction. The y-intercept for the 50:50 ratio for those variables reported relative to the reference variable is calculated by adding the value in the y-intercept column for the variable of interest to the value in the y-intercept column for the reference variable. The closer the summed y-intercept is to zero is an indication that the presence:absence ratio is closer to 50:50.

To determine whether the presence:absence ratios among the remaining variables statistically differ from each other, the values contained in the table were used to calculate the z-value (a measure of standard deviation providing guidance as to whether to reject the null hypothesis: “Is the presence:absence ratio for variable x equal to the presence:absence ratio for variable y?”) and from the z-values, the p-values were calculated (a measure of the probability that the null hypothesis is falsely rejected).

Example GLM modeling results for presence:absence based on individual predictive variables are included in the Results section of this report. Also included is an additive example where more than one predictor variable was included in the model, and an interaction model whereby the interactive effects of multiple predictor variables was modeled. The results from these examples can be used to guide deeper inquiry into the particulars generating the illustrated relationships at the aggregated levels used here.

Example R code to model FishPresence in the contemporary dataset:

1. using a single predictor variable: Tide Phase
glm.TideC <- glm(FishPresence ~ Tide, data=data_contemporary, family=binomial)
2. using a single predictor variable: Diel State
glm.DielC <- glm(FishPresence ~ Diel, data=data_contemporary, family=binomial)
3. using two additive predictor variables: Tide Phase and Diel State
glm.Tide_DielC <- glm(FishPresence ~ Tide + Diel, data=data_contemporary, family=binomial)
4. using two interactive predictor variables: Tide Phase and Diel State
*glm.Tide_DielCx <- glm(FishPresence ~ Tide * Diel, data=data_contemporary, family=binomial)*

Once the hierarchy of models was generated, an analysis of variance using the chi test was run to evaluate whether the higher complexity (modeling with more than one variable: additive or modeling with more than one variable: interactive) produced a better fitting model than those models lower in the hierarchy.

Example R code:

```
anova(glm.TideC, glm.Tide_DielC, glm.Tide_DielCx, test = "Chi")
```

R coding to implement the GLM modeling is included in the scripts with this document, along with an Excel spreadsheet containing the calculations to calculate the z-values required for calculating the p-value indicating statistical difference between variable pairs that do not include the baseline.

While using the GLM to generate a model by which to predict fish presence:absence using the spatial and temporal variables in the dataset, the relationship of the density of fish to these variables is also of interest. An analysis using the magnitude of S_v (non-zero) values was undertaken to gain insights into the relationship of our proxy for fish density (S_v) to the spatial and temporal variables.

[Analyses – Fish Density \(using \$S_v\$ as proxy\)](#)

To investigate the relationship of the magnitude of relative fish density to the spatial and temporal variables, an analyses of variance (ANOVA) was implemented in R using the non-zero backscattering values of the “20-m dataset” (n=25,536). ANOVA is a robust statistical tool used to test whether there are statistical differences between the means of two or more independent groups. While the calculations for all previous analyses and visualizations were done with the data in its linear form, for the ANOVA analyses the data used in the calculations was the log form (S_v : mean volume backscattering strength) rather than the linear form (s_v : volume backscattering coefficient) (Equation 1). The distribution of the residuals of the linear-form did not approach normality, but the distribution of the residuals of the log-transformed

data (S_v) approached normality and therefore more closely conformed to the normality assumption required by ANOVA.

The ANOVA was used to test the mean of the relative fish densities (non-zero S_v values) for statistical differences between the groupings within the predictor variables. The null hypothesis tested was whether the mean of the S_v values were equal as grouped within the predictor variable levels. The test statistic reported for ANOVA, the f-value, provided a statistical measure of whether the mean of each of those group levels were equal. The f-value tends to be greater when the null hypothesis is false. The p-value was used to assess whether the result was statistically significant. Whereas an ANOVA reports whether a significant difference is present, it doesn't report between which groups a significant difference was found. Therefore, a Tukey HSD (honestly significant difference) test was run. This multiple comparison procedure and statistical test is commonly run in conjunction with an ANOVA as a post-hoc analysis to find the means that are significantly different from each other.

To test that the ANOVA result was robust, a permutation test with 10,000 iterations was implemented in R in which the assignment of the S_v values to the categories within an explanatory variable were randomized. The resulting f-values were compared to the f-value garnered from the initial ANOVA run and the resulting p-value computed. The purpose of the permutation test was to evaluate the probability of observing an f-value magnitude equal to or greater than the f-value from the original ANOVA if the grouping labels were randomized. The null hypothesis tested here was: "There is no statistical difference in the group means of the observed S_v values than would be found in the group means if the assignment of the S_v values to the groups were randomized." Therefore, a resulting "significant" probability ($p < 0.05$) indicated that the original groupings of S_v values were not likely to occur by chance and that the ANOVA result from the original test was robust. A probability result (p-value) of $1e-4$ (i.e. 0.0001 or 1 in 10,000) indicates that of the 10,000 permutations, in no case was the f-value equal to or greater than the original ANOVA f-value results.

Sample sizes with particularly pronounced imbalances in the count of observations can cause statistical testing to become sensitive to very small and inconsequential differences. Given that categories within some explanatory variables had very pronounced differences in the number of observations, an estimated marginal means (EMM) test was implemented in R. The purpose of calculating EMM was to mitigate the effects of imbalances in the number of observations by estimating what the marginal means would be if the number of observations had been balanced. The EMM were then tested for differences. A test for difference is then carried out with the equally weighted means. "emmeans" as implemented in R uses a confidence level of 0.95 and a significance level (alpha) of 0.05. The EMM model was populated with the model results from the ANOVA. The estimation of the marginal means and the subsequent test for differences will be referred to as the "estimated marginal means test" herein.

Note that while the EMM test addresses the mathematical imbalances, the underlying assumption is that there is no bias implicit in the difference in the amount of time spent sampling: for example, one hour of observations at slack tide (defined as the half hour preceding and following the predicted high or low slack) versus five hours of observations during the periods of flooding or ebbing flow. To test for the presence of bias versus biological differences inherent in the different flow regimes, these analyses can be run again using a selection of one hour's data from the flood and ebb time periods, such as the hour prior to and following the designated slack period and then run again using the hour at peak flow for the ebb and flood flow regime.

For the analyses implemented here, while the mean of the log-transformed data would be difficult to convert into biologically meaningful information, the calculated (or estimated) mean does provide a baseline against which the significance of the differences in relative fish density relationships between the explanatory group levels can be measured. In a log-transformed state, the high outliers (orders of magnitude) are de-emphasized such that the mean of the log-data is lower in magnitude than the mean of the linear-data log transformed (i.e. converted to S_v for reporting). Therefore, the log-means as reported in the tables associated with the fish density analyses were lower than the linear-means reported in the Data Visualizations section of this report.

A compact letter display (CLD) table was generated using the EMM results. For each of the categories within the predictor variable, the CLD tables report the EMMs, standard error, degrees of freedom, lower and upper boundaries of the confidence interval, and a "group number". (Note: although the command to display the table is "cld" (i.e. compact letter display), R uses group numbers rather than group letters.) If a group number appears in one row only, the EMM of the associated category is statistically different from the EMMs of all other categories. If a group number is reported in more than one row, the EMMs of the associated categories do not statistically differ.

The EMM along with bars indicating the confidence interval were plotted. Generally, when comparing two parameter estimates, in this case the EMMs, it is always true that if the confidence intervals do not overlap, then the difference between those statistics (the EMMs) will be significant. However, the converse is not true. That is, one cannot determine the statistical significance of the difference between two statistics based on overlapping confidence intervals. Therefore, to indicate the statistical comparison between the estimated marginal means, the comparison interval was also plotted. Where the comparison intervals overlap, the difference between the EMM was not statistically significant.

To provide a visual representation of the data underlying the ANOVA analyses, the data in their S_v (log) form were plotted as notched boxplots for each category within the explanatory variable examples.

Notched Boxplots

The boxplots included with the results for ANOVA analyses follow the conventions as described in the Exploratory Data Visualizations methods section of this report with the following exceptions. The “notched” form of the boxplot was used, and all calculations were made with the data in its log form (S_v). Relative to the exploratory data visualization boxplots that were calculated using the linear-form data (s_v) and plotted with a log-scale y-axis, calculating the boxplot using the log-form data does not affect the position of the upper and lower boundaries of the box or the placement of the minimum, maximum, or median magnitude, but calculating the mean and the length of whiskers using the log-data does affect their positions.

If you compare the plots calculated in log-form to the plots calculated in linear-form, you’ll note that in the linear form there are far more outliers plotted beyond the ends of the whiskers and that the mean of the log-transformed data plots closer to the median. The mean on the notched boxplots are plotted as a star to indicate that the underlying calculation (mean of the log-transformed data) is different than the underlying calculation of the Data Visualizations boxplots for which the mean was calculated using the linear-form data and then transformed to the log form for display (plotted as an open square on those boxplots).

The notches included in the notched boxplots indicate the confidence interval around the median. Although not a formal test, if the notches of two boxes do not overlap it indicates that the plotted data were not from the same or similar populations and there is “strong evidence” (95% confidence interval) that their medians differ. Horizontal dashed lines were added to the boxplots outlining the boundaries of the notches to assist in visualizing the notch overlap or the lack thereof.

Results

The results presented here are examples of data inquiry that can provide information relevant to understanding the historical and contemporary datasets. The data used in these example data inquiries are highly aggregated (e.g. single-level aggregations by study area, survey, tide phase, or diel state). Deeper understanding of the data underlying these examples can be obtained with further exploration as aggregate-level relationships may differ markedly from less highly aggregated data (e.g., survey by tide phase or survey by transect or transect by tide phase).

Data Visualizations

The log-transformed non-zero relative fish density value (S_v) contained in the “20-m dataset” were nearly normal in their distribution with a few high values resulting in a mean (-87.1 dB) slightly greater (~12% in linear terms) than the median (-87.6 dB) (Figure 3). The distribution of

the data in its linear form (S_v) does not approach normality (not shown). The mean of the data calculated in its linear form and converted to its log form (S_v) for reporting is -70.1 dB, greater than the median by a factor of 56.

Throughout the Results section, you'll note that outliers tend to be high values rather than low values. While this could be an artifact of setting a minimum threshold for the data integration, the abundance (and therefore density) distribution of marine animals tends to be clustered. Therefore, it might not be unexpected for the distributions of relative fish density to include large numbers of low-density values with proportionately less high-density values resulting in outliers at high values.

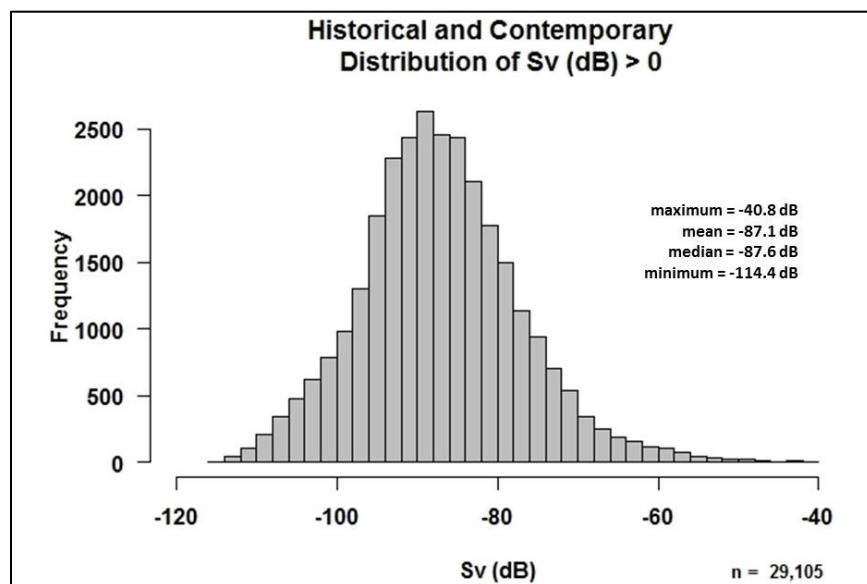


Figure 3. Frequency distribution of non-zero historical and contemporary S_v values. Data shown are the data exported from Echoview integrated over the full water column binned in 20-m along-shiptrack horizontal bins for the historical and contemporary datasets (excluding zeros).

Contemporary surveys generally recorded a wider range of S_v values than the historical surveys while possessing generally lower median values (Figure 4 and Figure 5). The distribution statistics for each survey are shown in Table 3.

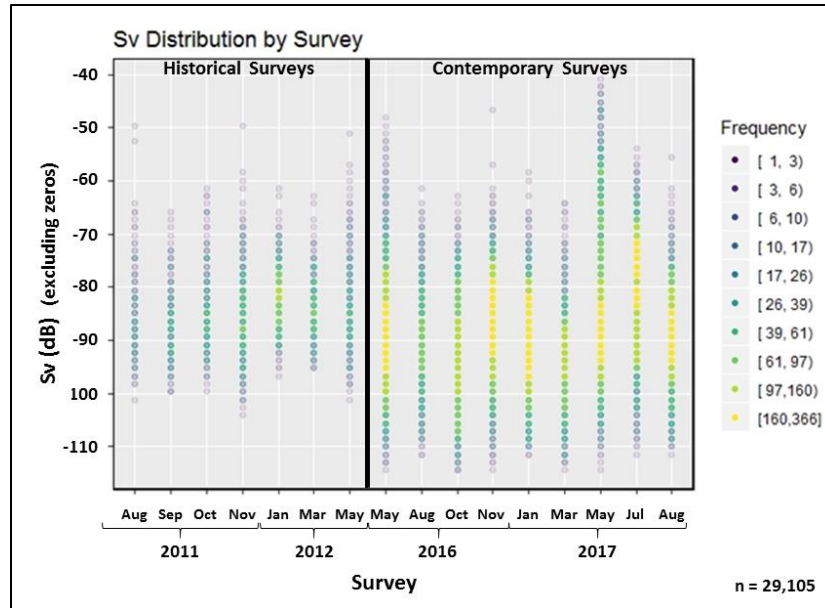


Figure 4. Distribution and frequency of historical and contemporary S_v values by survey. Data shown are the data exported from Echoview (excluding zeros) integrated over the full water column binned in 20-m along-shiptrack distances for each survey.

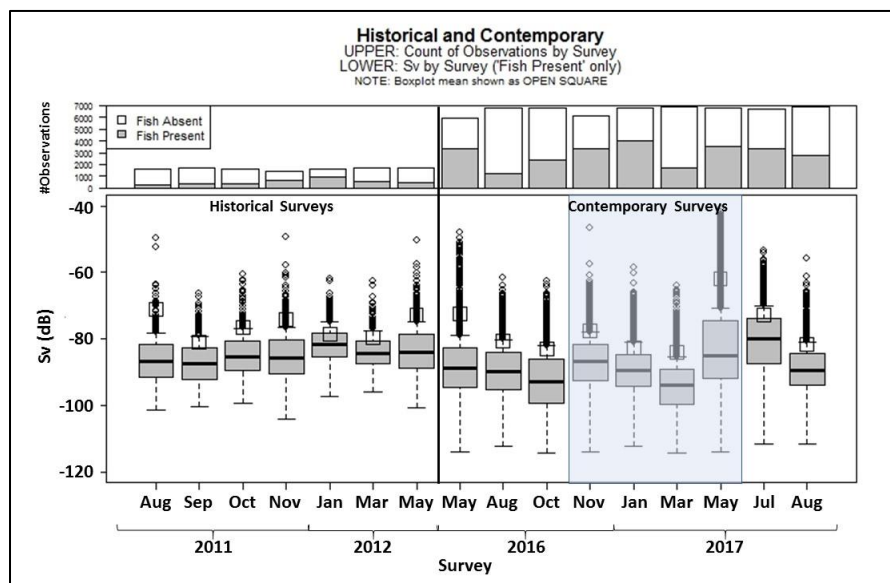


Figure 5. Distribution of historical and contemporary S_v values by survey. Data shown are the data exported from Echoview integrated over the full water column binned in 20-m along-shiptrack distances for each survey. Data from all transects are aggregated within each survey. **Top:** Top of bar indicates the total number of observations for each survey. Axis range: 0 to 7,000. Shaded portion indicates number of non-zero observations ($n = 29,105$). White portion indicates number of zero observations ($n = 41,911$). **Bottom:** Boxplots of non-zero S_v observations by survey. See text for description of boxplot. Shaded portion of right-hand bottom plot demarcates surveys when a TISEC was in place in the CLA study area.

Table 3. Distribution statistics for each survey. Statistics were calculated in linear form (s_v) and converted to the log form (S_v) for reporting. Non-zero datapoints only.

	2011 Aug	2011 Sep	2011 Oct	2011 Nov	2012 Jan	2012 Mar	2012 May	2016 May	2016 Aug	2016 Oct	2016 Nov	2017 Jan	2017 Mar	2017 May	2017 Jul	2017 Aug
n (non-0)	267	343	393	678	911	526	451	3319	1190	2344	3371	3998	1698	3562	3322	2732
maximum	-49.5	-66.4	-60.7	-49.5	-62.0	-62.7	-50.4	-48.1	-61.7	-62.5	-46.5	-58.5	-63.8	-40.8	-53.5	-55.8
median	-86.9	-87.3	-85.5	-85.8	-81.8	-84.5	-84.1	-88.8	-89.7	-92.8	-86.6	-89.4	-94.0	-88.0	-80.0	-89.5
mean	-71.0	-81.1	-76.6	-74.2	-78.6	-79.8	-72.7	-72.5	-80.1	-83.1	-77.7	-82.8	-84.1	-62.0	-72.8	-81.8
minimum	-101.5	-100.4	-99.2	-104.1	-97.4	-95.9	-100.6	-113.8	-112.1	-114.4	-113.9	-112.1	-114.3	-113.8	-111.6	-111.5

Although differing in detail between surveys and the number of observations substantially differing between study areas, at this level of detail the data subsetted by Study Area (CLA and reference) suggests that as the range of S_v values vary from survey to survey in the CLA study area, the reference study area follows generally similar trends (Figure 6a and 6b).

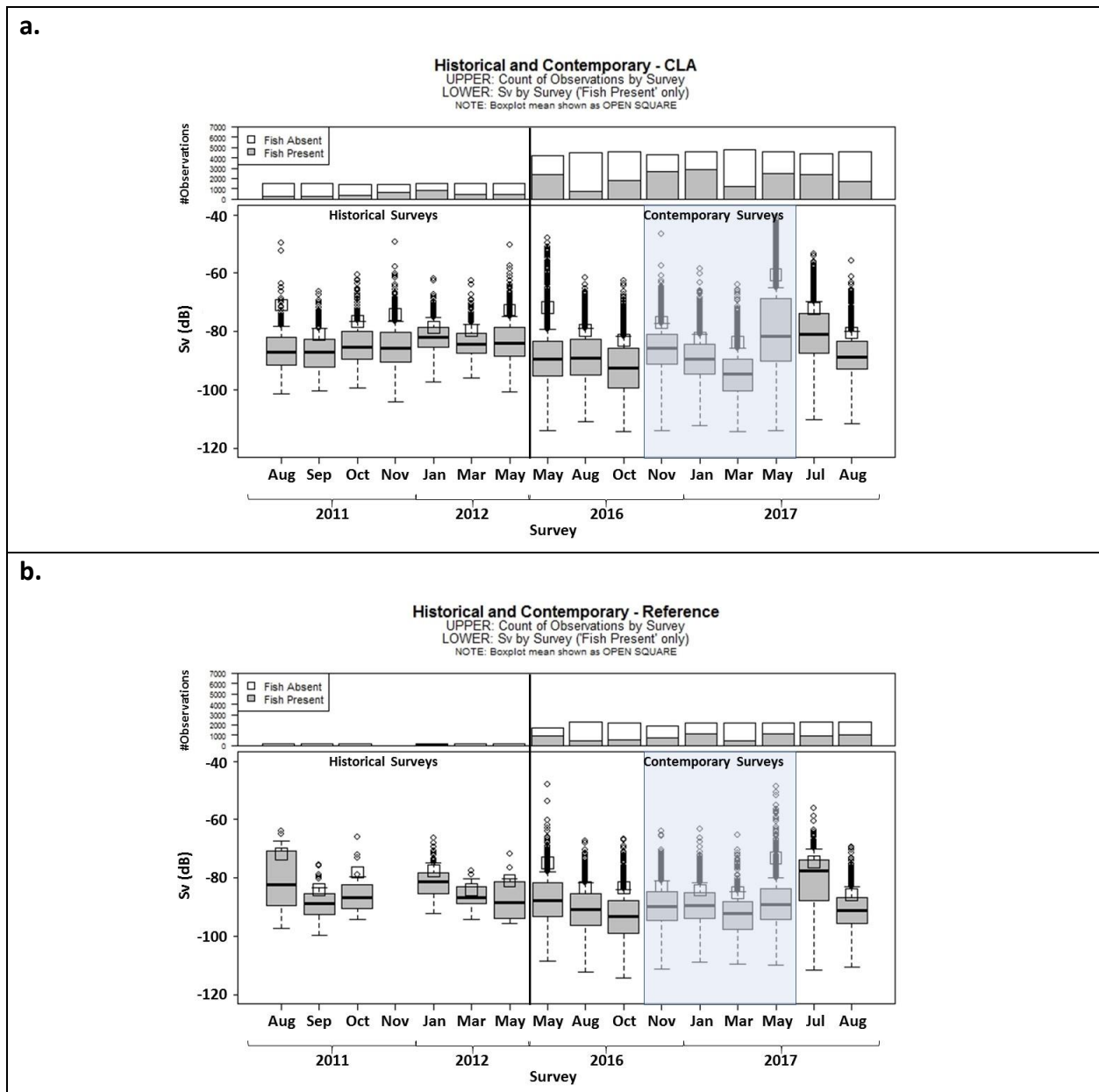


Figure 6. Distribution of historical and contemporary S_v values for the CLA and reference study areas grouped by survey. Data shown are the data exported from Echoview integrated over the full water column binned in 20-m along-shiptrack distances for each survey. Data from all transects are aggregated within each survey. **(a)** S_v values observed in the CLA study area. **(b)** S_v values observed in the reference study area. No data was reported for the reference study area during the historical Nov 2011 survey. (See #6 to Table A1 in Appendix A for more information.) **Top:** Top of bar indicates the total number of observations for each survey in the respective study area. Axis range: 0 to 7,000. Shaded portion indicates number of non-zero observations ($n_{CLA} = 21,481$, $n_{Ref} = 7,624$). White portion indicates number of zero observations ($n_{CLA} = 29,211$, $n_{Ref} = 12,700$). **Bottom:** Boxplots of non-zero S_v observations by survey in the respective study area. See text for description of boxplot. Shaded portion of right-hand bottom plots demarcate surveys when a TISEC was in place in the CLA study area.

Using the same “20-m dataset” as above, the data were aggregated and boxplots plotted to examine spatial groupings: Research Program (Figure 7a), and Study Area (Figure 7b), and environmental groupings: Tide Phase (Figure 7c), and Diel State (Figure 7d).

The range of backscattering values observed during the contemporary surveys was greater than those observed during the historical surveys (Figure 7a). While the median of the historical dataset was higher than that of the contemporary (Figure 7a), within the contemporary dataset there were a sufficient number of observations which were orders of magnitude greater than its median making the mean for the contemporary dataset higher than for the historical dataset. Using S_v as our proxy for relative fish density, these results indicated that backscatter from higher densities of fish were observed during the contemporary surveys than during the historical surveys. These observations gleaned from the highly aggregated data (by research program) were consistent with the lower-level aggregation by survey (Figure 5) and survey by study area (Figure 6).

There was a wider range of variability of the S_v values, and therefore inferred wider range of relative fish density, in the CLA than in the reference Study Area. In addition to the wider range of fish densities, the CLA Study Area had fish densities higher than that found in the reference Study Area. The differences in the ranges of the integrated mean volume backscattering strength and therefore differences in the ranges of fish densities found in both study areas was approximately a factor of 5.5. (Figure 7b).

The maximum S_v and range of S_v across the ebb, low, and flood tide phases were within less than 2 dB of each other. This indicates generally similar results during each of those tide phases relative to the high slack observations, which exhibited a maximum S_v value and range of S_v an order of magnitude less than the other three tide phases (Figure 7c).

There were much greater differences in the distribution of fish densities across diel states (Figure 7d) than was seen across the tidal phases. Maximum relative density of fish observed during day and night were approximately two orders of magnitude greater than the maximum recorded for dawn or dusk. In spite of those substantially greater maximum fish densities, the mean densities were within approximately one order of magnitude to each other, and the median densities were all within 3 dB (within a factor of two) across the diel states. Therefore, the diel states with the very high fish density observations included sufficient numbers of low fish density observations to reduce the variability in the measures of central tendency (mean and median) across the diel states.

In the visualizations presented here, the data were highly aggregated such that the details of the range of S_v observations by spatial and temporal detail are hidden. The visualization of the data aggregated by diel state therefore, illustrates the value of examining the data in

aggregated form (e.g. Figure 7) and the need to examine the data in lower-level aggregations in order to gain insight as to the source of distinctive range of S_v observations such as those at dawn and dusk.

Approximately 600 non-zero data points, each, comprised the dawn and dusk portions of the non-zero dataset whereas the day and night portions included ~14,000 non-zero datapoints each. Therefore, the question arises as to whether the difference in range of S_v observations by diel state was an artifact of sample size or a record of biological behavior. The dawn and dusk sampling periods constituted 4.3% of the total observations (71,016). The non-zero dawn and dusk observations (1,275) plotted here (Figure 7d) at 4.4% of the total non-zero observations (29,105) is proportional to the entire dataset. In other words, the presence:absence ratio within the dawn and dusk time periods is equivalent to the average presence:absence ratio for the entire dataset. While this fact is not sufficient to address the “artifact vs. biology” question, as first cut, it eliminates the question as to whether the dawn and dusk time periods were periods of particularly low fish presence, and thereby possibly periods of particularly low relative fish density.

Remembering that non-zero observations encompassed nearly eight orders of magnitude, that the upper end of the dawn and dusk observations peak approximately two orders of magnitude below those for day and night warrants closer inspection. Given that the range of the distribution of S_v observations across tide phases do exhibit such a marked difference, at first glance there is not sufficient evidence to hypothesize that the dawn and dusk sampling periods were predominantly on a particular tide phase. Although the maximum observation during high slack was approximately an order of magnitude lower than the maximum of the other tide phases, the dawn/dusk maximum observations were lower still, by another order of magnitude.

Further exploration of the dawn/dusk data is warranted in order to gain insights as to whether the distinctive dawn and dusk range of S_v observations were an artifact of sampling or a biological signal. Did the sampling regime work out such that lower fish densities would be expected because of the environmental setting during which dawn and dusk sampling was executed? Possibilities to explore are: plotting the dawn/dusk data by survey (i.e. are the data predominantly recorded in a period of lower fish density?) or plotting by transect (i.e. are the data predominantly recorded on particular transects for which lower fish density dominates?) or given that the dawn/dusk time periods are seasonally approximately 30 to 40 minutes long, random sampling the dataset in 30 or 40 minute time-blocks may help shed light on the source of the distinctive ranges of S_v observations recorded during the dawn and dusk time periods.

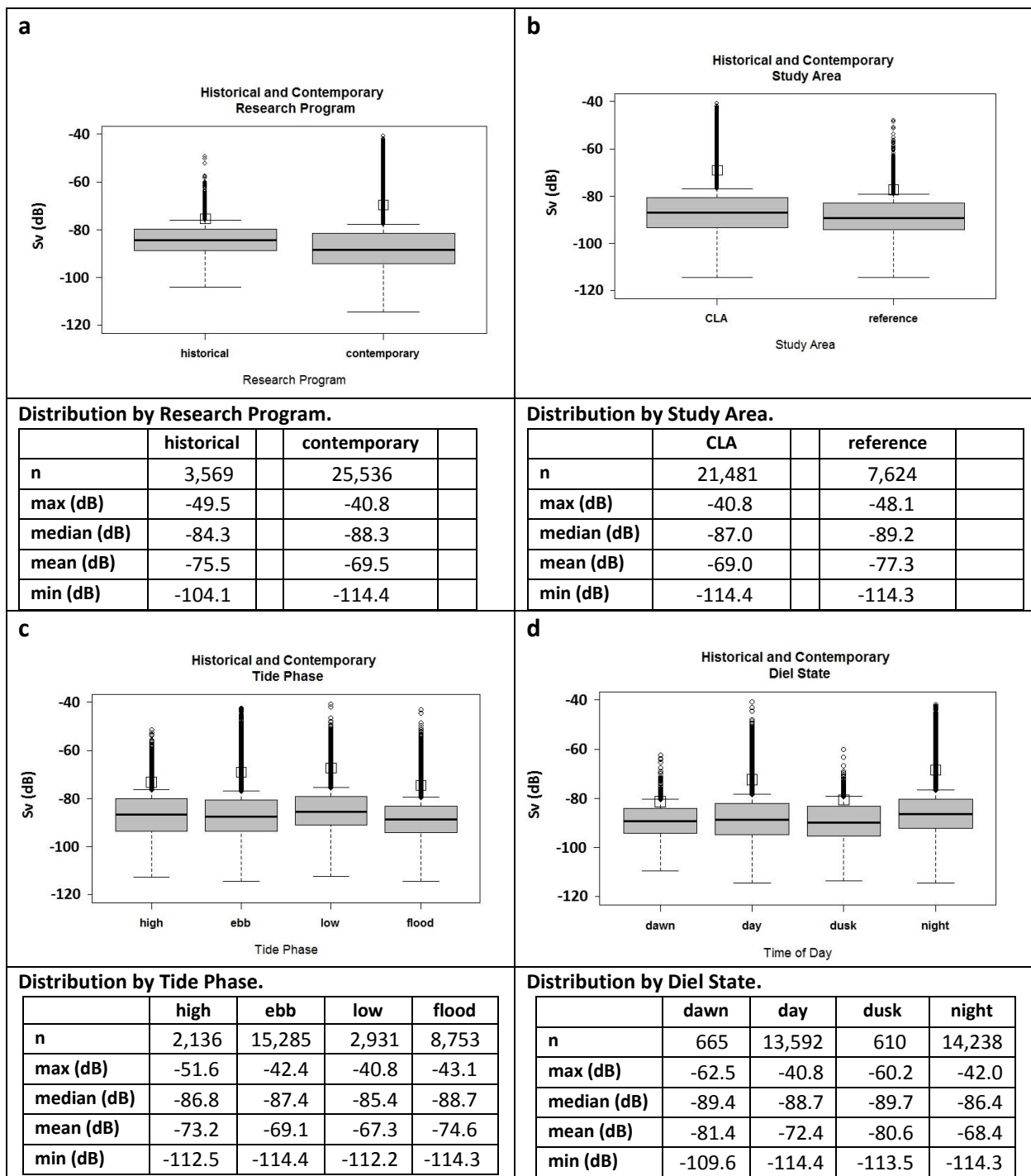


Figure 7. Distribution of historical and contemporary S_v values for spatial and environmental groupings. (a) by Research Program: historical and contemporary, (b) by Survey Area: CLA and reference, (c) by Tide Phase: ebb, flood, high, and low, (d) by Diel State: dawn, day, dusk, and night. Data shown are the data exported from Echoview (excluding zeros) integrated over the full water column binned in 20-m along-shiptrack horizontal bins. See text for description of boxplot.

In addition to single-level groupings as illustrated in Figure 7, a multi-level grouping example is included here. The multi-level example included data aggregated so as to examine the S_v distribution in both the CLA and reference study areas while a TISEC device was in place in the CLA (Figure 8). Given that no TISEC device was in place during the time periods included in the historical dataset, the data associated with “TISEC Present” were observations from the contemporary dataset.

Although the minimum S_v value, the median, and interquartile range in the CLA site, with and without the presence of a TISEC device, are nearly indistinguishable (Figure 8a), the maximum observed S_v value in the CLA study area was greater by a factor of five while the TISEC device was present. In contrast, in the reference site (Figure 8b) there was a compression of the interquartile range and the maximum observed S_v was 10% less during the same time period. Changes in S_v values can be indicators of change in the aggregation densities of fish or change in the assemblages and therefore, changes in fish sizes passing under the echosounder. To gain insight into the potential influences that may have generated the observed changes in S_v , one must look both to changes in the behavior of the fish present (e.g. aggregating densities) and to the seasonal changes (e.g. fish assemblages or fish sizes) encapsulated by these time periods with and without the TISEC device. Some insights can be gained by examining the underlying data (such as transect-level which is explored further below) and *a priori* information for clues as to possible factors influencing the data at these summary levels.

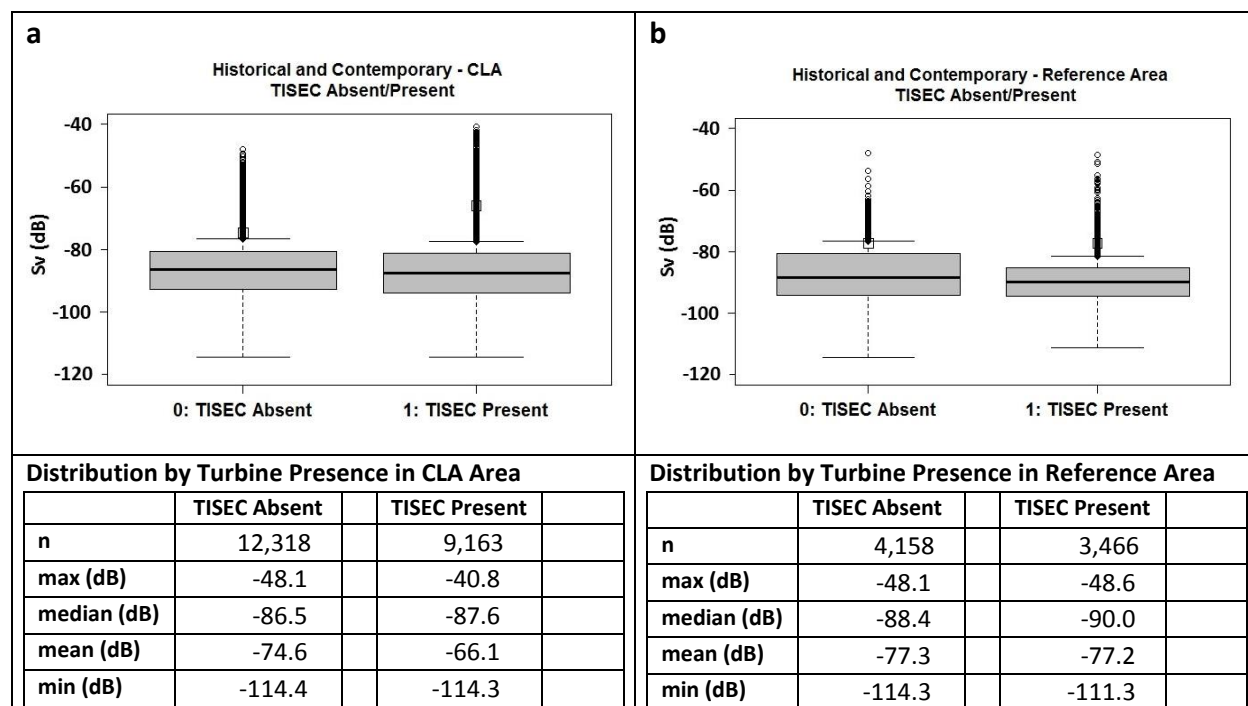


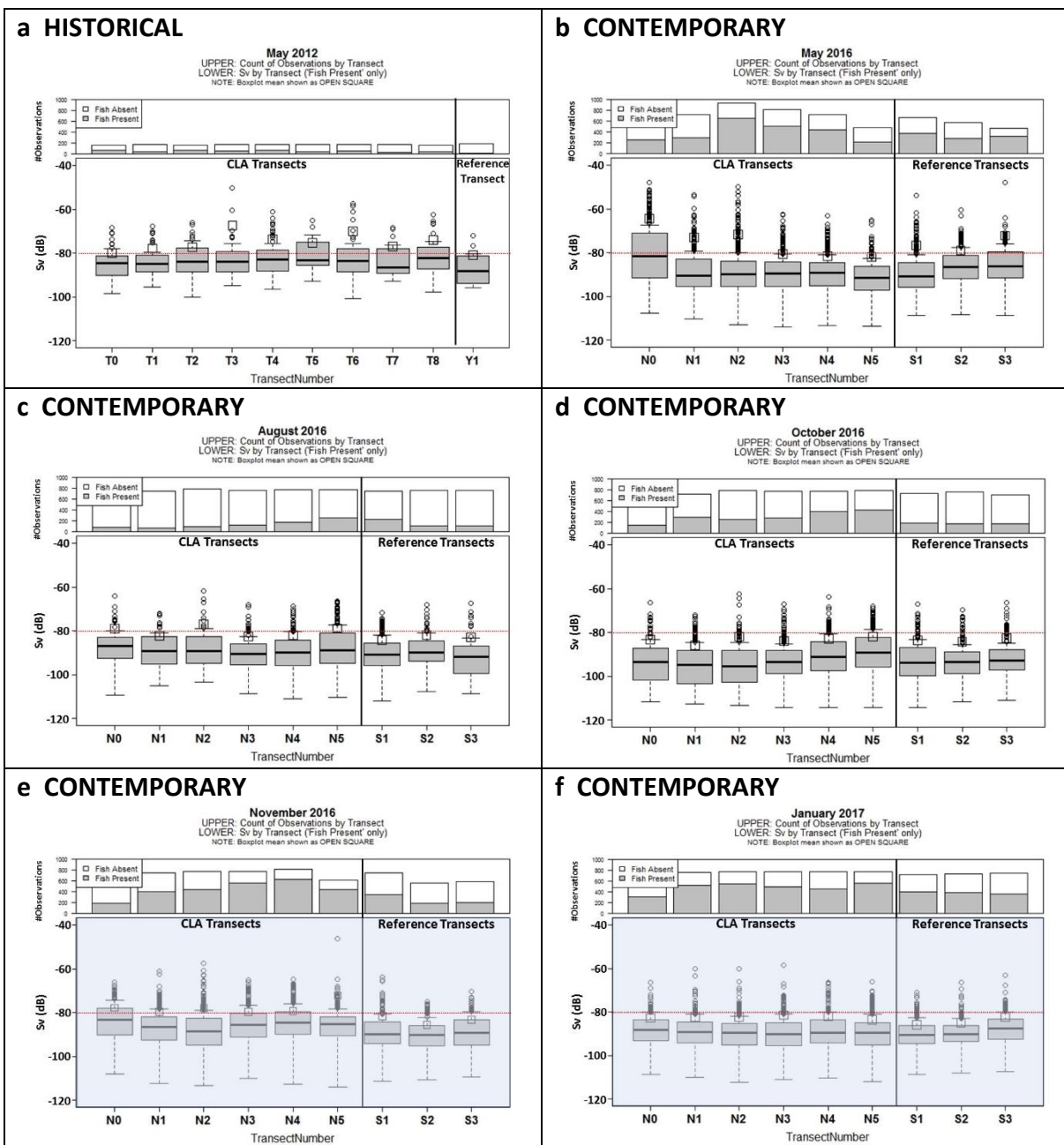
Figure 8. Distribution of S_v values without and with a TISEC emplaced in CLA. S_v distributions and distribution statistics for both the (a) CLA and (b) Reference study areas are shown. Data shown are the data exported from Echoview (excluding zeros) integrated over the full water column binned in 20-m along-shiptrack horizontal bins. See text for description of boxplot.

To examine the underlying data for cues that suggest what data should be examined at finer scales, the distribution of S_v values by survey was scrutinized (Figure 5), as was the distribution of S_v values by survey within the CLA and within the reference study area (Figure 6). It is evident from those data that May 2017 had a strong influence on the maximum values observed in the aggregated “TISEC present in CLA” S_v distribution (Figure 8a). And it is noted that May appears to be a month with a notably wider range of observed S_v values both overall (Figure 5) and within the individual study areas (Figure 6), particularly during the contemporary surveys (May 2016 and May 2017). The S_v distribution for May 2012 in the historical dataset is not so markedly different from the remaining historical surveys as are the May surveys in the contemporary dataset, and certainly not in the reference study area. However, the maximum S_v observed in each of the three May surveys are among the five highest integrated values observed in the entire dataset. Nov 2011 and Nov 2016 exhibit the remaining two magnitudes of integrated S_v that make up the five highest. Aug 2011 is also within the top five, exhibiting a magnitude equivalent to Nov 2011.

Given the pattern of higher mean volume backscattering strength (S_v) and therefore potentially higher fish densities during May surveys, attributing the higher S_v observed during the “TISEC present” phase (Figure 8a) cannot be attributed to the presence of the TISEC without further investigation. Higher fish densities during May surveys as was noted by Daroux and Zydlewski (2017), may have been associated with adult alewife (*Alosa pseudoharengus*) spring spawning migrations and the presence of Atlantic herring (*Clupea harengus*) and striped bass (*Morone saxatilis*) (Baker *et al.*, 2014). Striped bass are common in the Minas Passage along the shoreline and they spawn in the head of the tide in May-June (Rulifson and Dadswell, 1995). Spring variation may also be linked to other species migrating into the Basin for the summer, such as Atlantic sturgeon (*Acipenser oxyrinchus*), American shad (*Alosa sapidissima*), American mackerel (*Scomber scombrus*), and rainbow smelt (*Osmerus mordax*) (Dadswell, 2010).

To place the “TISEC present” surveys in context, and particularly the May 2017 survey, the observed S_v for all of the contemporary surveys plus the May 2012 survey were aggregated by transect and plotted (Figure 9). Although there was variability from transect to transect and survey to survey, of note were the transects nearest to the north shore in the contemporary May surveys (May 2016 and May 2017). In both cases the data for the northern-most transects (N0, N1, N2) suggest a wider range of S_v values to include high values markedly different from other transects within the respective survey and among surveys. The segregation of the high values within those northern-most transects may indicate that the shallower areas are regions of easier fish movement. Within the “TISEC present” surveys (Nov 2016, Jan 2017, Mar 2017, May 2017) the distribution of S_v values for May 2017 stand out as distinctly different in range, magnitude, and spatial distribution from the other “TISEC present” surveys. This evidence suggests that the S_v values aggregated at the coarse scale of “TISEC present-absent” (Figure 8) are likely a function of seasonal and inter-annual variation. May, with its particularly high and

wide-range of observed S_v values and apparently distinctive spatial pattern, appears to be an important month for surveying to continue to gather time-series data to help with interpretation.



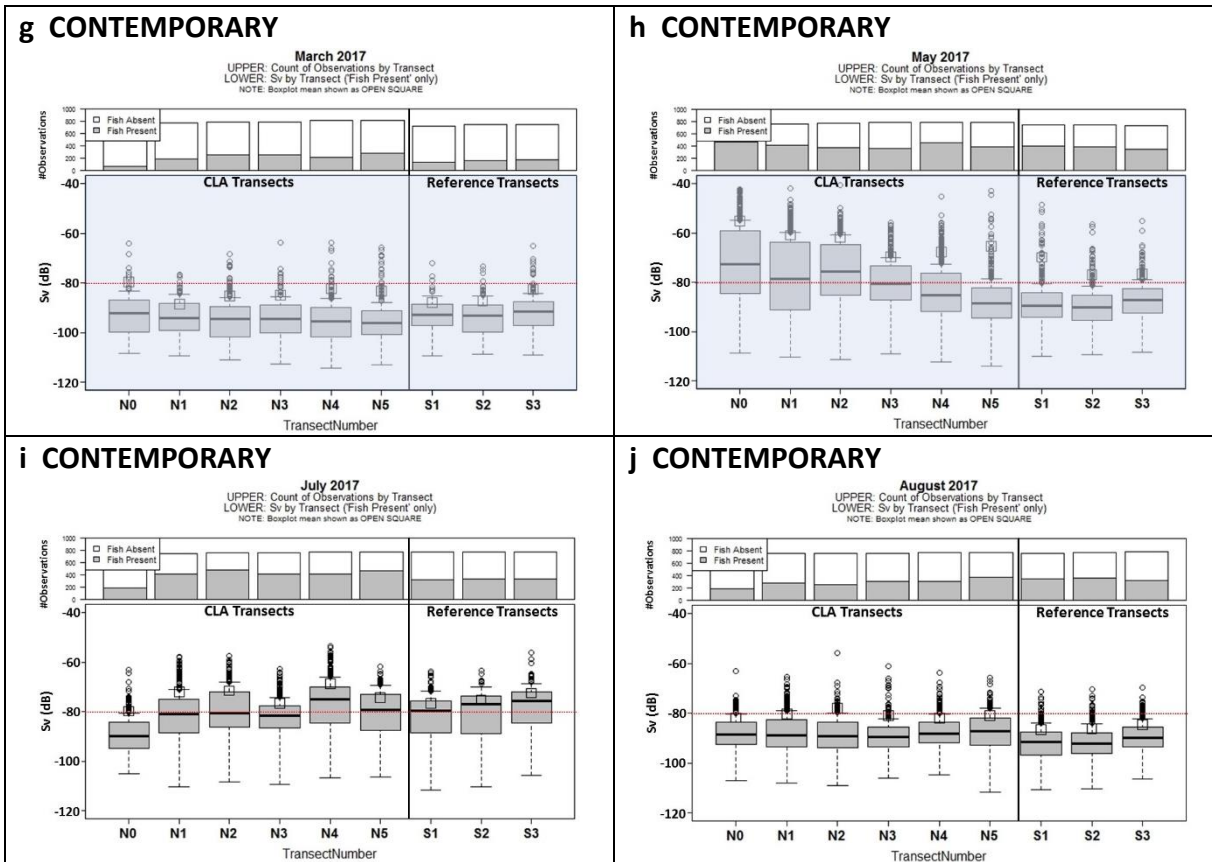


Figure 9. Distribution of S_v values by Transect for Contemporary Surveys and May 2012. S_v distributions by Transect for (a) May 2012, (b) May 2016, (c) August 2016, (d) October 2016, (e) November 2016, (f) January 2017, (g) March 2017, (h) May 2017, (i) July 2017, and (j) August 2017. **Top:** Top of bar indicates the total number of observations for each transect in the respective survey. Axis range: 0 to 1,000. Shaded portion indicates number of non-zero observations. White portion indicates number of zero observations. **Bottom:** Boxplots of non-zero S_v observations by transect in the respective survey. See text for description of boxplot. **Shaded Surveys** (Nov 2016, Jan 2017, Mar 2017, and May 2017) are surveys conducted while a TISEC was in place. **Red Line:** A red line is placed at -80 dB for reference across all surveys.

Analytical Approach: Fish Presence:Absence

Given the preponderance of zeros in the dataset (59%) and the range of nearly eight orders of magnitude for the non-zero values, two separate analyses were selected to facilitate exploration of the dataset. The first analysis modeled fish presence:absence in relation to the spatial and temporal explanatory variables and is presented in this section, Analytical Approach: Fish Presence:Absence. The second analysis investigated the ranges of relative fish density (S_v values) in relation to the spatial and temporal explanatory variables and is presented in the next section of this report, Analytical Approach: Fish Density. For robust decision-making, we suggest that the results of both analyses (presence:absence and magnitude of relative fish density) be considered together with the characteristics of the underlying data.

Presented here are examples of the results of the modeling of fish presence when implementing the binary logistic model using the GLM command in R. The model was populated with counts of the fish presence:absence observations and a variety of categorical predictor variables. As noted above, the model output includes a table in which the first line of data is reported relative to a 50:50 presence:absence ratio. While a 50:50 ratio is not intrinsically of biological interest, the 50:50 ratio provides a baseline against which the significance of the differences in fish presence relationships to the explanatory variables can be measured.

It should be noted that large sample sizes can cause statistical testing to become sensitive to even very small, inconsequential differences resulting in statistical significance for small and uninteresting effects. The effect is particularly pronounced when there is an imbalance in the count of observations. Therefore, multiple views of the fish presence:absence data is provided in this section to provide the reader with a more robust understanding of the context in which to interpret the meaningfulness of the statistical results. For example, as shown below (“Survey” section) the fish presence:absence ratio for the May 2016 and Nov 2016 surveys was identified as not statistically different (presence: 56.2% and 54.9%, respectively) whereas the ratio for May 2016 and Jan 2017 surveys differed statistically (presence: 56.2% and 58.9%, respectively). In this case, depending on the question at hand, the statistical significance of the differences, 56.2% and 58.9%, may be deemed to be of practical importance or not. On the other hand, cases where differences do not reach the level of statistical significance may provide decisive insights. For example, the presence:absence ratio for three transect pairs (N2:N3, N4:N5, S2:S3) were not statistically different as shown below (“Transect” section). Therefore, if the decision at hand is an issue of cost savings on individual surveys (such as to increase survey frequency without adjusting the survey budget), the statistical results provide some guidance as to consider adjusting the survey design to include one of each pair rather than both.

Note that the underlying data used for these modeling examples are highly aggregated. Aggregate-level relationships of the fish presence:absence ratio to predictor variables such as Research Program, Study Area, Tide Phase, etc. may differ markedly from less highly aggregated data such as by transect within a survey, and thereby the strength of predictors may change. A script containing the R coding to implement the GLM modeling is included with this document along with sufficient commenting to allow one to explore relationships or interactive predictor variables.

GLM Output

For each GLM modeling result, three tables and one figure are presented. A stacked bar plot provides a visualization of the presence (“1”) and absence (“0”) counts for each category within the explanatory variable. Accompanying the bar plot is a table enumerating those counts and their associated percentages. The table is presented to assist in developing inquiries deeper

into the data. Additionally, a table reporting the GLM output and a table summarizing the statistical significance levels are included.

To assist with understanding the GLM output, an explanation of the result table is provided here. The purpose of running the GLM was to produce the coefficients that describe the model of the data, and the parameters by which to quantify the statistical significance of the results. Thereby the GLM output table reports the data needed to *calculate* the estimated y-intercept for each category within the explanatory variable (the “estimate” column) and reports the associated standard error and p-value. A y-intercept of “0” indicates a presence:absence ratio of 50:50. For y-intercepts other than zero, the magnitude of the estimated y-intercept is indicative of how close to, or far from, 50:50 is the presence:absence ratio. The sign of the y-intercept indicates the direction of the ratio: ‘+’ indicates more “present” observations than “absent”, whereas ‘-’ indicates more “absent” observations than “present”.

The category listed in the first row of the table is referred to as the “baseline” category. The data in the remaining rows of the table are relative to the baseline category. The data reported for the baseline category are indicative of that category’s presence:absence ratio relative to 50:50. Therefore the estimate reported for the first row (baseline) is the y-intercept for that category. The estimate values reported in all remaining rows of the table are relative to the baseline. To determine the magnitude of the y-intercept for a category other than the baseline, the estimate reported for that category must be added to the y-intercept reported for the baseline. If the category’s reported estimate has the same sign as the baseline y-intercept, the sum will be greater than that reported for the baseline indicating the presence:absence ratio for the category is in the same direction as that of the baseline, but with a larger difference between presence and absence. Depending on the magnitude of the category’s reported estimate, if the sign is opposite to that of the baseline, the presence:absence ratio for the category may in the same direction as the baseline but closer to 50:50 (i.e. the sum of the y-intercept for the baseline and the category are closer to zero than the baseline y-intercept) or with its opposite sign, if the magnitude of the estimate for the category is greater than that of the baseline, the presence:absence ratio for the category will be reverse that of the presence:absence ratio of the baseline (i.e. greater “present” observations in the category if “absent” observations were greater than “present” in the baseline).

The p-value recorded in the first row of the R GLM-output table reports the statistical significance of the difference from 50:50 that is the fish presence:absence ratio for that category. All other p-values report the statistical significance of the difference of the fish presence:absence ratio for that category relative to the baseline category presence:absence ratio. A two-way table summarizing the p-values reported to two decimal places is also presented. For tables with more than two rows of categories, the statistical significance among the pairs of categories that do not include the baseline were calculated separately and are reported in the summary two-way table. See caption for Table 5 for more information.

Although the ratio of presence:absence for the “20-m dataset” was 41:59, finer-scale aggregations at the category level within the explanatory variables revealed the spatial and temporal categories for which the presence:absence ratio approached 50:50 or for which “absent” observations were exceeded by “present” (Table 4). Further examination of the data is warranted to determine if the reported presence:absence ratios hold at finer scales. For example: the presence:absence ratio for “night” as aggregated over all contemporary surveys was 52:48. Before generalizing this feature, aggregating the diel data by survey will provide the information to confirm whether or not “present” counts exceeded “absent” counts in every case, seasonally, or on some other time scale. Other finer-scale aggregations of data may also provide insights such as diel by transect.

Table 4: Fish Presence:Absence as Percentage by Explanatory Variable Category. The fish presence (“1”) and absence (“0”) as percentage of total observations for each category within the explanatory variables included in this report. Column pairs are grouped with decreasing “presence” percentages moving left to right in the table. **Black bolded** percentages in left-most columns indicate presence:absence ratio ~50:50. **Red bolded** percentages in left-most columns indicate presence:absence ratio where presence > absence. Full dataset (n = 71,016) was used for research program explanatory variable. All remaining explanatory variables are based on contemporary data only (n = 59,669). See text under “Research Program” below for more information.

Explanatory Variable	Category					>50%		50%	50%		51%-59%		60%-69%		70%-71%		80%-89%	
		0	1	100%	0	1	0	1	0	1	0	1	0	1	0	1	0	1
Research Program	historical	68.5%	31.5%	100.0%									68.5%	31.5%				
	contemporary	57.2%	42.8%	100.0%							57.2%	42.8%						
Study Area	CLA	55.1%	44.9%	100.0%							55.1%	44.9%						
	reference	61.6%	38.4%	100.0%									61.6%	38.4%				
Tide Phase	high	63.0%	37.0%	100.0%									63.0%	37.0%				
	ebb	50.7%	49.3%	100.0%			50.7%	49.3%										
	low	63.2%	36.8%	100.0%									63.2%	36.8%				
	flood	62.2%	37.8%	100.0%									62.2%	37.8%				
Diel State	dawn	54.5%	45.5%	100.0%							54.5%	45.5%						
	day	65.0%	35.0%	100.0%									65.0%	35.0%				
	dusk	62.8%	37.2%	100.0%									62.8%	37.2%				
	night	47.5%	52.5%	100.0%	47.5%	52.5%												
Survey	2016-May	43.8%	56.2%	100.0%	43.8%	56.2%												
	2016-Aug	82.4%	17.6%	100.0%													82.4%	17.6%
	2016-Oct	65.2%	34.8%	100.0%									65.2%	34.8%				
	2016-Nov	45.1%	54.9%	100.0%	45.1%	54.9%												
	2017-Jan	41.1%	58.9%	100.0%	41.1%	58.9%												
	2017-Mar	75.5%	24.5%	100.0%											75.5%	24.5%		
	2017-May	47.9%	52.1%	100.0%	47.9%	52.1%												
	2017-Jul	50.5%	49.5%	100.0%			50.5%	49.5%										
Transect	2017-Aug	60.2%	39.8%	100.0%									60.2%	39.8%				
	N0	69.1%	30.9%	100.0%									69.1%	30.9%				
	N1	57.6%	42.4%	100.0%							57.6%	42.4%						
	N2	53.4%	46.6%	100.0%							53.4%	46.6%						
	N3	53.2%	46.8%	100.0%							53.2%	46.8%						
	N4	50.4%	49.6%	100.0%			50.4%	49.6%										
	N5	48.5%	51.5%	100.0%	48.5%	51.5%												
	S1	58.7%	41.3%	100.0%							58.7%	41.3%						
	S2	63.1%	36.9%	100.0%									63.1%	36.9%				
	S3	63.2%	36.8%	100.0%									63.2%	36.8%				

Research Program

During both research programs (historical and contemporary) counts of fish presence observations were exceeded by counts of fish absence (Table 5 and Table 7). For the baseline category (historical), the deviation of the fish presence:absence ratio from 50:50 was statistically significant ($p < 2e-16$; Table 5). The fish presence:absence ratio during the contemporary program, although higher than during the historical was still less than 50:50 and was statistically different from the historical fish presence:absence ratio (Table 5).

When considered in conjunction with the S_v distributions within the historical and contemporary datasets (Figures 4 and 5), the data suggest that not only does fish presence differ between the two research programs (historical and contemporary), but also in range of values. This is explored in the next Results section (Analytical Approach: Relative Fish Density).

Table 5. Generalized Linear Model Output of Fish Presence by Research Program. The value in the “Estimate” column for row one indicates the estimate of the y-intercept coefficient for that category. “Zero” would indicate a fish presence:absence ratio of 50:50. A negative value indicates that the count of observations of fish absence was higher than the count of observations of fish presence. The corresponding p-value reported in the last column indicates the statistical significance level of the difference of the observed presence:absence ratio from 50:50 for that category. Any additional rows are reported relative to the category in the first row (“the baseline category”). In this example, we add the “estimate” of the baseline category (“historical” in this case) plus the estimate of the category of interest (“contemporary” is our only choice in this table): $-0.77901 + 0.48884 = -0.29017$. The resulting negative estimate of the y-intercept for the contemporary category (-0.29017) tells us that the presence:absence ratio for “contemporary” is still such that the number of “absent” observations exceeds the number of “present” observations, but at a lower ratio than the historical (i.e. -0.29017 (contemporary) is closer to zero than -0.77901 (historical)). The p-value reported for contemporary is a measure of the significance of the difference in the presence:absence ratio for that category (contemporary) relative to the baseline category listed in row one (historical). Summary for this table: “historical” presence:absence ratio is statistically different from 50:50 with more “absent” observations than “present” observations. The “contemporary” presence:absence ratio is statistically different than for the “historical” category, although like the historical category, there were more “absent” observations than “present” observations but by a lower ratio. This table description is referenced for all GLM Output tables in this section.

Coefficients			
	Estimate	Std. Error	Pr(> z)
historical	-0.77901	0.02022	<2e-16
contemporary	+0.48884	0.02185	<2e-16

Table 6. Summary Two-way Table of the Statistical Significance of Differences in Pairs of Fish Presence:Absence Ratios. Statistical significance is reported as p-value to two decimal places. Black box with white lettering in column one of row one is the p-value representing the statistical significance of the difference for that variable of the fish presence:absence ratio relative to 50:50. White (statistically significant: $p < 0.05$) and gray (not statistically significant: $p > 0.05$) cells contain the p-value quantifying the statistical significance of the difference in fish presence:absence ratios of the two categories (as listed in the corresponding column header and row name). Gray cells not shown here will be present in other two-way tables in this section. When there are only two categories in the table, the p-value quantifying the statistical difference for the second category relative to the first. When there

are more than two categories in a table, the p-values reporting the statistical significance of the presence:absence ratios between all pairs that did not include the baseline category were calculated as a separate step. Solid black cells along the diagonal and below are cells of the redundant pairs. The two-way has been included for all explanatory variables, including those with only two rows, in order to standardize the reporting for all variables. This table description is referenced for all Summary Two-Way tables in this section.

	historical	contemporary
historical	0.00	0.00
contemporary		

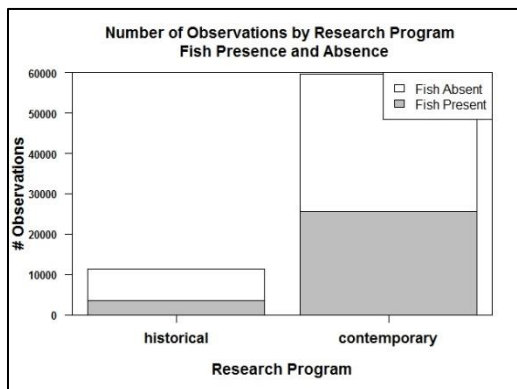


Figure 10. Fish Presence:Absence Observations by Research Program. Top of bar indicates the total number of observations by research program. Shaded portion indicates the number of observations assigned a value of “1” (i.e. integrated S_v by “20-m” bin $\neq 0$). White portion indicates number of observations assigned a value of “0” (i.e. integrated S_v by “20-m” bin = 0). Total number of observations = 71,016. See Table 7 for detailed quantification.

Table 7. Research Program Fish Presence:Absence Observations. Left side of the table contains the count of fish presence:absence observations by category. Right side of the table contains the corresponding percentages. Fish Presence = “0” designates “absence”: no observations above the thresholds were observed in the “20-m” data bins (i.e. $S_v = 0$). Fish Presence = “1” designates “presence”: observations above the thresholds were observed in the “20-m” data bins (i.e. S_v is any value other than zero). Where present, **bolded black values** (none shown here) highlight ratios ~50:50 and **bolded red values** (none shown here) highlight ratios where the count of “present” observations exceeded the count of “absent” observations.

Fish Presence	historical	contemporary	TOTAL	historical	contemporary	TOTAL
0	7,778	34,133	41,911	68.5%	57.2%	59.0%
1	3,569	25,536	29,105	31.5%	42.8%	41.0%
TOTAL	11,347	59,669	71,016	100.0%	100.0%	100.0%

In light of the findings suggesting a significant difference in the proportions of fish presence in the contemporary vs. historical datasets further modeling of fish presence by spatial, temporal, and environmental variables was conducted using the **contemporary dataset only**. In the R scripts included with this document, there is coding that can be used to drill down into the

datasets to further explore whether the differences between the historical and contemporary datasets were a function of time or an artifact of the differing characteristics of survey design.

There were substantive differences in survey characteristics between the historical and contemporary surveys. In addition to the survey design characteristics outlined in the Methods section of this report, differences in the execution of the survey design may contribute to differences in the resulting recorded data. For example, there is evidence that suggests that the vessel speed during the historical surveys may have been substantively higher than during the contemporary surveys. At faster vessel speeds, it is possible to miss fish higher in the water column where the acoustic beam is narrower. To test this, the vessel speed can be calculated in Echoview for both the historical and contemporary datasets, and with the known beam widths of the transducers, and ping rates for each survey, one can calculate the depth in the water column where the beam swath overlaps. The volume of water above that depth between pings is not sampled. If that volume substantially differs between the research programs, it may indicate that artifacts due to the execution of the survey may have contributed to the statistically differing results.

Other differences between the research program surveys may have also contributed to differences in the recorded observations of backscatter: differences in the length of transect, single passes over transects during the historical surveys rather than the “with” and “against” passes during the contemporary surveys, or the distribution of observations particularly over the diel state. For more information concerning differing characteristics of survey design and execution, please see Tables A1, A2, A3, and A4 in Appendix A, particularly Table A3.

Study Area

In both study areas (CLA and reference), counts of fish presence observations were exceeded by counts of fish absence (Table 8 and Table 10). For the baseline category (CLA), the deviation of the fish presence:absence ratio from 50:50 was statistically significant ($p < 2e-16$: Table 8). Like the CLA, data collected in the reference Study Area recorded more counts of “absent” than “present”, but at a higher ratio than in the CLA (Table 10). The difference in the fish presence:absence ratio in the reference study area was statistically different from the ratio in the CLA study area ($p < 2e-16$: Table 8).

The number of observations and presence:absence ratios (Table 10) by study area provide a good case study for looking deeper into the question of whether an imbalance in the number of observations is unduly generating a statistically significant difference when the numerical differences are small and inconsequential. There were twice as many observations in the CLA study area than there were in the reference study area (Table 10 and Figure 11) and the difference in the presence:absence ratios were deemed statistically significant (Table 8). It is left to the reader to discern whether the difference in the presence:absence ratios (55:45 and

62:38, respectively) are of practical importance when considering the functioning of the ecosystem within Minas Passage.

Table 8. Generalized Linear Model Output of Fish Presence by Study Area – Contemporary Surveys Only. See text and the caption for Table 5 for more information.

Coefficients			
	Estimate	Std. Error	Pr(> z)
CLA	-0.20398	0.01001	<2e-16
reference	-0.27042	0.01787	<2e-16

Table 9. Summary Two-way Table of the Statistical Significance of Differences in Pairs of Fish Presence:Absence Ratios – Contemporary Surveys Only. See caption for Table 6 for more information.

	CLA	reference
CLA	0.00	0.00
reference		

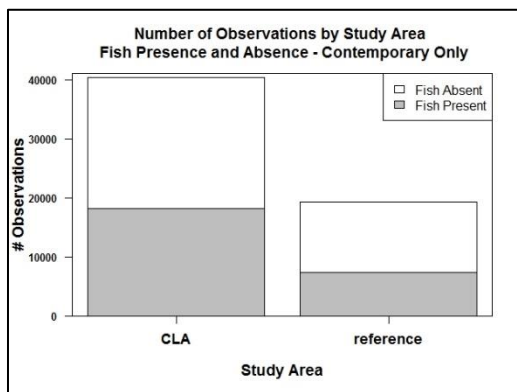


Figure 11. Fish Presence:Absence Observations by Study Area – Contemporary Surveys Only. Top of bar indicates the total number of observations by study area. Shaded portion indicates the number of observations assigned a value of “1” (i.e. integrated S_v by “20-m” bin $\neq 0$). White portion indicates number of observations assigned a value of “0” (i.e. integrated S_v by “20-m” bin = 0). Total number of observations = 59,669. See Table 10 for detailed quantification.

Table 10. Fish Presence:Absence Observations by Study Area – Contemporary Surveys Only. Left side of the table contains the count of fish presence:absence observations by category. Right side of the table contains the corresponding percentages. Fish Presence = “0” designates “absence”: no observations above the thresholds were observed in the “20-m” data bins (i.e. $S_v = 0$). Fish Presence = “1” designates “presence”: observations above the thresholds were observed in the “20-m” data bins (i.e. S_v is any value other than zero). Where present, bolded black values highlight ratios ~50:50 and bolded red values highlight ratios where the count of “present” observations exceeded the count of “absent” observations.

Fish Presence	CLA	reference	TOTAL		CLA	reference	TOTAL
0	22,236	11,897	34,133		55.1%	61.6%	57.2%
1	18,133	7,403	25,536		44.9%	38.4%	42.8%
TOTAL	40,369	19,300	59,669		100.0%	100.0%	100.0%

Tide Phase

The counts of “absent” observations exceeded counts of “present” observations for the high-slack, low-slack, and flooding tide phases, whereas the presence:absence counts for the ebb tide phase was nominally 50:50. The presence:absence ratio for the high-slack tide phase (the “baseline” category in this case) significantly differed from 50:50 ($p < 2e-16$; Table 11 and Table 13). Among the four tide phases, the presence:absence ratios for the following pairs were not statistically different: high-low ($p=0.83$), high-flood ($p=0.33$), flood-low ($p=0.43$) (Table 12). The presence:absence ratio for the ebb tide phase statistically differed ($p=0.00$) from each of the other three tide phases: high-ebb, low-ebb, flood-ebb (Table 12).

The presence:absence ratios across the three statistically similar tide phases (high, low, and flood) are surprisingly close (“absent” = 63.0%, 63.2%, and 62.2%) (Table 13). The data, at this highly aggregated level suggest that the **highest probability of observing backscatter from fish occurs during the ebbing tide** when the presence absence ratio is nearly 50:50 (“absent”=50.7%) (Table 13). Before generalizing this finding from the highly aggregated data, exploration of the data aggregated at finer scales should be considered. In addition, if entrained air is particularly evident on specific tides, one must consider the challenges of recording backscatter from fish when entrained air is present in the water column. Further analysis at the detailed level of examining the echograms in Echoview for the influence of entrained air obfuscating backscatter from fish may be required. Included in the script for automating exports from Echoview is coding that exports the depth of the bottom line along the shiptrack as well as the depth of the turbulence line. These can be used to estimate the proportion of the water column lost to entrained air.

Table 11. Generalized Linear Model Output of Fish Presence by Tide Phase – Contemporary Surveys Only. See text and the caption for Table 5 for more information.

Coefficients			
	Estimate	Std. Error	Pr(> z)
high	-0.53156	0.029431	<2e-16
ebb	+0.50300	0.031852	<2e-16
low	-0.00842	0.038541	0.827
flood	+0.03159	0.032721	<3.3e-01

Table 12. Summary Two-way Table of the Statistical Significance of Differences in Pairs of Fish Presence:Absence Ratios – Contemporary Surveys Only. See caption for Table 6 for more information.

	high	ebb	low	flood
high	0.00	0.00	0.83	0.33
ebb			0.00	0.00
low				0.43
flood				

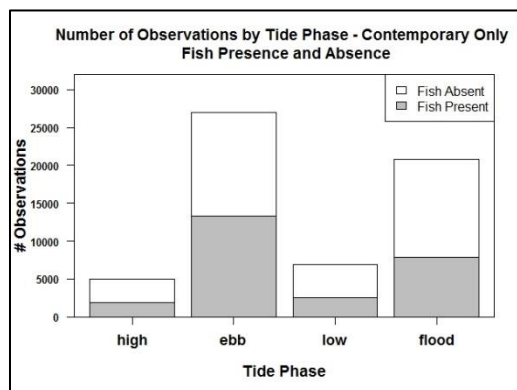


Figure 12. Fish Presence:Absence Observations by Tide Phase – Contemporary Surveys Only. Top of bar indicates the total number of observations by tide phase. Shaded portion indicates the number of observations assigned a value of “1” (i.e. integrated S_v by “20-m” bin $\neq 0$). White portion indicates number of observations assigned a value of “0” (i.e. integrated S_v by “20-m” bin = 0). Total number of observations = 59,669. See Table 13 for detailed quantification.

Table 13. Fish Presence:Absence Observations by Tide Phase – Contemporary Surveys Only. Left side of the table contains the count of fish presence:absence observations by category. Right side of the table contains the corresponding percentages. Fish Presence = “0” designates “absence”: no observations above the thresholds were observed in the “20-m” data bins (i.e. $S_v = 0$). Fish Presence = “1” designates “presence”: observations above the thresholds were observed in the “20-m” data bins (i.e. S_v is any value other than zero). Where present, bolded black values highlight ratios ~50:50 and bolded red values highlight ratios where the count of “present” observations exceeded the count of “absent” observations.

Fish Presence	high	ebb	low	flood	TOTAL		high	ebb	low	flood	TOTAL
0	3,119	13,676	4,386	12,952	34,133		63.0%	50.7%	63.2%	62.2%	57.2%
1	1,833	13,291	2,556	7,856	25,536		37.0%	49.3%	36.8%	37.8%	42.8%
TOTAL	4,952	26,967	6,942	20,808	59,669		100.0%	100.0%	100.0%	100.0%	100.0%

Diel State

Night is the first category for which the count of fish “present” exceeds the count of “absent” (52.5%:47.5%) (Table 16). Counts of “absent” exceeded counts of “present” for the remaining three diel states (dawn: 54.5%:45.5%, day: 65.0%:35.0%, dusk: 62.8%:37.2%) (Table 16). The fish presence:absence ratio for night was statistically different ($p = 0.00$) than the fish presence:absence ratios for dawn, day, and dusk (Table 15). The fish presence:absence ratios for the following pairs were statistically different: dawn-day ($p = 0.00$) and dawn-dusk ($p = 0.00$) (Table 15). The presence:absence ratio for the following pair was not statistically different: dusk-day ($p = 0.35$, Table 15). The distribution of observations (Table 16) suggest that the **probability of observing fish presence is highest at night (52.5%) and dawn (45.5%)**. Before

generalizing the finding of higher fish presence at night, aggregating the diel data by survey will provide information to confirm whether or not “present” counts exceeded “absent” counts in every case, seasonally, or on some other time scale. Other finer-scale aggregations of data may also provide insights such as diel by transect.

Table 14. Generalized Linear Model Output of Fish Presence by Diel State – Contemporary Surveys Only. See text and the caption for Table 5 for more information.

Coefficients			
	Estimate	Std. Error	Pr(> z)
dawn	-0.18051	0.05771	0.00176
day	-0.43615	0.05890	1e-13
dusk	-0.34421	0.07962	<2e-05
night	+0.28122	0.05905	<2e-06

Table 15. Summary Two-way Table of the Statistical Significance of Differences in Pairs of Fish Presence:Absence Ratios – Contemporary Surveys Only. See caption for Table 6 for more information.

	dawn	day	dusk	night
dawn	0.00	0.00	0.00	0.00
day			0.35	0.00
dusk				0.00
night				

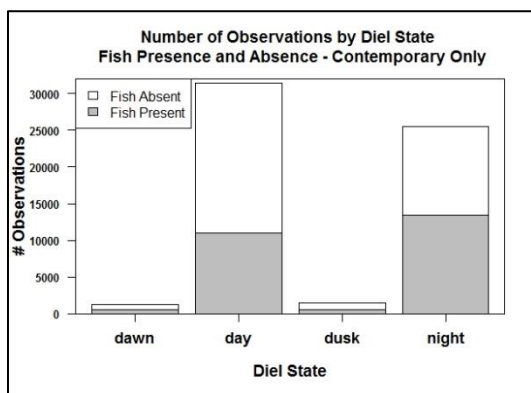


Figure 13. Fish Presence:Absence Observations by Diel State – Contemporary Surveys Only. Top of bar indicates the total number of observations by diel state. Shaded portion indicates the number of observations assigned a value of “1” (i.e. integrated S_v by “20-m” bin $\neq 0$). White portion indicates number of observations assigned a value of “0” (i.e. integrated S_v by “20-m” bin = 0). Total number of observations = 59,669. See **Table 16** for detailed quantification.

Table 16. Fish Presence:Absence Observations by Diel State – Contemporary Surveys Only. Left side of the table contains the count of fish presence:absence observations by category. Right side of the table contains the corresponding percentages. Fish Presence = “0” designates “absence”: no observations above the thresholds were observed in the “20-m” data bins (i.e. $S_v = 0$). Fish Presence = “1” designates “presence”: observations above the thresholds were observed in the “20-m” data bins (i.e. S_v is any value other than zero). Where present, bolded black values highlight ratios ~50:50 and bolded red values highlight ratios where the count of “present” observations exceeded the count of “absent” observations.

Fish Presence	dawn	day	dusk	night	TOTAL		dawn	day	dusk	night	TOTAL
0	660	20,443	894	12,136	34,133		54.5%	65.0%	62.8%	47.5%	57.2%
1	551	11,034	529	13,422	25,536		45.5%	35.0%	37.2%	52.5%	42.8%
TOTAL	1,211	31,477	1,423	25,558	59,669		100.0%	100.0%	100.0%	100.0%	100.0%

Survey

There were four surveys for which the count of “present” observations exceeded the count of “absent” observations (May 2016, Nov 2016, Jan 2017, May 2017) and one survey (Jul 2017) for which the fish presence:absence ratio was nominally 50:50 (Table 19b). The presence:absence ratios for all surveys were statistically different from each other ($p < 0.05$) except for one pair of surveys for which the ratios were not statistically different: May 2016-Nov 2016 ($p=0.16$, Table 18).

The survey results provide a good case study for using ecosystem knowledge and additional analyses to inform interpretations of the statistical results. For example, although the May 2016 and Nov 2016 fish presence:absence ratios are not statistically different (Table 18), the assemblage of fish moving through Minas Passage during May will be very different from the fish assemblage during November. In addition, there are another two survey pairs for which the fish presence:absence ratios were statistically different (Table 18) but for which the p-values were greater than 0.00 unlike all remaining pairing of surveys and therefore may warrant further investigation to inform interpretations of the statistical results: Oct 2016-May 2017 ($p=0.03$) and May 2017-Jul 2017 ($p=0.04$). For example, the movement of diadromous fish into and out of Minas Passage in the spring and fall may influence these patterns (Baker *et al.*, 2014; Dadswell, 2010; Rulifson and Dadswell, 1995).

The seasonal variation in the fish presence:absence ratio (Table 19b) may suggest that more frequent sampling (such as sequential days) is warranted during those months with higher fish presence in order to increase the likelihood of capturing the extremes of the fish movement.

Table 17. Generalized Linear Model Output of Fish Presence by Survey – Contemporary Surveys Only. See text and the caption for Table 5 for more information.

Coefficients			
	Estimate	Std. Error	Pr(> z)
2016 May	+0.24916	0.02623	<2e-16
2016 Aug	-1.79009	0.04133	<2e-16
2016 Oct	-0.87936	0.03663	<2e-16
2016 Nov	-0.05208	0.03668	0.16
2017 Jan	+0.11131	0.03601	0.00
2017 Mar	-1.37565	0.03831	<2e-16
2017 May	-0.16577	0.03569	3e-6
2017 Jul	-0.27002	0.03583	5e-14
2017 Aug	-0.66120	0.03600	<2e-16

Table 18. Summary Two-way Table of the Statistical Significance of Differences in Pairs of Fish Presence:Absence Ratios – Contemporary Surveys Only. See caption for Table 6 for more information.

	2016 May	2016 Aug	2016 Oct	2016 Nov	2017 Jan	2017 Mar	2017 May	2017 Jul	2017 Aug
2016 May	0.00	0.00	0.00	0.16	0.00	0.00	0.00	0.00	0.00
2016 Aug			0.00	0.00	0.00	0.00	0.00	0.00	0.00
2016 Oct				0.00	0.00	0.00	0.03	0.00	0.00
2016 Nov					0.00	0.00	0.00	0.00	0.00
2017 Jan						0.00	0.00	0.00	0.00
2017 Mar							0.00	0.00	0.00
2017 May								0.04	0.00
2017 Jul									0.00
2017 Aug									

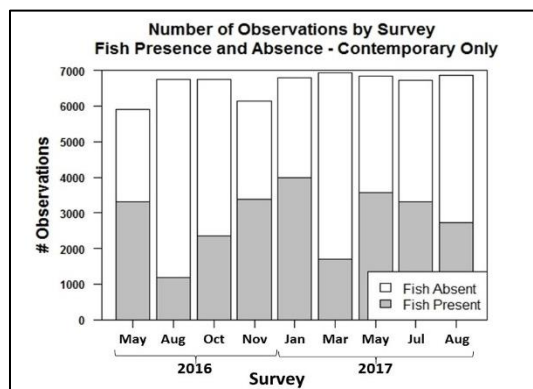


Figure 14. Fish Presence:Absence Observations by Survey – Contemporary Surveys Only. Top of bar indicates the total number of observations by survey. Shaded portion indicates the number of observations assigned a value of “1” (i.e. integrated S_v by 20-m bin $\neq 0$). White portion indicates number of observations assigned a value of “0” (i.e. integrated S_v by 20-m bin = 0). Total number of observations = 59,669. See Table 19 for detailed quantification.

Table 19. Fish Presence:Absence Observations by Survey – Contemporary Surveys Only. (a) Count of fish presence:absence observations by category and **(b)** the corresponding percentages. Fish Presence = “0” designates “absence”: no observations above the thresholds were observed in the “20-m” data bins (i.e. $S_v = 0$). Fish Presence = “1” designates “presence”: observations above the thresholds were observed in the “20-m” data bins (i.e. S_v is any value other than zero). Where present, **bolded black values** highlight ratios ~50:50 and **bolded red values** highlight ratios where the count of “present” observations exceeded the count of “absent” observations.

(a) Fish Presence	2016 May	2016 Aug	2016 Oct	2016 Nov	2017 Jan	2017 Mar	2017 May	2017 Jul	2017 Aug	TOTAL
0	2,587	5,556	4,402	2,768	2,788	5,238	3,277	3,392	4,125	34,133
1	3,319	1,190	2,344	3,371	3,998	1,698	3,562	3,322	2,732	25,536
TOTAL	5,906	6,746	6,746	6,139	6,786	6,936	6,839	6,714	6,857	59,669

(b) Fish Presence	2016 May	2016 Aug	2016 Oct	2016 Nov	2017 Jan	2017 Mar	2017 May	2017 Jul	2017 Aug	TOTAL
0	43.8%	82.4%	65.2%	45.1%	41.1%	75.5%	47.9%	50.5%	60.2%	57.2%
1	56.2%	17.6%	34.8%	54.9%	58.9%	24.5%	52.1%	49.5%	39.8%	42.8%
TOTAL	100.0%	100.0%	100.0%	100.0%	100.0%	100.0%	100.0%	100.0%	100.0%	100.0%

Transect

There was one transect for which the count of “present” observations exceeded the count of “absent” observations (N5: 51.5%:48.5%) and one transect for which the fish presence:absence ratio was 50:50 (N4) (Table 22b). Three pairs of adjacent transects (N2-N3, N4-N5, S2-S3) were not statistically different from each other ($p > 0.05$) in their fish presence:absence ratios (Table 21). The presence:absence ratio for N0 ($p = 0.00$) was statistically different from all other transects (Table 21). And the presence:absence ratios for one pair of cross-channel transects (S1:N1) were not statistically different ($p = 0.92$, Table 21). The presence:absence ratio of all other transect pairings were statistically different ($p < 0.05$, Table 21). These pairs were explored further in the results on relative fish density is examined later in this Results section.

The S1:N1 pair is of note given their placement across the channel from each other unlike the adjacent placement of all other pairs. The S1:N1 pairing may be of interest from a habitat-use perspective to explore further (e.g. are these transects in similar bathymetric settings such that the pairing provides insight into environmental characteristics that influence fish movement?). Investigation of the adjacent pairings may provide similar insights, but in addition may be of practical significance for survey design (e.g. when circumstances require excluding the time required to survey two transects or if in the interest of increasing survey frequency under the same budget, select one transect from two different pairs rather than two transects from the same pair).

The transect data is highly aggregated, i.e., all data collected for each transect during the first nine surveys of the contemporary research program are grouped for the following analyses. While caution is advised in using these results for decisions, the results from the highly aggregated data identify relationships warranting further investigation for ecosystem understanding.

Table 20. Generalized Linear Model Output of Fish Presence by Transect – Contemporary Surveys Only. See text and the caption for Table 5 for more information.

Coefficients			
	Estimate	Std. Error	Pr(> z)
N0	-0.80471	0.02786	<2e-16
N1	+0.49911	0.03723	<2e-16
N2	+0.67069	0.03661	<2e-16
N3	+0.67618	0.03678	<2e-16
N4	+0.78895	0.03674	<2e-16
N5	+0.86519	0.03725	<2e-16
S1	+0.45274	0.03743	<2e-16
S2	+0.26843	0.03803	1e-12
S3	+0.26212	0.03822	7e-12

Table 21. Summary Two-way Table of the Statistical Significance of Differences in Pairs of Fish Presence:Absence Ratios – Contemporary Surveys Only. See caption for Table 6 for more information.

	N0	N1	N2	N3	N4	N5		S1	S2	S3
N0	0.00	0.00	0.00	0.00	0.00	0.00		0.00	0.00	0.00
N1			0.00	0.00	0.00	0.00		0.37	0.00	0.00
N2				0.92	0.02	0.00		0.00	0.00	0.00
N3					0.03	0.00		0.00	0.00	0.00
N4						0.13		0.00	0.00	0.00
N5								0.00	0.00	0.00
S1									0.00	0.00
S2										0.92
S3										

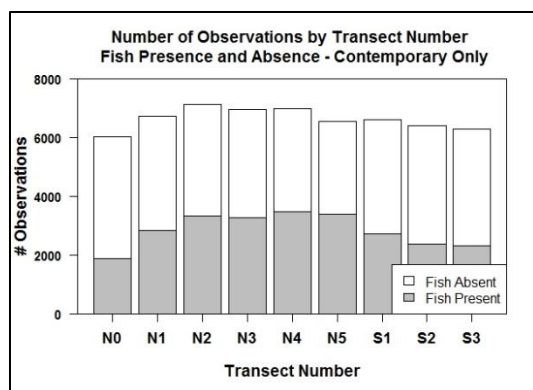


Figure 15. Fish Presence:Absence Observations by Transect – Contemporary Surveys Only. Top of bar indicates the total number of observations by transect. Shaded portion indicates the number of observations assigned a value of “1” (i.e. integrated S_v by “20-m” bin $\neq 0$). White portion indicates number of observations assigned a value of “0” (i.e. integrated S_v by “20-m” bin = 0). Total number of observations = 59,669. See Table 22 for detailed quantification.

Table 22. Fish Presence:Absence Observations by Transect – Contemporary Surveys Only. (a) Count of fish presence:absence observations by category and **(b)** the corresponding percentages. Fish Presence = “0” designates “absence”: no observations above the thresholds were observed in the “20-m” data bins (i.e. $S_v = 0$). Fish Presence = “1” designates “presence”: observations above the thresholds were observed in the “20-m” data bins (i.e. S_v is any value other than zero). Where present, **bolded black values** highlight ratios ~50:50 and **bolded red values** highlight ratios where the count of “present” observations exceeded the count of “absent” observations.

(a)											
Fish Presence	N0	N1	N2	N3	N4	N5		S1	S2	S3	TOTAL
0	4,168	3,866	3,803	3,706	3,517	3,176		3,876	4,045	3,976	34,133
1	1,864	2,848	3,326	3,259	3,462	3,374		2,726	2,366	2,311	25,536
TOTAL	6,032	6,714	7,129	6,965	6,979	6,550		6,602	6,411	6,287	59,669

(b)											
Fish Presence	N0	N1	N2	N3	N4	N5		S1	S2	S3	TOTAL
0	69.1%	57.6%	53.4%	53.2%	50.4%	48.5%		58.7%	63.1%	63.2%	57.2%
1	30.9%	42.4%	46.6%	46.8%	49.6%	51.5%		41.3%	36.9%	36.8%	42.8%
TOTAL	100.0%	100.0%	100.0%	100.0%	100.0%	100.0%		100.0%	100.0%	100.0%	100.0%

Example: Modeling with Additive and Interactive Explanatory Variables

Presented here is an example of using an ANOVA with a Chi-Square test to discern whether more complexity in the modeling provides a better fit to the data. For example, to predict fish presence:absence by tide phase or by tide phase and diel state (where tide and diel effects add to one another) or by tide phase * diel state (where tide and diel interact). Reduction of the deviance is an indication of the improvement of the model fit obtained by adding additional terms.

Modeling fish presence:absence using tide phase + diel state (additive) provides a statistically significant better fit to the data ($p < 2.2e-16$; Table 23) than by tide phase alone. Modeling fish presence:absence using tide phase * diel state (interaction) provides again, a better fit given that the deviance for the interactive model is less than that of the additive model (Table 23). The fit is a statistically significant better fit ($p < 2.2e-16$; Table 23). Therefore, variance in the fish presence:absence data is better explained using the complexity of the interaction of the two explanatory variables. To investigate the influence of the variety of explanatory variables and their additive versus interactive impact, more explanatory variables can be added and the ultimate model could be made very complex.

Table 23. Analysis of Deviance Table – Contemporary Surveys Only. Fish presence:absence during the contemporary surveys ($n=59,669$) was modeled using a single explanatory variable (Model 1: FishPresence ~ Tide Phase), model with two additive explanatory variables (Model 2: FishPresence ~ Tide Phase + Diel State), and modeled with two interactive explanatory variables (Model 3: FishPresence ~ Tide Phase * Diel State).

	Resid. Df.	Resid. Dev	Df	Deviance	Pr(>Chi)
Model 1	59665	80626			
Model 2	59662	78799	3	1827.66	< 2.2e-16
Model 3	59655	78475	7	324.06	< 2.2e-16

Analytical Approach: Relative Fish Density (as inferred from S_v)

The analysis examples presented in this section investigated the mean of relative fish density in relation to the spatial and temporal explanatory variables. ANOVA, Tukey HSD, and permutation tests were implemented to test for significant differences in the mean of S_v as grouped by explanatory variable categories. An estimated marginal means test was used to mitigate the imbalance of number of observations between the groupings within an explanatory variable and a final ANOVA was then used to test for differences between those means. The log form of backscattering (S_v) was used in these analyses because the distribution of residuals of the log-transformed data more closely approached normality than did the residuals of the data in their linear form.

When using the log-transformed data, the influence of extreme outliers (orders of magnitude) is de-emphasized when calculating the mean relative to using the data in their linear form. In some cases, the apparent sequence of categories within an explanatory variable may shift when ordered by magnitude of the mean (EMM vs. linear mean). The means by Research Program is an example of the re-ordering (Table 26). The goal of this section of analyses was to demonstrate examples by which statistical differences or similarities in relative fish density could be identified over space and time. Although the linear mean has been included in the tables below for ease of comparison, the relationship between categories in terms of relative magnitudes of fish density are more appropriately addressed using the boxplots and tables in the Data Visualization section of this report.

For each explanatory variable example, three tables and two figures are presented. One table reports the f-value and p-value results from the initial ANOVA test and reports the f-value level tested with the permutation tests and the resulting p-value. The second table reports the p-value results from the Tukey HSD test portraying the categories within the explanatory variables for which the difference in the mean were statistically significant. The third table contains the R output from the estimation of the marginal means and their difference testing: the estimated marginal mean, standard error, degrees of freedom, lower confidence level, upper confidence level, and compact letter (number) display groupings. A graph onto which are plotted the estimated marginal mean, the confidence interval (95%), and the comparison range is included, along with notched boxplots providing a visual representation of the data used in these analyses.

To provide additional information, the range of the confidence interval and the number of observations within each grouping were added to the estimated marginal means tables. You'll note that the confidence interval is smaller when the sample size (n) is larger. As was noted with the presence:absence analyses, large sample sizes can cause statistical testing to become sensitive to very small differences resulting in statistical significance for small and uninteresting effects. The sample size effect is particularly pronounced when there is an imbalance in the count of observations. Therefore, the statistical results in this section should not be interpreted

in isolation but considered in the context of other analyses in this report and the ecosystem questions at hand to determine the meaningfulness of the results in a biological context.

The notched boxplots were generated using the relative fish density data in its log-transformed state (S_v). The near co-location of the mean and the median on these plots is an indication that the distribution of the log-transformed data approaches normality, whereas the mean, when calculated in its linear form, was not co-located with the median, an indication of the influence of the extreme outliers in the linear data. (See boxplots generated from the data in its linear form in the Data Visualizations section of this report.)

Research Program

The mean of the relative fish density observations during the contemporary surveys differed significantly from the mean of the historical survey data (ANOVA: $f=393.8$, $p=0.00$; Table 24). This was corroborated by the permutation test ($p=1e-4$; Table 24) and the estimated marginal means test for which the results do not group the two categories indicating statistically significant differences in the estimated marginal means (Table 26). The 95% confidence intervals for the medians (Figure 17) and the comparison ranges (Figure 16) of each of the research programs do not overlap, providing additional evidence of differences between the data of the two research programs. The EMM (Table 26) for the historical dataset was higher than that of the contemporary dataset whereas as the inverse was true when evaluating the linear mean (Table 26). In light of the findings of a statistically significant difference in the observations of the relative fish densities in the contemporary vs. historical datasets, the analyses of relative fish density by spatial, temporal, and environmental variables was conducted using the **contemporary dataset only**.

Table 24. Statistical Results from ANOVA and Permutation Tests for Research Program. (LEFT): The f -value and p -value reported under the ANOVA heading are the results from the ANOVA when run with non-zero S_v observations from the “20-m dataset”. p -value < 0.05 indicates that there was a statistically significant difference in the mean of the S_v values by category within the explanatory variable. The ANOVA does not indicate between which set of means. When there are only two categories within the explanatory variable the two categories with statistically different means is self-evident. For explanatory variables with greater than two categories, finding the pairs of categories with and without statistical differences in the means can be found in the Tukey HSD results table. (RIGHT): The f -value threshold for the permutation test is reported as is the resulting p -value. For the 10,000 permutations of the observed S_v values randomly assigned to the categories within the explanatory variable, the p -value indicates the number of resulting f -values of equal or greater value than that listed as f -value test. A p -value of $1e-4$ indicates that no resulting f -values were equal to or greater than the f -value results from the original ANOVA, providing confidence that the original ANOVA results are robust.

ANOVA			Permutation Test	
f-value	p-value		f-value test	p-value
393.8	0.00		≥ 393.8	$1e-4$

Table 25. Tukey HSD Results for Research Program. Whereas the ANOVA is not designed to indicate between which categories the means are or are not statistically significant, the Tukey HSD was implemented to provide that information. For the pair of categories indicated by the column header and the row name, the statistical significance of the difference of the means is reported. Boxes are shaded gray where the *p*-value is less than 0.05. Boxes are not shaded when the *p*-value is greater than 0.05. Black boxes are redundant pairs.

	historical	contemporary
historical		0.00
contemporary		

Table 26. Estimated Marginal Mean and Compact Letter Display for Research Program. Results from the “emmean” computation as reported by R: The computed estimated marginal means (emmean) using the modeled data from the ANOVA are reported, along with the standard error (SE), degrees of freedom (df), lower confidence level (lower.CL), upper confidence level (upper.CL), and grouping (group). If a group number appears in one row only, the estimated marginal mean of the associated category (row name) is statistically different from the estimated marginal means of all other categories. If a group number is repeated in more than one row, the estimated marginal means of the associated categories do not statistically differ. To provide additional information, the range of the confidence interval and the number of observations (*n*) are included. Significance level used to determine group: $\alpha = 0.05$. Confidence level used: 0.95. The rows are ordered from lowest estimated marginal mean to highest.

RESEARCH PROGRAM	emmean (dB)	SE (dB)	df	lower.CL (dB)	upper.CL (dB)	group	CL range (dB)	n	min S _v (dB)	max S _v (dB)	mean S _v (linear)
contemporary	-87.53	0.06197	29103	-87.65	-87.41	1	0.24	25,536	-114.4	-40.8	-69.7
historical	-84.02	0.16576	29103	-84.35	-83.70	2	0.65	3,569	-104.1	-49.5	-75.5
TOTAL								29,105			

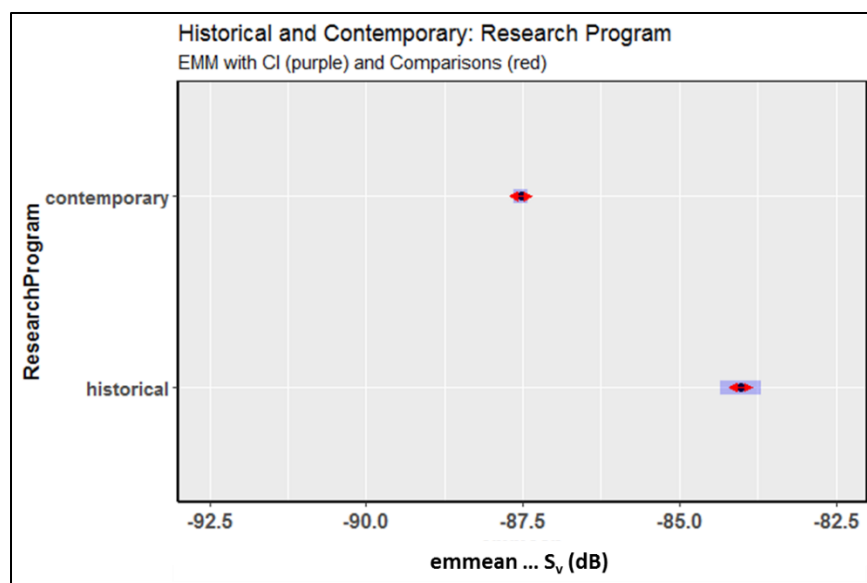


Figure 16. Estimated Marginal Mean with Confidence Interval and Comparisons. Graph displays results from the estimated marginal mean table. Black dot: estimated marginal mean. Purple bar: range from lower confidence level to upper confidence level (95% confidence interval). Red arrows: comparison range. Where the comparison levels (red arrows) overlap, the difference between the estimated marginal means is not statistically significant. Where the comparison levels (red arrows) do not overlap, the difference between the estimated marginal means is statistically significant. x-axis minimum and maximum has been standardized to encompass the full range necessary for all data reported in this section.

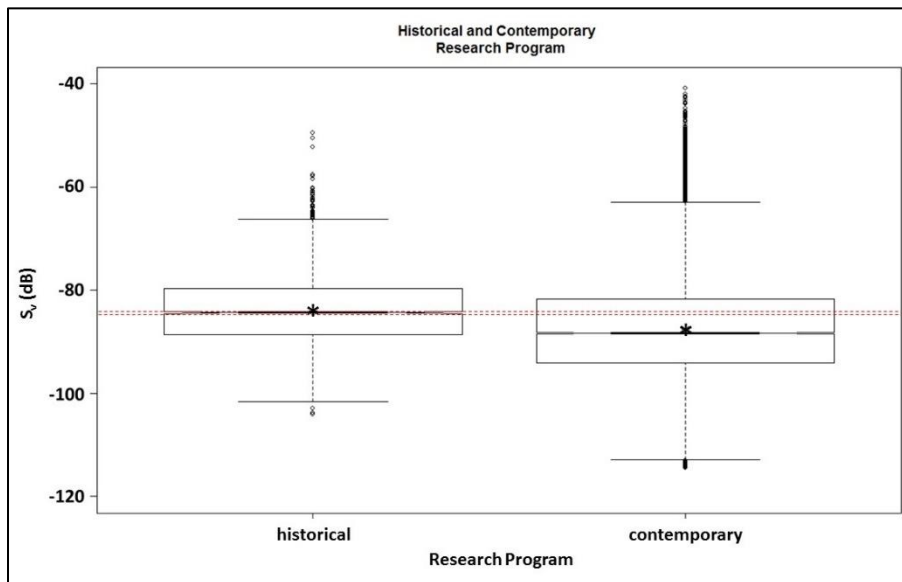


Figure 17. Notched Boxplot for Research Program. Notched boxplots of non-zero relative fish density values were calculated from "20-m dataset". Boxplot construction was the same as in the Data Visualizations section with the following exceptions. All calculations were done using backscatter in its log form (S_v). Mean of the log values is plotted as star. Median plus the confidence interval around the median is expressed as the notch. While not a formal test, if the notches from two boxes do not overlap it is "strong evidence" (95% confidence interval) that the medians differ. Colored horizontal dashed lines were added to guide the eye between box notches. Where the mean and median overlap, distribution of the data approaches normality. Therefore, note that the distribution of the data much more closely approaches normality when log-transformed (S_v) relative to the data in its linear form (s_v). (See boxplots of the linear data in the Data Visualizations section of this report.) Notched boxplots of similar ranges and similar shapes indicate that the variances are equal. The boxplots are presented in order to provide visual representation of the data used in these analyses.

Study Area

Generally, relative fish density was greater in the CLA than the reference site. The mean of the relative fish density observations in the reference study area differed significantly from the mean in the CLA study area (ANOVA: $f=164.4$, $p=0.00$; Table 27). This was corroborated by the permutation test ($p=1e-4$; Table 27) and the estimated marginal means test for which the results do not group the two categories indicating statistically significant differences in the estimated marginal means (Table 29). The 95% confidence intervals for the medians (Figure 18)

and the comparison ranges (Figure 19) of each of the study areas do not overlap providing additional evidence of differences between the observations in each study area.

Table 27. Statistical Results from ANOVA and Permutation Tests for Study Area – Contemporary Only. (LEFT): The *f*-value and *p*-value reported under the ANOVA heading are the results from the ANOVA when run with non-zero *S_v* observations from the “20-m dataset”. *p*-value < 0.05 indicates that there was a statistically significant difference in the mean of the *S_v* values by category within the explanatory variable. The ANOVA does not indicate between which set of means. When there are only two categories within the explanatory variable the two categories with statistically different means is self-evident. For explanatory variables with greater than two categories, finding the pairs of categories with and without statistical differences in the means can be found in the Tukey HSD results table. (RIGHT): The *f*-value threshold for the permutation test is reported as is the resulting *p*-value. For the 10,000 permutations of the observed *S_v* values randomly assigned to the categories within the explanatory variable, the *p*-value indicates the number of resulting *f*-values of equal or greater value than that listed as *f*-value test. A *p*-value of 1e-4 indicates that no resulting *f*-values were equal to or greater than the *f*-value results from the original ANOVA, providing confidence that the original ANOVA results are robust.

ANOVA		Permutation Test	
f-value	p-value	f-value test	p-value
164.4	0.00	>= 164.4	1e-4

Table 28. Tukey HSD Results for Study Area – Contemporary Only. Whereas the ANOVA is not designed to indicate between which categories the means are or are not statistically significant, the Tukey HSD was implemented to provide that information. For the pair of categories indicated by the column header and the row name, the statistical significance of the difference of the means is reported. Boxes are shaded gray where the *p*-value is less than 0.05. Boxes are not shaded when the *p*-value is greater than 0.05. Black boxes are redundant pairs.

	CLA	reference
CLA		0.00
reference		

Table 29. Compact Letter Display for Study Area – Contemporary Only. Results from the “emmean” computation as reported by R: The computed estimated marginal means (emmean) using the modeled data from the ANOVA are reported, along with the standard error (SE), degrees of freedom (df), lower confidence level (lower.CL), upper confidence level (upper.CL), and grouping (group). If a group number appears in one row only, the estimated marginal mean of the associated category (row name) is statistically different from the estimated marginal means of all other categories. If a group number is repeated in more than one row, the estimated marginal means of the associated categories do not statistically differ. To provide additional information, the range of the confidence interval and the number of observations (*n*) are included. Significance level used to determine group: alpha = 0.05. Confidence level used: 0.95. The rows are ordered from lowest estimated marginal mean to highest.

STUDY AREA	emmean (dB)	SE (dB)	df	lower.CL (dB)	upper.CL (dB)	group	CL range (dB)	n	min <i>S_v</i> (dB)	max <i>S_v</i> (dB)	mean <i>S_v</i> (linear)
reference	-88.81	0.11870	25534	-89.05	-88.58	1	0.47	7,403	-114.3	-48.1	-77.2
CLA	-87.01	0.07584	25534	-87.16	-86.86	2	0.30	18,133	-114.4	-40.8	-68.4
TOTAL								25,536			

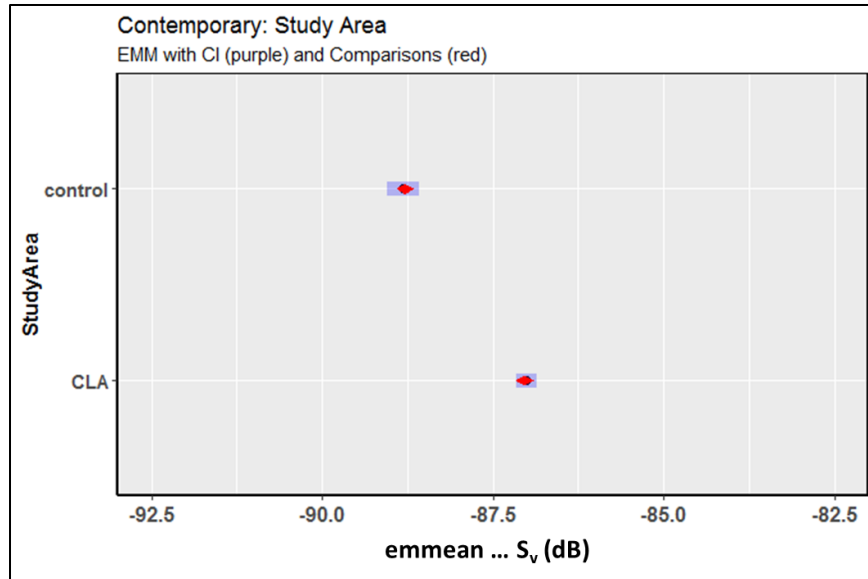


Figure 18. Estimated Marginal Mean with Confidence Interval and Comparisons for Study Area – Contemporary Only. Graph displays results from the estimated marginal mean table. Black dot: estimated marginal mean. Purple bar: range from lower confidence level to upper confidence level (95% confidence interval). Red arrows: comparison range. Where the comparison levels (red arrows) overlap, the difference between the estimated marginal means is not statistically significant. Where the comparison levels (red arrows) do not overlap, the difference between the estimated marginal means is statistically significant. x-axis minimum and maximum has been standardized to encompass the full range necessary for all data reported in this section.

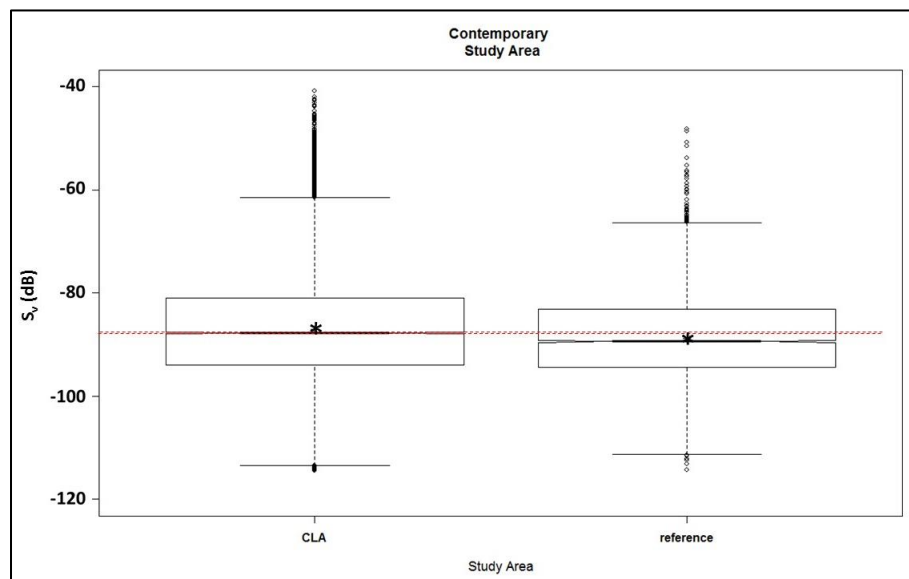


Figure 19. Notched Boxplot for Study Area – Contemporary Only. Boxplot of non-zero relative fish density data. Boxplot was calculated with the data in its log form (S_v) and are presented in order to provide visual representation of the data used in these analyses. See text and caption for Figure 17 for more information.

Tide Phase

There was a significant difference between the mean S_v values for at least one pairing of tide phases (ANOVA: $f=131.2$, $p=0.00$; Table 30) which was corroborated by the permutation test ($p=1e-4$; Table 30). The Tukey HSD test elaborated as to which tide phase pairings were found to have statistical differences between their means: high:low, high:flood, ebb:low, ebb:flood, low:flood. The only pairing for which the difference in the mean of the S_v values was not significant was the ebb:high pair (Table 31). These findings were corroborated by the estimated marginal means test for which the results pair ebb:high (Group 2; Table 32). The 95% confidence intervals (boxplot notches) for the medians overlap for the ebb and high-slack tide phases (Figure 21) as do the comparison ranges (Figure 20) whereas the median notches and comparison ranges do overlap for any other tide phase pairings.

As was noted in the Methods section of this report, the purpose of calculating the EMMs was to mitigate the effects of imbalances in the number of observations between categories within an explanatory variable. The underlying assumption in that approach is that there is no bias implicit in the sampling. There may be such a bias in the tide data. No data was collected during low-slack or high-slack along certain transects during the contemporary surveys: S1, S2 and N4, N5, S2, S3 respectively (Figure A3 in Appendix A). All data from those respective transects were excluded from the low-slack and high-slack analyses.

Table 30. Statistical Results from ANOVA and Permutation Tests for Tide Phase – Contemporary Only. (LEFT): The f -value and p -value reported under the ANOVA heading are the results from the ANOVA when run with non-zero S_v observations from the “20-m dataset”. p -value < 0.05 indicates that there was a statistically significant difference in the mean of the S_v values by category within the explanatory variable. The ANOVA does not indicate between which set of means. When there are only two categories within the explanatory variable the two categories with statistically different means is self-evident. For explanatory variables with greater than two categories, finding the pairs of categories with and without statistical differences in the means can be found in the Tukey HSD results table. (RIGHT): The f -value threshold for the permutation test is reported as is the resulting p -value. For the 10,000 permutations of the observed S_v values randomly assigned to the categories within the explanatory variable, the p -value indicates the number of resulting f -values of equal or greater value than that listed as f -value test. A p -value of $1e-4$ indicates that no resulting f -values were equal to or greater than the f -value results from the original ANOVA, providing confidence that the original ANOVA results are robust.

ANOVA			Permutation Test	
f-value	p-value		f-value test	p-value
131.2	0.00		>= 131.2	1e-4

Table 31. Tukey HSD Results for Tide Phase – Contemporary Only. Whereas the ANOVA is not designed to indicate between which categories the means are or are not statistically significant, the Tukey HSD was implemented to provide that information. For the pair of categories indicated by the column header and the row name, the statistical significance of the difference of the means is reported. Boxes are shaded gray where the p-value is less than 0.05. Boxes are not shaded when the p-value is greater than 0.05. Black boxes are redundant pairs.

	high	ebb	low	flood
high		1.00	0.00	0.00
ebb			0.00	0.00
low				0.00
flood				

Table 32. Compact Letter Display for Tide Phase – Contemporary Only. Results from the “emmean” computation as reported by R: The computed estimated marginal means (emmean) using the modeled data from the ANOVA are reported, along with the standard error (SE), degrees of freedom (df), lower confidence level (lower.CL), upper confidence level (upper.CL), and grouping (group). If a group number appears in one row only, the estimated marginal mean of the associated category (row name) is statistically different from the estimated marginal means of all other categories. If a group number is repeated in more than one row, the estimated marginal means of the associated categories do not statistically differ. To provide additional information, the range of the confidence interval and the number of observations (n) are included. Significance level used to determine group: alpha = 0.05. Confidence level used: 0.95. The rows are ordered from lowest estimated marginal mean to highest.

TIDE	emmean (dB)	SE (dB)	df	lower.CL (dB)	upper.CL (dB)	group	CL range (dB)	n	min S _v (dB)	max S _v (dB)	mean S _v (linear)
flood	-89.09	0.1147	25532	-89.32	-88.87	1	0.45	7,856	-114.32	-43.11	-74.28
ebb	-87.19	0.0882	25532	-87.37	-87.02	2	0.35	13,291	-114.40	-42.37	-68.65
high	-87.17	0.2375	25532	-87.65	-86.72	2	0.93	1,833	-112.53	-51.59	-72.72
low	-84.75	0.2011	25532	-85.14	-84.35	3	0.79	2,556	-112.25	-40.78	-66.79
TOTAL								25,536			

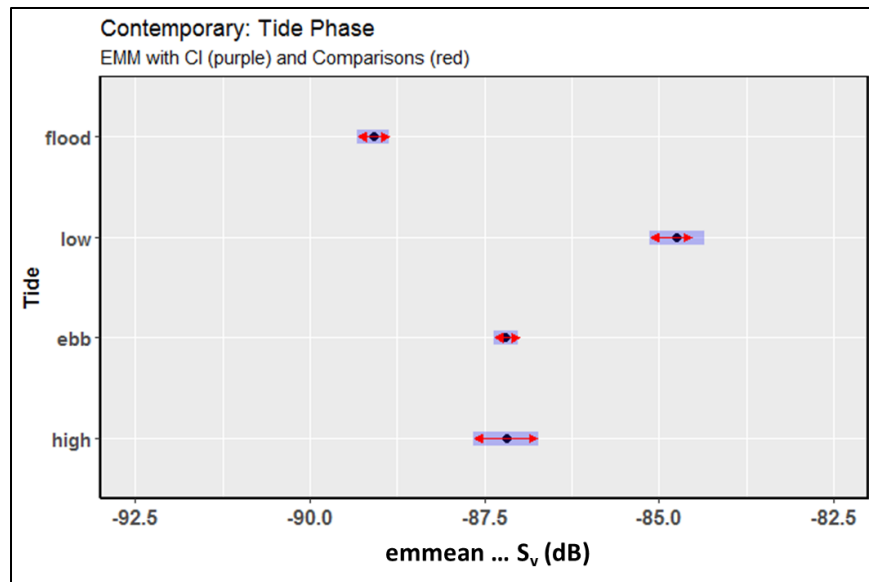


Figure 20. Estimated Marginal Mean with Confidence Interval and Comparisons for Tide Phase – Contemporary Only. Graph displays results from the estimated marginal mean table. Black dot: estimated marginal mean. Purple bar: range from lower confidence level to upper confidence level (95% confidence interval). Red arrows: comparison range. Where the comparison levels (red arrows) overlap, the difference between the estimated marginal means is not statistically significant. Where the comparison levels (red arrows) do not overlap, the difference between the estimated marginal means is statistically significant. x-axis minimum and maximum has been standardized to encompass the full range necessary for all data reported in this section.

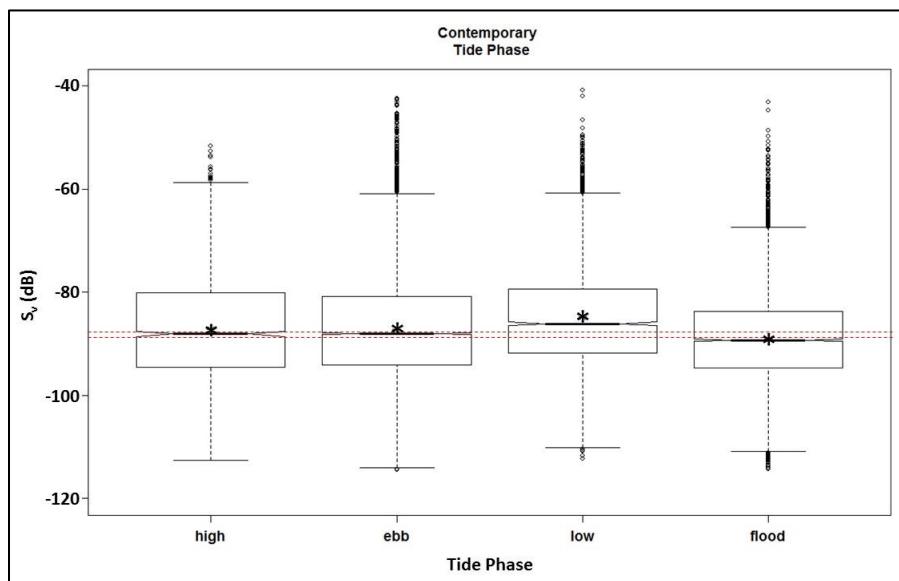


Figure 21. Notched Boxplot for Tide Phase – Contemporary Only. Boxplot of non-zero relative fish density data. Boxplot was calculated with the data in its log form (S_v) and are presented in order to provide visual representation of the data used in these analyses. See text and caption for Figure 17 for more information.

Diel State

There was a significant difference between the mean S_v values for at least one of the pairing of the diel states (ANOVA: $f=200.5$, $p=0.00$; Table 33) which was corroborated by the permutation test ($p=1e-4$; Table 33). Pairwise statistical differences between their means: dawn: day, dawn:night, day:night, dusk:night (Table 34, Tukey HSD test). There were two pairings for which the difference of the means were not statistically significant: dawn:dusk, day:dusk (Table 34). These findings were corroborated by the estimated marginal means test for which the results group dawn:dusk (Group 1) and day:dusk (Group 2) (Table 35). The 95% confidence intervals (boxplot notches) for the medians (Figure 23) and the comparison ranges (Figure 22) overlap in the same pattern: dawn:dusk and day:dusk. There were no overlaps for any of the other diel pairings.

As was noted in the Methods section of this report, the purpose of calculating the EMMs was to mitigate the effects of imbalances in the number of observations between categories within an explanatory variable. The underlying assumption in that approach is that there is no bias implicit in the sampling. There may be such a bias in the diel data. No data was collected during dawn or dusk on a low-slack tide during the contemporary surveys (Figure A3 in Appendix A), thereby excluding all low-slack tide measurements from the dawn or dusk analyses. Similarly, certain transects were not traversed during dawn or dusk during the contemporary surveys: N3, N4 and N5, S1, S2 respectively (Figure A3 in Appendix A).

Table 33. Statistical Results from ANOVA and Permutation Tests for Diel State– Contemporary Only. (LEFT): The f -value and p -value reported under the ANOVA heading are the results from the ANOVA when run with non-zero S_v observations from the “20-m dataset”. p -value < 0.05 indicates that there was a statistically significant difference in the mean of the S_v values by category within the explanatory variable. The ANOVA does not indicate between which set of means. When there are only two categories within the explanatory variable the two categories with statistically different means is self-evident. For explanatory variables with greater than two categories, finding the pairs of categories with and without statistical differences in the means can be found in the Tukey HSD results table. (RIGHT): The f -value threshold for the permutation test is reported as is the resulting p -value. For the 10,000 permutations of the observed S_v values randomly assigned to the categories within the explanatory variable, the p -value indicates the number of resulting f -values of equal or greater value than that listed as f -value test. A p -value of $1e-4$ indicates that no resulting f -values were equal to or greater than the f -value results from the original ANOVA, providing confidence that the original ANOVA results are robust.

ANOVA			Permutation Test	
f-value	p-value		f-value test	p-value
200.5	0.00		>= 200.5	1e-4

Table 34. Tukey HSD Results for Diel State – Contemporary Only. Whereas the ANOVA is not designed to indicate between which categories the means are or are not statistically significant, the Tukey HSD was implemented to provide that information. For the pair of categories indicated by the column header and the row name, the statistical significance of the difference of the means is reported. Boxes are shaded gray where the p-value is less than 0.05. Boxes are not shaded when the p-value is greater than 0.05. Black boxes are redundant pairs.

	dawn	day	dusk	night
dawn		0.00	0.47	0.00
day			0.44	0.00
dusk				0.00
night				

Table 35. Compact Letter Display for Diel State – Contemporary Only. Results from the “emmean” computation as reported by R: The computed estimated marginal means (emmean) using the modeled data from the ANOVA are reported, along with the standard error (SE), degrees of freedom (df), lower confidence level (lower.CL), upper confidence level (upper.CL), and grouping (group). If a group number appears in one row only, the estimated marginal mean of the associated category (row name) is statistically different from the estimated marginal means of all other categories. If a group number is repeated in more than one row, the estimated marginal means of the associated categories do not statistically differ. To provide additional information, the range of the confidence interval and the number of observations (n) are included. Significance level used to determine group: alpha = 0.05. Confidence level used: 0.95. The rows are ordered from lowest estimated marginal mean to highest.

DIEL	emmean (dB)	SE (dB)	df	lower.CL (dB)	upper.CL (dB)	group	CL range (dB)	n	min S _v (dB)	max S _v (dB)	mean S _v (linear)
dawn	-90.61	0.43144	25532	-91.46	-89.77	1	1.69	551	-109.6	-62.5	-82.1
dusk	-89.72	0.44032	25532	-90.59	-88.86	12	1.73	529	-113.5	-63.2	-81.6
day	-89.05	0.09641	25532	-89.24	-88.86	2	0.38	11,034	-114.4	-40.8	-72.0
night	-86.07	0.08742	25532	-86.24	-85.90	3	0.34	13,422	-114.3	-42.0	-68.2
TOTAL								25,536			

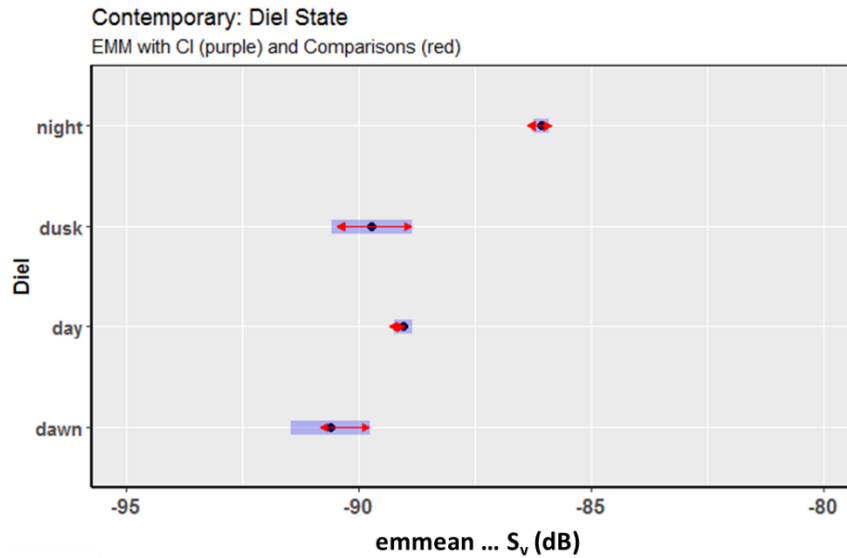


Figure 22. Estimated Marginal Mean with Confidence Interval and Comparisons for Diel State – Contemporary Only. Graph displays results from the estimated marginal mean table. Black dot: estimated marginal mean. Purple bar: range from lower confidence level to upper confidence level (95% confidence interval). Red arrows: comparison range. Where the comparison levels (red arrows) overlap, the difference between the estimated marginal means is not statistically significant. Where the comparison levels (red arrows) do not overlap, the difference between the estimated marginal means is statistically significant. x-axis minimum and maximum has been standardized to encompass the full range necessary for all data reported in this section.

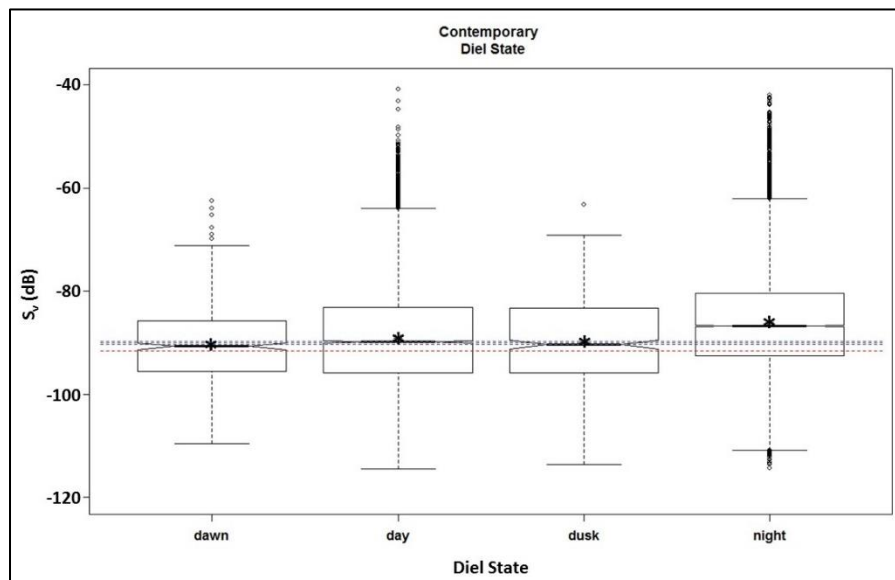


Figure 23. Notched Boxplot for Diel State – Contemporary Only. Boxplot of non-zero relative fish density data. Boxplot was calculated with the data in its log form (S_v) and are presented in order to provide visual representation of the data used in these analyses. See text and caption for Figure 17 for more information.

Survey

There was a statistically significant difference between the mean of the S_v values for at least one pairing of the surveys (ANOVA: $f=575.2$, $p=0.00$ Table 36) corroborated by the permutation test ($p=1e-4$; Table 36). All survey pairings were found to have statistical differences between their means, except for three pairings for which the difference in the survey means was not statistically significant: Aug 2016:Jan 2017, Aug 2016:Aug 2017, Jan 2017:Aug 2017 (Table 37). These findings were corroborated by the estimated marginal means test for which the results group the Aug 2016, Jan 2017, and Aug 2017 surveys (Group=3, Table 38) and shown by the overlap in the comparison ranges (Figure 24). Whereas the analysis using the means and the estimated marginal means grouped the three surveys together, the 95% confidence intervals around the median suggest that May 2016 may be included in the grouping established by the means (Aug 2016, Jan 2017, and Aug 2017; Figure 25).

Table 36. Statistical Results from ANOVA and Permutation Tests for Survey – Contemporary Only. (LEFT): The f -value and p -value reported under the ANOVA heading are the results from the ANOVA when run with non-zero S_v observations from the “20-m dataset”. p -value < 0.05 indicates that there was a statistically significant difference in the mean of the S_v values by category within the explanatory variable. The ANOVA does not indicate between which set of means. When there are only two categories within the explanatory variable the two categories with statistically different means is self-evident. For explanatory variables with greater than two categories, finding the pairs of categories with and without statistical differences in the means can be found in the Tukey HSD results table. (RIGHT): The f -value threshold for the permutation test is reported as is the resulting p -value. For the 10,000 permutations of the observed S_v values randomly assigned to the categories within the explanatory variable, the p -value indicates the number of resulting f -values of equal or greater value than that listed as f -value test. A p -value of $1e-4$ indicates that no resulting f -values were equal to or greater than the f -value results from the original ANOVA, providing confidence that the original ANOVA results are robust.

ANOVA			Permutation Test	
f-value	p-value		f-value test	p-value
575.2	0.00		≥ 575.2	$1e-4$

Table 37. Tukey HSD Results for Survey – Contemporary Only. Whereas the ANOVA is not designed to indicate between which categories the means are or are not statistically significant, the Tukey HSD was implemented to provide that information. For the pair of categories indicated by the column header and the row name, the statistical significance of the difference of the means is reported. Boxes are shaded gray where the p-value is less than 0.05. Boxes are not shaded when the p-value is greater than 0.05. Black boxes are redundant pairs.

	2016 May	2016 Aug	2016 Oct	2016 Nov	2017 Jan	2017 Mar	2017 May	2017 Jul	2017 Aug
2016 May		0.00	0.00	0.00	0.00	0.00	0.00	0.00	0.00
2016 Aug			0.00	0.00	1.00	0.00	0.00	0.00	1.00
2016 Oct				0.00	0.00	0.00	0.00	0.00	0.00
2016 Nov					0.00	0.00	0.00	0.00	0.00
2017 Jan						0.00	0.00	0.00	0.87
2017 Mar							0.00	0.00	0.00
2017 May								0.00	0.00
2017 Jul									0.00
2017 Aug									

Table 38. Compact Letter Display for Survey – Contemporary Only. Results from the “emmean” computation as reported by R: The computed estimated marginal means (emmean) using the modeled data from the ANOVA are reported, along with the standard error (SE), degrees of freedom (df), lower confidence level (lower.CL), upper confidence level (upper.CL), and grouping (group). If a group number appears in one row only, the estimated marginal mean of the associated category (row name) is statistically different from the estimated marginal means of all other categories. If a group number is repeated in more than one row, the estimated marginal means of the associated categories do not statistically differ. To provide additional information, the range of the confidence interval and the number of observations (n) are included. Significance level used to determine group: alpha = 0.05. Confidence level used: 0.95. The rows are ordered from lowest estimated marginal mean to highest.

SURVEY	emmean (dB)	SE (dB)	df	lower.CL (dB)	upper.CL (dB)	group	CL range (dB)	n	min S _v (dB)	max S _v (dB)	mean S _v (linear)
2017 Mar	-94.01	0.2289	25527	-95.54	-93.64	1	1.90	1,698	-114.3	-63.8	-84.1
2016 Oct	-92.55	0.1948	25527	-92.93	-92.16	2	0.77	2,344	-114.4	-62.5	-83.1
2017 Jan	-89.74	0.1492	25527	-90.04	-89.45	3	0.59	3,998	-112.1	-58.5	-82.8
2016 Aug	-89.59	0.2734	25527	-90.13	-89.05	3	1.08	1,190	-112.1	-61.7	-80.7
2017 Aug	-89.40	0.1805	25527	-89.75	-89.05	3	0.70	2,732	-111.6	-55.8	-81.8
2016 May	-88.36	0.1637	25527	-88.68	-88.04	4	0.64	3,319	-113.8	-48.1	-72.5
2016 Nov	-87.03	0.1625	25527	-87.35	-86.71	5	0.64	3,371	-113.9	-46.5	-77.7
2017 May	-82.39	0.1580	25527	-82.70	-82.08	6	0.62	3,562	-113.8	-40.8	-62.0
2017 Jul	-80.90	0.1636	25527	-81.22	-80.58	7	0.64	3,322	-111.6	-53.5	-72.8
TOTAL								25,536			

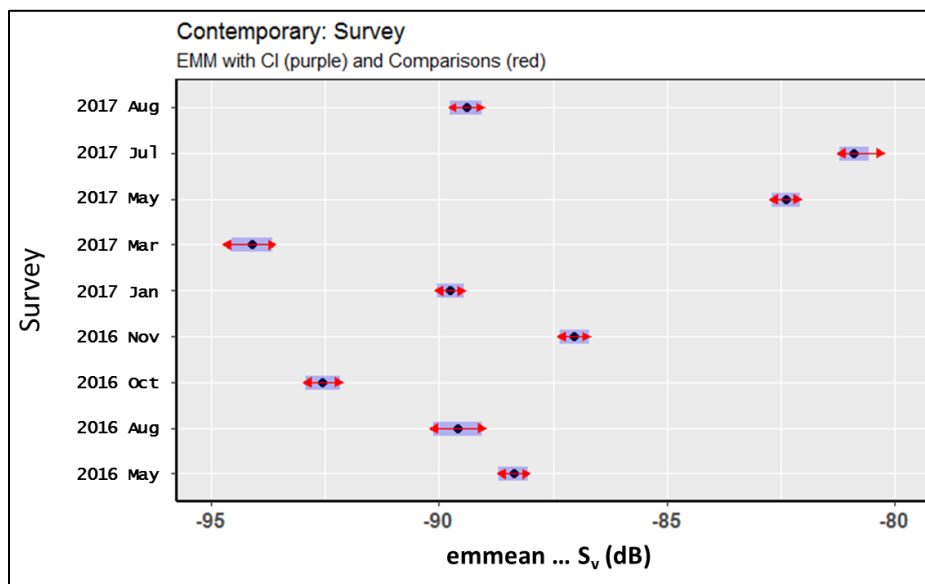


Figure 24. Estimated Marginal Mean with Confidence Interval and Comparisons by Survey – Contemporary Only. Graph displays results from the estimated marginal mean table. Black dot: estimated marginal mean. Purple bar: range from lower confidence level to upper confidence level (95% confidence interval). Red arrows: comparison range. Where the comparison levels (red arrows) overlap, the difference between the estimated marginal means is not statistically significant. Where the comparison levels (red arrows) do not overlap, the difference between the estimated marginal means is statistically significant. x-axis minimum and maximum has been standardized to encompass the full range necessary for all data reported in this section.

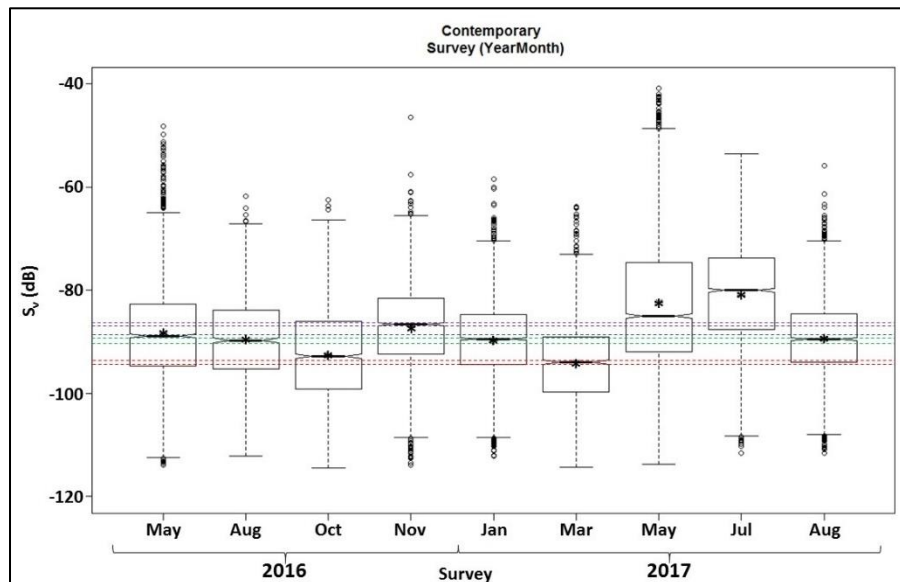


Figure 25. Notched Boxplot by Survey – Contemporary Only. Boxplot of non-zero relative fish density data. Boxplot was calculated with the data in its log form (S_v) and are presented in order to provide visual representation of the data used in these analyses. See text and caption for Figure 17 for more information.

Transect

There was a statistically significant difference between the mean of the S_v values for at least one pairing of the transects (ANOVA: $f=61.9$, $p=0.00$ Table 39) corroborated by the permutation test ($p=1e-4$; Table 39). The ANOVA f -value of 61.9 is the lowest of, and substantially lower than, the f -value results from the ANOVA tests for the variety of explanatory variable examples included in these analyses. Of the 36 possible transect pairings, 11 pairings were not found to have statistical differences between their means: N1:N2, N1:N4, N1:S3, N2:N3, N2:N4, N2:S3, N3:N5, N3:S3, N4:S3, N5:S3, S1:S2 (Table 40). As with the fish presence:absence analysis, transect N0 alone is statistically different than all other transects (Table 40). The means for all remaining possible transect pairs were statistically different. These findings were corroborated by the estimated marginal means test for which the results group the following transect pairs: S1:S2 (Group 1), N3:N5:S3 (Group 2), N2:N3:S3 (Group 3), N1:N2:N4:S3 (Group 4) with the estimated marginal mean for transect N0 statistically different than the estimated marginal mean for all other transects (Table 41). The 95% confidence intervals around the medians suggest two groupings and two singular transects: S1:S2, N1:N2:N3:N5:S3, and N0 and N4 respectively (Figure 27).

Table 39. Statistical Results from ANOVA and Permutation Tests by Transect – Contemporary Only. (LEFT): The *f*-value and *p*-value reported under the ANOVA heading are the results from the ANOVA when run with non-zero *S_v* observations from the “20-m dataset”. *p*-value < 0.05 indicates that there was a statistically significant difference in the mean of the *S_v* values by category within the explanatory variable. The ANOVA does not indicate between which set of means. When there are only two categories within the explanatory variable the two categories with statistically different means is self-evident. For explanatory variables with greater than two categories, finding the pairs of categories with and without statistical differences in the means can be found in the Tukey HSD results table. (RIGHT): The *f*-value threshold for the permutation test is reported as is the resulting *p*-value. For the 10,000 permutations of the observed *S_v* values randomly assigned to the categories within the explanatory variable, the *p*-value indicates the number of resulting *f*-values of equal or greater value than that listed as *f*-value test. A *p*-value of 1e-4 indicates that no resulting *f*-values were equal to or greater than the *f*-value results from the original ANOVA, providing confidence that the original ANOVA results are robust.

ANOVA			Permutation Test	
f-value	p-value		f-value test	p-value
61.9	0.00		>= 61.9	1e-4

Table 40. Tukey HSD Results by Transect – Contemporary Only. Whereas the ANOVA is not designed to indicate between which categories the means are or are not statistically significant, the Tukey HSD was implemented to provide that information. For the pair of categories indicated by the column header and the row name, the statistical significance of the difference of the means is reported. Boxes are shaded gray where the *p*-value is less than 0.05. Boxes are not shaded when the *p*-value is greater than 0.05. Black boxes are redundant pairs.

	N0	N1	N2	N3	N4	N5		S1	S2	S3
N0		0.00	0.00	0.00	0.00	0.00		0.00	0.00	0.00
N1			0.98	0.04	1.00	0.00		0.00	0.00	0.69
N2				0.40	0.86	0.01		0.00	0.00	1.00
N3					0.01	0.94		0.00	0.00	0.97
N4						0.01		0.00	0.00	0.41
N5								0.00	0.00	0.32
S1									0.96	0.00
S2										0.00
S3										

Table 41. Compact Letter Display by Transect – Contemporary Only. Results from the “emmean” computation as reported by R: The computed estimated marginal means (emmean) using the modeled data from the ANOVA are reported, along with the standard error (SE), degrees of freedom (df), lower confidence level (lower.CL), upper confidence level (upper.CL), and grouping (group). If a group number appears in one row only, the estimated marginal mean of the associated category (row name) is statistically different from the estimated marginal means of all other categories. If a group number is repeated in more than one row, the estimated marginal means of the associated categories do not statistically differ. To provide additional information, the range of the confidence interval and the number of observations (n) are included. Significance level used to determine group: alpha = 0.05. Confidence level used: 0.95. The rows are ordered from lowest estimated marginal mean to highest.

STUDY AREA	emmean (dB)	SE (dB)	df	lower.CL (dB)	upper.CL (dB)	group	CL range (dB)	n	min S _v (dB)	max S _v (dB)	mean S _v (linear)
S1	-89.59	0.1944	25527	-89.97	-89.21	1	0.76	2,726	-114.3	-48.6	-76.4
S2	-89.25	0.2086	25527	-89.66	-88.84	1	0.82	2,366	-111.5	-56.6	-79.7
N5	-88.10	0.1747	25527	-88.45	-87.76	2	0.69	3,374	-114.2	-43.1	-73.1
N3	-87.78	0.1778	25527	-88.13	-87.44	23	0.69	3,259	-114.1	-56.0	-76.9
S3	-87.46	0.2111	25527	-87.88	-87.05	234	0.83	2,311	-111.1	-48.1	-76.5
N2	-87.23	0.1760	25527	-87.58	-86.89	34	0.69	3,326	-113.4	-40.8	-69.9
N1	-86.95	0.1902	25527	-87.33	-86.58	4	0.75	2,848	-112.5	-42.0	-68.7
N4	-86.87	0.1725	25527	-87.20	-86.53	4	0.67	3,462	-114.4	-45.4	-73.7
N0	-83.63	0.2351	25527	-84.09	-83.17	5	0.92	1,864	-111.5	-42.4	-60.9
TOTAL								25,536			

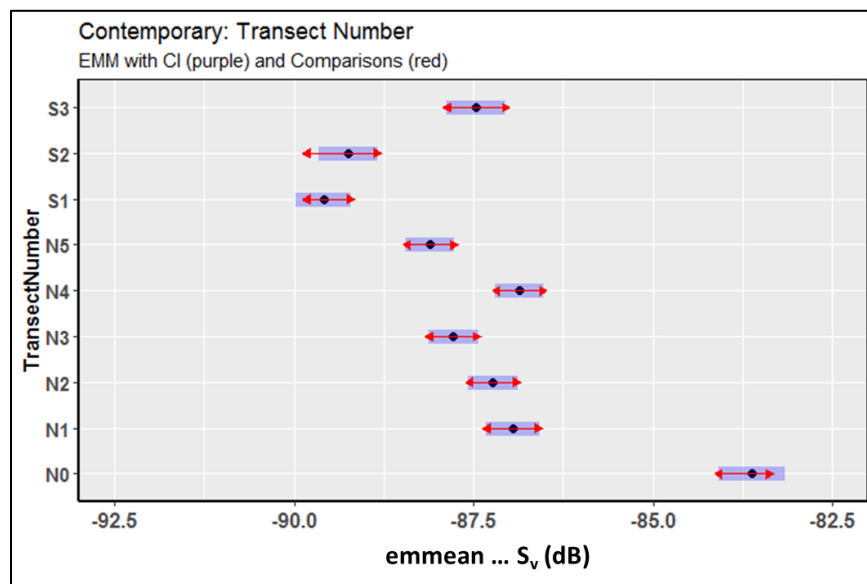


Figure 26. Estimated Marginal Mean with Confidence Interval and Comparisons by Transect – Contemporary Only. Graph displays results from the estimated marginal mean table. Black dot: estimated marginal mean. Purple bar: range from lower confidence level to upper confidence level (95% confidence interval). Red arrows: comparison range. Where the comparison levels (red arrows) overlap, the difference between the estimated marginal means is not statistically significant. Where the comparison levels (red arrows) do not overlap, the difference between the estimated marginal means is statistically significant. x-axis minimum and maximum has been standardized to encompass the full range necessary for all data reported in this section.

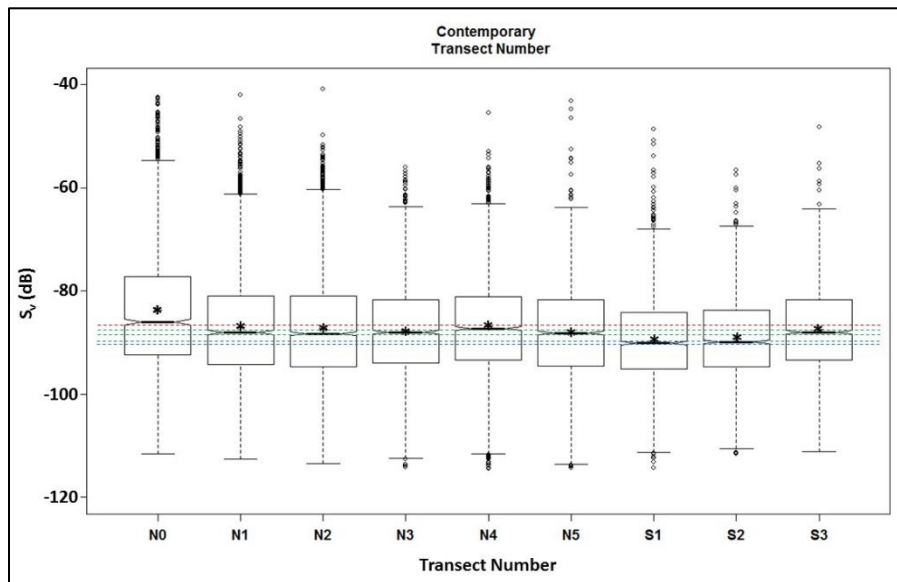


Figure 27. Notched Boxplot by Transect – Contemporary Only. Boxplot of non-zero relative fish density data. Boxplot was calculated with the data in its log form (S_v) and are presented in order to provide visual representation of the data used in these analyses. See text and caption for Figure 17 for more information.

Table 42. Results Summary Table – Contemporary Only. Left three columns: number of observations (n) for fish absence (n:0), fish presence (n:1), category total (n:all). Percent columns: see caption to Table 4. P:A: Results from Presence:Absence analyses. Values indicate statistical groupings. “1” indicates the category with the highest percent of “present” observations within the Explanatory Variable. max S_v : checkmark indicates the category with the highest fish density observation (S_v) within the Explanatory Variable. data range: checkmark indicates the category with the widest range between the maximum and minimum fish density observation (S_v), “w” indicates the category with the widest range between the upper and lower whisker positions. EMM: compact letter display indicating groupings from the fish density analyses. “1” indicates category with the highest estimated marginal mean. Numeral groupings reported here are in opposite order as reported in the individual Results tables where “1” indicated category with the lowest estimated marginal mean. Median: compact letter display indicating groupings defined by overlap of the notch ranges in the notched boxplots. “1” indicates category with the highest median S_v .

See table on the next page.

See previous page for Table Description.

Explanatory Variable	Category									>50%		50%	50%			< 50%		P:A	max S _v	data range	EMM	median
		n:0	n:1	n:all		0	1	100%		0	1	0	1		0	1						
Research Program	historical	7,778	3,569	11,347		68.5%	31.5%	100.0%							68.5%	31.5%		2			1	1
	contemporary	34,133	25,536	59,669		57.2%	42.8%	100.0%							57.2%	42.8%		1	√	vw	2	2
Study Area	CLA	22,236	18,133	40,369		55.1%	44.9%	100.0%							55.1%	44.9%		1	√	vw	1	1
	reference	11,897	7,403	19,300		61.6%	38.4%	100.0%							61.6%	38.4%		2			2	2
Tide Phase	high	3,119	1,833	4,952		63.0%	37.0%	100.0%							63.0%	37.0%		2		w	2	2
	ebb	13,676	13,291	26,967		50.7%	49.3%	100.0%				50.7%	49.3%					1		√	2	2
	low	4,386	2,556	6,942		63.2%	36.8%	100.0%							63.2%	36.8%		2	√		1	1
	flood	12,952	7,869	20,808		62.2%	37.8%	100.0%							62.2%	37.8%		2			3	3
Diel State	dawn	660	551	1,211		54.5%	45.5%	100.0%							54.5%	45.5%		2			3	3
	day	20,443	11,034	31,477		65.0%	35.0%	100.0%							65.0%	35.0%		3	√	vw	3,2	2
	dusk	894	529	1,423		62.8%	37.2%	100.0%							62.8%	37.2%		3			2	2,3
	night	12,136	13,422	25,558		47.5%	52.5%	100.0%		47.5%	52.5%							1			1	1
Survey	2016-May	2,587	3,319	5,906		43.8%	56.2%	100.0%		43.8%	56.2%							2			4	4
	2016-Aug	5,556	1,190	6,746		82.4%	17.6%	100.0%							82.4%	17.6%		8			5	5
	2016-Oct	4,402	2,344	6,746		65.2%	34.8%	100.0%							65.2%	34.8%		6			6	6
	2016-Nov	2,768	3,371	6,139		45.1%	54.9%	100.0%		45.1%	54.9%							2			3	3
	2017-Jan	2,788	3,998	6,786		41.1%	58.9%	100.0%		41.1%	58.9%							1			5	5
	2017-Mar	5,238	1,698	6,936		75.5%	24.5%	100.0%							75.5%	24.5%		7			7	7
	2017-May	3,277	3,562	6,839		47.9%	52.1%	100.0%		47.9%	52.1%							3	√	vw	2	2
	2017-Jul	3,392	3,322	6,714		50.5%	49.5%	100.0%				50.5%	49.5%					4			1	1
	2017-Aug	4,125	2,732	6,857		60.2%	39.8%	100.0%							60.2%	39.8%		5			5	5
Transect	N0	4,168	1,864	6,032		69.1%	30.9%	100.0%							69.1%	30.9%		5		w	1	1
	N1	3,866	2,848	6,714		57.6%	42.4%	100.0%							57.6%	42.4%		3			2	3
	N2	3,803	3,326	7,129		53.4%	46.6%	100.0%							53.4%	46.6%		2	√	√	23	3
	N3	3,706	3,259	6,965		53.2%	46.8%	100.0%							53.2%	46.8%		2			34	3
	N4	3,517	3,462	6,979		50.4%	49.6%	100.0%				50.4%	49.6%					1			2	2
	N5	3,176	3,374	6,550		48.5%	51.5%	100.0%		48.5%	51.5%							1			4	3
	S1	3,876	2,726	6,602		58.7%	41.3%	100.0%							58.7%	41.3%		3			5	4
	S2	4,045	2,366	6,411		63.1%	36.9%	100.0%							63.1%	36.9%		4			5	4
	S3	3,976	2,311	6,287		63.2%	36.8%	100.0%							63.2%	36.8%		4			234	3

DISCUSSION

Presented above was a data visualization and analytical *approach* designed to provide a methodology to explore the hydroacoustic data collected in Minas Passage to answer questions pertinent to the needs of FORCE personnel. It was 3-pronged:

- 1) *exploratory data visualization*: to gain an understanding of the underlying historical and contemporary data available for spatial and temporal analysis
- 2) *fish presence:absence*: to investigate the relationship between the spatial and temporal distribution of the presence of fish and the predictor variables
- 3) *relative fish density (using S_v as proxy)*: to investigate the relationship of the magnitude of relative fish density to spatial and temporal variables

This approach was undertaken to gain insights on the probability of recording observations of fish presence and to understand the relative density of fishes, in time and space. The predictor or explanatory variables for fish presence and density that could be evaluated were categorical: temporal (historical vs. contemporary, or by survey), spatial (CLA vs. reference study area, or by transect), and environmental (tide phase, diel state, or with and against predicted tidal flow).

The data used for the analyses included seven surveys conducted during the historical research program (Aug 2011 – May 2012) and nine surveys conducted during the contemporary research program (May 2016 – Aug 2017). The post-processed data was exported from Echoview in 20-m along-shiptrack distance bins integrated over the whole water column, the “20-m dataset”.

Data from the contemporary dataset were used for the analysis examples presented in this report. This approach was taken because statistical differences between the historical and contemporary dataset were found with both the presence:absence analysis and the relative fish density analysis. In addition, there were sufficient differences in the survey design and execution that deeper investigation into those differences is warranted before combining the datasets for analysis.

It should be noted that there were categorical gaps within the dataset. For example, there were no data collected during *dawn or dusk on a low-slack tide* during the nine contemporary surveys. Similarly, there were *transects* within the contemporary dataset for which no data was collected during dawn and dusk and during high and low slack tide periods. Should FORCE want to understand the dynamics of fish presence and relative density across these spatial and temporal categories, a detailed analysis of the data gaps in light of the questions pertinent to FORCE could help guide discussions concerning potential changes to the survey plan.

Within the contemporary dataset, where the number of categories within an explanatory variable exceeded two, the statistical results of the presence:absence analysis generally differed from that of the relative fish density analysis in terms of which of the categories statistically differed or not. These findings suggest that the presence:absence ratio of observations was not necessarily an indicator of the relative density of fish passing under the transducer. Selected findings are summarized in the Executive Summary.

The analysis examples included in this report were designed to provide an initial understanding of the data relative to the explanatory variables at a highly aggregated level and to demonstrate the approach. The results provide insights to form inquiries that could be conducted to dig deeper into the data at finer scales in order to answer pertinent questions. The results found using the data at finer scales can also be used to confirm whether insights from the highly aggregated data can be generalized or are a function of analyses using such highly aggregated data. For example: the results show that fish presence exceeds fish absence at night when the data is aggregated over the entire contemporary dataset, but this may not hold when examined on the finer levels of e.g. season, where behavior of the fish may differ on that temporal scale or on a spatial scale (e.g. transect). Much more investigation can and should be done using the scripts included with this document.

Further inquiries into the data that could be considered:

- 1) In both analytical approaches (fish presence:absence and relative fish density), the contemporary dataset was found to statistically differ from the historical dataset. The source of the difference may be one of natural variability or the difference may have also been influenced by the differences in survey design and execution. For example: historical transect length was nominally 1 km whereas the transect lengths during the contemporary surveys were nominally 2 km, during the historical survey each transect was traversed once during each grid pass (i.e. either with or against the direction of tide flow) whereas the transects were traversed twice during the each grid pass of the contemporary surveys (i.e. both with and against the direction of tide flow). In addition, between the two research programs there was a strong imbalance in the proportion of observations collected over the diel states (historic: day =78%, night=18%. contemporary: day=53%, night=43%). Deeper investigation into the sources influencing the statistical differences between the historic and contemporary datasets may provide insights as to whether analyses for the two datasets should remain separate.
- 2) Large imbalances in the count of observations between categories can cause statistical testing to become sensitive to very small, inconsequential differences resulting in statistical significance for small, uninteresting effects. In addition to the statistical effect is the question of whether the shortened window of observations that result in the smaller counts of observations generated a bias in the dataset. For example, the high and low slack tide periods are designated as the half-hour prior to and following the time of predicted slack for a total of one hour each occurring twice per day. Consequently, the count of observations for the two periods of running tides (ebb and flood) are an order of magnitude larger than the count of observations during the slack periods. One test that may be of interest is to select an hour of data from the ebb and flood

periods and rerun the tide phase analyses. The selected hour could be the hour adjacent to the slack period, and then again select an hour during the peak of flow.

- 3) For the 30 categories within the six variables analyzed, six categories had fish “present” counts that exceeded “absent” (night, May 2016, Nov 2016, Jan 2017, May 2017, N5) and for three categories the ratio of presence:absence was nominally 50:50 (ebb, Jul 2017, N4). “Absent” counts exceeded “present” counts for the remaining 21 categories (Table 4). Before generalizing findings from highly aggregated data, inquiries into the data at finer scales is warranted, including the night example referenced above and other distinctions in the dataset.
- 4) It was noted in the Analytical Approach: Fish Presence:Absence section of this report that there were pairings of transects for which there were not statistical differences in the presence:absence ratio. While it was suggested that those findings may provide guidance if transects need to be skipped for time or if there is an effort to increase survey frequency under the same budget constraints, the results in the Analytical Approach: Relative Fish Density suggest that there may be a different set of transect pairings for which there are or are not statistical differences. Given that there is the suggestion of transect pairings at this level of highly aggregated data, those findings should be investigated at finer scales.
- 5) The high value outliers should be explored to understand the particular states of an explanatory variable associated with observations of high fish density.

While the analytical approach presented here did provide insight using data summarized over spatial and temporal scales, and deeper inquiries at finer levels of summarized data will provide new understandings or confirmation of the findings at the summarized levels, more data needs to be collected to be able to draw larger inferences. In particular, the dataset needs to continue to be built such that multi-year data in comparable months are available. In addition, given the absence of a seasonal pattern and the preponderance of statistical differences between surveys, it may be advisable to increase sampling frequency within each month, sampling on consecutive days in order to get a finer scale understanding of the patterns and variability of fish presence and density in Minas Passage.

During the re-analysis of these data, it came to light that the echosounder gain settings during the contemporary surveys were not appropriately calibrated. After consultation with acoustic-community leaders it was determined that a post-hoc methodology by which to correct the calibrations was not available (McGarry and Zydlewski, 2018). Consequently, the echosounder gain settings have been standardized to the Simrad default settings (McGarry and Zydlewski, 2018; 2019). The calibration procedures were subsequently updated starting with Survey 15. Because appropriate calibration is fundamental to quantitatively compare survey results over time, distinguishing the contemporary dataset containing surveys with valid calibrations from

those with the standardized calibration parameters is advised. Distinguishing the datasets will allow for the analyses to be combined or separated as appropriate.








Literature Cited

- Baker, M., M. Reed, A. Redden (2014). "Temporal Patterns in Minas Basin Intertidal Weir Fish Catches and Presence of Harbour Propoise during April – August 2013." ACER, Wolfville, NS, Tech. Rep. 120.
- Dadswell, M. (2010). Occurrence and migration of fishes in Minas Passage and their potential for tidal turbine interaction. Technical Report.
- Daroux, A., G.B. Zydlewski (2017). Final Report: Marine Fish Monitoring Program Tidal Energy Demonstration Site – Minas Passage. Submitted to Fundy Ocean Research Center for Energy, 16 October 2017. 34 pp.
- Daroux, A., L.P. McGarry, G.B. Zydlewski (2017). Marine Fish Monitoring at FORCE: Report on processing and analysis of surveys from May, July and August 2017. Submitted to Fundy Ocean Research Center for Energy, 29 December 2017. 16 pp.
- MacLennan, D.N., P.G. Fernandes, J. Dalen (2002). A consistent approach to definitions and symbols in fisheries acoustics. ICES Journal of Marine Science, 59: 365-369.
- Melvin, G.D., N.A. Cochrane (2014). Investigation of the Vertical Distribution, Movement and Abundance of Fish in the Vicinity of Proposed Tidal Power Energy Conversion Devices. Final Report, OEER/OETR Research Project 300-170-09-12.
- McGarry, L.P., G.B. Zydlewski (2019). Notes for EK80 CW Calibration Settings for FORCE. Submitted to Fundy Ocean Research Center for Energy, 02 February 2019. 4 pp.
- McGarry, L.P., G.B. Zydlewski (2018). Calibration Quality Control. Submitted to Fundy Ocean Research Center for Energy, 22 June 2018. 10 pp.
- Rulifson R., M. Dadswell (1995). Life history and population characteristics of striped bass in Atlantic Canada. Transactions of the American Fisheries Society, 124(4), 477-507.

APPENDIX A: Technical Notes

Historical Survey Detail

Table A1: Historical Surveys. Each survey consists of three to twelve repeats of the grid defined by the following transect lines: T0, T1, T2, T3, T4, T5, T6, T7, T8, Y1, X1, Y2⁷. Only data collected from “T” and “X” transects were included for analysis. Additional notations are listed below.

Survey 9,11,12,13	Month ^{0,3}	Start date	Start time ^{2,5}	End date	End time ^{2,5}	Day/ Night ^{5,7}	Temperature (°C)	Turbine presence	Moon Phase Tide Range
1	Aug 2011 (4:3)	2011-08-22	11:45 (08:45)	2011-08-22	21:28 (18:28)	D	15.4	No	 7 m
2	Sep 2011 (4:3)	2011-09-19	10:55 (07:55)	2011-09-19	20:23 (17:23)	D	15.7	No	 8 m
3	Oct 2011 (4:3)	2011-10-03	09:53 (06:53)	2011-10-03	20:18 (17:18)	D	15.0	No	 10 m
4 ⁶	Nov 2011 (3:3)	2011-11-22	14:22 (10:22)	2011-11-22	22:32 (18:32)	D	10.3	No	 11 m
5 ¹⁰	Jan 2012 (10:9)	2012-01-25	18:32 (14:32)	2012-01-26	16:15 (12:15)	D/N	3.6	No	 11 m
6 ⁴	Mar 2012 (12:11)	2012-03-19	14:23 (11:23)	2012-03-20	13:33 (10:33)	D/N	2.5	No	 9 m
7 ¹⁰	May 2012 (5:4)	2012-05-31	12:09 (09:09)	2012-05-31	23:12 (20:12)	D	9.5	No	 10 m
8	Jun 2012 ¹								

⁰ **September 2010:** a datasheet for a September 2010 survey is included in the historical datasheets provided by Dr. Melvin. But no echosounder data for that survey was delivered to UMaine. See Melvin and Cochrane (2014) for reporting that includes that survey.

¹ **June 2012:** according to the datasheet, 10 grids were executed on June 25-26, 2012, but only data for one partial grid was received with the transfer of the “Melvin” data to UMaine. Because only one partial grid of data is available, the survey has been excluded from the analytical work. Note that an event that may be of interest: “extremely high fish concentrations” is noted on page 16 of Melvin and Cochrane (2014) but unavailable for inclusion in the work herein.

² Echosounder data and the associated datasheets were recorded with “time” set to GMT (Greenwich Mean Time). Testing of tide height change per echograms and predicted tide height change confirmed that GMT is the correct designation of time for the historical “Melvin” data and is also consistent with reporting in Melvin and Cochrane (2014). “Time” associated with the echo integrated data was converted to local time after export from Echoview. “Time” as designated on the datasheet was converted to local time to ensure that tide, diel, and “with/against” stages were appropriately assigned. Time in parentheses in Table A1 is Local Time.

Note: If further analysis requires subsequent metadata merges with the historical data, use the “Time Offset” feature in the Echoview Fileset Properties to set the conversion (3 or 4 hours depending on time of year) from GMT time at which the data was collected to local time before executing the exports. Then any additional

exports of the historical datasets can be directly merged with the historical datasheet for which “time” has already been converted to local time.

³Numbers in parentheses in the Month column are the **number of partial:complete grids** executed for the survey. Three was the minimum number of complete grid passes in the historical surveys. To standardize the number of grid passes per historical survey, three grid passes were included in the data used for analyses. Complete grid passes were evaluated and three were selected to maximize “good” data (e.g. selecting grids with lesser entrained air where possible, etc.). One exception is the Nov 2011 survey during which no data were reported in the reference study area. So although three complete grid passes were executed, incomplete passes without the reference study area data have been included in the analyses. (Data were collected in the reference Study Area but not transferred to the University of Maine.) The grids selected for inclusion in the analyses in this report are the following:

Aug 2011: 1,2,3

Sep 2011: 1,2,3

Oct 2011: 1,2,3

Nov 2011: 1,2,3 <- NOTE: no data was available from the reference study area during this survey⁶

Jan 2012: 5,8,9

Mar 2012: 7,10,11

May 2012: 2,3,4

Detailed notes regarding data quality of grid passes can be found in the “20170519 Datasheet_Melvin WORKG” tab of the *20170519 Datasheet_Melvin WORKING20190115LPM.xlsx* spreadsheet. See also the “Datasheet Documentation” tab in the *20190115 AllDataParseToMonthly_MelvinONLY_20mBinsFullWaterColumn.xlsx*. Final grid selection notes are in: *MelvinGridNOTES.xlsx*.

⁴For survey **March 2012**, the datasheet lists 12 grid passes but T5, T7, and T8 were populated with zeros on the datasheet for particular grids (#3 and #12). Therefore, Grids #3 and #12 are **not complete grids** and should not be included in the grids selected for analysis. See *MelvinGridNOTES.xlsx* for more detailed information for grids in **all historical surveys**.

⁵**Start Time, End Time, and Day/Night** are reported for the entirety of each survey dataset, whereas a subset of the data (three complete grid passes for each survey) were used in analyses. Therefore, Start Time, End Time, and Day/Night as represented in the analyses may differ from what is reported here. See *MelvinGridNOTES.xlsx* for more detailed information for grids in **all historical surveys**.

⁶**Nov 2011:** No .raw data were provided for the **reference transect**. Raw data for the cross-channel transects (X1 and X2) were included – but not the connecting reference transect. Therefore, although 3 complete grid passes were executed during data collection, the data provided for analyses were not 3 complete grid passes for Nov 2011. Given that analyses presented in this report did not include historical data aggregated at scales finer than “research program”, the data for the CLA study area for November 2011 were included in the analyses.

⁷Note the **predominance of day coverage**. Percentages reported here for CLA and reference transects only.

Detail for entire historical dataset...

Dawn: 3%, Day: 69%, Dusk: 2%, Night: 26%

Detail for (complete) grids included in 2019 analysis...

Dawn: 3%, Day: 78%, Dusk: 1%, Night: 18%

⁸There is an **inconsistency in the reference and cross-channel transect notations** in Melvin and Cochrane (2014). Table 4 therein refers to the reference transect as Transect X1 and the cross-channel transects as Transect Y1 and Transect Y2. Table A5-9 and the narrative on page 16 refer to the reference transect as Transect Y1 and the cross-channel transects as Transect X1 and Transect X2. It appears that the X1 in Table 4 was in error. Given that

the datasheets used for these analyses were constructed from the Table A5-9, the **reference transect is referred to as Transect Y1 in this document.**

- ⁹ In the historical dataset, **passes over each transect** were in **one direction only** (“with” OR “against” tidal stream flow). Whereas passes over each transect in the cotemporary dataset were executed twice; once “with” AND once “against”.
- ¹⁰ Surveys in **Jan 2012** and **May 2012** include transects during which the vessel traversed partway across the transect length and then **returned to the start of the transect** following which the transect was surveyed in its entirety. The data from the initial partial transect were excluded from analyses via edits to the start and end times of the transects in the datasheet Excel file used for the metadata merge. Given that these exceptions were not noted in the datasheet .pdfs received with the historical dataset, and that the start and end times on those datasheets encompassed the whole effort for that transect rather than limiting the start and end times to the one clean traverse across the transect, the partial transect would not have been excluded from the analytical dataset if the cruise tracks hadn’t been plotted confirming the spatial extent of the data. If one doesn’t catch this particular exception, then both “with” and “against” data would be included although the metadata merged would have labeled the direction as either “with” or “against” as specified by time-of-day.
- ¹¹ **GPS values** are particularly erratic in the historic dataset. Caution should be exercised when analyzing data specified by the recorded latitude and longitudes.
- ¹² The historical data used in the analyses included in this report were as exported from Echoview 7 by Aurelie Daroux.
- ¹³ In the historical dataset, the **data collection file** was run as **one long file** for the entire survey. Implications: (a) the .raw files imported to Echoview define the data for the entire survey, precluding the ability to generate Echoview files for individual transects or grids, (b) for processing historical data by transect once the data is exported from Echoview requires accuracy in the start and end of each transect line as defined by the time entries in the datasheets, (c) “along” data is included in the Echoview exports and therefore needs to be explicitly excluded at a later point in the processing. (For the contemporary data exported from Echoview, the Echoview files for the “along” transects were excluded from the export process thereby eliminating the necessity to explicitly exclude “along” later in the processing.) Note that the time entries in the original historical datasheets were not sufficiently accurate to exclude data from the transits between transects. LPM produced a new datasheet for the historical data with more tightly defined start and end times for the transects. LPM made two passes at this process for all 7 of the historical surveys. The results are visualized here:

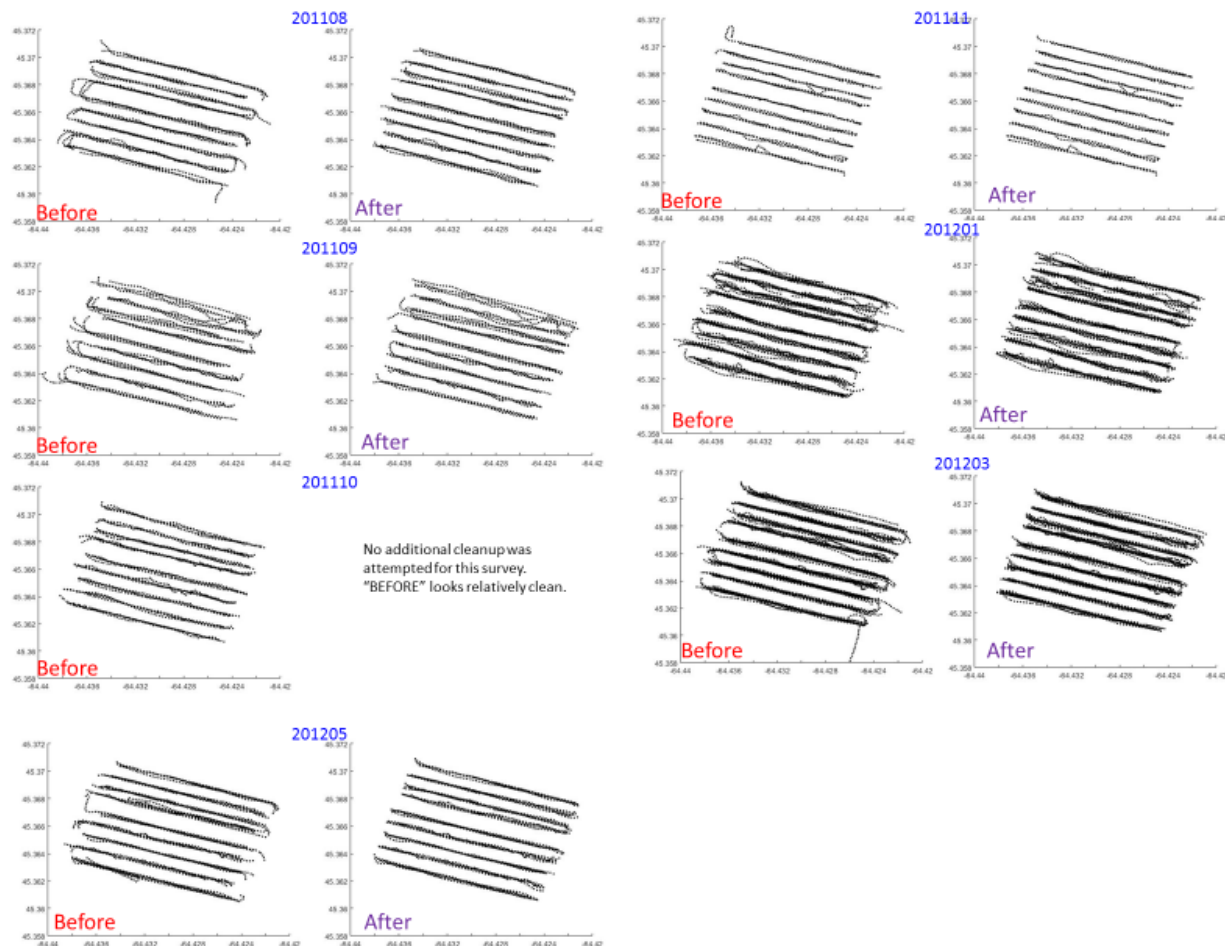











Figure A1. CLA Transect Lines in the Historical Dataset. Because the echosounder data was collected in one long .raw file, the definition of the ends of the transect lines were completely dependent on the start and end times defined in the datasheet. Shown here for the “20-m dataset” are the definitions of the transect lines based on an unedited datasheet (“Before”) and the edited datasheet (“After”) after two passes at refining start and end times. Each dot representing a 20-m along-shiptrack distance bin.

Summary of Historical Survey Dataset Reprocessing since December 2017 report (Daroux *et al.* 2017)

1. no changes were made to the data exported from Echoview (#12 above)
2. definition of the ends of the transects in the metadata file were adjusted to remove “20-m bins” associated with transits between transects (#13 and Figure A1 above).
3. time recorded at GMT in the metadata file was converted to local time and environmental metadata (tide phase, diel state, “with/against”, etc.) reassigned based on local time (#2 above)
4. time in the exported Echoview files was converted from GMT to local time (#2 above)
5. partial Jun 2012 survey data was excluded from analyses (#1 above)
6. complete versus incomplete grid passes were documented and in conjunction with review of echograms for bad data and excessive turbulence, three grids for each survey were selected for inclusion in the analyses (#3 above)
7. partial repeats of transects were identified and the metadata file edited in order to exclude the partial passes (#10 above)

Contemporary Survey Detail

Table A2: Contemporary Surveys. Each survey consists of 4 repeats of the grid defined by the following transect lines: N0, N1, N2, N3, N4, N5, South_CW^L, S1, S2, S3, North_FM with calibration files. Only data collected from “N” or “S” transects were included in analyses. Additional information and notes regarding where data differs from the standardized grid are included in the notations are below.

Survey	Month ^Z	Start date	Start time ^A	End date	End time	Day/ Night ^T	Temperature (°C)	Turbine presence	Moon Phase Tide Range
1	May 2016 B,C,D,E,O,Q,R,Y	2016-05-28	06:01	2016-05-29	05:35	D/N	7	No	 10 m
2	Aug 2016 C,E,R,Y	2016-08-13	09:09	2016-08-14	07:40	D/N	15	No	 7 m
3	Oct 2016 C,D,F,M,P,R,Y	2016-10-07	05:45	2016-10-08	04:21	D/N	15	No	 8 m
4	Nov 2016 E,G,H,HH,P,R,QQ,S,Y	2016-11-24	08:38	2016-11-25	09:07	D/N	8.0	Yes	 8 m
5	Jan 2017 C,G,H,HH,R,RR,Y	2017-01-21	06:55	2017-01-22	05:55	D/N	1.5	Yes	 7 m
6	Mar 2017 P,R,Y	2017-03-21	08:24	2017-03-22	06:04	D/N	4	Yes	 7 m
7	May 2017 I,R,Y	2017-05-04	19:57	2017-05-05	18:21	D/N	5	Yes (free spinning)	 9 m
8	Jul 2017 I,J,R,Y	2017-07-03	21:34	2017-07-04	19:09	D/N	12	No	 8 m
9	Aug 2017 I,R,Y	2017-08-30	18:53	2017-08-31	17:37	D/N	15.7	No	 7 m

^A Time recorded here and in the .raw files is local time at Minas Passage.

^B Raw data collected in passive for **AC/DC test** in addition to standard grid

^C Raw data collected for **stationary data** in addition to standard grid

^D Raw data collected for **transects in addition to** standard grid

^E Raw data collected for **unspecified test** in addition to standard grid

^F Raw data collected for **ping rate test** in addition to standard grid

^G **Both South and North transects** (CW and FM respectively) were done on the east side of the grid

^H Raw data collected for **“T” transect** between N2 and N3 in addition to standard grid

^{HH} **“T” transect** looks like it means: **“Turbine”**. As of April 24, 2018, how the “turbine” data is labeled in the digital datasheets has not been standardized (i.e. should they be classified as “with/against” or “stationary” or simply “turbine” given that in some cases they weren’t stationary – but weren’t doing actual transects in an effort to run over the turbine multiple times).

^I Transect execution for **South CW and North FM were reversed** (i.e. the actual transects were: South FM and North CW). See note “L” below for more information.

^J **Survey 8** raw data collected for **GR1-N0** and the **first file of GR1-N1**: The set of transect coordinates that were stored in the ship’s plotter were deleted before the start of this survey. “Helper” gave the captain old coordinates. GR1-N0 is indeed offset (Figure A2a). It falls about midway between where it should be (N0) and the next transect N1. Both GR1-N0 transects (“with” and “against”) were excluded from analytical processing. The N1 segment falls within the cloud of N1 transects for Grid 1 from each of the contemporary Surveys 1 through 9. So all the GR1-N1 data is included for processing.

- ^L To alleviate the nightmare that is the **North/South CW/FM** issue and filenames, the “along” transects have been **excluded from analytical processing** (i.e. the “along” were not intended to be included in analyses and therefore were not included in the “alldata” files.) NOTE that North/South confusion for surveys 7,8, and 9 cascades throughout the processing steps. i.e. .raw file names = South when they were actually traveling North. The EV file names were corrected to correspond to the actual direction of travel, but when the .vbs script exports the data from EV, the script incorporates the .raw file name rather than the EV filename, and hence we’re back to files with names that don’t correspond to the actual direction of travel.
- ^M Survey 03 has both **North/South CW**. As of January 2018, only the South CW files have been imported into Echoview. Therefore, there is more “along” CW data available than is indicated by the number of “along” EV files. (But again, “along” data were excluded from analytical processing for this report.)
- ^N **Oct 2016** includes one transect labeled **Grid 5**. This data is excluded from analysis.
- ^O **Entrained air** so severe and persistent through the water column that sections of transects are assigned as bad data regions and eliminated from any effort to ascertain whether fish are present. (e.g. Survey1_GR3_N1W.EV and Survey1_GR3_N1A.EV) Note: To distinguish passive data regions from actual bad data regions, each were assigned a different type of bad data region within Echoview.
- ^P During transect **GR4_N2A** for surveys **Oct 2016, Nov 2016, Mar 2017**, there is a feature that **looks non-biological** (derelict gear? a tether?). In all 3 cases the time is within 30 minutes of slack (low) and is located at 45 22.166'N 64 26.195'W or thereabouts. Given the consistency of location and feature, the signals were designated as a bad data/no data region in each of the 3 surveys. 45 22.166' N 64 26.195' W 45 22.161' N 64 26.201' W 45 22.170' N 64 26.213' W The ?tether? rises about 8 m off the seafloor and is 50+ m long.
- ^Q **Survey 1 skipped transects**. There are a lot of .raw files per transect (20+). Datasheet .docx has a note that the transects should be shortened. Taking too long. Specifically GR2_N2A took 3 hours (cruisetrack looks like they got caught in an eddy). Lots of entrained air. There are 746 .raw files associated with that transect. GR2_N4A is missing from .raw files and is not listed on the datasheet. There are no notes on the datasheet as to why that transect was skipped. However, they went directly into South_CW therefore must be skipped transects to make up time. They did one transect (S1W) on the control site and then went into North_FM and started GR3. See *SimradFilesPerTransect.xlsx* for details as to which were skipped, etc.
- ^{QQ} Survey 4 **didn’t end file for GR2_N5A** and began heading south to control site **skipping N5W**. In Echoview, only one file is included for N5A so as to exclude the cross-channel transit. No Echoview file was created for the skipped N5W.
- ^R Data collection procedures for **calibration** data were insufficient to provide reliable calibration parameters. For more information see the **Calibration Quality Control Report issued June 22, 2018** and the **Notes for EK80 CW Calibration Settings issued February 2, 2019**.
- ^{RR} Special consideration for **this calibration**: Collection range window included nearfield. (Min range set at 1.2 m whereas the nearfield/farfield boundary used is 1.7 m.)
- ^S **Nov 2016. Skipped transects for time – and started GR4 still in FM.**
- ^T **Day/Night coverage** detail for CLA and control transects: Dawn: 2%, Day: 53%, Dusk: 2%, Night: 48%
- ^Y Note that for Survey 10 and prior of the Contemporary surveys, the **files names** (e.g. GR1_N0A and GR1_NOW) were labeled “against” and “with” respectively based on the conceptual plan for the grid, rather than based on whether the tide was flooding or ebbing. The merge of the EV exported data with the datasheet has corrected the data internal to the “alldata” files (i.e. the WithAgainst column is consistent with direction of predicted tide), leaving the file names disconnected from the physical attributes of the tidal flow.
- ^Z Review the **trackline positions and direction of travel** for the “along” transects before you use them for analyses. Somewhere along the way the grid lost its shape in terms of the locations at which the “along” transects are recorded. (See screenshots in “A2b” below.)

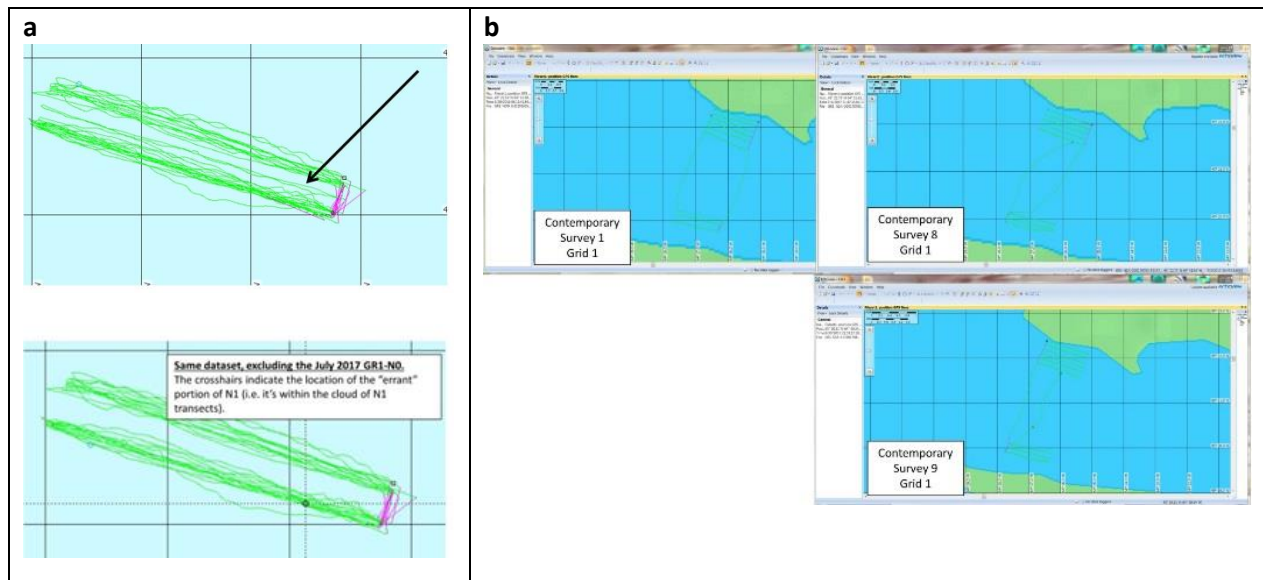


Figure A2. Contemporary Dataset Notes. (a) Physical location of the two transects (N0 and the first pass of N1) for survey 8 (July 2017) that were executed under old coordinates, relative to plotted transects N0 and N1 from grids one through four for surveys one through nine. The arrow points to the “with” and “against” transects of the errant N0. N0 is distinctly between its assigned location and the location of N1. If the transects are nominally assigned 200 m apart, this one is 100 m apart. N0 for that grid pass is therefore excluded from analysis. The errant N1 plots within the cloud of N1 locations from surveys 1 through 9 and therefore was included in analyses. Notation “J” above. (b) Grid shape as defined in survey 1 is not held for surveys 8 and 9. Given that “along” transects are outside the scope of the analytical work described in this document, no further action or investigations was required (e.g. determining how many of the 9 contemporary surveys have compromised grid shapes). However, if the “along” is used in subsequently analyses, be sure to examine the position of the “along” transects to determine whether the data is appropriate to include. Notation “Z” above.

Summary of Contemporary Survey Dataset Reprocessing (since December 2017 report (Daroux et al. 2017))

1. data was exported from Echoview 7 where processing for EK80 data was still in beta testing to Echoview 8 as recommended by Echoview
2. top and bottom lines within Echoview were adjusted to eliminate gaps that cause spurious data in the export
3. within Echoview, “bad data” regions were redefined for consistency: passive data was defined as bad data-empty water and regions of backscatter from non-biological targets were defined as bad data-no data. Use of the two definitions specifies which portions of the transect were excluded due to passive data collection versus portion of the transects lost to entrained air or other non-biological targets
4. all Echoview files (~72 per survey) were reviewed and corrected for errors in .raw data inclusion (e.g. “with” and “against” within the same EV file, data from more than one transect within the same EV file, etc.)
5. upon discovery of the calibration issues, extensive testing and then consultation with acoustic-community leaders was undertaken in order to determine if a post-hoc solution was available. Where one was not forthcoming, worked extensively with Echoview in an effort to create and test a post-hoc solution. When it was deemed that a final solution was not imminent, worked

with acoustic-community leaders to settle on an approach that would allow analyses to move forward (McGarry and Zydlewski, 2018).

6. once the approach to standardize the calibration parameters was identified (McGarry and Zydlewski, 2019) new Echoview calibration files (.ecs) were created for all nine contemporary surveys
7. Echoview export script was extensively updated to include export of EV file metadata with the export of the EV data for analyses
8. Echoview exports for all transect data for all nine surveys was executed including data, EV metadata, and EV files for archiving the data in the state used for these analyses
9. metadata (datasheet) files were completely reworked to correct errors and to reassign “with/against” based on predicted tidal phase (original entered was a combination of predicted tidal phase and perceived tidal phase in the field)
10. developed and tested new scripts to automate steps to prepare EV exported data for analyses (see Appendix C for more description of the scripts)
11. incorporated some data quality control tests into the scripts based on issues found in the December 2017 data and scripts. Some of these are articulated in “Notes” and “Cautions” below. See scripts for complete list of data quality control tests
12. worked with University of Maine statistician to develop a statistically rigorous approach to analyzing the hydroacoustic data from Minas Passage

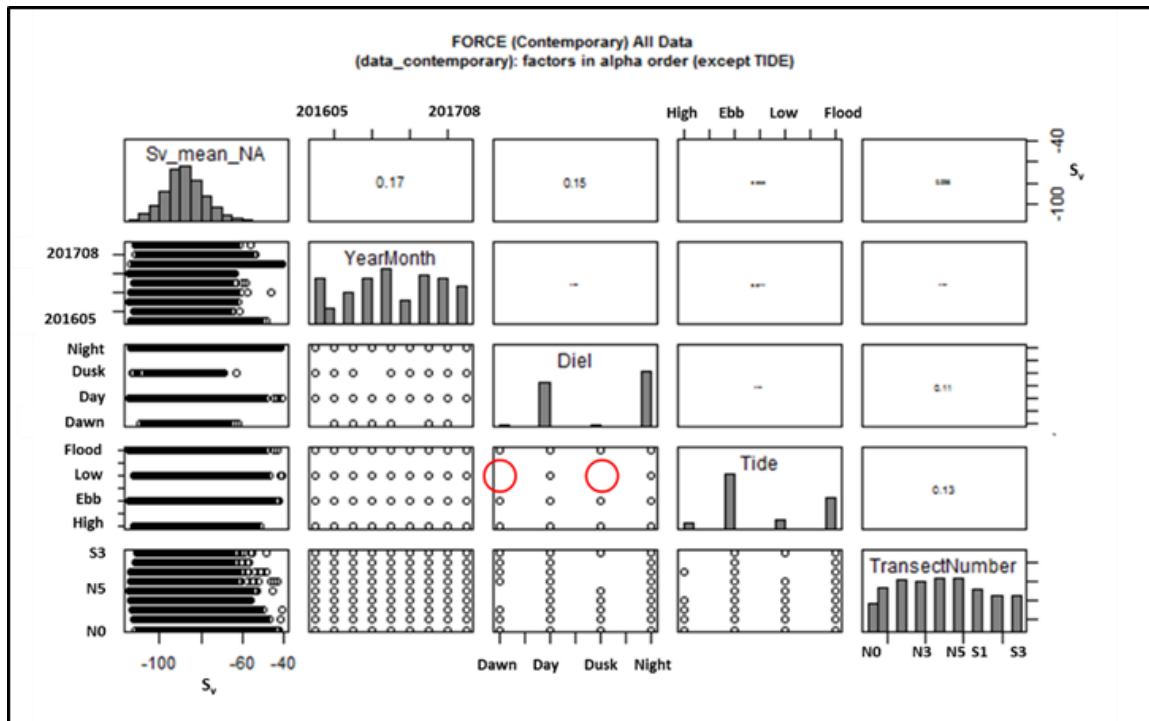


Figure A3: Panel Plot - Contemporary Surveys Only. Panel plot of non-zero S_v values and selected variables contained within the contemporary portion of the “20-m dataset”. Histograms on the diagonal: only the x-axis is associated with the histograms (i.e. the heights are relative heights of the number of non-zero S_v observations within the individual variable). Dot plots below the diagonal are read with both x and y axes as indicated by the categories in the histograms of the associated row and column. For example: the plot with the two red circles is a Diel-by-Tide plot. As per the x-axis labels, from left to right: dawn, day, dusk, night. As per the y-axis labels, from bottom to top: high, ebb, low, flood. Therefore, the two red circles highlight that no data was collected during low slack at either dawn or dusk. Note that there are gaps in transects by tide phase, and gaps in transects by diel state. Correlations among the pairs are posted in panels above the diagonal. Font size is indicative of magnitude of each correlation. Coding to generate this plot is included in the R scripts: `SCRIPT2019 20mBinAnalysis.R`. **Caution:** There may be an upper limit to the number of categories that can be shown within a variable. For example: when this plot was generated for the full dataset (historical plus contemporary), the histogram values for the first two surveys (YearMonth) were summed and shown as one bar.

Survey Characteristics – Historical and Contemporary Surveys

Table A3: Contemporary and Historical Surveys. *Survey characteristics.*

	Historical/Melvin	Contemporary/FORCE
Number of Surveys	7	9
Target	1 or 2 full tide cycle: 12-24 hours	2 full tide cycles: 24 hours thereby encompassing tide cycles both day and night
Vessel Speed-Over-Ground (Nominal or Actual)	should be investigated	should be investigated
Number of Complete Grid Passes per Survey	3 – 11 (one survey also includes a partial 12 th grid pass)	4
Grid Length	~1 km	~ 2 km
Number of Transects	CLA: 9 reference: 1	CLA: 6 reference: 3
Transect Direction Relative to Tidal Flow	data collection for every transect was executed once: “with” tidal flow or “against”	data collection for every transect was executed twice: “with” tidal flow and “against”
Diel Distribution of Data Collection (<i>Historical “Analytical” describes the distribution of data in the grids selected for inclusion in analyses.</i>)	...Dataset... Entire Analytical Dawn: 3% 3% Day: 69% 78% Dusk: 2% 1% Night: 26% 18%	...Dataset... Entire = Analytical Dawn: 2% Day: 53% Dusk: 2% Night: 43%
Tide Distribution of Data Collection (<i>Historical “Analytical” describes the distribution of data in the grids selected for inclusion in analyses.</i>)	...Dataset... Entire Analytical Low: 11% 17% Flood: 34% 27% High: 6% 6% Ebb: 49% 50%	...Dataset... Entire = Analytical Low: 12% Flood: 35% High: 8% Ebb: 45%

Table A4: Contemporary and Historical Surveys – Year, Month, Tide Range. Shaded and hatched boxes indicate months in which hydroacoustic survey data was collected. Hatched shading indicates the surveys during which a turbine was present in the CLA study area. Number within the shaded box indicates the tide range (in meters) predicted for survey days.

	2011	2012	2016	2017
January		11		7
February				
March		9		7
April				
May				9
June		10	10	
July				8
August	7		7	7
September	8			
October	10		8	
November	11		8	
December				

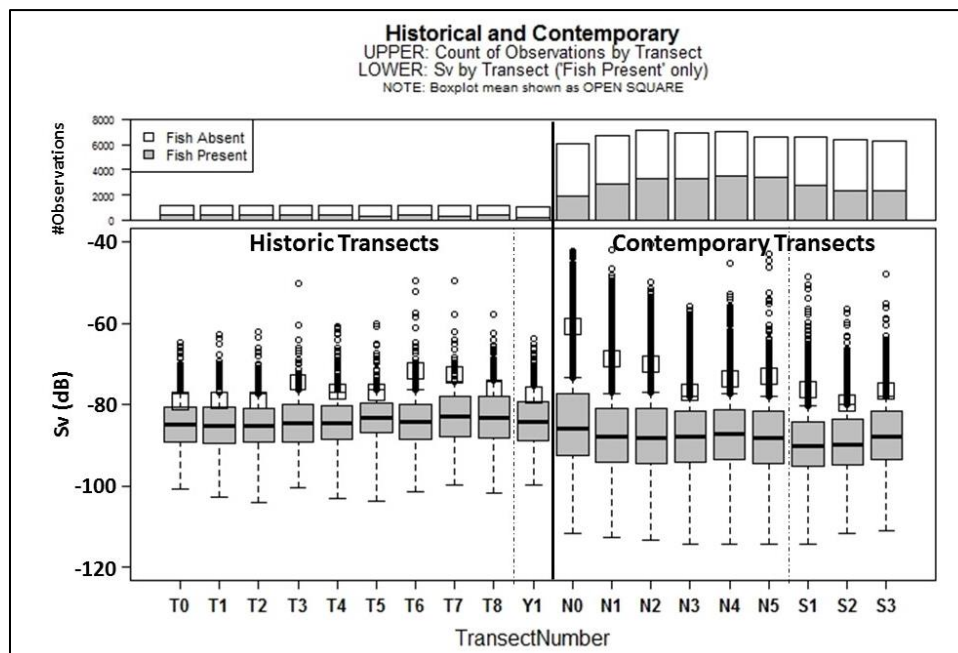


Figure A4: Distribution of S_v values by Transect for Historical and Contemporary Datasets. Data shown are the data exported from Echoview integrated over the full water column binned in 20-m along-shiptrack distances (the “20-m dataset”). The data is highly aggregated. Each transect represents all data in the “20-m dataset” used in the analyses contained in the report. Top: Top of bar indicates the total number of observations for each survey. Axis range: 0 to 8000. Shaded portion indicates the number of non-zero observations ($n = 29,105$). White portion indicates the number of zero observations ($n = 41,911$). Bottom: Boxplots of non-zero S_v observations by transect. See text in the Explanatory Data Visualizations section of report for description of boxplot.

Survey Design Notes – Contemporary Surveys

The original grid plan was designed such that four complete grid passes were completed within 24-hours resulting generally in two grid passes during day, executing one full grid during ebbing tide and one full grid during flooding tide, and two grid passes during night, again with one full grid during ebbing tide and one full grid during night. For each grid, every 1.8-km transect was traversed twice, once “with” the direction of tidal flow, and once “against” the direction of tidal flow, before moving to the next transect. The surveys were scheduled to begin on the ebbing tide with the EK80 echosounder set to record in “continuous wave” (CW) mode, starting by traversing transect N0 in the direction “with” the ebbing tide. Each successive transect, N0 to N5, were occupied in order (both “with” and “against”). Then a southward across-channel transect was executed terminating near Passage’s southern coastline. This cross-channel transect was designated “South_FM” to indicate that the direction of travel was southward across the channel and that the data would be collected with the EK80 echosounder set to record in “frequency modulated” mode. Upon completion of the southward transect, the EK80 echosounder was returned to its “continuous wave” mode, and three reference transects, S1 to S3, were each executed twice: once “with” and once “against” the direction of tide flow. To finish the grid, a northward return transect “North_CW” returned the vessel to N0. One grid pass consisted of one full set of all transects.

Note that the original grid plan called for the south across-channel transect to be conducted in continuous wave mode (South_CW) and the northward return transect in frequency modulated mode (North_FM). However, this convention was not consistently met during surveys 1 through 9. For example: in survey 3 both North and South transects were executed in CW mode and the two modes (FM and CW) were interchanged for surveys conducted in May, July, and August 2017. **In future surveys the convention should be standardized.** Note that there is now a mismatch between the echosounder .raw filenames and the contents of the .raw files. When constructing the Echoview files for the cross-channel data, extra caution is required to ensure that the intended data (regardless of the .raw filename) is included.

EV Exported Data Notes – Historical and Contemporary

- Interval: start ping differs between historical (Melvin) and contemporary (FORCE) surveys
 - Historical: Interval starts with the first ping regardless of whether there was a good GPS location associated with it
 - Contemporary: Interval starts with first ping for which good GPS location was available. So some pings may be skipped
 - SIGNIFICANCE: Where there were missing GPS locations for those start pings in the historical data, the GPS location for the initial Interval(s) (e.g. 20-m along-shiptrack bins) were populated with 999 for both longitude and latitude. For the contemporary dataset, the initial few pings without a good GPS location were designated as Interval 0, allowing the EV export to calculate the appropriate GPS location for the remaining contemporary Intervals
- Interval: 0
 - Interval “0” only occurs if there is no GPS associated with the very first ping recorded in the Echoview file AND the “Start interval numbering from the first ping in the echogram” box is checked in the Grid tab of the Variable Properties.
- Passive and Bad Data definitions
 - were assigned two different bad data types so that the portions of the echogram excluded from analysis could be distinguished between exclusion of noise/turbulence vs. passive data collection
- “Along” data for the contemporary dataset was excluded from analysis at a different processing stage than for the historical dataset.
 - contemporary: new data files were created for each transect during a survey, thereby facilitating the creation of individual Echoview files for each transect. Therefore, “along” and any other non-standard grid data were excluded simply by not exporting any echo integration data from EV files associated with any non-standard grid data
 - historical: generally survey data was collected in one file, thereby making it impossible to segregate standard grid data from non-standard grid data at the Echoview stage. Therefore, “along” data and partial grid data were included in the echo integration exports from Echoview and succeeding steps (e.g. the merge with the metadata, and included in the appending of the historical dataset with the contemporary dataset to create the “alldata” file). Exclusion of the “along” and unwanted grids was executed by explicit command in the R scripting resulting in the “data_subsetMaster” dataframe used for analysis.

APPENDIX B: Notes Going Forward

Cautions – Analytical

- **threshold settings in EV** were -66 dB (minimum integration (S_v) threshold) and -60 dB (minimum target strength (TS) threshold), changes to these settings for future surveys will alter the comparability of the data.
- **depth of transducer** (historical and contemporary) is listed at 0 m (i.e. no offset for the depth at which transducer is deployed).
 - Therefore “depths” reported are “range from transducer” unless some offset is applied to data outside of EV. (No offset has been applied to the data processed here.)
 - Therefore, in order to keep the datasets consistent in future analysis, if the same deployment configuration is used (boat and pole mount) depth of transducer should continue to be reported at 0 m.
 - Best Practice: the depth of the transducer should be recorded on the data sheet for each survey, and that offset from the surface entered into Echoview. By doing so, data recorded using differing deployment methods (e.g. different boat, different polemount) can be directly compared by depth. “Range” from transducer face is still available in Echoview even when offset for the depth of the transducer has been entered.

Cautions – Data Processing Procedures

- need to be super cautious **working in .csv or .xlsx**
 - “time” as exported from Echoview includes hh:mm:ss.SSS. However, it is not uncommon for the hours component to be lost when using .csv files (number formatting is not embedded in a .csv file).
 - also found that the decimal seconds got dropped in the .csv file – those decimal seconds can be important for getting lines of data in chronological order
 - Excel will sometimes split the contents of the “EV_filename” column across two columns which results in an offset of the contents of all following columns relative to the column headers
- it’s an **easy check in EV** to plot the cruise track within each EV file.
 - This can function as a quality control that you’ve imported only the .raw files actually associated with that transect regardless of the filename, etc.
 - Also serves as a quality control that .raw files were appropriately labeled. (Example: Nov 2016 .raw file for GR2_N5A wasn’t closed and renamed before turning south for the “along” transect. Therefore when creating the N5A EV file including .raw files by filename only, “along” data would be included in the N5A transect.)
 - Also serves as a quality control for any exceptions to the standardized survey plan
 - for example: two of the historical surveys include transects during which the vessel traversed partway across the transect length and then returned to the

start of the transect, following which the transect was surveyed in its entirety. These exceptions were not noted in the datasheets and the start and end times in the datasheets encompassed the whole effort for that transect rather than limiting the start and end times to the one clean traverse across the transect. The results of not discovering this excursion from the survey plan is that for each of those transects, both “with” and “against” data would be included in analysis although the metadata merge would assign the direction as either “with” or “against”.

- The **EV export** scripts are written such that the export includes all data categories available (making for lots of columns not used in our analyses), the logic is that if we ever want to do analyses using additional data columns, they’d already be in the exported files thereby eliminating the “version control” issue (i.e. any additional analysis would be done with equivalently processed data)
 - REMINDER: the number of columns exported, when all columns is selected in EV, changes from EV version to EV version. So processing the data based on column header names rather than column position is vital to keep consistency in the data.
 - REMINDER: you need to select ALL columns in EV (it’s not the default)
 - See the Export tab in the EV File Properties
 - Be sure to include the ALL columns setting in the EV template to ensure that those settings are in place for all EV files created for the project.
- **Minimum Surface Exclusion Line** was set to 1.7 m for all surveys (historical and contemporary) except for May 2012 which was set to 1.5
- The **deadzone** for a 7° 120 kHz echosounder with a 1.024 ms pulse length operating in seawater is 0.8 m at 10 m depth and 1.0 m at 100 m depth. When defining the bottom line within Echoview, a minimum of a 1-m stepback is recommended in order to exclude the deadzone from the data used for analyses.
- Make sure the **bottom line (and top line)** has no gaps in EV. Otherwise, “data” gets included in the automated exports from below bottom (or above top). (See next comment.)
- The early versions of the **Echoview template** introduced a “**smoothing**” to the bottom (or top) line after bottom (or top) edits. This generated two challenges (1) the smoothing algorithm commonly introduced erratic behavior in the bottom (or top) line and (2), the result commonly introduced data to the analysis that in truth we were trying to exclude (a “+1” depth bin - “data” that we don’t want)
 - In August 2018, UMaine sent FORCE a revised Echoview template that incorporates the smoothing before the manual edits of the bottom and top lines thereby eliminating the extraneous “+1 m” “data”

Cautions – Datasets

- Historical (Melvin)
 - datasheets and raw files are recorded in GMT (whereas contemporary (FORCE) are recorded in local time)
 - LPM proofed GMT by comparing tide height change for each of the Melvin surveys (2011-2012) per echogram (assuming recorded time was GMT and then assuming recorded time was Local) against predicted tide height change, and found that when assuming GMT, the tide height change per echogram closely corresponded to predicted tide height change (within +/- 2 m) whereas the tide height change differed substantially from predicted tide height change when assuming the recorded time was local (up to +/- 16 m)
- Contemporary (FORCE)
 - despite settings of 4 pings per second, apparently only 2 pings per second are being recorded
 - make sure any reporting reports the actual pings-per-second achieved

Cautions – Data Collection (Simrad) and Data Processing (Echoview) Software

As with the release of all new hydroacoustic scientific instruments such as the EK80, there is a lag between the release of the instrument and the time at which the research community has vetted its operation, including the operation of its data collection and calibration software and resultantly the updates required of the processing software. Therefore, it is not unexpected that new releases including corrections and refinements will be forthcoming for the EK80 software provided by Simrad and Echoview. Please keep your software up-to-date with the latest releases.

APPENDIX C: Data Export and Processing Scripts

Please review the extensive comments in the script files for more detail than is listed here.

Export Scripts

20190225 Script_exportEV8_MASTER run20190225.vbs

Purpose: export the following

- a. data
- b. metadata
- c. jpgs
- d. archiving files from Echoview

Output:

- a. .csv data files of the full suite of Echoview variables in a variety of user-defined cell sizes (e.g. 20-m along-shiptrack distance integrated over the full water column). REMINDER: exclude the EV files associated with “along” at this stage.
- b. .jpg files of the raw and processed echograms associated with the data contained in the .csv data files
- c. .txt files documenting approximately 140 Echoview settings associated with each of the .csv data files (e.g. colorbar settings for the echogram .jpgs among others)
- d. .csv files of the line depth of the “turbulence line” and the “bottom line” by which to calculate the proportion of the water column lost to turbulence
- e. .jpg of the cruise track over which the data in the .csv files were collected showing S_v mean alongtrack distinguishing regions designated as bad-data/no-data (designates bad-data/turbulence regions) and bad-data/empty-water (designates for passive data region)
- f. .evd files: an Echoview format that hardcodes data values based on settings at the time of export. The script is set to export the “data without turbulence” variable (i.e. the variable we use for analysis). Can be used to hardcode an archive of the data in the condition it was at the time of the automated export
- g. .ev files: a copy of the Echoview file for archiving. Gives you a fully operational copy of the Echoview file and all its variables to archive in its state at the time of the export in case future edits are required. Leaving you the original EV file for “exploring” if necessary. (i.e. the archived EV file leaves no question as to which EV files (and therefore settings) generated the exports)

Processing Scripts

SCRIPT2019 AppendCSV_20m.R

Purpose: To prepare for merge with metadata (“datasheet”),

- a. import and append the “20m dataset” transect .csv data files exported from Echoview for a single survey
- b. populate “Transect” metadata column (i.e. “GR1_NOA” which is read from the names of each of the imported .csv files)
- c. populate DateTime columns as yyyyymmdd.decimaltime to mitigate the .csv issue where “hour” gets dropped from the time column
- d. perform critical data quality control tests (failed status requires script termination)
- e. populate the data quality checks variable

Output:

- a. data file of the appended .csv data files for the survey
- b. .csv file holding the data quality checks for review
- c. archive the workspace

SCRIPT2019 MergeCSV_20m.R

Purpose: To prepare for analyses by associating (merging) metadata with S_v thereby placing S_v in a meaningful ecological context

- a. import appended survey data file (.csv) and metadata file (“datasheet” .csv)
- b. populate additional data file columns (e.g. linear version of S_v , FishPresence, etc.)
- c. using start and end date-time as the parameters by which to match metadata to data file, populate the metadata columns in the data table
- d. perform data quality control tests (e.g. test for failed matches, for “along” (excluded from these analyses, and for misspellings coming from the user produced metadata (datasheet) file

Output:

- a. count of failed matches signifying that start and end times in the metadata files (“datasheet” .csv) may need attending to (script prints instructions on how to find the data lines that failed to match with the metadata start/end times)
- b. count of the data bins that matched to “along” (rather than CLA or reference) signifying that start and end times in the metadata file may need attending to (check_along variable holds the detail by which to find those lines that matched to “along”)
- c. .csv file of the survey data merged with metadata (diel state, tide phase, study area, “with/against”, etc.)
- d. print to Console the unique values of a variety of columns within the newly merged dataset for user’s review (1) for confirmation that the merged data is as expected (i.e. all from the correct survey, etc.), (2) for missing data (e.g. no “day” etc.), or (3) for misspellings
- e. .csv file holding the merged data for the survey
- f. archive the workspace

SCRIPT2019 AppendAlldata.R

Purpose: To append the merged survey data onto the alldata .csv file

- a. import newly appended survey data and the alldata .csv files
- b. append survey data to alldata

Output:

- a. "alldata" .csv with latest merged survey data appended at the bottom
- b. archive the workspace

SCRIPT2019 20mBinAnalysis.R

Purpose: Generate data visualizations and execute analyses using S_v and

Presence:Absence data

Output:

- a. plots ready for examination and/or saving as .jpg, .png, .tiff, or .pdf
- b. analytical results printed to the Console and available as a dataframe for export

Processing Notes:

- a. some data quality checks are performed here for which output is printed to Console rather than to a file. These should be reviewed at time of running the script.

APPENDIX D: Additional Files Transferred with this Report

Files referenced in Appendix A

- 20170519 Datasheet_Melvin WORKING20190115LPM.xlsx
- 20190115 AllDataParseToMonthly_MelvinONLY_20mBinsFullWaterColumn.xlsx
- MelvinGridNOTES.xlsx
- SimradFilesPerTransect.xlsx

Merged and Appended “alldata” File for Import into R Processing Scripts

- 20190304_alldata_Grid_20mBinFullWaterColumn_thruSurvey09_201708.csv

Files Documenting Calculations for Significance Between Categories that do not include the baseline (“reference”) category in presence:absence analyses

- 20190501_significanceCalcs.xlsx

Data Files

- Echoview post-processing files for historical and contemporary surveys
- Echoview calibration files (.ecs) for historical and contemporary surveys
- Echoview export (data) files for historical surveys
- Echoview export (data, metadata, and archiving) files for contemporary surveys
- metadata (“datasheet”) files for historical and contemporary surveys

APPENDIX E: Glossary and Abbreviations

ANOVA: analysis of variance

a statistical procedure used to analyze the differences among group means in a sample

CLA: Crown Lease Area

located in Minas Passage

CLD: compact letter display

a compact presentation of the results of multiple comparisons

although the name references “letter”, R uses numbers to indicate groupings

dB: decibel

3 dB: a 3 dB change in S_v (the log form) is equivalent to a doubling or halving in linear terms

10 dB: a 10 dB change in S_v (the log form) is equivalent to a change by an order of magnitude in linear terms

20 dB: a 20 dB change in S_v (the log form) is equivalent to a change by two orders of magnitude in linear terms

EMM: estimated marginal mean

when there are pronounced differences in the number of observations, the estimated marginal mean is a way to estimate what the mean would be if the number of observations were balanced

EV: Echoview Software

industry-standard software used to post-process hydroacoustic data preparing it for analyses

GLM: Generalized Linear Model implemented in R for binary logistic regression

GMT: Greenwich Mean Time

used interchangeably with UTC (Coordinated Universal Time)

R: an integrated suite of software facilities for data manipulation, calculation, and graphical display

S_v : mean volume backscattering strength

the log form of a fundamental hydroacoustic measurement

unit: dB re 1 m^{-1}

a proxy for relative fish density

relationship to s_v is shown in Equation 1

s_v : **volume backscattering coefficient**

the linear form of a fundamental hydroacoustic measurement

unit: m^{-1}

relationship to S_v is shown in Equation 1

TISEC: Tidal In Stream Energy Conversion device

an device engineered to convert tidal energy to electricity

Appendix V

Passive acoustic monitoring in tidal channels and high flow environments

Passive Acoustic Monitoring in Tidal Channels and High Flow Environments

Report for OERA/FORCE, The Pathway Program

David R. Barclay, PhD
Department of Oceanography
Dalhousie University
1355 Oxford St., Halifax, Nova Scotia, B3H 4R2
e-mail: dbarclay@dal.ca

I. Introduction

This report provides an overview of methods, data processing techniques, and equipment used to make passive acoustic measurements in tidal channels. The acoustic field is measured in these energetic environments to characterize the natural noise field, quantify contributions by tidal energy and other human deployed devices, and to detect and localize vocalizing marine animals, the latter being the primary objective of interest in this report. No commercially available, purpose built acoustic monitoring systems have been designed for operation in turbulent tidal channels, estuaries, or rivers, despite a growing body of underwater acoustic field work being carried out in the context of environmental impact assessment of tidal energy extraction. However, a number of technologies designed for more benign oceanographic conditions have been experimentally deployed in high flow environments, including conventional cabled or autonomous hydrophone and analogue-to-digital instrument packages, internally recording hydrophones with digital interfaces, autonomous and cabled hydrophone or vector sensor arrays, and integrated hydrophone and data processing systems for marine animal detection. Flow noise, natural ambient noise, sensor size and geometry, and deployment method all have an effect on the detection efficiency of passive acoustic systems. Experimental results and system performances are compared across all instrument package types, deployment methods, and study areas.

The primary scientific and engineering challenge while working in a turbulent flow environment is the identification and mitigation, either through mechanical or signal conditioning means, of the pseudo-sound (flow noise) generated by pressure fluctuations due to turbulent flow on the surface of the hydrophone. The magnitude, spectral shape, and bandwidth of the flow noise depends on the flow speed and effective shape of the hydrophone. Mechanical solutions are proposed, such as the deployment of sensors on Lagrangian drifting floats in place of fixed moorings, and the use of flow shields, baffles, and vibration isolation mounts to minimize the flow noise generated. Coherent processing of acoustic signals recorded on multiple sensors has also been demonstrated as a method to reduce incoherent flow noise while providing gain to acoustic signals propagating in the water.

In tidal channels and rivers, flow noise can potentially mask true propagating sound into the 10's of kilohertz band, with increasing intensity with decreasing frequency. This makes the characterization of ambient noise and quantification of turbine and industrial noise challenging to measure and reduces the effective range of detection of vocalizing marine animals.

The similarity between the deployment of passive acoustic systems in tidal channels and from moving vessels is suggested, the latter being the subject of several decades of research while the former is still in relative infancy. Novel uses of autonomous vehicles may also present a solution to the large field effort required for sustained, flow noise free, passive acoustic monitoring in high flow environments.

Tidal turbines could become an important source of ambient noise in tidal channels through cavitation and motor or mechanical noise (Wang, 2007). Turbine anthropophony could affect animal navigation, communication, predator-prey detections (Lombardi, 2016), and marine life cycles (Pine, 2012). Moreover, turbine-generated sound could be damaging to fish tissue (Halvorsen, 2011). If substantive, these effects would threaten near-field and far-field ecosystem health, stressing the need for rigorous environmental impact assessments in the tidal power sector.

The report is organized as follows: Section II discusses the physics of flow noise and potential methods of identification and mitigation; Section III surveys studies in passive acoustic monitoring in high flow environments that have been previously carried out and compares the two primary methods of deployment (fixed and drifting sensors); Section IV describes marine animals of interest and compares the methods and instruments for detecting, classifying, and localizing them; Section V provides a summary, recommendations, and conclusions.

II. Flow noise and self-noise identification and mitigation

A. Flow noise

Turbulent flows occupy a wide range of frequencies and wavenumber domains, with broad spatial and temporal variability. The advective nonlinearity of turbulent flows, combined with the variety of effective shapes that a sensor and instrument housing may present, makes them unpredictable in space and time and contributes to their complex nature (M. Van Dyke, 1982) (Finger, 1979). As such, it is difficult to reliably model flow noise.

Bassett (Bassett, 2013), applied the findings from three Strasberg papers on hydrodynamic flow noise and wind screen noise (Strasberg, 1979, 1984, 1988) to predict the upper frequency limit for flow noise, noting that it is related to the wavelengths of the spatial velocity fluctuations and the mean velocity of the flow, u , by $f = |u| \eta^{-1}$, where η is the Kolmogorov microscale. The microscale describes the length scale at which viscosity overcomes the turbulent fluctuations, and is practically related to the dissipation rate, ϵ , and the kinematic viscosity, ν , by $\eta = (\nu^3/\epsilon)^{0.25}$. While the viscosity difference between sea water and fresh water is small ($\sim 90\%$), the dissipation rate has large variability, with reported peak dissipation rate of $2 \times 10^{-3} \text{ m}^2 \text{ s}^{-3}$ at Admiralty Inlet, Washington (Thomson 2012), and order $1 \times 10^{-3} \text{ m}^2 \text{ s}^{-3}$ measured in Grand Passage, Nova Scotia (Guerra-Paris, 2019), both several orders of magnitude greater than typical rates in the open ocean. For the particular case of Admiralty Inlet, WA, the maximum theoretical frequency at which flow-noise is expected was 10 kHz. In practice, the scale of the sensor itself plays an important role in lowering that upper frequency limit.

In the idealized circumstance of an infinitesimally small sensor, flow noise would follow a spectral slope of $f^{5/3}$, behaviour that is analogous by Kolmogorov's turbulence theory. This flow noise is not to be confused with wind-generated noise that produces $f^{5/3}$ spectral slopes at higher frequencies (Knudsen, 1948). Bassett et al. (Bassett, 2014) identifies $f^{5/3}$ flow noise below 20 Hz and describes steepened spectral slopes, f^m where $m > 5/3$, at low-to-mid frequencies. Lombardi (Lombardi, 2016) identifies these steep spectral slopes in measurements from the Grand Passage tidal channel. The flow noise that produces f^m is a result of small-scale turbulence being averaged out across the surface of a finite sized hydrophone, typically several orders of magnitude larger than the microscale, which dampens (or reduces) the measured flow noise as frequency increases.

B. Identification of flow noise

Flow noise is always 'red' (decreasing in intensity with increasing frequency), so the upper limit of the flow noise bandwidth, or the critical frequency where the intensity of the flow noise is equal to the intensity of the true sound or noise, is of primary interest. Below the critical frequency, flow noise masks the true sound that would otherwise be measured by the sensor, while above the

critical frequency the measurement can be considered to be uncontaminated by flow noise. Flow noise and natural, wave driven noise in the ocean have spectra that obey power laws, where the former depends on the length scale of the sensor. To determine the critical frequency, a break in the slope of the spectrum can be found computationally, or by inspection. This method is generally employed and carries with it some level of uncertainty.

When measurements are made with two or more sensors, the spatial coherence between them may be used to identify the critical frequency with high accuracy (Auvinen, 2019). Propagating ambient noise is highly correlated between two hydrophones placed less than a few wavelengths away. Additionally, propagating noise at wavelengths sufficiently large relative to sensor spacing produces very high coherence at low frequencies, since the hydrophones become effectively co-located. Conversely, flow noise is a source of incoherence, as pseudo-sound is uncorrelated between sensor, thus flow noise is marked by low coherence while ambient noise is marked by high coherence (Barclay, 2013). At low frequencies (below frequencies corresponding to half the sensor separation) the transit of this coherence boundary, from flow noise (incoherent) to ambient noise (coherent) provides a precise metric for describing the upper extent of the flow noise bandwidth.

In some instances, co-located measurements of static and Lagrangian (drifting) hydrophones have been made to determine the upper bandwidth limit of flow noise on the static device, assuming the free drifting sensor is flow noise free.

C. Mitigation strategies for flow noise

The dampening effect associated with sensor size can be exploited by choosing a cut-off frequency above which true sound must be measured and designing the receiver's surface to have an area on the order of the corresponding acoustic wavelength in the fluid. In the case of recording turbine noise over a bandwidth of interest with respect to fish and other low-frequency sensing marine life (~10 - 100's of Hz), the scale of such a sensor becomes impracticable. However, this mechanism has been theoretically developed and proposed for underwater surveillance applications. Ko demonstrated, for the particular case of flush mounted hydrophones as you might find on the hull of a submersible, that a careful choice of sensor shape, the application of an elastomer layer, and the combination of single hydrophones into an array can further reduce the effects of noise induced by a turbulent boundary layer flow (Ko, 1992, 1993). He further claims that the arrangement of array elements, including interelement spacing has little effect on the performance of the flow noise suppression.

For the case of tidal turbine monitoring, Auvinen (Auvinen, 2019) and Worthington (Worthington, 2014) demonstrated that linear arrays can be used to reduce flow noise in open channel turbulent flow. As the flow noise is generated locally on each sensor, it is independent from one sensor to the next, while true propagating sound will appear coherent across the array. By coherently averaging the received signals across the array, the flow noise is suppressed while the true sound is amplified.

Another method to reduce the impact of flow noise is to use a flow shield and isolation system where the hydrophone is encased in a larger structure, either semi-permeable with a very low hydraulic conductivity, or impermeable and oil-filled. These types of systems should have three purely mechanical effects on the reduction of pseudo-sound. Firstly, the flow of water over the

hydrophone is eliminated by the shield acting as a baffle, along with any flow noise normally generated on the surface of the hydrophone. Vibrational noise will be generated on the shield, but as it is larger than the hydrophone, the upper frequency limit of flow noise is effectively lowered. Lastly, the hydrophone is suspended inside the shield using an isolation system that aims to minimize the vibrational energy transferred from the shield to the sensor. Without isolation, the flow shield may be wholly ineffective (Porskamp, 2015). These types of systems are extremely effective for in-air flow noise reduction, are commercially available, and seen in use by professional recording studios, and television news-people reporting in adverse weather conditions. It should be noted that conventional dynamic in-air microphones are not as sensitive as a ceramic hydrophone to vibrational energy propagating through the housing of the sensor, so an isolation system is usually not required and a fuzzy wind-sock attached directly fixed to the microphone can be quite effective. This is not the case with ribbon microphones or ceramic sensors, that should always employ suspension systems.

The spring constant needed for an effective isolation and suspension system is dictated by the wavelength. The resonance of the isolation system must be half the lowest desired resolvable (flow noise free) frequency. For frequencies on the order of 10^2 Hz, in water, where wavelengths are 5 times larger than in air, the suspension system becomes unreasonably large, as does the flow shield that encases it. As the size of the flow shield increases, so does the drag on the entire system and the problem is only practically tenable with careful engineering (e.g. dashpot suspension, hydrodynamic flow bodies). Additionally, the use of flow shields lowers the sensitivity of the hydrophone, requiring re-calibration, and reducing the effective listening range of a receiver (Malinka, 2015).

A simple method to minimize flow noise is to place the recording system in a region where flow speeds are minimized, such as very near the seabed, or out of the flow channel. In both cases, transmission loss between the turbine, animal, or source of interest must be well understood in order to determine a source level, or detection efficiency, as the study may require. As previous reports have identified (Environmental Effects Monitoring Programs, Fundy Ocean Research Center for Energy, March 2016), transmission loss in turbulent shallow water environments with high tidal flow is not well understood and must be further investigated. In the case of the depth-dependence of background (turbine-less) noise in Minas Passage, a comparison of median pressure spectral densities between a bottom-mounted recording with a steel and neoprene flow shield, a free-drifting near surface hydrophone with a simple suspension system, and two static mid-water column mounted hydrophones with no-shields or suspension was made (Martin, 2018). The measurements between the drifter and bottom mounted system were the most in agreement. The upper frequency limit of flow noise on the bottom mounted system was 60 Hz, while the unshielded mid-water column phones had an upper frequency flow noise contamination limit of, optimistically, 600 Hz. Most importantly, the agreement between the drifter and the bottom mounted system suggests that the depth-dependence of ambient noise is minimal over the band of 60 Hz – 1 kHz.

To better understand the sound propagation loss in a turbulent tidal channel and thus the effective horizontal ranges of sources such as turbines, marine animals, active sonars, and passive acoustic monitoring systems, one experiment has been carried out in Admiralty Inlet, Washington, and two experiments were carried out in Grand Passage, Nova Scotia. The Admiralty Inlet experiment showed reduced transmission loss during slack tide and compared the results to geometric spreading laws. In Grand Passage, 2015, a drifting source was deployed near moored

hydrophones to determine the effective listening radius under different flow conditions and baffling arrangements, for that particular arrangement of receivers. In 2018, an active source and set of three receivers at distances between 100 m and 1.1 km were moored in Grand Passage. Linear frequency modulated sweeps, and pure tones were played every 30 minutes in an effort to quantify the effects of tidal state and mean and turbulent flow speed on transmission loss (Wilson, 2019). The analysis of the collected data is underway, along with the development of a validated transmission loss model for turbulent high mean flows.

D. Self-noise

Other forms of self-noise should also be taken into consideration when designing an experiment in a high flow environment. Systems suspended from surface floats will experience wave induced noise caused by vertical motion in the water column, unless an adequate isolation and suspension system is employed. Additionally, though drifting systems do an adequate job of removing the effects of the mean flow noise, the finite size of the drifting system may be subject to flow noise created by system motion due to turbulent flow and vertical shear. One method employed to avoid this flow noise, or instrument motion noise, is to deploy the sensor inside of a drogue (Wilson, 2014). Moored systems with subsurface floats will suffer from cable strum, and noise induced by mooring knock down unless vortex shedding fairings, hydrophone isolation and suspension systems, and hydrodynamic floats are used. Bottom-mounted systems near the seabed are susceptible to turbidity currents. In high flow environments, sands and gravel have been observed to generate noise through contact directly on the instrument housing (Martin, 2018).

E. Conclusions

A review of the basic physics of flow noise, identification, and mitigation techniques for passive acoustic measurement methods in tidal channels has the following conclusions:

- 1) Due to high dissipation rates in tidal channels, flow noise can potentially mask sound over a very large bandwidth (0 – 10 kHz).
- 2) The bandwidth of flow noise contamination can be generally identified by looking for regions of changing slope in the noise spectrum, or more accurately by investigating the frequency dependent spatial coherence between adjacent sensors in an array. Comparisons between drifting measurements and static measurements can also be used to identify flow noise bandwidth
- 3) Increasing the size of a sensor lowers the upper frequency limit at which flow noise masks a measurement.
- 4) Measuring sound with a coherently averaged array of sensors lowers the upper frequency limit at which flow noise masks a measurement.
- 5) Placing shielded sensors near the bottom boundary where flow speeds are reduced mitigates flow noise.
- 6) The depth-dependence of ambient noise in a shallow water tidal channel (Minas Passage) is negligible over the band 100 Hz – 1 kHz. Transmission loss modelling in turbulent media is poorly understood.

III. Sensor deployment configurations

In 2013, two review papers were written covering all published acoustic environmental monitoring activity, the first by Robinson and Lepper based in the United Kingdom (Robinson, 2013) and the second by Copping et al., based in the United States of America (Copping, 2013). The latter study resulted in the Tethys database, an online resource collecting papers in the peer-reviewed and grey literature on the topic of marine energy extraction, and environmental monitoring and impacts. Both surveys discuss wave energy and tidal energy conversion devices, system source levels, installation noise levels including pile driving, and methods used for passive acoustic monitoring.

For this report, the work of Robinson & Lepper and Copping is updated and expanded, summarizing the various passive acoustic monitoring efforts in tidal channels, consisting of ambient noise baseline measurements, turbine operational noise, construction and installation noise, and planned transmissions, presented in Table 1. The configuration of equipment employed for each measurement campaign is classified generally as 1) boat drifting, 2) buoy drifting, 3) bottom moored or mounted, or 4) turbine mounted single hydrophones, pairs, or larger (vertical, horizontal, or two dimensional) arrays. The objectives of the ensemble of studies at each site are described as either background, construction, or operational noise measurements, along with some selected publications describing the results. In certain cases, detection of marine animals or planned transmissions from user deployed sources are described. This table attempts to be exhaustive and up-to-date.

Table 1. Summary of deployment locations, passive acoustic monitoring equipment configurations employed, acoustic measurement type, and associated references.

Tidal Energy Noise Monitoring Campaigns			
Location	Methodology used	Measurements	References
Lynmouth, UK	Drifting boat hydrophone	Operational noise	(Parvin et al 2005) (Richards et al 2007) (Faber Maunsell & Metoc 2007).
Strangford Lough, UK	Drifting boat hydrophone	Operational noise	(Nedwell and Brooker, 2008) (Kongsberg, 2010) (Götz et al, 2011)
Fall of Warness, Orkney, UK	Drifting boat hydrophone Drifting buoy hydrophone	Background noise, Construction noise, Operational noise.	(Wilson et al, 2010) (Aguatera 2010, 2011) (Wilson, 2014) (Beharie and Side, 2011)
Cobscook Bay, Maine, USA	Drifting buoy with pair of vertically separated hydrophones	Operational noise.	(CBTEP, 2012)
Kvalsund, Western Finnmark, Norway	Drifting boat hydrophone	Operational noise	(Akvaplan-niva, 2009)
East River, New York, USA	Towed hydrophones	Operational noise	(OES, 2013)

Admiralty Inlet, Puget Sound, USA	Bottom mounted hydrophone, Drifting buoy with vertical pair of hydrophones, Drifting boat hydrophone, Drifting vertical line array.	Background noise, Operational noise, Planned transmissions	(Bassett, 2010, 2013, 2014) (Polagye, 2012) (Copping et al 2013) (Xu, 2012)
Minas Passage, Bay of Fundy, Canada	Drifting buoy hydrophone, Bottom moored system, Turbine mounted system, Moored subsurface float, Boat deployed horizontal array.	Background noise, Free spinning turbine noise.	(Martin, 2012) (Martin, 2018) (Tollit, 2013) (Auvinen, 2019)
Schottel, Queen's University Belfast Tidal Test Site in Portaferry, Northern Ireland	Drifting buoy hydrophone	Background noise, Operational noise including free spinning and braking.	(Schmitt, 2015)
River Turbine, Iguigig, Alaska, USA	Drifting spar buoy hydrophone	Operational noise	(Polagye, 2015)
Site Expérimental Estuarien National pour l'Essai et l'Optimisation Hydrolenne (SEENOH), Bordeaux, France	Drifting boat hydrophone	Background noise, Installation noise, Operational noise	(Bald, 2015) (Giry, 2018)
Cook Inlet, Alaska, USA	Moored directional array, Moored hydrophone	Background noise, Beluga whale monitoring	(Worthington, 2014)
Ramsey Sound, UK	Boat deployed partial drifting hydrophone with subsurface float and weight, 12 element turbine mounted array	Background noise, Cetacean detection and localization	(Broudic, 2012a, 2012b) (Willis, 2012) (Malinka, 2018)
Grand Passage, Canada	Bottom moored hydrophone, Drifting buoy hydrophone Turbine mounted hydrophone	Background noise, Planned transmissions	(Malinka, 2015) (Wilson, 2019)
West Scotland (Sound of Islay, Scarba, the Great Race, Gulf of Corryvreckan, Kyle Rhea, the Sound of Sleat)	Moored C-PODs Drifting C-PODs Moored vertical line array Bottom mounted hydrophone, Towed hydrophone array, Drifting hydrophone.	Porpoise detection and localisation Baseline noise, Construction noise, Operational noise	(Wilson, 2013) (Macaulay, 2017) (Benjamins, 2016) (EMEC, 2012) (Benjamins, 2017)
Mississippi River, Memphis, Tennessee, USA	Moored hydrophone Drifting hydrophone	Background noise, Operational noise.	(Bevelhimer, 2016)
Sequim Bay, Washington, USA	Bottom mounted vector sensor array	Test tones	(Raghukumar, 2019)

At the 17 study sites presented, each representing a larger number of individual experiments, measurement campaigns and studies, seven studies employed moored or bottom mounted systems, 14 used drifting buoy or boat measurement, and six have used drifting and moored hydrophones, in some cases simultaneously as a means of quantifying flow noise. Six sites have been studied using directional arrays or pairs of hydrophones to incorporate directional information of the noise field, perform localization of marine animals, or to suppress flow noise.

Many early studies used drifting boat deployed hydrophones, though self-noise generated by surface motion and boat noise such as lapping of waves against the hull and topside activity were identified as significant contaminants in the acoustic records. Hydrophones deployed under drifting buoys with isolation and suspension systems, drogues, or catenary sections were employed in later studies to improve the reduction of surface motion noise, and the associated turbulent flow noise. In general, these types of measurements are described as having the highest fidelity to the true sound field and this claim is often substantiated by the demonstration of relatively reduced flow noise and motion induced noise levels on subsequently collected sets of data.

In a subset of cases, comparisons between moored recorders and drifting recorders are used to quantify the performance of flow noise suppression on static systems. Operationally, bottom mounted systems provide the ability to monitor a single point in space for a long period of time (even indefinite), while drifting systems measure a snapshot (typically on the order of minutes) of the noise field over wider area. The advantages and disadvantages of these two methods must be put in context of the monitoring program being designed.

For example, in quantifying turbine generated noise, flow noise suffered by a static system tends to mask the frequencies (10's - 100's of Hz) of interest, therefore favouring a labour intensive and carefully executed drift measurement campaign. For the detection and localization of marine animals such as porpoise and Beluga, the band of interest is outside of the flow noise contaminated acoustic regime and moored or even turbine mounted sensors are adequate. For monitoring harbor porpoises and other odontocetes, C-PODs (autonomous echolocation loggers), were popularly employed as both drifters and moored units, and found to be reasonably effective in both configurations.

In the case of continuous real-time monitoring, a cabled moored or mounted system is the only option, thus methods of flow noise suppression must be employed if the objective is to record turbine generated noise. No standard flow shield design has been proposed, and results from flow shield experiments are mixed, sometimes reducing flow noise (Raghukumar 2019, Bassett 2013), sometimes reducing sensitivity with no effect on flow noise over the band of interest (Malinka 2015, Porskamp 2015). A number of custom-built arrays were deployed in tidal channels with various motivations; however, the use of large diameter horizontal arrays has not been well investigated. A significant body of literature and expertise concerning ship towed passive sonar systems has been developed over the last century, including analytical theories for the prediction of flow noise for sensors placed in oil filled elastomeric tubes (e.g. Corocos, 1963, Knight, 1996). A study of towed array design knowledge could lead to significant advances in flow noise suppression from stationary hydrophone systems in tidal channels, through both improved isolation, and signal processing.

Digital hydrophones, which are now manufactured by a number of North American and international companies, are preferable for permanently cabled static observation systems because of their ability to optically transfer data at high speeds and with little signal attenuation, though this was only demonstrated in a single report. Digital hydrophones, particularly the OceanSonics icListen, were a popular choice for deployment in tidal channels, likely because of their compact form factor.

The field intensive requirement of drifter deployments is seen as a major drawback from an otherwise ideal technology. One proposed solution is the automation of drifting passive acoustic

monitoring systems. Research is underway using Unmanned Aerial Vehicles (UAVs) to make underwater noise measurements using dip sonars (Lloyd, 2017). The use of a station-keeping autonomous hovercraft with a deployable acoustic sensor has also been proposed (Barclay, 2019). Both technologies could potentially provide duty cycled long term monitoring of tidal energy sites, without the interference of flow noise.

Polagye (2014) and Lepper (2016) mention the importance of particle motion (as opposed to pressure) measurements due to the physiological sensitivity of some marine animals to particle velocity as opposed to pressure. An array of vector sensors, capable of resolving particle motion and pressure, was deployed in a single study (Raghukumar, 2018, 2019), demonstrating the ability to resolve directional information in the sound field while identifying flow noise contamination. However, this system operated with a limited acoustic bandwidth of 50 Hz - 5 kHz, reducing its ability to resolve vocalizing animals of interest, particularly echolocation clicks.

IV. Detection, classification, and localization of marine animals

Several scientific objectives were met in the studies listed in Section III, Table 1. The objectives of interest for this report are the detection, classification, and localization of vocalizing marine animals. In order to understand which passive acoustic instruments are best suited to these tasks, and future work on animal presence, population density estimate, and animal-turbine interaction, the published studies were surveyed to determine which marine animals were detected in the study area, the passive acoustic instrument used to make the detection, and the relative performances of these instruments. In these comparisons, an effort is made to understand factors that will influence the detection efficiency of the instrument, such as flow noise (or current flow speeds), ambient noise with special attention paid to sediment generated noise on the seafloor, reverberation, the propagation environment, sensor placement, and sensor deployment methodology. In considering these factors, and by estimating their relative effects, the performance of the sensors can be compared more directly.

A. Marine animals of interest

In order to best understand detection performance, the bandwidth of the marine animal vocalizations must be known. Over the ensemble of study sites, the known presence by acoustic detection of marine animals is summarized in Table 2, along with the relevant bandwidth of interest for each animal and instrument used to make the detection.

Table 2. Survey of acoustically detected marine animals in tidal channels, characteristics of sounds produced, and instrument packages used for detection.

Marine animals detect at tidal energy sites			
Marine animal	Study site(s) present	Characteristics of vocalizations	Instrument used
Dolphins (bottlenose, Risso's, short-beaked common, Atlantic white-sided and white-beaked dolphin)	Ramsay Sound, Minas Passage	Clicks: with root mean square bandwidths of 23–54 kHz, centred at ~ 90kHz Whistles, varying bandwidth: low 10's of kHz	C-POD Turbine mounted hydrophones
Harbour porpoise	Great Race, Scarba, Sound of Islay, Minas Passage, Admiralty Inlet, Kyle Rhea	Clicks: centred at 130 kHz with 16kHz bandwidth. Highly directional (beam pattern 9.5 to 16 degrees).	C-POD (bottom mounted, SUB moored, drifting) Boat drifting vertical line array Drifting hydrophones
Beluga Whale	Cook Inlet	Clicks with bandwidths of 40 – 120 kHz Non-echolocation calls: 2.0 to 5.9 kHz	EAR C-POD DASAR

It should be noted that animals such as the harbour and grey seals, and humpback, fin, and minke whales have been visually observed in Minas Passage but have never been acoustically detected, despite acoustic monitoring with some regularity. In most cases, the presence of these animals is rare, their calls are sporadic and infrequent, and simply may not have coincided with a passive acoustic survey. However, these animals produce sound mostly below 1 kHz, and always below 5 kHz where masking from flow noise may also be contributing to the absence of detections. It is difficult to conclude which factor is playing the limiting role in the lack of acoustic observations of these animals.

Over the band of 5 kHz – 10's of kHz, beluga non-echolocation calls and dolphin whistles should be detected in tidal channels where these animals are present. The limited number of studies on these animals do not report many detections of these types of calls, though it is difficult to conclude if that is due to the limited presence and call rates coupled with the sparsity of data sets, or the frequency band and potential masking of the calls.

The endangered Southern Resident killer whale are frequently visually observed in Admiralty inlet, WA (Snohomish PUD, 2012). These animals produce echolocation clicks centered at 60 kHz with bandwidths of 50 kHz, as well as social vocalizations in the band 1 – 6 kHz. A modelling study found that passive acoustic detection range of the whales in the tidal channel reduces by 90% during flood and ebb tides strong enough for turbine operation, relative to slack tide (Bassett, 2013). This proposed mechanism of the reduction of this range is masking by sediment generated noise. No published acoustic observations of the killer whales at this site have been reported.

Passive acoustics monitoring may also be used to detect fish (Luczkovich, 2008). However, in all cases the combination of low source levels (typically around 130 dB re 1 μ Pa) and their frequency band (100's of Hz) makes the detection of fish in high flow environments very unlikely due to flow noise masking. No passive acoustic observations of fish have been reported in the studies listed in Table 1.

The majority of passive acoustic monitoring studies of marine animals in tidal channels are centered on the detection, classification, and localization of harbour porpoises, dolphins, and belugas using their echolocation clicks. These short duration signals have reasonably wide bands (10 – 50 kHz) and are centered at relatively high frequencies (90 – 130 kHz).

B. Instrument and detection rates comparison studies

A limited number of passive acoustic instrument packages have been used to detect marine animals in tidal channels. Since the primary signals of interest are echolocation clicks, the data recording packages suitable for detection must have high sampling rates, above 250 kHz, and thus large memory capacity for storing the raw pressure time series. Acoustic data collected as raw pressure time series must be processed for detection, classification, and localization using either commercially available software or using custom detection algorithms. A popular choice amongst researchers was the use of PAMGUARD, an open source software managed by Sea Mammal Research Unit at the University of St Andrews in Scotland. The software allows automated detection and classification of marine animals sounds in the time series, and recently, localization modules have been added to its library.

One established alternative to these separate hardware (recording) and software (detection and classification) systems is the development of stand-alone instruments, where the pressure time series is analyzed in real-time given some prescribed criteria which provides classification of clicks, and then discarded, while the meta-data is stored. Chelonia Ltd. has manufactured three generations of this class of instrument called the PORpoise Detector (POD): the T-POD, the digital C-POD, and most recently the C-POD-F, which allows storage of the full wave form of each detection. In the case of the C-POD, the instrument used in the majority of studies surveyed here, the time and duration of each detected click are recorded. Clicks are detected using a proprietary algorithm and classified using the KERNO classifier (also proprietary) which identifies the echolocating species.

These two classes of systems have been deployed in drifting, moored, bottom mounted and turbine mounted configurations, and used to detect, classify, and located porpoises, dolphins, and belugas in tidal channels and have been shown to have very different performances.

A study in the relatively benign environment of the Baltic Sea found that a co-located C-POD detected between 21 – 94% of the click trains detected by PAMGUARD applied to broadband recordings made on a SoundTrap, a conventional pressure time series recorder produced by Ocean Instruments (Sarnocinska, 2016). The reduced rate of detection was due to many factors, but the primary one was that PAMGUARD detects individual clicks, while C-POD detects trains of clicks using patterns in the inter-click intervals as well as characteristics of the clicks; a more restrictive and discerning detection algorithm. All trains of four clicks or less are ignored by the C-POD, for

example, which greatly reduces false positives. PAMGUARD's click detection algorithm compares energy in narrow-band filters whereas the C-POD employs a zero-crossing algorithm.

The large spread in the detection ratio of the two systems was the result of very poor correlation between the detection rates in time. In the research paper, one proposed explanation is that the signal excess required for a positive detection on the C-POD is larger than that of PAMGUARD's algorithm. Although this would impact the detection ratio between instruments and provide a non-zero intercept when calculating the linear regression between relative performance, this would not cause poor correlation at higher signal excess levels than the minimum detection threshold, shown as the large spread in the scatter plot presented in Fig. 2 of (Sarnocinska, 2016). The study also observed that when only a few animals were in the study area, the C-POD tends to report a detection rate of zero as compared to a non-zero rate reported by PAMGUARD, which suggests either that hydrophone sensitivity (detection range) is higher on the SoundTrap, or that the rate of false positives could be very high (order 10^3 clicks per minute) on the SoundTrap, although this seems unlikely.

The lack of a consistent linear relationship between the detection rate in clicks-per-minute of the C-POD and SoundTrap-PAMGUARD highlights the fact that data collected on these two classes of systems cannot be directly compared. Instead, the difference between acoustic sensitivities and detection efficiencies must be understood. By accounting for the effective listening range and detection efficiencies, it is conceivable that a method for inter-data comparison may be developed.

Another study in a non-tidal environment comparing a co-located C-POD and a Digital acoustic MONitoring (DMON) recorder (Woods Hole Oceanographic Institute) found that C-PODs reported a small number of false detections, with false positive rates ranging between 1% and 4% for individual units (Roberts, 2015). In this case, the researchers compared recorders using 'detection positive minutes', per unit time. With this metric, it was found that C-PODs performed with a high accuracy and low spread in detection ratio relative to the time series recorder (72%–91%) over a period of ~ 8 hours. The authors also show that this performance ratio depends on the unit time over which detection positive minutes are computed.

A study in Monterey Bay, California found very good agreement between the number of echolocation-clicks per hour detected on a co-located SoundTrap and C-POD (Jacobson, 2017). In this case, the pressure time series data were analyzed using an in-house built detector and filtering scheme and found 13% more echolocations than the C-POD.

A comparative study of harbour porpoise detection rates between a C-POD housed within streamlined SUB buoy suspended 3 m above the seafloor, two bottom platform mounted C-PODs, and a co-located conventional passive acoustic recorder, the icListen (OceanSonics) was carried out in 2014 in the Minas Passage (Porskamp, 2015). High-flow induced noise in the caused the C-POD's maximum recordable clicks per minute to be exceeded, resulting in 'lost time', and thus under-detected porpoise click trains. This effect was greater on the SUB buoy C-POD than the bottom mounted units. This may be due to flow noise, sediment generated noise, mooring noise (including noise generated by the mooring being blown down against the bottom). The latter is the most likely since it is expected that sediment generated noise would be greater or equal in intensity near the bottom so would contribute equally to lost time on both recorders, and, while flow increases with decreasing depth, it is not likely to be significant at frequencies above 10 kHz.

Reports of saturation of the C-POD detection buffer due to sediment generated noise have been made by researchers in Admiralty Inlet and previously in Minas Passage (Tollit, 2013).

The bottom mounted C-PODs detected roughly 10 times more detection minutes per day than the subs mounted C-POD, while the icListen detected five times more detection minutes per day than the co-located C-PODs. Another comparison experiment in Minas Passage also observed a factor of 10 increase in the number of detection minutes on an icListen as compared to the C-POD (Tollit, 2013). This is either due to the software analysis technique applied to the icListen time series (i.e., the detection algorithm), or greater flow and/or electronic noise present in the C-POD recording. The flow noise generated on both instruments is likely similar, as the physical dimensions of the two co-located instruments are similar. The receiving sensitivity of the C-POD is -211 dB re 1V/ μ Pa and the icListen is -169 dB re 1V/ μ Pa. Though these reported sensitivities are significant, the detection stage of each package also contributes to the disparity between measurements.

A study in Kyle Rhea was carried out with deployments of C-PODs moored 5 m from the bottom along the edge of the channel (in an effort to protect the instruments from the full force of the flow) and drifters comprised of a surface float and a C-POD mounted on a Lagrangian drogue 5 m below the surface (Wilson, 2013). Additionally, a pair of HS150 (Sonar Research & Development) hydrophones were towed 100 m behind a boat through the study area in a separate acoustic and visual survey. The hydrophone data was analyzed using PAMGUARD to detect clicks, which were classified manually. The moored C-PODs suffered from lost time due to high background noise, while the co-incident drifting C-PODs did not, suggesting that flow noise is causing the buffer saturation on the moored units, or that the moored units were placed in areas of high background (sediment generated) noise. Comparisons with the towed array are limited in this study, but generally it was found that the drifting C-PODs had the highest detection rates.

Comparisons of the ability of a C-POD, duty cycled Ecological Acoustic Recorders (EAR, Oceanwide Science Institute), and the Directional Autonomous Seafloor Acoustic Recorder (DASAR, Greenridge Scientific) to detect Beluga whales in the tidal energy site in Cook Inlet, Alaska were made (Worthington, 2014). Detections from the raw acoustic data were found using an in-house developed whistle detector, with a human verification step to eliminate false positives. In order to reduce the complication of recorder specific detection efficiency comparison, the meta-data were decimated to detections per hour across all three devices and presented in the final report as detections per month, and detection days per month. Even with this further data processing step, the agreement between devices was poor, with the C-POD outperforming the DASAR and EAR by a factor of two in December, March, and April, while the reverse is true in November and January. To further cloud data interpretation, the C-POD only detected echolocation clicks, while the DASAR and EAR only detected social Beluga vocalizations since their sampling frequency was too low to detect the echolocation signals.

A drifting pair of icListen recorders and a pair of C-PODs were deployed in Minas Passage on a single float spanning the upper 20 m of the water column (Adams, 2018). The drifting C-PODs suffered no lost time due to buffer filling, which supports a hypothesis that flow noise or mooring generated noise is responsible for triggering false detections. Sediment generated noise was not reported on in the study, but the acoustic time series data could be analyzed to investigate the depth-dependence and spatial variability of such noise. The detection minutes on the icListen were between 4-5 times greater than on the C-PODs. In this case, an in-house developed software

package ‘Coda’ was used to detect clicks in the raw time series data. Again, it is difficult to determine if the relatively poor detection performance of the C-POD is due to hardware (lower hydrophone sensitivity) or software (more stringent detection algorithm) since the instrument is effectively a closed system.

In general, the standard C-POD detection limit of 4096 clicks min⁻¹ can be easily exceeded during deployment in tidal channels. This has been extensively reported in the above described studies that employ moored and bottom mounted C-PODs, as well as several drifter deployments (Benjamins, 2016, Wilson, 2013). This may be due to sediment generated noise, mooring noise, or flow noise, though the physics of the latter seems unlikely. More work is needed to determine the primary cause of lost time for both deployment configurations of C-PODs in the different areas of study.

C. Detection Range Estimation

A direct comparison of detection range between an icListen and a C-POD in a low-noise, shallow water environment at 69 kHz showed that the combined sensitivity of the C-POD hydrophone and click-detection algorithm is lower than the icListen (Tollit, 2013, Porskamp, 2013). It is not possible to determine if this is due to hardware or software as the C-POD is a closed system. The range test described in the text lacks sufficient detail to describe a generalized detection efficiency ratio, but for this particular case the icListen was able to detect the signal to the maximum tested range of 500 m, while the C-POD’s maximum detection range was 375 m.

It was reported that a C-POD could detect echolocations in 5 m water depths, in a calm estuary, at a distance of 933 +/- 75 m (Roberts, 2015). This was demonstrated with little consistency in the study, with the C-POD reliably demonstrated a detection range of 300 m. Detection ranges of T-PODs and C-PODs in similar benign environments have been reported as ~ 200 – 300 m (Kyhne et al. 2008, 2012).

Using a mean empirically derived porpoise click source level and a high-frequency transmission loss model, receive levels can be used to estimate source-receiver distance and thus a detection range. This method was used to conclude that the detection range of an icListen deployed in the Minas Passage FORCE site had a mean of ~275 m and a typical daily maximum of 500 m (Porskamp, 2013). Detection ranges of C-PODs at the EMEC site were reported to be < 150 m (Benjamins, 2017). Deployment of a C-POD in Admiralty Inlet showed detections of ‘landmark’ click trains (where the C-POD itself is the target of the echolocation) at a distance of 90 m (Polagye, 2012).

The theoretical maximum on-axis detection range for these vocalisations is proposed to be less than 500 m under the assumptions of a relatively modest maximum source level (Villadsgaard et al., 2007), spherical spreading, and a detection threshold of 120 dB re 1 µPa. This range is dictated by the high sea water absorption coefficient at 130 kHz, which varies as f^2 (i.e., at 13 kHz, the absorption is 2 orders of magnitude weaker!). However, in tidal channels attenuation due to bubble scattering and turbulent mixing may decrease detection ranges further, though more research is needed to quantify this effect.

Improving the understanding of high frequency sound transmission in tidal environments will allow better estimates of detection ranges of any passive acoustic sensor and provide clarity

to past date and future studies. For example, Tollit (2013) reported that the deeper the C-POD unit, the higher the number of porpoise detections in the Minas Passage, based on a data set of 7 SUB buoy mounted C-PODs. This may be due to the larger effective listening volume of the sensor deployed in deeper water, lower background noise level with increasing depth at 10's and 100's kHz (Moore, 2016), or by porpoise usage of the passage.

D. Localization

Only two three-dimensional (3D) localization studies have been carried out to date. A 3D distribution of seven hydrophones mounted to a turbine was used to detect and localize porpoises and dolphins (Malkina, 2018). The estimated the range of the system was between 20 - 200 m for sound sources with source level 178 – 205 dB re 1 μPa_{p-p} respectively, where an 8 dB signal excess (SE) level was assumed for the detector. It was further estimated that the probability of detection and localization was below 50% for ranges of greater than 20 m, and 10% at 50 m. A large aperture vertical array of eight hydrophones deployed from a drifting ship was combined with a small quad array to localize in 3D and gave a detection range of 200 m (Macaulay, 2017).

E. Performance summary and recommendations

Results from the few passive acoustic instrument comparison tests for the detection of marine animals in tidal channels provide a basis for some recommendations. Hydrophones with greater sensitivity have larger detection ranges, which lead to higher detection rates. Additionally, instruments that record the pressure time series which is then analyzed by a click detector (PAMGUARD, Coda) have much higher click-per-minute detection rates, and generally higher detection positive minutes per unit time, regardless of environment or deployment configuration. In some cases, the detection positive minutes time-base can confound comparison results between C-PODs and other devices. Direct comparison of detector performance is difficult to impossible, since the C-POD performance is the result of a coupled hardware (hydrophone sensitivity, electronic noise floor) and software (detector efficiency, false positive filter) system.

C-PODs are typically programmed to limit the number of detections per minute, causing 'lost time' when that limit is reached before a minute is through. In tidal channels, lost time can be above 90%.

Masking by flow noise and mooring noise decreases detection rates on bottom moored C-PODs, while masking by sediment generated noise and mooring noise decreases detection rates on bottom moored, SUB moored, and drifting C-PODs. The inability to distinguish between these masking sources confounds the performance comparison between drifting and bottom mounted sensors. In general, drifting C-PODs were found to have the least lost time, followed by bottom mounted C-PODs, with mooring deployed C-PODs performing the worst.

The C-POD-F may be able to reduce lost time – this claim is made by promotional material (C-POD & C-POD-F.ppt retrieved from the Chelonia website) but is not clearly explained. C-POD-F will be able to record wave forms (or pressure time series) at sampling rates up to 1 MHz, when detections are made. This will help solve the uncertainty behind masking noise processes.

The detection range of a C-POD or a hydrophone system at relevant frequencies in a tidal channel has not been directly measured. Measurements in benign environments showed that both

the icListen (at 69 kHz) and the DMON (using porpoise clicks) outperformed the C-POD. A typical value for a hydrophone detection ranges of porpoise clicks in a tidal channel is between 100 and 300 m. 3D localizing arrays were only able to operate successfully out to 90 m for a 7-element volumetric array, and 200 m for an 8-element linear array.

Considering these findings, the recommended approach for passive monitoring of porpoise in a tidal channel is to use a bottom mounted or drifting compact hydrophone with an acoustic bandwidth of at least 150 kHz, such as the icListen HF or SoundTrap 300, to collect pressure time series. PAMGUARD has been shown to perform well as a detector and classifier. The acoustic bandwidths of the DASAR and EAR are too small to be effective. As shown in Section III, there are many other hydrophone and data acquisition systems that are capable of making these measurements, but we have so far limited the discussion to instruments that have been demonstrated in these environments. Potentially suitable commercially available systems for animal detection in tidal environments are the Reson TC4014-5, Magrec HPO3 hydrophones, though those would need to be connected to a data acquisition system. Suitable complete systems include the AMAR G4 (JASCO), the ORCA Acoustic Recorder (Seiche), and the TR-ORCA or TR-Porpoise (Turbulent Research). Some of these systems, as well as the SoundTrap and icListen, allow multiple sensors to be configured into arrays, demonstrably useful for studies where localization is needed.

The choice between drifting and bottom mounted deployments depends on available survey effort, and observational objectives. For the detection of high frequency echolocation clicks, flow noise should be minimized by all means available, though the icListen and SoundTrap have demonstrated their ability to detect clicks without flow noise mitigation from bottom mounted platforms. For the detection of animals that vocalize at lower frequency, flow noise reduction strategies must be developed.

V. Conclusions

Overall, a wide assortment of hydrophone and data acquisition systems were used in the studies listed in Table 1. A small number of systems have demonstrated detections of animals (harbour porpoise, dolphins, beluga) in tidal channels. By surveying the ensemble of studies that describe the performance of these systems in tidal channels and in other ocean environments where comparison studies have been made, some conclusions are reached. The ideal system has the highest sensitivity, best mitigation of flow noise, and records the entire pressure time series. Practically speaking, these systems can be bottom deployed for long term monitoring without flow noise reduction, and they will be able to detect animals at ranges of 150 – 300 m in tidal channels. Compact hydrophone and data acquisition systems that record the pressure time series outperform C-PODs and provide higher data analysis capability. The C-POD-F may reduce the technological gap between these two classes of instruments, but this has not yet been demonstrated.

Additionally, it was found that the deployment configuration is the most important factor to consider when pairing passive acoustic technology with monitoring objectives. Drifting buoy suspended systems with appropriate vibration isolation and an underwater drogue provide the least contaminated measurement, while requiring a large field effort. Fixed systems provide continuous monitoring, but methods in flow noise suppression, both mechanical and signal processing, must be advanced. It is suggested that the towed array literature be consulted to improve flow shield and static system design. The current best performing static system appears to be the bottom

mounted, shielded hydrophones, though they are susceptible to noise generated by mobile sediments colliding with the instrument body. Autonomous vehicles may also propose a solution for long-term high-fidelity monitoring programs, though considerable technological development is needed.

References:

- Adams, M. J. (2018). *Application of a multi-hydrophone drifter and porpoise detection software for monitoring Atlantic harbour porpoise (Phocoena phocoena) activity in and near Minas Passage*. Honours Thesis, Acadia University
- Auvinen, M.A., Barclay, D.R. (2019) *Performance of a passive acoustic linear array in a tidal channel*, IEEE-JOE, in revisions
- Barclay, D. R., & Buckingham, M. J. (2013). *Depth dependence of wind-driven, broadband ambient noise in the Philippine Sea*. The Journal of the Acoustical Society of America, 133(1), 62-71.
- Barclay, D.R., (2019) *Ambient Noise in the Ocean*, Dalhousie University Department of Physics seminar series.
- Bassett, C., (2013) *Ambient noise in an urbanized tidal channel*, Ph.D. dissertation, University of Washington, [http://depts.washington.edu/pmec/docs/Bassett \(2013\) - Ambient Noise in an Urbanized Tidal Channel.pdf](http://depts.washington.edu/pmec/docs/Bassett%20(2013)%20-%20Ambient%20Noise%20in%20an%20Urbanized%20Tidal%20Channel.pdf)
- Bassett, C., Thomson, J., & Polagye, B. (2010). *Characteristics of underwater ambient noise at a proposed tidal energy site in Puget Sound*. In OCEANS 2010 MTS/IEEE SEATTLE (pp. 1-8). IEEE.
- Bassett, C., Thomson, J., Polagye, B. (2013). *Sediment-generated noise and bed stress in a tidal channel*. Journal of Geophysical Research: Oceans, 118(4), 2249-2265.
- Bassett, C., Thomson, J., Dahl, P. H., Polagye, B., (2014) *Flow-noise and turbulence in two tidal channels*, The Journal of the Acoustical Society of America, vol. 135, no. 4, pp. 1764–1774.
- Beharie, R., Side, J., (2011) *Sub-Sea Acoustic Monitoring - North-West mooring leg installation for the Scotrenewables SR250*, Report commissioned by Scotrenewables from International Centre for Island Technology, Report No. 2011/04/SR, 2011.
- Benjamins, S., Dale, A., van Geel, N., & Wilson, B. (2016). *Riding the tide: use of a moving tidal-stream habitat by harbour porpoises*. Marine Ecology Progress Series, 549, 275-288.
- Benjamins, S., van Geel, N., Hastie, G., Elliott, J., & Wilson, B. (2017). *Harbour porpoise distribution can vary at small spatiotemporal scales in energetic habitats*. Deep Sea Research Part II: Topical Studies in Oceanography, 141, 191-202.
- Bevelhimer, M. S., Deng, Z. D., & Scherelis, C. (2016). *Characterizing large river sounds: Providing context for understanding the environmental effects of noise produced by hydrokinetic turbines*, The Journal of the Acoustical Society of America, 139(1), 85-92.
- Broudic, M., Croft, N., Willis, M., Masters, I., & Sei-Him, C. (2012). *Comparison of underwater background noise during Spring and Neap tide in a high tidal current site:*

Ramsey Sound. In Proceedings of Meetings on Acoustics ECUA2012 (Vol. 17, No. 1, p. 070104). ASA.

Broudic, M., Croft, T. N., Willis, M. R., Masters, I., & Cheong, S. H. (2012). *Long Term Monitoring of Underwater Noise at a Proposed Deployment Site of a Tidal Stream Device*, In Proceedings of the 4th International Conference on Ocean Energy.

Copping, A., Hanna, L., Whiting, J., Geerlofs M., Grear, M., Blake, K., Coffey, A., Massaua, M., Brown-Saracino J., Battey, H. (2013) *Environmental Effects of Marine Energy Development around the World for the OES Annex IV*, (Online), Available: www.ocean-energy-systems.org.

Cobscook Bay Tidal Energy Project (2012) *Cobscook Bay Tidal Energy Project*; http://mhk.pnnl.gov/wiki/index.php/Cobscook_Bay_Tidal_Energy_Project

Corcos, G. M. (1964). *The structure of the turbulent pressure field in boundary-layer flows*, Journal of Fluid Mechanics, 18(3), 353-378.

EMEC (2013) *Shapinsay Sound Tidal Test Site: Acoustic Characterisation*, Harland, E. J. EMEC Report ref. CBA044/12 Issue 4, January 2013.

Finger, R. A., Abbagnaro, L. A., & Bauer, B. B. (1979). *Measurements of low-velocity flow noise on pressure and pressure gradient hydrophones*. The Journal of the Acoustical Society of America, 65(6), 1407-1412.

Fogarty, L. C. (2012). *Listening in the fast lane: Detecting harbour porpoise activity in the Minas Passage*. Honours Thesis, Acadia University

Giry, C., Bald, J., Uriarte, A., (2018), *Underwater sound on wave & tidal test sites: improving knowledge of acoustic impact of Marine Energy Convertors*, Proceedings of the International Conference on Ocean Energy, Cherbourg, France

Guerra-Paris, M. (2019), personal communication

Halvorsen, M., Carlson, T., Copping, A., (2011) *Effects of tidal turbine noise on fish*, PNNL Report-20787 for US Dept of Energy, WA, DC: by Pacific Northwest National Laboratory, Sequim, WA, pp. 1–41.

Jacobson, E. K., Merkens, K. P., Forney, K. A., & Barlow, J. (2017). *Comparison of harbor porpoise (Phocoena phocoena) echolocation clicks recorded simultaneously on two passive acoustic monitoring instruments*. NOAA Technical memorandum.

Knight, A. (1996). *Flow noise calculations for extended hydrophones in fluid-and solid-filled towed arrays*. The Journal of the Acoustical Society of America, 100(1), 245-251.

Knudsen, V. O., Alford, R., Emlin, J. (1948) *Underwater ambient noise*, J. Mar. Res., vol. 7, pp. 410–429.

- Ko, S. H. (1993). *Performance of various shapes of hydrophones in the reduction of turbulent flow noise*. The Journal of the Acoustical Society of America, 93(3), 1293-1299.
- Ko, S. H., & Schloemer, H. H. (1992). *Flow noise reduction techniques for a planar array of hydrophones*. The Journal of the Acoustical Society of America, 92(6), 3409-3424
- Kyhn, L., Tougaard, J., Teilmann, J., Wahlberg, M., Jørgensen, P. B., and Bech, N. I. (2008). *Harbour porpoise (Phocoena phocoena) static acoustic monitoring: laboratory detection thresholds of T-PODs are reflected in field sensitivity*, Journal of the Marine Biological Association of the United Kingdom, 88(06), 1085 - 1091.
- Kyhn, L., Tougaard, J., Thomas, L., Duve, L.R., Stenback, J., Amundin, M., Desportes G., (2012). *From echolocation clicks to animal density—Acoustic sampling of harbor porpoises with static dataloggers*, J. Acoust. Soc. Am., 131(1), 550-560.
- Lepper, P. A., Robinson, S. P. (2016). *Measurement of Underwater Operational Noise Emitted by Wave and Tidal Stream Energy Devices*. In The Effects of Noise on Aquatic Life II (pp. 615-622). Springer, New York, NY.
- Lloyd, S., Lepper, P., Pomeroy, S. (2017). *Evaluation of UAVs as an underwater acoustics sensor deployment platform*. International journal of remote sensing, 38(8-10), 2808-2817.
- Lombardi, A., (2016). *Soundscape characterization in Grand Passage, Nova Scotia, a planned in-stream tidal energy site*”, M.Sc. Thesis, Dalhousie University.
- Lombardi, A. R., Hay, A. E., Barclay, D. R. (2016). *Soundscape characterization in a dynamic acoustic environment: Grand Passage, Nova Scotia, a planned in-stream tidal energy site*. In Proceedings of Meetings on Acoustics 4ENAL (Vol. 27, No. 1, p. 005001). ASA.
- Luczkovich, J. J., Mann, D. A., Rountree, R. A. (2008). *Passive acoustics as a tool in fisheries science*. Transactions of the American Fisheries Society, 137(2), 533-541.
- Macaulay, J., Gordon, J., Gillespie, D., Malinka, C., Northridge, S. (2017). *Passive acoustic methods for fine-scale tracking of harbour porpoises in tidal rapids*. The Journal of the Acoustical Society of America, 141(2), 1120-1132.
- Malinka, C., Hay, A., Cheel, R. (2015). *Toward acoustic monitoring of marine mammals at a tidal turbine site: Grand Passage, NS, Canada*. Proc. of EWTEC, 1-10.
- Malinka, C. E., Gillespie, D. M., Macaulay, J. D., Joy, R., Sparling, C. E. (2018). *First in situ passive acoustic monitoring for marine mammals during operation of a tidal turbine in Ramsey Sound, Wales*. Marine Ecology Progress Series, 590, 247-266.
- Martin, B., Vallarta, J. (2012). *Acoustic Monitoring in the Bay of Fundy*. JASCO Document 00393, Version 1.1. Technical Report for FORCE.

Martin, B., Whitt, C., and Horwich, L. (2018). *Acoustic Data Analysis of the OpenHydro Open-Centre Turbine at FORCE: Final Report*. Document 01588, Version 3.0b. Technical report by JASCO Applied Sciences for Cape Sharp Tidal and FORCE

Moore, D., Barclay, D. R. (2016). *Modelling the performance of fish tag monitoring stations on the Scotian Shelf*. The Journal of the Acoustical Society of America, 139(4), 2172-2172.

Ocean Energy Systems (2013), *2013 Annual Report*, from: <https://www.ocean-energy-systems.org/publications/oes-annual-reports/>

Pine, M. K., Jeffs, A. G., Radford, C.A., (2012) *Turbine sound may influence the metamorphosis behaviour of estuarine crab megalopae*, PLoS One, vol. 7, no. 12, p. e51790.

Polagye, B., Bassett, C., Wood, J., Barr, S. *Detection of tidal turbine noise: A preinstallation case study for Admiralty Inlet*. Puget Sound, Washington (USA). Unpublished

Polagye, B., Thomson, J., Bassett, C., Graber, J., Cavagnaro, R., Talbert, J., Reay-Ellers, A., Tollit, D., Wood, J., Copping, A., (2012) *Study of the acoustic effects of hydrokinetic tidal turbines in Admiralty Inlet, Puget Sound*, U. S. Department of Energy, Tech. Rep.

Polagye, B., A. Copping, R. Suryan, S. Kramer, J. Brown-Saracino, and C. Smith. (2014) *Instrumentation for Monitoring Around Marine Renewable Energy Converters: Workshop Final Report*. PNNL-23110 Pacific Northwest National Laboratory, Seattle, Washington.

Polagye, B. (2015). *Acoustic characterization of a hydrokinetic turbine*, Oregon State University Scholar's Archive.

Porskamp, P. (2013). *Passive acoustic detection of harbour porpoises (Phocoena phocoena) in the Minas Passage, Nova Scotia, Canada*. Honours thesis, Acadia University, Wolfville, NS.

Porskamp, P., Broome, J., Sanderson, B., Redden, A. (2015). *Assessing the performance of passive acoustic monitoring technologies for porpoise detection in a high flow tidal energy test site*. Canadian Acoustics, 43(3).

Raghukumar, K., Spada, F., Chang, G., Jones, C. (2018). *Initial field trials of the NoiseSpotter: an acoustic monitoring and localization system*. Presented at the Marine Energy Technology Symposium, Washington, D.C. 30 April - 2 May.

Raghukumar, K., Chang, G., Spada, F. W., Jones, C. A. (2019). *Performance characteristics of a vector sensor array in an energetic tidal channel*. Offshore Technology Conference. doi:10.4043/29425-MS

Roberts, B. L., Read, A. J. (2015). *Field assessment of C-POD performance in detecting echolocation click trains of bottlenose dolphins (Tursiops truncatus)*. Marine Mammal Science, 31(1), 169-190.

Robinson S.P., Lepper P.A. (2013) *Scoping study: review of current knowledge of underwater noise emissions from wave and tidal stream energy device*. The Crown Estate, London

Sarnocinska, J., Tougaard, J., Johnson, M., Madsen, P. T., Wahlberg, M. (2016). *Comparing the performance of C-PODs and SoundTrap/PAMGUARD in detecting the acoustic activity of harbor porpoises (Phocoena phocoena)*. In Proceedings of Meetings on Acoustics 4ENAL (Vol. 27, No. 1, p. 070013). ASA.

Schmitt, P., Elsaesser, B., Coffin, M., Hood, J., Starzmann, R. (2015). *Field testing a full-scale tidal turbine part 3: Acoustic characteristics*. In European Wave and Tidal Energy Conference 2015.

Snohomish PUD, (2012) *Admiralty Inlet Pilot Tidal Project*, FERC project no. 12690, Tech. rep., Public Utility District No. 1 of Snohomish County.

Sousa-Lima, R. S., Norris, T., Oswald, J., Fernandes, D. (2013). *A Review and Inventory of Fixed Autonomous Recorders for Passive Acoustic Monitoring of Marine Mammals*. Aquatic Mammals 39(1):23–53. DOI: 10.1578/AM.39.1.2013.

Thomson, J., Polagye, B., Durgesh, V., Richmond, M. (2012). *Measurements of turbulence at two tidal energy sites in Puget Sound, WA (USA)*, IEEE J. Ocean. Eng., 37(3), 363–374, doi:10.1109/JOE.2012.2191656

Tollit, D., Redden, A. (2013). *Passive acoustic monitoring of cetacean activity patterns and movements in Minas passage: pre-turbine baseline conditions*. Acadia Centre for Estuarine Research (ACER), Acadia University, Offshore Energy Research Association of Nova Scotia (OERA), and SMRU Consulting.

Van Dyke, M., (1982) *An album of fluid motion*. Parabolic Press Stanford, 1982, vol. 176.

Villadsgaard, A., Wahlberg, M., Tougaard, J. (2007). *Echolocation signals of wild harbour porpoises, Phocoena phocoena*. J. Exp. Biol. 210(1), 56–64.

Wang, D., Atlar, M., Sampson, R., (2007) *An experimental investigation on cavitation, noise, and slipstream characteristics of ocean stream turbines*, Proceedings of the Institution of Mechanical Engineers, Part A: Journal of Power and Energy, vol. 221, no. 2, pp. 219–231.

Willis, M.R., Broudic, M., Haywood, C., Masters, I., Thomas, S. (2012), *Measuring Underwater Background Noise in High Tidal Flow Environments*, Journal of Renewable Energy, doi:10.1016/j.renene.2012.01.020

Wilson, B., Benjamins, S., Elliott, J. (2013). *Using drifting passive echolocation loggers to study harbour porpoises in tidal-stream habitats*. Endangered Species Research, 22(2), 125–143.

Wilson, B., Lepper, P. A., Carter, C., Robinson, S. P. (2014). *Rethinking underwater sound-recording methods to work at tidal-stream and wave-energy sites*. In Marine Renewable Energy Technology and Environmental Interactions (pp. 111-126). Springer, Dordrecht.

Wilson, C., Maxner, E., Martin, B., Lawrence, C. (2019) *Data Quality Assurance Report: 2018 OERA Grand Passage*. Document 01750, Version 1.0. Technical report by JASCO Applied Sciences for Offshore Energy Research Association of NS.

Worthington, M. (2014). *Acoustic Monitoring of Beluga Whale Interactions with Cook Inlet Tidal Energy Project* (No. Final Scientific Report). ORPC Alaska, LLC, Anchorage, AK.

Xu, J., Deng, Z. D., Martinez, J. J., Carlson, T. J., Myers, J. R., Weiland, M. A. (2012). *Broadband acoustic environment at a tidal energy site in Puget sound*. Marine Technology Society Journal, 46(2), 65-73.

Appendix VI

Imaging sonar review for marine environmental monitoring around tidal turbines

Imaging sonar review for marine environmental monitoring around tidal turbines

Report for OERA/FORCE, Pathway 2020

June 14, 2019

James Joslin, PhD
Applied Physics Laboratory
University of Washington
1013 NE 40th Street, Seattle, WA 98105
e-mail: jbjoslin@uw.edu

I. Introduction

Environmental monitoring of tidal turbines can provide valuable information on interactions between devices and marine animals that is necessary for the sustainable development of this resource. Information from early turbine deployments can help inform environmental impact assessments and mitigate risks for larger future deployments. Collecting and interpreting useful information from these high energy environments however poses many challenges to underwater instrumentation and data processing. Of the efforts to perform this type of monitoring over the last decade there have been a higher number of instrumentation or data collection failures than projects that succeeded in their monitoring goals. For future monitoring projects at these sites to be successful, lessons must be taken from previous efforts and experience from successful projects is invaluable.

In anticipation of upcoming turbine deployments in the Minas Passage, Bay of Fundy, the Offshore Energy Research Association (OERA) and the Fundy Ocean Research Center for Energy (FORCE) have put together the 'Pathway Program' to establish a suite of integrated environmental monitoring sensors for monitoring bottom-deployed turbines and floating tidal energy platforms. The first phase of this program involves a comprehensive literature review for different instrument classes that may be incorporated in the final monitoring solution. This review of imaging (or multibeam) sonars is an attempt to summarize the capabilities of these instruments for monitoring tidal turbines and the lessons learned from previous efforts. By assembling this information during this Phase, the 'Pathway Program' will reduce the development timeline and increase the capabilities of the integrated instrumentation suite.

For environmental monitoring at tidal energy sites imaging sonars can offer high resolution imagery in turbid waters without the need for artificial illumination. There are currently more than a dozen commercially available imaging sonars that have been developed for use in high energy marine environments. Each of these instruments varies in functional range, resolution, field of view, and mechanical configuration. The most typical applications of these sonars is for underwater vehicle navigation and situational awareness. Due to the nature of most use cases, not all sonars have been designed for long term deployments without regular maintenance. Similarly, most use cases do not require the sonar control software to be integrated on a multi-instrument platform with other active acoustics. For these reasons, many of the commercially available sonars are not well suited for monitoring tidal turbines and the best options are those that have been demonstrated on previous projects.

Acoustic imagery from these sonars has many advantages over optical imagery although classification of targets is generally more difficult. Data processing techniques are currently under development to allow real-time target detection, tracking, and, ultimately, classification. However, every monitoring project varies in environmental conditions and instrument configuration, thus requiring tuning of target detection algorithms. The final classification step of targets generally requires information from a secondary sensor, such as optical camera, an echosounder, or an ADCP.

This report presents a summary of the literature review followed by an overview of the most relevant commercially available imaging sonars. Section IV provides a summary of six applications of imaging sonars for similar use cases. Sections V and VI discuss key considerations for the integration of the sonar into the instrument platform and lessons learned from previous deployments. Finally the

report concludes with the best-in-class recommendations and a list of the references used in the literature review.

II. Literature Review Summary

The use of imaging sonars for environmental monitoring in high current environments is documented in the literature by approximately 20 different relevant journal publications and project reports. These publications are spread across a range of applications that may be categorized by the deployment type, duration, target monitoring goals, and methods of data acquisition and processing. The three main categories for deployment methods are downward looking from a surface vessel, on a purpose built bottom lander, or integrated into the turbine structure. Depending on the deployment configuration, these monitoring projects typically last from less than one day up to several months. The monitoring goals for each project are often defined by regulatory requirements or project developer's interest in retiring perceived risks. To date, most monitoring projects have continuously acquired data throughout the deployment and used a combination of manual review and automated processing in post. Section IV of this report provides further details on 6 of the most relevant application of imaging sonars for tidal turbine monitoring along with the references for each case.

While the documentation of applications in the literature presents many of the best methods for using imaging sonars, many of the key considerations for successful integration and lessons learned from previous projects come from failures, which often remain undocumented. The most common of these challenges lie in the durability of the instruments for long term deployments and in the software for data collection and processing. All too many monitoring projects have either failed outright or been terminated early because of instrument failure and prohibitively high maintenance costs. In many cases, choosing the optimal instrument settings for data acquisition is not possible prior to deployment. Similarly, development of data processing software is not possible until the data is available. For these reasons, much of the data collected to date is either of low value or remains unprocessed. In an attempt to prevent such issues, this report presents key considerations and lessons learned from previous deployments that are both found in the literature and from the author's personal experience.

III. Imaging Sonars

For this review, 18 different commercially available imaging sonars from 10 developers are summarized in the technology assessment rubric. Specifications for each sonar may be found in the instrumentation manual and used to assess the instruments suitability for monitoring tidal turbines. Given that every monitoring project has distinct requirement, which may change over the course of the project, the best sonar for each application will also vary. In addition to the general specification, manufacturers typically list common applications of their instruments which indicate their primary target markets. More information on the applications of these sonars for turbine monitoring are found in publications from each project.

a. General Specifications for Turbine Monitoring

The specifications summarized in the technology assessment rubric were selected because they have the greatest impact on the monitoring capabilities of each imaging sonar. Table 1 provides a summary of these specifications for the 6 most relevant sonar producers. These specifications include the operating frequency, field of view or swath angles, functional range, I/O trigger option, and software

development kit (SDK) option. In general, the functional range of the sonar is determined by the operational frequency and the field of view and resolution are a function of the number of beams. The options for an input trigger or SDK are critical for instrument integration on a multi-instrument platform and for software customization. Finally, specific applications of each sonar are presented for reference.

Table 1 - Summary table of most relevant imaging sonars with general specifications

Sonar	Frequency	FOV	Range	Trigger	SDK?	Applications
Tritech Gemini	720 kHz	120 x 20 deg	<120 m	Yes	Yes	Vessel surveys, SeaGen, AMP
Teledyne BlueView	900/2250 kHz	130 x 20 deg	<100 / <10 m	Yes	Yes	AMP, vessel surveys
Kongsberg Mesotech	500 kHz	120 x 3, 7, 15, or 30 deg	<150 m	Yes	No	AMP, vessel surveys
Blueprint Subsea Oculus	375 or 750/1200 or 1200/2100 kHz	130 x 20 deg or 70 x 12 deg or 60 x 12 deg	<200 or <120 / <40 or <30 / <10 m	Yes	Yes	Vessel surveys
Imagenex Delta T	260 kHz	120 x 10 deg	<150 m	Yes	Yes	FLOWBEC
Sound Metrics Aris	1200/700 or 1800/1100 or 3000/1800 kHz	28 x 14 deg or 28 x 14 deg or 30 x 15 deg	<80 / <35 or <35 / <15 or <15 / <5 m	No	No	ORPC, Verdant RITE

IV. Previous Applications

While imaging sonars are a common tool for marine operations with many broad applications, there are relatively few applications that are relevant to tidal turbine monitoring. The following sections present summaries of 6 applications that are described in the literature and have the highest relevance to this program.

a. Vessel Surveys

Mounting imaging sonars on a pole over the side of a surface vessel is a common method for conducting bathymetry or marine life surveys (Melvin and Cochrane, 2015, Parsons et al., 2014 and 2017, ORPC Maine 2014, Grippo et al., 2017). Figure 1 shows the sonar configuration and vertical field of view and Figure 2 shows sample data for such a survey from Parsons et al. 2017. This study was performed with a Tritech Gemini sonar using the native software for data acquisition and processing. Similar surveys have also been conducted using the sonar in conjunction with a fisheries echosounder.

This combinations allows for fish classification with the echosounder and then tracking with the imaging sonar when targets can be co-registered between the two data streams. Advantages of this type of survey include the ability to cover a large area and the motion of the sonar can allow for 3D reconstruction. The primary draw backs of vessel surveys are the sort duration of operations and that the constantly changing field of view complicates background subtraction for automated data processing. The short duration of deployments does simplify sonar maintenance and allow for continuous data collection, eliminating the need for real-time target detection and tracking algorithms.

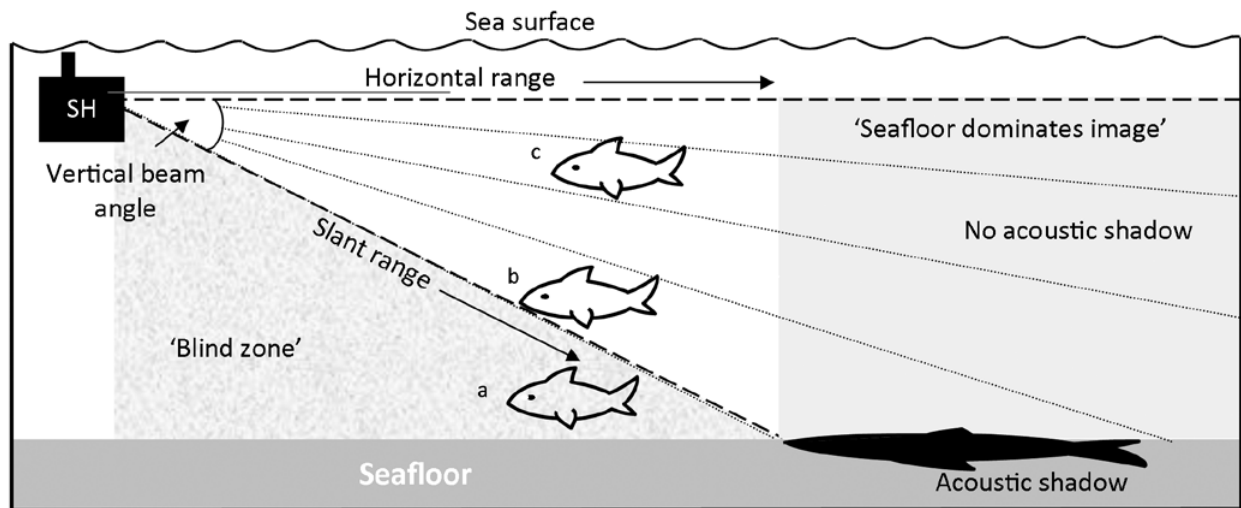
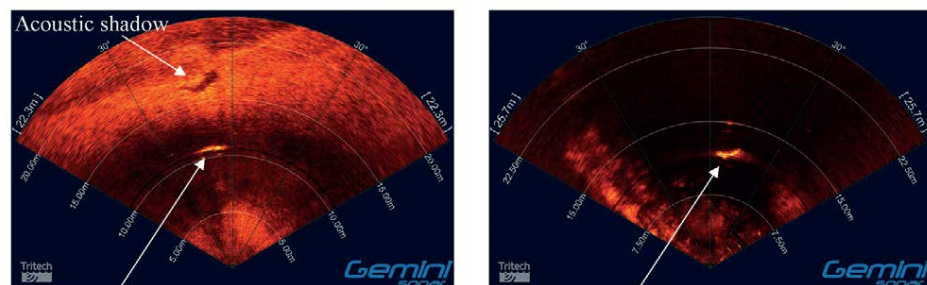


Figure 1 - Example of vessel based sonar configuration from Parsons et al. 2014



2.7 m Great White at 11m in 7.5 m of water 2.7 m Great White at 11 m in 15 m of water

Figure 2 - Example data from survey to track sharks in Australia from Parsons et al. 2014

b. FLOWBEC-4D Platform

The FLOW, Water column and Benthic Ecology-4D platform (FLOWBEC-4D) is used by researchers in the UK for monitoring at tidal and wave energy sites (Williamson et al., 2016 and 2017). This system, shown in Figure 3, integrates the Imaginex 837A Delta T imaging sonar with the EK60 multi-frequency echosounder, an ADV, and a fluorometer with a large battery bank for autonomous deployments. Figure 4 shows an example of a processed data sequence with the imaging sonar and echosounder tracking biological targets on the approach of a tidal turbine. The battery bank is sized to allow for continuous data collection for 2 week deployments with rapid 1 day turnarounds to span the full neap tidal cycles. Deployment and recovery of this platform has been demonstrated to place the package within 50 m of

the tidal turbine structure. The deployments to date have allowed for target detection and tracking algorithm development to simplify post processing of the data collected.

The Imaginex 837A Delta T sonar was originally selected for this platform due to previous in-house experience with the sonar, relatively low instrument cost, and low power draw and data bandwidth. The previous in-house experience simplified the integration of the sonar into the platform and ensured synchronization with the EK60 echosounder. The low power and bandwidth requirements similarly made this sonar better suited to the autonomous battery powered platform. The mounting of the sonar on the platform provides a field of view that allows for target co-registration with the echosounder and tracking up to the turbine structure. The narrow angle of the swaths of both the sonar and echosounders, however, result in a narrow horizontal area of the turbine being monitored.



Figure 3 - FLOWBEC platform during deployment at EMEC from Williamson et al. 2017.

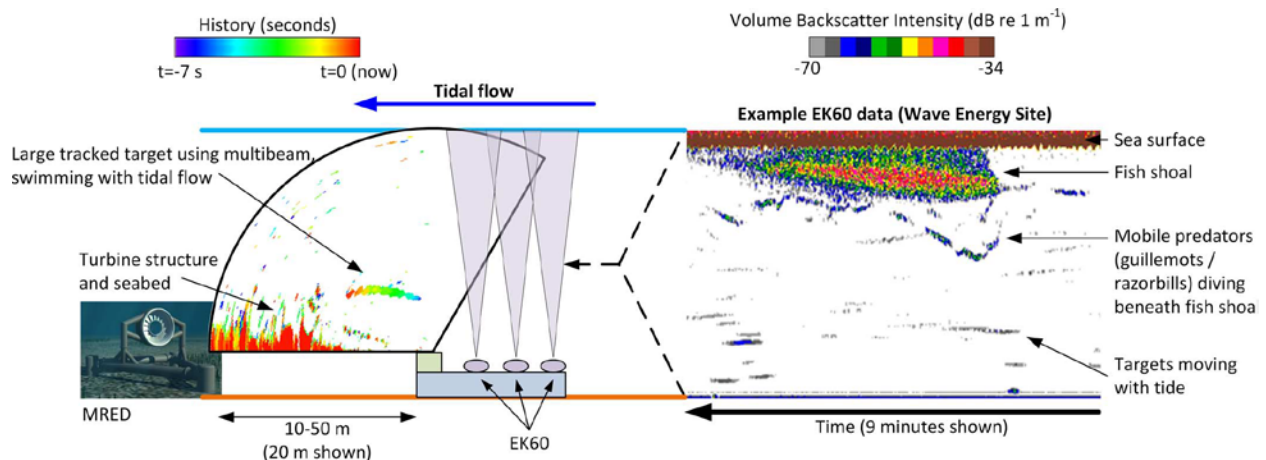


Figure 4 - Example data from FLOWBEC deployment from Williamson et al. 2017.

c. SeaGen, Strangford Lough

Harbor seal and porpoise monitoring for the SeaGen turbines in Strangford Lough is the longest duration environmental monitoring program with imaging sonars (G. Hastie, 2013). For this project, a Tritech Gemini sonar was integrated with the turbine structure as shown in Figures 5 and 6. Throughout the turbine operations, if harbor seals or porpoises were detected close to the turbines operations were shut down to avoid potential blade strikes although no such interactions were ever detected. This

monitoring project represented the first of its kind to use an imaging sonar and allowed Tritech to implement autonomous real time target detection and tracking algorithms in their software.

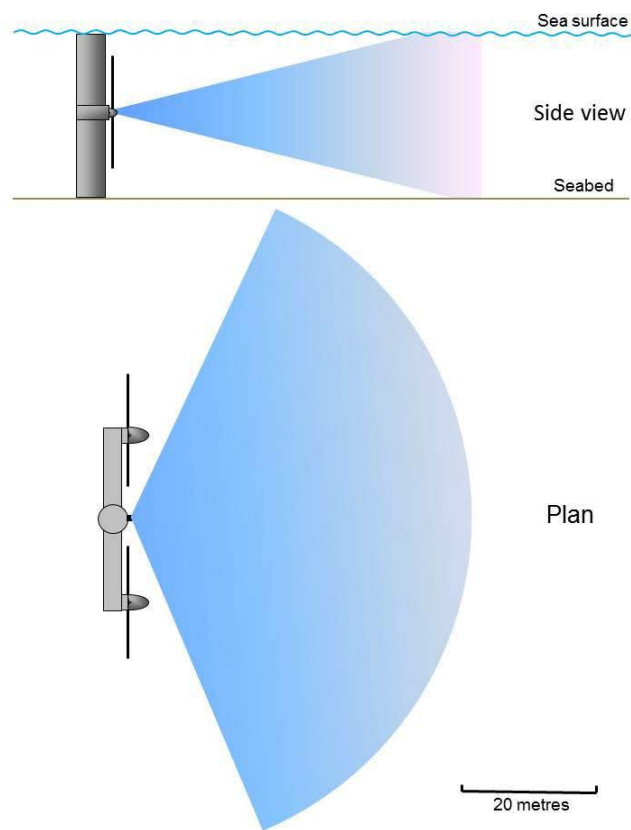


Figure 5 - Sonar configuration on SeaGen turbines from Hastie, 2013.

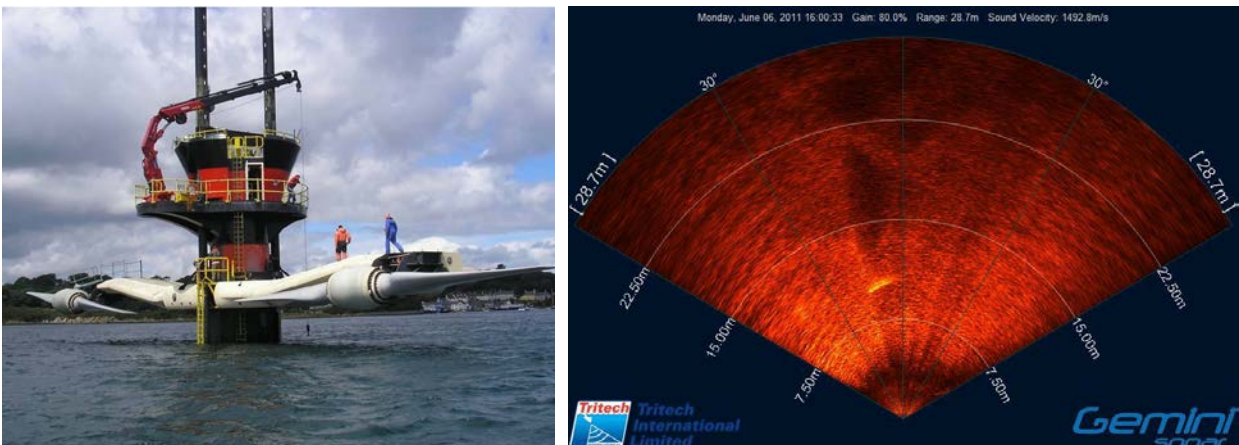


Figure 6 – SeaGen Turbines in Strangford Lough and example imagery of a seal at 10 m from Hastie, 2013.

d. ORPC, Cobscook Bay

Ocean Renewable Power Company (ORPC) has performed extensive monitoring for all of their turbine deployments to date. In 2012, two Sound Metrics DIDSON imaging sonars were used on their turbine test platform to monitor for fish passage through or around their turbine (Viehman et al., 2014).

Figure 7 shows the sonar configuration from the vessel-based test platform looking down and through the turbine in both fore and aft positions. Figure 8 shows an example of annotated data from the deployment with sample fish tracks. These DIDSON imaging sonars have the highest resolution of commercially available instruments which allows for individual fish tracking and classification. Conversely, these sonars have a narrow field of view and short range compared to most others. For this application data was collected continuously for 22 hours with manual post processing. Additional vessel based surveys for fish abundance using echosounders around ORPC turbines in Cobscook Bay are described in Grippo et al., 2017.

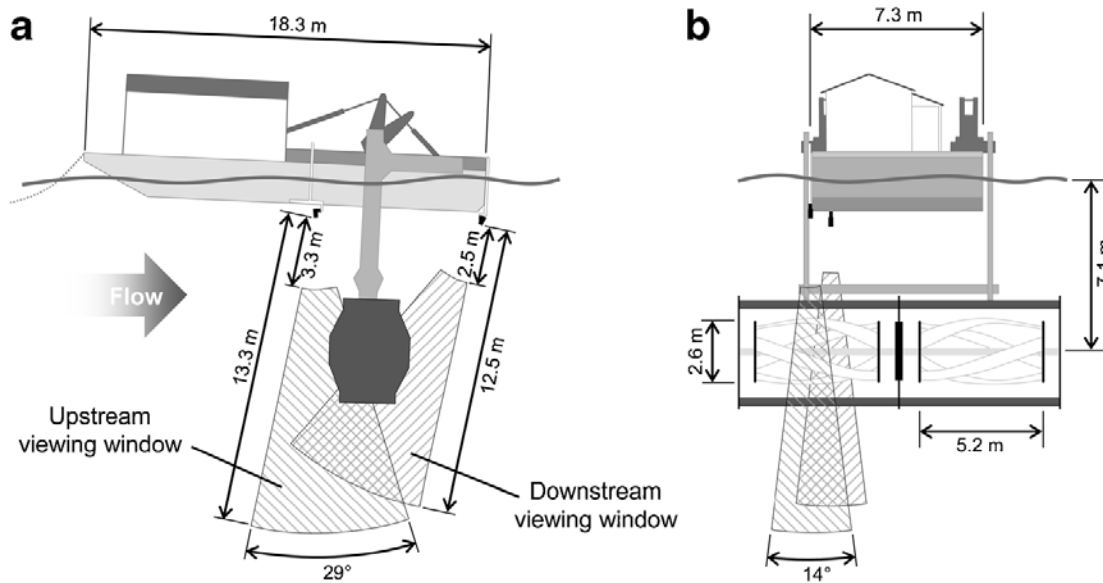


Figure 7 - Sonar configurations on ORPC turbine test platform from Viehman et al., 2014.

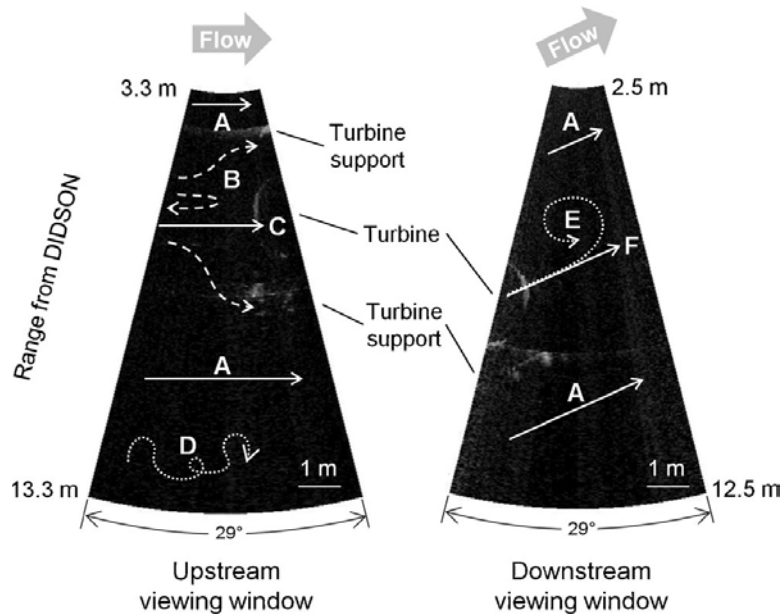


Figure 8 - Example of annotated data with fish passage from Viehman et al., 2014.

e. Verdant, RITE Project

The tidal turbine deployment for the Verdant RITE project incorporated a Sound Metrics DIDSON camera on a standalone bottom mounted platform approximately 12 m from the turbine base (Bevelhimer et al., 2016). For this application the sonar was mounted on a pan and tilt platform to allow the field of view to be aimed throughout the deployment as shown in Figure 9. The monitoring objective of the sonar was to observe fish behavior relative to the turbine and look for avoidance. Although the turbine itself failed after the first few days of the deployment, the sonar continued to collect data continuously for 19 days. The data processing effort was led by Oak Ridge National Laboratory and evaluated autonomous processing algorithms for fish detection and tracking.

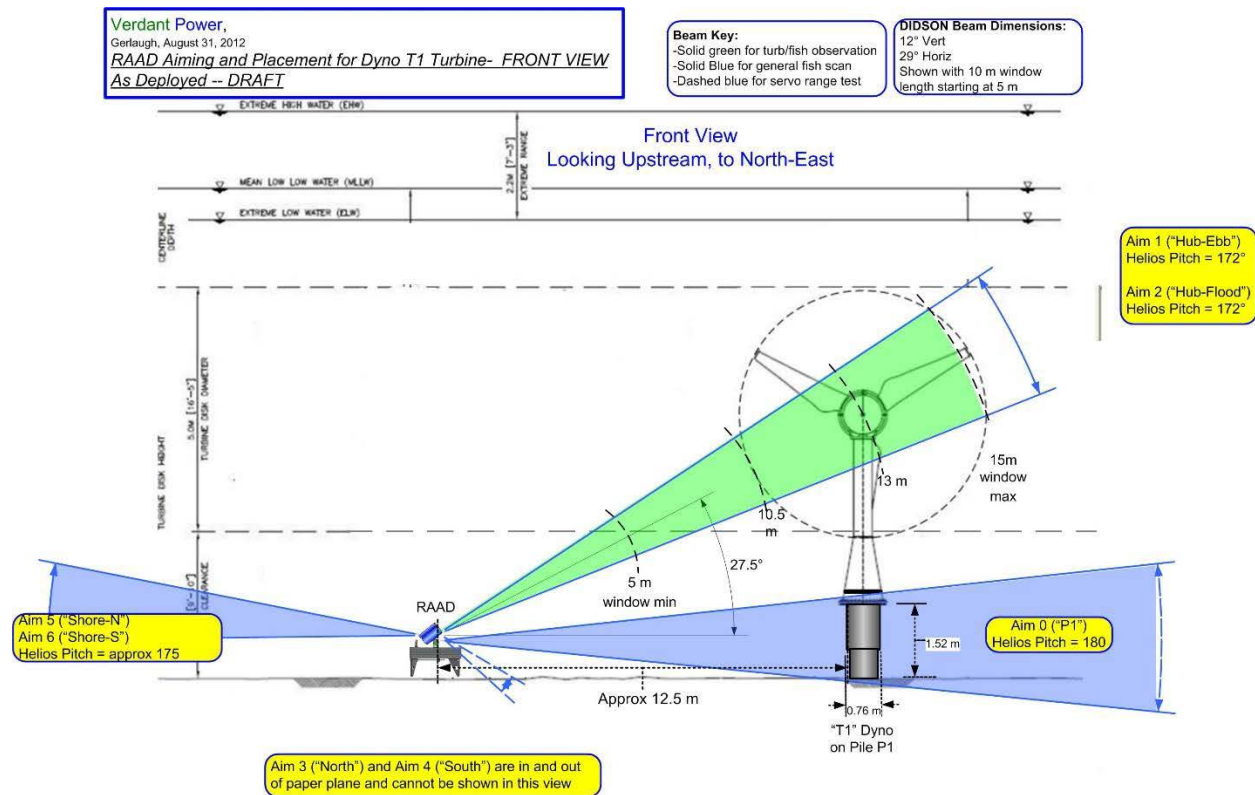


Figure 9 - Deployment configuration of sonar and turbine for Verdant RITE project from Bevelhimer et al., 2016.

f. AMP Platform

The Adaptable Monitoring Package (AMP) is an integrated instrumentation platform under development at the University of Washington since 2011 for environmental monitoring at tidal energy sites (Cotter et al., 2017). The most recent deployment of the AMP, shown in Figure 10, was at the Pacific Northwest National Labs Marine Science Laboratory in Sequim Bay, Washington from January to May 2019. This system integrates a Tritech Gemini sonar, a BlueView sonar, a WBTmini splitbeam echosounder, stereo optical cameras with strobe lights, and ADCP, four icListen hydrophones, a Vemco fishtag receiver, a water clarity sensor, antifouling wipers and UV lights, an inertial measurement sensor, and a tilt motor for the instrument head. This system integrates both the Gemini and BlueView sonars to take advantage of the long and short relative ranges of the two instruments. The objective of the deployment in Sequim bay was to evaluate the systems monitoring capabilities and improve real time target detection, tracking, and classification algorithms. Due to the high bandwidth of the sensors on the

AMP, imaging sonar data is processed in real time to detect targets of interest and trigger the optical camera lights and data archival. This real-time approach to initial data processing avoids data mortgages and simplifies any post processing steps required. Throughout this 135 day deployment the system was operational for 97% of the time and performed real time target detection, tracking, and triggering on schools of fish, seals, diving sea birds, and squid.

In addition to this Sequim Bay deployment, the AMP has been deployed in various configurations twice previously in Sequim Bay, off the coast of Newport, Oregon at the PacWave site, and in Kaneohe Bay, Hawaii at WETS for a total of over two years of in water testing. Due to the author's personal experience in the development of the AMP, many of the key considerations and lessons learned presented in Sections V and VI reference this system.



Figure 10 - 3G-AMP prior to deployment in Sequim Bay, WA, Jan 2019.

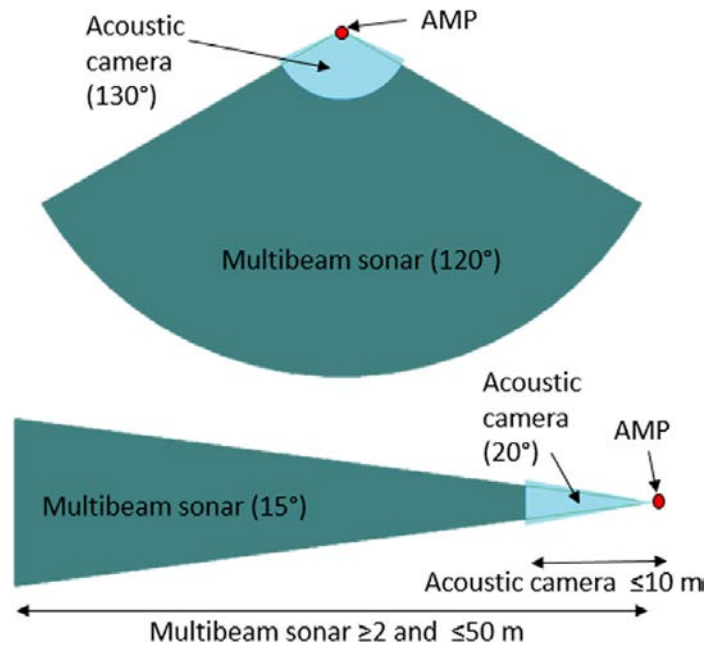


Figure 11 - Sonar configuration on the AMP from Cotter et al., 2017.

V. Key Considerations for Use of Imaging Sonars for Turbine Monitoring

The successful integration of imaging sonars for tidal turbine monitoring relies on an understanding of the sonar operations and of the environmental conditions at the deployment site. Given the exceptionally strong currents in Minas Passage, the best suited instruments will be the most durable with demonstrated performance in similar conditions. The following sections presents an overview of some of the key considerations for integrating the sonar in a multi-instrument platform for this site.

a. Mounting and Orientation

The ideal imaging sonar orientation depends heavily on the location and size of the turbine and the monitoring objectives. As evidence by the applications described in Section IV, the sonar swath may be oriented to look across the turbine, out in front of or behind the turbine, with a vertical or horizontal orientation, and either from a bottom or surface platform. Each configuration presents unique challenges and benefits that are difficult to predict prior to testing. If the monitoring objective is for individual fish passage, a high resolution sonar will need to be mounted in close proximity to the turbine. Alternatively, if the monitoring objective is to cover the full turbine area, a configuration such as shown in Figure 12 may be necessary.

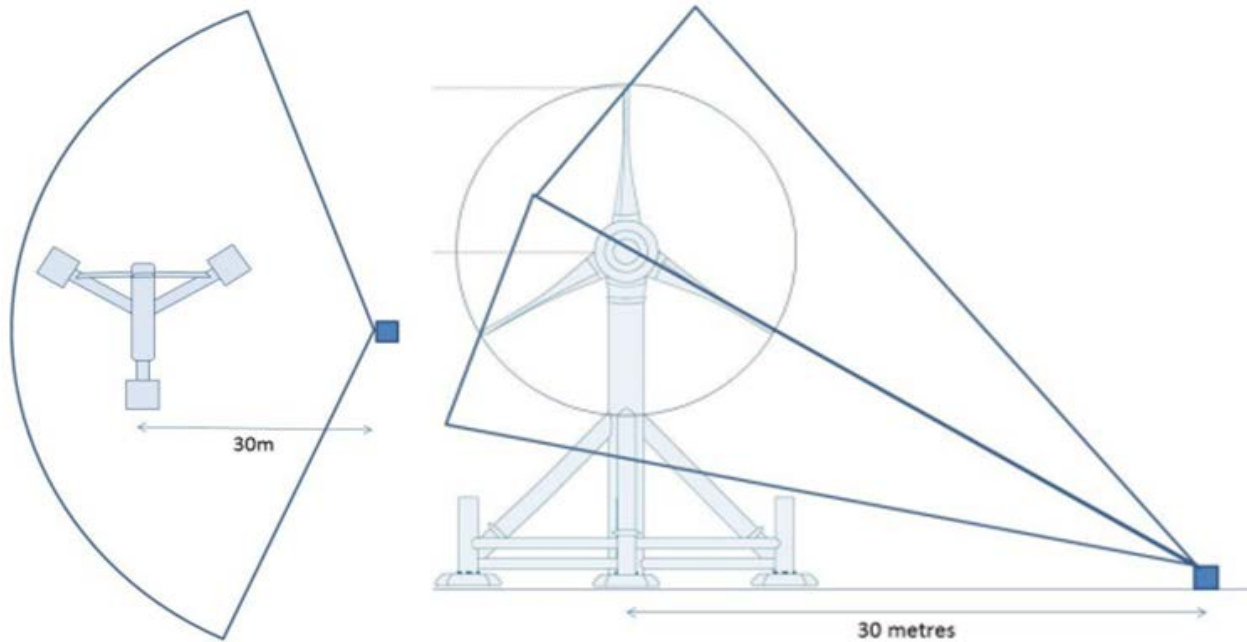


Figure 12 - Example of sonar orientation relative to turbines for Pentland Firth Meygen Project

b. Electrical and Communications Connections

The typical connections for imaging sonars provide the instrument power, use Ethernet communications protocols, and have optional I/O lines for triggering. On some sonars, the optional trigger input requires a second connector (Gemini and M3). In the case where two connectors are required, they may often be “wyed” into a single cable for connection to a control bottle using a 13 pin power and Ethernet connector. For proper operation, the power supply and Ethernet connections should be optically isolated in the control bottle with relay control to power cycle the instrument. Prior to deployment, IP addresses should be established for each instrument to ensure proper network control and data transfer.

c. Software for Instrument Control and Data Acquisition

All instrument developers have custom software for controlling their sonar and acquiring data. In order to integrate multiple instruments on a single platform and optimize for monitoring performance, customization is required that is typically beyond the native software capabilities. For this reason, sonars with manufacturer supported SDKs are more suitable to platform integration. For the AMP, instrument control and data acquisition software has been developed using National Instruments LabView for both the BlueView and Gemini imaging sonars.

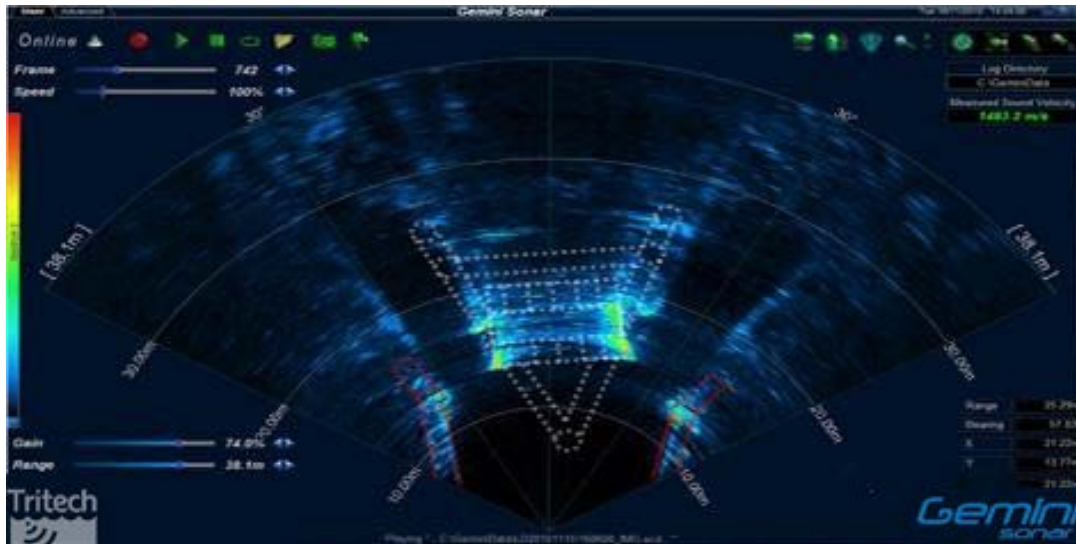


Figure 13 - Example screenshot from Tritech Seanet Pro software.

d. Software for Data Processing

The development of automatic data processing algorithms is an active area of research for most tidal turbine monitoring projects. The most recent publications on these methods have demonstrated the ability to detect and track targets with some ability to automatically classify between biologic and non-biologic classes. This classification level of processing typically relies on information from multiple instruments, such as shown in Figure 14, where the AMP targets from the imaging sonar could be classified by the optical imagery (Cotter et al., 2017). Implementation of data processing techniques should leverage previous efforts in this area to reduce processing and reporting timelines.

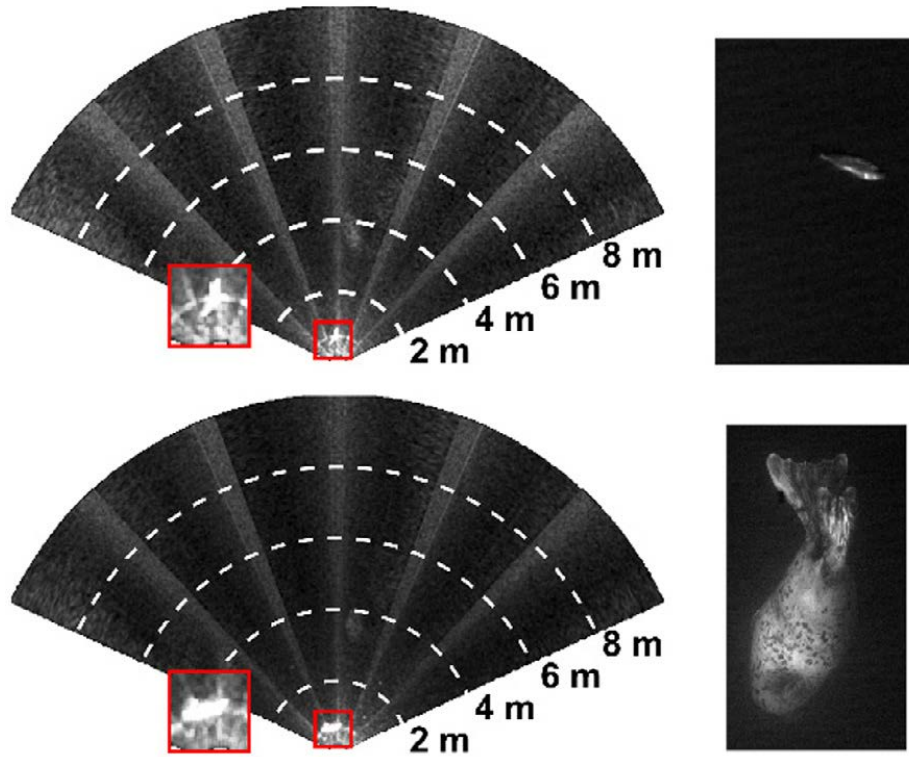


Figure 14 - Examples of AMP data of seal and fish detection and classification with optical cameras from Cotter et al., 2017.

VI. Lessons Learned from Previous Applications

The following sections present some of the primary lessons learned from previous imaging sonar deployments. These examples are included in this report to help guide this programs development of its multi-instrument monitoring platform.

e. Biofouling

Long term deployments of instrumentation in the marine environment are guaranteed to result in biofouling that will eventually inhibit data collection. While growth on sonar transducers does not inherently degrade the imagery, the growth can cause damage to sensitive components over time. Figure 15 shows examples of extreme biofouling from the most recent AMP deployment in Sequim Bay. In this case, the system was deployed in only 6 m of water for over 4 months through the most productive time of the year. The best solution to prevent biofouling is a regular maintenance interval that does not allow macro fouling to form. For the more sensitive components of instrumentation, such as optical view ports and transducers, biofouling wipers (ZibraTech Inc.) and UV lights (AML) are effective. Some transducer elements may also be coated with antifouling paint or high content zinc oxide paste. For less sensitive components of the platform, copper or vinyl tape may be used to coat surfaces to either inhibit growth or easily remove growth after recovery.



Figure 15 - Example of extreme biofouling from recent AMP deployment with UV lights on sonar transducers

f. Corrosion

Since the most typical applications of imaging sonars are for short term deployments, corrosion on the instrument or its connectors should be anticipated. Figure 8 shows examples of corrosion on an anodized aluminum housing and on the locking sleeves of a sonar's connectors from previous AMP deployments. Mitigation of this type of corrosion is best performed by the elimination of dissimilar metal contact and ground faults throughout the instrumentation package. If it is not possible to eliminate all dissimilar metal contact (for example, if you are delivered a sonar with a titanium housing and stainless steel connectors) a sacrificial anode should be added to prevent corrosion of sensitive components. For aluminum housings, a zinc anode may be used and for stainless steel housings, a mild steel anode may be better to limit the rate of the anode's corrosion.



Figure 16 - Examples of corrosion on anodized aluminum housing and connectors with dissimilar metals

g. Image Noise from Acoustic and Electrical Interference

Sonar integration on a multi-instrument platform can result in interference from other active acoustic sources and electrical noise. Figure 17 shows an example of electrical interference on a BlueView sonar in the form of thin radial lines that only appeared when the strobe lights for the optical cameras were triggered. This type of interference is typically due to DC power converters that operate at frequencies similar to the imaging sonars. Changes in power output provided by these converters can produce noise in the sonar imagery. To avoid this type of noise, the power supplied to the sonar should be isolated and filtered. To avoid cross talk between active acoustic instruments, synchronization of the instrument controls is necessary to interweave pings. This type of control typically requires the sonar to have an input trigger option that can be synchronized with a central controller.

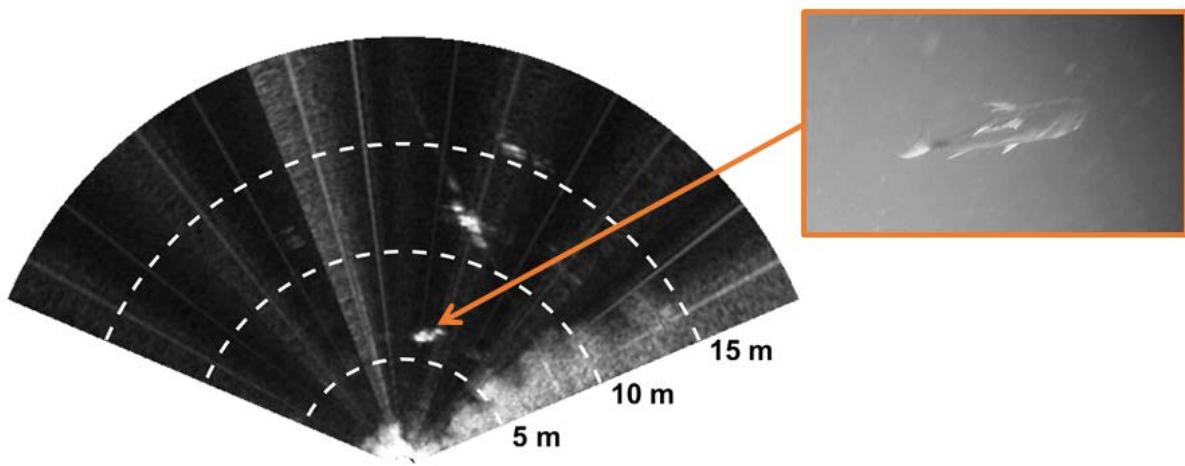


Figure 17 - Example data from BlueView deployment where thin radial lines appear when strobe lights fire

h. Image Noise from Environmental Conditions

High current sites often result in large turbulent vortices and bubble clouds or debris deep in the water column. These non-biological targets complicate environmental monitoring as they can mask actual targets of interest and impede automatic target detection algorithms. Similarly, moving targets in the sonar field of view (such as turbine blades or the water surface) or a sonar mounted to a moving platform, can result in large changing reflections in the sonar image. Figure 18 shows an example of multiple noise sources on a BlueView sonar mounted to a surface buoy. For these reasons, integration of the sonar on a bottom mounted platform that is within the waters depth to the side of the turbine will most likely result in the highest quality imagery (similar to the configuration in Figure 12).

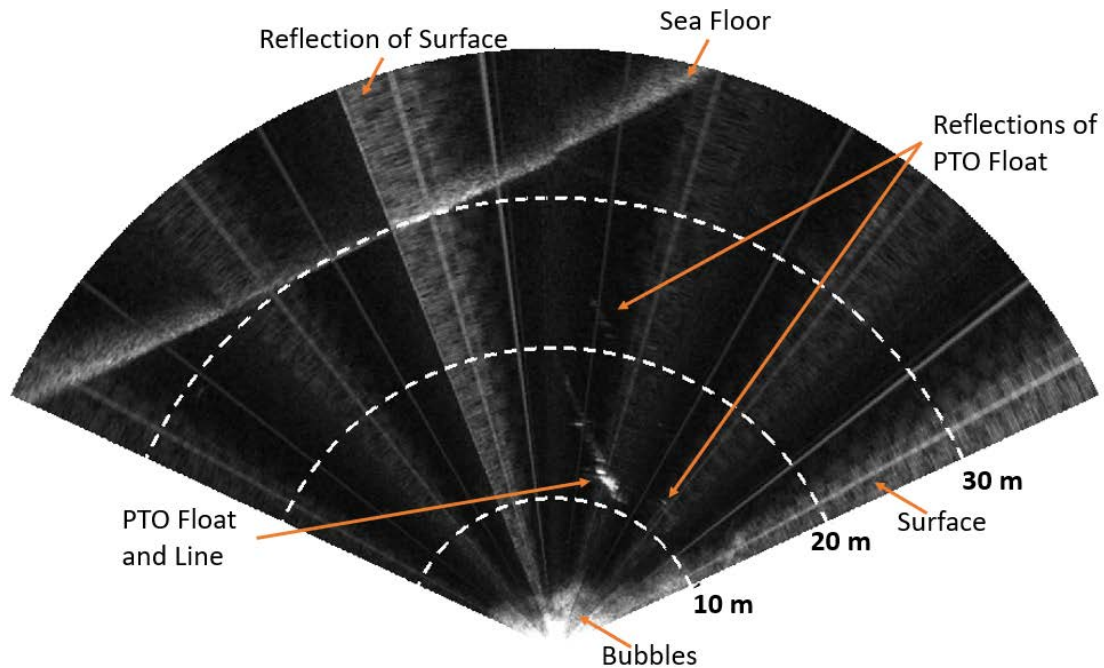


Figure 18 - Example data from BlueView deployment with multiple targets creating non-biologic triggers

i. Sonar Sound Levels

Another active area of research for turbine monitoring with imaging sonars is the marine animal response to the noise produced by the sonar. Although sonars operational frequencies are well above the hearing levels of marine animals, the sonars do typically produce some sound across all frequencies as shown in Figure 19. Due to this lower frequency sound, it is possible that marina animal behavior may be affected. While the sound levels are not typically high enough to be of concern, further research is needed in this area to fully classify behavioral changes that are detected by imaging sonars.

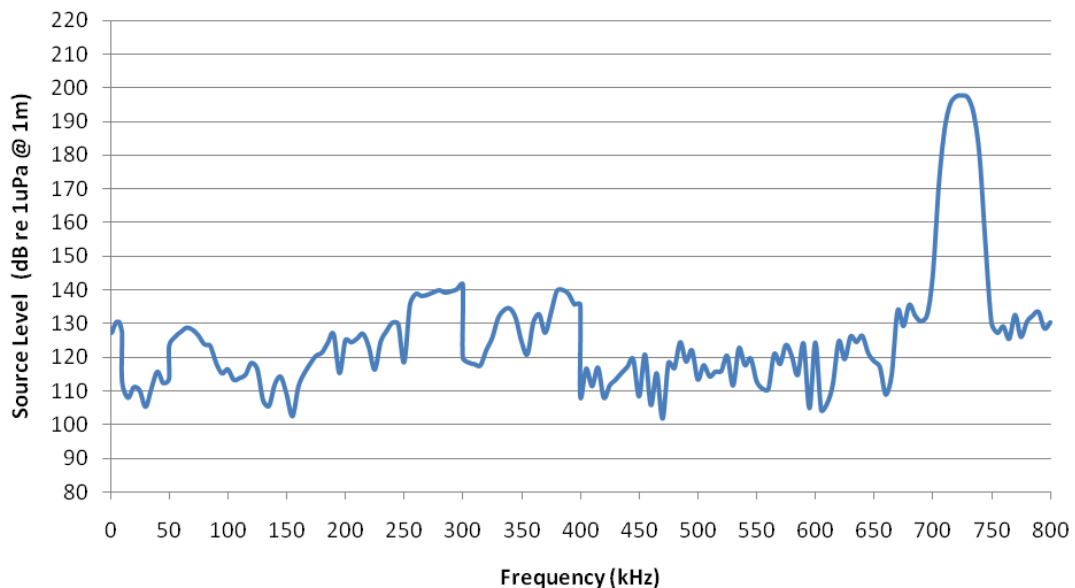


Figure 19 - Source level of Tritech Gemini from G. Hastie Report

VII. Summary and Recommendations

This literature review shows that imaging sonars can be an effective tool for environmental monitoring of tidal turbines but successful application requires careful consideration of the integration methods. Previous efforts have successfully used imaging sonars on both bottom and surface mounted platforms to monitor for fish, seals, porpoises, and diving sea birds. Target classification from imaging sonars is best achieved by pairing the sonar data stream with optical cameras or fisheries echosounders. Although custom software development may be required for instrument control, data acquisition, and data processing, these tools can greatly decrease manual review and processing delays. The following sections presents an overview of the best-in-class recommendation and the application methods.

j. Best-in-Class Sonar Recommendations

Commercially available imaging sonars that are best suited for tidal turbine monitoring in Minas Passage are the most robust and have had the most successful use cases. In addition, these sonars should offer both an optional input trigger line and SDK to be integrated on a multi-instrument platform with other active acoustics. For these reasons, the recommendation for the best-in-class imaging sonars is the Tritech Gemini 720is and the Teledyne BlueView M900/2250 as shown in Figure 20. These sonars have the broadest demonstrated use cases for tidal turbine monitoring with optional input triggers and SDKs. Depending on the range and resolution requirements of the monitoring objectives the benefits of each sonar will vary. The Gemini will be better suited for longer range application with lower resolution requirements while the BlueView will provide higher resolution at closer ranges. Although these sonars are recommended by this report, other monitoring objectives or prior in-house experience may dictate the preference for another instrument.



Figure 20 - Best-in-class imaging sonar recommendations, the Tritech Gemini 720is and the Teledyne BlueView M900/2250

k. Application Recommendations

While every tidal turbine monitoring application is different, there are some universal recommendations that should be considered for the development of this platform. The first of these recommendations is that the monitoring objectives for the platform should be clearly outlined prior to system development to ensure the required capabilities are achieved. Second, the software integration and data processing options may drive the instrument selection process. Without the software in place to perform the data processing, long delays in acquiring useful information from the platform should be expected. Third, the mounting and deployment orientation will have a large impact on the image quality. For this reason it is important to design flexibility into the overall system to allow for alternative

instrument configurations. Forth, proper consideration should be given for electrical isolation, corrosion resistance, and biofouling mitigation to ensure long term performance of the platform. Finally, pre-deployment testing in similar environments with easier maintenance options is essential to avoid costly failures during critical deployments.

VIII. References

- B. J. Williamson *et al.*, "A Self-Contained Subsea Platform for Acoustic Monitoring of the Environment Around Marine Renewable Energy Devices—Field Deployments at Wave and Tidal Energy Sites in Orkney, Scotland," in *IEEE Journal of Oceanic Engineering*, vol. 41, no. 1, pp. 67-81, Jan. 2016. doi: 10.1109/JOE.2015.2410851
- B. J. Williamson, S. Fraser, P. Blondel, P. S. Bell, J. J. Waggitt and B. E. Scott, "Multisensor Acoustic Tracking of Fish and Seabird Behavior Around Tidal Turbine Structures in Scotland," in *IEEE Journal of Oceanic Engineering*, vol. 42, no. 4, pp. 948-965, Oct. 2017. doi: 10.1109/JOE.2016.2637179
- Williamson, B.; Fraser, S.; Blondel, P.; Bell, P.; Waggitt, J.; Scott, B. (2016). Integrating a Multibeam and a Multifrequency Echosounder on the Flowbec Seabed Platform to Track Fish and Seabird Behavior around Tidal Turbine Structures. Paper Presented at the 4th Marine Energy Technology Symposium (METS), Washington DC, USA.
- Jha, S. (2016). Tidal Turbine Collision Detection: A review of the state-of-the-art sensors and imaging systems for detecting mammal collisions. Report by ORE Catapult. pp 50.
- Francisco, F.; Sundberg, J. (2019). Detection of Visual Signatures of Marine Mammals and Fish within Marine Renewable Energy Farms using Multibeam Imaging Sonar. *Journal of Marine Science and Engineering*, 7(1), 1-19.
- Verfuss, U.; Gillespie, D.; Gordon, J.; Marques, T.; Miller, B.; Plunkett, R.; Theriault, J.; Tollit, D.; Zitterbart, D.; Hubert, P.; Thomas, L. (2018). Comparing methods suitable for monitoring marine mammals in low visibility conditions during seismic surveys. *Marine Pollution Bulletin*, 126, 1-18.
- Giorli, G. (2017). Combining Passive Acoustics and Imaging Sonar Techniques to Study Sperm Whales' Foraging Strategies. *Journal of the Acoustical Society of America*, 142(3).
- Dual stacked Tritech Gemini vertical and horizontal swath (Sparling et al. 2016)
- Grippio, M.; Shen, H.; Zydlewski, G.; Rao, S.; Goodwin, A. (2017). Behavioral Responses of Fish to a Current-Based Hydrokinetic Turbine Under Multiple Operational Conditions: Final Report. Report by Argonne National Laboratory (ANL) and University of Maine. pp 49.
- Viehman, H. a., & Zydlewski, G. B. (2014). Fish Interactions with a commercial-scale tidal energy device in the natural environment. *Estuaries and Coasts*, 38(Suppl 1), S241–S252. <https://doi.org/10.1007/s12237-014-9767-8>
- Bevelhimer, M.; Colby, J.; Adonizio, M.; Tomichuk, C.; Scherelis, C. (2016). Informing a Tidal Turbine Strike Probability Model through Characterization of Fish Behavioral Response using Multibeam Sonar Output. Report by Oak Ridge National Laboratory (ORNL). pp 75.
- Melvin, G.; Cochrane, N. (2015). Multibeam Acoustic Detection of Fish and Water Column Targets at High-Flow Sites. *Estuaries and Coasts*, 38(1), 227-240.

- ORPC Maine (2014). Cobscook Bay Tidal Energy Project: 2013 Environmental Monitoring Report. Report by Ocean Renewable Power Company (ORPC). pp 502.
- Hastie, G. (2013). Tracking Marine Mammals Around Marine Renewable Energy Devices Using Active Sonar. Report by SMRU Consulting. pp 99.
- Parsons, Miles JG, et al. "Detection of sharks with the Gemini imaging sonar." *Acoustics Australia* 42.3 (2014): 185-190.
- Parsons, Miles JG, et al. "Imaging marine fauna with a Tritech Gemini 720i sonar." *Acoustics Australia* 45.1 (2017): 41-49.
- Lieber, Lilian & Williamson, Benjamin & Jones, Catherine & Noble, Leslie & Brierley, Andrew & Miller, Peter & Scott, Beth. (2014). INTRODUCING NOVEL USES OF MULTIBEAM SONAR TO STUDY BASKING SHARKS IN THE LIGHT OF MARINE RENEWABLE ENERGY EXTRACTION.
- E. Cotter and B. Polagye. Automatic Classification of Biological Targets in a Tidal Channel using a Multibeam Sonar. In prep.
- Cotter, E., Murphy, P., and Polagye, B. (2017) Benchmarking sensor fusion capabilities of an integrated instrumentation package, *International Journal of Marine Energy*, doi: 10.1016/j.ijome.2017.09.003.
- Cotter, E.; Murphy, P.; Bassett, C.; Williamson, B.; Polagye, B. (2019). Acoustic characterization of sensors used for marine environmental monitoring. *Marine Pollution Bulletin*, 144, 205-215.

Appendix VII

Final Report: Scientific echosounder review for instream tidal turbines

Final Report: Scientific Echosounder Review for In-Stream Tidal Turbines

Prepared for: Offshore Energy Research Association of Nova Scotia

Prepared by: John K Horne, University of Washington

Service agreement: 190606

Date submitted: August 2019

Objectives:

The overall goal of this exercise is to evaluate features and performance of current and future scientific echosounders that could be used for biological monitoring at in-stream tidal turbine sites. Specific objectives include:

1. Reviewing literature for desired characteristics of scientific echosounders used in marine renewable energy monitoring applications.
2. Communicating with scientific echosounder manufacturer representatives to confirm current and future performance features of scientific echosounders.
3. Evaluating and reporting findings.

Introduction and Overview

Environmental monitoring is a required component of Marine Renewable Energy (MRE) licensing and operations throughout the world. Biological monitoring at instream tidal sites is the most challenging of all MRE industry sectors due to challenges associated with sampling. Biological monitoring at MRE sites is constrained by hydrodynamics that limits traditional sampling (i.e. nets) due to high water flow velocities and remote sensing (i.e. active acoustics) that is constrained by entrained air and turbulence. As a result, little historical data are typically available to characterize biological constituents, and the choice, timing, and deployment of monitoring equipment requires additional planning compared to less dynamic environments.

The primary challenge when choosing any remote sensing instrument is maximizing the signal to noise data ratio. This generic statement has three relevant components when using active acoustics to monitor aquatic animals at instream tidal sites: near boundary interfaces, target resolution, and target detection (i.e. false targets). Returned or backscattered energy (i.e. echoes) from animals (e.g. fish, macrozooplankton) close to any interface (e.g. surface, bottom) may coincide with strong reflections from the interface. Integration of backscatter from the interface will lead to large overestimates of aquatic animal densities (MacLennan et al. 2004; Totland et al. 2009). To minimize bias due to interface inclusion a layer close to the interface is excluded from the integration (often called the acoustic deadzone). To compensate for the exclusion of targets within the acoustic deadzone, echo integrals are positively scaled by a correction factor to compensate for targets that were not included in the echo integrals (e.g. Ona and Mitson 1996; Lawson and Rose 1999; McQuinn et al. 2004).

The extent of the acoustic deadzone can be minimized by reducing the duration of the transmitted acoustic pulse. Reduction of the pulse duration also maximizes the resolution of detected targets. The extent of the deadzone is determined by the sound speed c multiplied by the pulse duration τ divided by 2 (i.e. $c\tau/2$). For a given c and τ , the backscattered energy from an interface will overlap that from any target less than a range of $c\tau/2$ from the interface. A short pulse duration also has the advantage of maximizing the resolution between any two targets. To resolve any two targets at slightly different ranges from a transducer (R_1 , R_2), the range

difference (i.e. $R_2 - R_1$) must exceed half the pulse duration to be resolve the two targets as single echoes.

The challenge of detecting focal from unwanted acoustic targets is exacerbated at MRE tidal turbine sites. Anything with a density different than water will reflect sound energy. These reflections will include energy from entrained air bubbles and water turbulence, two features commonly encountered around tidal turbine devices. Two strategies are available to minimize detections from unwanted targets: avoid resonance frequencies of entrained air bubbles, and maximize signal-to-noise ratios (SNR) of backscattered energy using wideband signals and matched filters. Backscattered energy from air bubbles at or near the resonant frequency can equal that backscattered by fish at the same frequency but in the geometric scattering region. The backscatter region of a target depends on the target dimensions L (and material properties) relative to the acoustic wavelength λ . If the L/λ ratio is close to 1, then the target falls within the resonance backscattering region. For a spherical target (e.g. air bubble) the backscattered energy increases approximately as the square of the sphere radius (Simmonds and MacLennan 2005). When the target is much larger than the wavelength (e.g. a turbulent or density front), the energy is reflected at the same angle of incidence. The acoustic resonance frequency of an air bubble can be found using the Minnaert (1933) equation where resonance is a function of the bubble radius a , the polytropic coefficient γ (i.e. expansion and contraction coefficient), ambient pressure p_A , and the density of water ρ .

$$f = \frac{1}{2\pi a} \left(\frac{3\gamma p_A}{\rho} \right)^{\frac{1}{2}}$$

This equation can also be used to estimate the resonant frequency of a bubble cloud with a as the bubble cloud radius and ρ the density difference between water and the bulk density of the bubble cloud (Greene and Wilson 2012). As an approximation under typical water conditions, this equation simplifies to $fa \approx 3.26 \text{ ms}^{-1}$, where f is the bubble resonant frequency. In practice knowing the distribution of bubble radii to then estimate bubble resonant frequency is rare. Bubble resonant frequencies typically range from hundreds of Hertz (Hz) to a few kilohertz (kHz). This contrasts to a range of scientific echosounder operating frequencies spanning 10's to 100's of kHz.

The ability to detect a target depends on the backscattered energy (i.e. echo) from the target being larger than the ambient noise level. Five different approaches can be used to maximize the probability of a received echo: increase source level; reduce range to targets; match transmit frequency to intended target resonance peak; increase SNR; and process data to remove noise. If the source level (i.e. power) of a signal is increased, then amplitude of returned echoes from all ambient noise is also increased and target detection may not be improved. Echo amplitudes can be increased by reducing the distance between the transducer and intended targets. This strategy may be possible at tidal turbine sites using bottom mounted instrument packages. As described

above, all targets have a resonant frequency. For fish this frequency is in the 110s of Hz to a few kHz range. This frequency range requires very large transducers, which introduces operational constraints and may also conflict with legislation and/or regulations imposed to protect marine mammal hearing (e.g. US Marine Mammal Protection Act 1972).

The most advantageous way to increase echo amplitude SNR from aquatic organisms is to combine broadband transmit signals with matched filters on the received echoes. Broadband pulses are frequency modulated (FM) where the transmit energy is distributed across a band of frequencies. Categories of broadband pulse types include linear (e.g. up and down sweeps) or nonlinear (e.g. parabolic, exponential) over time. These signals are often called ‘chirp’ signals as they sound like the chirp of a bird when played through a speaker. Broadband pulses consist of several cycles over the frequency bandwidth of the instrument but the energy within the pulse is not distributed evenly across all frequencies. The strategy of increasing target resolution by reducing pulse duration (see above for details) will reduce the overall SNR at long ranges as the total energy within each pulse will result in lower amplitude echoes. To balance the tradeoff between high target resolution and low SNR, broadband FM chirp signals are often combined with a matched filter that results in a pulse compression and maximizes the SNR. Matched filtering is a demodulation technique with linear time invariant filters (Van Vleck and Middleton 1946) in environments with stochastic additive noise. The matched filter delays frequencies within the transmit signal so that the pulse is compressed in time and increased in amplitude (Erhenberg and Torkelson 2000). The resulting pulse duration τ is a function of the bandwidth BW of the frequency range ($f_2 - f_1$):

$$\tau = \frac{1}{f_2 - f_1} = \frac{1}{BW}$$

The resulting SNR amplitude ratio gain is proportional to the square root of the number of independent samples in the coded signal (Clay and Medwin 1997). A conservative estimate results in a 15 dB gain over a comparable continuous wave transmit pulse (Ehrenberg and Torkelson 2000).

The final approach to increasing echo amplitudes of acoustic targets is to process the backscatter data to remove noise. Ambient noise removal can be achieved by increasing the noise threshold so that only targets with a minimum acoustic size are processed, include an ambient noise filter, mask unwanted targets, or extract targets from within noise features. A noise threshold will filter all backscattered energy below an analyst-chosen. The challenge is to choose the appropriate threshold to exclude unwanted targets. Many equations are available that have used empirical data to quantify relationships between acoustic size (i.e. echo amplitude) and animal size, typically indexed using animal length. The standard form of the equation to convert acoustic size, measured as Target Strength (TS, units dB) and fish body length (L, units m) is:

$$TS = m \log L + b$$

where the slope m and intercept b are constant for a given species. A large effort has gone into determining m and b values for many groups of fishes (e.g. see Tables 6.3 – 6.6 in Simmonds and MacLennan 2005). Values of m generally range between 18 and 30 while b values can range from the -80s to -50s depending on species and life history stage.

Development of acoustic data processing software (e.g. Echoview, LSSS, SonarX) has increased the number of filtering techniques available to remove unwanted targets. A variety of techniques have been developed to remove noise (e.g. Korneliussen 2000; DeRobertis and Higginbottom 2007; Ryan et al. 2015) and isolate target groups (e.g. Sato et al. 2015). As one example, a bitmap mask can be applied to the data to isolate targets of interest. A bitmap mask changes the sample value to an arbitrary value (e.g. -999) for samples that do not meet the filter criteria, while leaving data values corresponding to true values unchanged. When bitmap mask(s) are applied to backscatter data, only intended targets remain in the modified data file. The final approach (Fraser et al. 2017) uses multifrequency acoustic data to delineate turbulent regions and then extracts biological targets from within these regions.

Technology Assessment Rubric

See attached file 190225 Technology Assessment Rubric jkh.xlsx

Echosounders to Eliminate from Consideration

Kaijo/Sonic: scientific market not a large part of business plan, limited support for instruments

Furuno: No active instrument development at this time

Imagenix: very limited support for instrument, limited use on alternate platforms

Summary and Recommendations

Instrumentation Category:	Echosounders
Prepared By:	Dr. John Horne
Affiliation:	University of Washington; School of Aquatic and Fishery Sciences
Completion Date:	8/21/2019
Best-in-Class Instrument(s) recommendation(s): Recommended best-in-class echosounder is the Kongsberg – Simrad EK80 scientific line of echosounders. EK80 echosounder models include the EK80, WBAT, WBT Mini, and the WBT Tube. All of these echosounders are built using a common architecture with shared design features: actively transmit in continuous wave (i.e. CW) or wideband mode and ‘listen’ in passive mode on 4 or 8 channels using singlebeam and/or splitbeam transducers. There are also differences among models that target different deployment strategies. The WBAT and WBTmini can be controlled using EK80 software and have an autonomous operation mode using the Mission Planner software. The WBAT and WBT Tube are housed in a pressure container rated to 1000 or 4000 metres. See Table X for a comparison of model options.	
Approaches to the physical use of the instrument: Multiple housing configurations enable multiple deployment strategies with this line of echosounders. The EK80 is designed for traditional vessel deployment with transducer(s) mounted in the hull, on a pole mount, or on a towbody. The WBAT pressure-rated housing is designed for autonomous deployments on moorings or in bottom instrumentation packages, while the WBT Tube are designed for alternate platform deployments on ROVs or AUVs with an external power supply. The WBT Mini configuration can be placed in a pressurized housing (e.g. underwater glider) or mounted in a small footprint package for surface deployments.	
Other key considerations: The combination of packaging flexibility, transmission pulse types, processing software options, and international community vetting make this current generation of Simrad echosounders the default choice for Marine Renewable Energy (MRE) applications.	
Software and data processing considerations for <i>best-in-class</i> instrument: The EK80 acquisition software is common among these echosounder models (and common to all Simrad sonars). The Mission Planner software is used with the WBAT and optionally with the WBT Mini. Data processing for all of the EK80-based echosounders can be completed using commercial software packages including: Echoview (www.echoview.com), LSSS (https://www.marec.no/products_iwf.htm), SonarX (http://folk.uio.no/hbalk/sonar4_5/), and recently developed open-source software ESP3 (https://sourceforge.net/p/esp3/wiki/ESP3/) and Matecho (https://org.uib.no/wplib/PREFACE%20Lanzarote2018%20S4%20P%20Perrot.pdf). For active acoustic data acquired at MRE site deployments, the most common processing software used is Echoview, followed by LSSS.	
Key Literature Reviewed for Future Reference	

Additional Information Sources

Jeff Condiotty Simrad (Jeff.Condiotty@km.kongsberg-us.com)

Tracey Steig HTI-Vemco-Innovasea (tracey.steig@innovasea.com)

Tim Acker BioSonics (Tacker@BioSonicsInc.com)

Jan Buermans and Steve Pearce ASL (jbuermans@aslenv.com, spearce@aslenv.com)

Appendices (if applicable)

See manufacturer specification sheet or

<https://www.simrad.com/www/01/NOKBG0240.nsf/AllWeb/941F9CBFD32D266EC1257C220047E755?OpenDocument>

<input checked="" type="checkbox"/>	Slide presentation outlining the contents of this report is attached.
-------------------------------------	---

<input checked="" type="checkbox"/>	I acknowledge that the information shared in this report may used in the Annex IV State of Science Report II (to be released 2020). All work used for the Annex IV Report will be cited appropriately.
-------------------------------------	--

INSTRUMENT CATEGORY SUMMARY AND *BEST-IN-CLASS* RECOMMENDATION

References

- Clay, C.S. and H. Medwin. 1977. *Acoustical Oceanography: Principles and Applications*. John Wiley & Sons, New York. 544 pp.
- De Robertis, A. and I. Higginbottom. 2007. A post-processing technique for estimation of signal-to-noise ratio and removal of echosounder background noise. *ICES J. Mar. Sci.* 64: 1282-1291.
- Erhenberg, J.E. and T.C. Torkelson. 2000. FM slide (chirp) signals: a technique for significantly improving the signal-to-noise performance in hydroacoustic assessment systems. *Fish. Res.* 47: 193-199.
- Fraser, S., V. Nikora, B.J. Williamson, and B.E. Scott. 2017. Automatic active acoustic target detection in turbulent aquatic environments. *Limnol. Oceanogr. Methods* 15:184–199.
- Greene, C.A. and P.S. Wilson. 2012. Laboratory investigation of a passive acoustics method for measurement of underwater gas seep ebullition. *J. Acoust. Soc. Am.* 131: EL61-EL66.
- Korneliussen R.J. 2000. Measurement and removal of echo integration noise. *ICES J. Mar. Sci.* 57: 1204-1217.
- Lawson, G.L., and G.A. Rose. 1999. The importance of detectability to acoustic surveys of semi-demersal fish. *ICES J. Mar. Sci.* 56: 370-380.
- MacClennan, D.N., P.J. Copland, E. Armstrong, and E.J. Simmonds. 2004. Experiments on the discrimination of fish and seabed echoes. *ICES J. Mar. Sci.* 61: 201-210.
- McQuinn, I.H., Y., Simard, T.W.F. Stroud, J.-L. Beaulieu, and S.J. Walsh. 2004. An adaptive, integrated “acoustic-trawl” survey design for Atlantic cod (*Gadus morhua*) with estimation of the acoustic and trawl dead zones. *ICES J. mar. Sci.* 62: 93-106.
- Minnaert, M. 1933. On musical air-bubbles and the sound of running water. *Philosophical Magazine* 16: 235-248.
- Ona, E., and R.B. Mitson. 1996. Acoustic sampling and signal processing near the seabed: the deadzone revisited. *ICES J. Mar. Sci.* 53: 677-690.
- Sato, M., J.K. Horne, S.L. Parker-Stetter, and J.E. Keister. Acoustic classification of coexisting taxa in a coastal ecosystem. *Fish. Res.* 172: 130-136.
- Simmonds, E.J. and D.N. MacLennan. 2005. *Fisheries Acoustics: Theory and Practice*, 2nd ed. Blackwell Science, Oxford. 437 pp.

Totland, A. G.O. Johansen, O.R. Godoe, E. Ona, and T. Torkelsen. 2009. Quantifying and reducing the surface blind zone and the seabed dead zone using new technology. ICES J. Mar. Sci. 66: 1370-1376.

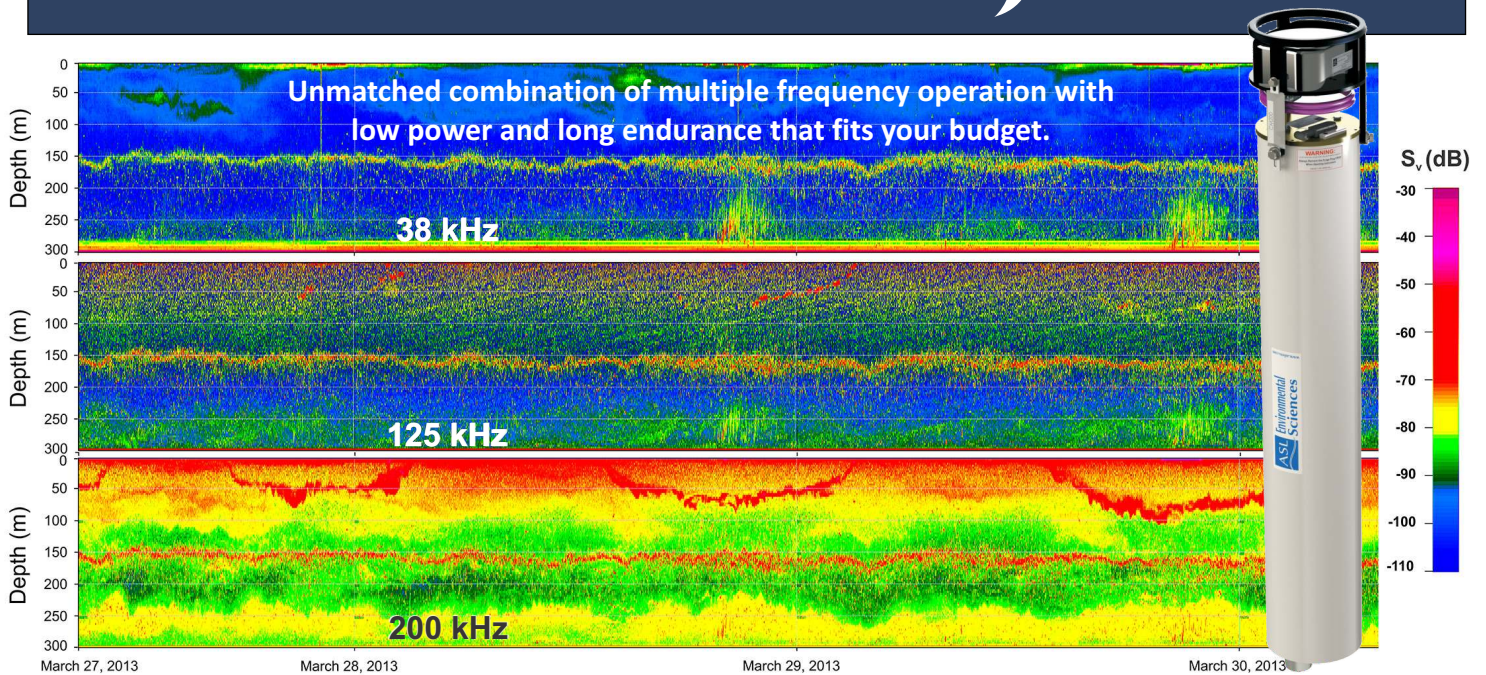
Van Vleck, J.H. and D. Middleton. 1946. A theoretical comparison of the visual, aural, and meter reception of pulsed in the presence of noise. Journal of Applied Physics 17: 940-971.

Appendices

Manufacturer instrument specification sheets are attached if available.

Acoustic Zooplankton Fish

ProfilerTM

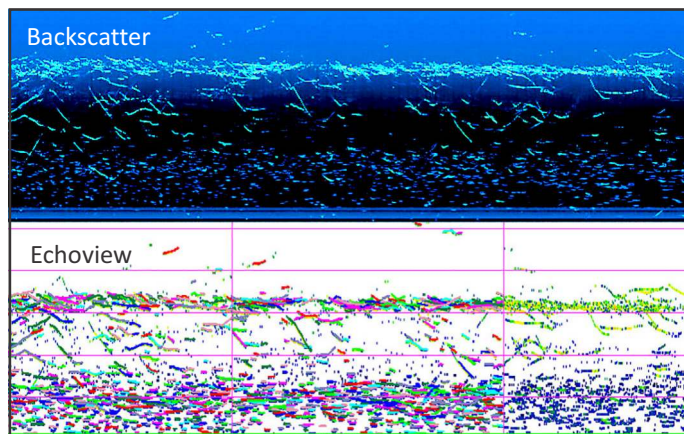


Applications

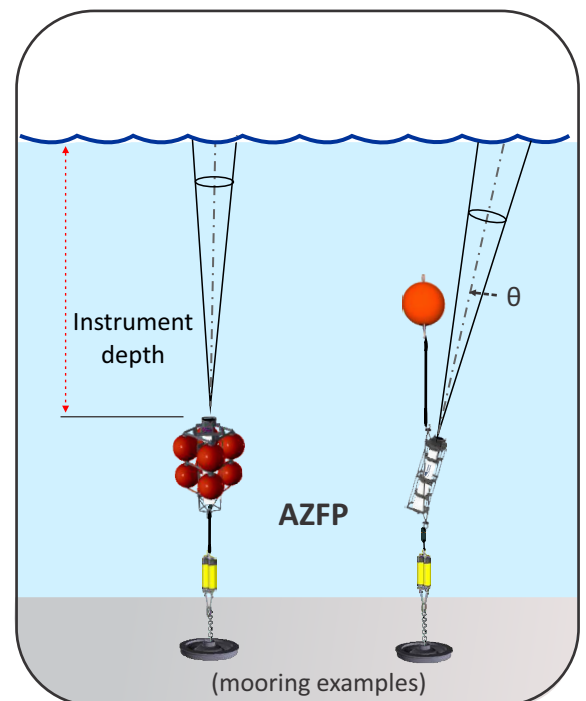
The Acoustic Zooplankton Fish ProfilerTM can monitor the presence and abundance of zooplankton and fish within the water column by measuring acoustic backscatter returns with ultrasonic frequencies. Other sonar targets realized from the sonar backscatter data include bubbles and suspended sediments.

Features

- Can collect data continuously for periods of up to one year at high temporal and spatial resolution.
- Available with up to four frequencies in a single transducer housing.
- Can be operated in bottom-mounted, upward looking mode or in downward looking mode from a buoy.



Backscatter data showing fish arches (Echoview software)



AZFP Specifications

- Deployment phases (12 max) by date or duration (with repeat & sleep)
- Configurable ping rate up to 1 Hz (depends on frequencies and range)
- A/D Digitization rate: 64,000, 40,000 or 20,000 Hz
- User selectable pulse length: 100 to 1000 microseconds
- Range lockout to ignore near targets
- Range averaging into bins (minimum bin size is 0.011m) and ping averaging over time
- Anodized aluminum underwater pressure housing rated to 600 m

TILT SENSOR

Range $\pm 45^\circ$ with an accuracy of $\pm 3^\circ$

DATA STORAGE

16 GB CompactFlash

SIZE

Pressure case: 170mm diameter x 1000mm long

POWER

Example with standard battery pack: ping for 150 days with 4 frequencies every 2 seconds over a 100 m range)

ACOUSTIC PERFORMANCE of the AZFP

Estimated Minimum Detectable Volume Backscatter Strength (dB)

Frequency (kHz)	Nominal Source Level(dB)	Nominal -3dB Beam Angle	1m	2m	5m	10m	20m	50m	100m	200m	300m	500m
38	208	12	-136	-130	-122	-116	-110	-101	-94	-87	-82	-74
67.5	205	10	-131	-125	-117	-110	-104	-95	-87	-77	-70	-58
125	210	8	-136	-129	-121	-115	-108	-98	-88	-75	-64	-
200	210	8	-130	-124	-115	-109	-102	-91	-79	-63	-48	-
333	211	8	-121	-115	-106	-100	-92	-79	-65	-43	-	-
455	210	7	-116	-110	-101	-94	-86	-71	-54	-	-	-
769	210	7	-106	-99	-90	-81	-71	-48	-	-	-	-
1250	211	7	-91	-83	-72	-61	-	-	-	-	-	-
2000*	212	7	-80	-71	-55	-	-	-	-	-	-	-

NOTES

- Sidelobes are -15 dB or better
- Limits of detectable volume backscatter strength are estimates; individual units may vary by +/- 3 to 4 dB
- Receiver dynamic range is >85 dB each channel (* receiver dynamic range is 75 dB for 2000 kHz)
- The above specifications are subject to change without prior notice
- Volume backscatter is calibrated to +/- 1dB, Sv resolution is +/-0.1 dB

SOFTWARE

- Includes AZFPLink to configure the instrument and plot hourly single frequency echograms
- AZFP's raw data format is compatible with Echoview and Sonar5
- AZFP's comma delimited ASCII format (CSV) is compatible with Matlab and other software.

OPTIONAL FEATURES

- 32 GB Compact Flash
- 1000 m rated versions
- RS422 serial communication with optical isolation for real-time applications
- Bottom frames
- Compact AZFP packages for Mid-ocean floats, gliders and AUVs and towed bodies
- Short pressure case without batteries
- Taut-line mooring frame
- Pressure Sensor
- Tilt pinger for use with bottom frame
- Deployment and recovery services
- Deepwater versions available up to 6000 m



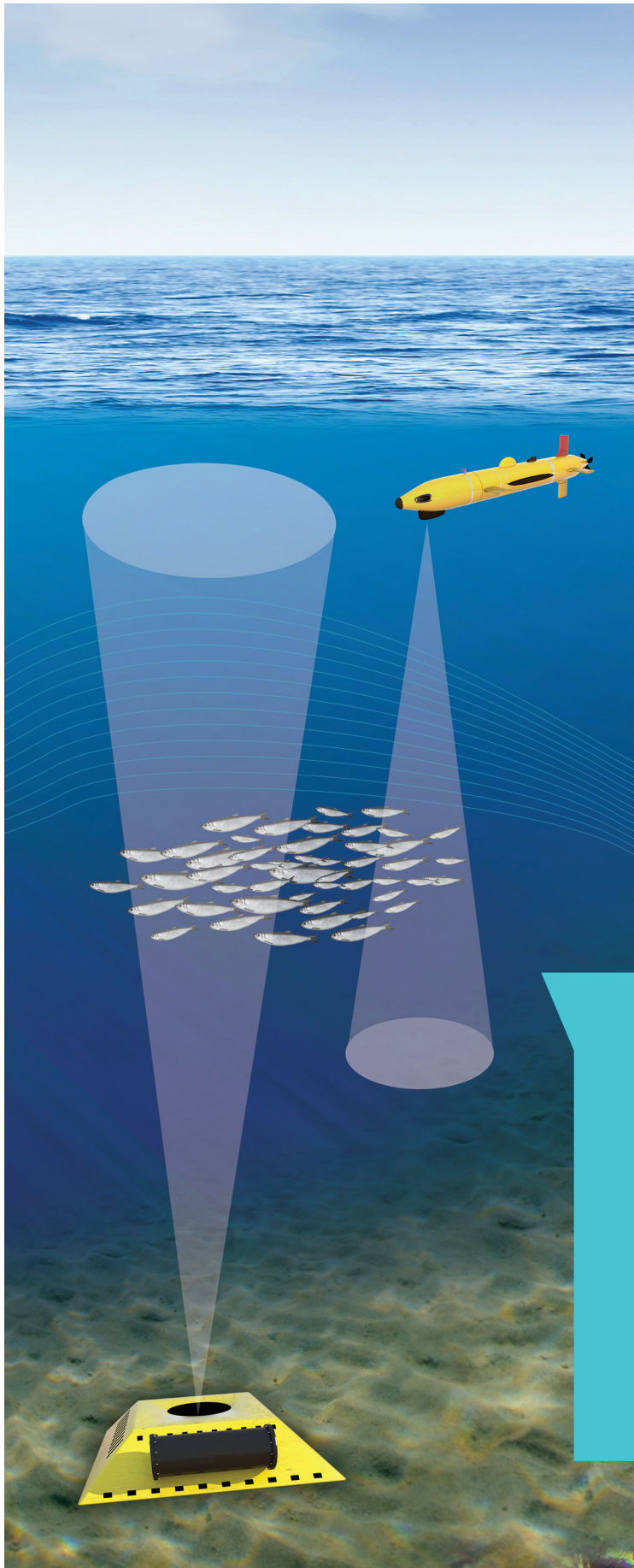
AUTONOMOUS SUBMERSIBLE ECHOSOUNDER

Applications

- Ideal for AUV or ROV instrumentation
- Deploy as a complete seafloor observatory system, tripod mount and batteries available
- Monitor migration and evaluate temporal patterns in distribution and abundance
- Gain insight into behavior variations and event response

Product Highlights

- Monitor and assess fish, marine mammals, zooplankton, other aquatic organisms
- Completely autonomous with no external cables
- Fully functional DT-X split beam echosounder packaged for seafloor or unmanned vehicle deployments
- Programmable duty-cycle and wake/sleep timer for extended deployments
- OEM version available for integration



DT-X SUB AUTONOMOUS SUBMERSIBLE ECHOSOUNDER

Performance Features

- System Noise Floor: Extremely quiet -140dB
- Dynamic Range: Greater than 160dB
- Adjustable Ring Rate: 0.01 to 30 pps
- Adjustable Pulse Duration: 0.1 to 1.0 ms
- Adjustable Range: >2000m
- Transmit Power: 100 to 1000 Watts RMS

Dimensions

- Housing: 10" diameter x 22" length
- Digital transducer:
 - 7.2" diameter x 6.25" (200, 420 kHz)
 - 10.3" diameter x 8.5" (38, 70, & 120 kHz)

Power System

- External Battery, 11-24 Volts DC
- SMART power control eliminates surges and ensures safe shut-down when power is low and reboot only after recharge

Communication and Data Storage

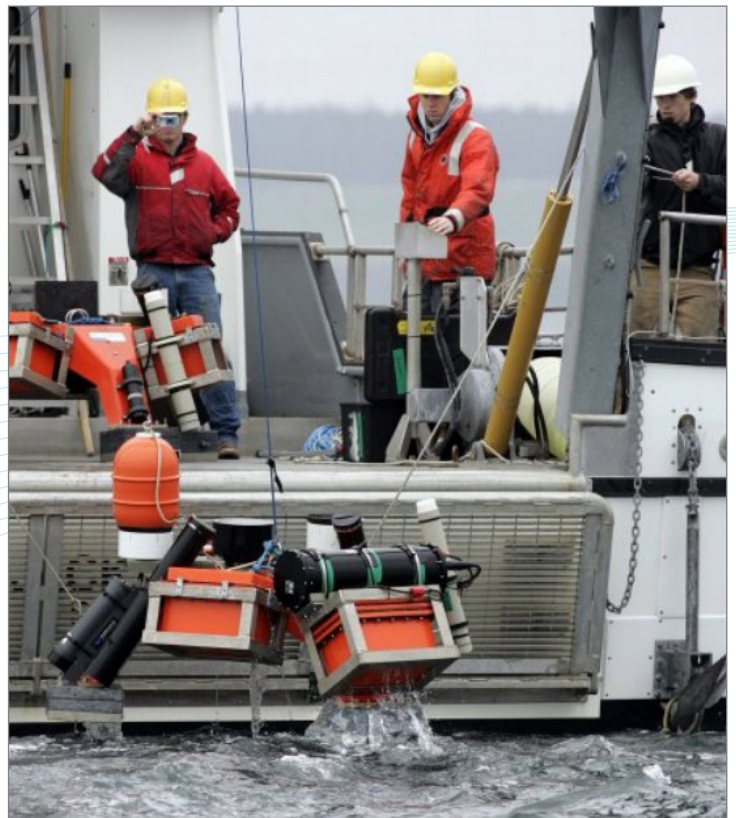
- High-capacity storage drives
- USB and Ethernet ports for echosounder configuration and data retrieval
- Integrated data storage and power management systems

Echosounder Unit

- Fully programmable
- Self diagnosis and calibration on start-up
- Fully selectable configuration options
- Integrated orientation sensor
- Programmable duty cycle

Transducer Options

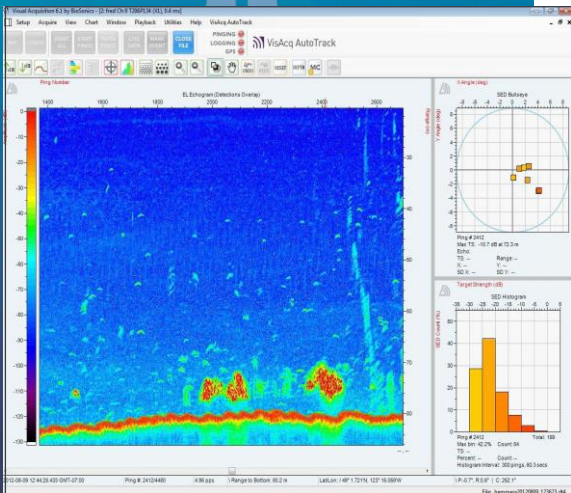
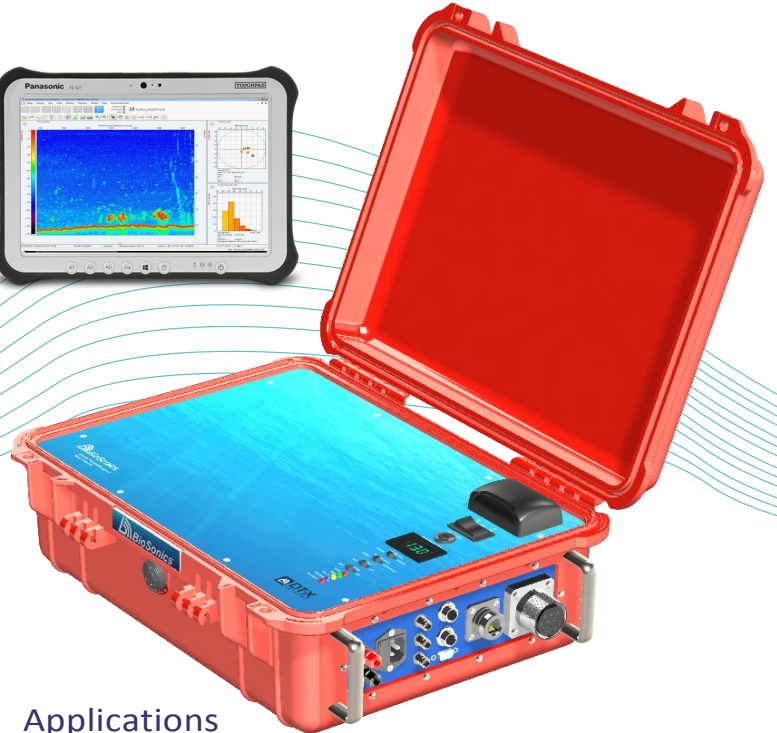
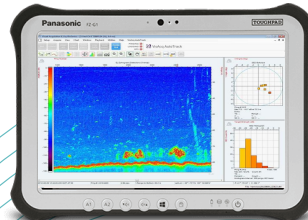
- Scientific split beam technology
- Wide range of standard frequencies for numerous fisheries and habitat assessment applications; 38, 70, 120, 200, 420, & 1000 kHz
- Ultra-low side lobes to -35 dB
- Multiple frequencies from a single echosounder



Fully rigged DT-X SUB as deployed for 5-week seafloor observatory mission.



AUTONOMOUS PORTABLE SCIENTIFIC ECHOSOUNDER

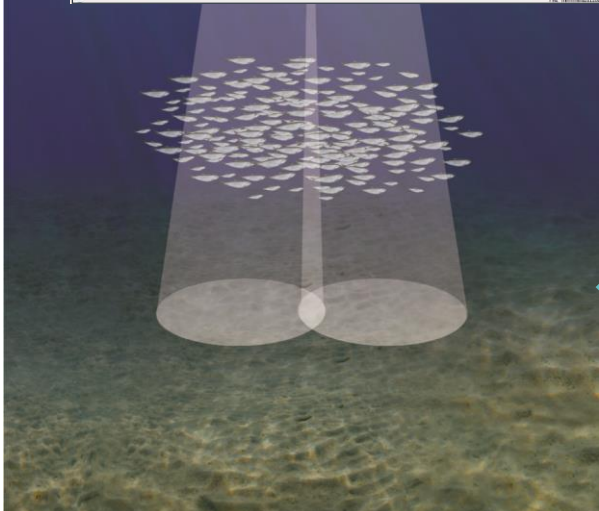


Applications

- Mobile surveys to assess fish population, biomass and size distribution
- Fixed-station monitoring at rivers, dams, water intakes
- ASV/USV surveys, surface buoys, and other unmanned or unattended deployments
- Fish passage, entrainment and migration studies
- Habitat mapping, seagrass, substrate classification and bathymetric surveys

Product Highlights

- Scientific split beam technology
- Operates with or without a PC or Tablet in autonomous mode
- Ultra-rugged IP67 metal connectors
- Log up to 30 days of data
- Programmable wake/sleep function
- Internal Wi-Fi router & DGPS, voltage monitor, and much more!



DT-X EXTREME AUTONOMOUS PORTABLE SCIENTIFIC ECHOSOUNDER

Echosounder Specifications

- Programmable LINUX-based embedded processor
- Wired or wireless ETHERNET control
- Real-time depth and speed output via NMEA 0183
- Internal DGPS with optional external interface
- Metal IP67 connectors
- High resolution, full color echogram
- System Noise Floor: Extremely quiet -140dB
- Dynamic Range: Greater than 160dB
- Selectable Ping Rates from 0.01 to 30 pps
- Selectable Pulse Duration: from 0.1 to 1.0 ms
- Split Beam Detection Range: 0.5 to 2,000 meters
- Transmit Power: 1000 Watts RMS
- Input Power: 11-26 VDC or 90-264 VAC
- Power Consumption:
Active mode: 30 Watts; Sleep mode: <1 Watt
- Weights and Dimensions
L: 49 cm (19") W: 39 cm (15") H: 19 cm (8"); Wt.: 11.4kg (22 lbs.)

Digital Transducer Specifications

- Signal digitization provides improved SNR and overall superior data quality
- Integrated Orientation Sensor included
- Wide range of frequencies:
 - 38, 70, 120, 200, 420, & 1000 kHz
- Scientific grade split beam or single beam
- Ultra-Low side lobes to -35 dB
- Network up to 10 separate transducers at various frequencies
- **NEW** stainless steel bulkhead and cable connectors
- Anodized aluminum housings
- Weights and Dimensions:
 - 200, 400, 1000 kHz**
D: 18 cm (7.2") H: 17 cm (6.3") W: 4kg (9.5 lbs.)
 - 38, 70, 120 kHz**
D: 26 cm (10.3") H: 22 cm (8.5") W: 14-17kg (30-38 lbs.)



BioSonics Data Collection, Data Analysis and Real-Time Reporting Software - INCLUDED!



Visual Acquisition Echosounder configuration and data collection/playback



Visual Analyzer Echo counting and echo integration for fish density and biomass estimation

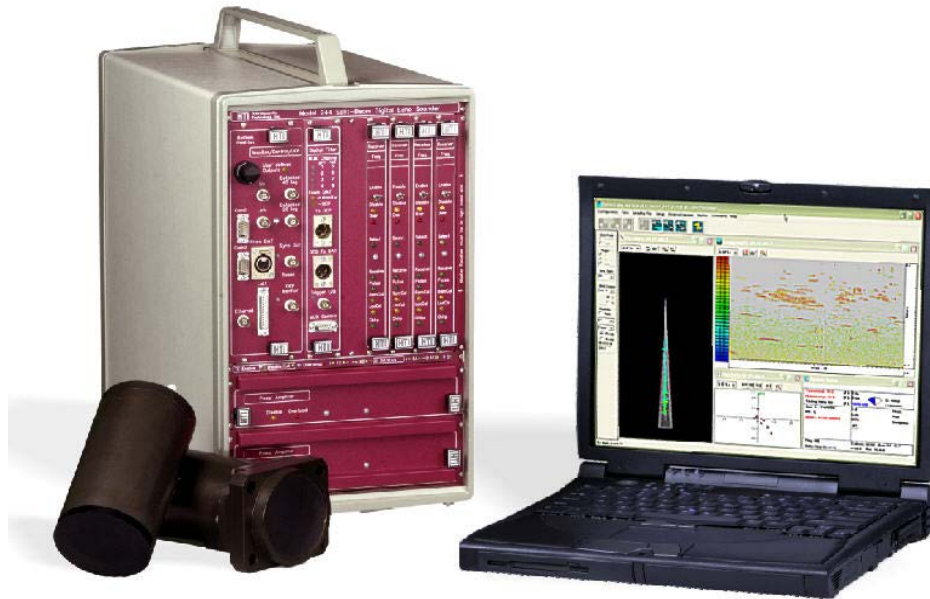


VisAcq AutoTrack Real-time processing and automated reporting for fisheries applications



Visual Habitat Aquatic habitat mapping and assessment, measure plant canopy height and % coverage, SAV and substrate classification

MODEL 244 MULTI-FREQUENCY SYSTEM



The HTI *Model 244 Multi-Frequency System* is a powerful digital split-beam/single-beam hydroacoustic system designed specifically for fisheries and plankton evaluations. Combining powerful digital signal processing hardware with a MS *Windows2000/XP*-based user interface, the *Model 244 System* produces results in real time, with multiple data display and storage options. The following components are housed in a single compact enclosure:

Digital Echo Sounder
Digital Data Tape Interface

Digital Chart Recorder
Digital Multiplexer

The menu-driven *Windows2000/XP* user interface permits the operator to enter calibration, operation, and data processing parameters, as well as select real-time data display and output options. Five levels of output data files (available individually or in combination) are written to disk, providing permanent data records ready to import into spreadsheets or data bases.

A Brief Overview:

- Sub-meter, three-dimensional resolution over time (e.g., once every second).
- Very high resolution: up to 1400 range strata as small as 10 cm, summary data available as frequently as every 6 sec, ping rate up to 50 pings/sec.
- Samples up to 16 transducers at up to 5 different frequencies from 38 kHz to 1 MHz.
- Either slow (timed) or fast multiplexing (alternating pings) sampling among transducers.
- Records the complete, raw, unthresholded digital split-beam samples.
- A compact, 12VDC-powered M241 Portable Digital Ech Sounder is also available.

HTI - HYDROACOUSTIC TECHNOLOGY, INC.

715 NE Northlake Way, Seattle, WA 98105 USA
Tel. 206.633.3383 | 206.633.5912 Fax
support@HTIsonar.com www.HTIsonar.com

MODEL 244 MULTI-FREQUENCY SYSTEM

Power Supply:	Nominal 120 VAC standard (240 VAC optional).
Dimensions:	500 mm length x 282 mm width x 522 mm height (19.7 x 11.1 x 20.6 inches).
Weight:	28 kg (62 lb) for 120 VAC version.
Operating Frequency:	Up to 16 transducers at 5 frequencies, in any combination of beam widths, split-beam (38, 60, 120, 200, 307, and 420 kHz) or single-beam (38-420 kHz, and 1 MHz).
Operating Temperature:	0-50°C (32-122°F).
Power Consumption:	200 watts without echogram PC printer; approximately 300 watts with printer.
Transmit Power:	38-200 kHz = 1000 watts, 300-420 kHz = 500 watts.
Dynamic Range:	Total dynamic range is 140 dB.
Chirp/FM Slide Option:	Increases non-reverberant signal-to-noise ratio by up to 15 dB (PW = 1.25, 2.5, 5.0 msec).
Transmit Level:	Output power is variable over a 9 dB range in 3 dB steps (+18 dB to +33 dB dep. on frequency).
Receiver Gain:	Overall receiver gain is adjustable in five 6 dB steps over a 24 dB range (-12, -6, 0, +6, +12 dB).
Time Varied Gain:	Simultaneous 20 log R + 2 <input type="checkbox"/> R and 40 log R + 2 <input type="checkbox"/> R functions. Spreadin
Receiver Blanking:	programmable to nearest 0.1 dB. Total TVG range is 120 dB. Start/end TVG 0.5-1000 m.
Pulse Width:	Start and stop range blanking is selectable to the nearest 0.1 m.
System Synchronization:	Selectable from 0.1 to 10 msec. Receiver bandwidth automatically adjusted to optimize system performance for the selected pulse width.
Bottom Tracking:	Externally or internally triggered. Internal rate varies from 0.5-50 pings/sec.
Signal Outputs:	Fixed, manual, and automatic bottom tracking modes.
	Detected outputs maximum calibrated output of 10 volts, suitable for display on oscilloscopes or chart recording. Undetected outputs maximum calibrated sine wave output of 20 volts peak-to-peak main beam, 10 volts peak-to-peak formed beams (at center frequency of 12 kHz). Suitable for use with data recorders. Four signal outputs can be user-designated from any of the following:
	20 log R detected out (composite beam)
	40 log R detected out (composite beam)
	Undetected composite beam, as well as undetected up, down, left, or right beam. One output displays processed strata/bottom/echo monitor w/selected echo indicators for o'scope.
Real Time Data Displays:	Echogram, echoscope, and several others, including
	System Status: Indicates operation, sample, data, file status, disk space, and GPS position.
	Fish Densities: Relative fish/plankton density by range bins.
	Total Echoes: Raw and tracked echoes by range bins.
	Stacked Bar Chart: Fish frequency vs. range (e.g, depth), and TS color bin.
	Horizontal Stacked Bar: Fish frequency vs. angle off axis, and TS color bin.
	Scatter Plot: Echo X-Y location (angle off axis) in the beam (also X-Z and Y-Z).
	3D Display: User-controlled rotation.
Angular Resolution:	<+/- 0.1° (6° beam width, 200 kHz), using quadrature demodulation.
Echo Integration:	Simultaneous digital echo integration in up to 1400 total range-dependent echo level thresholds:
	Number of echo integration layers: 1400 total surface locked (100 bottom locked optional).
	Ping based (i.e., specific number of pings), or time based (i.e., number of minutes).
Target Tracking:	Simultaneous three-dimensional echo target tracking with real-time screen displays:
	Real-time updates of important values (at selectable intervals): mean target strength of tracked targets, cumulative number of echoes received, current bottom depth.
	Up to 1400 total range-dependent echo level thresholds.
Multiplexer:	<i>Digital Multiplexer</i> samples up to 16 transducers optionally. Switching by time (i.e., slow multiplexing), or ping-by-ping (i.e., fast multiplexing).
Digital Chart Recorder:	Internal <i>Digital Chart Recorder</i> , using a PC printer to create echograms.
Data Recording:	Complete recording of the digital split-beam samples directly to disk (optional) or Digital Audio Tape (DAT) recorder via <i>Digital Tape Interface</i> .
Transducers:	See <i>Model 540 Split-Beam Transducer</i> specification sheet for beam widths, maximum depths, and available cable lengths. All HTI transducers are preamplified to maximize signal-to-noise ratio.
Positioning:	GPS position recorded to data file or to DAT (GPS unit not included).
Remote Operation:	Modem and communication software permits full remote operation, data transfer, and quality control of the <i>Model 244 System</i> from anywhere in the world with reliable telephone communication.
Computer Requirements:	Minimum desktop 2 GHz, 128 MB RAM (256 MB recommended), <i>Windows2000/NT</i> , 50 GB HD (100 GB recommended), <i>Lantastic</i> . Contact HTI for more detailed specifications.
Note:	Specifications subject to change without notice.



852 Echo Sounder 6000 m
445-040 MARCH 2006-REVISED MAY 2017

IMAGENEX MODEL 852 ULTRA-MINIATURE 6000 m ECHO SOUNDER

APPLICATIONS:

- ROV Navigation
- Diving Support
- Inspection
- Search & Recovery

FEATURES:

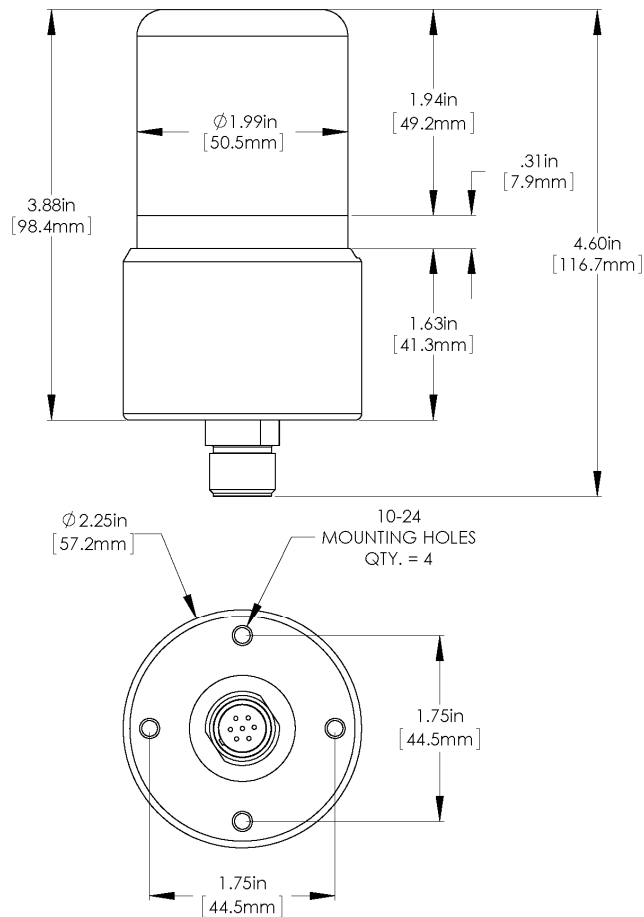
- Ultra-miniature size is ideal for mounting on today's micro ROV's
- Low cost
- Direct connection to laptop computer
- External trigger available

The Model 852 Digital Echo Sounder was designed for use with the smallest of ROV's. For maximum flexibility, the unit requires approximately 1.5 Watts from 24 VDC, or optional 48 VDC. Serial communication is utilized, RS-485 or RS-232 at 115.2 kbps. The maximum operating range is 50 meters.



HARDWARE SPECIFICATIONS:	
FREQUENCY	675 kHz or Optional 330 kHz
TRANSDUCER BEAM WIDTH	9° x 9° (20° conical for 330 kHz)
RANGE RESOLUTION	20 mm
MIN. DETECTABLE RANGE	500 mm
MAX. OPERATING DEPTH	6000 m
MAX. CABLE LENGTH	1000 m on typical twisted shielded pair
INTERFACE	RS-485 @ 115.2 kbps (RS-232 optional)
CONNECTOR*	IE55-1204-BCR
POWER SUPPLY	22 – 30 VDC at less than 1.5 Watts Optional 40 – 56 VDC
DIMENSIONS	See drawing
WEIGHT: In Air	0.53 kg (1.2 lbs)
In Water	~0.34 kg (~0.75 lbs)
MATERIALS	6AL4V Titanium, PVC, Epoxy
FINISH	Natural

SOFTWARE SPECIFICATIONS:	Win852.exe
WINDOWS™ OPERATING SYSTEM	Windows™ XP, Vista, 7, 8, 10
MODES	Echosounder
RANGE SCALES	5 m, 10 m, 20 m, 30 m, 40 m, 50 m
EXTERNAL INPUT	Depth, Heading, Turns
FILE FORMAT	(filename).852
RECOMMENDED MINIMUM COMPUTER REQUIREMENTS:	100 MHz Pentium 16 MB RAM 1 GB Hard Disk 800 x 600 x 256 colour graphics



ORDERING INFORMATION:		
6000 m UNIT	Standard	852-000-142
330 kHz	Option	-001
RS-232	Option	-006
40 – 56 VDC	Option	-013
External Trigger*	Option	-023

*External Trigger option comes with MKS(W)-307-BCR connector.

Product and company names listed are trademarks or trade names of their respective companies.



853 ES with Data Logger

445-076 JANUARY 2011-REVISED MARCH 2012

IMAGENEX MODEL 853 SCIENTIFIC ECHO SOUNDER with DATA LOGGER

APPLICATIONS:

- Seaglider Installation
- ROV, AUV & UUV
- Offshore Oil & Gas
- Surveying
- Scientific Research
- Fisheries Research

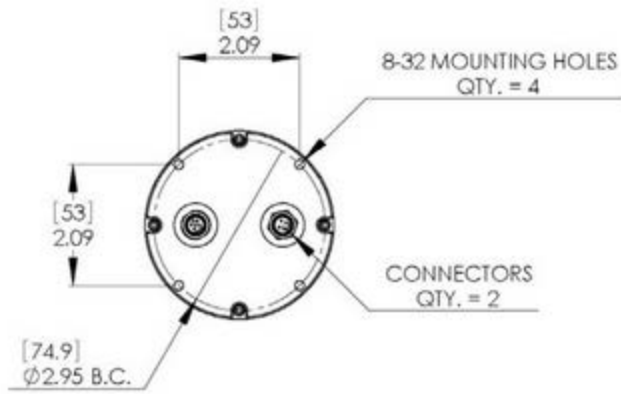
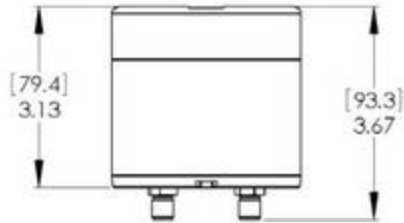
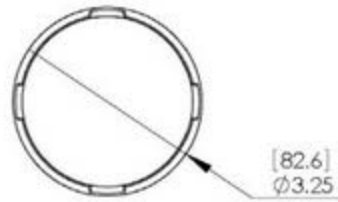
FEATURES:

- Programmable
- High performance
- Low power
- Simple set-up and installation
- Digital telemetry
- 25, 50 or 100 m operation
- Compact size
- Communication format available to user
- USB Data download



HARDWARE SPECIFICATIONS:	
FREQUENCY	120 kHz
TRANSDUCER	Conical
TRANSDUCER BEAM WIDTH	10°
TRANSDUCER SOURCE LEVEL	210 dB re 1 μ Pa @ 1 m (nominal)
TRANSDUCER RECEIVE SENSITIVITY	-180 dB re 1 V/ μ Pa (nominal)
RECEIVE BANDWIDTH	10 kHz
PULSE LENGTH	100 μ s
MAXIMUM INPUT LEVELS	with 20 dB Gain: 35 mV _{RMS} with 40 dB Gain: 3.5 mV _{RMS}
NOISE FLOOR	with 40 dB Gain: -96 dB re 1 V _{RMS}
RANGE BINS	200
DATA STORAGE	200 Days before Download
MIN. DETECTABLE RANGE	0.5 m
MAX. DETECTABLE RANGE	100 m
MAX. OPERATING DEPTH	1000 m
MAX. CABLE LENGTH	15 m (RS-232), 3 m (USB)
TELEMETRY/ PROGRAMMING INTERFACE	RS-232 Serial Interface @ 115.2 kbps (or as ordered)
DOWNLOAD INTERFACE	USB
CONNECTORS	Impulse IEW55-1004-BCR / IEW55-1006-BCR
POWER SUPPLY	22 – 32 VDC at less than 0.25 Watts (Glider mode only)
TEMPERATURE	-5 to +35 °C (operational) -40 to +50 °C (storage)
DIMENSIONS	See drawing
WEIGHT: In Air	~ 1 kg (2.2 lbs)
In Water	~ 0.55 kg (1.2 lbs)
MATERIALS	6061-T6 Aluminum, PVC
FINISH	Hard Anodize

SOFTWARE SPECIFICATIONS:	Programming/Download/Viewing program: Win853.exe
WINDOWS™ OPERATING SYSTEM	Windows™ XP, Vista, 7
MODES	Normal (interrogate to ping) Glider (one ping every 4 seconds) Stand Alone (one ping per second)
RANGE SCALES	25 m, 50 m, 100 m
FILE FORMAT	(filename).853
RECOMMENDED MINIMUM COMPUTER REQUIREMENTS:	2 GHz Pentium 4 256 MB RAM 20 GB Hard Disk 1024 x 768 screen resolution



**ORDERING
INFORMATION:**

1000 m UNIT	Standard	853-000-140
-------------	----------	-------------

Product and company names listed are trademarks or trade names of their respective companies.

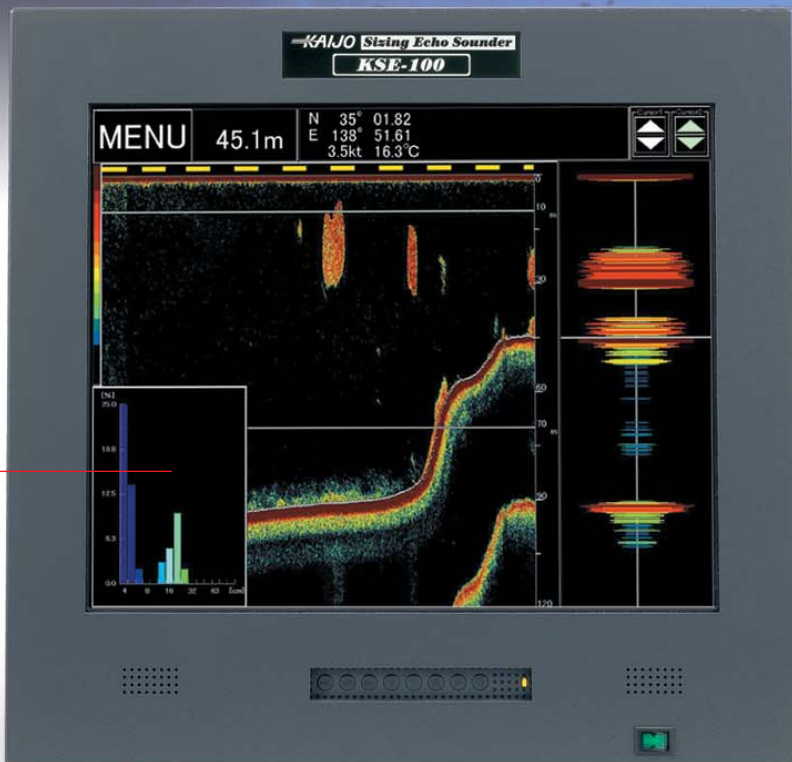
853 ES with Data Logger
445-076

IMAGENEX
www.imagenex.com

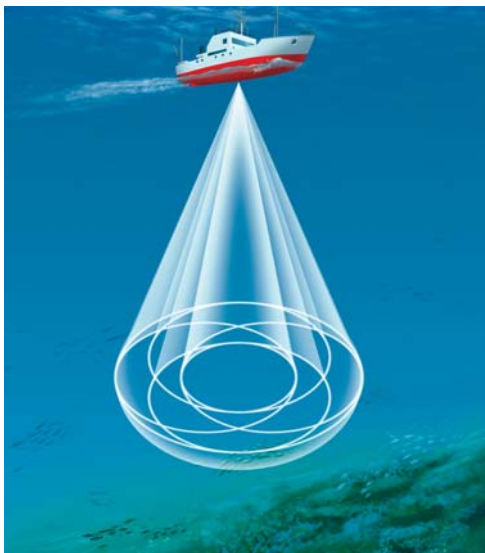
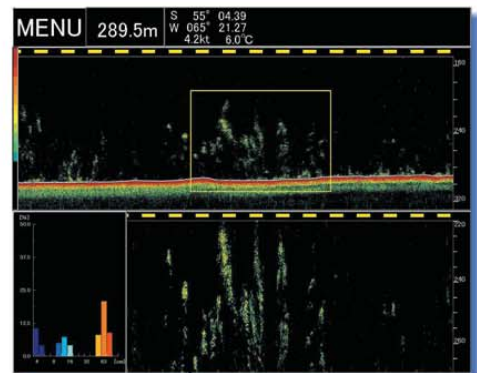
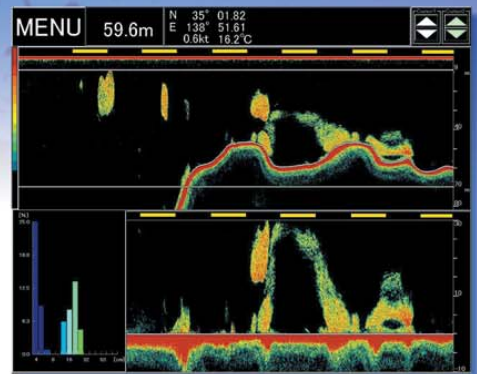


KSE-100

Kaijo Sonic Sizing Echo Sounder with Split beam transducer



Bar graph of fish size and frequency(%)
with split beam technology



The latest Technology! High Performance split beam fish- sizing echo sounder

Features:

- Easy control using a trackball
- High precision digital TVG
- LCD monitor with high resolution picture
- Selectable display area enclosed by Graphic User Interface
- Instant saving and retrieval for user settings

Kaijo Sonic Sizing Echo Sounder with Split beam transducer **KSE-100**

Specification

Operation: Menu operation by a trackball
Display: High resolution 17" LCD color monitor
Display composition:

Fish length graph	Display of the fish length in a selected area
Standard picture	Single picture/split picture display(Max.3pictures)
Enlarged split picture	Expanded picture, Sea bottom fixed picture(non-display available)
Information	Navigation information data, Command display
Menu	Operation menu in a variety of settings

Fish length graph: Graph types Bar Graph
Measurement range: Max. 600m
Fish length range: Max. 200cm
Selected range: Operational range, Depth layer, Depth layer from sea bottom
Range: 5 - 2000m(setting in each 10m step)
Shift: 0 - 3000m(setting in each 10m step)
Scale: Selected by m.fathom
Color: 16colors
Color expansion: 5 steps
Clutter: 16 steps
TVG: Fish school mode, optional mode
Marker: Minute, time, distance(3 kinds)
Picture-advance speed: 2 times, 1 time, 1/2 time, 1/5 times. pause(4 kinds)
Interference removal: Correlation way
Memorized function: Settings storage(2 kinds), picture memorize(6 kinds)
Character: Vertical cursor(2 kinds), horizontal cursor, A scope
 Net finder water depth display

Information: Navigation information(latitude, longitude, ship speed, water temperature, net finder, water depth), operation command display

Language: English,Japanese(set by KAIJO SONIC before shipment)

Outer synchronization: Synchronous input, output trigger(TTL level or current)

Navigation info. Input: NMEA0183(latitude, longitude, GLL, fish speed VTG, water temperature, MTW)
 IF-17 Interface format(Latitude, longitude, water temperature)
 I-50 net finder signal(Net finder water depth)

Navigation info. output: NMEA0183(fish finder sea depth DBT)

Frequency: 38kHz, 70kHz

Transducer: Split beam way, transmission output 3kw

Standard system composition:

Composition	Measurement(W x H x D)	Weight
I-125 Display	340 x 369 x 157mm	4.1kg
PRC-45 Processor	365 x 470 x 141mm	13kg
Track ball	119 x 190 x 60mm	0.3kg
SR-78 TX/ RX	387 x 565 x 330mm	40kg
T-178 Transducer	342.5 x 134mm	27kg
T-181 Transducer	200 x 220 x 120mm	20kg

Operating conditions: PRC-45 processor(AC100V, 200VA, 0 ~ 50)
 SR-78 TX/RX(AC100V, 800VA, -5 ~ 55) *Option:AC220V

Fish finder option

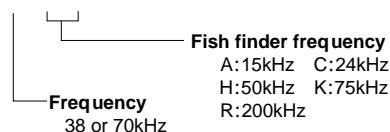
Frequency: 15, 24, 50, 75, 200kHz

Number of connection: Max. two frequencies

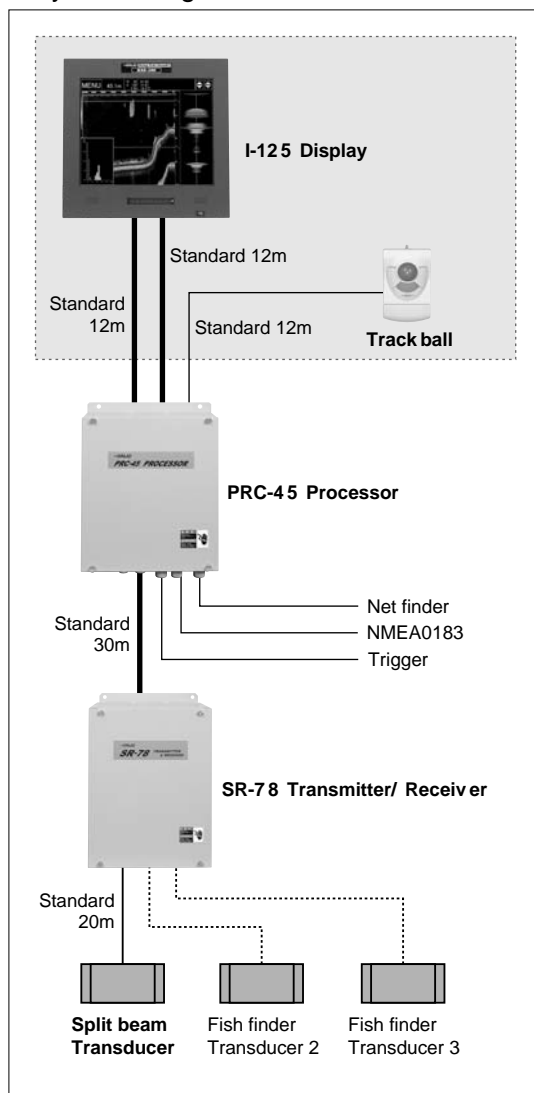
Transducer: Single beam

Transmission output: 2 kw

Type
KSE-100-



System diagram



SAFETY PRECAUTION: Please be sure to read the Instruction Manual before operating
 Specifications are subject to change without prior notice for improvement.

KAIJO



ISO 14001

KAIJO SONIC CORPORATION

HEAD OFFICE

3-1-5, SAKAE-CHO HAMURA-SHI, TOKYO, JAPAN 205-8607

TEL.81-42-555-6080 FAX.81-42-579-5171

URL <http://www.kaijasonic.co.jp> E-mail info@sonic.kaijo.co.jp

OVERSEAS MARKETING & SALES DIVISION

9TH FLOOR, KANDABASHI PARK BLDG,

1-19, KANDA-NISHIKICHO CHIYODA-KU, TOKYO, JAPAN 101-0054

TEL.81-3-3294-7615 FAX.81-3-3294-7663

OVERSEAS DISTRIBUTOR

KAIJO CORPORATION

SEOUL BRANCH TEL 82-2-563-3345 ~ 6 FAX 82-2-563-3347

TAIPEI BRANCH TEL 886-2-2709-3538 FAX 886-2-2704-8907

Signature100



Long-range current profiler designed for combined current profile and biomass measurements

The Signature100 combines a four-beam current profiler operating at 100 kHz with an optional scientific echosounder.

Both the current profiler and the biomass measurements have an effective range of 300-400 m providing unprecedented insight into the dynamics of zooplankton, krill or even schools of fish. Likewise, acoustic tracer material can give new insight into small-scale physical processes.

Signature100



Highlights

- ✓ 300–400 m current profiling range
- ✓ Optional center beam with 70–120 kHz echosounder

Applications

- ✓ Detection of krill in the water column
- ✓ Cost-effective current profile measurements at mid-range
- ✓ Plankton migration studies
- ✓ Upwelling and downwelling studies
- ✓ Internal waves
- ✓ Suitable for buoy mounting with internal AHRS

Technical specifications

→ Water velocity measurements

Maximum profiling range	300-400 m*
Cell size	3-15 m
Minimum blanking	TBA
Maximum number of cells	200
Velocity range (along beam)	User-selectable 2.5 or 5.0 m/s
Minimum accuracy	1% of measured value \pm 0.5 cm/s
Velocity precision	Broadband processing, consult instrument software
Velocity resolution	0.1 cm/s
Max sampling rate	1 Hz (1/2 Hz at max output power)

*Maximum range depends on acoustic scattering conditions.

→ HR option (on 5th beam only)

Velocity range	N/A
Cell size	N/A
Profiling range	N/A
Range velocity limitations	N/A

→ AD2CP Measurement modes*

Single	Average
Concurrent	Average and echosounder
Alternate	N/A

* US Patent 8223588

→ Echo Intensity (along slanted beams)

Sampling	Same as velocity
Resolution/dynamic range	0.5 dB/70 dB
Transducer acoustic frequency	100 kHz

→ Echo Intensity (along slanted beams)

Number of beams	4 slanted at 20°, optional vertical beam for echosounder
Beam width	6.1° (slanted)

→ Echosounder option

Transducer acoustic frequency	70–120 kHz
Transducer beam width	15° @ 70 kHz, 8.7° @ 120 kHz
Resolution	0.375–4 m
Number of bins	1800
Transmit pulse length	0.5–6 ms
Transmit pulse	Monochromatic 70 kHz, 90 kHz and 120 kHz or frequency chirp (90 kHz, 50% BW)
Transmit power	1.2–120 W, adjustable
Chirp signal processing	Pulse compression or binned frequency response
Raw complex data storage	Configurable rate
Resolution/dynamic range	0.01 dB / 130 dB
Linearity	TBA

→ Wave measurement option

AST frequency	N/A
AST max distance	N/A
Maximum wave measurement depth	N/A
Height range	N/A
Accuracy/resolution (Hs)	N/A
Accuracy/resolution (Dir)	N/A
Period range	N/A
Cut-off period (Hs)	N/A
Cut-off period (dir)	N/A
Sampling rate (velocity and AST)	N/A

→ Ice measurement option

Parameters

N/A

→ Sensors

Temperature	Thermistor in head (sampled at meas. rate)
Temp. range	-4 to +40 °C
Temp. accuracy/resolution	0.1 °C/0.01°C
Temp. time response	2 min
Compass	Solid-state magnetometer (Max 1 Hz sample rate)
Accuracy/resolution	2° for tilt < 30°/0.01°
Tilt	Solid-state accelerometer (Max 1 Hz sample rate)
Accuracy/resolution	0.2° for tilt < 30°/0.01°
Maximum tilt	Full 3D
Up or down	Automatic detect
Pressure	Piezoresistive (sampled at meas. rate)
Standard range	0–1500 m (inquire for options)
Accuracy/precision	0.1% FS / Better than 0.002% of full scale

→ AHRS option

Accelerometer dynamic range	± 2 g
Gyro dynamic range	± 250°/sec
Magnetometer dynamic range	± 1.3 Gauss
Pitch and roll range/resolution	± 90° (pitch) ± 180° (roll) / 0.01°
Pitch and roll accuracy	± 2° (dynamic)*, ± 0.5° (static, ±30°)
Heading range/resolution	360°, all axis / 0.01°
Heading accuracy	± 3° (dynamic) ² , ± 2° (static, tilt < 20°)
Sampling rate	Same as measurement rate (up to 1 Hz)

* Dynamic specifications depends on the type of motion

→ Data recording

Capacity	16 GB, 64 GB or 128 GB (inquire for larger capacity)
Data record	Consult instrument software

→ Data recording

Mode	Stop when full
------	----------------

→ Real-time clock

Accuracy

Clock retention in absence of external power	1 year. Rechargeable backup battery
--	-------------------------------------

→ Data communications

Ethernet	10/100 Mbits Auto MDI-XTCP/IP, UDP, HTTP protocols Fixed IP/DHCP client/AutoIP, UPnP
----------	---

Serial	Configurable RS-232/RS-422 300–1250000 bps
--------	--

Recorder download baud rate	20 Mbit/s (Ethernet only) - 1 GB in 6 minutes
-----------------------------	---

Controller interface	ASCII command interface over Telnet and serial
----------------------	--

→ Connectors

Depending on configuration	MCBH6F (Ethernet), MCBH8F (serial), MCBH2F-G2 (pwr), optional Souriau M-series metal connector for online use (14M)
----------------------------	---

→ Software

Functions	Deployment planning, instrument configuration, data retrieval and conversion (for Windows®)
-----------	---

→ Power

DC input	15–48 V DC
----------	------------

Maximum peak current	1.5 A
----------------------	-------

Max. average consumption at 1 Hz	15 W
----------------------------------	------

Typical average consumption*	2 W
------------------------------	-----

Sleep consumption	100 µA, power depending on supply voltage
-------------------	---

Transmit power per beam	4–200 W, adjustable levels
-------------------------	----------------------------

Ping sequence	Multiplexing or parallel
---------------	--------------------------

* 10 min. avg. profile, 1 cm/sec hor. prec., max cell size, max power, long range mode. Consult SW for other configurations

Current profiler

Signature100



→ Batteries

Internal

One or two 540 Wh alkaline or 1800 Wh lithium

Signature100



→ Batteries

Duration	Depending on configuration, consult software
----------	--

→ Environmental

Operating temperature	-4 to +40 °C
Storage temperature	-20 to +60 °C
Shock and vibration	IEC 60068-1/IEC 60068-2-64
EMC approval	IEC 61000
Depth rating	1500 m

→ Materials

Standard model	POM with titanium fasteners. Titanium/POM transducer cups
----------------	---

→ Dimensions

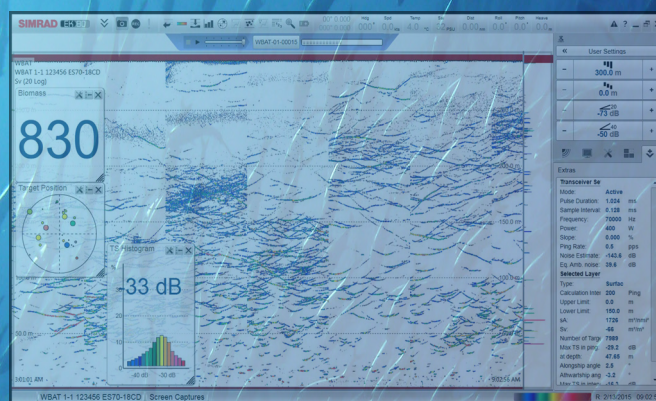
Maximum diameter	460 mm
Maximum length with room for internal batteries	765 mm (2 batteries)
Maximum length without room for internal batteries	N/A

→ Weight

In air, no battery	37.5 kg
In water, no battery	13 kg
Battery	10.0 kg (2x540 Wh), 5.8 kg (2x1800 Wh)

Simrad WBAT

Wideband Autonomous Transceiver



WBAT is a “cutting edge” subsea innovation rising from a need to monitor marine life and detect oil and gas leaks at virtually any corner of the world.

Description

The Simrad WBAT system is at the forefront of monitoring marine life capable of being submerged to a maximum depth of 1500 meters and prolonged periods of up to 15 months.

When deployed, the WBAT is self-contained and will record data with the acoustic settings at the given time intervals.

Between data recording events the WBAT will be in “deep sleep”, conserving energy and extending battery life.



The WBAT Transceiver comprises a rugged cylinder providing all necessary transmitter and receiver electronics, a battery and the necessary interface and control circuitry.

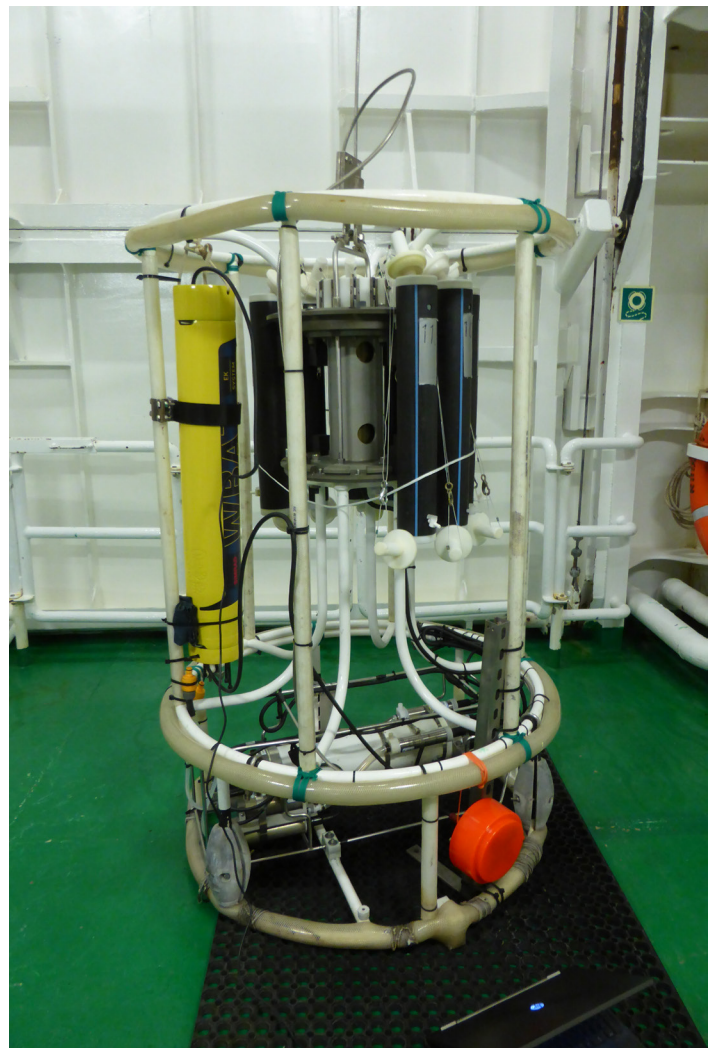
Key features

- Autonomous all-in-one echo sounder
- Advanced mission control
- Internal battery and data storage
- More than 1 year deployment
- Depth rated to 1500 m
- Frequencies from 30 to 500 kHz
- Connects two split-beam or four single-beam transducers
- Chirp and CW pulse forms
- Standardized Simrad® EK80 raw data format
- Built in calibration tool
- Wide range of transducers available

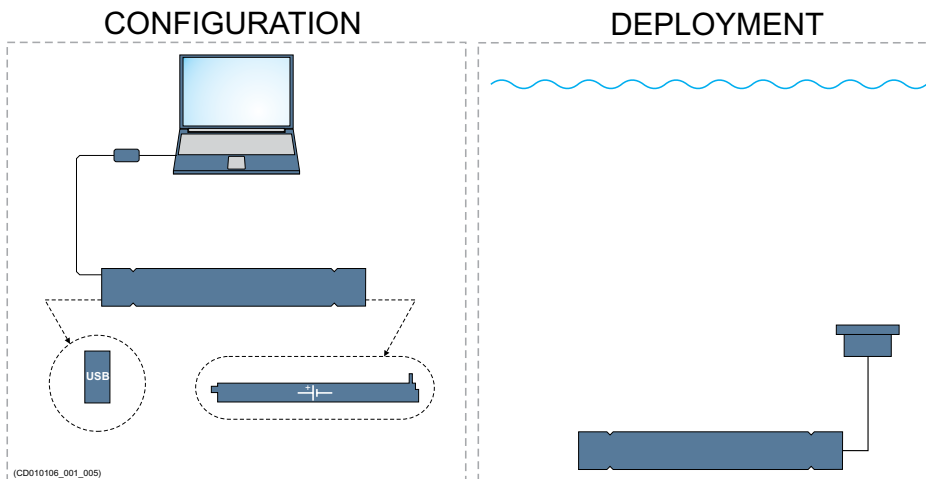
Typical applications

- Ocean observatories
- Fish migration studies
- Long-term biological studies
- Improved fish stock assessment
- Water column profiling
- Instrumentation on ROVs and AUVs

WBAT mounted on Conductivity-Temperature-Depth sensor unit.

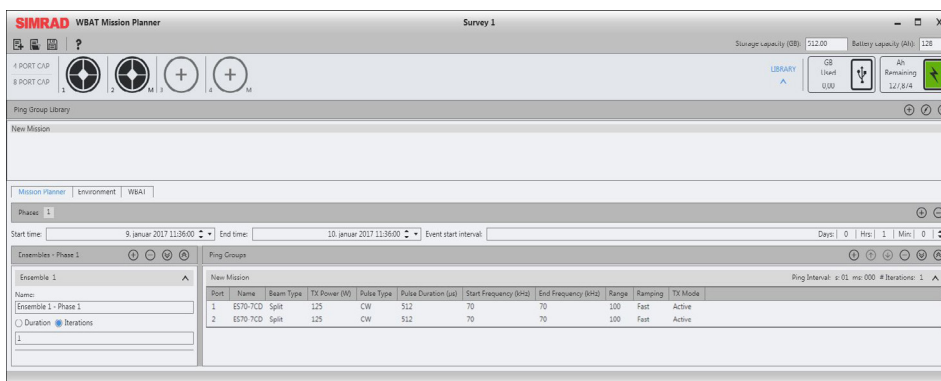


Mission Planning



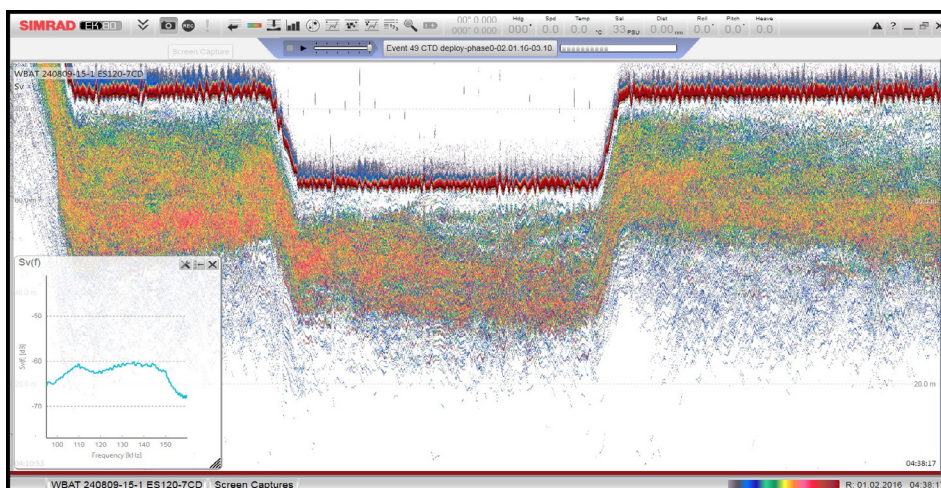
A WBAT system consists of an autonomous transceiver, one or more transducers and Mission Plan software.

Regardless if the data is collected from the ship sounders, a profiling probe, or from other platforms; the echo sounders use the same data format.



Mission Planner user interface

An advanced mission control software gives the operator a full spectre of parameters to chose from. Once uploaded into the transceiver the unit will record the data based on the acoustic settings.



The data from the system can be viewed and calibrated with the EK80 software as the RAW data format used by these products are identical.

EK80 echogram playback of krill from Antarctica. (Screen capture kindly provided by British Antarctic Survey, UK)

Technical specifications

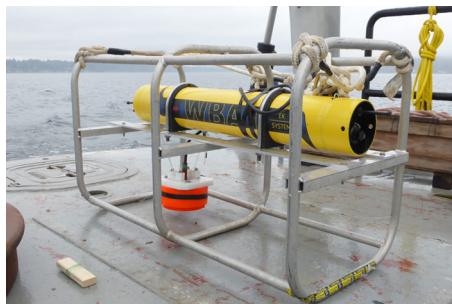
- Physical dimensions: 100 x 16.6 cm
- Weight in air/water: 25/12 kg
- Operational frequency: 30-500 kHz
- Max Transmit power: 250 W per channel with 70Ω load at 38 kHz
- No. of channels: Four independent channels
- Pulse types: CW, FM, Active, Passive
- Pulse lengths: 128 μs to 2 ms
- Transducer types: Single and/or split-beam
- Multiplexing: Built in multiplexer on each channel
- DC voltage: 14 V (internal battery)
- Battery capacity: 128 Ah
- Current consumption active: 350 mA
- Current consumption inactive: 1.5 mA
- Control: Pre-planned mission
- External interface: RS-422
- Depth rating Transceiver: 1500 meters
- Data format: Same as EK80
- EK 80 SW: Replay, calibration
- Calibration: Calibration tool built into the mission planner. Data calibration in EK80 or 3rd party processing software.
- License required: No



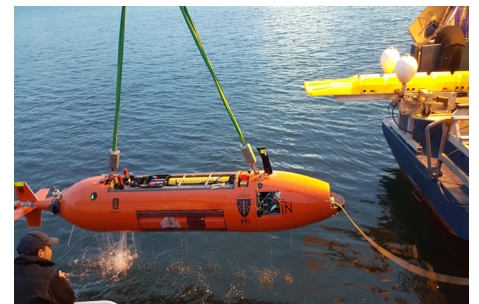
WBAT assembled with transducer mount



WBAT testing onboard NOAA/Saildrone platform San Francisco Bay, CA.



WBAT calibration on Lake Washington Seattle, WA.



WBAT mounted on HUGIN Oslofjord, Norway

Simrad

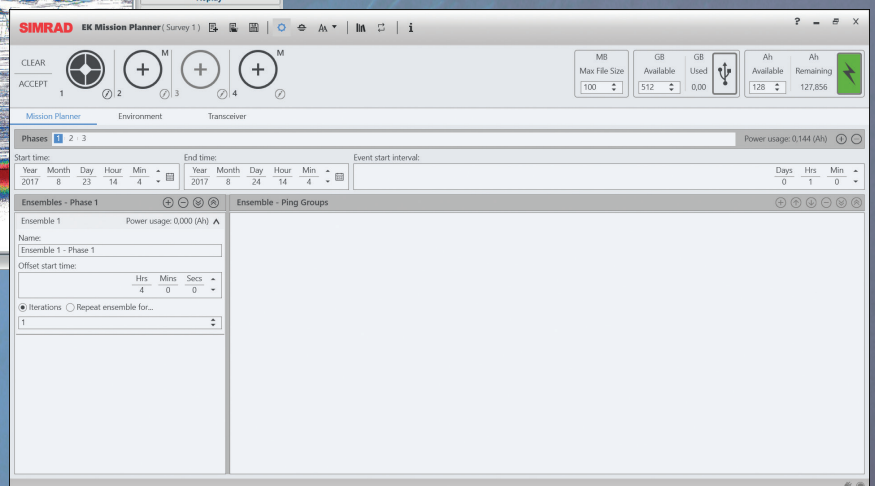
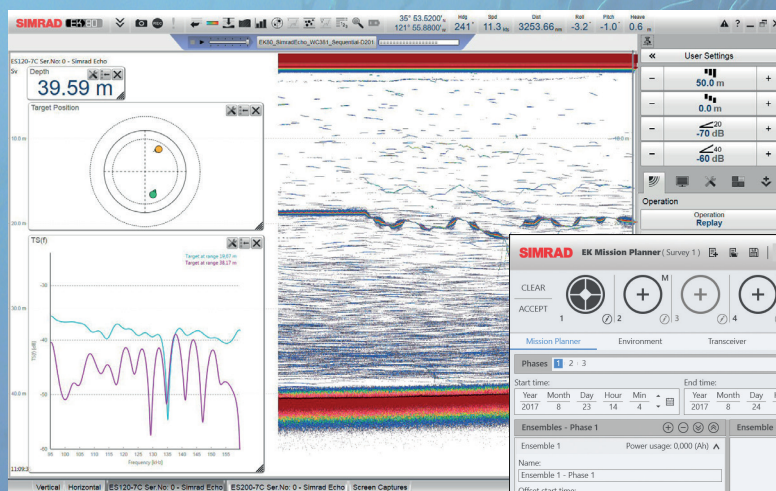
Kongsberg Maritime AS
Strandpromenaden 50
P.O.Box 111
N-3191 Horten, Norway

Telephone: +47 33 03 40 00
Telefax: +47 33 04 29 87
www.simrad.com
simrad.sales@simrad.com

SIMRAD

Simrad WBT Mini

Miniature wide band echo sounder transceiver



www.simrad.com

TECHNOLOGY FOR SUSTAINABLE FISHERIES

SIMRAD

The WBT Mini is a compact version of the highly efficient Wide Band Transceiver (WBT) used by marine research vessels all around the world. Its compact size and energy efficient design makes it perfect as a portable echo sounder or for installation on a wide range of platforms.

Description

The WBT Mini supports chirp (FM) and continuous wave (CW) pulse forms. It contains four individual transceiver channels with multiplexing functionality, allowing for flexible setup of split- or single beam transducer configurations.

The WBT Mini is contained in a splash proof cabinet and the robust design allows long-term deployment in challenging environments.

The WBT Mini can be operated in two different modes: EK80 mode or Autonomous mode.

EK80 mode

In this mode, the WBT Mini is used with a computer running the EK80 echo sounder software. The EK80 software provides full control of the WBT mini via Ethernet in real time. When used in EK80 mode .RAW echosounder data will be recorded to the computer disk(s).

This mode requires one or more EK80 software licenses.

Autonomous mode

In this mode, the WBT Mini is programmed to perform a predefined mission. A mission will normally record data in intervals over a period of time using specific acoustic settings. The mission plan is designed using the EK Mission Planner software and downloaded to the WBT Mini before mission start.

When used in Autonomous mode the high resolution .RAW data are stored internally and retrieved after mission completion.

During a mission the WBT Mini can be remotely controlled and monitored by sending operational commands and receiving downsampled data using the serial line interface.

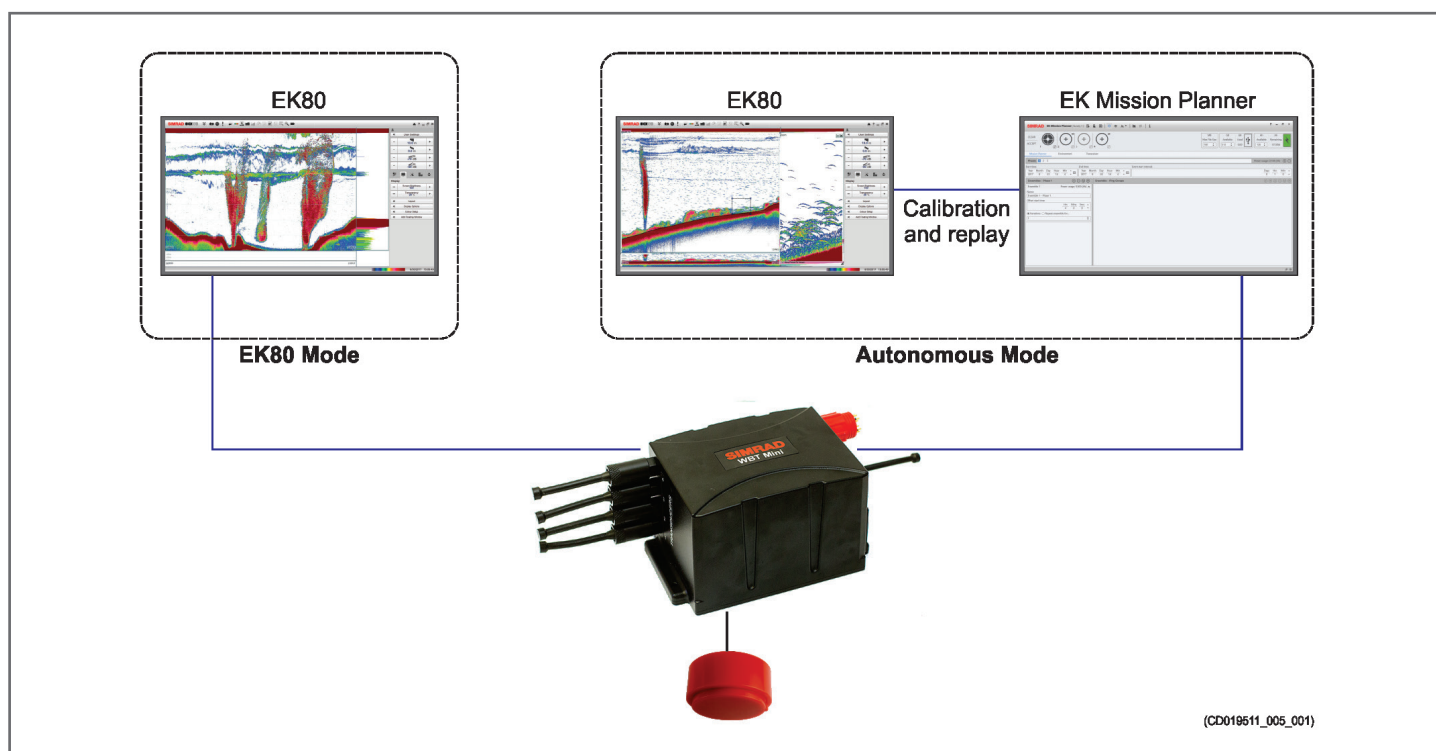
The Autonomous mode is an option that can be purchased separately.

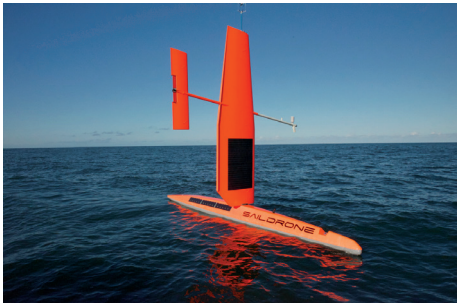
Key features

- A member of the Simrad EK80 wideband echo sounder family
- Rugged and compact design
- Splash Proof
- Operates in EK80 or Autonomous mode
- Four independent channels with built-in multiplexing available
- Built in calibration tool
- Low power consumption
- Wide range of transducers available

Typical applications

- Unmanned Surface Vehicles
- Autonomous Underwater Vehicles
- Autonomous Underwater Gliders
- Portable configurations
- Fixed installations in challenging environments

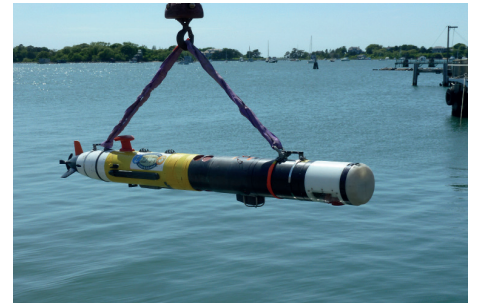




WBT Mini onboard a Sairdrone
(Image courtesy of Sairdrone)



WBT Mini onboard the Jolner USV

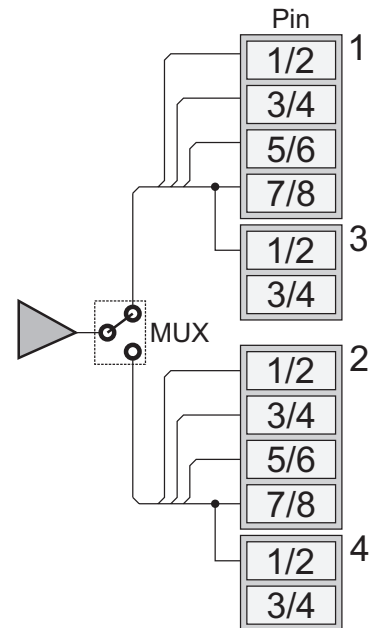


WBT Mini onboard the Remus AUV

Transducers and multiplexing

The WBT Mini has four transducer connectors. There are two 8-pin connectors (identified as 1 and 2) and two 4-pin connectors (3 and 4).

- Connector 1 is the main connector. It is always used.
- Connector 2 is used for multiplexing with connector 1.
- Connector 3 is used to add an extra single-beam transducer when a 3-sector split-beam transducer is connected to connector 1
- Connector 4 is used for multiplexing with connector 3.



Technical specifications

Performance specifications

- Frequency range: 30 – 500 kHz
- Pulse duration: 64 – 2048 μ s
- Pulse forms: CW + FM (Linear up-sweep)
- Maximum transmit power: 1000 W @ 55 Ω
- Number of channels: 4 (With multiplexer: 8)
- Transducer options: Single beam/Split beam
- Memory capacity (Autonomous mode): 512 GB

Weight and outline dimensions

- Outline dimensions:
Depth: 145 mm
Width: 289 mm
Height: 127 mm
- Weight: 5.4 kg

Power requirements

- Voltage requirement: 12 – 16 VDC
 - Power consumption:
Active: 38 / 120 / 333 kHz: 6 / 3 / 3 W(*)
Passive: 2 W
Standby: <0.02 W (Autonomous mode)
 - Maximum current: 2.5 A (Peak)
- (* @ Maximum tx power, 1 ms pulse duration, and 2 ping/second)

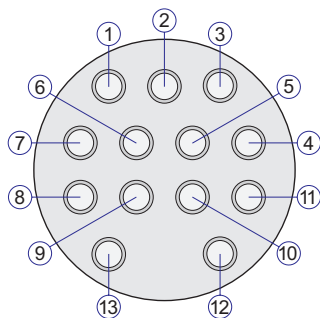
Environmental requirements

- Operational temperature: -15 to 55 $^{\circ}$ C
- Storage temperature: -20 to 70 $^{\circ}$ C
- Ingress protection (IP) rating: IP67
- Enclosure material: Aluminium

All specifications are maximum ratings. We are continuously working to improve the quality and performance of our products. The technical specifications may be changed without prior notice.

Power and Ethernet

Connector type: MacArtney male DBH13MAS

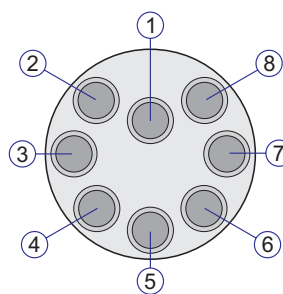


Seen towards the connector

- 1 +15 VDC (Black)
 - 2 Screen
 - 3 Ground (White)
 - 4 RJ45/8 (Brown*)
 - 5 RJ45/7 (Brown/White*)
 - 6 RJ45/4 (Blue*)
 - 7 RJ45/5 (Blue/White*)
 - 8 RJ45/2 (Orange*)
 - 9 RJ45/1 (Orange/White*)
 - 10 RJ45/6 (Green*)
 - 11 RJ45/3 (Green/White*)
 - 12 N/C (Red)
 - 13 N/C (Green)
- *Twisted pairs

Serial RS-422

Connector type: MacArtney female MCBH8F

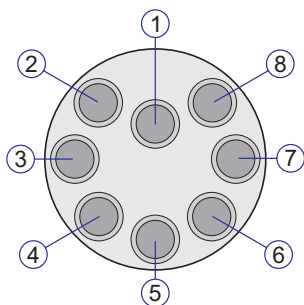


Seen towards the connector

- 1 WBT Mini RxD+ (Black)
- 2 WBT Mini RxD- (White)
- 3 WBT Mini TxD- (Red)
- 4 WBT Mini TxD+ (Green)
- 5 Ground (Orange)
- 6 N/C (Blue)
- 7 N/C (White/Black)
- 8 N/C (Red/Black)

Transducer 8-pin

Connector type: MacArtney female MCBH8F

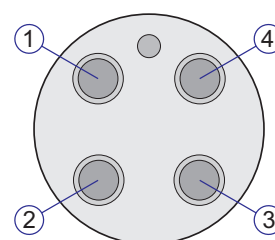


Seen towards the connector

- 1 Channel 1+ (Black)
- 2 Channel 1- (White)
- 3 Channel 2+ (Red)
- 4 Channel 2- (Green)
- 5 Channel 3+ (Orange)
- 6 Channel 3- (Blue)
- 7* Channel 4+ (White/Black)
- 8* Channel 4- (Red/Black)

Transducer 4-pin

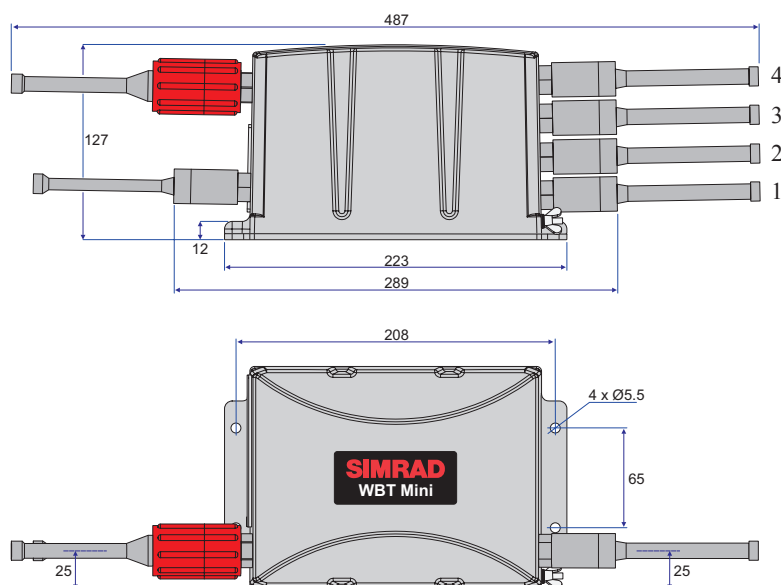
Connector type: MacArtney female MCBH4F



Seen towards the connector

- 1* Channel 4+ (Black)
- 2* Channel 4- (White)
- 3 N/C (Red)
- 4 N/C (Green)

*Pins 7 and 8 on the 8-pin transducer connector are connected in parallel with pins 1 and 2 on the 4-pin transducer connector.



422357 / Rev. B / August 2017

Simrad

Kongsberg Maritime AS
Strandpromenaden 50
P.O.Box 111

Telephone: +47 33 03 40 00
Telefax: +47 33 04 29 87
www.simrad.com

SIMRAD

Technology Assesment
Rubric
Instrument / Sensor
Category:

No.	Instrument/ Sensor Type	Commercially Available (Can)		Manufacturer(s)/ Vendor(s)	Description and Target Use	Target or Typical Use	Other Use(s)?	Capabilities & Limitations	Anticipated Range	Sector(s) Use	Experience/ Robustness in High Flows			Experience with High Flows	Software Considerations	
		CA	R&D?			survey=census, distribution, possible size frequency		CW=continuous wave transmit pulse	dependent on frequency and power input		0-3 m/sec	3-5 m/ sec	5+ m/sec		Required or Additional Software	Data Processing & Analysis Considerations
	Simrad EK80	x		Kongsberg/Simrad	shipboard surface mount, needs power	survey		CW, multifrequency, broadband, matched filter, splitbeam	max 900 m	all sectors but autonomous	x		x (previous generation echosounder EK60)	Bay of Fundy Survey (Melvin), Admiralty Inset (Horne), the Fall of Warness Scotland (Williamson)	Acquisition, Processing (Echoview, LSSS, SonarX)	Python packages for data processing under development (e.g. echopy, ESP3, PyEcholab); R package for Echoview scripting; MatLab package Matecho
	Simrad WBAT	x		Kongsberg/Simrad	autonomous, underwater mount, battery included	survey/monitoring		CW, multifrequency, broadband, matched filter, splitbeam	max 450 m	autonomous deployments only	x	x	x	Admiralty Inlet (Horne), Bay of Fundy (FORCE)	Acquisition, Processing (Echoview, LSSS, SonarX)	Python packages for data processing under development (e.g. echopy, ESP3, PyEcholab); R package for Echoview scripting; MatLab package Matecho
	Simrad WBT Tube	x		Kongsberg/Simrad	underwater mount needs power	survey/monitoring		CW, multifrequency, broadband, matched filter, splitbeam	max 450 m	ROV and AUV, could be used on mooring and bottom packages	x				Acquisition, Processing (Echoview, LSSS, SonarX)	Python packages for data processing under development (e.g. echopy, ESP3, PyEcholab); R package for Echoview scripting; MatLab package Matecho
	Simrad WBT Mini	x		Kongsberg/Simrad	surface or pressurized container mount, needs power	monitoring		CW, multifrequency, broadband, matched filter, splitbeam	max 450 m	surface and glider deployments	x				Acquisition, Processing (Echoview, LSSS, SonarX)	Python packages for data processing under development (e.g. echopy, ESP3, PyEcholab); R package for Echoview scripting; MatLab package Matecho
	HTI Model 244	x		HTI Vemco	shipboard surface mount, needs power	survey/monitoring		multifrequency, wideband with matched filter, splitbeam	max 800 m	all sectors but autonomous	x				Acquisition, Processing (Echoview, SonarX)	
	BioSonics DTX Extreme	x		BioSonics	shipboard surface mount, needs power	survey/monitoring		CW, multifrequency, splitbeam	max 2000 m	all sectors but autonomous	x				Acquisition, Processing (Echoview, SonarX)	
	BioSonics DTX Extreme Sub	x		BioSonics	pressurized container mount, battery included	survey/monitoring		CW, multifrequency, splitbeam	max 2000 m	autonomous deployments only	x	x		Admiralty Inlet (Horne)	Acquisition, Processing (Echoview, SonarX)	
	ASL AZFP	x		ASL	autonomous, underwater mount, battery included	survey/monitoring		CW, multifrequency, single beam only	max 500 m	moorings and bottom mojnted packages	x	x		Chukchi Sea (Horne), Saanich Inset (Sato)	Acquisition, Processing (Echoview)	some MatLab and Python development
	ASL AZFP glider	x		ASL	autonomous, pressurized container mount, needs power	survey/monitoring		CW, multifrequency, single beam only	max 500 m	glider only	x				Acquisition, Processing (Echoview)	some MatLab and Python development
	Nortek Signature 100	x		Nortek	autonomous, underwater mount, battery included	survey/monitoring	ADCP included	multifrequency choice with wideband	max 400 m	new instrument, initial focus on moorings	x	?		Bransfield Strait (Reiss)	Acquisition	MatLab processing

	Kaijo/Sonic KSE-100			Sonic	shipboard surface mount, needs power	survey		CW, multifrequency, splitbeam	max 2000 m	limited use in Japanese surveys	x					Acquisition, Processing (Echoview)	
	Furuno FQ80			Furuno	shipboard surface mount, needs power	survey		CW, split beam; file format not directly supported		historic use in Japan, no longer available	x						FQ80 Analyser software converts to HAC format, then Echoview
	Imagenix 852/853	x		Imagenix	surface or pressurized container mount, needs power	survey/monitoring		CW, single frequency 120 kHz, single beam	max 100 m	limited use in autonomous gliders	x						MatLab processing

Supplemental / Other Details	References/ Web Links
NOAA effort for NetCDF format for data archive	https://www.simrad.com/www/01/NOKBG0240.nsf/AllWeb/941F9CBFD32D266EC1257C220047E755?OpenDocument
NOAA effort for NetCDF format for data archive	see spec sheet
NOAA effort for NetCDF format for data archive	see spec sheet
NOAA effort for NetCDF format for data archive	see spec sheet
no active development on instruments,	see spec sheet
broadband echosounder under development (due 2020)	see spec sheet
broadband echosounder under development (due 2020)	see spec sheet
second generation echosounder under development (due 2020)	see spec sheet
second generation echosounder under development (due 2020)	see spec sheet
potential development of alternate platform (e.g. glider) version (date unknown)	see spec sheet

	see spec sheet
not heavily supported, calibration difficult	see spec sheet

Appendix VIII

Active sonar environmental monitoring for Fundy tidal energy project



TECHNICAL SERIES

ACTIVE SONAR ENVIRONMENTAL MONITORING FOR
FUNDY TIDAL ENERGY PROJECT

A Panel Discussion by Subject Matter Experts

Spring 2019



Centre for Ocean Ventures and Entrepreneurship (COVE)

The Centre for Ocean Ventures and Entrepreneurship (COVE) is an ocean tech business hub that encourages collaboration across sectors to connect local, national and international companies in the ocean industry. We are a catalyst in creating the world's next commercial and revolutionary ocean tech advances by bringing together people, ideas, industry and research.

Strategically located on the Halifax Harbour, more than 55 companies are located at COVE, ranging from small ocean technology start-ups to large companies. The companies are focused on all sectors of the ocean economy – transportation, energy, the capture fishery & aquaculture, marine tourism, and defence & security. The programs, facilities and services offered through COVE bring the ocean technology cluster together to advance the competitive position of members in the global ocean industry.

For more information visit www.coveocean.com

Table of Contents

Foreword	5
Introduction.....	6
Discussion Summary.....	8
Appendix A: Post-meeting SME submissions	13

Foreword

The COVE Technical Series investigates and advances ocean technology challenges that potentially hold market value and are of interest to COVE tenants, stakeholders and ocean industry as a whole. This study, ***Active Sonar Environmental Monitoring for Fundy Tidal Energy: A Panel Discussion by Subject Matter Experts***, provides input on the current and near-future capability of active acoustic instrumentation, devices, and techniques for environmental monitoring in highly turbulent marine environments.

The support of the Ocean Technology Council of Nova Scotia (OTCNS) www.otcns.ca and the provincial and federal governments for this event and related activity is acknowledged. Irving Shipbuilding Inc. is a foundational contributing sponsor to COVE's programming and to IORE, the Institute for Ocean Research Enterprise.

This work was undertaken and its report prepared by Dr. Paul Hines of Hines Ocean S&T to whom we are grateful. He may be contacted as below:

Dr. Paul Hines
Hines Ocean S&T Consulting Inc.



phone: +1 (902) 809-0559
email: phines50@gmail.com



Government
of Canada

Gouvernement
du Canada



Introduction

The **Centre for Ocean Ventures and Entrepreneurship (COVE)** held a round-table discussion on active sonar technology and its underlying science with a select group of subject matter experts, on May 23rd 2019. This is in line with COVE's mandate to bring together people across ocean-industry sectors and research areas to identify and tackle ocean technology challenges with market potential. This round-table was a contribution to a broader set of projects related to environmental monitoring being planned within 'The Pathway'—a new initiative by the Offshore Energy Research Association of Nova Scotia (**OERA**) and The Fundy Ocean Research Center for Energy (**FORCE**). The goal of the meeting was to provide input on the current and near-future capability of active acoustic instrumentation, devices, and techniques for environmental monitoring in highly turbulent marine environments.

Problem statement: Tidal power is recognized as a clean, renewable source of energy. However, environmental monitoring of these systems can pose unique challenges. Underwater acoustic devices are a primary tool for monitoring fish and marine mammals. However, in environments such as the Bay of Fundy, the utility of these devices is severely restricted due to the high tidal flow-rates, and the subsequent eddies, whirlpools and vortices that entrain air bubbles well below the surface. Previous studies have shown that the high ambient background noise in this turbulent flow severely limits the utility of passive acoustic monitoring devices. Active sonar is a potential option but the entrained air interferes with transmission of active sonar signals, *and* causes high reverberation against which to detect the target echoes.

Objective: The goal of the round-table was to convene a panel of experts in active sonar technology *and its underlying science*, to discuss the limitations of existing technologies in these environments. Also under consideration, is whether these limits are imposed by the physics of the environment, or are simply artifacts of current active sonar technologies, which have not been optimized for these specific conditions.

Outcomes: The discussion is captured in this summary report and identifies the key points of the meeting and specific science and technology (S&T) questions that should be addressed to reach the stated objective. The goal is to have this report distributed to the attendees and stakeholders within a few weeks of the meeting. Moreover, the S&T questions that are identified herein may be used to guide the direction of funded research projects which are forthcoming as part of 'The Pathway' program.

Following this introduction, the meeting participants are identified and a summary of the panel discussion is presented. Post meeting comments provided by some of the subject matter experts (SME) are contained in Appendix A at the end of this report.

MEETING LOGISTICS AND OVERVIEW

The meeting was conducted at the COVE North Building, 4th floor conference room B. Video conferencing allowed remote attendees to "see and be seen" and contributed to their high level of engagement in the discussions. Table I lists the SMEs invited to the panel discussion as well as the other attendees and their primary roles. Entries in grey note SMEs who were unable to attend. Names followed by "R" were remote attendees.

Table I: Subject Matter Experts and other attendees to the panel meeting.

Name	Affiliation	Subject Matter Expertise (partial)
David Barclay	Dalhousie	TL modelling, ambient noise
Alex Hay	Dalhousie	Ocean acoustics, remote measurement of turbulence in tidal channels
Bruce Armstrong	GeoSpectrum	Transducer design
Sara Stout-Grandy	Vemco	Fish tagging and tracking
Craig Brown	NSCC	Ocean mapping, remote sensing, env. monitoring
Chris Loadman	TR	Sonar receiver design, signal processing
Jinshan Xu	DFO	General acoustics, physical oceanography, fish acoustics
Ian Church	UNB	Ocean mapping, hydrodynamic modelling
Olivier Beslin	UEMS	Turbulent Boundary Layer, towed arrays
Brendan Harvey	UEMS	DCL, towed arrays, sonar
Joe Hood	GeoSpectrum	PD-PFA, DCL
Ron Kessel, R	SAL	TL modelling, HF sonar, high-res sonar
Tom Weber, R	UNH	Fish sonar, bubble scattering
Andone Lavery, R	WHOI	AUV navigation in turbulent rivers
John Horne, R	UW-SAFS	HF sonar for fish monitoring
Name	Affiliation	Role
Paul Hines	HOST	Moderator/Chair
Dan Hasselman	FORCE	Supporting Context/Co-chair
Tyler Boucher	FORCE	Supporting Context
Tony Wright	FORCE	Observer
Alisdair McLean	OERA	Observer/Stakeholder
Luiz Faria	OERA	Observer/Stakeholder
Shawna Eason	NSDOE	Observer/Stakeholder
Leslie Munro	COVE	Meeting support
Cal Murphy	COVE	Meeting support
Kylee Weir	COVE	Meeting support

A simple agenda (shown in Table II) was distributed prior to the meeting to provide some general guidance to the discussion and ensure time was spread over several topics of interest. The agenda was accompanied with the six questions show below. These questions were used to motivate discussion; however, the discussion was not limited to addressing these questions.

- Q1. Are existing linear acoustic models sufficiently accurate for this environment (small amplitude, and more importantly, no rotational flow, i.e. $\text{Curl} = 0$)?
- Q2. Does entrained air represent a physical limit or can we design systems around it?
- Q3. Are active sonars at their functional limits, or are they just poorly matched to work in turbulent flow?
- Q4. Will we get more traction from increasing Signal, or decreasing Noise?
- Q5. Will we get more traction from improving hardware (sensors) or improving software (DCL?)
- Q6. What should we be measuring/modelling *right now* to fast track progress in this topic?

Table II: Proposed meeting agenda.

Time (ADT)	Event	Name	Comments
11:30-12:15	Lunch	Local Participants	
12:15	Assemble	All	
12:30	Opening remarks	Hines, Hasselman	Review problem statement and context
12:40	Panel Introductions	Hines	Introduction of relevant expertise of participants
13:00-16:00	Moderated Panel Discussion		
13:00	Part 1: Challenges of the Physical Environment		
13:45	Part 2: Technology Solutions: Current Capability and Ongoing Development		
14:30	Part 3: The Key S&T Questions (Experiment and Theory)		
15:30	Part 4: Wrap Up		

Discussion Summary

The SME's represent a broad range of expertise necessary to tackle the very challenging objective laid out in the introduction. The round table meeting was an active and engaging technical discussion with all participants contributing clearly articulated, deep technical insights throughout the three and one-half hour exchange.

Following opening remarks from the moderator and a short welcome from Mr. Alisdair McLean of OERA the technical exchange began. First, a short presentation on the technical challenge was provided by Dr. Daniel J. Hasselman. This reinforced the problem statement identified in the introduction. The environmental monitoring program includes hydroacoustic fish surveys done using transects across the test site and across the bay using an EK80 split beam echosounder to do a 24-hour survey (2 ebb/flood cycle). The video output from Echoview contains a substantial amount of backscatter noise from the entrained air bubbles and sediment throughout much of the water column. Separating the signal (fish echoes) from the noise (scatter from bubbles and sediment) is the primary challenge.

The discussion began by considering whether linear acoustic models are sufficiently accurate for this environment. David Barclay responded that although there may be some flow-related effects, he felt the linear acoustic models in place were adequate to tackle the problem. Scatter from bubbles was the real issue. The SMEs agreed with this observation.

Ron Kessel made a clear distinction between turbulence and entrained sediment and bubbles. Turbulence will not generate scatter; its only relevance is that it entrains sediment and air bubbles which cause scatter. (Moderator note: Turbulence will also raise the ambient noise background which may or may not be the limiting factor in active sonar. In the present case however, volume reverberation from the bubbles is likely the limiting factor.) He suggested that the best way to monitor fish in the immediate vicinity of a turbine (20 m to 50 m) is to reduce bubble noise. High-resolution multi-beam imaging sonars might be considered (e.g., BlueView P450, RESON Seabat 7128, and possibly the much shorter range and much higher-frequency DIDSON sonar). High resolution imaging sonars:

1. dramatically decrease the volume V for bubble backscatter (smaller region of interest and the very narrow beamwidths of multibeam imaging sonars (0.5 to 1.5 degrees). It is expected that bubbles will not be a problem, but this is must be tested *in situ*.
2. give nearly visual-quality scene-rendering with fish evident (presumably restrictions on fish body and schools size apply), with the immediate understanding and impact that visual scenes have for non-experts concerned about impact on fish.
3. should be positioned with the sonar line of sight perpendicular to fish-path into turbine, to maximize the target strength (broadside) of fish.

Jinshan Xu raised concerns that the sonar location for FORCE's mobile fish surveys may be too close to the ship hull and may have contributed to the entrained air observed on Echograms. Ultimately, the panel felt that this was a fairly standard approach and bubble scattering was due to turbulence from the flow, not from the ship hull. Tom Weber felt that measurements should be made as deep as possible to reduce bubble density. Dan Hasselman noted that the flow can be energetic enough to entrain bubbles all the way through the 20 m water column.

It was suggested that lowering frequency would reduce the scatter from bubbles. John Horne cautioned that going down in frequency could impact marine mammals (MM). After a short discussion, it was concluded that the harbour porpoise is the only MM in the area, and we should first see if we can select a frequency that maximizes the signal-noise ratio (SNR) for this problem and then deal with MM mitigation for the harbour porpoise as required.

Joe Hood and Brendan Harvey contributed substantially to an important discussion on signal processing that was on-going throughout the meeting. Several important points came out of this:

1. Echoview is the standard for fishery acoustics but the video displays substantially compress the dynamic range from as much as 24 bits down to about 8 bits. Doing this throws away a

substantial amount of information. Fortunately, Echoview does enable one to access the raw data. Much of the raw acoustic data collected for the tidal energy project has been stored. FORCE will enquire as to the release conditions on the data. This data should be mined to see if there are better approaches to detection, classification, localization and tracking (DCLT).

2. There may be gains obtained by using more complex time-frequency signals than current systems use. This includes optimizing (or at least improving) the center frequency, the bandwidth, and the pulse type of the transmitted signals.

3. Classification, rather than simple detection, should be investigated. Currently much of the classification is done manually by visually assessing the data. Do fish echoes have features that make it look different than the scatter which would help identify fish? Tracking may also help reduce false alarms. (Note that the small field of view that would be a by-product of the very short range sonar suggested earlier would adversely effect tracking.) John Horne noted that tracking work is being done by tagging fish and sending them through scale models of a tidal device this summer.

4. There was general consensus that we are probably not at the limit of technology but commercially available technology might not be suited for this application. In general, try to avoid using consumer grade (COTS) software. Data is being processed and information might not fully convey the total information that is gathered. Accessing the raw data will enable analysis using scientific algorithms written in high level languages such as IDL or Matlab to see if improvements can be made.

John Horne provided some background on monitoring: Biomass estimates are based on echo integration. Must look at pulse widths and frequencies. Detectability probability of frequent targets. Split beam algorithms for single targets. During tidal cycle you will have echo integration as opposed to echo counting of individual targets. Densities will be species-dependent. Aggregations that you would see through tidal cycle will depend on combination of species and turbulence and tidal state. Colour palette might be biasing interpretation of data. Full digital data is available that can be used for full analytic capability from EK80. To look at detection of fish in turbulent zones he recommended the paper by Fraser et al. (Automatic active acoustic target detection in turbulent aquatic environments, 2017 in *Limnology and Oceanography: Methods*).

John Horne said that current detection in the fish acoustics field uses Target strength first–amplitude-based to discriminate frequencies; 2nd is multi-frequency differencing – differences in wavelengths and direction of targets. With availability of broadband signals there is renewed interest in full spectrum or partial spectrum comparisons. What's come from that is machine learning and AI for characterization of unique signatures. Constructive and destructive interference on fish bladder from fish body and outside sources. Body plus swim bladder returns from an animal must be considered and swim bladder cannot be the only defining characteristic.

Craig Brown strongly advocated for ground truth validation of any detection and classification estimates.

Sara Stout-Grandy noted that Vemco/Innovasea and Acadia University (Dr. Anna Redden in the Acadia Tidal Energy Institute) are pursuing some funding to use machine learning on active sonar detections to identify fish around turbines. Dr. Redden has already done a lot of work around turbines in the Bay of Fundy with Vemco's fish tracking equipment. (Note: Machine learning for this purpose is also being worked on in Norway by Niels Hendergard at IMR.)

There was some discussion on monitoring animal-device interactions vs. monitoring population effects (domain monitoring) which require different approaches. While monitoring in other jurisdictions (i.e. United Kingdom) suggests that turbine interactions with individual marine animals are relatively rare, the nature of these interactions in the Bay of Fundy has yet to be quantified and needs to be addressed. Domain monitoring—are the devices affecting the long term health of the population—is far more critical. The species of special status are particularly important (salmon and sturgeon in the case of Fundy). Some feel that the inshore fishing community is against anything going in the water and DFO is not taking a constructive role in managing this process.

David Barclay suggested developing a fluid-acoustic coupled model. Could we go from theory to a model without doing any experimental work, and still feel confident in its performance? Alex Hay responded that we have basic information on turbulence models as a function of flow speed using characteristic measures of turbulence. There is enough information to provide input to such a model although some assumptions would still need to be made. You could have a basis for how the fluid would behave statistically in relation to the sonar. The question is, how will the fish behave relative to the turbulence? What scales of turbulence affect the fish? What is the relationship between turbulence and fish detection other than the presence of bubbles? Answers to these questions could be used as a performance prediction tool to determine subsequent monitoring equipment requirements.

Although the SMEs covered much of the primary expertise needed for the discussion, the consensus was that, given that Echoview is the standard for fishery acoustics, it would be helpful to have had a technical expert on Echoview present at the discussion. Sara Stout-Grandy suggested someone from HTI-Vemco in Seattle as a candidate and Dan Hasselman suggested Haley Viehman. Dan Hasselman suggested a fish-behaviour specialist would be helpful to understand their behaviour around bubbles. It was noted that some species refuse to cross bubble curtains and cetaceans will often form a bubble cloud to surround fish schools to trap them. *Could this technique be used to direct fish away from the turbines?*

Meeting Wrap up: To conclude the meeting the Moderator asked each SME to provide closing comments. Many of the comments were echoed around the table, so they are not attributed to a single SME. These comments are summarized below:

1. A coupled fluid-acoustic model with a short range experiment to validate for single device interaction should be developed.

2. Reprocess the existing raw data using non-COTS software to see if improved detection and classification can be achieved. Survey data from the FORCE site using multibeam data could be useful as well.
3. An approach to wide area monitoring (vs. single turbine monitoring) should also be considered as it is an obvious next-step in environment monitoring.
4. Bottom-mounted sonar data should be processed and analyzed and compared with the ship-based transect data. Differences between these data could help with our understanding of the monitoring challenge.
5. Validation of targets (fish) will be challenging, but is nonetheless critical. An optical system will be deployed along with a multibeam system to provide ground-truth data in an upcoming project with OERA. Ocean mapping might provide context for signal processing.
6. Use multi-frequency EK. Crowd-source the data analysis.
7. Experiment with various waveforms, frequencies and bandwidths, to see what kind of information can be extracted. A thorough review the literature should be done to understand what has already been done.
8. Long term monitoring is important to understand how population is affected. Fixed systems are more efficient for long term modelling.
9. Get statistical models of scattering from fish vs bubbles. For single-device monitoring, one can reduce volume scattering by bringing sonar closer to the targets, or reduce the operating frequency. Depends on target area of fish and field of view. Check with manufacturers to see who wants to test their equipment at the site to get access to equipment. (Note, some nearfield device testing work has been done by a group off Oregon Coast for wave energy test centre.)
10. Examine if there is a threshold at which the bubble field entirely obscures the fish signal.

Appendix A: Post-meeting SME submissions

Dr. David Barclay recommended the following paper on scattering from mixed assemblages:

1. Wu-Jung Lee and Timothy K. Stanton, "Statistics of Echoes From Mixed Assemblages of Scatterers with Different Scattering Amplitudes and Numerical Densities," *J. Oceanic Eng.*, **39**, no. 4, p. 740, 2014.

Dr. John Horne recommended the following papers for information on domain monitoring:

2. John K. Horne and Dale A. Jacques II, "Determining representative ranges of point sensors in distributed networks," Springer International Publishing AG, part of Springer Nature 2018, p. 347, May 2018.
3. Hannah L. Linder and John K. Horne, "Evaluating statistical models to measure environmental change: A tidal turbine case study," **84** p. 765, *Ecological Indicators*, 2018.
4. Hannah L. Linder, John K. Horne, and Eric J. Ward, "Modeling baseline conditions of ecological indicators: Marine renewable energy environmental monitoring," **83** p. 178, *Ecological Indicators*, 2017.
5. Lauren E. Wiesebron, John K. Horne, Beth E. Scott, Benjamin J. Williamson, "Comparing nekton distributions at two tidal energy sites suggests potential for generic environmental monitoring," *Intl. J. Marine Energy*, **16**, p. 235, 2016.
6. Lauren E. Wiesebron, John K. Horne, and A. Noble Hendrix, "Characterizing biological impacts at marine renewable energy sites," *Intl. J. Marine Energy*, **14**, p. 27, 2016.

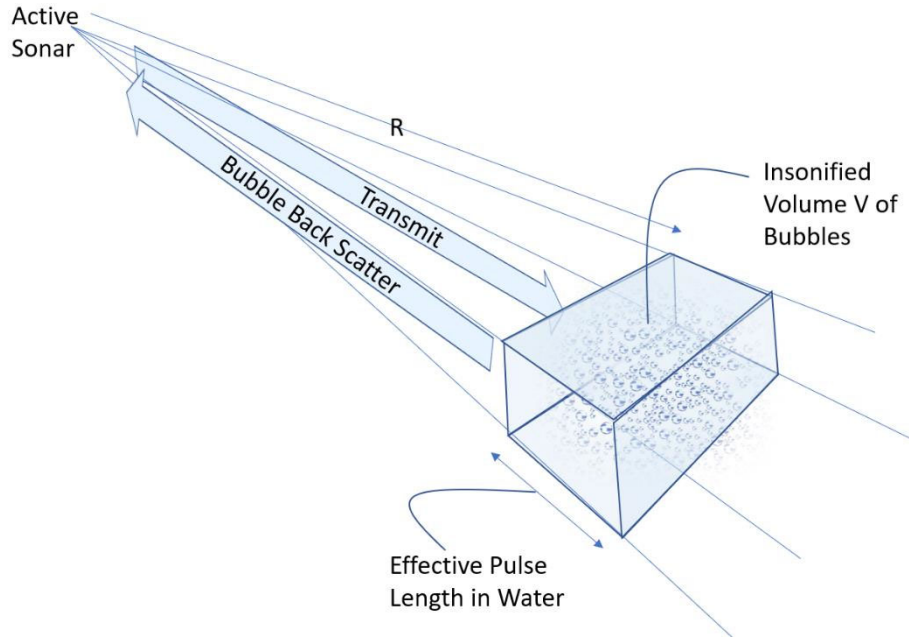
Dr. Sara Stout-Grandy submitted the six seed questions contained in the agenda to her colleagues at HTI-Vemco in Seattle (<http://www.htisonar.com/>). They have about 30 years of experience using their echosounder around DAMs to monitor/track fish around them. Below are their replies:

- a. Q1. Are existing linear acoustic models sufficiently accurate for this environment? (small amplitude, and more importantly, no rotational flow, i.e. $\text{Curl} = 0$). The propagation model (I think) this question is addressing is probably not that important for our work. We would probably locate the transducers so that fish targets were 10s of meters (not hundreds of meters) way from the transducer. Over those distances, arrival times and amplitudes would not be altered that much. Most of the parameters we might consider for species identification would be related to aggregations of returning echoes (tracks), or possibly relative amplitudes of discrete frequencies. What might come into play is Doppler shift of the echoes if the fish targets are moving very fast. Another possibility would be variability in amplitude or variability in pulse length of echoes.
- b. Q2. Does entrained air represent a physical limit or can we design systems around it? Yes air is a serious problem— although lower frequencies may allow limited improvement in some cases. Also, forward scattering has been used to retrieve at least some data in very poor acoustic environments, although only presence/absence is likely to be available.
- c. Q3. Are active sonars at their functional limits, or are they just poorly matched to work in turbulent flow? There are certainly areas that could be explored, but these are primarily in the data processing end – not so much the physical sound transmission and reception aspect of the signals. Looking at multiple channels and Doppler shifts (as the HR3 tag receiver does) might be one such avenue to go down.

- d. Q4. Will we get more traction from increasing Signal, or decreasing Noise? Either way would help! Our challenge has always been that the electronics have very low noise and is insignificant compared to the environmental noise – which we cannot control. I’m not sure about how some sort of active noise-cancelling scheme might work with narrow-band acoustics, but maybe there is something there. We have been successful at increasing signal by using wide-band signals (FM slide) and matched filter processing – perhaps there are more aggressive ways to use these techniques to get better results.
- e. Q5. Will we get more traction from improving hardware (sensors) or improving software (DCL?) I think that the software side is where significant advances will come – in terms of capabilities. Sensors are well developed – although the best ones are still expensive. Improvements to hardware will likely be to bring the price down.
- f. Q6. What should we be measuring/modelling *right now* to fast track progress in this topic? Water velocities and physical mounting, aiming, and coverage requirements have always been major challenges. Knowledge about species present, behavioral data, and fish sizes is also helpful.

Dr. Ron Kessel of Seamout Analytics (<https://seamountanalytics.ca/>) submitted the following observations to the panel shortly after the meeting closed.

The troublesome fish-masking phenomenon illustrated at the outset of the workshop, for an echo sounder using the Echoview software, was variously attributed to “bubbles”, “turbulence”, “noise”, “reverberation”, and “volume scattering”. The worst term is *turbulence*. It is like using the term “wind” for clouds in the sky. Turbulence below super sonic speeds is invisible to sonar except insofar as the turbulence happens to entrain bubbles, sediments, or thermal/salinity/density contrasts. The best terms are *volume reverberation* or *volume scattering*, which expressly feature in the sonar equation (R. Urick, Principles of Underwater Sound, 3rd Ed). Volume scattering strength for wind-wave injected bubbles is included in the sonar equation by Medwin and Clay for instance (Medwin and Clay, Fundamentals of Acoustical Oceanography). When bubbles mask targets as in the echo- sounder data, the sonar is *reverberation limited*.



Signal to Noise Ratio: Assuming spherical beam spreading, the received signal (in dB) from fish decreases by the two-way propagation loss $-2 \times 10 \log_{10} R = -40 \log_{10} R$, while the backscatter from a uniform bubble cloud is the combined effect of the two-way propagation loss and the increasing size of the scattering volume $-40 \log_{10} R + 10 \log_{10} R^3 = -10 \log_{10} R$. The signal-to-noise ratio (SNR) for fish in a uniform bubble cloud therefore decreases as $-40 \log_{10} R + 10 \log_{10} R = -30 \log_{10} R$. SNR for fish in a uniform bubble therefore decreases by 9 dB for every doubling of range. This is a severe range limitation. It applies for conical echo-sounder beams as well.

Bubbles also increase the sonar propagation losses through a bubble cloud. This is bubble extinction (cf. Medwin and Clay, *Fundamentals of Acoustical Oceanography* or Kessel, "Bubble Extinction Model", Maritime Way Scientific Technical Note, 16-May-2017). If bubbles are confined to the sea surface, then bubble extinction can decrease the received fish signal owing to higher two-way propagation losses through the bubble cloud. Bubble extinction does not change the conclusions in point 2 above because extinction affects the fish signal and bubble backscatter levels to the same degree in a uniform bubble cloud.

Volume backscatter from bubbles decreases as the:

- a. insonified volume V decreases, by:
 - i. increasing the sonar resolution (narrowing the sonar beam);
 - ii. decreasing the effective pulse length in the water (increasing the sonar bandwidth);
 - iii. decreasing the survey range R , by surveying/monitoring a smaller water volume, such as in the immediate vicinity of a turbine for instance.
- b. sonar frequency is decreased—whose benefit generally is countered somewhat (perhaps entirely?) by the increasing beam width (insonified volume) that attends lower-frequency sonar when size and cost are constrained.

Monitoring of fish in the immediate vicinity of a turbine, on distances on the order of 20 m to 50 m, using high-resolution multi-beam imaging sonars might be considered (e.g., BlueView P450, RESON Seabat 7128, and possibly the much shorter range and much higher-frequency DIDSON sonar). High resolution imaging sonars:

- a. dramatically decrease the volume V for bubble backscatter owing to both the smaller region of interest and the very narrow beam widths of multibeam imaging sonars (on the order of 0.5 to 1.5 degrees). It is expected that bubbles will not be a problem, but this is must be tested in situ.
- b. give near visual quality scene rendering with fish evident (presumably restrictions on fish body and schools size apply), with the immediate understanding and impact that visual scenes have for non-experts concerned about impact on fish.
- c. should be positioned with the sonar line of sight perpendicular to fish-path into turbine, to maximize the target strength of fish at risk.

Tracking: Imaging sonars are rather like video cameras, with a frame rate equal to the ping-rate of the sonar. Tracking of fish amounts to tracking of high-contrast objects in video imagery. A simple back-of-the-envelope task-based configuration design, coordinating sonar resolution, coverage area, ping rates (frame rate for imaging sonar) could be carried out (Kessel, Pastore, Crawford, and Crowe “Commercial Imaging Sonars for Observing Underwater Intruders”, proceedings of the Waterside Security 2008 (WSS2008), Aug 2008).

My experience with the sonar manufacturer’s is that they would be happy to provide COVE a loaner sonar for trials.

EchoView: One point to be made about the EchoView viewing of an echosounder echograph is that *any* visual rendering loses echograph information. Why? Because the human eye can discriminate only about 256 monochromatic contrast levels in an image, hence 8 bits of contrast information, in three colours (RGB), which is far below the 24-bit information generally contained in an echograph. High glints in an echograph are usually clipped very severely in visual rendering for instance, losing the information that glints carry. This is not a criticism of EchoView. It is a shortcoming of *any* visual rendering of an echograph by any means. It could be that changing the EchoView rendering parameters far outside their usual regime, or, leaving EchoView aside and applying customized image or signal processing to the echograph, may (emphasize *may*) bring fish out for detection amid bubbles under some conditions.

Appendix IX

Passive acoustic monitoring in a tidal energy environment:
Comparing acoustic data from three measurement positions in
the Minas Passage



Passive Acoustic Monitoring in a Tidal Energy Environment

Comparing Acoustic Data from Three Measurement Positions in the Minas Passage

Submitted to:

Dan Hasselman
Fundy Ocean Research Centre for Energy
(FORCE)

Authors:

Colleen Wilson
Bruce Martin

13 September 2019

P001146-005
Document 01774
Version 2.1

JASCO Applied Sciences (Canada) Ltd
Suite 202, 32 Troop Ave.
Dartmouth, NS B3B 1Z1 Canada
Tel: +1-902-405-3336
Fax: +1-902-405-3337
www.jasco.com



Suggested citation:

Wilson, C.C. and S.B. Martin. 2019. *Passive Acoustic Monitoring in a Tidal Energy Environment: Comparing Acoustic Data from Three Measurement Positions in the Minas Passage*. Document 01774, Version 2.1. Technical report by JASCO Applied Sciences for Fundy Ocean Research Centre for Energy (FORCE).

Disclaimer:

The results presented herein are relevant within the specific context described in this report. They could be misinterpreted if not considered in the light of all the information contained in this report. Accordingly, if information from this report is used in documents released to the public or to regulatory bodies, such documents must clearly cite the original report, which shall be made readily available to the recipients in integral and unedited form.

Executive Summary

Passive acoustic monitoring (PAM) is expected to be an important component of environmental management plans around marine hydro-kinetic energy sites, including tidal turbines. There are two main roles envisioned for PAM: 1) measuring sound emitted by turbines to determine the distance at which it may injure or disturb marine life and 2) monitoring the presence of vocalizing marine animals (especially porpoises) and how they interact with the turbines. In both roles, it is important to understand the noise levels from true sounds in the environment and pseudo-noise generated by flow around the hydrophones used to record the data.

Previous work analyzed data from drifting, turbine-mounted hydrophones and autonomous hydrophones during the first deployment of the OpenHydro Open-Centre turbine at the Fundy Ocean Research Centre for Energy (FORCE) site in Minas Passage, NS. It was demonstrated that drifting hydrophones had the lowest noise levels, as expected, but they were limited to measurement durations on the order of minutes. Drifters are well suited for determining the acoustic propagation loss for sound emitted by the turbine because drifters can measure sound levels as a function of range as they move past the turbines. Flow noise on hydrophones fixed to the turbine platform depended on the height of the hydrophone off the seabed, where higher hydrophones had more flow noise. Flow noise measured by the hydrophone on top of the turbine extended as high as 10 kHz in frequency. An autonomous hydrophone on the seabed had lower flow noise sound levels than the turbine mounted hydrophones. Relationships between flow speed, current direction, and turbine operating mode were developed that allow users to predict sound levels for future applications. The previous work was unable to compare sound levels before and after the turbine was installed since data were not recorded prior to the turbine installation.

This report analyzes data collected from June to November 2018. Data were available from a JASCO Autonomous Multichannel Acoustic Recorder (AMAR) in the same autonomous mooring used in 2016. The AMAR data is available for the entire June-November period. Data are also available for parts of September 2018 from icListen hydrophones mounted on the turbine and an icListen hydrophone mounted on a FAST platform 60 m from the Open-Centre turbine. The turbine was installed in late July 2018 and ceased operating on 9 Aug 2018.

The objectives of the current analysis were to further compare the noise levels at different measurement locations. A secondary objective was to further analyze how the turbine contributed to the soundscape using the limited data available. Similar to the previous results, the measured sound levels due to flow noise increased with the height of the hydrophone off the seabed. The hydrophone on top of the turbine was most affected by flow-induced noise—out to ~2.5 kHz at the 90th percentile of flow speed. For comparison, the two least affected locations ('Aft' turbine hydrophone and the autonomous AMAR hydrophone) were only affected by flow noise out to 160 Hz. All hydrophone positions measured approximately the same spectral and decidecade sound levels for frequencies above their flow noise cut-offs. The ambient sound above the flow cut-off frequencies also increased with current speed; however, these changes were likely due to increases in entrained bubbles and sediment movement.

When the turbine was present (and presumably free spinning) the sound levels increased in the 30–1000 Hz band. The flow-induced noise on the 'aft' and autonomous recorders was low enough to successfully measure the sound from the turbine; however, the FAST platform and 'stbd' locations had floor noise levels high enough that they would have had difficulty quantifying the turbine noise in free spinning mode.

The flow-induced noise at all recording locations were similar above 3 kHz and therefore all locations are equally appropriate for detecting porpoise.

There were two unexpected results: 1) the decidecade sound pressure levels on the turbine 'aft' hydrophone were up to 30 dB quieter than the same type of hydrophone in the 'stbd' location and 2) the decidecade sound pressure levels on the autonomous recorder were up to 20 dB quieter after the neoprene cover designed to protect the hydrophone from flow was removed.

Contents

EXECUTIVE SUMMARY	I
1. INTRODUCTION	1
2. GENERAL METHODS	2
2.1. Data Collection	2
2.2. Data Analysis	3
2.3. Recorder Calibration	3
3. RESULTS	4
3.1. Acoustic Doppler Current Profiler (ADCP) Data	4
3.2. Turbine-mounted icListen Results	4
3.3. Platform icListen Results	5
3.4. HFM AMAR Results	5
4. DISCUSSION	6
4.1. Comparison of Recording Locations	6
4.2. Correlation of Hydrophone and ADCP data	9
LITERATURE CITED	14
APPENDIX A. DETAILED METHODS	A-1
APPENDIX B. RESULTS	B-1
APPENDIX C. DECIDECAD E SOUND PRESSURE LEVEL TABLES	C-1

Figures

Figure 1. Recorder locations	2
Figure 2. Water depths and total root-mean-square (rms) water speeds at the first 0.5 m bin (near-bottom) measured by the Acoustic Doppler current profiler (ADCP).....	4
Figure 3. Comparison of all hydrophones at each percentile at all measured frequencies.	7
Figure 4. Band SPL at each calculated decidecade band frequency for the specified percentiles.	8
Figure 5. Aft hydrophone correlogram	10
Figure 6. Starboard hydrophone correlogram.....	11
Figure 7. Top hydrophone correlogram	11
Figure 8. FAST platform hydrophone correlogram	12
Figure 9. HFM AMAR hydrophone correlogram	13
Figure A-1. General arrangement drawing for the Open-Centre Turbine showing the locations of the icListen hydrophones.	A-2
Figure A-2. FAST platform with two icListen hydrophones.	A-3
Figure A-3. Platform orientation	A-3
Figure A-4. High Flow Mooring (HFM) design.	A-4
Figure A-5. Inside the high-flow mooring.	A-5
Figure A-6. Cover of the JASCO High Flow Mooring.	A-5
Figure A-7. Split view of a G.R.A.S. 42AC pistonphone calibrator with an M36 hydrophone	A-6
Figure B-1. (Top) in-band SPL and (bottom) spectrogram for the Aft hydrophone for 7–22 Sep 2018.....	B-1
Figure B-2. (Top) Exceedance percentiles and mean of the decidecade band SPL and (bottom) exceedance percentiles and probability density (grayscale) of 1-min PSD levels	B-2
Figure B-3. Cadence spectrogram for the hours since high tide, for the Aft Hydrophone for 7–22 Sep 2018.....	B-3
Figure B-4. (Top) in-band SPL and (bottom) spectrogram for the Starboard hydrophone for 7–22 Sep 2018.....	B-4
Figure B-5. (Top) Exceedance percentiles and mean of the decidecade band SPL and (bottom) exceedance percentiles and probability density (grayscale) of 1-min PSD levels	B-5
Figure B-6. Cadence spectrogram for the hours since high tide, for the Starboard hydrophone for 7–22 Sep 2018.....	B-6
Figure B-7. (Top) in-band SPL and (bottom) spectrogram for the Top hydrophone for 7–22 Sep 2018..	B-7
Figure B-8. (Top) Exceedance percentiles and mean of the decidecade band SPL and (bottom) exceedance percentiles and probability density (grayscale) of 1-min PSD levels	B-8
Figure B-9. Cadence spectrogram for the hours since high tide, for the Top hydrophone for 7–22 Sep 2018.....	B-9
Figure B-10. (Top) in-band SPL and (bottom) spectrogram for the FAST platform hydrophone for 7–22 Sep 2018.....	B-10
Figure B-11. (Top) Exceedance percentiles and mean of the decidecade band SPL and (bottom) exceedance percentiles and probability density (grayscale) of 1-min PSD levels	B-11
Figure B-12. Cadence spectrogram for the hours since high tide, for the FAST platform hydrophone for 7–22 Sep 2018.	B-12
Figure B-13. (Top) in-band SPL and (bottom) spectrogram for the AMAR hydrophone for July to November 2018.	B-13
Figure B-14. (Top) Exceedance percentiles and mean of the decidecade band SPL and (bottom) exceedance percentiles and probability density (grayscale) of 1-min PSD levels	B-14

Figure B-15. Cadence spectrogram for the hours since high tide, for the AMAR hydrophone July to November 2018.	B-15
Figure B-16. (Top) in-band SPL and (bottom) spectrogram for the AMAR hydrophone during the pre-turbine operation period, 1–22 Jul 2018.	B-16
Figure B-17. (Top) Exceedance percentiles and mean of the decidecade band SPL and (bottom) exceedance percentiles and probability density (grayscale) of 1-min PSD levels compared to the limits of prevailing noise (Wenz 1962) for the AMAR hydrophone during the pre-turbine operation period, 1–22 Jul 2018.	B-17
Figure B-18. Cadence spectrogram for the hours since high tide, for the pre-turbine operation AMAR hydrophone, 1–22 Jul 2018.	B-18
Figure B-19. (Top) in-band SPL and (bottom) spectrogram for the AMAR hydrophone during the turbine operation period, 22 Jul to 9 Aug 2018.	B-19
Figure B-20. (Top) Exceedance percentiles and mean of the decidecade band SPL and (bottom) exceedance percentiles and probability density (grayscale) of 1-min PSD levels compared to the limits of prevailing noise (Wenz 1962) for the AMAR hydrophone during the turbine operation period, 22 Jul to 9 Aug 2018.	B-20
Figure B-21. Cadence spectrogram for the hours since high tide, for the turbine operation AMAR hydrophone, 22 Jul to 9 Aug 2018.	B-21
Figure B-22. (Top) in-band SPL and (bottom) spectrogram for the AMAR hydrophone during the post-turbine operation period, ~25 Aug to 30 Oct 2018.	B-22
Figure B-23. (Top) Exceedance percentiles and mean of the decidecade band SPL and (bottom) exceedance percentiles and probability density (grayscale) of 1-min PSD levels compared to the limits of prevailing noise (Wenz 1962) for the AMAR hydrophone during the post-turbine operation period, ~25 Aug to 30 Oct 2018.	B-23
Figure B-24. Cadence spectrogram for the hours since high tide, for the post-turbine operation AMAR hydrophone, ~25 Aug to 30 Oct 2018.	B-24

Tables

Table 1. Recording dates, mounting locations and sample rates of each hydrophone.	2
Table 2. Summary of the effects of flow speed on flow-induced noise cut-off frequency and increase in sound levels.	9
Table A-1. Data from the turbine-mounted icListen.	A-1
Table A-2. Data from the platform icListen.	A-2
Table A-3. AMAR deployment locations	A-3
Table A-4. HF AMAR recording schedule	A-4
Table C-1. Aft hydrophone decidecade band percentile values	C-1
Table C-2. Starboard hydrophone decidecade band percentile values	C-2
Table C-3. Top hydrophone decidecade band percentile values	C-3
Table C-4. FAST platform hydrophone decidecade band percentile values	C-4
Table C-5. HFM (pre-turbine) hydrophone decidecade band percentile values	C-5
Table C-6. HFM (turbine on) hydrophone decidecade band percentile values	C-6
Table C-7. HFM (post-cover loss) hydrophone decidecade band percentile values	C-7

1. Introduction

Passive acoustic monitoring (PAM) is expected to be an important component of environmental management plans around marine hydro-kinetic energy sites, including tidal turbines. There are two main roles envisioned for PAM: 1) measuring sound emitted by turbines to determine the distance at which it may injure or disturb marine life and 2) monitoring the presence of vocalizing marine animals (especially porpoises) and how they interact with the turbines. In both roles, it is important to understand the noise levels from true sounds in the environment and pseudo-noise generated by flow around the hydrophones used to record the data.

Martin et al. (2018) analyzed data from drifting, turbine-mounted hydrophones and autonomous hydrophones during the first deployment of the OpenHydro Open-Centre turbine at the Fundy Ocean Research Centre for Energy (FORCE) site in Minas Passage, NS. They demonstrated that drifting hydrophones had the lowest noise levels, as expected, but they were limited to measurement durations on the order of minutes. The report concluded that drifters are well suited for determining the acoustic propagation loss for sound emitted by the turbine because drifters can measure sound levels as a function of range as they move past the turbines. Flow noise on hydrophones fixed to the turbine platform depended on the height of the hydrophone off the seabed, where higher hydrophones suffered from higher levels of flow-induced noise. Flow noise measured by the hydrophone on top of the turbine extended as high as 10 kHz in frequency. The autonomous hydrophone had lower flow noise measurements than the turbine mounted hydrophones. Relationships between flow speed, current direction, and turbine operating mode were developed that allow users to predict sound levels for future applications.

The Martin et al. (2018) report was unable to compare sound levels before and after the turbine was installed since data were not recorded prior to the turbine installation. The data also contained few porpoise detections, which was unsurprising because porpoise activity typically peaks in May to June, and the data were recorded in November and December 2016.

This report analyzes data collected from June to November 2018. Data were available from a JASCO Autonomous Multichannel Acoustic Recorder (AMAR) in the same autonomous mooring used in 2016. The AMAR data were available for the entire June-November period; however, approximately halfway through the period the neoprene cover was torn from the mooring cover. Data were also available for parts of September 2018 from icListen hydrophones mounted on the turbine and an icListen hydrophone mounted on a FAST platform 60 m from the Open-Centre turbine. The turbine was installed in late July 2018 and ceased operating on 9 Aug 2018.

This report aims to:

1. Compare sound levels at measurement locations using the 1-minute power spectral density (PSD) and decidecade sound pressure levels to determine frequencies impacted by flow noise in the 10th, 25th, 50th, 75th, and 90th percentiles.
2. Evaluate the performance of the hydrophones with respect to flow noise and system noise.
3. Compare the sound levels in Minas Passage without the turbine, with the turbine free-spinning, and with the turbine stationary.
4. Examine the impact of the loss of the neoprene cover from the AMAR high-flow-mooring.

Section 2 provides an overview of the methods employed for data collection and analysis, which are explained in more detail in Appendix A. Section 3 provides the high-level results obtained, with supplemental figures provided in Appendix B. Section 4 contains a comparison of the spectral percentiles and decidecade percentiles between monitoring positions and sensors.

2. General Methods

This section summarizes the measurements and the analysis performed on the data. Detailed methods including information on the recorders is contained in Appendix A.

2.1. Data Collection

Acoustic data were recorded using a JASCO AMAR housed in a high-flow mooring, two autonomous icListen hydrophones on a FAST platform, and four cabled icListens mounted on the Open-Centre turbine. The recorders were deployed for different durations and had different sampling protocols (Table 1). The turbine was deployed in 23 Jul by OpenHydro; it stopped rotating on 9 Aug. The AMAR was located ~130 m to the side of the turbine, while the FAST platform was located 60 m on the ebb side of the turbine (Figure 1).

Table 1. Recording dates, mounting locations and sample rates of each hydrophone.

Hydrophone ID	Recording start	Recording end	Sample rate (kHz)
Turbine icListen 1–1678–Starboard	07 Sep 2018	30 Sep 2018	512
Turbine icListen 2–1404–Port	--	--	--
Turbine icListen 3–1677–Top	07 Sep 2018	30 Sep 2018	512
Turbine icListen 4–1406–Aft	05 Sep 2018	30 Sep 2018	512
FAST icListen 1–1247	07 Sep 2018	22 Sep 2018	8
FAST icListen 2–1405	07 Sep 2018	22 Sep 2018	8
AMAR	28 Jun 2018	1 Nov 2018	32 kHz for 300 sec 375 kHz for 60 sec Sleep for 300 sec

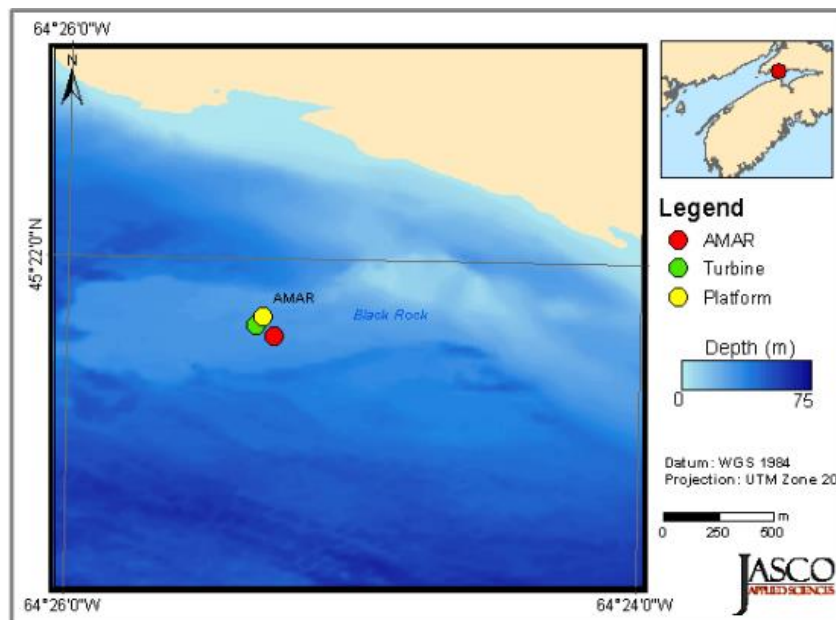


Figure 1. Recorder locations. JASCO deployed the AMAR (red), OpenHydro deployed the turbine with hydrophones mounted on it (green), and FORCE deployed the FAST platform (yellow).

2.2. Data Analysis

The objectives of this data analysis were to compare the 1-minute power spectral density and decidecade sound pressure levels to determine frequencies impacted by flow noise in the 10th, 25th, 50th, 75th, and 90th percentiles. This comparison is effective for evaluating hydrophone performance with respect to flow noise and system noise and for examining the impact of the loss of the neoprene cover for the autonomous recorder. The acoustic metrics used for these analyzes were 1-minute broadband sound pressure levels (SPL), power spectral density (PSD), and decidecade-band SPL. One-minute statistics were used to match the time resolution of the current speed and turbine state data set.

The metrics used throughout this report are *level* quantities. This means that they are ten times the logarithm (base 10) of an acoustic field quantity divided by its reference value, and the units have the form 'dB re 1 μPa^2 ' (see ISO 2017). A result, a 10 dB increase in the level is equivalent to multiplying the acoustic measurement by 10.

The following results are presented in Appendix A:

- **Combined ambient SPL and spectrogram versus time plots:** The broadband and decade band results represent SPL in 1-minute periods as averages of 1-second Hanning-windowed spectra with 50% overlap. The results are presented in five frequency bands: first the broadband 10–50000 Hz, and then the following bands: 10–100 Hz, 100–1000 Hz, 1000–10000 Hz, and 10000–50000 Hz.
- **Decidecade band levels and spectral level plots:** The 1-minute power spectral density averages are displayed at 5th, 25th, 50th, 75th, and 95th percentile levels, referred to as L_5 , L_{25} , L_{50} , L_{75} , and L_{95} , respectively. By ANSI (American National Standards Institute) standard, L_5 is the sound level only exceeded 5% of the time, and it is therefore larger than L_{95} (ANSI S1.43-1997 R2007). L_{50} is commonly referred to as the median. The frequency range displayed spans the acoustic bandwidth of the recording. The decidecade band levels are calculated similar to the spectral levels, except the 1-minute spectra are first integrated within the decidecade bands between 10 Hz and 50 kHz, which are then displayed at 5th, 25th, 50th, 75th, and 95th percentile levels. The mean band levels are also shown.
- **Cadence plots:** The data are examined in 10-minute steps throughout one day (i.e., from 0:00–0:10, 0:10–0:20, ..., 23:50–24:00). Each 10-minute step is comprised of ten 1-minute bins. The median value is calculated from these bins for a given time each day. For example, in a 30-day month, the daily L_{50} for 12:00–12:10 is the median of the ten 1-minute samples each day for all 30 days (from 300 1-minute samples). Plotting the daily cadences can reveal patterns associated with human activity, such as from ferries and other regularly-scheduled vessel passages.

2.3. Recorder Calibration

The AMAR instrumentation used in this study was calibrated before and after each use (see Appendix A.2). Calibrations were validated after data collection and before data analysis to verify instrument performance, as a standard part of JASCO's ISO 9001 Quality Management System. Data from other instrumentation were analyzed according to manufacturer-supplied calibration information.

3. Results

3.1. Acoustic Doppler Current Profiler (ADCP) Data

A Teledyne Workhorse ADCP mounted on the turbine recorded water depths, total rms water speeds and direction throughout the acoustic recording period (Figure 2). The water speeds were measured at the 1st and 10th, 0.5 m bins above the transducer. The ADCP had a 1.6 m blanking distance, and data was provided by FORCE with mounting unknown. These speeds and depths were used to correlate with sound level recordings in decade bands, to relate flow and flow noise.

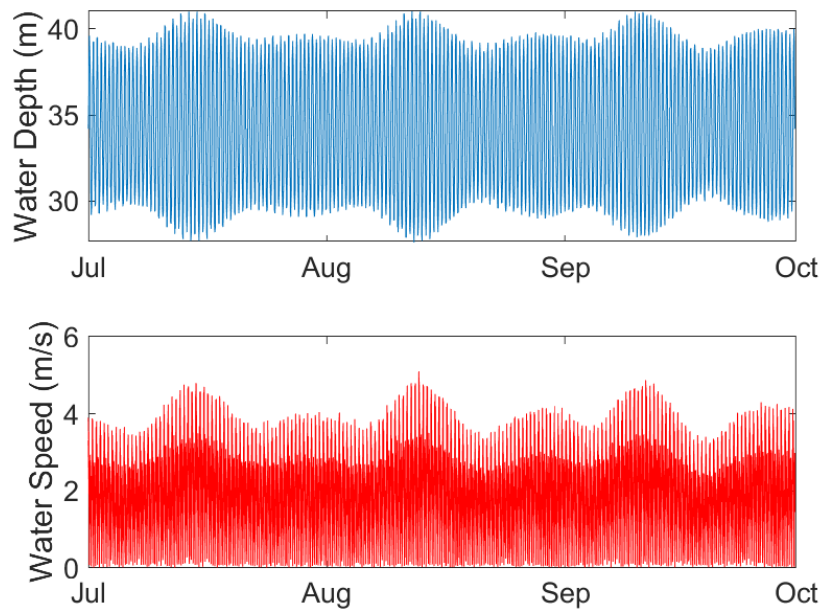


Figure 2. Water depths and total root-mean-square (rms) water speeds at the first 0.5 m bin (near-bottom) measured by the Acoustic Doppler current profiler (ADCP). Colour variation in the water speed panel are a result of flood/ebb asymmetry and superimposing of absolute speeds.

3.2. Turbine-mounted icListen Results

Three icListen hydrophones recorded data during September 2018, at locations 'Aft', 'Top', and 'Stbd' (see Figure A-1 and Table A-1). The turbine was not in operation when the icListens were recording. Appendix B.1 contains detailed figures of the sound levels for the icListen hydrophones on the turbine.

The Aft hydrophone recorded much lower sound levels than any other recorder (Figures B-1 to B-3), particularly in the lower frequencies below ~1000 Hz. Further investigation is needed for this hydrophone, potentially with regards to the mounting location and whether that may have caused it to be protected from flow noise.

The Top and Stbd hydrophones recorded high levels of low-frequency sound (Figures B-4 to B-9), which we attribute to the high-flow environment. The tidal signal was very clear, including an increase/decrease of sound levels corresponding to the increase/decrease of current velocities. Both hydrophones recorded slightly higher values on the flood tide, and much decreased sound levels during slack tide. The Top hydrophone levels were higher than the Starboard by approximately 20 dB at frequencies below 1000 Hz. Since this hydrophone is mounted at the top of the turbine and tidal velocity decays with depth, it would be subjected to higher flows, which could have caused the increased flow noise. Above approximately

1000 Hz, the Starboard had slightly higher values than the turbine, which may be attributed to the sediment interaction noise being important at the near-bottom Starboard hydrophone but not at the top.

3.3. Platform icListen Results

The platform deployed by FORCE was located 60 m northeast of the turbine. It was equipped with two hydrophones, only one of which was analyzed in detail (icListen 1247, Figures B-10 to B-12). The second hydrophone (icListen 1405) had flow induced noise levels ~15 dB higher than the hydrophone that was analyzed.

The recorded levels were similar to the Starboard hydrophone; however, there was a time alignment delay of approximately 6.5 hours. This error was detected in the data provided to JASCO by FORCE and the source of the error is unknown. The time delay was accounted for during correlation but not in the cadence plot (Figure B-12). Therefore, the recorded sound levels that were slightly higher on the ebb than flood would have been adjusted by approximately half a tidal cycle to align with the platform hydrophone results. The 10–100 Hz band had the highest SPL, which again can be attested to flow noise.

3.4. HFM AMAR Results

The HFM (High Flow Mooring) AMAR was deployed for 4 months, starting on 28 June 2018 (see Table 1), and was located 130 m southeast of the turbine (Figure 1). The turbine was operational between 23 Jul 2018 and 9 Aug 2018 and was recorded by the AMAR. Upon retrieval, it was discovered that the neoprene cover over the mooring had come off (Figure A-6). There was a change in the recorded sound levels in the 10–100 Hz band around 21 Aug with a reduction of PSD below 100 Hz, and a stronger spring-neap cycle which suggest that this is when the cover came off (Figure B-13). There was also a 40 minute data gap, which was unexpected as the recording schedule sleep was only for 5 minutes.

The AMAR results were further analyzed by comparing separately the pre-turbine operational, operational and post-operational periods (the post operational period was also when the neoprene cover was suspected to have come off). Before the turbine was operating (Figures B-16 to B-18), the dominant sound was in the 10–100 Hz decade band, which can be attributed to flow noise. The SPL in this band are approximately 20 dB higher than the other bands. The flood tide had slightly higher values than the ebb.

While the turbine was operating (Figures B-19 to B-21), SPL in higher decade bands increased, particularly the 100–1000 Hz band, and a peak around 150 Hz appears in the percentile plot for L_{mean} , L_{75} , and L_{95} . This peak was also apparent in the percentile plots in Figures 3 and 4. Here again, the flood tide had greater SPL values than the ebb. The increase in SPL was likely caused by a combination of noise from the turbine itself, as well as the additional turbulence introduced by the turbine (the AMAR is downstream of the turbine on the flood).

After the turbine was operating (Figures B-22 to B-24), the 10–100 Hz band SPL were reduced to below even the pre-turbine operation levels. The flood tide continued to have higher SPL than the ebb.

4. Discussion

4.1. Comparison of Recording Locations

The L_1 , L_5 , L_{10} , L_{25} , L_{50} , L_{75} , L_{90} , L_{95} , and L_{99} percentiles and L_{mean} were compared for all hydrophones in Figures 3 and 4, with the decidecade values used in Figure 4 provided in Tables B-1 to B-7. The HFM AMAR was split into three segments: before the turbine was operating, while the turbine was operating, and after the time at which the neoprene cover was suspected to have come off (turbine was off during this time). It is important to note that L_1 and L_{99} levels only occur for ~1 minute every 2 hours— i.e., they are rare.

Flow-induced noise has a characteristic spectral shape that decays as frequency^{-5/3} (Kolmogorov 1941). The frequencies in Figures 3 and 4 where the slope of the spectra change marks where the effects of flow-induced noise around the hydrophone no longer dominates and other sound sources become important. The other main noise sources are wind and wave action as well as sediment movement noise (Bassett et al. 2013). In Figures 3 and 4, the 1st percentile does not show any Kolmogorov $f^{-5/3}$ dependence, which indicates that this percentile is associated with very calm periods at slack tide, with no other sound sources of note. The 5th percentile shows a slight $f^{-5/3}$ spectrum below 100 Hz for the turbine top hydrophone, but otherwise this data may be considered as the baseline quiet ambient spectrum. By comparing the other spectra to the 5th percentile it is possible to determine: 1) the frequencies affected by flow noise as a function of current speed; 2) how flow increases the total sound levels as a function of current speed; and 3) the frequencies at which the turbine contributes to the soundscape more than the other sources.

The frequencies affected by flow noise and the increase in sound levels above that frequency as a function of flow speed are summarized in Table 2 using the decidecade sound pressure levels (Figure 4, Appendix C). Note that flow speed is directly proportional to sound level, and hence the sound level percentiles, as shown in Section 4.2. The location most affected by flow-induced noise was the hydrophone on top of the turbine which was affected out to 2.5 kHz; for comparison the two least affected hydrophones ('Aft' turbine hydrophone and the autonomous AMAR hydrophone) were only affected by flow noise out to 160 Hz. All hydrophone positions measured approximately the same spectral and decidecade sound levels for frequencies above their flow noise cut-offs. Compared to the 5th percentile decidecade sound pressure levels, the decidecade SPLs were up to 5 dB higher at the 10th percentile, 16–24 dB higher at the 50th, and 28–35 dB higher at the 90th. There were two un-expected results: 1) the decidecade flow-induced noise sound pressure levels on the turbine 'aft' hydrophone were up to 30 dB quieter than the same type of hydrophone in the 'stbd' location; 2) the decidecade flow-induced noise sound pressure levels on the autonomous recorder were up to 20 dB quieter after the neoprene cover came off.

When the turbine was present (and presumably free spinning) the sound levels increased in the band of 30–1000 Hz. The maximum increase in decidecade sound pressure level occurred at 160 Hz with an increase of 30 dB at the 90th percentile. This result is similar to the those reported in Martin et al. (2018), which also indicated that the turbine produces sound in the 400–8000 Hz frequency band when generating power. The flow-induced noise on the 'aft' and autonomous recorders were low enough to successfully measure the sound from the turbine when free-spinning. The FAST platform and 'stbd' locations have very similar flow-induced noise profiles. Both of these locations, as well as the 'top' locations would have difficulty quantifying the turbine noise in free-spinning mode but would be effective location for monitoring turbine sound when generating power, based on the results in Martin et al. (2018). This difference reflects the increase in sound levels with height off the seabed at lower frequencies.

The flow-induced noise at all recording locations were similar above 3 kHz and therefore all locations are equally appropriate for detecting porpoise.

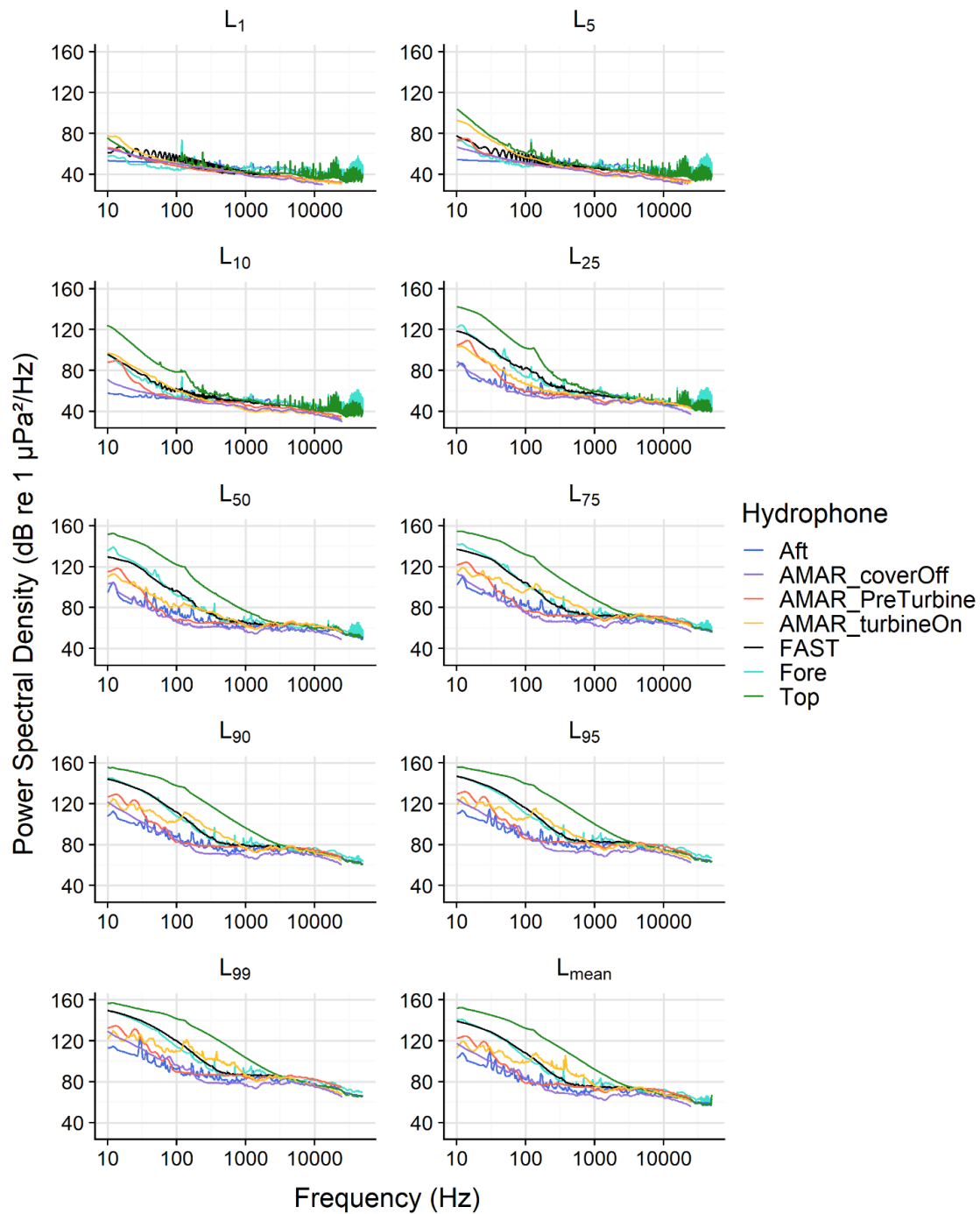


Figure 3. Comparison of all hydrophones at each percentile at all measured frequencies.

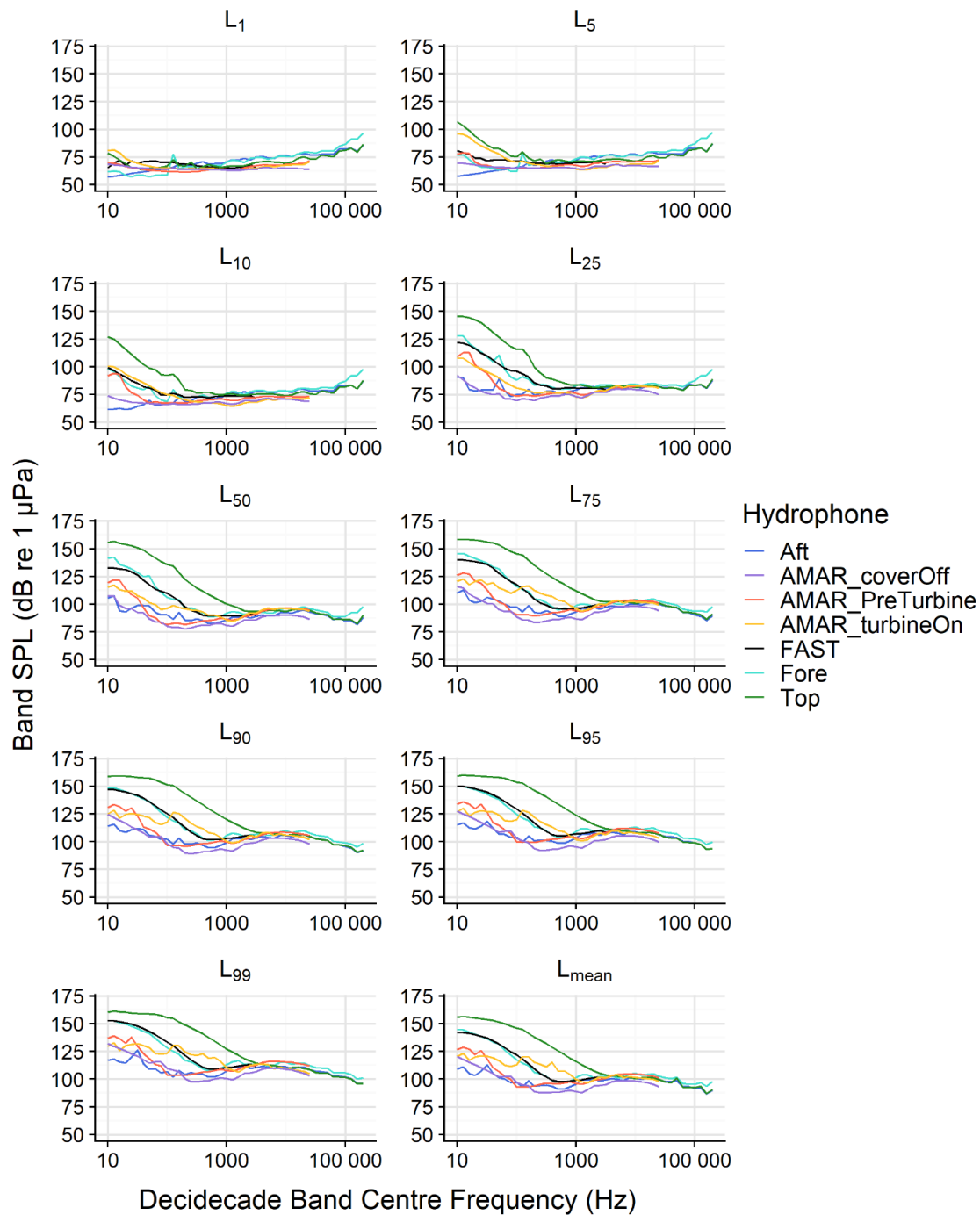


Figure 4. Band SPL at each calculated decade band frequency for the specified percentiles. Values appear in Tables C-1 to C-7. The hydrophone mounted on the top of the turbine recorded elevated band SPL from 10–2500 Hz. When the turbine was in operation, there was a peak in the 125–200 Hz range.

Table 2. Summary of the effects of flow speed on flow-induced noise cut-off frequency and increase in sound levels. These results were computed using the decidecade band sound pressure levels (Figure 4)

Hydrophone position	Metric	L_{10}	L_{50}	L_{90}
Aft	Flow-induced noise cut-off frequency band	10 Hz	50 Hz	160 Hz
	Increase in decidecade band SPL	<3 dB	20–24 dB	28–32 dB
AMAR–Cover Off	Flow-induced noise cut-off frequency band	16 Hz	50 Hz	160 Hz
	Increase in decidecade band SPL	< 3 dB	18–26 dB	27–34 dB
AMAR–Cover On	Flow-induced noise cut-off frequency band	40 Hz	80 Hz	80 Hz
	Increase in decidecade band SPL	<3 dB	18–26 dB	22–28 dB
FAST Platform	Flow-induced noise cut-off frequency band	63 Hz	315 Hz	400 Hz
	Increase in decidecade band SPL	3–5 dB	18–22 dB	32–35 dB
Forward Starboard	Flow-induced noise cut-off frequency band	50 Hz	315 Hz	500 Hz
	Increase in decidecade band SPL	< 3 dB	16–22 dB	28–32 dB
Turbine Top	Flow-induced noise cut-off frequency band	160 Hz	1000 Hz	2500 Hz
	Increase in decidecade band SPL	3–5 dB	21–28 dB	30–35 dB

4.2. Correlation of Hydrophone and ADCP data

Correlograms were generated for each hydrophone, comparing the decade band SPL, water depth, and flow speed from the ADCP, with the flood and ebb tide compared separately. The water depth is measured in metres, and the speed is measured in the first ADCP bin, which is nearest to the bottom.

The three hydrophones mounted on the turbine (Aft, Stbd, and Top) had strong positive relationships between all decade bands and the water speed, and a weak positive relationship with the water depth. The relationship with the depth may have been weaker due to spring neap cycles causing variations in water depth, whereas the water speed at the near bottom remained more consistent with time (for a given stage of the tidal cycle). The strength of the relationship between water speed and decade band SPL did not show much variation between decade bands (Figures 5–7). We had expected that the lower frequencies would have a stronger relationship due to increased flow noise.

For the platform hydrophone the time stamp appears to have been off by 6.5 hours. After adjusting the time stamps, the decade bands had a strong positive relationship with each other and with the water speed, and a weakly positive relationship with water depth (Figure 8).

The high-flow mooring was further separated for comparing the times when the turbine was and was not operating (Figure 9). Overall, there were strong positive relationships between different decade bands, and between decade bands and water speed. There were weak to medium positive relationships between the decade bands and the water depth. When the turbine was operating, the relationship between the decade band and the water speed weakened slightly, particularly in the 100–1000 Hz band (Figure 9). This may have been due to the turbine operational sounds masking the sound affiliated with water speed. Note that a thorough analysis of sound levels as a function of flow speed, direction, and turbine operating

state could not be performed since the turbine only operated in free-spinning mode for a limited period of time. A full analysis was performed using the 2016/17 data (Martin et al. 2018).

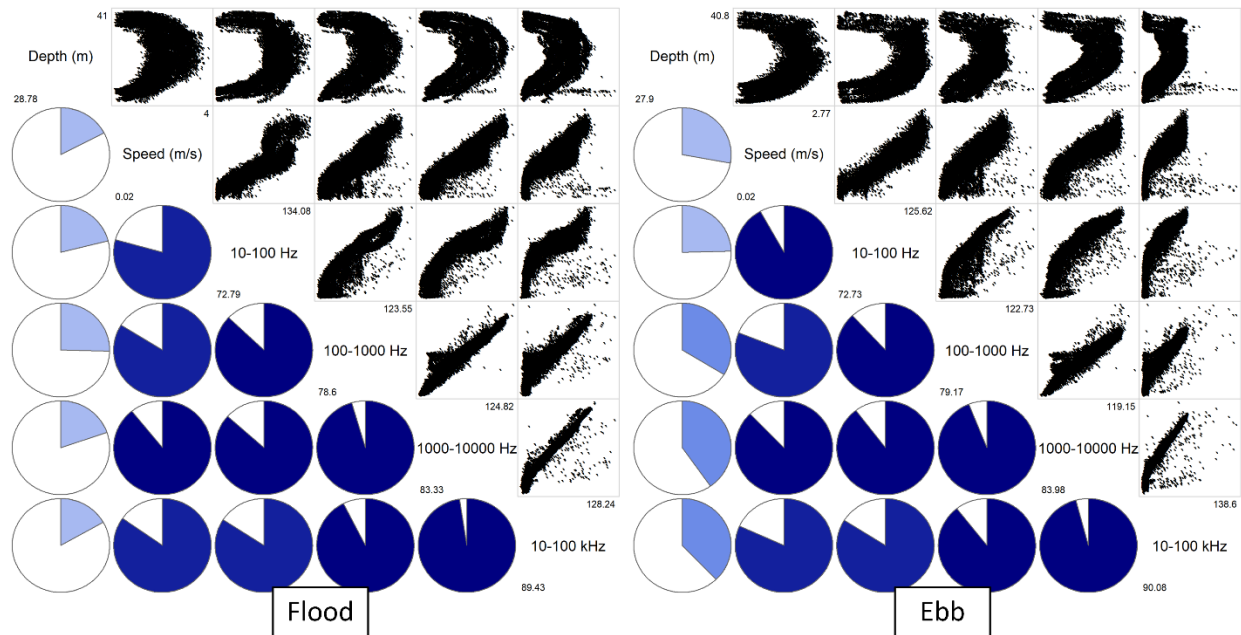


Figure 5. Aft hydrophone correlogram, which depicts the degree of correlation between variables, separated by tidal flow direction. Two types of variables are shown: 1-minute sound pressure levels in decade band SPL and two environmental variables (water speed and water depth). The diagonal of the figure identifies the variables. The top-right triangles are scatterplots of pairs of variables. The lower left triangles are disks representing the degree of correlation between variables. Blue represents a positive correlation, and red a negative correlation. The amount of the pie that is filled and the shading represent the degree of correlation from +1 (full blue) to -1 (full dark red). No negative correlations were found in the data.

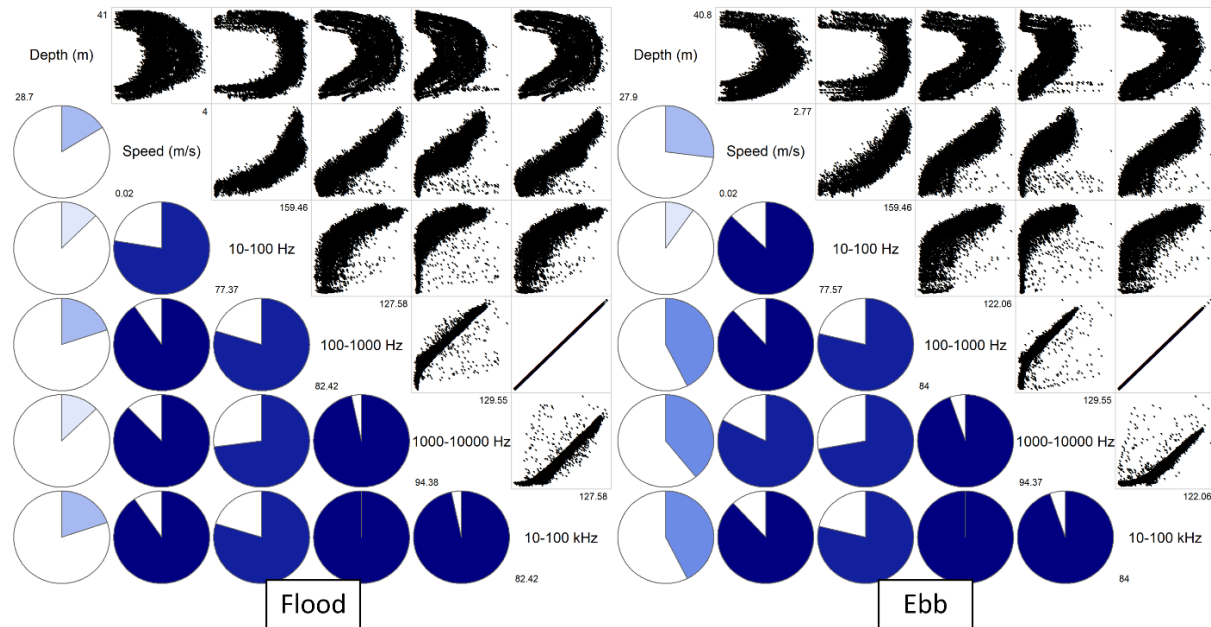


Figure 6. Starboard hydrophone correlogram, which depicts the degree of correlation between variables, separated by tidal flow direction. Two types of variables are shown: 1-minute sound pressure levels in decade band SPL and two environmental variables (water speed and water depth). The diagonal of the figure identifies the variables. The top-right triangles are scatterplots of pairs of variables. The lower left triangles are disks representing the degree of correlation between variables. Blue represents a positive correlation, and red a negative correlation. The amount of the pie that is filled and the shading represent the degree of correlation from +1 (full blue) to -1 (full dark red). No negative correlations were found in the data.

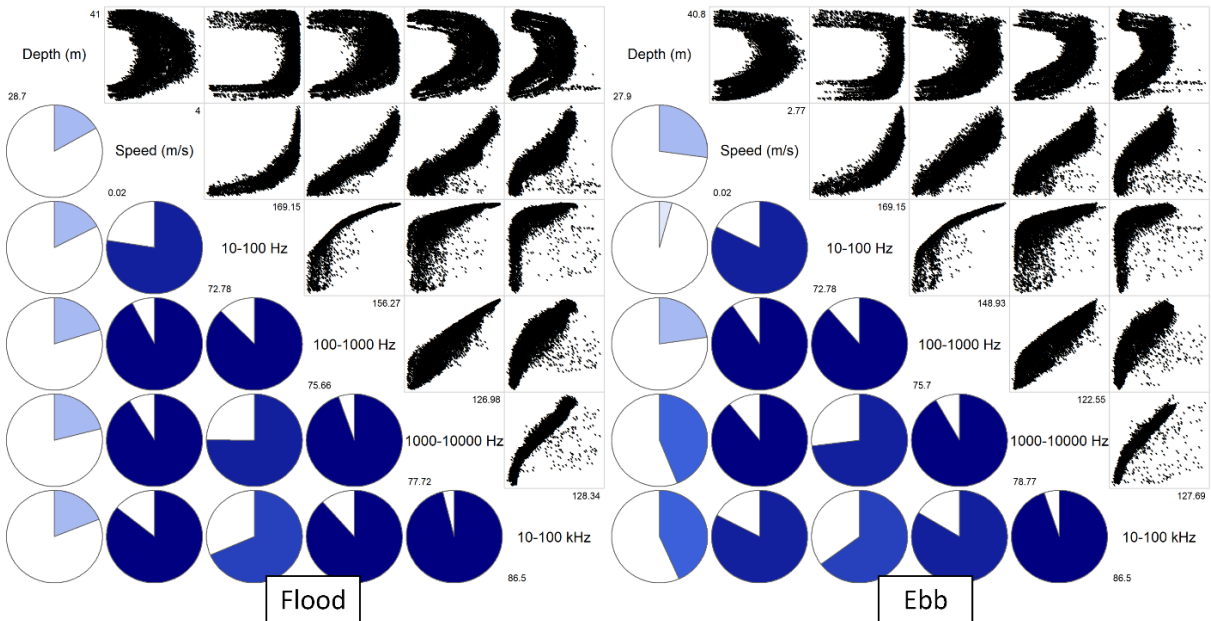


Figure 7. Top hydrophone correlogram, which depicts the degree of correlation between variables, separated by tidal flow direction. Two types of variables are shown: 1-minute sound pressure levels in decade band SPL and two environmental variables (water speed and water depth). The diagonal of the figure identifies the variables. The top-right triangles are scatterplots of pairs of variables. The lower left triangles are disks representing the degree of correlation between variables. Blue represents a positive correlation, and red a negative correlation. The amount of the pie that is filled and the shading represent the degree of correlation from +1 (full blue) to -1 (full dark red). No negative correlations were found in the data.

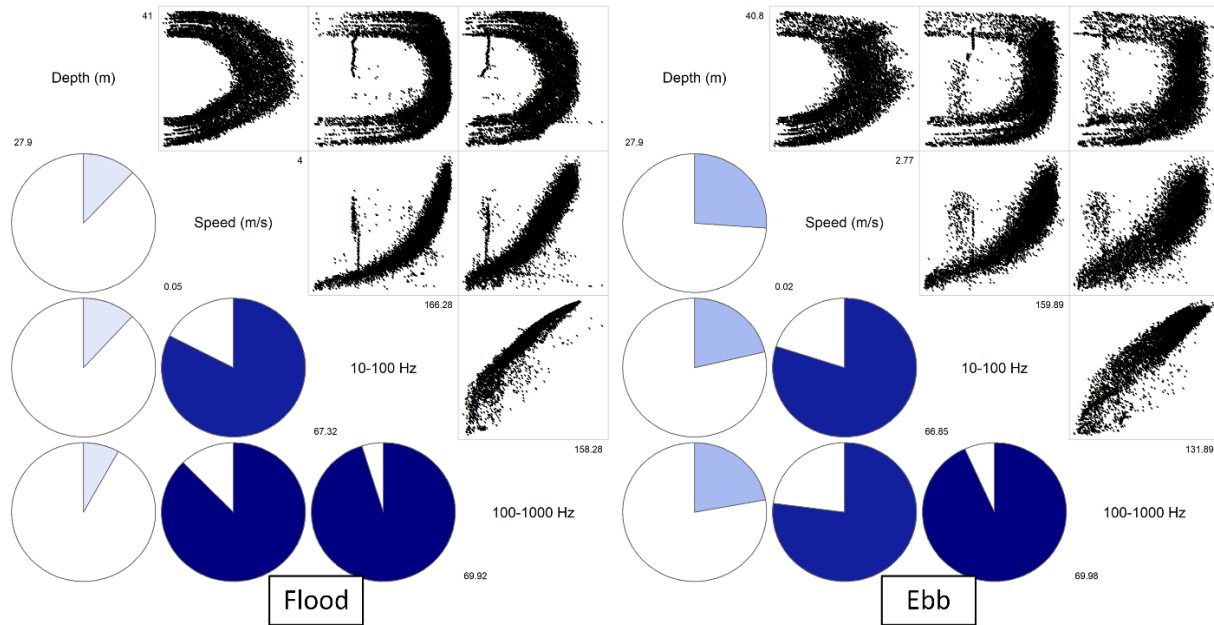


Figure 8. FAST platform hydrophone correlogram, which depicts the degree of correlation between variables, separated by tidal flow direction. Two types of variables are shown: 1-minute sound pressure levels in decade band SPL and two environmental variables (water speed and water depth). The diagonal of the figure identifies the variables. The top-right triangles are scatterplots of pairs of variables. The lower left triangles are disks representing the degree of correlation between variables. Blue represents a positive correlation, and red a negative correlation. The amount of the pie that is filled and the shading represent the degree of correlation from +1 (full blue) to -1 (full dark red). No negative correlations were found in the data.

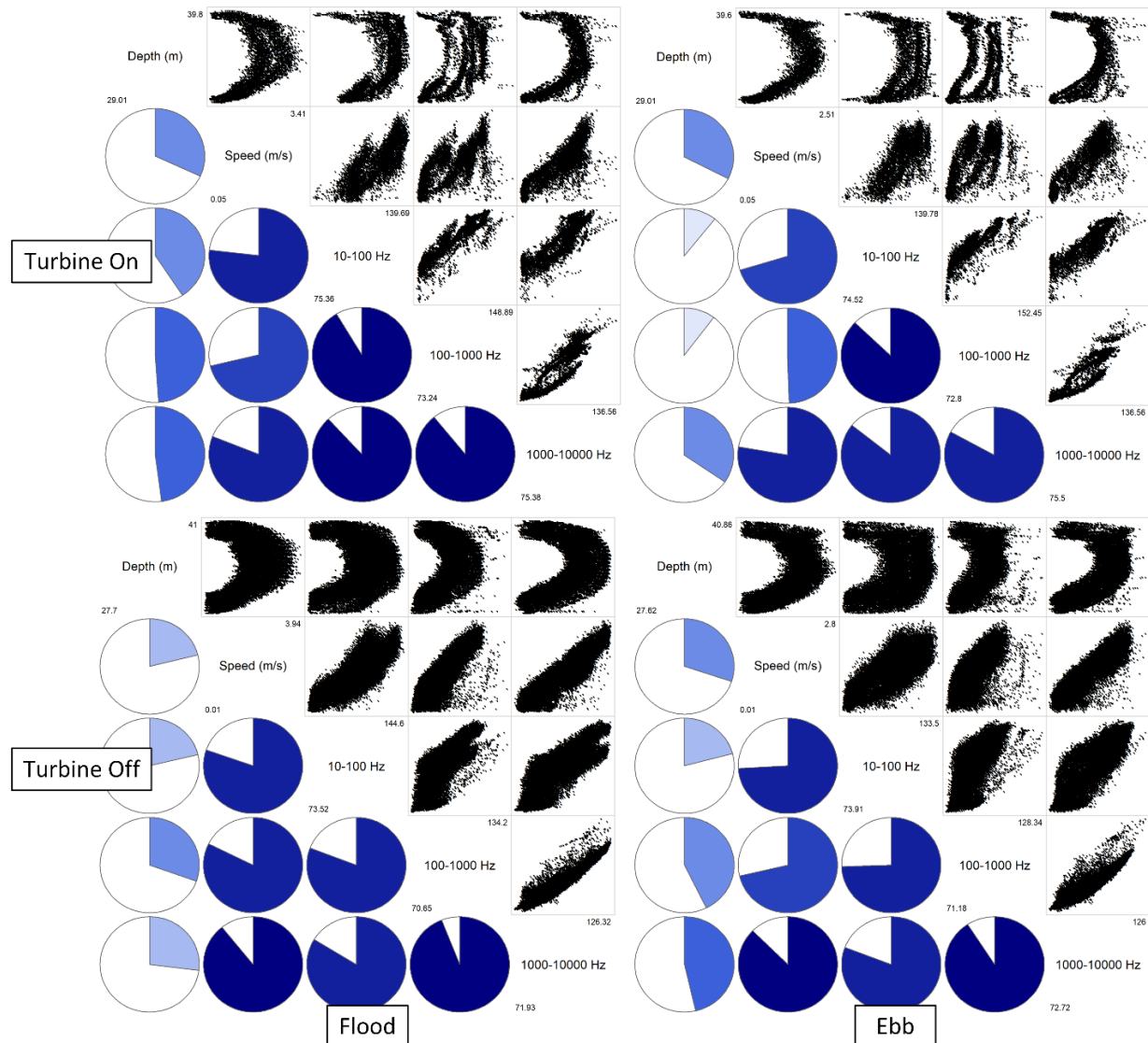


Figure 9. HFM AMAR hydrophone correlogram, which depicts the degree of correlation between variables, separated by tidal flow direction. Two types of variables are shown: 1-minute sound pressure levels in decade band SPL and two environmental variables (water speed and water depth). The diagonal of the figure identifies the variables. The top-right triangles are scatterplots of pairs of variables. The lower left triangles are disks representing the degree of correlation between variables. Blue represents a positive correlation, and red a negative correlation. The amount of the pie that is filled and the shading represent the degree of correlation from +1 (full blue) to -1 (full dark red). No negative correlations were found in the data.

Literature Cited

- [ISO] International Organization for Standardization. 2017. *ISO 18405:2017. Underwater acoustics – Terminology*. Geneva. <https://www.iso.org/standard/62406.html>.
- ANSI S1.43-1997. R2007. *American National Standard Acoustical Terminology*. American National Standards Institute, NY, USA.
- Bassett, C., J. Thomson, and B. Polagye. 2013. Sediment-generated noise and bed stress in a tidal channel. *Journal of Geophysical Research* 118(4): 2249-2265. <https://doi.org/10.1002/jgrc.20169>.
- Kolmogorov, A. 1941. The Local Structure of Turbulence in Incompressible Viscous Fluid for Very Large Reynolds' Numbers. *Proceedings of the USSR Academy of Sciences (Doklady Akademii Nauk SSSR)* 30: 301-305.
- Martin, B., L. Horwich, and C.J. Whitt. 2018. *Acoustic Data Analysis of the OpenHydro Open-Centre Turbine at FORCE: Final Report*. Document Number 01588, Version 3.0 Technical report by JASCO Applied Sciences for Cape Sharp Tidal and FORCE.
- Wenz, G.M. 1962. Acoustic Ambient Noise in the Ocean: Spectra and Sources. *Journal of the Acoustical Society of America* 34(12): 1936-1956. <https://doi.org/10.1121/1.1909155>.

Appendix A. Detailed Methods

This section contains details on the recorder configuration, deployment and recording schedule. The general methods, including data collection and analysis details appear in Section 0.

A.1. Recorder Configurations

A.1.1. icListen Turbine Hydrophones

Table A-1. Data from the turbine-mounted icListen.

icListen ID	Data start	Data end	Sample rate (kHz)
Hydrophone 1–1678–Starboard	07 Sep 2018	30 Sep 2018	512
Hydrophone 2–1404–Port	--	--	--
Hydrophone 3–1677–Top	07 Sep 2018	30 Sep 2018	512
Hydrophone 4–1406–Aft	05 Sep 2018	30 Sep 2018	512

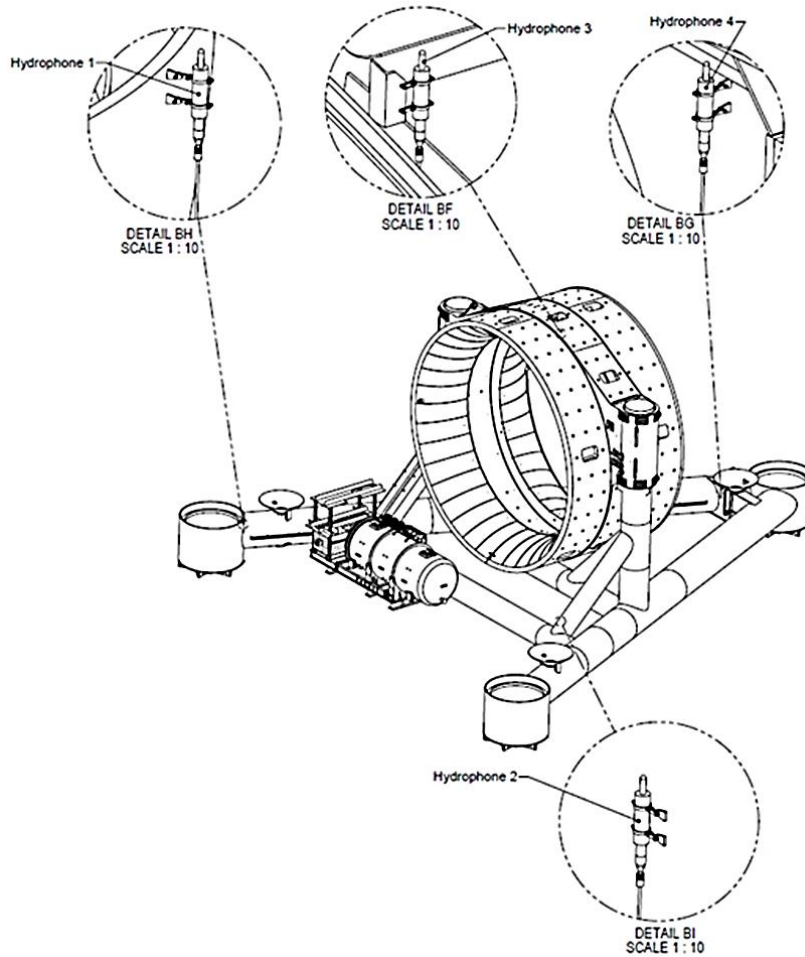


Figure A-1. General arrangement drawing for the Open-Centre Turbine showing the locations of the icListen hydrophones. Hydrophone 1 was 8 m from the turbine rim. The cylinder at the lower left side of the turbine rim is the Turbine Control Centre. The hydrophone naming used in this report are shown in Table A-1.

A.1.2. icListen FAST Platform Hydrophone

Table A-2. Data from the platform icListen.

icListen ID	Data start	Data end	Sample rate (kHz)
Hydrophone –1247–Platform	07 Sep 2018	22 Sep 2018	8
Hydrophone –1405–Platform	07 Sep 2018	22 Sep 2018	8



Figure A-2. FAST platform with two icListen hydrophones.

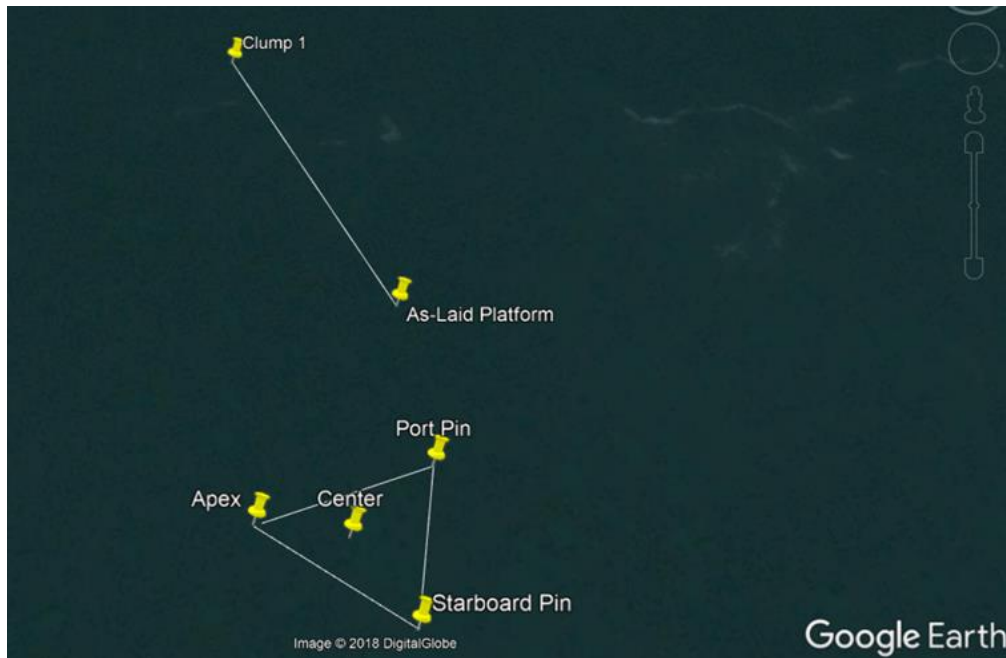


Figure A-3. Platform orientation

A.1.3. HFM AMAR

Table A-3. AMAR deployment locations

Location	Latitude	Longitude	Depth (ft)
HFM AMAR	45°21.806"N	64°25.275"W	~95
Clump Weight	45°21.766"N	64°25.228"W	~95

Table A-4. HF AMAR recording schedule

Duration (s)	Action
300	Record at 32 kHz, channel 1
60	Record at 187.5 kHz, channel 9
300	Sleep

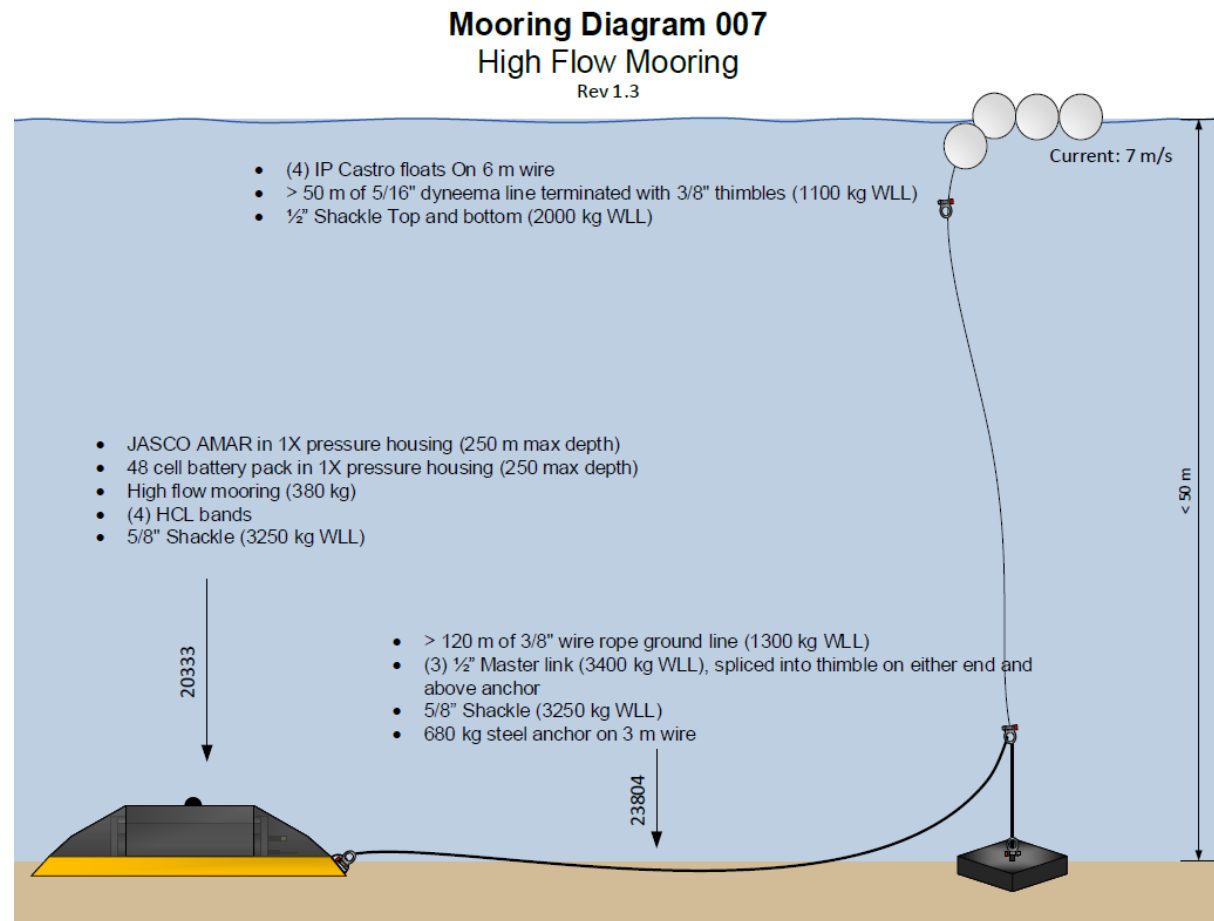


Figure A-4. High Flow Mooring (HFM) design.

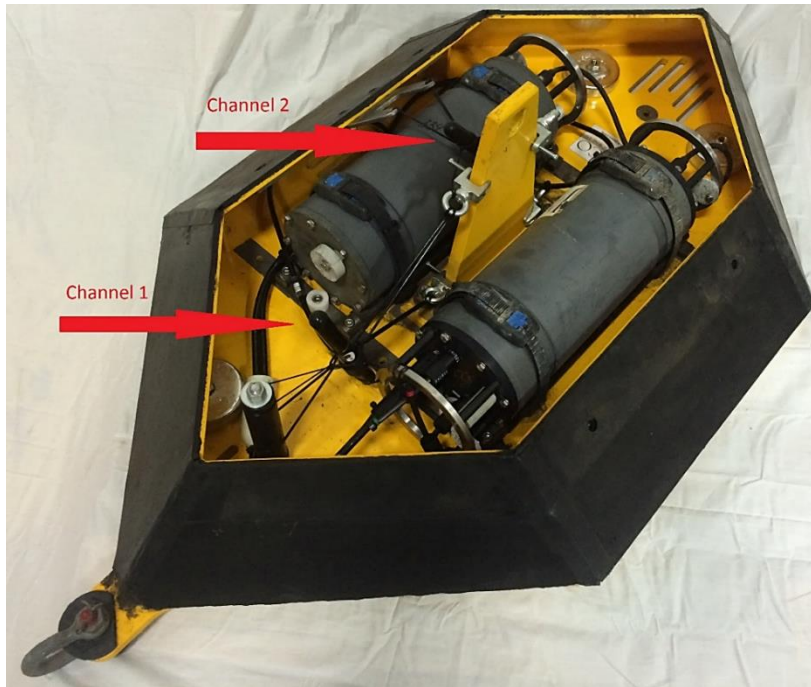


Figure A-5. Inside the high-flow mooring. Hydrophones are shown with red arrows.

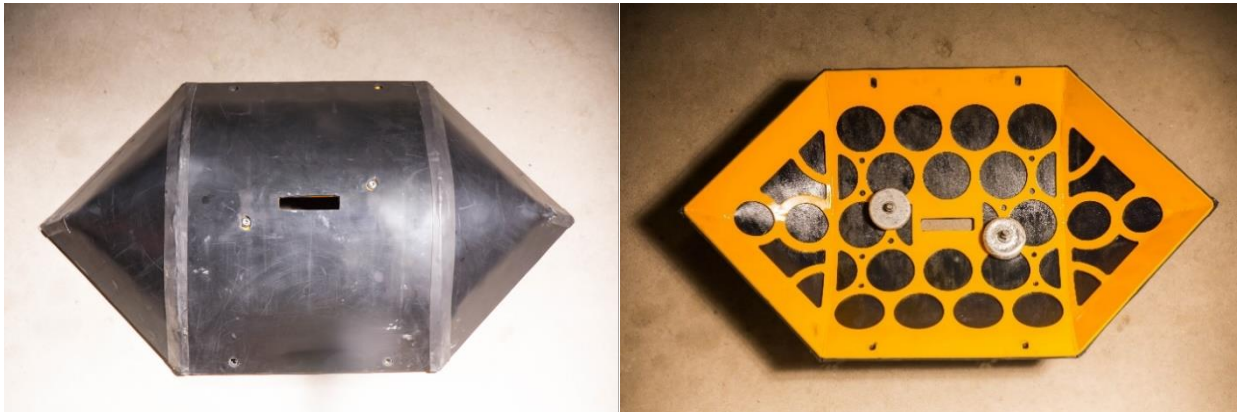


Figure A-6. Cover of the JASCO High Flow Mooring. (Left) top view of the neoprene cover. (right) View from underneath showing cut-outs in the metal structure to allow for sound transmission.

A.2. Recorder Calibrations

Each AMAR was calibrated before deployment with a pistonphone type 42AC precision sound source (G.R.A.S. Sound & Vibration A/S; Figure 16). The pistonphone calibrator produces a constant tone at 250 Hz at a fixed distance from the hydrophone sensor in an airtight space with known volume. The recorded level of the reference tone on the AMAR yields the system gain for the AMAR and hydrophone. To determine absolute sound pressure levels, this gain is applied during data analysis. Typical calibration variance using this method is less than 0.7 dB absolute pressure.



Figure A-7. Split view of a G.R.A.S. 42AC pistonphone calibrator with an M36 hydrophone Manufacturers' calibrations were used for the icListen data.

Appendix B. Results

This section contains the spectrograms, percentiles and cadence plots for the Aft, Stbd, Top (discussed in Section 0), FAST platform (Section 3.3) and HFM AMAR (Section 3.4) hydrophone recordings.

B.1. Turbine-mounted icListens

B.1.1. Aft Hydrophone

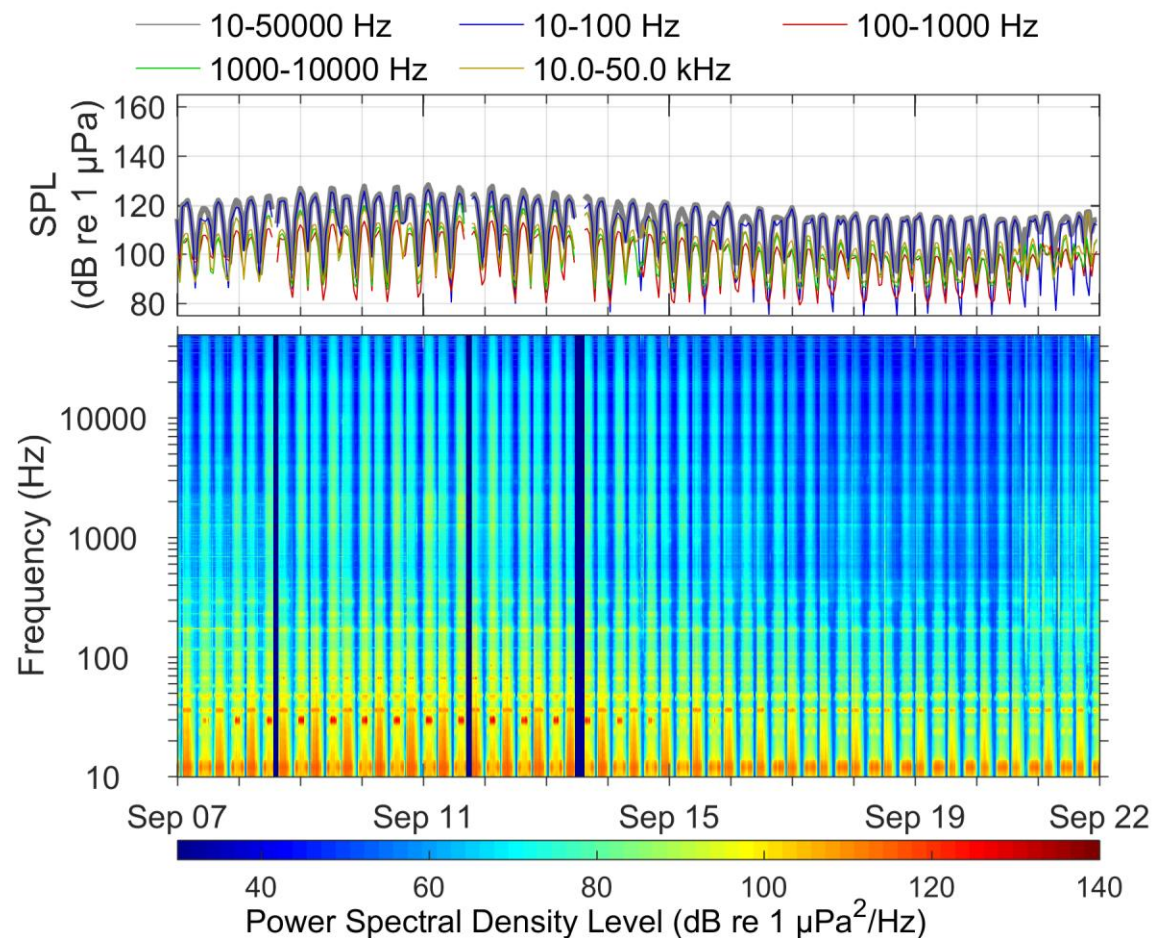


Figure B-1. (Top) in-band SPL and (bottom) spectrogram for the Aft hydrophone for 7–22 Sep 2018.

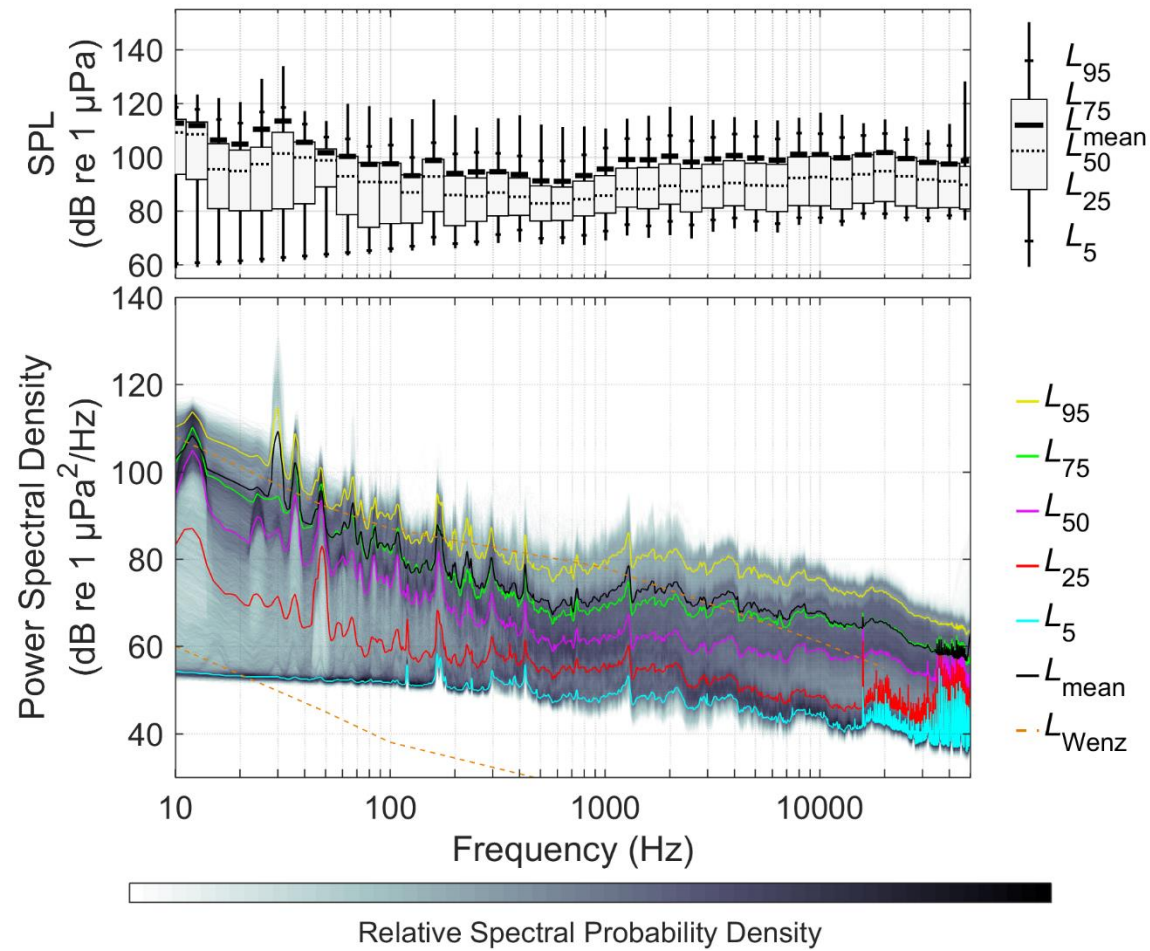


Figure B-2. (Top) Exceedance percentiles and mean of the decade band SPL and (bottom) exceedance percentiles and probability density (grayscale) of 1-min PSD levels compared to the limits of prevailing noise (Wenz 1962) for the Aft hydrophone for 7–22 Sep 2018.

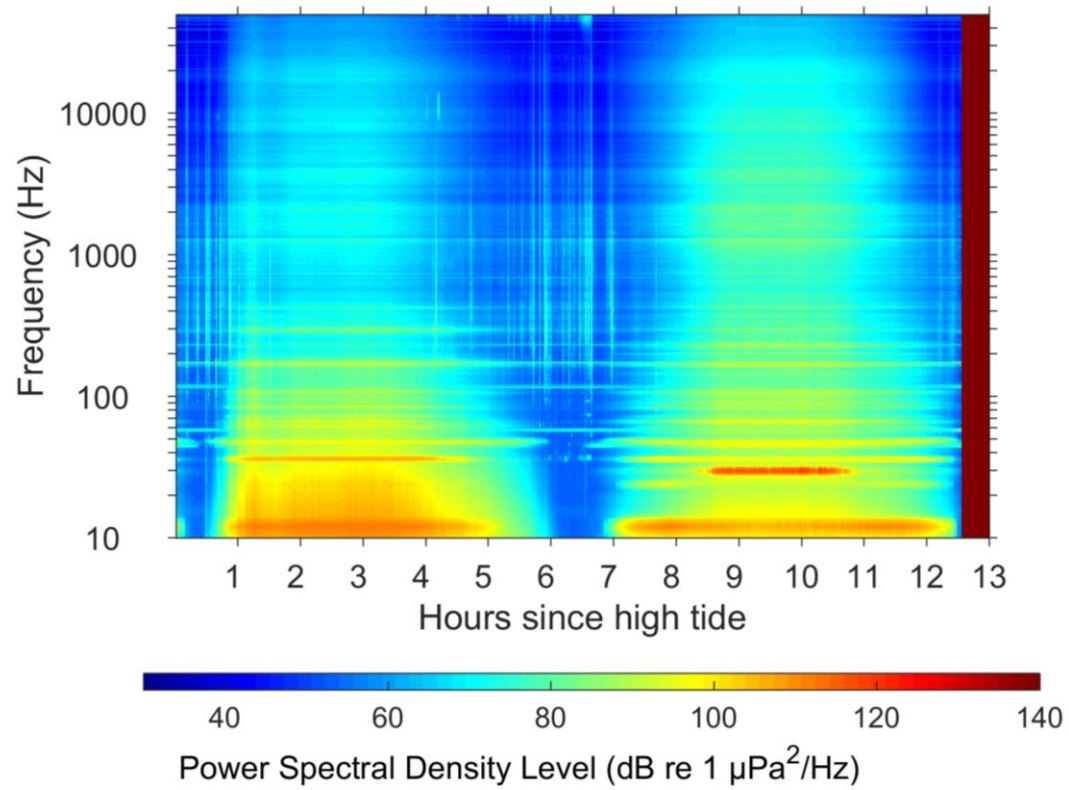


Figure B-3. Cadence spectrogram for the hours since high tide, for the Aft Hydrophone for 7–22 Sep 2018.

B.1.2. Stbd hydrophone

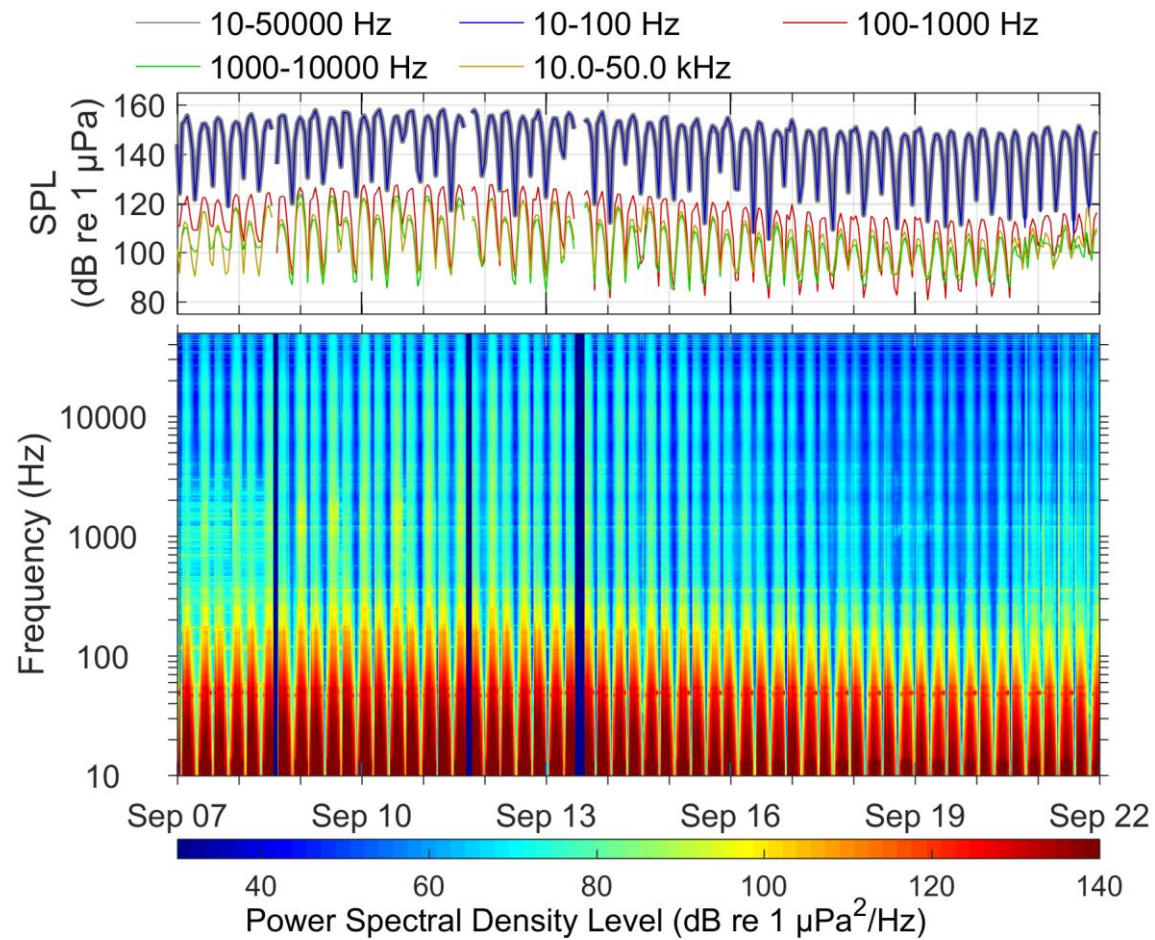


Figure B-4. (Top) in-band SPL and (bottom) spectrogram for the Starboard hydrophone for 7–22 Sep 2018.

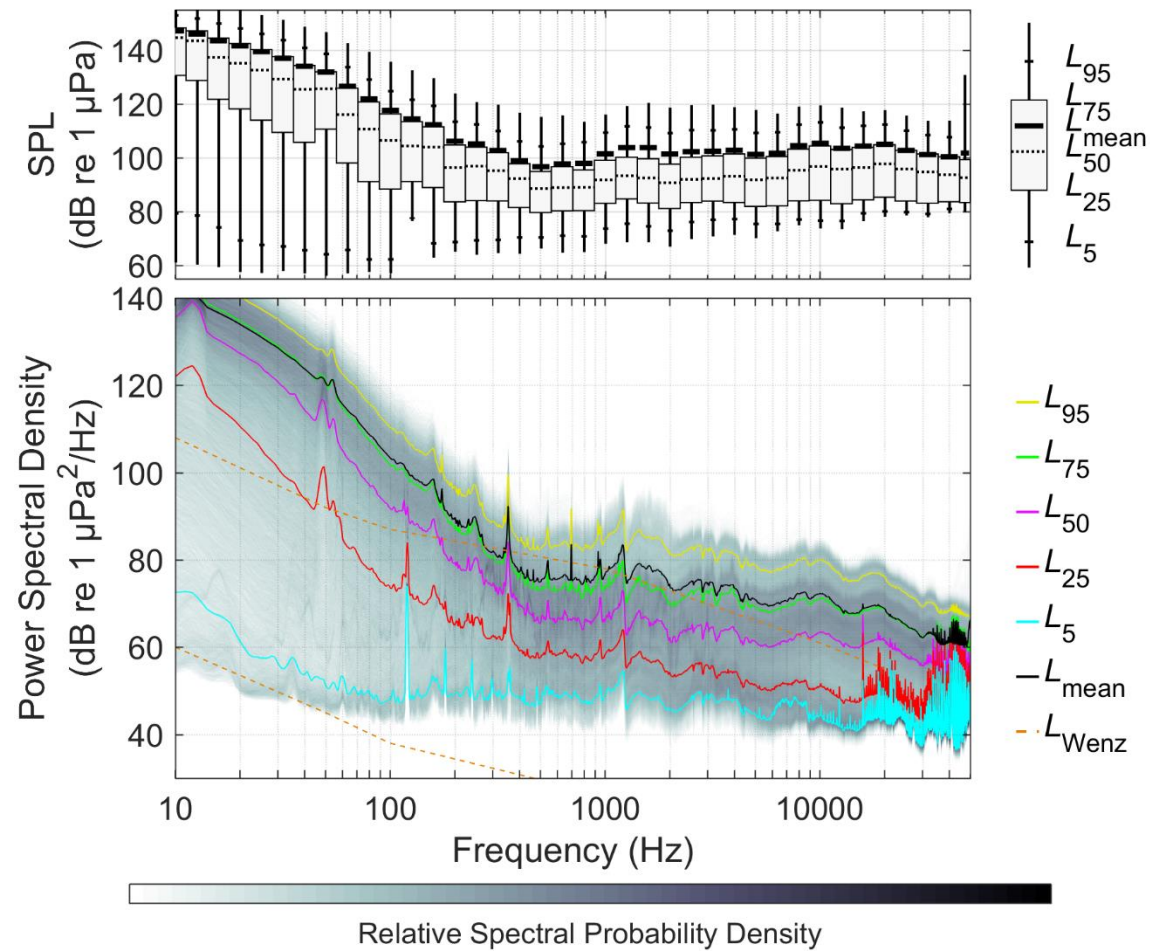


Figure B-5. (Top) Exceedance percentiles and mean of the decade band SPL and (bottom) exceedance percentiles and probability density (grayscale) of 1-min PSD levels compared to the limits of prevailing noise (Wenz 1962) for the Starboard hydrophone for 7–22 Sep 2018.

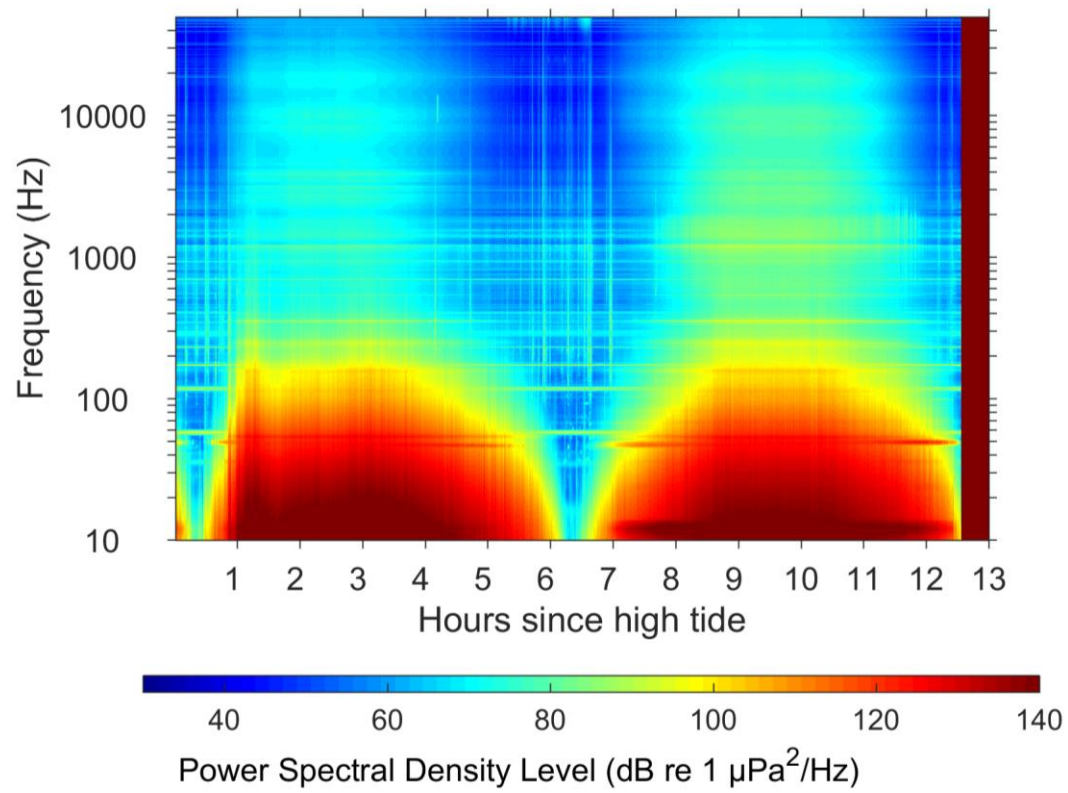


Figure B-6. Cadence spectrogram for the hours since high tide, for the Starboard hydrophone for 7–22 Sep 2018.

B.1.3. Top Hydrophone

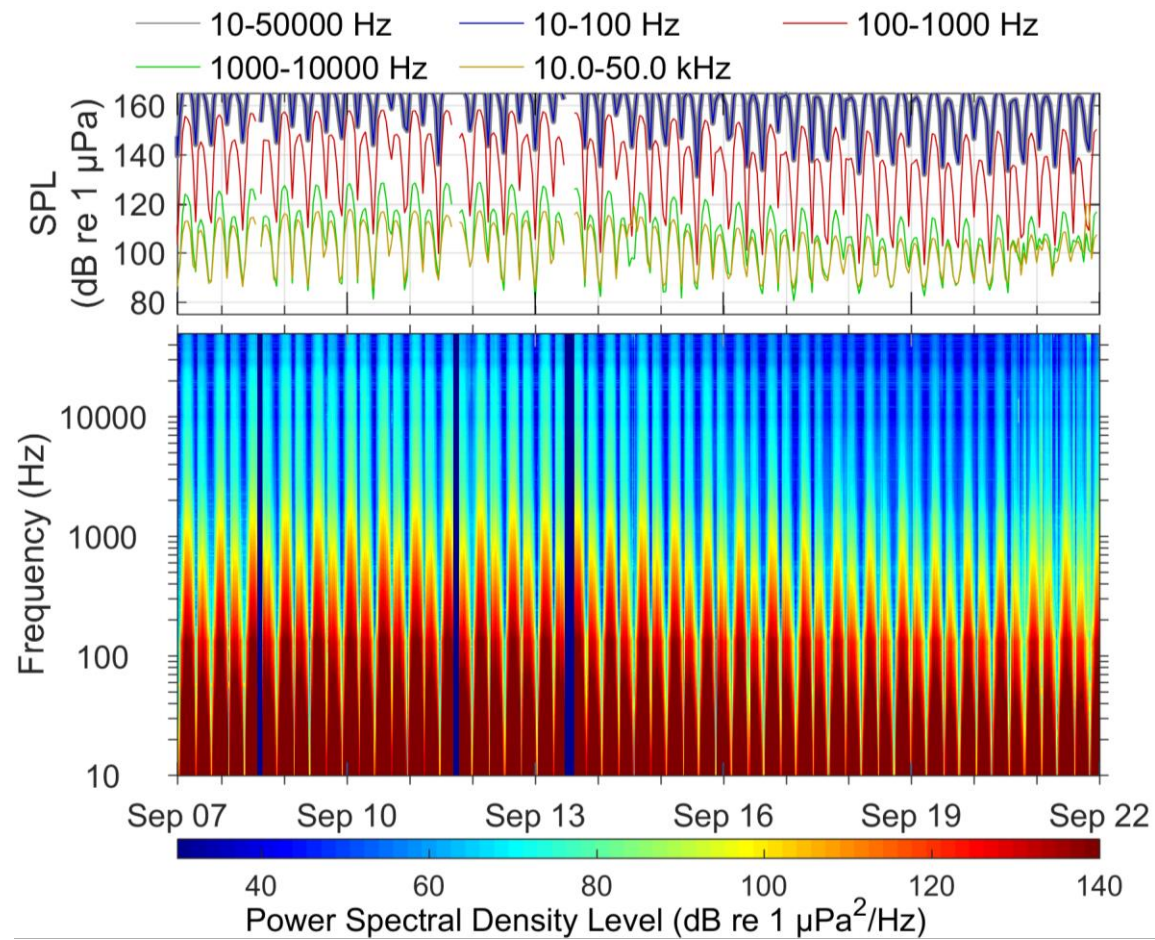


Figure B-7. (Top) in-band SPL and (bottom) spectrogram for the Top hydrophone for 7–22 Sep 2018.

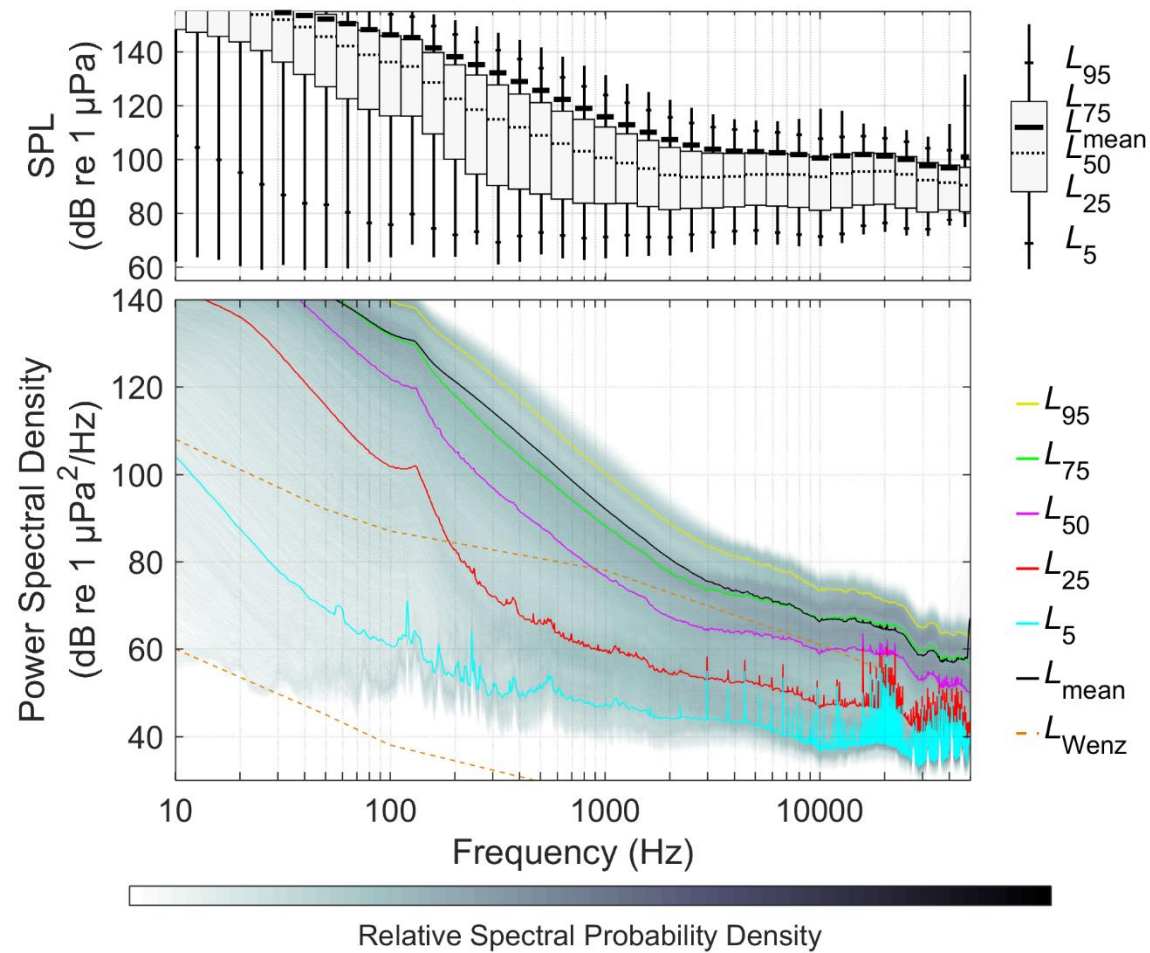


Figure B-8. (Top) Exceedance percentiles and mean of the decade band SPL and (bottom) exceedance percentiles and probability density (grayscale) of 1-min PSD levels compared to the limits of prevailing noise ((Wenz 1962) for the Top hydrophone for 7–22 Sep 2018.

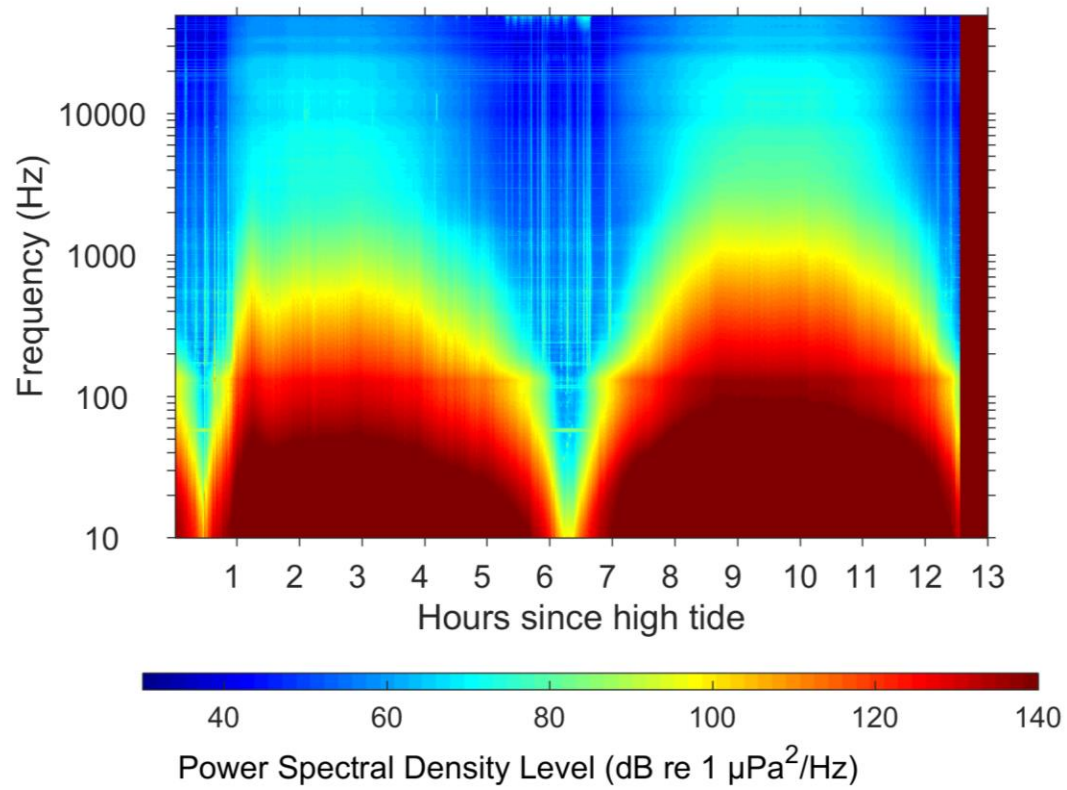


Figure B-9. Cadence spectrogram for the hours since high tide, for the Top hydrophone for 7–22 Sep 2018.

B.2. FAST Platform icListen

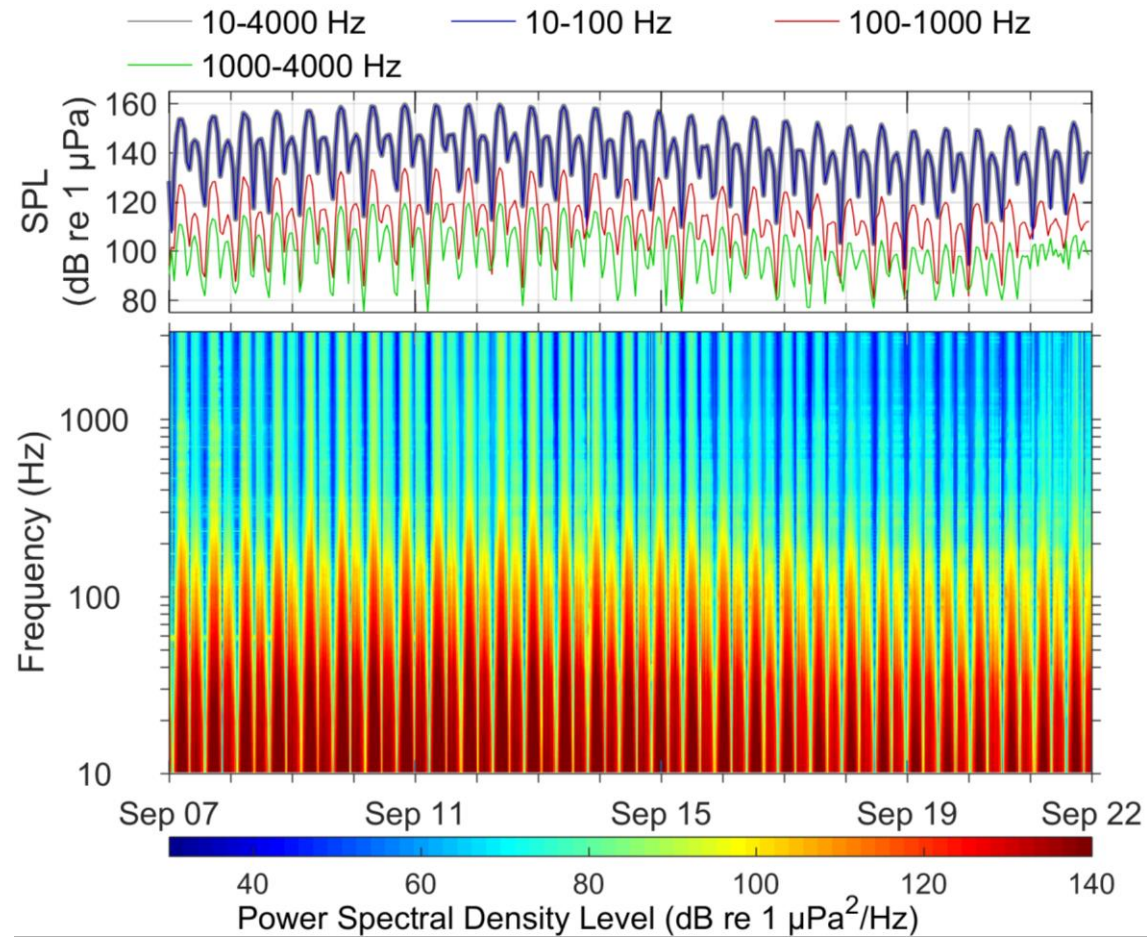


Figure B-10. (Top) in-band SPL and (bottom) spectrogram for the FAST platform hydrophone for 7–22 Sep 2018.

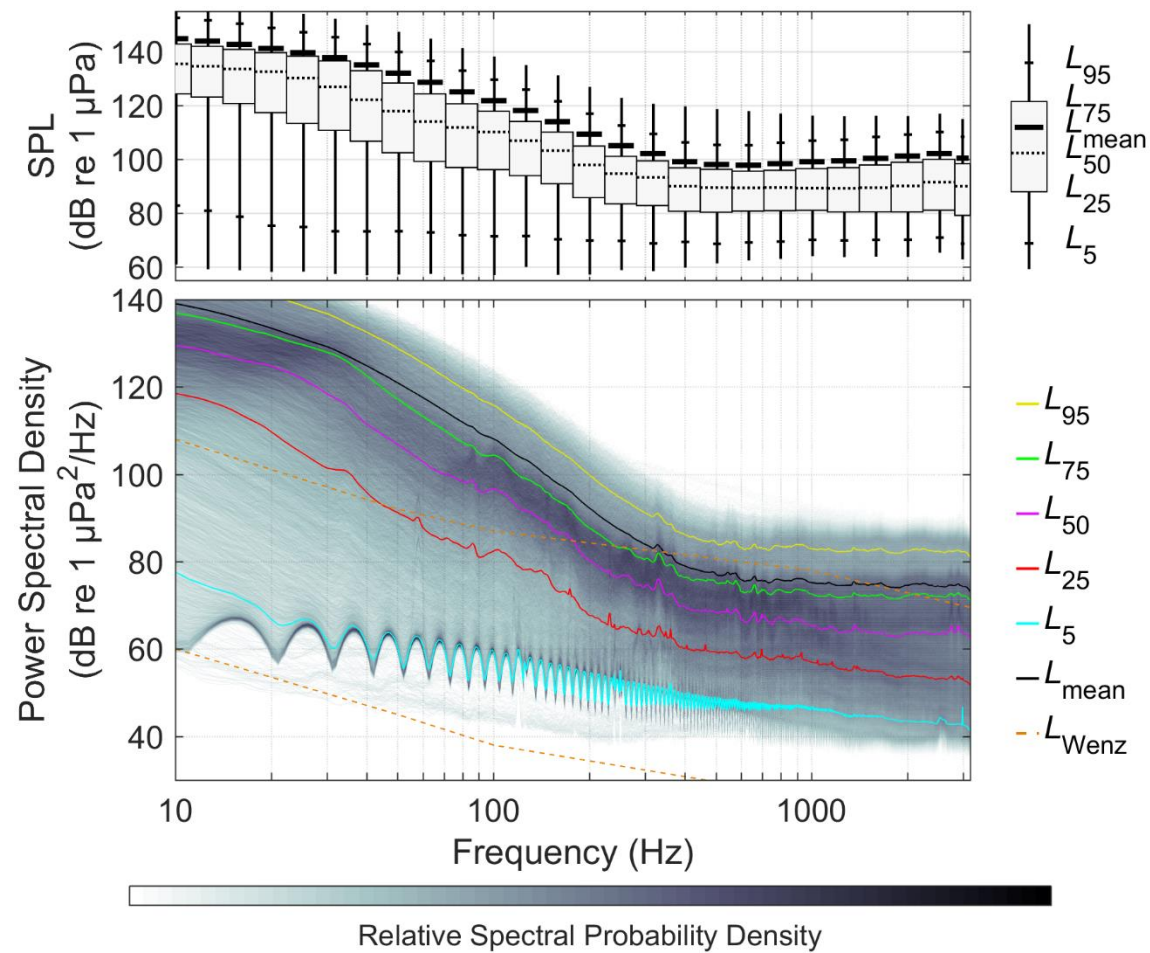


Figure B-11. (Top) Exceedance percentiles and mean of the decidecade band SPL and (bottom) exceedance percentiles and probability density (grayscale) of 1-min PSD levels compared to the limits of prevailing noise (Wenz 1962) for the FAST platform hydrophone for 7–22 Sep 2018.

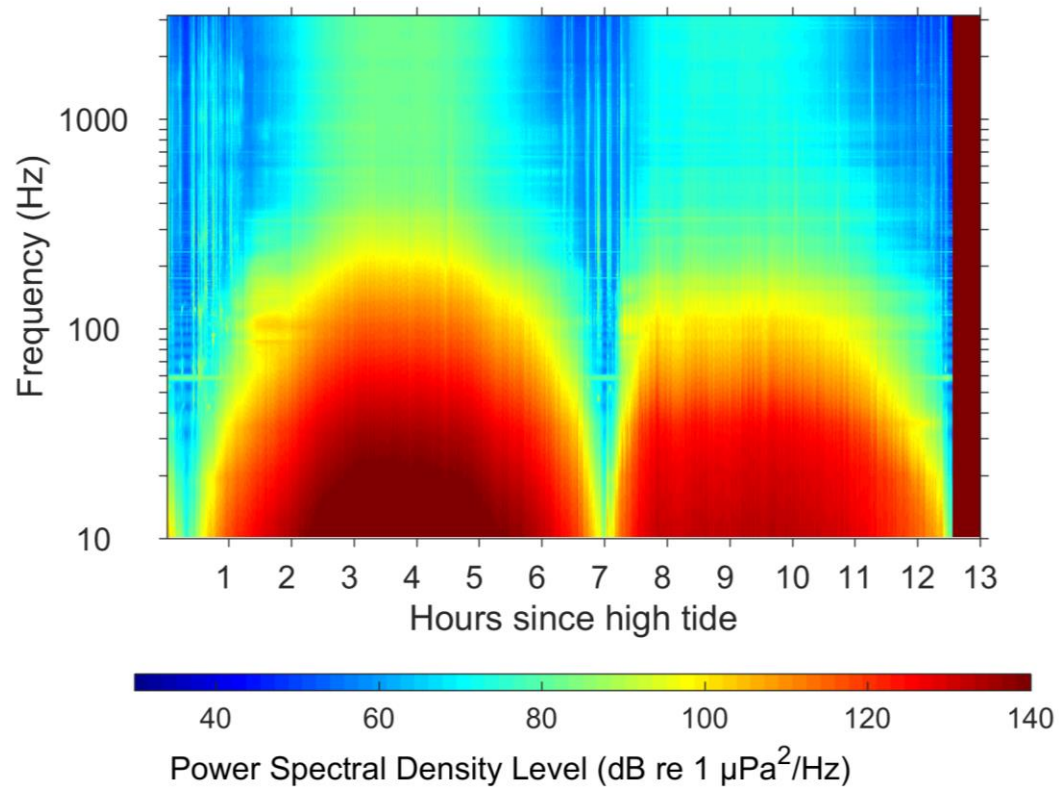


Figure B-12. Cadence spectrogram for the hours since high tide, for the FAST platform hydrophone for 7–22 Sep 2018.

B.3. HFM AMAR

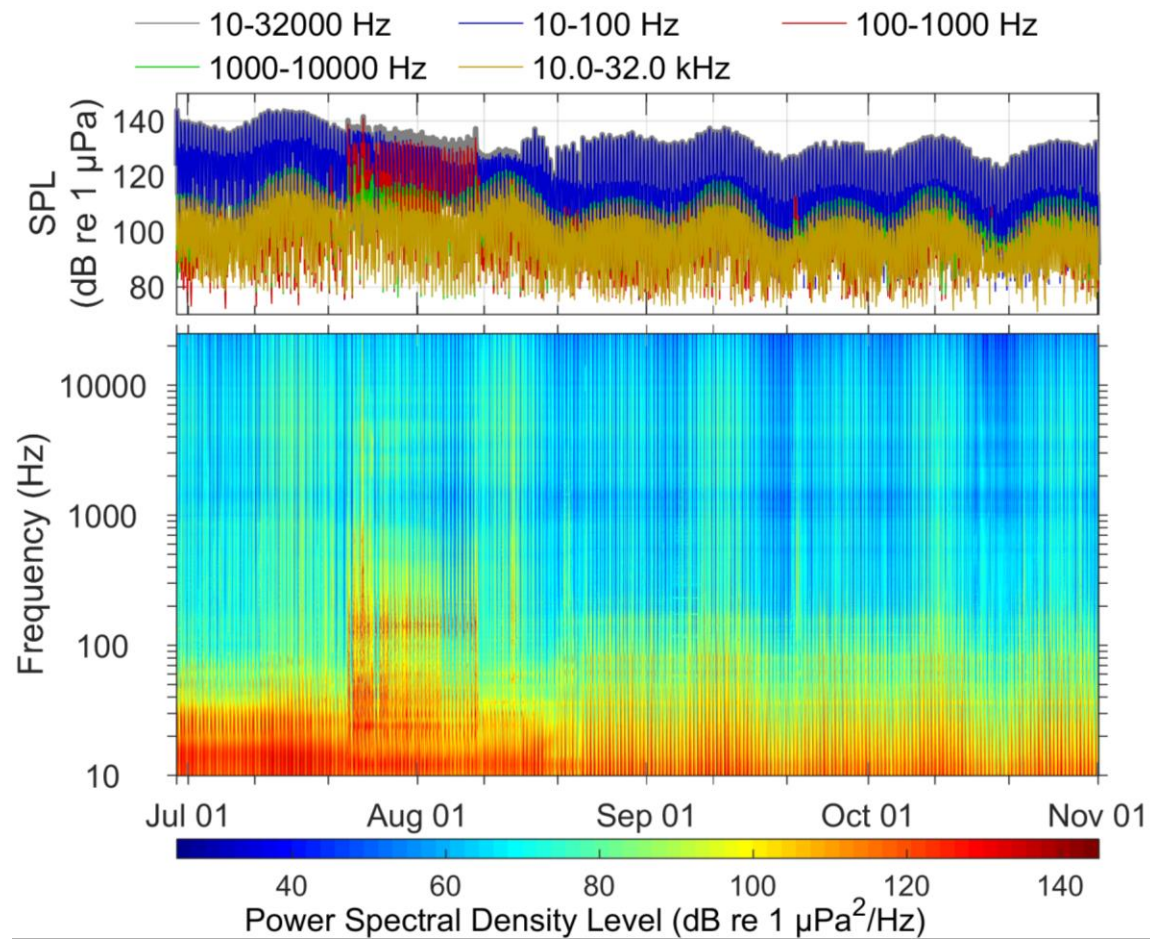


Figure B-13. (Top) in-band SPL and (bottom) spectrogram for the AMAR hydrophone for July to November 2018.

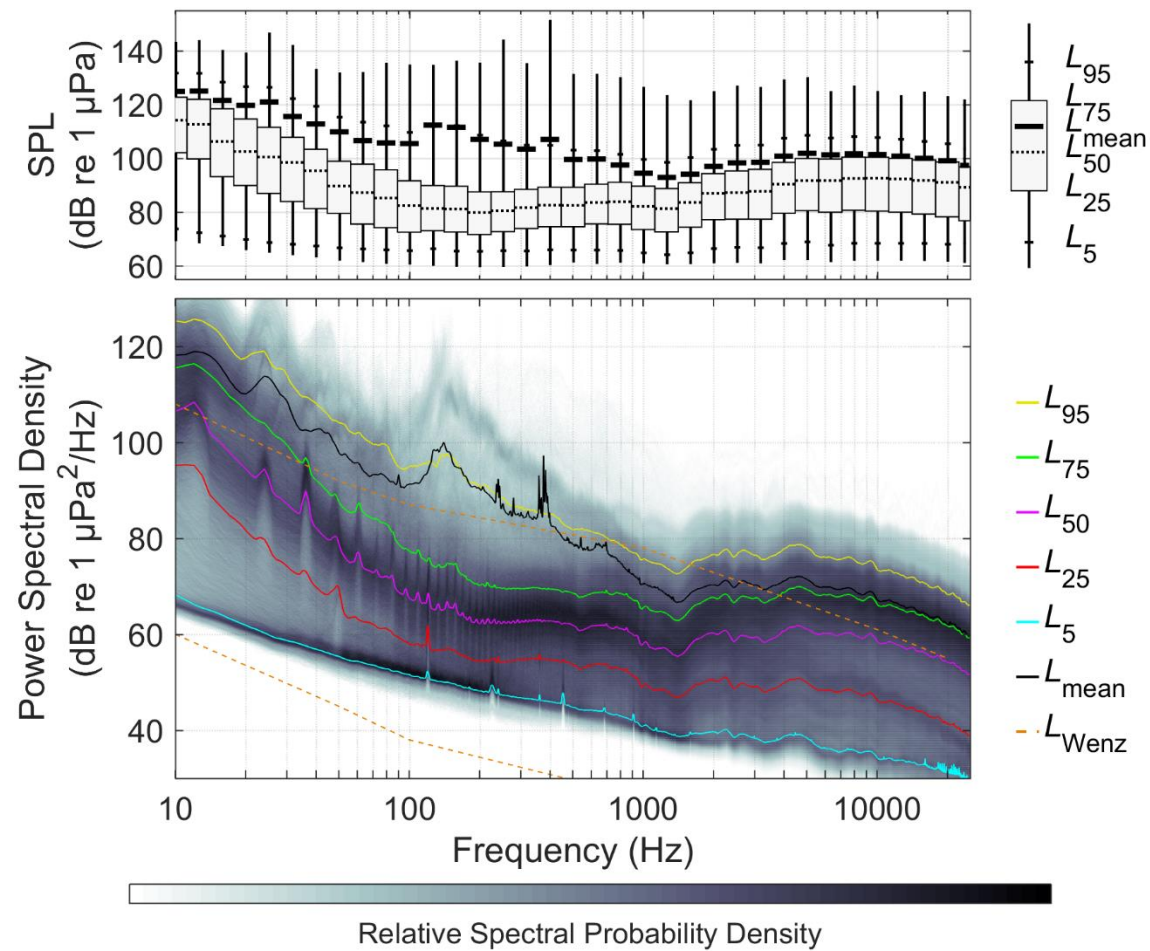


Figure B-14. (Top) Exceedance percentiles and mean of the decidecade band SPL and (bottom) exceedance percentiles and probability density (grayscale) of 1-min PSD levels compared to the limits of prevailing noise (Wenz 1962) for the AMAR hydrophone July to November 2018.

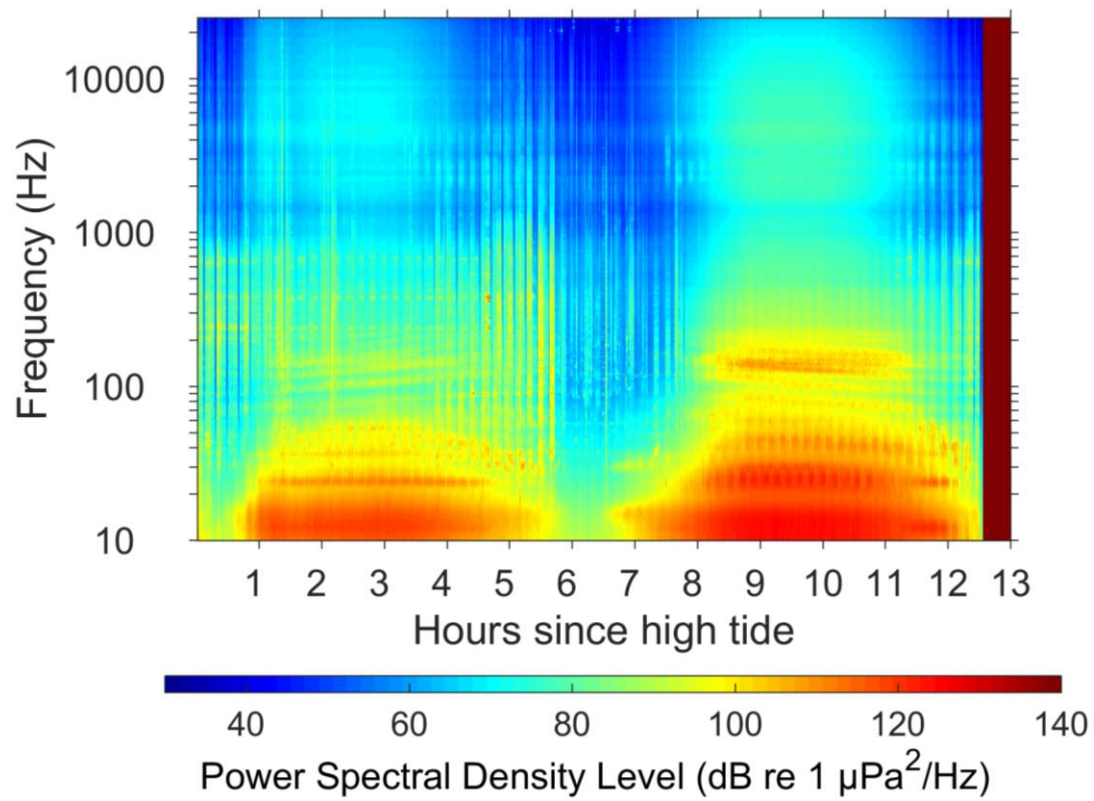


Figure B-15. Cadence spectrogram for the hours since high tide, for the AMAR hydrophone July to November 2018.

B.3.1. Pre-Turbine Operation

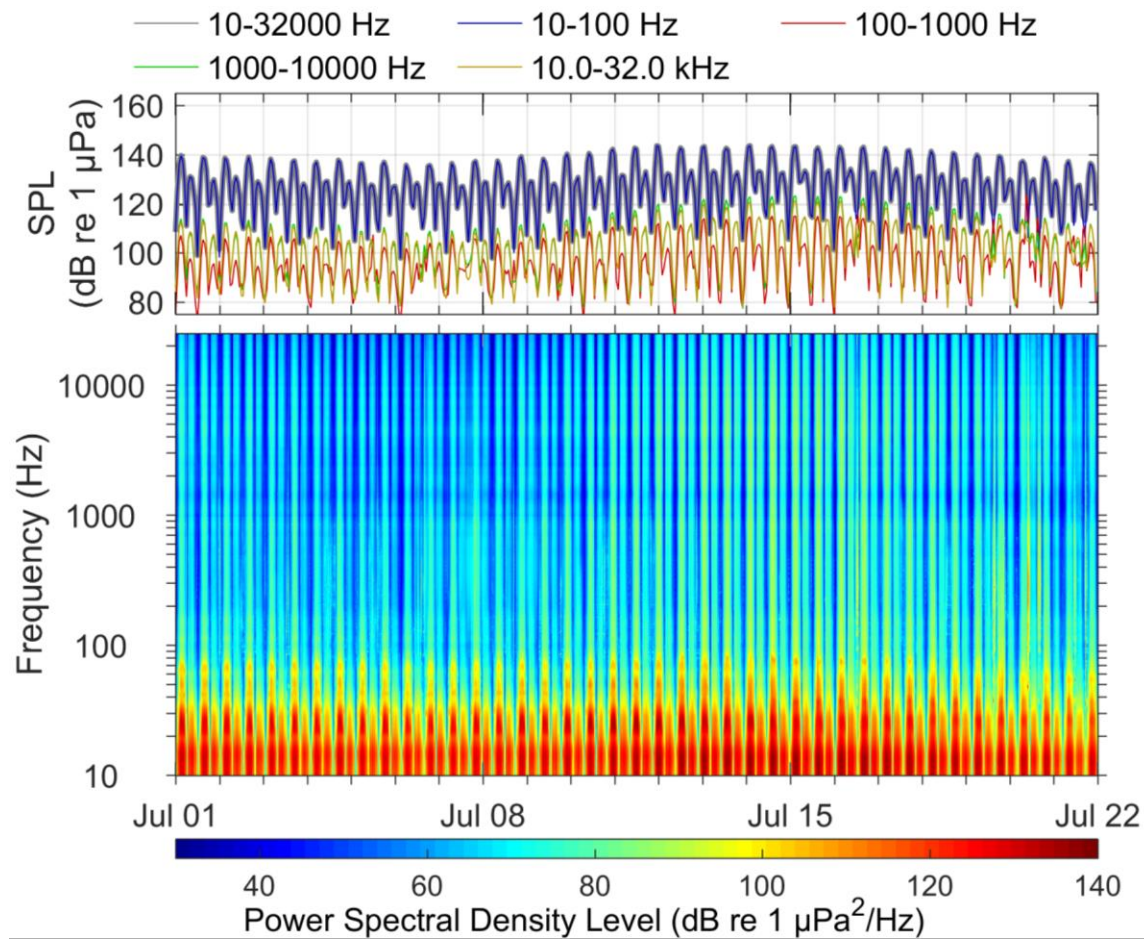


Figure B-16. (Top) in-band SPL and (bottom) spectrogram for the AMAR hydrophone during the pre-turbine operation period, 1–22 Jul 2018.

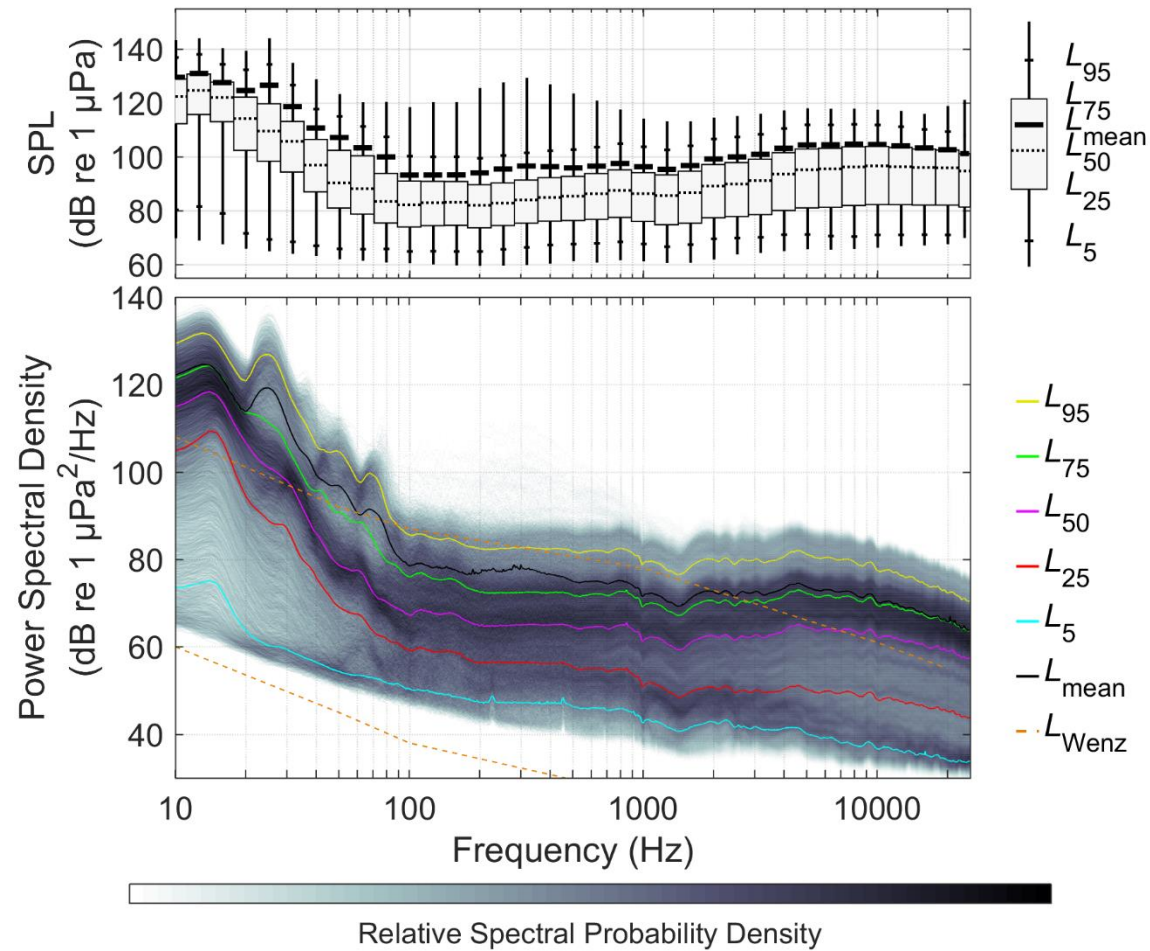


Figure B-17. (Top) Exceedance percentiles and mean of the decade band SPL and (bottom) exceedance percentiles and probability density (grayscale) of 1-min PSD levels compared to the limits of prevailing noise (Wenz 1962) for the AMAR hydrophone during the pre-turbine operation period, 1–22 Jul 2018.

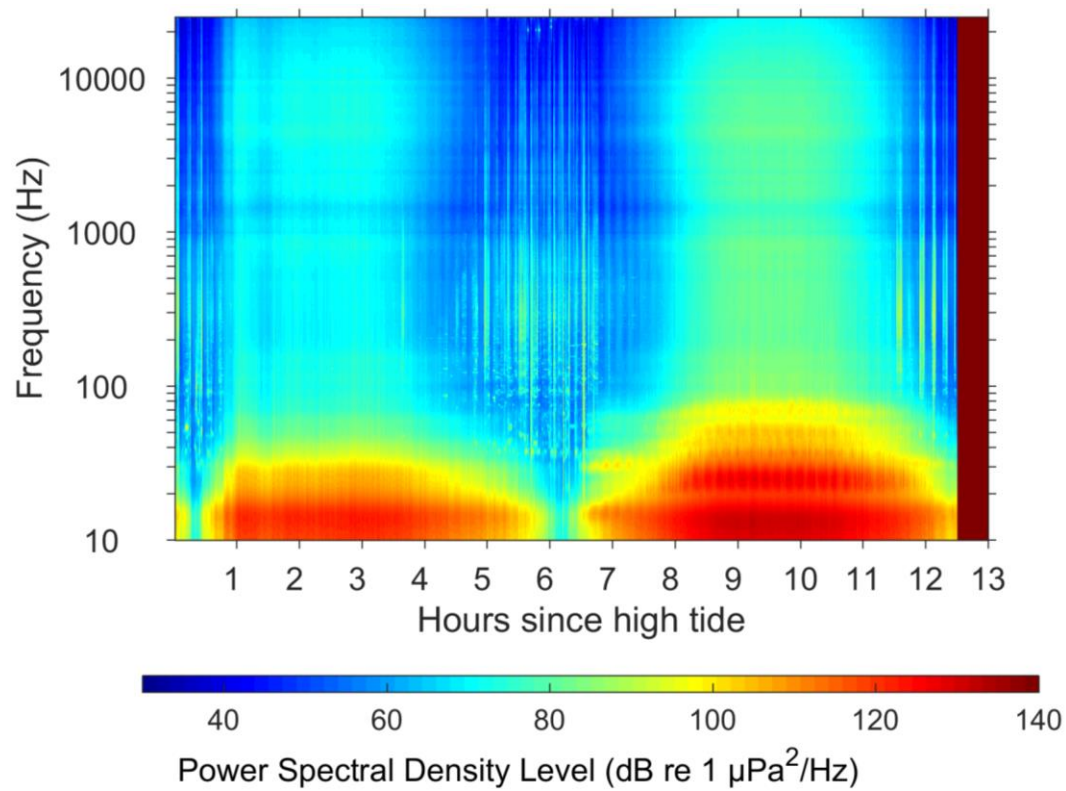


Figure B-18. Cadence spectrogram for the hours since high tide, for the pre-turbine operation AMAR hydrophone, 1–22 Jul 2018.

B.3.2. Turbine Operation

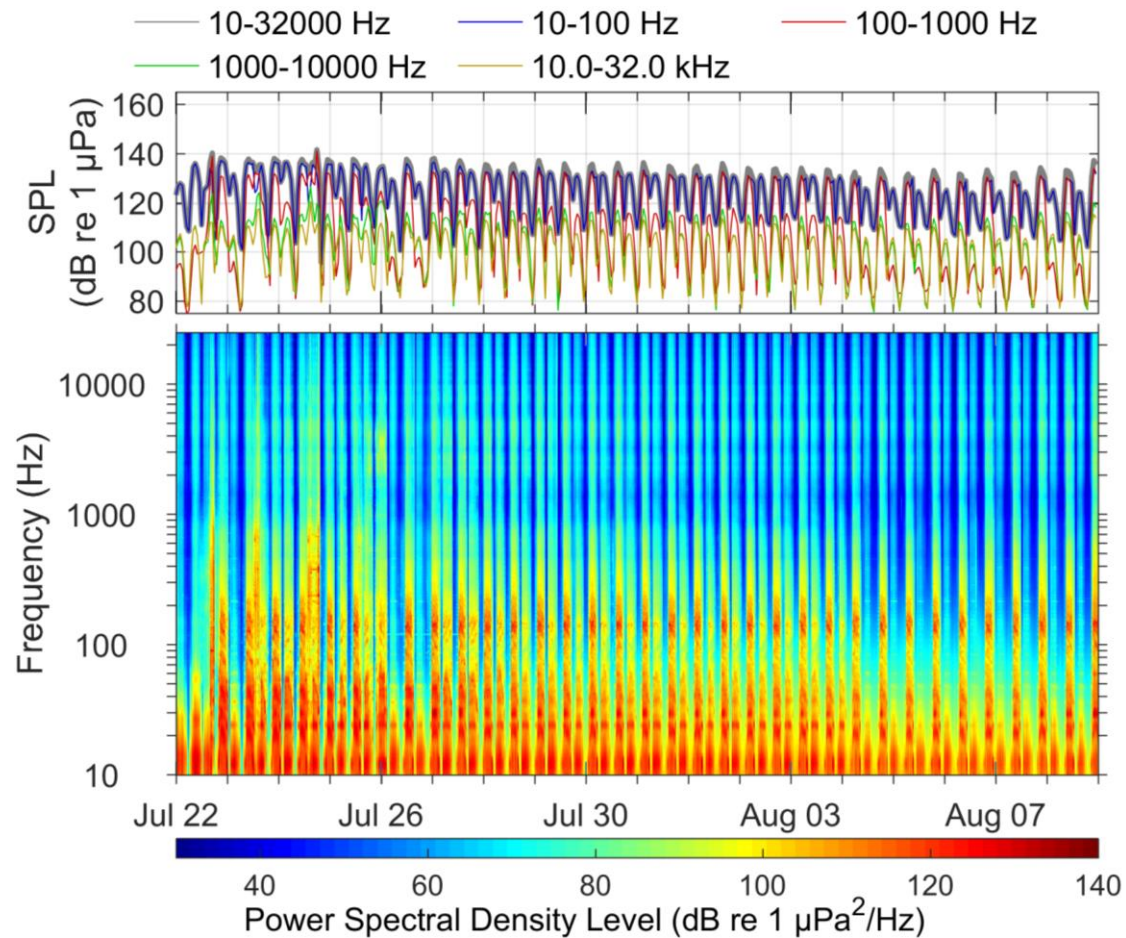


Figure B-19. (Top) in-band SPL and (bottom) spectrogram for the AMAR hydrophone during the turbine operation period, 22 Jul to 9 Aug 2018.

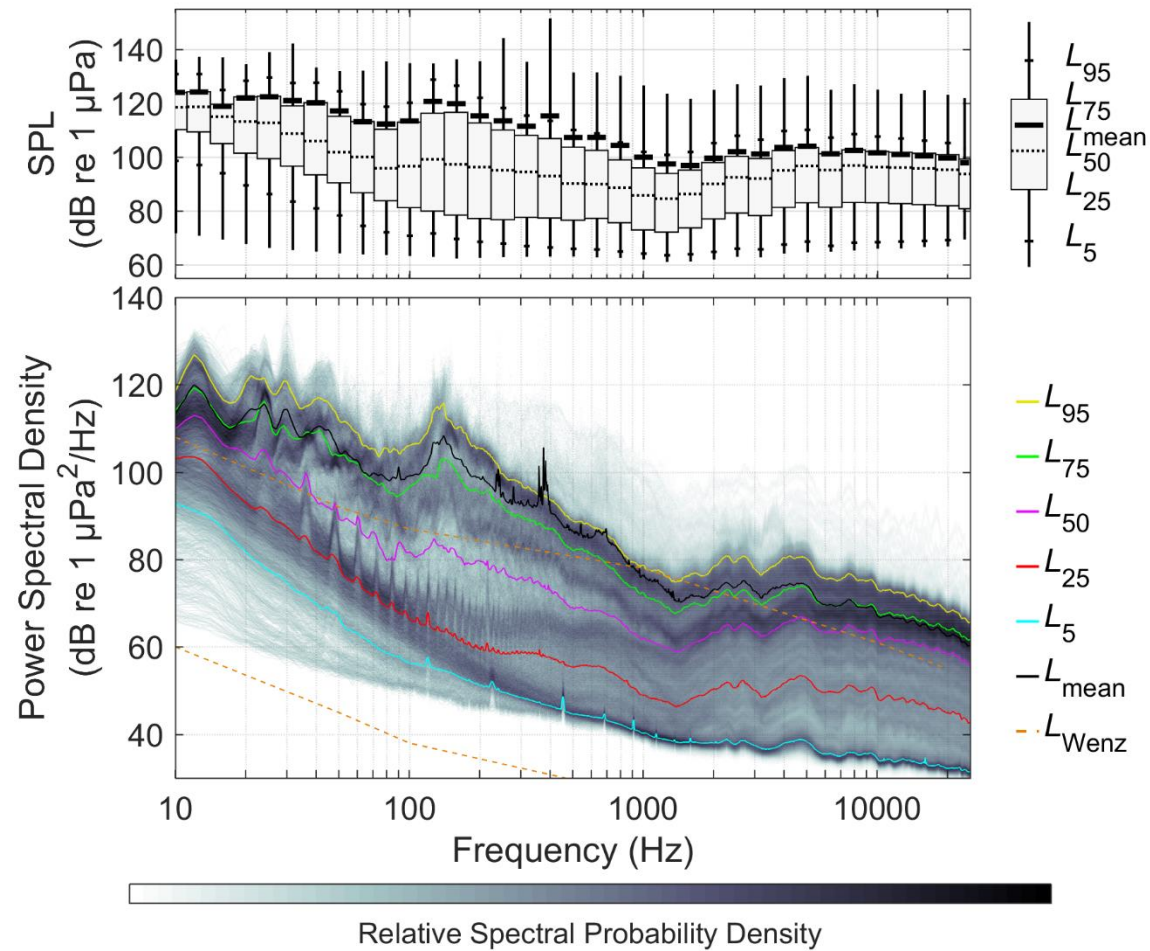


Figure B-20. (Top) Exceedance percentiles and mean of the decidecade band SPL and (bottom) exceedance percentiles and probability density (grayscale) of 1-min PSD levels compared to the limits of prevailing noise (Wenz 1962) for the AMAR hydrophone during the turbine operation period, 22 Jul to 9 Aug 2018.

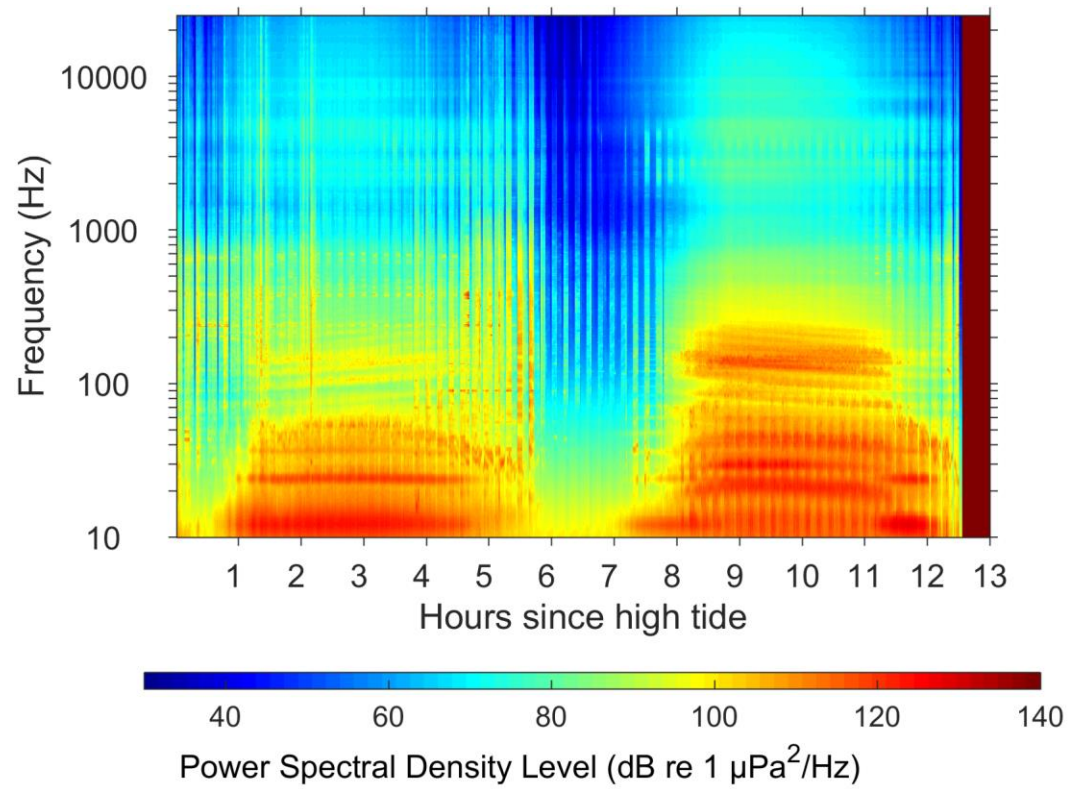


Figure B-21. Cadence spectrogram for the hours since high tide, for the turbine operation AMAR hydrophone, 22 Jul to 9 Aug 2018.

B.3.3. Post-Turbine Operation

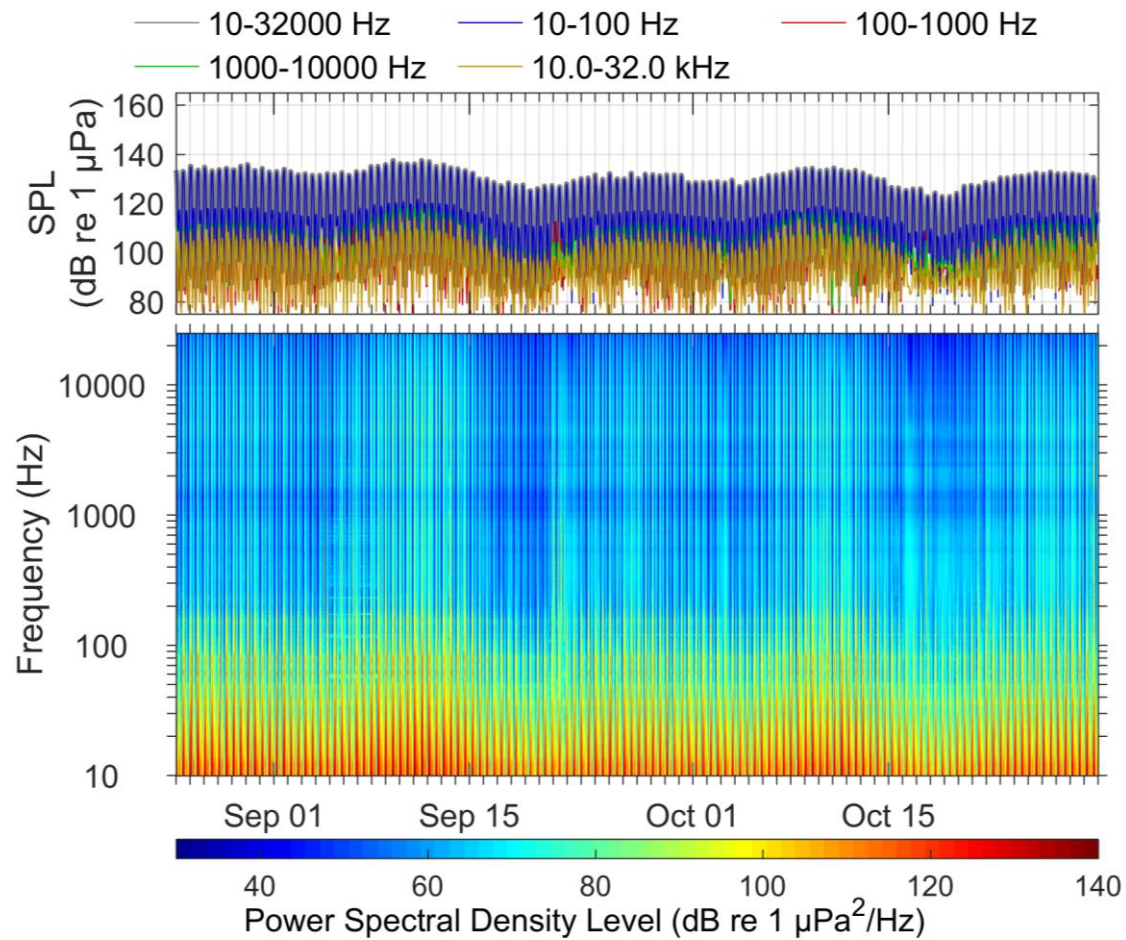


Figure B-22. (Top) in-band SPL and (bottom) spectrogram for the AMAR hydrophone during the post-turbine operation period, ~25 Aug to 30 Oct 2018.

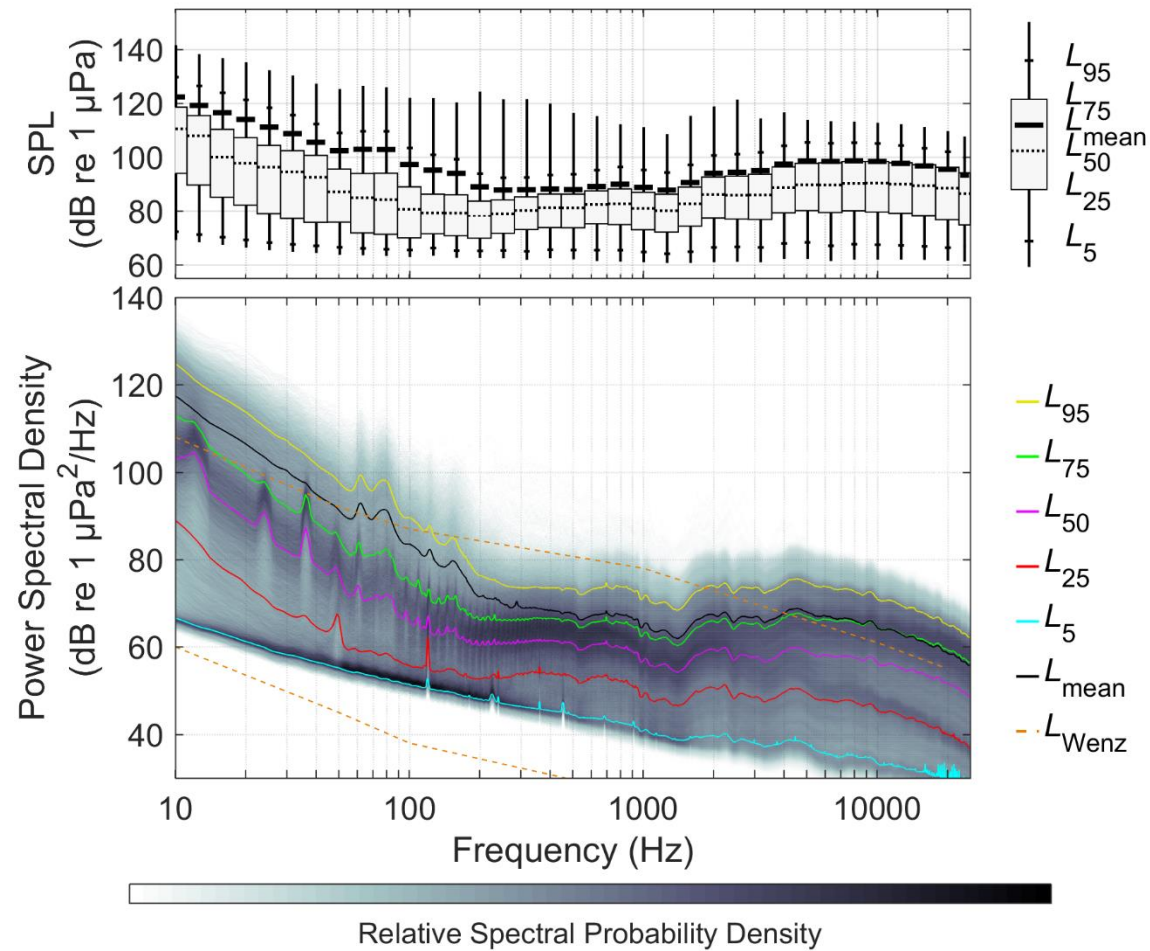


Figure B-23. (Top) Exceedance percentiles and mean of the decidecade band SPL and (bottom) exceedance percentiles and probability density (grayscale) of 1-min PSD levels compared to the limits of prevailing noise (Wenz 1962) for the AMAR hydrophone during the post-turbine operation period, ~25 Aug to 30 Oct 2018.

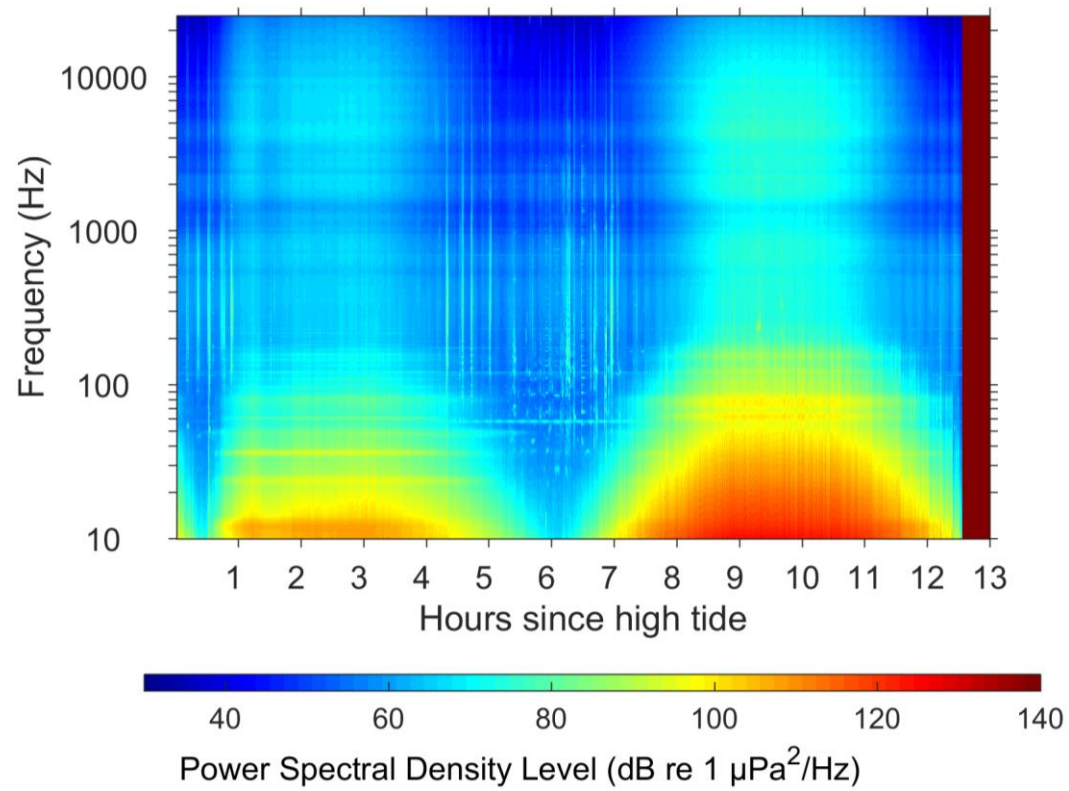


Figure B-24. Cadence spectrogram for the hours since high tide, for the post-turbine operation AMAR hydrophone, ~25 Aug to 30 Oct 2018.

Appendix C. Decidecade Sound Pressure Level Tables

Table C-1. Aft hydrophone decidecade band percentile values

band	min	1st	5th	10th	25th	50th	75th	90th	95th	99th	max	mean
1	49.14	53.36	60.32	67.08	84.74	96.11	101.6	104.77	106	107.81	110.49	100.02
1.3	50.14	54.36	61.32	68.08	85.74	97.11	102.6	105.77	107	108.81	111.49	101.02
1.6	50.05	52.97	58.39	65.48	84.97	97.58	103.54	106.92	108.2	110.21	113.4	102.09
2	50.44	52.68	55.82	63.87	85.07	98.36	104.53	107.96	109.28	111.39	114.69	103.12
2.5	51.34	52.93	55.43	63.16	84.72	98.63	105.25	108.84	110.14	112.1	115.94	103.9
3.2	51.73	53.02	54.78	61.73	83.72	98.72	106.03	109.7	111.02	112.91	117.06	104.69
4	52.39	53.62	55.1	61.48	82.24	97.9	106.35	110.33	111.77	113.6	116.85	105.16
5	53.45	54.6	56.01	62.32	82.96	98.64	107.2	111.24	112.69	114.59	117.65	106.05
6.3	53.87	55.22	56.26	61.34	80.16	95.64	105.89	111.08	113.01	115.36	118.47	105.77
7.9	54.8	56.09	57.05	61.52	84.03	96.06	105.94	111.48	113.55	116.05	119.46	106.22
10	55.9	56.91	57.81	61.56	90.58	105.53	109.9	113.81	115.22	117.07	120.39	109.02
12.6	56.87	57.72	58.52	61.68	90.42	107.77	112.82	115.82	116.81	118.19	121.36	111.08
15.8	57.62	58.49	59.22	62.5	79.51	94.26	103.69	109.83	112.48	115.5	120.54	104.88
20	58.46	59.29	59.93	61.3	78.41	92.94	101.4	108.52	111.29	114.45	119.16	103.53
25.1	59.44	60.13	60.76	62.25	78.9	96.34	102.45	110.69	114.02	119.53	125.14	107.2
31.6	60.1	60.97	61.59	64.3	79.33	99.05	106.31	111.81	118.37	126.26	133.78	112.91
39.8	60.94	61.76	62.35	65.75	79.18	98.72	104.8	111	112.09	113.84	117.03	105.14
50.1	61.87	62.58	63.15	69.89	88.83	98.64	102.8	105.78	107.05	108.96	112.92	101.34
63.1	62.85	63.52	63.94	65.13	78.39	92.49	99.93	104.75	106.51	109.3	119.79	100.01
79.4	63.52	64.28	64.78	65.58	73.28	90.31	97.51	102.11	103.57	105.62	118.92	96.87
100	64.13	65.08	65.63	66.76	74.99	90.47	97.54	102.4	104.25	106.68	114.32	97.3
125.9	64.93	65.91	66.59	67.74	75.19	86.54	93.06	97.72	99.48	101.84	113.55	92.72
158.5	66.97	68.4	70.04	71.93	79.59	92.68	99.03	103.42	105.25	107.8	121.42	98.64
199.5	65.83	66.78	67.57	68.72	74.18	85.64	92.74	97.91	100.74	104.15	115.54	93.53
251.2	66.91	67.61	68.36	69.63	75.92	85.22	92.02	97.91	101.67	105.9	110.84	94.33
316.2	67.93	69.5	71.07	72.48	78.01	86.72	94.21	99.09	101.31	104.52	114.32	94.46
398.1	68.35	70.86	72.78	73.85	78.2	85.14	92.14	96.88	100.3	104.52	115.49	93.4
501.2	67.49	68.69	69.64	70.94	76.16	82.73	89.21	94.62	98.51	102.13	112.04	91.07
631	67.48	68.89	69.99	71.37	76.35	82.77	88.8	94.58	98.51	102.07	111.14	90.91
794.3	67.25	69.01	70.82	72.58	78	84.23	91	96.8	100.76	104.27	111.32	93.06
1000	68.94	70.62	72.41	74.19	79.12	85.63	93.03	99.11	103.31	107.09	110.56	95.48
1258.9	70.81	72.58	74.85	76.36	81.35	88.15	95.85	102.43	106.82	110.94	114.24	99.02
1584.9	69.96	72.31	74.32	75.91	80.73	88.09	96.06	102.48	106.67	110.72	115.35	98.94
1995.3	70.96	73.72	76.05	77.61	82.44	89.29	97.41	103.77	107.97	112.26	118.68	100.32
2511.9	69.65	72.2	74.74	76.19	79.55	87.33	95.72	101.93	106.02	109.57	115.44	98.11
3162.3	72.15	74.76	76.62	77.9	81.01	88.99	97.3	103.34	107.28	110.41	113.86	99.27
3981.1	73.44	75.52	77.31	78.45	81.85	90.33	98.62	104.65	108.54	111.59	114.89	100.54
5011.9	72.23	74.34	76.09	77.2	80.38	89.46	97.69	103.76	107.64	110.62	113.77	99.63
6309.6	71.93	73.73	75.2	76.28	79.71	89.32	97.31	102.96	106.7	109.6	113.65	98.82
7943.3	74.71	76.35	77.54	78.45	81.93	92.17	99.96	105.48	108.91	111.49	114.63	101.05
10000	75.15	76.66	77.56	78.33	81.84	92.58	100.24	105.51	108.68	111	116.51	100.92
12589.3	74.29	75.33	76.11	76.87	80.67	91.87	99.4	104.41	107.25	109.42	115.73	99.69
15848.9	76.7	77.98	78.99	79.73	82.8	93.6	100.84	105.67	108.03	110.21	112.6	100.77
19952.6	76.83	78.04	78.88	79.6	83.43	94.73	101.88	106.61	108.77	110.98	114	101.67
25118.9	76.11	77.04	77.68	78.35	81.8	92.87	99.8	104.4	106.45	108.62	111.33	99.44
31622.8	75.7	76.81	77.43	78	81.02	91.65	98.42	102.94	104.92	107.09	110.11	98
39810.7	76.69	77.61	78.2	78.67	81.17	91.01	97.71	102.23	104.31	106.55	112.3	97.39
50118.7	76.52	77.38	77.99	78.48	80.63	89.63	96.49	101.14	103.69	106.06	128.14	98.65
63095.7	76.64	77.46	77.89	78.18	79.44	85.94	92.67	97.53	100.33	102.84	108.02	93.02
79432.8	80.83	82.39	83.16	83.55	84.45	87.33	92.29	97.07	100.02	102.82	108.65	92.99
100000	81.55	82.16	82.42	82.63	83.04	85.03	90.45	95.66	98.94	101.88	110.19	91.72
125892.5	82.31	83.04	83.32	83.48	83.84	84.95	89.09	94.11	97.35	100.49	122.75	91.99
158489.3	79.13	79.85	80.13	80.28	80.63	81.7	85.35	90.15	93.22	96.32	102.91	86.53
199526.2	84.25	85.48	86.92	87.26	87.68	88.36	89.84	91.95	93.76	96.12	104.41	89.74

Table C-2. Starboard hydrophone decidecade band percentile values

band	min	1st	5th	10th	25th	50th	75th	90th	95th	99th	max	mean
1	58.35	75.4	87.5	103.54	121.94	133.03	138.19	141.24	142.54	144.47	147.59	136.64
1.3	59.35	76.4	88.5	104.54	122.94	134.03	139.19	142.24	143.54	145.47	148.59	137.64
1.6	57.58	73.94	86.76	104.63	123.75	135.35	140.83	143.86	145.11	146.88	150.12	139.18
2	57.15	72.38	86.45	105.19	124.69	136.38	141.98	145.04	146.26	148.08	151.63	140.34
2.5	56.61	70.61	85.76	105.35	125.34	137.23	142.98	146.11	147.4	149.37	153.38	141.41
3.2	55.65	65.26	84.85	105.41	125.95	138.07	143.95	147.13	148.5	150.61	154.92	142.44
4	55.03	60.78	82.75	104.67	126.04	138.6	144.61	147.91	149.38	151.6	156.04	143.23
5	56.02	61.53	83.45	105.38	126.87	139.48	145.51	148.83	150.29	152.52	156.98	144.14
6.3	55.25	58.72	78.33	102.03	125.64	138.93	145.27	148.65	150.22	152.8	157.36	144
7.9	56.44	59.78	77.82	101.18	125.77	139.2	145.59	149.03	150.63	153.19	157.86	144.36
10	58.19	61.62	76.59	98.26	127.58	141.38	145.52	148.75	150.36	153.04	157.08	144.43
12.6	58.32	62.32	77.08	95.65	127.67	142.59	145.97	148.54	150.08	152.63	157.01	144.58
15.8	57.75	61.72	72.76	90.94	120.61	136.01	143.08	146.87	148.54	151.22	155.65	142.1
20	56.12	58.22	68.42	86.5	117.22	133.97	141.29	145.24	146.9	149.65	153.96	140.41
25.1	55.82	57.44	65.92	82.66	113.33	131.75	139.35	143.43	145.12	147.9	152.14	138.57
31.6	56.75	58.84	65.72	80.85	108.7	128.53	136.86	141.21	142.98	145.73	150.54	136.28
39.8	56.24	58.33	64.53	79.24	104.56	124.83	133.8	138.5	140.36	143.17	148.14	133.51
50.1	55.44	57.41	63.6	82.47	110.42	125.47	131.68	136.26	138.26	141.16	146.35	131.52
63.1	56.51	58.48	65.3	73.91	97.86	115.81	125.63	131.15	133.43	136.75	142.28	126.3
79.4	57.19	58.89	61.91	70.16	90.89	110.47	120.56	126.41	128.84	132.42	139.09	121.67
100	56.73	58.68	61.91	68.72	88.01	106.15	116.03	122	124.51	128.19	135.48	117.33
125.9	76.44	77.35	77.75	79.37	91.03	104.23	113.24	118.92	121.38	124.93	132.34	114.28
158.5	61.76	64.21	67.61	72.76	88.77	103.88	111.43	116.91	119.23	122.45	129.5	112.16
199.5	64.86	66.31	68.51	72.25	83.43	96.25	104.64	110.66	113.27	116.92	123.77	106.01
251.2	63.79	66.27	69.18	72.64	84	96.81	103.88	109.76	112.37	115.65	120.64	105.05
316.2	64.46	66.37	69.23	72.64	83.48	94.9	101.44	106.95	109.51	112.69	119.58	102.29
398.1	64.2	66.37	70.36	74.74	81.46	92.18	97.74	103.32	106.08	109.29	116.7	98.82
501.2	66.17	67.84	70.11	72.28	79.56	88.48	94.84	101.05	104.17	107.33	115.13	96.61
631	64.64	67.61	70.94	73.3	80.21	88.85	96.62	102	105.18	108.29	115.71	97.65
794.3	64.85	67.3	70.69	73.28	80.28	88.94	95.41	101.99	105.7	109.1	113.29	97.85
1000	67.96	70.58	73.56	76.09	83	91.74	99.02	105.44	109.28	112.83	115.98	101.4
1258.9	68.51	72.34	75.44	77.9	84.66	93.26	100.16	107.6	111.67	115.66	119.21	103.76
1584.9	68.52	71.49	74.45	76.71	83.12	92.46	99.62	106.7	111.24	116.49	120.37	103.77
1995.3	66.89	70.24	72.85	75.01	81.09	90.68	97.62	104.78	109.14	113.49	118.61	101.39
2511.9	69.75	73.73	76.07	77.7	83.32	91.95	100.19	106.35	110.26	113.32	119.55	102.25
3162.3	70.73	74.44	76.91	78.66	83.87	92.23	100.68	106.47	110.15	113.32	119.74	102.38
3981.1	71.31	74.63	77.17	78.82	83.34	93.08	101.41	107.01	110.57	113.55	118.8	102.77
5011.9	70.08	72.92	75.33	77.14	81.91	91.81	99.87	105.53	109.21	112.01	117.76	101.27
6309.6	72.69	74.18	75.37	76.99	82.1	92.44	100.44	105.99	109.48	112.23	116.45	101.66
7943.3	74.82	76.07	77.01	78.55	83.97	95.36	103.21	108.9	112.32	115	119.01	104.47
10000	73.71	75.49	76.61	78.18	84.16	96.72	104.39	110	113.18	115.69	119.47	105.37
12589.3	73.46	75.37	76.5	77.76	82.91	95.76	103.08	108.27	111.16	113.32	118.61	103.49
15848.9	76.43	77.94	79.35	80.14	84.34	96.39	103.86	109.15	111.86	114.12	117.31	104.3
19952.6	78.06	79.17	80.04	80.83	85.33	97.7	104.84	109.92	112.36	114.56	117.7	104.99
25118.9	78.52	79.24	79.74	80.26	83.92	95.78	102.77	107.61	110.01	112.18	115.69	102.73
31622.8	77.89	78.61	79.13	79.63	83.09	94.72	101.4	106.03	108.42	110.5	113.79	101.2
39810.7	79.39	80.47	80.99	81.38	83.63	93.71	100.36	105.1	107.65	109.88	113.83	100.37
50118.7	79.76	80.72	81.07	81.38	83.33	92.6	99.3	104.31	107.09	109.56	130.81	101.73
63095.7	79.41	80.36	80.62	80.83	81.9	88.77	95.41	100.48	103.5	106.13	112.34	96.05
79432.8	83.73	84.72	85.04	85.22	85.71	88.64	94.36	99.52	102.83	105.73	113.26	95.47
100000	85.71	86.62	86.9	87.04	87.28	89.02	93.83	98.99	102.52	105.5	113.38	95.27
125892.5	90.22	91.11	91.67	91.76	91.96	92.29	94.23	97.99	101.17	104.21	129.55	96.73
158489.3	90.45	91.11	91.93	92.02	92.1	92.23	92.99	95.25	97.65	100.26	109.35	93.59
199526.2	96.03	96.58	97.39	97.52	97.67	97.77	97.91	98.54	99.55	101.19	114.45	98.09

Table C-3. Top hydrophone decidecade band percentile values

band	min	1st	5th	10th	25th	50th	75th	90th	95th	99th	max	mean
1	75.1	94.85	111.35	121.66	134.16	141.93	149.35	153.9	155.14	156.24	157.83	148.33
1.3	76.1	95.85	112.35	122.66	135.16	142.93	150.35	154.9	156.14	157.24	158.83	149.33
1.6	74.26	95.12	113.25	124.31	137.55	145	151.19	155.56	156.67	157.66	158.95	150.12
2	73.23	95.4	114.17	125.48	138.86	146.25	152.14	156.44	157.51	158.51	159.82	151.06
2.5	71.46	94.69	114.62	126.58	140.44	147.78	152.9	156.91	157.91	158.8	160.19	151.7
3.2	64.06	93.44	115.03	127.66	141.86	149.15	153.74	157.35	158.25	159.12	160.49	152.36
4	59.57	90.63	114.81	128.21	143.26	150.73	154.51	157.39	158.19	158.98	159.85	152.85
5	60.24	91.22	115.55	129.14	144.28	151.82	155.52	158.26	159.05	159.79	160.66	153.79
6.3	55.48	84.1	112.11	128.33	145.16	153.43	156.36	157.85	158.35	158.9	159.79	154.13
7.9	56.39	82.44	110.81	128.47	145.74	154.47	157.24	158.45	158.85	159.42	161.03	154.93
10	58.84	78.52	106.88	127.02	145.74	155.84	158.09	158.87	159.24	160.35	162.1	155.77
12.6	61.08	75.63	103.07	124.72	145.3	156.72	158.76	159.41	160.01	161.16	163	156.46
15.8	61.5	72.37	98.9	120.54	144.21	154.92	158.25	159.23	159.58	160.72	162.97	155.7
20	59.17	69.16	94.08	115.75	142.46	153.88	157.75	159.05	159.42	160.08	162.68	155.17
25.1	57.52	65.52	89.93	111.43	139.69	152.76	157.02	158.65	159.12	159.65	162.11	154.48
31.6	59.51	64.73	85.98	106.67	135.53	151.08	156.16	158.01	158.59	159.2	160.58	153.6
39.8	57.74	63.48	83.1	102.24	131.11	148.64	155.27	157.56	158.17	158.77	159.62	152.73
50.1	58.96	64.63	82.59	98.62	126.59	145.14	153.41	157.06	157.86	158.66	159.56	151.61
63.1	59.01	64.85	79.94	97.41	122.19	141.72	150.5	155.84	157.17	158.38	159.64	150.01
79.4	61.46	65.6	75.93	93.09	118.25	138.53	147.65	153.38	155.4	157.17	158.98	147.84
100	62.86	66.78	75.27	92.35	115.8	135.85	145.57	151.46	153.49	155.38	157.46	145.91
125.9	68.13	72.16	79.58	93.4	115.87	134.32	144.3	150.65	152.75	154.56	156.55	145
158.5	63.39	67.68	74.11	87.64	109.36	128.46	139.56	146.86	149.33	151.41	153.68	141.29
199.5	63.47	66.81	71.6	79.32	99.93	122.36	134.99	143.32	146.28	148.75	151.51	137.96
251.2	68.24	70.4	73.07	78.46	94.39	118.36	131.22	140.09	143.48	146.26	149.33	135.08
316.2	60.82	64.36	68.99	76.27	90.14	114.75	127.53	136.68	140.39	143.56	146.89	132.02
398.1	61.81	66.24	71.38	76.96	88.84	111.81	124.18	133.22	137.19	140.65	144.3	128.85
501.2	64.58	68.22	72.68	77.06	87	108.83	120.98	129.71	133.81	137.41	141.54	125.55
631	63.08	66.86	71.59	75.52	85.13	105.75	117.81	126.35	130.36	134.09	138.05	122.19
794.3	62.5	65.74	70.59	74.6	83.61	102.92	114.79	123.23	127.02	130.59	134.74	118.89
1000	63.1	66.41	71.07	75.22	83.46	100.51	111.95	120.26	123.85	127.35	131.22	115.74
1258.9	63.8	67.08	71.71	75.69	83.56	98.52	109.41	117.43	120.98	124.23	128.04	112.82
1584.9	64.01	66.81	71.04	74.73	82.41	96.52	106.97	114.72	118.22	121.3	124.95	110.04
1995.3	64.16	67.11	70.95	74.17	81.24	94.09	104.36	112.06	115.54	118.5	122.04	107.33
2511.9	65.5	68.7	72	75.03	81.72	93.37	102.95	109.98	113.44	116.19	119.12	105.23
3162.3	66.73	70.17	72.86	75.26	81.91	93.26	102.27	108.5	111.88	114.32	116.66	103.74
3981.1	67.98	70.89	73.16	75.46	82.26	93.61	102.13	107.76	111.02	113.22	114.88	103.01
5011.9	68.22	71.3	73.51	75.84	82.9	94.32	102.35	107.63	110.56	112.83	114.4	102.83
6309.6	68.23	70.63	72.76	75.24	82.57	94.4	102.19	107.24	109.96	112.15	114.1	102.4
7943.3	67.61	69.95	71.99	74.65	82.09	94.28	101.82	106.62	109.07	111.15	114.97	101.71
10000	67.63	69.52	71.28	73.75	81.03	93.48	100.79	105.41	107.62	109.62	118.77	100.48
12589.3	68.84	70.52	72.25	74.65	81.98	94.71	101.82	106.34	108.27	110.24	118.01	101.29
15848.9	72.02	73.77	75.26	76.79	82.96	95.45	102.45	106.78	108.58	110.61	113.2	101.73
19952.6	72.98	75.29	76.3	77.36	83.27	95.53	102.2	106.21	107.81	109.79	112.13	101.19
25118.9	71.65	73.3	74.23	75.55	81.83	94.4	100.99	104.91	106.47	108.42	110.86	99.92
31622.8	71.48	73.14	74	75.08	80.35	92.21	98.73	102.57	104.09	106.03	108.42	97.6
39810.7	75.37	76.87	77.64	78.18	81.13	91.28	97.79	101.72	103.33	105.43	113.1	96.82
50118.7	74.76	76.04	76.72	77.33	80.5	90.34	97	101.13	103.01	105.52	131.5	100.83
63095.7	74.03	75.25	75.88	76.39	78.58	86.34	93.12	97.43	99.5	101.84	106.15	92.63
79432.8	79.36	80.55	81.23	81.62	83.11	86.76	92.65	97.01	99.37	101.86	107.19	92.55
100000	80.05	81.22	81.75	82.02	82.94	86.08	92.06	96.55	99.11	101.67	111.29	92.27
125892.5	81.57	82.87	83.28	83.52	84.3	86.1	90.59	94.79	97.33	100.08	125.09	93.56
158489.3	78	79.3	79.77	80.06	80.84	82.55	86.49	90.66	93.15	95.71	102.9	86.81
199526.2	83.82	86.73	87.37	87.8	88.73	90.24	91.31	92.48	93.87	95.77	104.92	90.74

Table C-4. FAST platform hydrophone decidecade band percentile values

band	min	1st	5th	10th	25th	50th	75th	90th	95th	99th	max	mean
1	61.6	75.89	87.68	100.24	115.78	124.06	130.23	134.98	136.79	138.76	144.12	129.86
1.3	62.6	76.89	88.68	101.24	116.78	125.06	131.23	135.98	137.79	139.76	145.12	130.86
1.6	64.21	74.61	88.83	101.65	118.14	126.94	134.11	138.85	140.5	142.37	146.5	133.55
2	64.98	72.88	89.39	102.28	119.19	128.16	135.56	140.29	141.91	143.78	147.61	134.96
2.5	66.34	72.08	89.62	102.89	120.06	129.36	137.08	142.34	143.92	145.74	149.49	136.84
3.2	61.48	70.3	89.58	103.47	120.94	130.47	138.46	144.09	145.72	147.5	151.14	138.51
4	57.55	70.08	88.29	103.85	121.49	131.31	139.3	145.96	147.84	149.76	152.71	140.29
5	58.35	70.88	88.98	104.64	122.38	132.23	140.19	146.91	148.88	150.85	153.56	141.29
6.3	57.47	69.17	84.36	102.7	121.95	132.42	140.06	147.25	149.91	152.7	155.58	142.12
7.9	59.11	68.12	83.44	101.83	122.21	132.96	140.49	147.64	150.33	153.24	156.41	142.59
10	58.79	65.54	80.6	99.07	121.83	132.94	140.3	147.38	150.11	152.98	155.92	142.34
12.6	57	69.5	79.06	96.53	121.32	132.72	140.05	147	149.77	152.64	155.02	142
15.8	57.18	72.02	77.46	93.43	119.48	131.93	139.32	146.03	148.9	151.94	154.74	141.18
20	56.58	67.39	74.08	90.57	116.33	131.25	138.33	144.61	147.56	150.78	153.83	139.92
25.1	57.13	71.65	73.91	87.54	112.53	129.39	137.24	143.21	146.21	149.44	153.01	138.61
31.6	56.45	69.29	71.57	85.07	109.88	126.25	135.84	141.67	144.64	147.89	151.56	137.04
39.8	55.94	70.69	72.19	81.85	106.3	121.7	132.48	139.23	142.27	145.74	149.27	134.54
50.1	56.49	71.32	72.41	80.92	101.95	117.52	127.95	135.91	139.46	143.16	146.88	131.52
63.1	56.87	71.45	72.55	79.05	98.82	113.66	124.01	132.31	136.23	140.24	144.52	128.27
79.4	56.83	70.27	71.1	74.69	96.68	111.54	120.36	128.7	132.65	136.84	141.06	124.77
100	56.55	70.32	71.15	74.95	95.87	109.85	117.63	125.48	129.35	133.63	137.94	121.57
125.9	59.83	70.1	71.1	75.94	93.63	106.72	113.87	121.67	125.74	130.06	134.81	117.97
158.5	56.69	69.09	70.11	74.54	90.75	103.07	109.97	117.37	121.39	125.93	131.02	113.81
199.5	56.97	68.52	69.53	72.35	85.59	97.78	104.81	112.72	116.86	121.52	126.82	109.23
251.2	58.62	68.21	69.61	72.9	83.33	94.58	100.98	108.32	112.45	117.17	122.71	104.96
316.2	58.3	67.17	68.66	73.28	82.68	93.16	99.31	105.59	109.32	113.92	120.5	102.07
398.1	59.61	66.64	69.22	72.82	80.58	89.95	96.73	102.64	106.19	110.59	119.55	98.99
501.2	61.22	65.99	68.53	71.99	80.27	89.38	96.18	101.73	105.28	109.17	118.55	97.96
631	62.29	65.55	69	73.16	80.68	89.31	95.51	101.71	105.2	109.01	117.85	97.72
794.3	62.93	65.24	69.36	73.53	80.82	89.42	95.82	102.25	106.1	109.58	116.92	98.29
1000	63.92	65.39	69.97	74.02	80.98	89.26	96.46	103.14	106.9	110.3	116.19	99.02
1258.9	63.61	65.13	69.77	73.34	80.39	89.19	96.84	103.23	107.21	110.84	115.93	99.39
1584.9	63.78	65.77	69.99	73.64	80.43	89.4	97.85	104.2	108.25	111.79	116.13	100.33
1995.3	63.72	65.98	70.04	73.5	80.41	90.07	98.86	105.14	109.13	112.56	116.01	101.18
2511.9	65.25	67.76	70.85	73.83	81.04	91.44	99.92	105.97	110.07	113.46	116.89	102.13
3162.3	62.81	65.73	68.61	71.75	79.12	90	98.35	104.29	108.33	111.66	114.94	100.41

Table C-5. HFM (pre-turbine) hydrophone decidecade band percentile values

band	min	1st	5th	10th	25th	50th	75th	90th	95th	99th	max	mean
1	87.2	89.38	91.28	93.88	105.39	118.36	125.51	129.98	132.46	135.69	140.1	125.48
1.3	88.2	90.38	92.28	94.88	106.39	119.36	126.51	130.98	133.46	136.69	141.1	126.48
1.6	85.46	87.75	89.64	92.62	105.09	117.7	124.93	129.49	132.15	135.51	139.7	125.1
2	83.99	86.21	88.08	91.33	104.92	117.35	124.66	129.29	132.01	135.44	139.85	124.96
2.5	82.8	84.98	86.9	91.02	104.94	117.03	124.28	128.99	131.71	135.16	139.3	124.62
3.2	79.38	81.88	84.15	90.52	104.79	116.37	123.59	128.42	131.07	134.5	138.39	123.99
4	75.6	78.08	81.18	90.24	104.61	115.63	122.63	127.52	130.09	133.4	137.6	123.04
5	76.19	78.68	81.85	91.08	105.56	116.47	123.48	128.34	130.91	134.21	138.36	123.86
6.3	68.65	70.91	77.29	90.55	106.24	115.91	122.63	127.5	130.05	133.2	136.47	122.95
7.9	67.76	70.2	77.19	91.08	107.44	117.07	123.69	128.71	131.27	134.33	137.71	124.11
10	67.18	69.61	77.5	91.98	109.19	119.33	125.84	131.01	133.74	136.73	140.29	126.45
12.6	66.86	69.38	79.1	94.16	112.76	122.09	128.29	133.26	135.94	138.85	142.17	128.7
15.8	65.98	68.36	78.33	92.91	112.63	121.46	127.14	131.44	133.69	136.57	139.73	126.93
20	64.63	66.33	70.53	82.05	101.55	113.39	120.79	127.43	129.75	132.35	135.88	122.21
25.1	63.71	65.24	68.09	76.65	97.19	108.69	119.02	130.46	133.67	137.92	143.7	125.92
31.6	63.09	64.7	67.51	74.19	93.93	105.33	112.78	123.02	126.26	129.81	134.71	118.24
39.8	62.4	63.92	66.26	70.08	86.57	96.62	105.99	113.31	117.2	122.76	128.62	110.25
50.1	61.3	62.95	65.15	67.78	80.47	89.78	101.9	111.31	114.61	118.57	122.95	106.77
63.1	60.85	62.78	65.07	68.52	78.35	87.93	100.12	108.38	110.6	113.21	119.75	102.78
79.4	60.25	62.31	65.28	67.6	74.96	83.03	93.46	103.53	107.23	111.88	120.33	99.78
100	60.05	62.01	64.48	67.18	73.55	81.74	90.56	96.81	99.85	103.62	117.83	92.85
125.9	59.76	61.82	64.65	67.39	74.13	82.65	90.59	96.55	99.71	103.52	119.97	92.96
158.5	59.39	61.65	64.57	67.49	74.33	82.92	90.62	96.57	99.82	103.72	119.98	93.07
199.5	59.24	61.45	64.53	67.17	73.39	81.82	89.44	95.62	99.24	103.51	125.29	93.81
251.2	59.39	61.76	65.4	68.18	74.28	82.63	90.1	96.44	100.29	104.3	127.41	95.25
316.2	59.59	61.74	66.17	69.04	75.21	83.83	91.2	97.43	101.33	105.34	129.19	96.45
398.1	60.12	62.7	67.08	69.97	75.96	84.78	92.12	98.12	102.11	106.26	126.78	96.2
501.2	61.14	63.55	67.47	70.38	76.23	85.27	92.63	98.51	102.59	106.71	123.45	95.79
631	60.6	63.51	67.78	70.75	76.67	86.2	93.68	99.58	103.54	107.72	120.82	96.45
794.3	61.46	64.44	68.34	71.48	77.41	87.44	95.08	100.8	104.77	109.01	117.51	97.44
1000	61.14	63.87	67.55	70.08	75.93	86.24	94.02	99.65	103.65	107.89	114.06	96.22
1258.9	60.47	63	66.54	69.57	74.73	85.57	93.22	98.51	102.55	107.05	113.1	95.26
1584.9	60.54	63.61	67.3	69.95	75.28	86.62	94.6	99.7	104	108.74	113.11	96.69
1995.3	61.83	65.37	69.52	71.76	77.3	89.11	97.09	102.15	106.54	111.17	114.5	99.14
2511.9	63.74	66.62	69.77	72.12	77.76	89.85	97.79	103.01	107.29	111.81	115.11	99.88
3162.3	64.22	67.22	70.04	72.23	78.48	91.12	99.07	104.22	108.29	112.56	115.92	100.87
3981.1	64.91	67.86	71.02	73.28	80.02	93.56	101.49	106.41	110.47	114.92	117.19	103.13
5011.9	65.64	68.08	71.08	73.39	81	95.14	102.88	107.71	111.81	115.91	117.96	104.33
6309.6	65.47	67.71	70.54	73	81.22	95.52	103.13	107.99	111.8	115.85	117.8	104.42
7943.3	65.73	67.52	70.37	72.9	81.89	96.22	103.65	108.38	112.01	115.95	117.83	104.68
10000	66.21	68.22	70.94	73.29	82.2	96.57	103.78	108.38	111.78	115.66	117.46	104.54
12589.3	66.74	68.55	70.94	73.07	82.19	96.28	103.44	107.98	111.11	115.07	116.98	104.04
15848.9	67.02	68.98	71.01	72.93	82.04	95.98	102.86	107.32	110.11	114.12	115.89	103.24
19952.6	67.49	69.11	70.92	72.74	82.02	95.85	102.47	106.76	109.3	113.22	118.82	102.58
25118.9	69.81	71.5	72.49	73.64	81.29	94.69	101.12	105.39	107.85	111.78	121.09	101.19

Table C-6. HFM (turbine on) hydrophone decidecade band percentile values

band	min	1st	5th	10th	25th	50th	75th	90th	95th	99th	max	mean
1	88.29	90.94	97.78	102.52	107.66	112.07	115.36	119.02	121.04	124.52	130.22	115.22
1.3	89.29	91.94	98.78	103.52	108.66	113.07	116.36	120.02	122.04	125.52	131.22	116.22
1.6	86.61	89.66	97.3	102.18	107.36	111.75	114.92	118.42	120.36	123.91	129.69	114.71
2	84.88	88.78	97.06	101.97	107.26	111.6	114.76	118.15	120.03	123.7	129.75	114.49
2.5	83.55	88.09	96.94	101.8	107.1	111.37	114.52	117.77	119.56	123.29	129.7	114.16
3.2	79.94	86.52	96.57	101.36	106.66	110.87	114.02	117.09	118.79	122.42	129.47	113.54
4	76.6	84.6	96.19	100.46	105.83	109.98	113.14	116.08	117.77	121.18	128.41	112.57
5	77.22	85.51	97.3	101.28	106.63	110.79	113.94	116.91	118.6	121.99	129.23	113.39
6.3	70.52	81.6	96.51	100.37	105.39	109.46	113.01	116.15	117.75	120.93	128.41	112.45
7.9	70.32	81.86	96.68	100.8	106.46	111.23	114.86	117.79	119.36	122.34	130.06	114.09
10	68.98	80.94	96.11	100.62	107.42	115.37	120.37	124.96	126.78	129.3	133.09	120.17
12.6	68.73	81.39	95.25	99.84	107.52	117.05	122.88	128.27	130.08	132.72	135.73	123.2
15.8	67.46	78.95	92.96	97.29	103.9	113.27	117.68	121.39	123.08	125.82	136.77	117.05
20	66.14	73.8	88.45	93.42	100.19	111.72	120.43	124.6	126.53	130.06	131.96	120.04
25.1	65.11	71.06	85.34	90.82	98.48	111.93	122.09	125.41	128.07	131.1	135.71	121.16
31.6	64.47	69.47	82.67	88.26	95.65	107.62	117.93	124.44	127.06	131.86	142.18	120.49
39.8	64.17	68.11	80.09	85.57	92.85	105.57	119.42	123.13	126.68	130.35	132.75	119.33
50.1	63.63	66.87	77.87	83.2	90.04	101.29	114.57	121.52	123.95	128.27	131.69	116.75
63.1	63.35	65.86	74.06	79.72	86.33	99.57	112.78	117.23	119.16	123.12	131.25	112.71
79.4	62.87	65	71.66	76.9	83.46	95.26	110.02	115.37	118.37	122.51	133.25	111.62
100	62.68	65	70.38	74.87	80.96	96.24	112.48	117.81	119.72	123.18	134.86	112.94
125.9	62.72	65	71.38	74.09	79.66	98.91	115.8	126.56	128.18	130.01	134.72	120.18
158.5	61.97	64.26	69.39	71.8	78.27	97.17	116.49	125.33	126.42	130.33	136.3	119.73
199.5	62.32	64.4	68.31	70.32	76.98	96.1	112.51	120.79	121.92	124.16	135.49	115.15
251.2	62.73	64.94	67.75	69.26	76.59	94.98	109.96	116.56	118.1	122.22	144.19	113.34
316.2	62.83	64.38	66.84	68.47	77.4	94.38	107.97	113.56	115.28	121.38	135.32	111.29
398.1	62.85	64.83	66.28	68.04	77.26	92.9	106.81	111.71	113.38	122.91	151.48	115.25
501.2	62.94	64.71	65.86	67.35	76.45	90.1	103.6	108.15	109.96	118.67	131.33	107.21
631	62.69	64.49	65.6	67.33	77.16	89.89	102.44	106.85	108.78	119.4	131.41	107.27
794.3	62.46	63.94	64.88	66.5	75.56	88.55	98.93	103.57	105.34	115.77	130.15	104.26
1000	61.93	63.32	64.11	65.13	72.88	85.72	95.92	100.24	101.86	110.4	126.55	99.91
1258.9	61.01	62.64	63.45	64.37	72.07	84.52	93.88	98.8	100.78	108.31	123.56	97.43
1584.9	61.15	63.09	63.83	65.51	73.64	86.23	95.13	99.98	101.84	106.51	121.59	96.83
1995.3	61.93	63.74	64.73	67.42	76.97	90.01	97.93	103.03	105.17	109.62	124.92	99.55
2511.9	62.92	64.71	65.95	68.26	79.16	92.43	100.26	105.62	107.9	112.75	127.07	101.97
3162.3	62.75	64.6	65.69	67.9	78.23	92	99.43	104.5	106.4	113.16	126.55	101.15
3981.1	64.08	66	67.46	69.61	81.26	95.01	102.4	107.65	109.69	113.66	129.32	103.55
5011.9	64.61	67.1	68.6	70.79	83	96.65	103.53	108.32	110.06	112.82	130.18	104.01
6309.6	64.81	66.01	66.98	69.75	81.34	95.16	101.23	105.59	107.21	109.36	124.97	101.19
7943.3	65.27	67.27	68.13	70.78	83.12	96.83	102.65	106.86	108.5	110.74	127.11	102.43
10000	65.91	67.46	68.34	70.92	83.02	96.27	102.06	106.06	107.59	109.55	125.03	101.54
12589.3	65.98	67.78	68.61	70.92	82.7	96.09	101.78	105.5	106.89	108.73	123.55	100.94
15848.9	66.54	67.99	68.84	70.95	82.3	95.74	101.37	104.75	106.1	107.95	124.76	100.44
19952.6	66.74	68.2	69.09	70.83	81.89	95.28	100.89	103.94	105.23	107.02	123.09	99.64
25118.9	69.35	70.84	71.62	72.57	80.78	93.7	99.24	102	103.2	105.05	121.92	97.86

Table C-7. HFM (post-cover loss) hydrophone decidecade band percentile values

band	min	1st	5th	10th	25th	50th	75th	90th	95th	99th	max	mean
1	75.42	77.2	80.09	83.14	95.18	107.14	113.81	118.19	120.54	124.48	133.16	114.01
1.3	76.42	78.2	81.09	84.14	96.18	108.14	114.81	119.19	121.54	125.48	134.16	115.01
1.6	74.74	76.25	78.76	82.28	95.94	108.04	114.86	119.52	121.98	126.05	133.9	115.36
2	74.03	75.53	77.69	81.75	96.4	108.49	115.43	120.31	122.84	126.93	134.53	116.13
2.5	73.18	74.78	76.93	81.18	96.53	108.79	115.87	121.06	123.69	127.81	135.65	116.85
3.2	71	73.28	75.44	80.19	96.49	108.9	116.24	121.82	124.56	128.7	136.65	117.57
4	69.38	71.35	73.07	78.23	95.55	108.41	116.15	122.39	125.17	129.26	136.39	118.01
5	70.11	72.08	73.77	78.92	96.25	109.17	116.95	123.28	126.08	130.18	137.34	118.9
6.3	67.18	69.1	70.3	74.85	92.73	106.8	115.59	123.08	126.09	130.2	137.81	118.68
7.9	67.61	69.19	70.36	74.68	92.48	106.74	115.99	124.01	127.12	131.37	138.7	119.68
10	66.69	68.63	69.85	73.98	92.05	107.59	116.2	124.47	127.7	132.08	139.38	120.24
12.6	66.25	68.09	69.22	71.51	88.29	107.32	114.45	121.72	124.84	129.4	136.75	117.66
15.8	65.77	67.61	68.69	70.31	83.77	98.8	109.12	119.01	122.59	127.47	135.21	115.19
20	64.95	66.7	67.83	69.12	81.05	96.28	106.09	116.36	120.2	125.37	134.21	112.86
25.1	64.35	65.91	67.09	68.14	78.05	95.83	103.67	113.34	117.39	122.89	131.28	110.26
31.6	63.85	65.5	66.63	67.69	76.15	92.56	100.87	110.79	114.86	120.77	129.72	107.93
39.8	63.56	65.04	66.28	67.27	74.98	92.15	100.25	107.77	111.76	117.45	126.63	104.97
50.1	63.1	64.63	65.84	66.91	75.54	86.76	95.18	104.25	108.53	114.58	124.63	101.89
63.1	62.98	64.41	65.57	66.25	71.3	84.33	93.37	104.43	109.1	115.39	126.06	102.43
79.4	62.8	64.19	65.33	66.04	70.92	83.95	93.81	104.9	109.43	115.61	125.69	102.65
100	62.57	63.97	65.12	65.76	69.65	80.33	88.7	98.32	103.15	109.83	121.78	96.96
125.9	63.11	64.91	65.93	67.04	71.25	79	85.96	94.99	100.65	108.26	121.65	94.94
158.5	62.3	63.84	65.02	65.81	70.59	78.99	85.84	94.04	99.06	106.83	120.16	93.84
199.5	62.27	63.81	64.9	65.63	69.64	77.73	83.46	89.72	93.7	100.4	124.17	88.77
251.2	62.24	64.13	65.16	66.11	71.51	78.71	83.93	89.12	92.15	97.69	121.09	87.66
316.2	61.7	63.75	64.88	66.35	72.95	80.03	85.05	89.78	92.26	97.47	121.51	87.76
398.1	62.24	64.13	65.43	67.32	73.72	81.11	86.14	90.74	93.2	98.3	119.81	88
501.2	61.93	64.02	65.35	67.38	73.65	81.06	86.14	90.92	93.54	98.8	116.36	87.86
631	61.28	63.65	65.32	67.89	75.14	82.29	87.37	92.36	95.05	100.2	115.17	88.95
794.3	61.13	63.48	65.34	68.1	74.86	82.57	88.14	93.51	96.28	101.37	112.13	89.85
1000	60.9	63.16	64.67	66.86	72.96	80.88	86.86	92.45	95.16	100.34	111.08	88.71
1258.9	60.6	62.72	64.05	66.07	72.09	80.04	86.15	91.6	94.21	99.23	108.49	87.71
1584.9	60.6	62.93	64.77	67.33	74.29	82.56	88.8	94.39	97.06	102.04	115.26	90.5
1995.3	60.94	63.69	66.36	69.61	77.31	86.01	92.54	97.94	100.6	105.36	118.75	93.95
2511.9	61.1	64.12	66.58	69.44	76.95	85.81	92.88	98.41	101.02	105.72	121.3	94.3
3162.3	60.88	63.87	66.38	69.07	76.8	85.88	93.61	99.25	101.73	106.54	114.33	94.98
3981.1	62.11	65.35	67.89	70.92	79.24	88.6	96.31	101.67	104.17	108.77	116.61	97.37
5011.9	62.09	65.68	68.26	71.56	80.08	89.64	97.62	102.97	105.41	109.85	113.84	98.55
6309.6	61.33	64.25	67.01	70.67	79.37	89.58	97.82	102.89	105.13	109.48	113.28	98.38
7943.3	61.91	65.02	67.61	71.31	80.01	90.2	98.31	103.17	105.33	109.49	113.12	98.59
10000	61.88	64.83	67.38	70.89	79.55	90.31	98.33	102.96	105.04	109.07	112.72	98.38
12589.3	61.9	64.74	67.14	70.56	79.05	89.94	97.85	102.32	104.3	108.09	112.18	97.67
15848.9	61.77	64.62	66.84	70	78.17	89.36	97.14	101.37	103.27	106.8	111.15	96.69
19952.6	61.42	64.23	66.29	69.14	76.74	88.43	96.17	100.11	101.95	105.2	109.62	95.44
25118.9	61.15	63.9	66.96	68.82	74.79	86.41	94.12	97.99	99.83	103	107.65	93.32